THE TRANSFERENCE OF AXIAL LOAD

FROM

REINFORCED CONCRETE COLUMNS TO BASES

BY

DHIAB KHIRBEET AL-SAJIR

B.Sc., A.M.I.C.E.

A THESIS SUBMITTED FOR THE DEGREE

OF

MASTER OF PHILOSOPHY

DEPARTMENT OF CIVIL ENGINEERING

UNIVERSITY OF ASTON

IN BIRMINGHAM

JANUARY 1976

SYNOPSIS

The research work described in this thesis is concerned with the transference of axial load from reinforced concrete column to concrete base. The load is transferred to the base by column longitudinal reinforcement, core concrete, and cover concrete.

The first stage is primarily concerned with the literature review, design, preparation, and testing of specimens, which are designed to show the effect of the following base slab properties on the transference of the axial load where H-T square twisted steel bars are used for base and column reinforcement :

(1) The overall depth (h) and therefore the bond length of the column bars.

(2) Amount of tensile steel reinforcement (A_s) and hence (p)

(3) The lateral dimensions (A x B).

The second stage is concerned with the results and calculations and shows how the above variations affected the transference of the axial load from the column steel to the base by anchorage bond and on the column strength as a whole.

From these calculations it is found that the British code uses conservative ultimate anchorage bond stresses and a low allowable stress for steel in compression where the American code uses high or sometimes unsafe ultimate anchorage bond stresses and a very high allowable stress for steel in compression. It is found that part of the column length is acting as an extra anchorage length for the column longitudinal steel in addition to the embedment length in the base slab concrete.

The third stage is concerned with the transference of axial load from column concrete to base and shows that this load is transferred

from the core concrete at a higher stress than that from the cover concrete. A three part addition formula is suggested to calculate the ultimate axial load transferrable from a short reinforced column to a concrete base according to the above finding.

Finally the distribution of the anchorage bond stress along the anchorage length is predicted. This shows that a parabola plus a constant gives the best fit with the experimental results and that the results are best related to $\sqrt{f_{cu}}$ rather than f_{cu}.

ACKNOWLEDGEMENTS

The author wishes to express his gratitude to his supervisor, Mr. A. W. Astill, B.Sc. C.Eng. F.I. Struct.E. for his help, guidance and encouragement throughout this research project, and Dr.L. H. Martin, B.Sc., Ph.D., C.Eng., M.I.C.E. for acting as advisor. The author also wishes to express his appreciation to: The Ministry of Communications (Iraqi Ports Administration) of the Republic of Iraq for providing the scholarship during the course of this work. Mr. W. Parsons, The Departmental Superintendent of the Civil Engineering Department at the University of Aston, together with all the technicians and secretarial staff of the same department, for their willing and useful advice during all the stages of this project.
Mrs. L. Perkins, for her excellent typing of the script.
Miss. P. Sage for reproducing the drawings with such a good care.
His parents, wife and Mr. M. Al-Sajir, for their patience, help and encouragement.

CONTENTS

Page No.

Page No.

LIST OF TABLES

LIST OF FIGURES

NOTATION

NOTE - Some of the symbols used in one place only defined where they occur and not included here.

A	Length of base slab.
A_c	Area of concrete.
A_s	Area of tension reinforcement (for bases).
A_{sc}	Area of longitudinal reinforcement (for columns).
A_{sv}	Cross-sectional area of the two legs of a link.
a_1, a_2	Lateral dimensions of the column.
B	Width of base slab.
B_{i-j}	Base no (j) from series (i).
b	Width of section.
C_{i-j}	Column no (j) from series (i).
d	Average effective depth of tension reinforcement (for bases).
E_c	Secant Modulus for concrete.
E_{ce}	Initial tangent Modulus of elasticity for concrete.
E_s	Modulus of elasticity for steel.
f_{bs}(ACI)	Anchorage bond stress (ACI 318-1971.)
f_{bs}(av.)	Average anchorage bond stress at failure of column (Test).
f_{bs}(CP110)	Anchorage bond stress (CP110:Part 1:1972 Table 22).
f_{bs}(max)	Maximum anchorage bond stress at failure of column (Test).
f_{bs}(theory)	Average ultimate anchorage bond stress (Theoretical).
f_c	Maximum average stress in the column concrete at failure.
$f'_c=0.8f_{cu}$	or as stated where it occurs.
f_{cu}	Compressive strength of concrete measured from 150 mm. cube.
f_s(av.)	Maximum average stress in column longitudinal reinforcement. Corresponding to ε_s (av.).

f_s(max)	Maximum maximum stress in column longitudinal reinforcement corresponding to ε_s (max.).
f_t	Tensile stress measured from 150 mm. x 300mm. cylinder splitting test for concrete.
f_1	Maximum compressive stress in the column core concrete at failure.
f_2	Maximum compressive stress in the column cover concrete at failure.
f_y	Yield stress of reinforcement taken as 0.2% proof stress or as specified in the equations.
h	Overall depth of base slab.
K =	$\frac{E_s}{E_{ce}}$ Stiffness of a reinforcing bar.
l	Anchorage length of the column longitudinal reinforcement.
P_{test}	Maximum axial load on column at failure (Test).
P_{ult}	Calculated ultimate axial load for column using eqn.(1).
P_1	Calculated ultimate axial load for column using eqn.(8).
P_2	Calculated ultimate axial load for column using eqn.(9).
P_3	Calculated ultimate axial load for column using eqn.(10).
R =	f_{bs} (av.) /f_{bs} (theory).
s_b	Spacing of bars c - c for base reinforcement.
T_{i-j}	Test no (j) from series (i).
v	Shear stress.
v_c	Ultimate shear stress in concrete.
w/c	Water cement ratio.
γ_m	Partial safety factor for strength.
ε_s (av.)	Average longitudinal strain measured on column longitudinal reinforcement at failure.

ε_s(max.)	Maximum longitudinal strain measured on column longitudinal reinforcement at failure.
ξ_s	Depth of slab factor (Table 14 CP110:Part 1: 1972).
ρ	$\frac{100\, A_s}{Bd}$, % of tensile reinforcement in base slab or = $\frac{100\, A_{sc}}{a_1\, a_2}$, % of column longitudinal reinforcement.
ν_c	Poisson's ratio $= \frac{\text{Lateral strain}}{\text{Longitudinal strain}}$
ϕ	Bar size.

CHAPTER 1.

INTRODUCTION, REVIEW OF PREVIOUS WORK AND THEORY

1.1. INTRODUCTION

Slabs, beams, columns and bases are the most important structural parts of any structure.

The behaviour of columns and bases has received a steadily increasing interest during the past sixty or seventy years, but most of the research done was concerning one of them in detail without the consideration or the effect of each part on the behaviour of the other.

The subject of the present investigation is to find how the axial load of a reinforced concrete column is transferred to a concrete base slab and what effect variation of each property has on the other.

1.2 LITERATURE REVIEW

A literature study of the subject under consideration revealed that a number of experimental and theoretical studies have been carried out by several investigators but they are either concerned with reinforced concrete slabs and footings or reinforced concrete columns, and some of the work is indirectly related to the subject.

1.2.1. WORK DONE ON REINFORCED CONCRETE FLAT SLABS AND BASES

Most of the work done on this topic is concentrated on punching shear, flexural strength and bond stress between slab concrete and its tensile reinforcement which can be defined as the transfer of load per unit surface area of a bar to the surrounding concrete. By punching shear is understood the failure of a flat slab or base slab around a column or other concentrated load, when the magnitude of the failure load is less than that corresponding to the available flexural strength which is based on the strength of the concrete section and the tensile reinforcement across it.

Numerous attempts have been made to present theoretically acceptable formulae for the calculation of bond stress, punching resistance and flexural strength which are also in satisfactory agreement with the experimental results.

Some of the work done on these three subjects which has relevant relation with the aim of this project, is listed below :-

The first extensive work done on column footings was reported by Talbot (1913). Altogether (114) wall footings and (83) column footings were tested to failure. In all the column footings the load was applied through a (12" x 12" x 12") concrete stub and they were supported on steel springs to simulate uniform upward pressure, twenty of the column footings failed by punching shear and the rest either by tension failure or bond failure between the slab reinforcement and the concrete, and one failed by crushing of the concrete stub.

Talbot's study of reinforced concrete footings has been of the utmost importance in the design practice of many countries throughout the World.

Bach and Graf (1915) reported a large number of slab tests which were designed mainly to study flexural strength. However, a few slabs failed in shear and Graf (1933) (1) reported a series of tests on slabs subjected to concentrated loads near the supports.

Graf (1938) (2) reported another series of tests on eight very thick slabs of which six had shear reinforcement.

Marshall (1944) reported his work on reinforced concrete column bases in which he studied the effect of the bed used on the strength of the base. The specimens were models from cement-sand mortar and three different beds were used, sand, rubber sheets and clay. The load applied at the centre through a 2" square steel block. The other part of the work is testing 2' square and 4" thick slabs using 4" square stanchion and the object of his work is to determine the effect of the reinforcement in the base on its strength.

Forsell and Halmberg (1946) reported shear tests of slabs and the shearing stresses were computed assuming a parabolic distribution across the depth of the slab, and the critical section was taken at a distance ($\frac{h}{2}$) from the loaded area.

Richart (1948) presented the results of a very extensive investigation on reinforced concrete footings. In his experiments he also used a concrete stub to act as a column, and steel springs to support the footings. (104) of the isolated footings failed in punching shear and the rest failed in the same way as those of Talbot (1913). The test results served as a basis for many of the empirical relationships which were derived later for punching shear and flexure.

Hognestad (1953) reported the results of an extensive re-evaluation of the shear failure of footings which were reported by Richard (1948). He suggested that the shearing stresses be computed at zero distance around the loaded area.

Elstner and Hognestad (1956) reported the results of tests on (36) slabs which were 6' square by six inches thick. Most of the slabs were supported along all four sides but a small number were supported on two sides only. The concrete strength, the amount of tension and compression reinforcement, shear reinforcement and the size of the column were varied.

Whitney (1957) presented an ultimate strength theory of shear which he based on re-evaluation of previously reported test results by Richart (1948) and Elstner and Hognestad (1956). He calculated the shearing strength at a critical section ($\frac{d}{2}$) from the perimeter of the loaded area.

Base (1959) published details of small-scale tests on (18) reinforced concrete slabs supported on four sides. It was concluded that the amount of tensile reinforcement and the resulting degree of flexural cracking effect the punching failure significantly, furthermore, the addition of compression reinforcement to the slabs apparently had little effect on the failure load.

Kinnunen and Nylander (1960) presented a valuable study of shear failure of slabs without shear reinforcement. That was the first real attempt to establish a theoretical method of analysis. The experimental work consisted of (61) circular slabs approximately 6' diameter and six inches thick. These specimens were supported around by the rods along the circumference and an upward vertical load was applied at the centrally placed circular column. The main variables in these tests were the type and amount of flexural reinforcement and the diameter of the column stub.

Moe (1961) presented the results of thirty-one slabs tested under vertical loading and twelve slabs tested under combined loading. All slabs were 6' square and six inches thick simply supported along the edges. The main variables were concrete strength, percentage of tensile reinforcement, column dimensions and shear reinforcement. By carrying out an extensive statistical study of most of the tests reported before (1961) Moe predicted the ultimate shearing strength of slabs with a good accuracy by an empherical formula.

Medina (1961) reported the results of four tests on 6' square slabs in which the main variable was the amount of shear reinforcement. Kinnunen (1963) represented an extension of the theory of Kinnunen and Nylander (1960) to apply to slabs with two-way reinforcement. In this instance, the dowel and tensile membrane effect were considered in estimating the increased load-carrying capacity of the slab.

Hognestad, Elstner and Hanson (1964) and Ivy (1966) reported two papers in which the shear strength in light-weight concrete was studied. The slabs were 6' square with six inchest total depth supported along four edges. Four specimens tested by Ivy (1966) had different dimensions. The main variables were percentage of reinforcement and type of concrete.

Hognestad, Elstner and Hanson (1964) related the shear strength of the slab to the splitting tensile strength of the concrete. The critical section is assumed to be located on the perimeter of the loaded area.

Long and Bond (1967) (1), (2), (3) presented small scale square slab tests. A theoretical method of analysis was developed from elastic thin plate theory. The slabs were subjected to vertical and combined loads. They studied the concrete under bi-axial state of compressive stress and different failure modes were recognized.

Tankut (1969) reported test results of two full scale flat slab structures. They were 21' square and four inches thick supported on nine columns. The slabs tested under combined loading which was due to a system of vertical jacks representing uniformly distributed load and to a line of horizontal load acting along one of the edges.

Stamenković (1969) published results of three feet square slabs tested under different types of load combinations. The interaction between vertical load and moment was studied by combined load tests and interaction relations are proposed for internal, edge and corner column.

Anis (1970) presented his work on shear strength of reinforced concrete flat slab without shear reinforcement. The theoretical solution he preposed includes solutions for edge, and corner column. The experimental part concentrated on these two cases since a lot of experiments were done for internal columns and axial loading.

Stamenković and Chapman (1972) reported their work on fifty-two three feet square by three inches thick slabs, with 5" x 5" and 3" x 6" column stubs above and below the slab. Ten of the tests were axialy loaded and the column stubs were reinforced.

Ir. M. Dragosvić and Ir. A. Vander Beukel (IBBC-TNO) (1974) reported their work on punching shear in which they calculated the circumference for the critical section for punching shear at ($\frac{d}{2}$) from the column. They showed that the punching resistance of a slab is independent of the percentage of its tensile reinforcement. They proposed an emperical solution for calculating the punching shear resistance for axialy loaded slabs which shows a very good agreement with Talbot (1913) and Richart (1948) experimental results on column footings which failed by punching shear. The solution is very simple to use and the formula is used to calculate the depth required to resist punching shear failure for this project, see equation (2).

Regan (1974) reported his work on design for punching shear in which he assumed that the perimeter critical for shear cracking is located at a distance (d) from the faces of the column then he computed the shear stresses obtained using his formula and the experimental results from Kinnunen and Nylander (1960) and compared them with CP110: Part 1: 1972 for axial loading and showed that the comparison is reasonable.

1.2.2. WORK DONE ON REINFORCED CONCRETE COLUMNS

Many researchers have done a lot of work on reinforced concrete columns to study the effect on their strength by varying their materials and geometrical properties.

Some of the work which is relative to this research program follows :-

Pfister and Mattock (1963) reported their work on lapped splices in concentrically loaded columns with high strength reinforcing bars. They calculate the ultimate strength by using an addition formula which is

$$\text{ultimate strength} = 0.85f'_c\ A_c + f_y A_{sc}$$

where f_y is the yield stress corresponding to a strain of 0.6% and f'_c is the 6" x 12" cylinder strength of the concrete.

They found generally that steel stresses calculated using the above formula are higher than those obtained by direct strain measurement.

They also indicated that some of the total force transferred by a lapped splice is transferred by end bearing between the bars and the concrete.

Sargin, Ghosh and Handa (1971) published their experimental investigation on the effect of lateral reinforcement upon the strength and deformation properties of concrete. The main variables were : concrete strength, size, spacing and grade of lateral reinforcement, strain gradient and thickness of cover. In the analysis they treated the laterally reinforced specimens as composite members consisting of core and cover.

Ghosh, Sargin and Handa (1971) reported their work on the effectiveness of cover in reinforced concrete compression member, they have tested fourteen specimens with no longitudinal reinforcement used in any of them, and the primary variable was the thickness of the cover.

Somerville (1971) presented his work on structural joints in precast concrete columns and beams. He used the addition formula to calculate the theoretical ultimate axial load for columns which was in the form :-

$$\text{ultimate axial load} = 0.75f_y A_{sc} + 0.67f_{cu} A_c .$$

He found generally that steel stresses calculated using the above formula are higher than those obtained by using direct strain measurements on the reinforcement. He also suggested that a proportion of the force in the longitudinal bars is transferred to the concrete by end bearing.

Somerville and Taylor (1972) reported the results of their work on joggled splices in columns altogether five specimens were tested in axial compression. The theoretical failure load was calculated for each specimen from strain compatibility consideration. They also indicate that some of the load in the bars was being transferred to the concrete by end bearing.

1.2.3. WORK DONE ON SUBJECTS WHICH ARE RELATED TO THIS PROJECT

1.2.3.1. WORK DONE ON BOND STRESS BETWEEN STEEL REINFORCEMENT AND CONCRETE

All the work done on this topic was concentrated on finding a value for bond stresses using steel reinforcement in tension and no experimental effort was made to find them using compression steel reinforcement, apart from the work done on lapped splices in compression which is listed earlier, and this work does not give the actual bond stresses since some of the force in the bars is transferred to the concrete by end bearing and this prevents the bar from slipping.

1.2.3.2. WORK DONE ON BEARING CAPACITY OF CONCRETE

The first work reported on the bearing capacity of concrete and rock is by Meyerhof (1953). Then Shelson (1957) published his work on bearing capacity of concrete in which he found that bearing capacity increases as the ratio of the footing area to loading area increases until this ratio reaches (30) then the bearing pressure reaches a limiting value. Au and Baird (1960) reported their work on the bearing capacity of concrete blocks. They have tested (60) specimens and they used two concrete mixes with different maximum aggregate size where the block area is 2-16 times the contact area.

They confirm that the bearing pressure increases as the ratio of the block area to the loaded area increases.

Ersoy and Hawkins (1960) in their discussion of the work done by Au and Baird(1960) suggested that the bearing capacity of the concrete will approach some limiting value as the ratio of the block area to the loaded area increases indefinitely.

1.2.4. EXISTING DESIGN SPECIFICATIONS

1.2.4.1. THE BRITISH CODE OF PRACTICE CP110: PART 1: 1972

1) Design of columns :- For short columns the ultimate axial load is

$0.4\ f_{cu}\ A_c + 0.67\ f_y\ A_{sc}$ (3.5.3 eqn (25)). From (3.11.6.5) the length of the lap in compression reinforcement should be at least equal to the anchorage length derived from (3.11.6.2) required to develop the stress in the smaller of the two bars lapped and should not be less than $20\ \phi + 150$ mm.

2) Design of bases :- For design of bases the code considered the following :-

a. Resistance to bending (3.10.4.1)

b. Shear (3.10.4.2)

c. Bond and anchorage (3.10.4.3)

1.2.4.2. EXPLANATORY BOOKS ON CP110: PART 1: 1972

1) Designed and detailed CP110: 1972 by Higgins and Hallington (1973), page (22). For the design of reinforced pad footing $f_y = 410\ N/mm^2$, $f_{cu} = 30\ N/mm^2$, and the column has 6-32 mm. ϕ bar as longitudinal reinforcement. They found that the required depth was 500 mm after considering shear, bending and local bond in the

slab reinforcement, the bond length needed for the column starter bars was ignored.

2) Concrete design to CP110 - simply explained by Allen (1974), page (201) example 15.1. For the design of square base having $f_{cu} = 25N/mm^2$, and using mild steel reinforcement for the base and no information was given on column reinforcement, he found that the required depth was 500 mm. after checking for bending, shear and anchorage bond for base reinforcement.

1.2.4.3. THE AMERICAN CODE OF PRACTICE ACI 318-71

In the design of bases the code specifies that the calculated shear stress at ($\frac{d}{2}$) from faces of the column (11.10.2) should not be greater than 4 $\sqrt{f'_c}$ psi where f'_c is the compressive strength of concrete in psi based on tests of 6" x 12" cylinders (11.10.3) and this shear stress has constant value throughout depth (d) and length of the critical perimeter at ($\frac{d}{2}$) from faces of the column.

All axial forces applied at base of column shall be transferred to the top of the supporting footing by compression in the concrete and by reinforcement of the column (15.6.1).

Where transfer of force is accomplished by reinforcement, the development length of the reinforcement shall be sufficient to transfer the compression to the supporting member (15.6.4) and this development length of a deformed bar in compression is $0.2\ f_y\ d_b\ /\ \sqrt{f'_c}$ but not less than $0.000\ 3\ f_y\ d_b$ or 8" (12.6) where f_y is the stress corresponding to a strain of 0.35% for $f_y > 60000$ psi (3.5) and d_b is the nominal diameter of bar.

Hooks shall not be considered effective in adding to the compression resistance of reinforcement (12.8.3 and 15.5.4).

1.2.5. DISCUSSION AND CONCLUSIONS

1) In CP110: Part 1: 1972 and the explanatory books for it by Higgins

and Hallington (1973) and by Allen (1974), the anchorage length for the longitudinal column reinforcement in the base was not mentioned at all while it is specifically stated in the ACI 318-71. Hence, if the anchorage bond stresses stated in CP110: Part 1: 1972 table (22) are to be used to calculate the anchorage length and then the base slab depth for the example solved by Higgins and Hallington (1973) page (22), assuming that the column bars are of type (1) specified in CP110: Part 1: 1972, it would be equal to (896.5 mm + cover) in stead of (500 mm) and if it is designed according to the ACI 318-71, it would be equal to (639.4 + cover). The ratio of the two calculated anchorage lengths is 1.4.

For the example solved by Allen (1974) a column design is done based on the cross-section given, using H.T steel bars type (1) having a characteristic strength $f_y = 410$ N/mm^2, and the characteristic strength of the concrete f_{cu} is 25 N/mm^2. 4-25 mm. Ø bars must be used for minimum reinforcement, hence using the same calculations done for the example solved by Higgins and Hallington (1973), it is found that the overall depth of the base slab is (788 mm + cover) using CP110: Part 1: 1972 and (547.2 + cover) using ACI 318-71 instead of 500 mm. The ratio of the two anchorage lengths calculated is 1.44. The ratio of the two calculated anchorage lengths increases as the value of f_{cu} decreases.

Therefore, we can conclude that punching shear and bending moment do not always govern the depth of the base slab.

Also the difference between designing according to the British code and the American one is large as we have seen from the previous examples and since I have not been able to find any experimental work on this subject, further clarification is needed.

2) The effect of (ρ) on the anchorage bond and shear stresses was not stated in the ACI 318-71 while it is stated in CP110: Part 1: 1972 for shear stresses only.

3) From the work done in (1.2.3.2.) we can see that the bearing capacity of the concrete increases as the ratio of the footing area to the column area increases and hence this might have a similar effect on the anchorage bond stresses, it may also justify a higher compressive stress in the concrete of the column if suitable links are used.

4) Many of the researchers suggested that some of the load is transferred from the longitudinal reinforcement to the concrete by end bearing. This also applies for columns with starter bars. Hence, the stresses in the starter bars may be smaller than in the main bars leading to a smaller anchorage length.

5) In all the previous experimental program the axial load was applied to the reinforced concrete slabs either through a concrete stub or a steel plate and even if a reinforced concrete stub is used it is over designed since the ratio of the failure load of the slab to the ultimate axial load of the column calculated by equation (1) is only 0.192, 0.178 for S1-60 and S1-70 of Moe (1961) tests respectively and the same ratio is 0.165, 0.228 for V/I/2 and V/Ir/1 of Stomenbović and Chapman (1972) tests respectively. Hence from these ratios we can conclude that the stresses in the column reinforcement are very small and hence the anchorage bond stresses are also small which means only a shallow depth is needed and that is why only shear or bending moment failures were noticed.

1.2.6. EXPERIMENTAL PROGRAM FOR THIS PROJECT

From the discussion and conclusions of the literature review, the topic of this research program becomes very important, and a lot of clarification is needed since there are so many variables affecting the transference of axial load from R.C. columns to bases. Due to the limit of time only the following have been investigated.

1) The effect of varying the overall depth of the base slab (h) on the transference of axial load from R.C. columns to bases and keeping all other variables constant.

2) The effect of varying the quantity of tensile steel reinforcement and the diameter of bars used for the same quantity of tensile steel in the base slab for a fixed (h) and the rest of variables are constant.

3) The effect of varying the lateral dimensions of the base slab (A and B) for a fixed value of (h) and other variables are constant.

1.2.7. DESIGN OF SPECIMENS

Each specimen consists of a reinforced concrete column and a reinforced concrete base slab or a plain concrete base slab. Due to the limitation of space in the testing rig, the total height of specimens is fixed at (1030 mm.) while the maximum length x bredth was 900 mm. x 900 mm.

Also due to the maximum loading capacity of the loading cell the column dimensions were chosen to be 200 mm. x 200 mm. in cross-section which is also a reasonable section for site work. The columns are designed according to CP110: Part 1: 1972 concerning the size and spacing of links. 4-20 mm. Ø H-T square twisted steel bars are used as column reinforcement which give Asc = 1257 mm^2. and it is 3.14% of the column cross-section area. This reinforcement and a chosen f_{cu} =

35 N/mm^2. still keep the failure load of the column within the capacity of the loading cell.

The bases have different dimensions and reinforcement for each series of tests.

The dimensions of the specimens are shown in fig. (1.1) where the details are in figs. (2.1, 2,3,4,5 and 6) for series (1), (2) and (3) respectively.

To avoid end bearing in the longitudinal reinforcement for the columns, the bars are continued straight to the bottom face of the slab and a hole in the base steel plate of 200 mm. x 200 mm. was made, see fig. (2.1). This hole allows the column longitudinal 20 mm ø bars to push through without end bearing and also to see if punching shear failure does occur along the periphery of the column and at what stress.

Failure of the base due to bending is avoided by supporting the base on a solid steel plate.

To avoid failure due to stress concentration at the top of the column the spacing of the links was reduced as shown in figs. (2.1, 3, 5).

To ensure that the steel and concrete of the column carried their proper share of load, the longitudinal bars were welded to the top steel plate.

1.2.8. <u>THEORY FOR CALCULATIONS</u>

1.2.8.1. <u>CALCULATED ULTIMATE AXIAL LOAD FOR COLUMN (P_{ult}).</u>

For the calculation of the theoretical ultimate axial load CP110: Part 1: 1972 uses stresses 0.4 f_{cu} for concrete and 0.67 f_y for steel in the addition formula.

The concrete factor is obtained from $\frac{0.67}{\gamma_m}$ where the 0.67 is introduced to allow for the difference indicated by a cube crushing test and the strength of the concrete in the structure. A cube is crushed between two parallel steel plates which restrain the lateral expansion of the concrete by friction and leads to artificially high results whereas the area which crushes in a structure is bounded by concrete which does not give the same restraint. Also a short specimen will always give a higher result than a longer one. γ_m is 1.5 which takes account of possible differences between the material in the actual structure and the strength derived from test specimens and it covers items such as insufficient compaction, difference in curing dirty casting conditions and segregation in transport. Hence $\frac{0.67}{1.5} f_{cu} = 0.4466 f_{cu}$ then reduced by 10% to allow for the accedental moment specified in code, therefore, the concrete stress becomes $0.4 f_{cu}$.

The steel stress factor is obtained from the maximum stress in compression $\left[(f_y / \gamma_m) / (1 + \frac{f_y}{2000 \gamma_m})\right]$ γ_m is 1.15 which takes account of corrosion and variations of cross-sectional area. Therefore, the factor is variable as the value of f_y varies and it is 0.74 for f_y = 410 N/mm^2, 0.784 for f_y = 250 N/mm^2 and 0.72 for f_y = 460 N/mm^2.

Hence a stress of $0.75 f_y$ is used for short column design reduced by 10% for the same reason as that for the concrete, the stress becomes $0.67 f_y$.

Somerville (1971) used $0.67 f_{cu}$ and $0.75 f_y$ to calculate the theoretical axial load of the columns in his experimental program. Therefore, for simplicity the addition formula is used to calculate P_{ult} in the same way as it is used in CP110: Part 1: 1972, except for the stress factors, that is

$$P_{ult} = 0.8 f_{cu} A_s + 0.9 f_y A_{sc} \quad \ldots\ldots\ldots\ldots\ldots\ldots\ldots\ldots\ldots\ldots\ldots (1)$$

The factor of 0.8 is used since the average value of f_c/f_{cu} for all the tests in the three series is 0.797 and this is well established from test results for a member of the same concrete as a cube. This factor is twice the code factor and about 1.2 x that used by Sommerville (1971).

The steel stress factor of 0.9 is used to fit the experimental results of T_{1-6} and this is not far from the ratios of $\frac{f_{s(av.)}}{f_y} = 0.85$ and f_s (max.) / f_y = 0.941, see table (3.3). This factor is 1.343 x that of the code and 1.2 x that used by Somerville (1971). This means that P_{ult} of equation (1) is 1.2 x P_{ult} calculated by Somerville (1971).

All these equations can be written in a general form which is

$$P_{ult} = \alpha \; f_{cu} \, A_c + \beta \; f_y \, A_{sc}$$

Where α and β are the factors tabulated in Table 1.1.

	(1)	(2)	(3)	(4)	(5)
	Equation (1)	Sommerville (1971)	CP110:Part 1 1972.	(1)/(2)	(1)/(3)
α	0.80	0.67	0.40	1.20	2.00
β	0.900	0.750	0.670	1.200	1.343

1.2.8.2. PUNCHING SHEAR STRENGTH OF BASE SLABS

The punching shear strength of the base slab is calculated using the same equation used by Ir.M. Dragosavić and Ir. A. Van Den Beukel (IBBC - TNO) (1974) since it is very simple to use and fits very well with Talbot (1913) and Richart (1948) test results.

Hence,

$$\text{The punching shear strength} = \left[(2a_1 + 2a_2) + \pi \; d\right] (1 + 0.05 \, f_{cu}) \, d \quad \text{.................................(2)}$$

where a_1 and a_2 are the lateral dimensions of the column.

Equation (2) is used to find the depth of slab required to resist punching shear failure so that it can be compared with the depth of slab required to resist anchorage bond failure between column longitudinal reinforcement and the base slab concrete.

Also to compare these results with the current codes of practice equations (3) and (4) are used for CP110: Part 1: 1972 and the ACI 318-71 respectively.

$$\text{Punching shear strength} = \xi_s \, v_c \left[(2a_1 + 2a_2) + 3\,\pi\, h\right] \, d \quad \ldots\ldots\ldots\ldots\ldots\ldots\ldots\ldots\ldots\ldots\ldots(3)$$

where ξ_s obtained from table (14) and v_c from table (5) of the British code.

and

$$\text{Punching shear strength} = \left[(2a_1 + 2a_2) + \pi\, d\right] \, 0.85 v_c \, d \quad \ldots\ldots\ldots(4)$$

where $v_c = 0.3352 \sqrt{f_c'}$ (11.10.3) of the American code.

1.2.8.3. ANCHORAGE BOND STRESSES

The anchorage bond stresses f_{bs}(av) and f_{bs}(max.) are assumed to be constant over the effective anchorage length, taken as the force in the bar divided by the product of the effective anchorage length (which is (h) in this case) and the effective perimeter of the bar. f_{bs} (av.) is calculated using the average force in the four bars of the column while f_{bs} (max.) is calculated using the maximum force in one of the four bars of the column.

To compare these results with the current codes of practice equations (5) and (6 a, b) are used for the British and American codes respectively.

$$\text{Anchorage length} = l = \frac{f_u\, \emptyset}{4\, f_{bs}(\text{CP110})} \quad \ldots\ldots\ldots\ldots\ldots\ldots\ldots\ldots\ldots(5)$$

where $f_u = \dfrac{2000\, f_y}{2000\, \gamma_m + f_y}$ and since the proof stress of the steel

control specimens is used for f_y therefore, the partial safety factor

γ_m = 1 instead of 1.15 as specified in the British code where γ_m = 1.15 is used for the calculations of the examples solved by Higgins and Hallington (1973) and Allen (1974). f_{bs} (CP110) is the anchorage bond stress obtained from Table (22) of the British code.

$$\text{Anchorage length} = l = \frac{0.23875\, f_y\, \phi}{\sqrt{f'_c}} \quad \text{......................(6.a)}$$

$$\text{or} \quad l = 0.427\, f_y\, \phi \quad \text{.......................................(6.b)}$$

or l = 203.2 mm. whichever the greater.

Where f_y is the stress corresponding to a strain of 0.35% for f_y exceeding 421.9 N/mm^2 (3.5) of the American code.

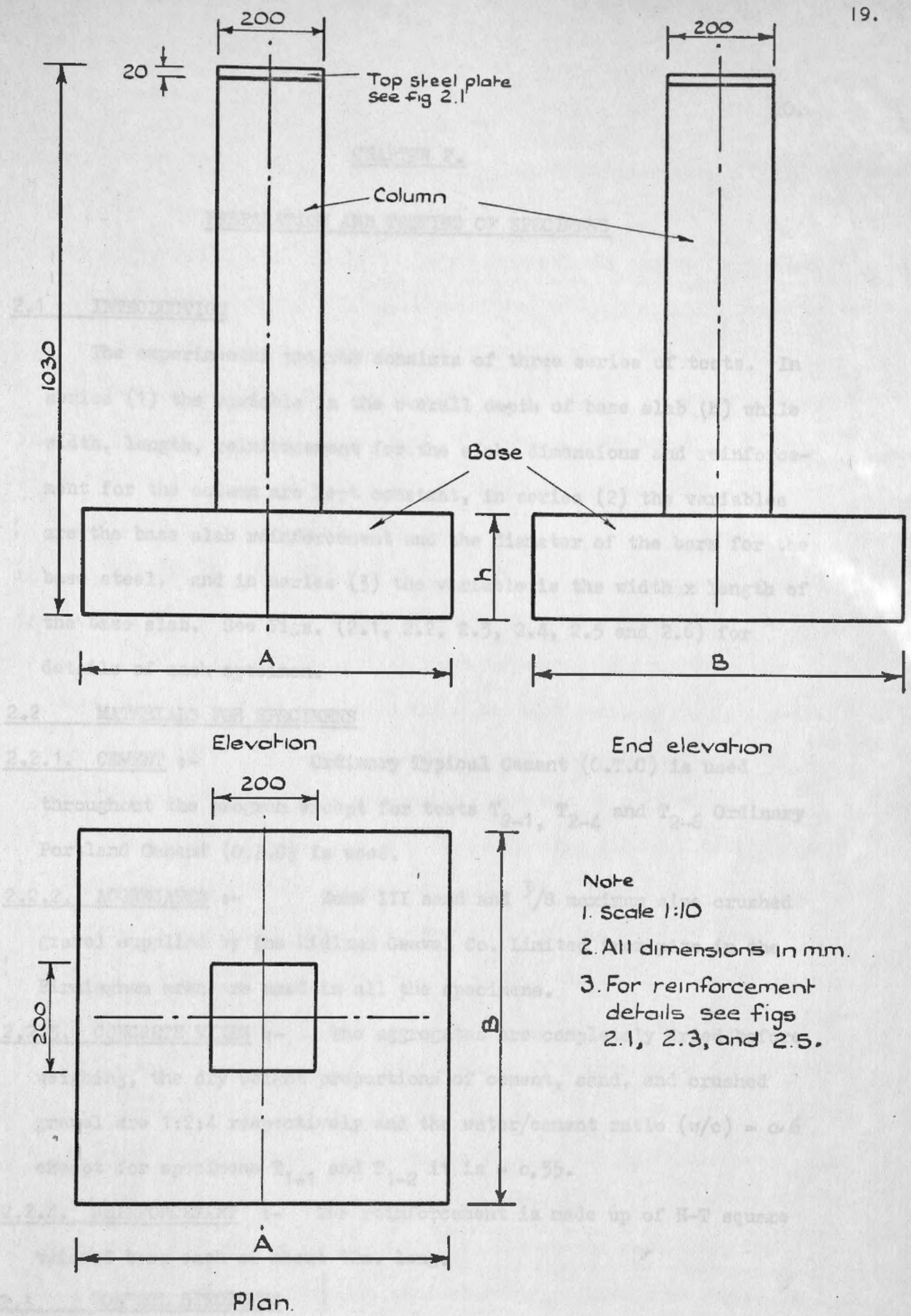

Fig. 1.1 General views for specimens of series 1.2. and 3

CHAPTER 2.

PREPARATION AND TESTING OF SPECIMENS

2.1 INTRODUCTION

The experimental program consists of three series of tests. In series (1) the variable is the overall depth of base slab (h) while width, length, reinforcement for the slab, dimensions and reinforcement for the column are kept constant, in series (2) the variables are the base slab reinforcement and the diameter of the bars for the base steel, and in series (3) the variable is the width x length of the base slab. See Figs. (2.1, 2.2, 2.3, 2.4, 2.5 and 2.6) for details of each specimen.

2.2 MATERIALS FOR SPECIMENS

2.2.1. CEMENT :- Ordinary Typical Cement (O.T.C) is used throughout the program except for tests T_{2-1}, T_{2-4} and T_{2-6} Ordinary Portland Cement (O.P.C) is used.

2.2.2. AGGREGATES :- Zone III sand and 3/8 maximum size crushed gravel supplied by The Midland Gravel Co. Limited from pits in the Birmingham area are used in all the specimens.

2.2.3. CONCRETE MIXES :- The aggregates are completely dried before weighing, the dry weight proportions of cement, sand, and crushed gravel are 1:2:4 respectively and the water/cement ratio (w/c) = 0.6 except for specimens T_{1-1} and T_{1-2} it is = 0.55.

2.2.4. REINFORCEMENT :- The reinforcement is made up of H-T square twisted bars each of about 12m. long.

2.3 CONTROL SPECIMENS

2.3.1. CONCRETE :- With each casting a set of concrete control specimens is cast. This consists of :-

(a) 4 - 5,150 mm. cubes from which f_{cu} is determined by averaging the testing results.

(b) 4,300 x 150 mm. cylinders. The stress-strain curves from which the secant modulus (E_c) calculated and poisson's ratio are obtained by testing two of the cylinders while the splitting tensile strength (f_t) is determined by testing the other two.

2.3.2. STEEL :- From each 12 m. bar a specimen 450 mm. long is tested in tension to determine the modulus of elasticity (Es), yield stress (f_y) and yield strain.

2.4 TESTING RIG AND MACHINES USED

2.4.1. TESTING RIG :- A photograph of the testing rig is shown in Fig. (2.7). The load is applied to the specimen by four hydraulic jacks through a steel platen on which the base steel plate is placed. The oil is pumped to these jacks by one pump through a four valve manifold by which the pressure on each jack can be controlled.

The maximum loading capacity of the testing rig is 8000 KN. The load reading is recorded from a calibrated dial gauge in the loading cell which is placed on the top steel plate of the column. The maximum capacity of the loading cell is 2000 KN. It has two 70 mm. thick steel plates and between them a steel sphere through which the load is applied. This arrangement ensures that axial load is applied to the column.

2.4.2 OTHER MACHINES USED :- The concrete cubes and cylinders are tested by a 3000 KN. Capacity Dension Compression Testing Machine and a Peekel strain recorder is used to record the strains in the concrete cylinders, while the reinforcement specimens are tested by a Denison Universal Testing Machine with a Baldwin automatic strain recorder which produces a load-extension graph. The strains in the reinforcement are measured by the Compulog Data Logger which prints the strains automatically for each load increment.

2.5. STRAIN AND DEFLECTION MEASUREMENTS

The strains in the H.T. square twisted reinforcing bars are measured by electrical resistance strain gauges which have either 6 mm. length, 2.14 gauge factor and 120 Ω gauge resistance or 5 mm. length, 2.04 gauge factor and same gauge resistance. These gauges are connected to the Compulog Data Logger.

The vertical and lateral strains in the concrete control specimens are measured by the electrical resistance strain gauges which have a gauge factor = 2.07, gauge resistance = 120 Ω and length = 60 mm. These gauges are connected to the Peekel strain recorder. All the electrical resistance strain gauges are manufactured by Tokyo Sokki Kenkyujo Co. Limited.

The longitudinal and lateral strains in the column are measured by 8" and 6" Demec gauges respectively.

The deflection of the base slab at the centre lines 105 mm. from faces of column and the upward movement of the loading platen (the total shortening of the specimen) are recorded from dial gauges reading to 0.001".

The position of all these gauges and their numbers are shown in Figs. (2.2, 2.4 and 2.6) for series (1), (2) and (3) respectively.

2.6. PREPARATION OF SPECIMENS

2.6.1 MOULDS :- The moulds used are made of wood and are divided into two parts, the first part is for the base and 50 mm. of the column height and the second part is the rest of the column height. See Fig. (2.8).

2.6.2 REINFORCEMENT

2.6.2.1. COLUMN REINFORCEMENT :- For all the three series of tests the longitudinal reinforcement consists of 4-20 mm. of H.T. square twisted bars each bar has a straight length of 1025 mm. ($\rho = 3.14$). The lateral reinforcement consists of 6 mm. Ø H.T. square twisted bars. The first link is 60 mm. above the top surface of the base slab followed by two links 200 mm. centre to centre. Near the top of the column for all specimens the link spacing is reduced to prevent local failure due to the stress concentration at the point of application of the load. See Fig. (2.1, 2.2, 2.3 and 2.5) for the spacing of these links. The measurement of bending dimensions of the links are according to B.S. 4466 - 1969.

The inside dimensions of all the links are 140 x 140 mm.

2.6.2.2. BASE SLAB REINFORCEMENT:- The base slab reinforcemt consists of 16 mm. Ø H.T. square twisted bars except T_{2-5} in which 25 mm. bars are used

The bending dimensions are in accordance with B.S. 4466 - 1969. For spacing of these bars see Figs. (2.1, 2.3 and 2.4).

2.6.3 TOP AND BASE STEEL PLATES :- The top plate is made of M- steel, 20 mm. thick and 200 x 200 mm. square, while the base plate is also M. steel but 12 mm. thick and 900 x 900 mm. square with a central hole 200 x 200 mm. square. See Fig. (2.1) for dimensions and position of holes for both plates and they are the same for all the specimens.

2.6.4 FIXING ELECTRICAL RESISTANCE STRAIN GAUGES ON THE REINFORCEMENT

After preparing the reinforcing steel bars for the specimens according to Figs. (2.1, 2.3 and 2.5), the exact positions of the gauges are marked out, then the areas on which the gauges are to be stuck are cleaned with emery cloth and further the areas are cleaned with "Genclene" and finally neutralized with an "Ammonia Solution".

The lower faces of the gauges are lightly rubbed with emery cloth to provide a key for the glue then dipped into "Genclene" to clean them and finally dipped into an Ammonia Solution.

When the gauges are dry a piece of sellotape is used to pick up one gauge by its upper face and placed in the exact position. The sellotape is peeled back from the non-connector end of the gauge until the whole of the gauge is held clear. The sellotape still stuck down will ensure that the gauge's position will not be altered.

A small blob of Permabond 102 contact cement glue is placed at the connector end of the gauge then it is rolled back down using finger pressure so that the glue squeezes under the whole of the gauge. A firm pressure is maintained over all the gauge for a minute then the sellotape is peeled back and the two connectors are soldered to the cables, sellotape is used to ensure that these connectors are insulated from the bars.

A dummy gauge is prepared in the same way on a small piece of steel bar and covered with Philips PR 9248/ 00 strain gauge sealing compound then embedded in 4" x 4" x 4" concrete cube.

The gauges on the 20 mm ø bars are placed in line with the longitudinal axis of the bar while those on the second link from the top surface of base slab are placed in line with the horizontal axis of each side of the link and at its centre on the top surface. The gauges on the base slab reinforcement are placed in line with the longitudinal axis of the bars on the bottom face and at the centre line of the base slab.

After fixing all the gauges on the reinforcing bars a layer of 5 mm. thick of Philips PR 9248/ 00 strain gauge sealing is used to protect the gauges from any moisture during casting of the specimens or afterwards, see Fig. (2.1, 2.2, 2.3, 2.4 and 2.5) for position and number of gauges for each specimen.

Apart from those T_{1-1} has 4-electrical resistance strain gauges fixed on the 4-20 mm. ϕ column bars at a 50 mm. level above the bottom face of the base slab and T_{1-2} has 4-electrical resistance strain gauges fixed on the 4-20 mm.ϕ column bars at 35 mm. level and another four at 120 mm. level.

2.7. CASTING AND CURING OF SPECIMENS

Each specimen is cast in two stages, first the base and 50 mm. of the column, then after 24 hours the rest of the column is cast.

2.7.1 FIRST CAST :-

The wooden mould for this cast is assembled and placed in position then the base is checked to be horizontal using a spirit-level. All the joints are sealed with plasticine to prevent any seepage of cement mortar or water after that the mould is oiled.

The reinforcemt cages are assembled and placed into position, then the longitudinal column reinforcements are checked by spirit-level to make sure that they are vertical before and during casting.

Due to the limiting capacity of the mixer the cast is made of two batches for all the specimens of series (2) and T_{1-1}, T_{1-2}, T_{1-3} and T_{3-2} from series (1) and (3) respectively while it is made of three batches for the rest of the specimens except T_{1-6} which is made of four batches and T_{3-1} which is made of one batch. Each batch is mixed for three minutes into the mixer then casting the first layer of the specimen took place, the layer is vibrated until there is no air bubbles on the surface using a Pooker vibrator, the same procedure is used for each layer. Four hooks are installed in the base slab to facilitate the lifting of the specimen after curing see Fig. (2.9).

The concrete control specimens are cast in the same way.

After the final layer, the upper face of the base slab and the control specimens is finished smoothly then covered with polythene sheets for twenty-four hours.

2.7.2 SECOND CAST :- Twenty-four hours after the first cast the 50 mm. part of the column is stripped of the mould then the top mould is assembled and its joints are sealed with plasticine. Then a thin layer of plasticine is placed around the 50 mm. part of the column at the surface of the base slab to prevent any leakage of cement mortar and water from the mould. The top mould is now placed and fixed in its exact vertical position and this is checked by spirit-level after that, 30 mm. concrete cubes are placed between the mould and the 20 mm ϕ bars to ensure exact cover and position of the steel cage, then the second cast is started and is made of one batch for all the specimens. After mixing the batch in the mixer for three minutes, the column is cast in layers, each one is vibrated using a Pooker vibrator. In the same time the control specimens are cast in the same way. After the last layer the 30 mm. concrete cubes are removed and the top of the column is levelled with the top of the mould. The specimen and control specimens are cured together under wet sacks and polythene. The sacks are soaked daily and the polythene is to prevent too rapid drying out.

2.8. PREPARATION OF SPECIMENS FOR TESTING :- After curing the specimen the polythene sheets and the wet sacks are removed, a thin layer of plaster of paris is placed on the top of the column under the top steel plate which is levelled by a spirit-level so that its top surface is horizontal.

The spote for the 8" and 6" Demec gauges are fixed onto the faces of the column using F.88 adhesive and their number and position as shown in Figs. (2.2, 2.4 and 2.6).

The specimen is then lifted with a forklift truck to the testing rig where the 5 mm. gap between the upper surface of the top steel plate and the top of the 20 mm. ϕ bars is filled by welding, after cleaning away the surplus plaster of paris to ensure that the bars will not slip upwards. The top surface of the weld is ground level with the top surface of the top steel plate. The specimen is then lifted into the test rig and mounted in position over the base plate which is on the top of the loading platen, making sure that the plan of the column coincides with the hole in the base plate.

A thin layer of plaster of paris is placed between the base slab and the base steel plate to ensure complete contact between them. To prevent the plaster of paris from entering the hole in the base plate a 5 mm. thick layer of plasticine is placed on the edges of the hole to seal it. The loading platen of the testing rig is levelled so that the column is vertical and this is checked by spirit level for all faces of the column.

The load cell is placed in position on the top steel plate at the centre of the column and the dial gauges on the base slab and under the loading platen corners are fixed as shown in Fig. (2.2).

The specimen is then ready for testing.

2.9 PREPARATION OF CONTROL SPECIMENS FOR TESTING

2.9.1. CONCRETE :- From each cast two 150 x 300 mm. cylinders are capped with plaster of paris to ensure a smooth horizontal top surface and four 60 mm. electrical resistance strain gauges are fixed at the mid height of each cylinder diametrically opposed using F.88 adhesive. Two are placed vertically and the other two circumferentially on the cylinder then the two connectors of each gauge are soldered to wires which are also connected to Peekel strain recorder.

2.10. TEST PROCEDURE FOR SPECIMENS

At zero load where the top of the loading cell is just touching the bottom face of the beam of the testing rig, the readings of the electrical resistance strain gauges are recorded by the Data Logger which is programmed to print the strains in the reinforcement directly for each loading. The horizontal and vertical Demec gauges reading which give the lateral and longitudinal strains in the column are recorded using 6" and 8" Demec gauges respectively. Finally the readings of the dial gauges on the base slab and under the loading platen are recorded.

The load is then increased by increments of 100 - 125 KN. and the readings are repeated until the specimen fails.

For each load increment the readings take about ten minutes. During the test any cracks appearing on the base or column are marked and their propogation for each load increment. After the test is completed the four sides of the specimen are photographed, then it is lifted and the pattern of cracks on the bottom face of the base slab are sketched and also photographed.

2.11 TESTING PROCEDURE OF CONTROL SPECIMENS

2.11.1. CONCRETE :- After the specimen is tested, the cubes are tested by the 3000 KN. Denison Machine and the crushing load is recorded, then the uncapped cylinders are tested to find the maximum splitting load and finally the capped cylinders are tested and the strains are recorded from the Peekel strain recorder for each load increment until failure of the cylinder.

All the tests are carried out in accordance with B.S. 1881 : Part 4: 1970, for testing of concrete except for E_c and ν_c tests.

2.11.2 STEEL :- The 450 mm. specimens are tested in the Denison Universal Testing Machine. Load-extension plots are obtained using Baldwin Automatic Strain Recorder.

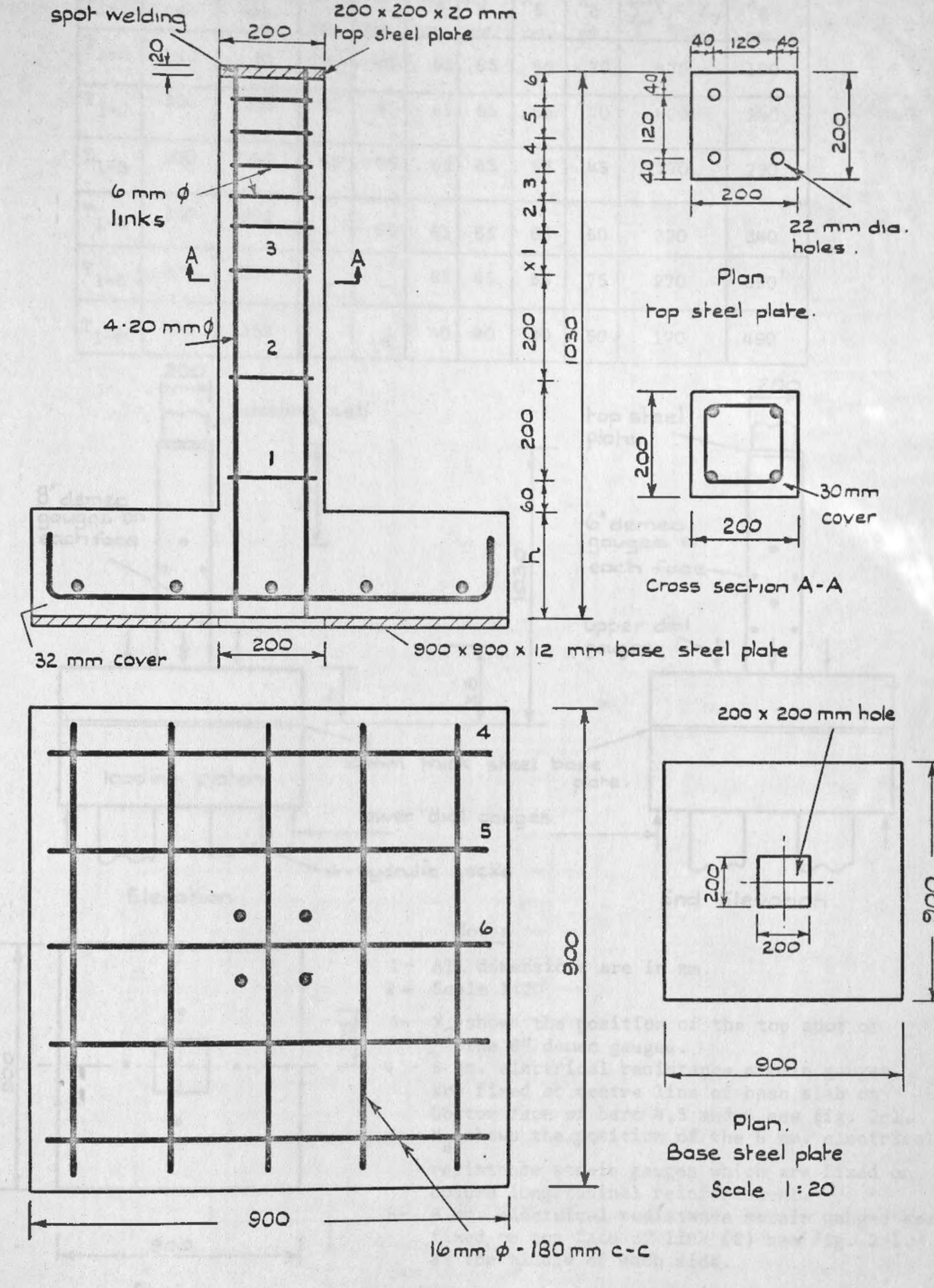

Fig. 2.1 Reinforcement details and dimensions for specimens. (series 1)

T_{i-j}	h. mm.	d. mm.	X_1 mm.	X_2 mm.	X_3 mm.	X_4 mm.	X_5 mm.	X_6 mm.	$\sum_1^6 X_i = X_7$ mm.	X_8 mm.
T_{1-1}	100	52	140	65	65	65	65	70	470	190
T_{1-2}	150	102	90	65	65	65	65	70	420	240
T_{1-3}	200	152	65	65	65	65	65	45	370	290
T_{1-4}	250	202	-	65	65	65	65	60	320	340
T_{1-5}	300	252	-	-	65	65	65	75	270	390
T_{1-6}	400	352	-	-	40	40	40	50	170	490

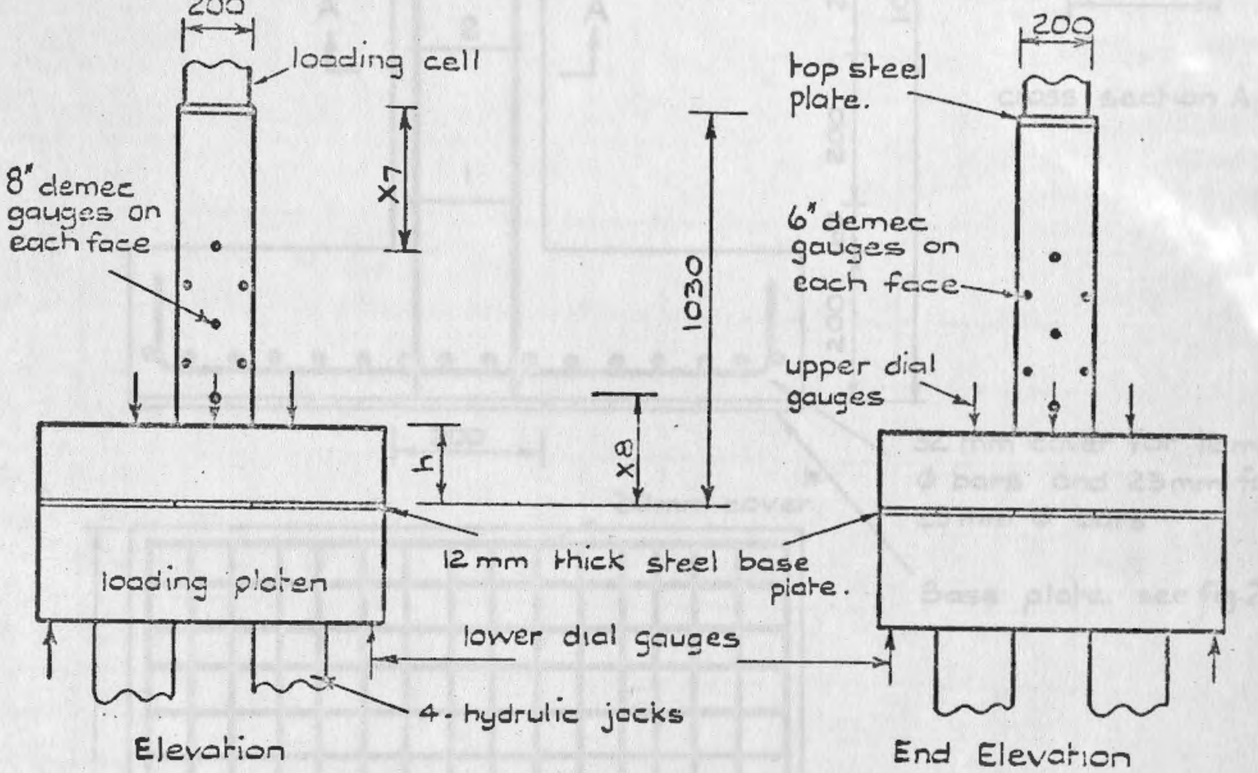

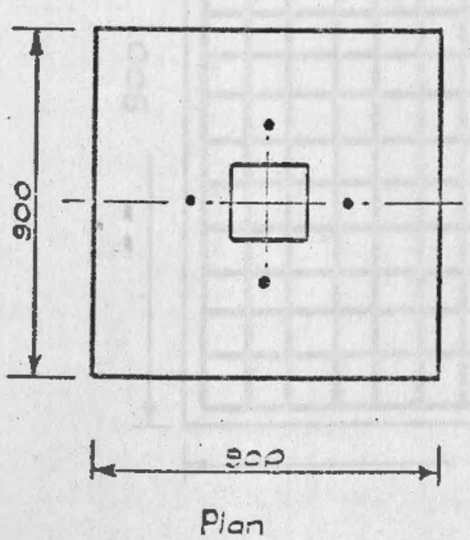

Notes

1- All dimensions are in mm.
2 - Scale 1:20
3- X_7 shows the position of the top spot of the 8" demec gauges.
4 - 6 mm. electrical resistance strain gauges are fixed at centre line of base slab on bottom face of bars 4,5 and 6 see fig. 2-1.
5 - X_8 shows the position of the 6 mm. electrical resistance strain gauges which are fixed on column longitudinal reinforcement.
6- 6 mm. electrical resistance strain gauges are fixed on top face of link (2) see fig. 2-1. at the middle of each side.

Fig. 2.2. Position of strain, Demec & dial gauges for each specimen (series . 1)

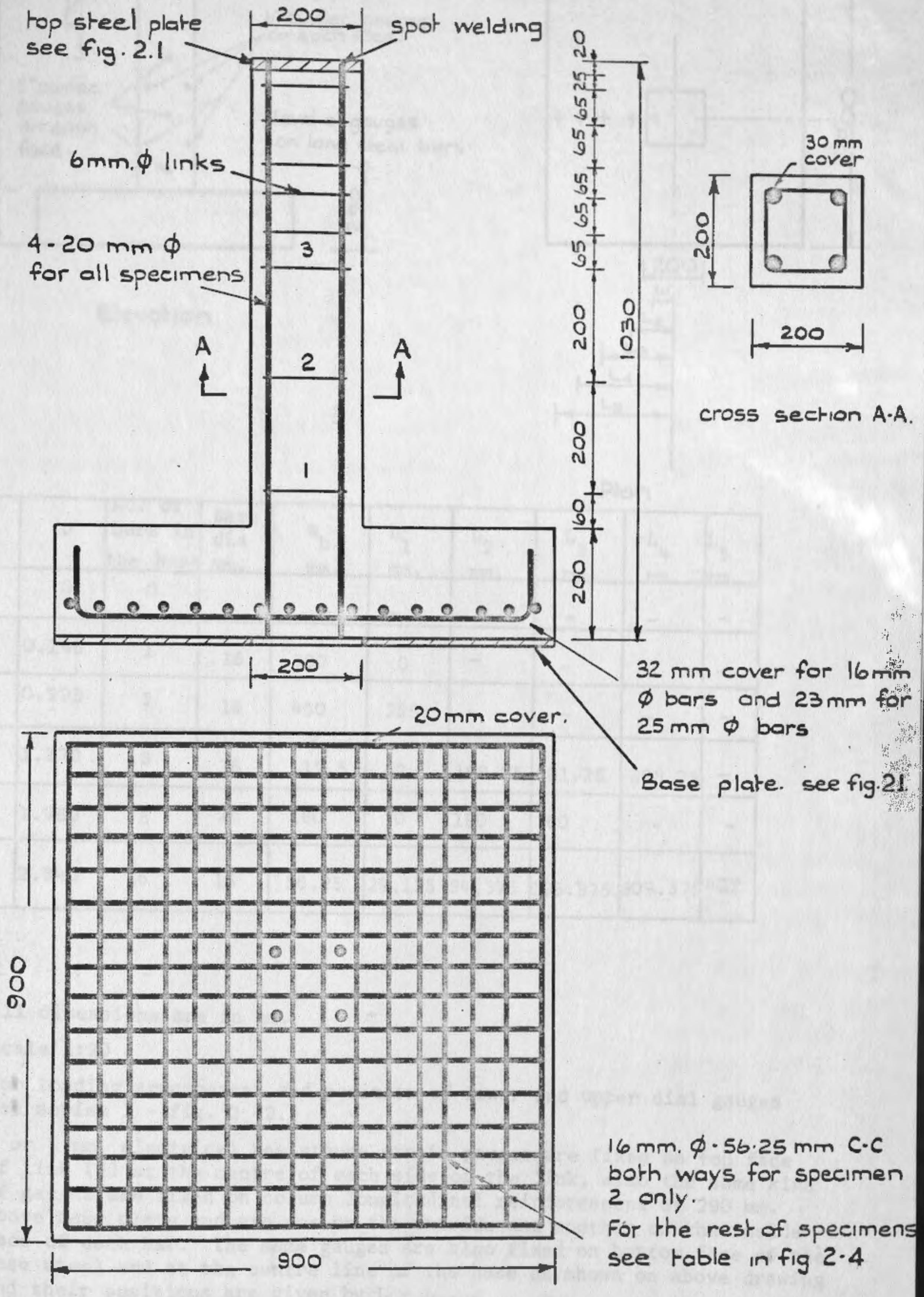

Fig. 2.3. Reinforcement details & dimensions for specimens (series. 2)

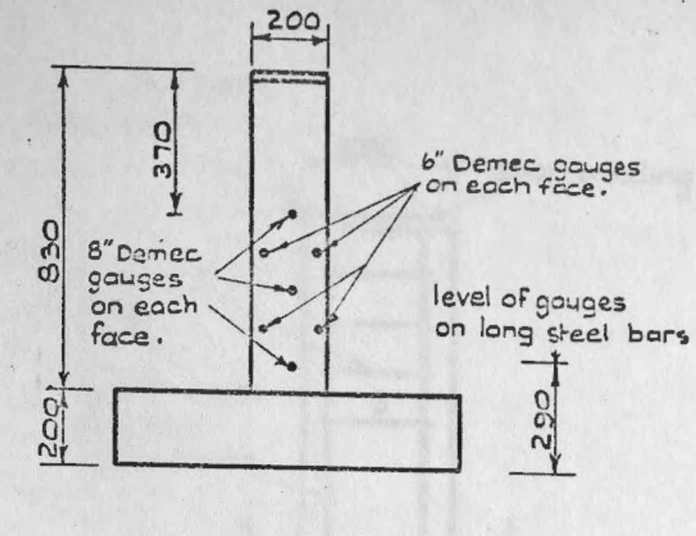

Elevation

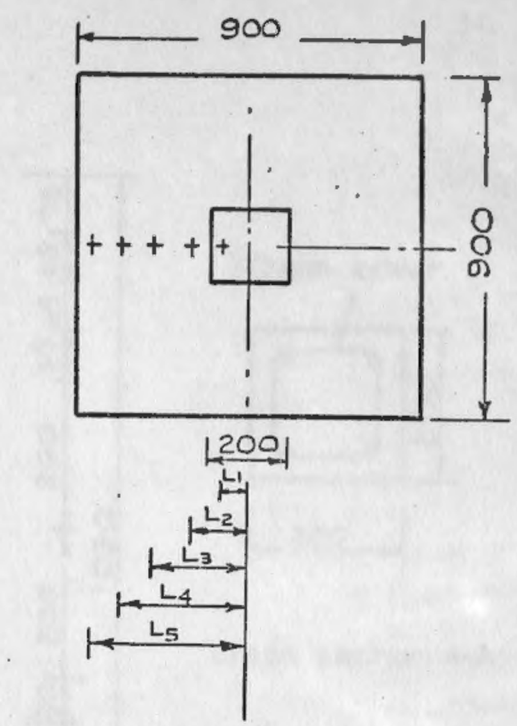

Plan

$T_{i \div j}$	ρ	No. of bars in the base	Bars dia mm.	s_b mm.	L_1 mm.	L_2 mm.	L_3 mm.	L_4 mm.	L_5 mm.
T_{2-1}	0	0	–	–	–	–	–	–	–
T_{2-2}	0.146	1	16	900	0	–	–	–	–
T_{2-3}	0.293	2	16	450	225	–	–	–	–
T_{2-4}	1.170	8	16	112.5	42	168.75	281.25	393.75	–
T_{2-5}	1.760	5	25	180	0	180	360	–	–
T_{2-6}	2.340	16	16	56.25	28.125	84.375	196.875	309.375	422

NOTES

1 - All dimensions are in mm.

2 - Scale 1:20

3 - For loading arrangement and position of lower and upper dial gauges see series 1 - fig. 2 -2.

4 - 6 or 5 mm. electrical resistance strain gauges are fixed on top face of link (2) at the centre of each side of the link, also the same kind of gauges are fixed on column longitudinal reinforcement at 290 mm. above base plate and are one on the outside and another on the inside face of each bar. The same gauges are also fixed on bottom face of the base steel and at the centre line of the base as shown on above drawing and their positions are given by $L_1 - L_5$.

Fig. 2.4. Position of strain, demec and dial gauges on each specimen.
(series . 2)

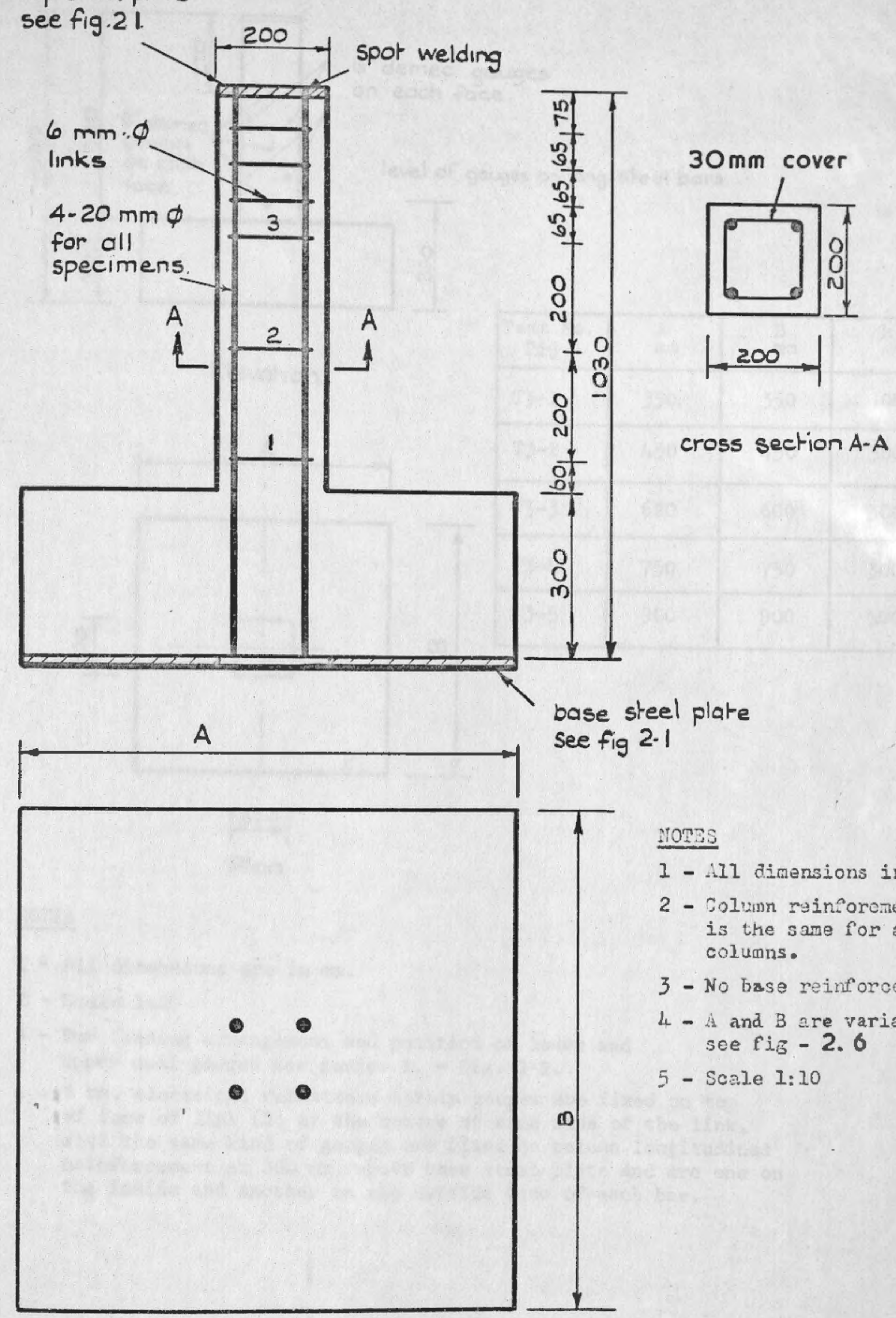

NOTES

1 - All dimensions in mm.

2 - Column reinforcement is the same for all columns.

3 - No base reinforcement

4 - A and B are variable see fig - 2. 6

5 - Scale 1:10

Fig. 2.5. Reinforcement details and dimensions for specimens (series - 3)

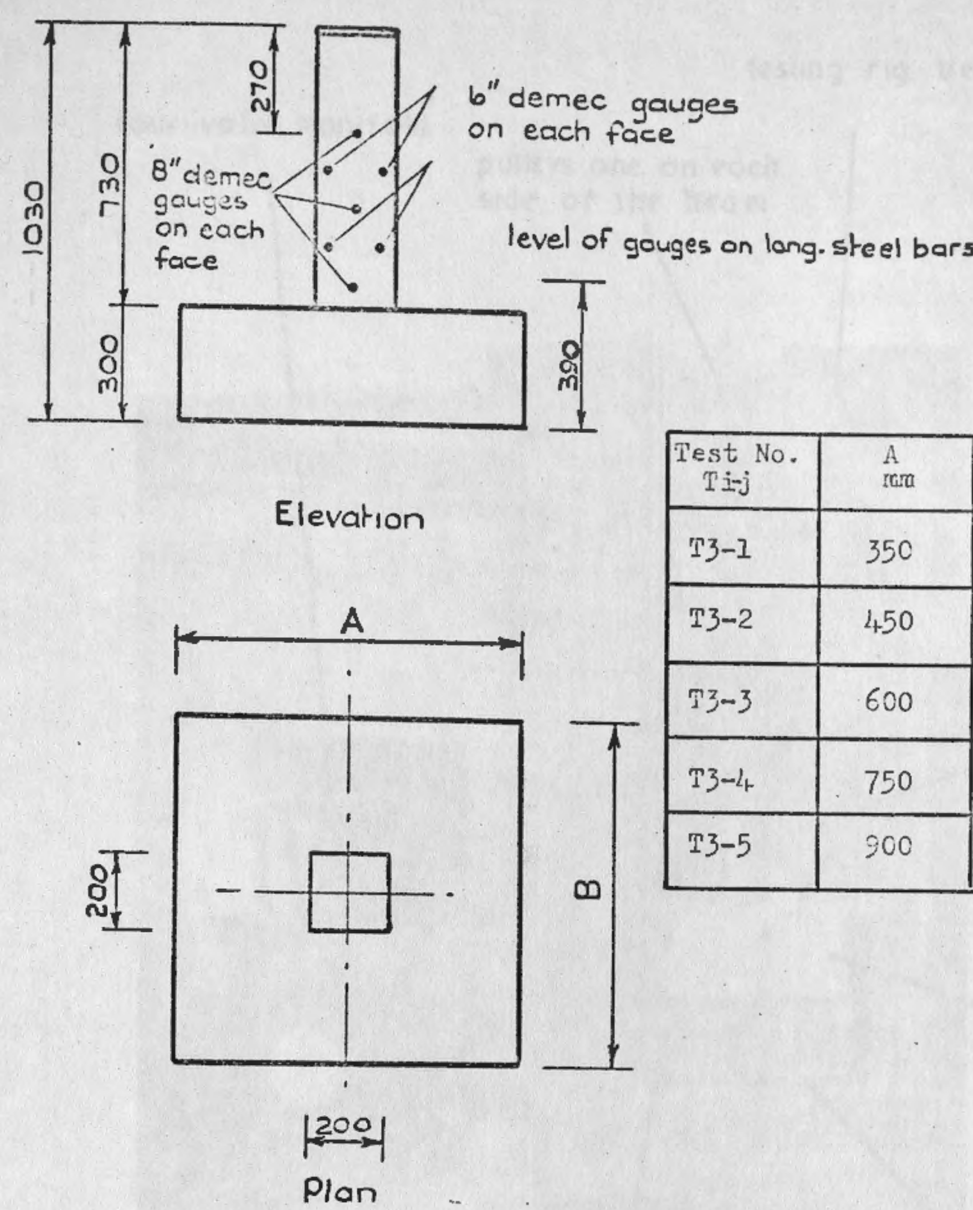

Test No. Ti-j	A mm	B mm	h mm
T3-1	350	350	300
T3-2	450	450	300
T3-3	600	600	300
T3-4	750	750	300
T3-5	900	900	300

NOTES

1 - All dimensions are in mm.

2 - Scale 1:20

3 - For loading arrangement and position of lower and upper dual gauges see series 1. - fig. 2-2.

4 - 5 mm. electrical resistance strain gauges are fixed on top of face of link (2) at the centre of each side of the link, also the same kind of gauges are fixed on column longitudinal reinforcement at 390 mm. above base steel plate and are one on the inside and another on the outside face of each bar.

Fig. 2.6. Position of strain, demec and dial gauges on each specimen. (series . 3)

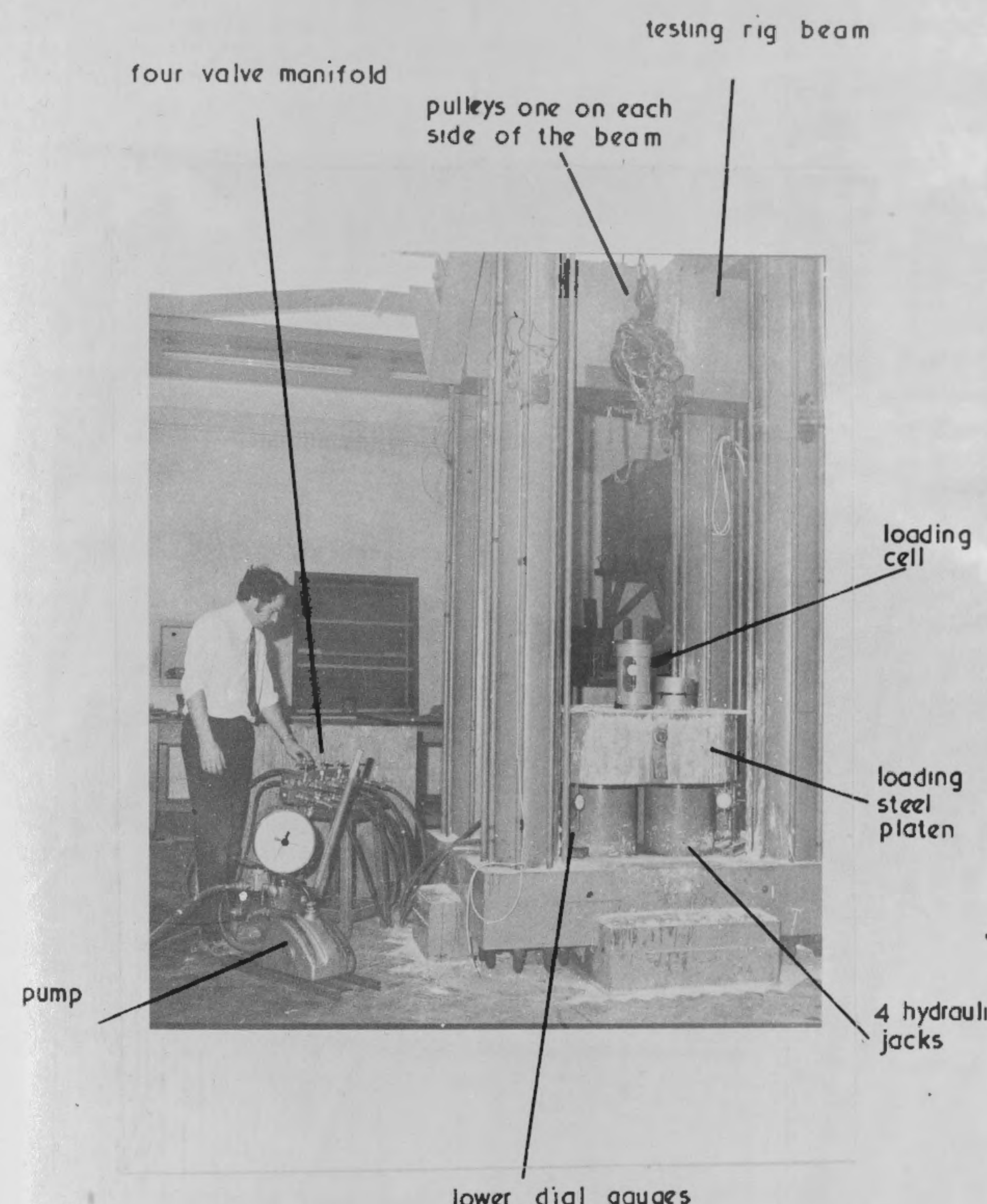

Fig .2.7 View of the testing rig

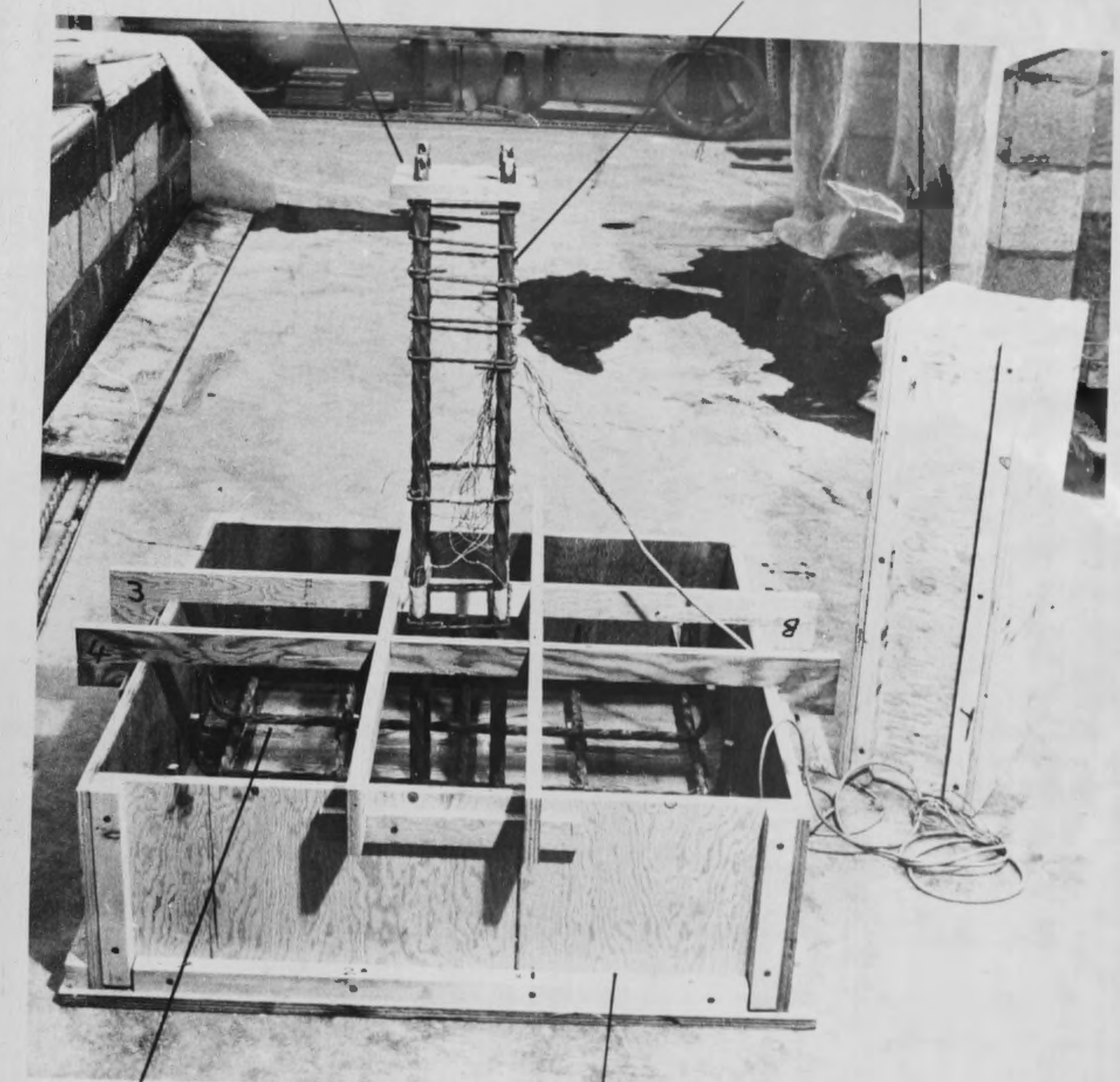

Fig. 2.8 View of reinforcing steel cages in position just before the first cast for one of the specimens

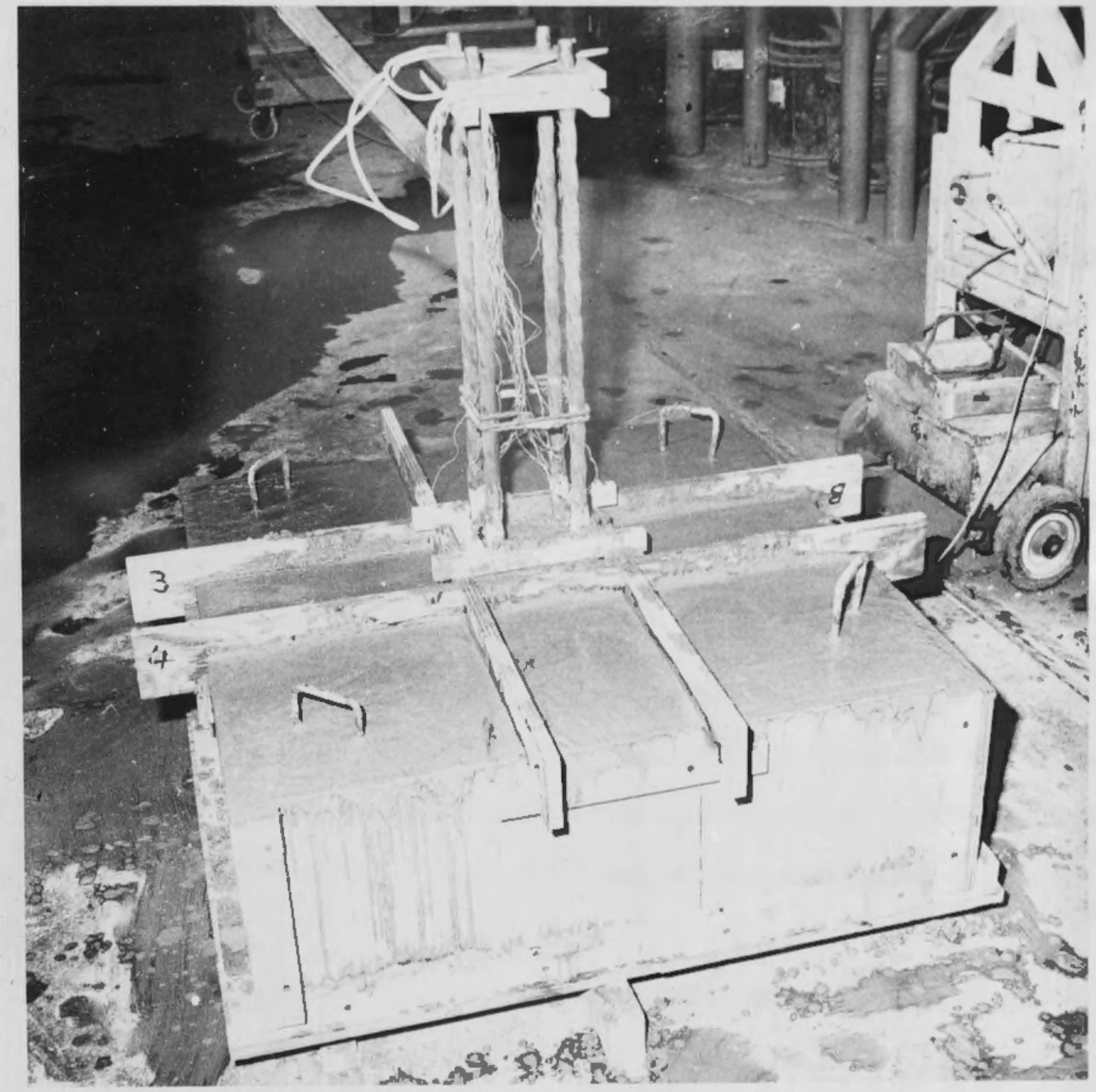

Fig. 2.9 View of one of the specimens just after the first cast

CHAPTER 3.

SERIES (1) RESULTS AND CALCULATIONS

3.1. INTRODUCTION

This series consists of six specimens each one has the same column dimensions, base lateral dimensions and reinforcement. The variable in this series is the overall depth of the base slab (h) which is 100, 150, 200, 250, 300, and 400 mm. for specimens T_{1-1}, T_{1-2}, T_{1-3}, T_{1-4}, T_{1-5}, and T_{1-6} respectively. All the details are in figs (2.1 and 2.2) in Chapter 2.

3.2. CONTROL SPECIMENS RESULTS

3.2.1. STEEL

For each specimen there are three control specimens one for the 20 mm.ø bar, the second for the 6 mm.ø bar and the third for the 16 mm. ø bar. The results of the tensile tests are as plotted in figs (3.1.a, b,c) and the values of (f_y) and (E_s) are tabulated in Table (3.1).

3.2.2. CONCRETE

The compresive cube strength (f_{cu}) for base and column concrete are obtained for each specimen from the 150 mm. cubes and the tensile strengths (f_t) are obtained from the uncapped cylinders. The water/cement ratio (w/c), mix proportion by weight, age of concrete and the above results are listed in Table (3.2).

From the capped cylinders result for base and column concrete of each specimen the axial stress is plotted against the longitudinal strain as shown in figs. (3.2.1a, 2a, 3a, 4a, 5a and 6a) for column concrete and figs. (3.2.1b, 2b, 3b, 4b, 5b and 6b) for base concrete. From these plots the average secant modulus (E_c) is calculated then the axial stress is plotted against (E_c) for both column and base concrete see figs. (3.2.1c, 2c, 3c, 4c, 5c and 6c). Also the axial stress is plotted against the lateral strain as shown in figs. (3.2.1d, 2d, 3d, 4d, 5d and 6d) for column concrete and figs. (3.2.1e, 2e, 3e, 4e, 5e, and 6e) for base concrete then the average Poisson's ratio (ν_c) is calculated by dividing the lateral strain by the longitudinal strain for each load increment and finally the axial stress is plotted against the Poisson's ratio (ν_c) for both column and base concrete as shown in figs. (3.2,1f, 2f, 3f, 4f, 5f and 6f).

3.3. SPECIMENS RESULTS

3.3.1. LONGITUDINAL STRAIN

For each specimen the average longitudinal strain is calculated from the results of the 8" Demec gauges on column concrete and from the electrical resistance strain gauges on column steel then the experimental axial load is plotted against the longitudinal strain measured on both concrete and steel as shown in figs. (3.3.1, 2, 3, 4, 5, and 6). Then the experimental axial load is plotted against longitudinal strain measured on all column's concrete as in fig. (3.3.b) and on all column's steel as in fig. (3.3.a).

3.3.2. LATERAL STRAIN

The experimental axial load is plotted against the average lateral strain calculated from the result of the 6" Demec gauges on column concrete and from the electrical resistance strain gauges on column link for each specimen as shown in figs. (3.4.1, 2, 3, 4, 5, and 6). Also the axial load is plotted against the lateral strain measured on column concrete for all specimens as in fig. (3.4.b) and against lateral strain measured on column link as in fig. (3.4.a).

3.3.3. STRAIN IN BASE SLAB REINFORCEMENT

The experimental axial load is plotted against the strain measured on the bottom face of the reinforcement for the base slab at the middle of the 16 mm.Ø bars for the lower layer as shown in figs. (3.5.1, 2, 3, 4, 5 and 6).

3.3.4. DEFLECTION OF BASE SLAB AND TOTAL SHORTENING OF SPECIMEN

The experimental axial load is plotted against the average upward deflection of base slab at 105 mm. from column faces on the centre lines of the base as shown in fig. (3.6) for all the specimens and then it is plotted against the total shortening of the specimen as in fig. (3.7) for all the specimens.

3.4. MODE OF FAILURE

Specimen T_{1-1} failed by punching shear failure of the base slab along the periphery of the column. The cracks first appeared on the bottom face of the slab then travelled outwards until they reach the outside then they propogate upwards for the full depth of the slab where they met the cracks on the top face of the slab as shown in figs. (3.8 and 3.9.1).

Specimen T_{1-2} failed by anchorage bond failure of the longitudinal column steel reinforcement with the base slab concrete. In this specimen the cracks on the bottom face of the base slab started first from the 20 mm.ϕ bars and they travel inwards and outwards until they meet each other inside the 4-20 mm.ϕ bars for the inside and until they reach the sides of the base for the outside then they extend upwards until they reach near the top of the base slab. The 20 mm.ϕ bars slip downwards then the column concrete failed by compression as shown in figs. (3.8 and 3.9.2.).

Specimen T_{1-3} failed in the same manner as T_{1-2} except the number of cracks on the bottom face of the base slab is fewer see fig. (3.8 and 3.9.3).

Specimen T_{1-4} also failed by anchorage bond failure as in T_{1-2} and T_{1-3} but in this test the cracks on the bottom face of the base slab only met inside the 4-20 mm.ϕ bars and did not travel far towards the outside direction, see fig. (3.8 and 3.9.4).

Specimen T_{1-5} failed in the same manner as T_{1-4} and the cracks on the bottom face of the base slab are even shorter. See figs. (3.8 and 3.9.5).

In specimens T_{1-3} to T_{1-5} the longitudinal 20 mm. Ø bars slipped downwards then the column concrete failed by compression.

Specimen T_{1-6} failed by yielding of the column longitudinal steel reinforcement and then the column concrete failed by compression. In this test there was no end slip of the 20 mm. Ø bars and no cracks on the base slab, see figs. (3.8 and 3.9.6).

In T_{1-2} - T_{1-6} the centre of the compression failure zone for column concrete is above the top of the base by about 310 mm. as an average for these tests.

3.5. CALCULATIONS

3.5.1. TABLE 3.3 AND GRAPHS

For each specimen the maximum experimental axial load (P_{test}) is recorded then using equation (1) the theoretical ultimate axial load ($P_{ult.}$) is calculated therefore, the ratio of (P_{test}/P_{ult}) is found.

From the maximum and average longitudinal strains measured on column reinforcement (ε_s max.) and (ε_s av.) respectively the axial load on each of the 20 mm. Ø bars is found for both (ε_s av.) and (ε_s max.) from that the average load taken by the longitudinal column reinforcement is calculated and subtracted from (P_{test}) and the result is divided by the concrete cross-sectional area (A_c) this gives (f_c) then the ratio of (f_c/f_{cu} for column concrete) is found, see example below for the calculations of T_{1-6}. The average and maximum anchorage bond stresses f_{bs} (av.) and f_{bs} (max.) respectively are calculated from the average and maximum axial load on the 20 mm. Ø bars. Then the ratios of (f_{bs} (av.) and f_{bs}(max.)) to (f_{cu} of base concrete) are calculated. In T_{1-1} and T_{1-2} the anchorage bond area subtracted from it the area of the water proof covering the strain gauges in the base slab on the column steel and this is 400 mm^2. for T_{1-1} and 800 mm^2 for T_{1-2}.

The average and maximum stresses in the 20 mm.ϕ column reinforcement f_s (av.) and f_s (max.) respectively are calculated from ε_s (av.) and ε_s (max.) then the ratios of f_s (av.) and f_s (max.) to f_y are found.

Using equation (6.a) and assuming $f'_c = 0.8\ f_{cu}$ the allowable anchorage bond stress f_{bs} (ACI) for the American code is found to be equal to (0.9366 f_{cu}). This value is calculated for all specimens. The ratios of f_{bs} (av.) / f_{bs} (ACI) and f_{bs} (ACI) / f_{cu} are found.

From CP110: Part 1: 1972 Table (22) the allowable anchorage bond stress corresponding to f_{cu} of base f_{bs} (CP110) is read for all the specimens then the ratios of f_{bs} (CP110) / f_{cu} and f_{bs} (av.) / f_{bs} (CP110) are found.

If the anchorage bond failure takes place entirely within the thickness of the base slab, for a base slab of zero thickness it might be expected that the column failure load would be given by the part of the column strength attributable to concrete only, on the assumption that the stress in the steel is zero. Then the ratio of($0.8\ f_{cu}\ A_c / P_{ult.}$) is calculated for all the specimens and the average value for T_{1-2} - T_{1-6} is 0.66 since T_{1-1} has different mode of failure. This ratio can represent a theoretical point whose $P_{test}/P_{ult.}$ = 0.66 at h = o.

All the above results and calculations are tabulated in Table (3.3).

The ratio of (P_{test}/P_{ult}) is plotted against the overall depth of the base slab (h) and the theoretical point whose co-ordinates are (0,0.66) is marked on this graph. A regression analysis is done for the results of T_{1-2}- T_{1-6} and the equation of the best straight line through these points is$\left(\frac{P_{test}}{P_{ult}}\right) = 0.77 + 0.55 \times 10^{-3}\ (h)$.

Then the results of T_{2-1} and T_{3-5} are plotted on the same graph. These specimens are a part of a series of tests with no steel reinforcement in the base slab. See fig. (3.10).

The ratios of f_{bs} (a.v), f_{bs} (max.), f_{bs} (CP110) and f_{bs} (ACI) to f_{cu} of base concrete are plotted against (h) as shown in fig. (3.11).

Example on f_c calculations for T_{1-6} :-

Reading from graph no. (3.1.a) for $\varepsilon_s = 2206 \times 10^{-6}$

Axial stress = 414 N/mm^2.

Load on steel = 414 x 1257/1000 = 512.4 KN -

Ptest = 1550 KN.

Load on concrete = 1550 - 521.4 = 1028.6 KN

A_c = 40000 - 1257 = 38743 mm^2.

Hence $f_c = \frac{1028600}{38743} = 26.58\ N/mm^2$. and $\frac{f_c}{f_{cu}} = \frac{26.58}{34.55} = 0.823$.

3.5.2. PUNCHING SHEAR

The depth required to resist punching shear failure using the properties of T_{1-6}. That is, axial load = 1550 KN and f_{cu} for base concrete = 34.55 N/mm^2.

Punching shear is considered so that the depth required can be compared with the anchorage length required to resist anchorage bond failure.

The depth required to resist punching shear is calculated according to the followings :-

1) CP110: Part 1: 1972

From tables (5) and (14) of CP110 code using T_{1-6} properties, $v_c = 0.35\ N/mm^2$.

Hence using equation (3) the required depth = 670.00 mm.

2) ACI 318 - 1971

The capacity reduction factor = 0.85

$f'_c = 0.8\, f_{cu} = 27.64\ \text{N/mm}^2$

Hence using equation (4) the required depth = 508.25 mm.

3) EQUATION (2)

Using equation (2) the required depth = 364.40 mm.

3.5.3. PUNCHING SHEAR ALONG THE PERIPHERY OF THE COLUMN

Speciment T_{1-1} failed by punching shear along the periphery of the column at a shear stress = $\frac{1285000}{80000}$ = 16.06 N/mm^2.

The ultimate shear stress from CP110: Part 1: 1972 tables (5) and (14) and the properties of T_{1-1} is equal to 1.144 N/mm^2.where from table (6) the maximum allowable shear stress = 4.4N/mm^2.

3.5.4. ANCHORAGE LENGTH FOR LONGITUDINAL COLUMN REINFORCEMENT

Specimen T_{1-6} failed by yielding of the column longitudinal reinforcement and hence its depth h = 400 mm. is also the anchorage length required to prevent anchorage bond failure (1). To compare this depth with the current codes of practice its properties are used and the following :-

1) CP110: Part 1: 1972

From table (22) of this code the anchorage bond stress = 2.93 N/mm^2. and the permissible stress in the column longitudinal reinforcement = $\frac{2000 \times 487.3}{2487.3}$

= 391.83 N/mm^2.

Hence using equation (5) gives

l = 669.01 mm.

2) ACI 318 - 1971

The yield stress corresponding to a strain of 0.35% for the T_{1-6} 20 mm. ∅ bars = 470 N/mm^2.

Hence equation (6.a) gives the maximum anchorage length, that is

l = 426.73 mm.

3.6 DISCUSSION OF SPECIMENS RESULTS AND CALCULATIONS

3.6.1. COLUMN LONGITUDINAL STRAIN

The graphs for strains measured on steel and concrete at the beginning of the tests are almost the same except for small difference which may be due to the different methods of measurement used in the test, then as the load increased the steel started to lose some strain which is the beginning of small slip after that the strain in the steel increased as the bar deformations began to be effective, then it slipped slightly more and as it is doing so the steel graph lags behind the concrete one until failure of the column concrete by compression. This applies for all the tests except T_{1-1} and T_{1-6}. In T_{1-1} the column did not fail although there was a difference between the steel and concrete strains as shown in fig. (3.3.1). In T_{1-6} the steel did not slip as in fig. (3.3.6) and the failure was due to yielding of the longitudinal steel reinforcement of the column, then compression failure of the column concrete. Figs. (3.3.1, 2) also show that the average reduction in strain and hence the average bond stress in the 20 mm. ∅ bars is not constant along the overall depth of the base slab (h). This confirms the findings of Mattes and Paulos (1968) and Paulos and Davis (1968) which states that at low values of K ($= \frac{E_s}{E_{ce}}$), and in this case $K < 10$, the bond stress (called shear stress in the references) is high at the top of the pile and low at the bottom of the pile, if we assume that the pile in the soil is similar to the steel bar in the concrete. The results of T_{1-1} and T_{1-2} also show that the bars undergo some bending and that the load reached the lower part of the bars only at the final stages of the test this is what Wilkins (1951) found for pullout test. For more details of this point, see Chapter (7).

The general shape of the graphs is the same for all specimens as is shown in fig. (3.3.a) for column steel and fig. (3.3.b) for column concrete.

3.6.2. COLUMN LATERAL STRAIN

Some of the graphs for column link have negative strain at the beginning of the test as in figs. (3.4.2, 4) and as the load increased both strains measured on concrete and column link increased and their values become almost the same, then at the final stages of the test, the column link graph lags behind the concrete one and at failure the strain measured on the column concrete is much greater than that measured on the column link even for T_{1-6} which has a different mode of failure.

The general shape of the graphs for all specimens is the same, see fig. (3.4.a) for strains measured on column link and fig. (3.4.b) for strains measured on column concrete.

3.6.3. STRAIN IN BASE SLAB REINFORCEMENT

The strains for each test are measured at the centre of the base slab and 180 mm, 360 mm. from the centre at the centre line on the bottom face of three different 16 mm. ϕ bars.

The shape of the graphs is the same for all tests except T_{1-1} in which the strains increased as the specimen failed, see fig. (3.5.1), this is because it has different mode of failure.

For T_{1-5} the strain gauges did not give consistent strain readings see fig. (3.5.5) and this might be due to some moisture entering the gauges.

Two of the strain gauges for T_{1-4} are damaged which are one at the centre of the slab and 180 mm. from it. The value of the strain measured on the bar at the centre of the base is higher than the one at 180 mm. from it, and this is higher than that at 360 mm. from the centre. The value of the strain at the centre is about three times that at 360 mm. from it at failure of the specimen, this means that the bending moment is not constant across a section taken at the centre line of the base slab. As the value of (h) increases, the measured strains for each specimen decreases see fig. 3.5.a.

3.6.4. UPWARD DEFLECTION OF BASE SLAB AND TOTAL SHORTENING OF SPECIMEN

The graphs of the average upward deflection of the base slab are shown in fig. (3.6), the shape of these graphs is almost the same and at early stages of the tests the deflection increased more rapidly than those at the end of the tests, after the early stages of the tests the graphs started to curve up as the load increased. The value of deflection at failure is smaller for bases with larger value of (h), except T_{1-1}.

The graphs of the total shortening of the specimen are almost straight lines until the final stages of the tests, when the shortening starts to increase rapidly due to the failure of the column.

As the value of (h) increased, the total shortening decreased for the same axial load, see fig. (3.7).

3.6.5. TABLE (3.3) AND GRAPHS

In Table (3.3) the average value of (f_c/f_{cu} for column) for all the specimens of series (1) except T_{1-1} is 0.814 and the average value of this ratio for all the experimental program is 0.797 hence the value of 0.80 used as a factor for ($f_{cu}A_c$) in eqn. (1). Also the maximum value of $f_s(av.)/f_y$ is 0.85 in T_{1-6}, but to make the ratio of $P_{test}/P_{ult} = 1$ for T_{1-6}, since its column failed by yielding of the column longitudinal steel. A factor of (0.9) is used for ($f_y A_{sc}$) in eqn. (1).

The maximum ratio of $f_s(max)/f_y = 0.941$ from T_{1-6} test results. Fig. (3.10) shows that the results of $T_{1-2} - T_{1-6}$ are reasonably near to a straight line whose equation is

$$(P_{test}/P_{ult}) = 0.77 + 0.55 \times 10^{-3} (h)$$

This line intercepts the ordinate axis at 0.77 and having a slope = 0.55×10^{-3}.

If the value of $P_{test}/P_{ult} = 0.66$ is substituted in the above equation, then h =-200 mm. This means that the origin of the graph is shifted - 200 mm. Also if a test on a base of zero thickness were considered, it would take a form similar to the following :-

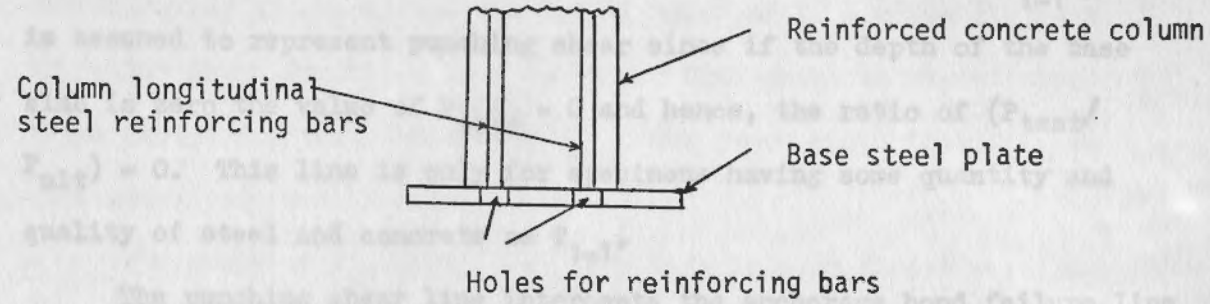

It seems probable that failure of the concrete would not occur at the level of base plate, but at some distance up the column, just as failure of the concrete occurred at some distance up the column in the tests conducted.

The reasons may be

1. Frictional restraint at the bearing surface provides an effective triaxial compression which enables the concrete to carry a higher compressive stress at the level of the plate than it can at some distance up from the bearing surface.

2. Until bond slip occurs between the bars and the concrete at the lower end of the column, concrete failure is unlikely to occur.

It may, therefore, be concluded that the effective anchorage bond length available for transfer of load from the column longitudinal bars to the base concrete includes not only that length of the bars in the base, but also a short length of the column. The concrete in the column being restrained by the base concrete as it is in the hypothetical case described above.

Hence for T_{1-2} - T_{1-6} tests the additional anchorage bond length is given by the above equation to be 200 mm. which is the same as the column dimension or the spacing of the links.

The average height of the centre of the compression failure zone above the top surface of the base slab for T_{1-2} - T_{1-6} is (310 mm.).

Increasing the depth (h) from 200 mm. to 400 mm. the column strength only increased by 11.5% compared with equation (1).

The other straight line passing through the origin and T_{1-1} point is assumed to represent punching shear since if the depth of the base slab is zero the value of P_{test} = 0 and hence, the ratio of (P_{test}/ P_{ult}) = 0. This line is only for specimens having some quantity and quality of steel and concrete as T_{1-1}.

The punching shear line intercepts the anchorage bond failure line at h = 110 mm. at which punching shear and anchorage bond failures occur at the same time.

Another line can be drawn through T_{2-1} and T_{3-5} for specimens without steel reinforcement in the base slab but this can only be relied upon if more tests are carried out to form another series. From the T_{2-1} and T_{3-5} results, it is possible that the line for slabs without steel reinforcement has smaller slopes than series (1) line or parallel to it.

Fig. (3.11) shows that the ratio of f_{bs} (av.)/f_{cu} for base for T_{1-2} is lower than that of T_{1-3} and that of T_{1-1} is almost the same as T_{1-1} although it failed by punching shear along the periphery of the column. This is because the measurement of strains on T_{1-1} and T_{1-2} column longitudinal reinforcement is done by using single electrical resistance strain gauge at each position whereon the rest of the tests two strain gauges are used at each position opposite to each other. After T_{1-3} the value of f_{bs}(av.)/f_{cu} of base decreases as (h) increases and the lowest value is that of T_{1-6} which is (0.15).

The graph of f_{bs}(max)/f_{cu} for base has the same shape as the above graph but the values are higher and the gap between the two results decreases as the value of (h) increases, this means that as (h) increases the load on the reinforcing steel is slightly uniform. These two graphs show that the experimental anchorage bond stresses are dependent on the anchorage length which is the same finding by Wilkins (1951) for pull-out tests. The graph of f_{bs} (CP110)/ f_{cu} is well below the experimental graphs and the lowest point of T_{1-6} gives (1.77) x the value given by CP110: Part 1: 1972. This graph is almost straight lines except for tests with high f_{cu}. The graph shows that British code gives very safe results.

The graph of f_{bs} (ACI) / f_{cu} for base is also almost straight lines except for high f_{cu} values. This graph shows that the anchorage bond stresses given by the American code are higher than the experimental values as in T_{1-5} and T_{1-6} and hence, gives unsafe results.

The ratio of f_c / f_{cu} for column for T_{1-4}, T_{1-5} and T_{1-6} are higher than those of T_{1-2} and T_{1-3}. This could be due to the increase in depth which gives less deformation in the column-base connection, and hence, stronger holding for column concrete. Also the steel in these tests carries more load due to the longer anchorage length and hence, gives more support to the column concrete.

3.6.6. PUNCHING SHEAR

1. Punching shear along the periphery of the column :- T_{1-1} failed by this kind of failure at a very high shear stress compared with those given by CP110: Part 1: 1972, and ACI 318 - 1971, see table below.

(1)	(2)	(3)	(4)	(5)	(6)	(7)
T_{1-1}	CP110 Tables					
N/mm^2	5 and 14 N/mm^2	6 N/mm^2	(1)/(2)	(1)/(3)	ACI N/mm^2	(1)/(6)
16.06	1.144	4.68	14.04	3.43	1.871	8.58

This means that this kind of punching shear failure is unlikely to occur except at a very high shear stress and using special loading arrangement.

2. Punching shear according to CP110: Part 1: 1972, ACI 318 - 1971 and equation (2) :- Using the properties of T_{1-6} and the above references the required depths to resist punching shear failure are listed in the following table.

(1)	(2)	(3)	(4)	(5)
Equation (2) mm.	Equation (3) (CP 110) mm.	(2) / (1)	Equation (4) (ACI) mm.	(4) / (1)
364.4	670.0	1.84	508.25	1.40

From this table it can be seen that the British code gives larger depths than the American code.

3.6.7. ANCHORAGE LENGTH

Since T_{1-6} just did not fail by anchorage bond failure, its depth (h) is used as reference to compare with the required anchorage length calculated according to the existing codes of practice, see table below.

(1)	(2)	(3)	(4)	(5)
T_{1-6} (h) mm.	Equation (5) (CP110) mm.	(2) / (1)	Equation (6.a) (ACI) mm.	(4) / (1)
400	669.01	1.67	426.73	1.07

From this table it can be noticed that the ratios of the anchorage lengths are not the same as the ratios of the anchorage bond stresses in Table (3.3) and this is because of the different allowable stresses in compression for the column longitudinal steel reinforcement as it is explained in the following table using T_{1-6} properties.

(1)	(2)	(3)	(4)	(5)	(6)
T_{1-6} f_s (av.) N/mm.^{2}	(1) In terms of f_y	CP110 allowable steel stress N/ mm.^{2}	(3) In terms of f_y	ACI allowable steel stress N/ mm.^{2}	(5) In terms of f_y
414	0.85 f_y	391.83	0.804 f_y	470	0.965 f_y

Where f_y = 487.3 N/mm^2.

This table shows that the American code uses a stress which is higher than the average experimental one and even higher than the maximum stress recorded on T_{1-6} longitudinal column reinforcemtn which is f_s (max) = 0.941 f_y and the British code uses a stress lower than the average experimental stress of T_{1-6}.

3.6.8 PUNCHING SHEAR AND ANCHORAGE LENGTH

If the specimens were loaded in a way so that punching shear failure and anchorage bond failure can occur, then using equation (2) it is found that at a depth less than 364.4 mm. and the properties of series (1) punching shear failure occurs before anchorage bond failure but for depths larger than 364.4 mm. and up-to 400 mm. anchorage bond failure is the governing criterion and for depths greater than 400 mm. the specimen will fail by yielding of the column longitudinal reinforcement.

If the specimen is designed according to CP110: Part 1: 1972, then it is found for the properties of T_{1-6} that punching shear failure governing the design by small difference where for the ACI 318 - 1971, it governs with a larger difference.

3.7. CONCLUSIONS

From the results and calculations of series (1) the followings are concluded.

(1) Punching shear failure along the periphery of the column is unlikely to occur, except at a very high shear stress, and under a special loading arrangement.

(2) The graph of the strength of columns measured by (P_{test}/P_{ult}) V. the overall depth of base slab (h) for specimens failed by anchorage bond failure can be represented by a straight line whose formula is

$$(P_{test}/P_{ult}) = 0.55 \times 10^{-3} (h) + 0.77$$

for $T_{1-2} - T_{1-6}$ properties and this shows that part of the column height is acting as extra anchorage length. Where for specimens failed by punching shear failure along the periphery of the column might be represented by a straight line passing through the origin whose formula is

$$(P_{test}/P_{ult}) = 7.38 (h) \times 10^{-3}$$

for specimens having the same properties as T_{1-1}.

(3) The bending moment across the section passing through the centre

line of the base slab is not constant, and it is higher at the centre than at the edges of the base slab.

(4) The experimental average and maximum anchorage bond stresses are dependent on the anchorage length (l) (The embedment length). The anchorage bond stress is not constant along the anchorage length but it is high at the top and low at the bottom of the anchorage length (l).

(5) The British code gives too conservative results for punching shear design where the American one also gives conservative value but more economical than the British one for low values of (ρ) in base.

(6) The American code uses higher values for allowable stresses in compression for the column longitudinal reinforcement than the experimental values where it uses unsafe anchorage bond stresses compared with the same experimental results for the type of reinforcement used in T_{1-6}.

The British code uses very conservative values of anchorage bond stresses and low allowable stress in compression for the column longitudinal reinforcement compared with the experimental results of T_{1-6}.

(7) Anchorage bond failure for the column longitudinal reinforcement must be considered in designing concrete bases.

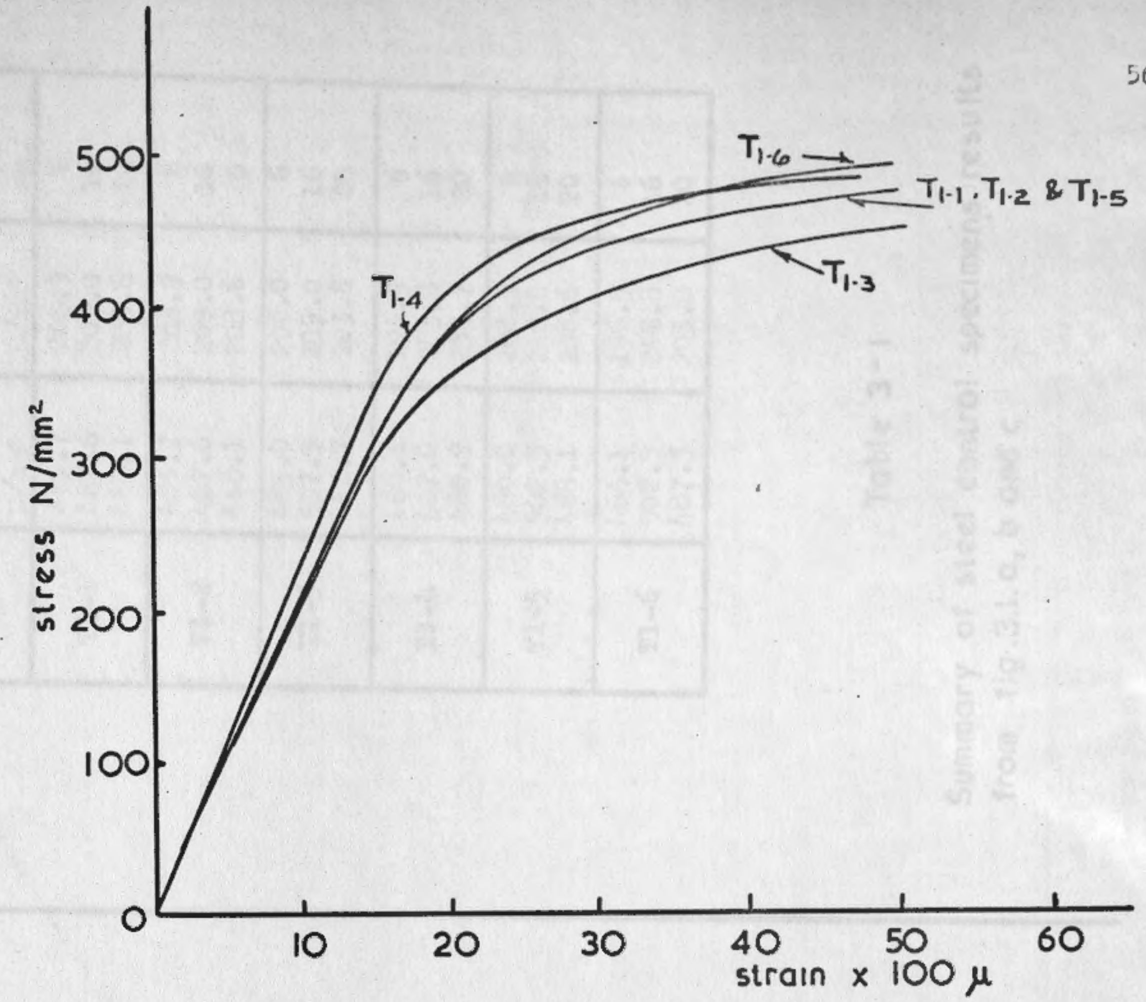

Fig. 3.1.a Stress v strain for 20 mm Ø H·T square twisted steel bars

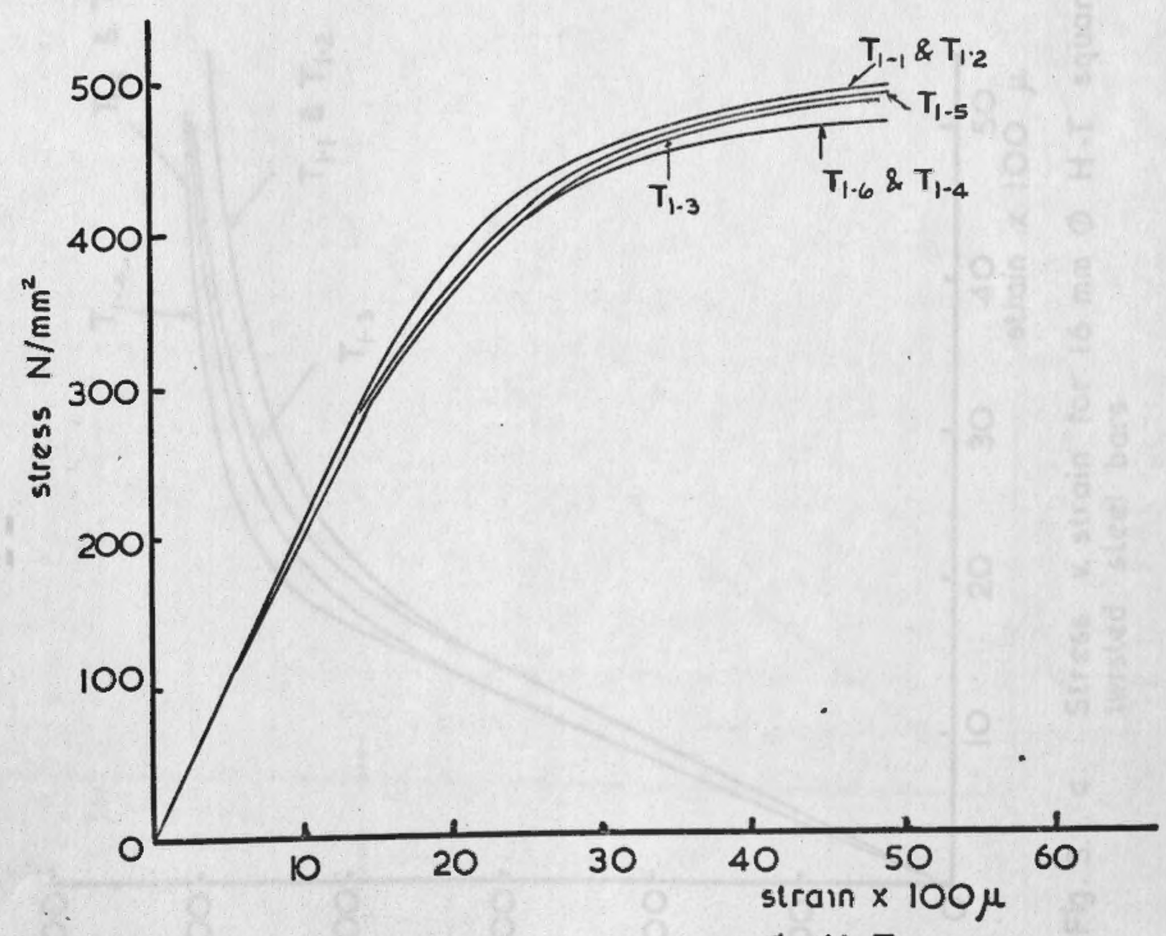

Fig. 3.1. b Stress v strain for 6 mm Ø H-T square twisted steel bars

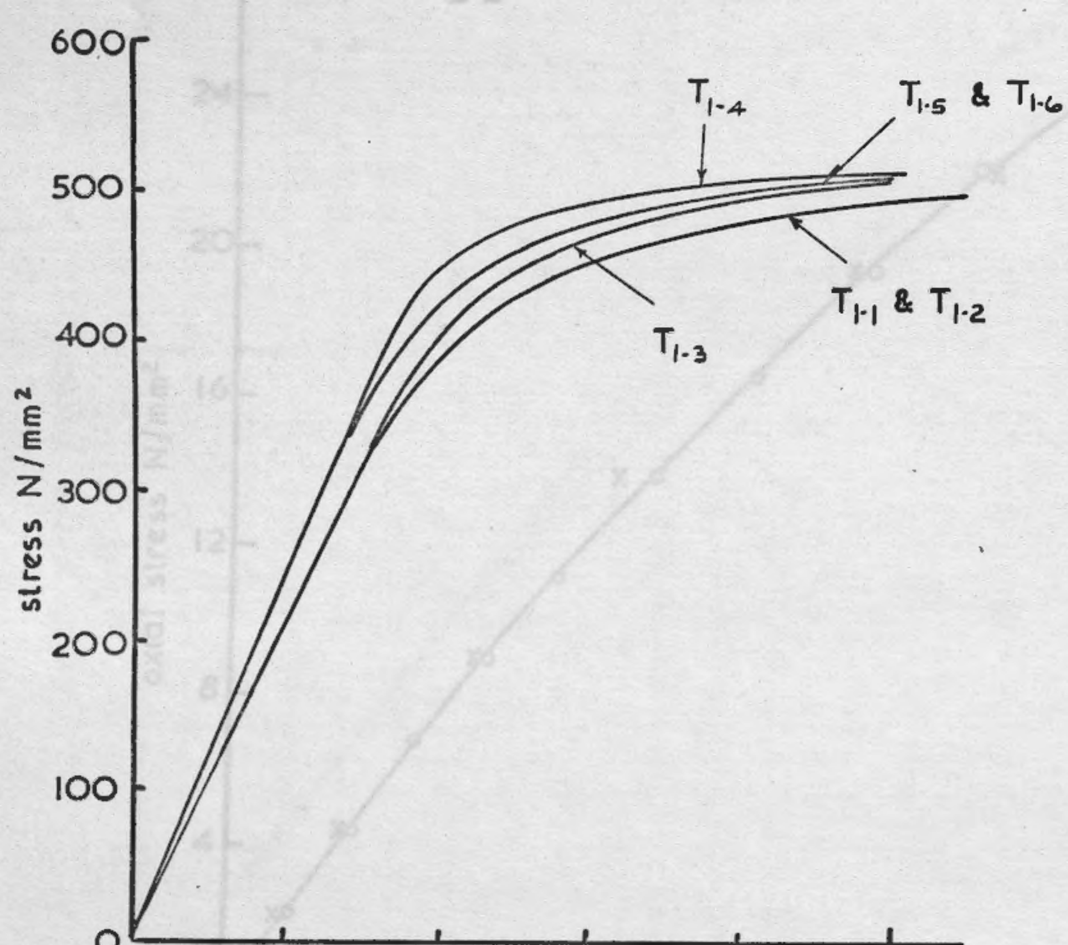

Fig. 3.1. c Stress v. strain for 16 mm Ø H-T square twisted steel bars

Test No. Tij	fy N/mm²	Es KN/mm²	Dia. of bar mm.
T1-1	485.7 487.6 468.1	208.9 209.0 208.6	6 16 20
T1-2	485.7 487.6 468.1	208.9 209.0 208.6	6 16 20
T1-3	485.0 507.5 442.7	200.0 209.0 203.8	6 16 20
T1-4	466.1 507.0 480.9	196.5 243.8 235.7	6 16 20
T1-5	480.0 502.5 468.1	208.9 248.8 208.6	6 16 20
T1-6	466.1 502.5 487.3	196.5 248.8 203.8	6 16 20

Table 3-1

Summary of steel control specimens results from fig.3.1.a, b and c

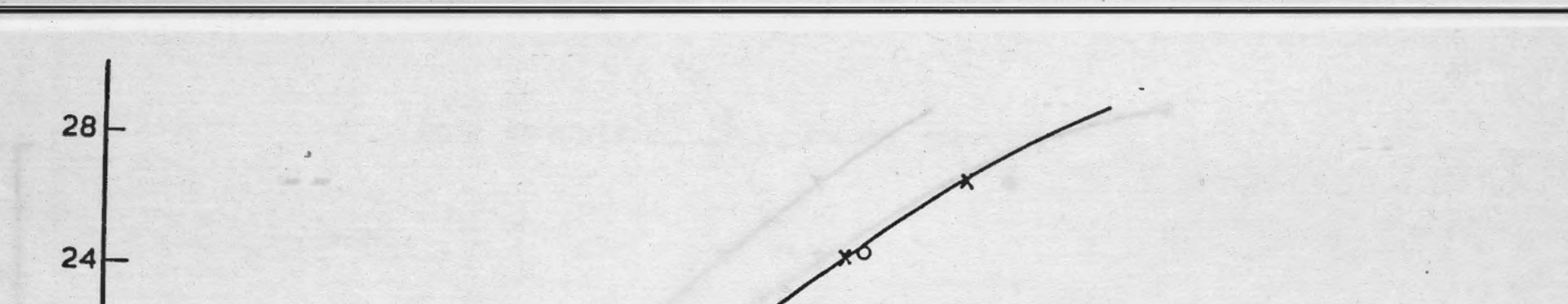

Fig 3.2. 1a. Axial stress v. longitudinal strain measured on cylinders for column concrete by electrical restance strain gauges

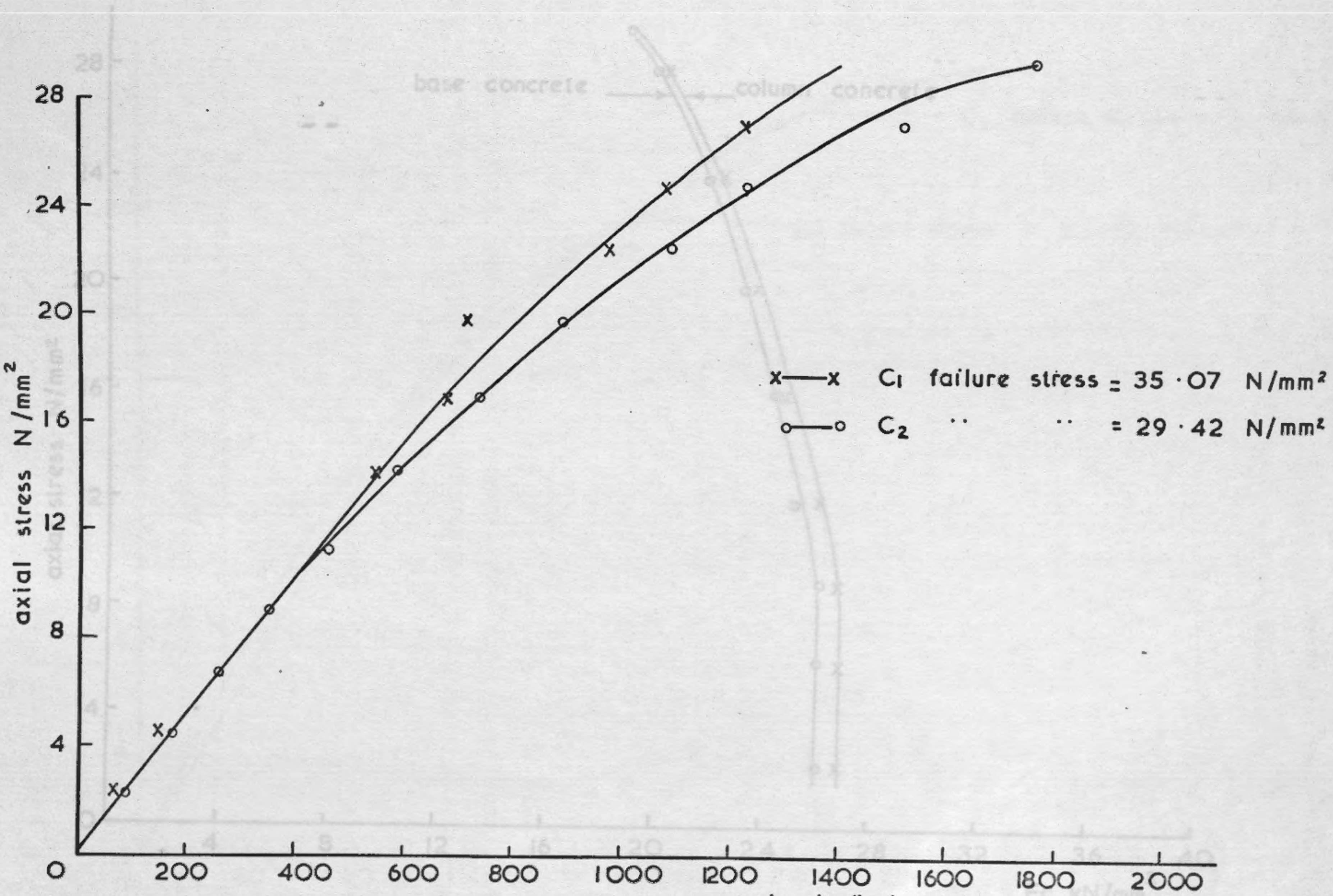

Fig. 3.2.1b. Axial stress v. longitudinal strain measured on cylinders for base concrete by electrical resistance strain gauges.

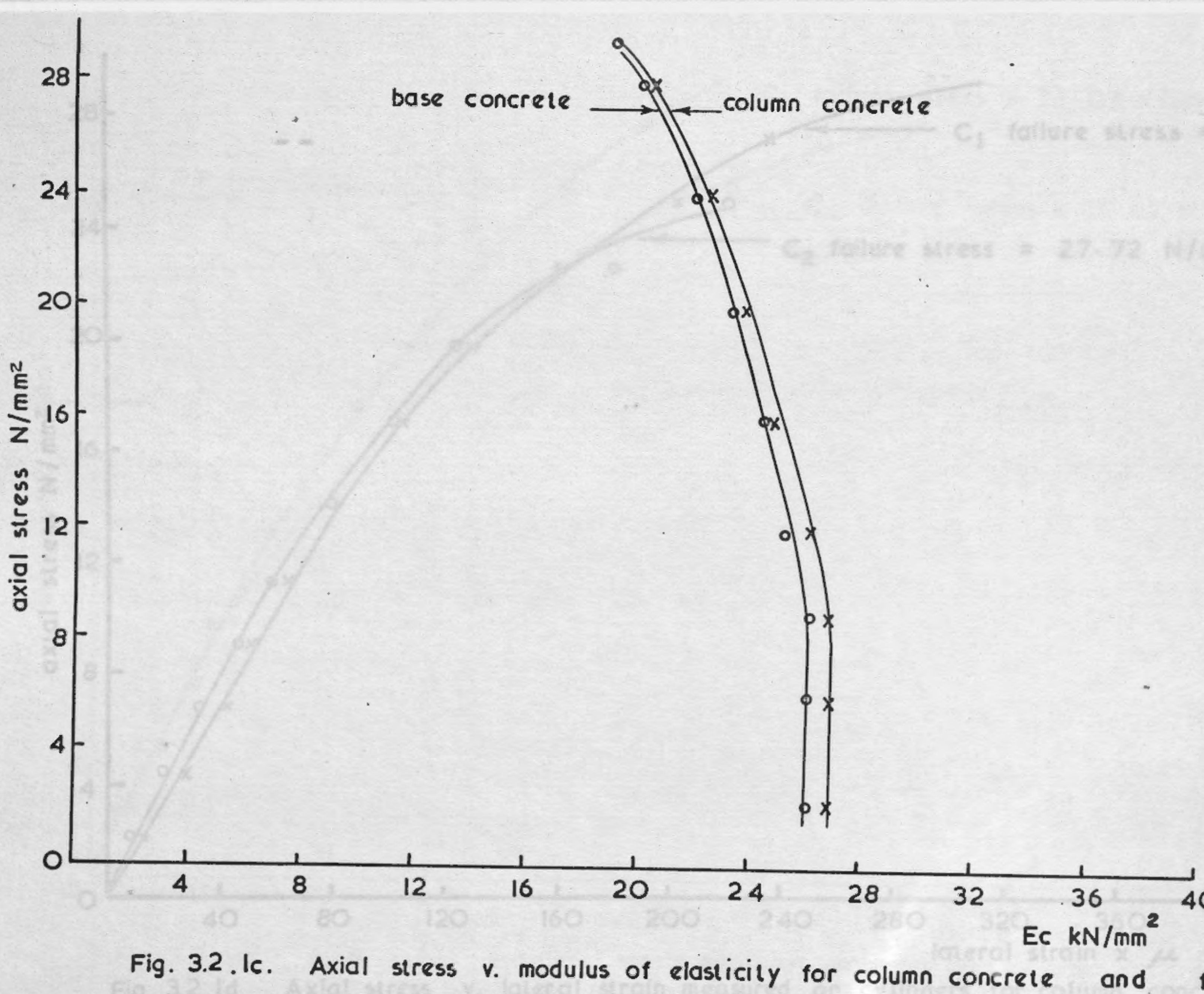

Fig. 3.2.1c. Axial stress v. modulus of elasticity for column concrete and for base concrete

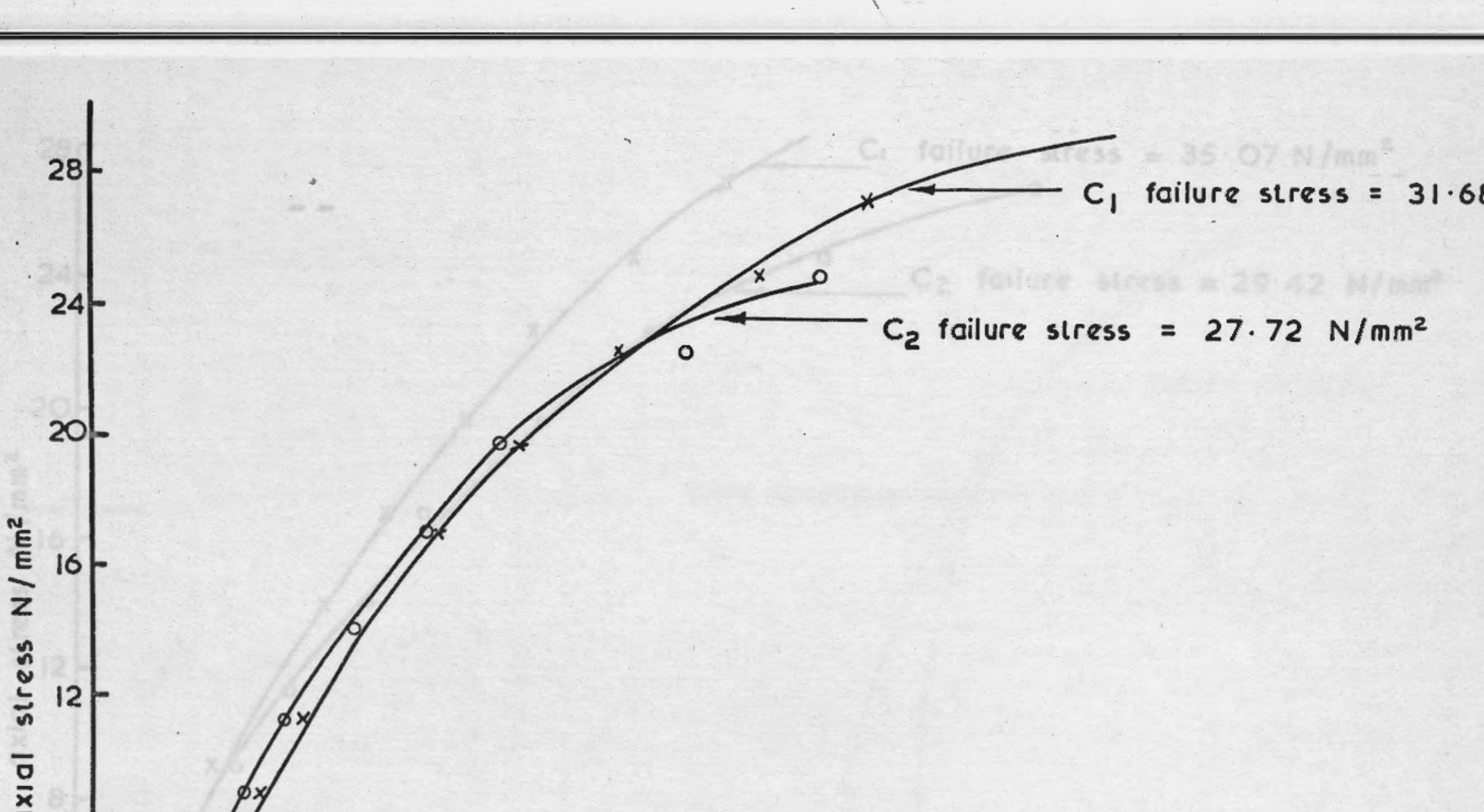

Fig. 3.2.1d Axial stress v. lateral strain measured on cylinders for column concrete by electrical resistance strain gauges.

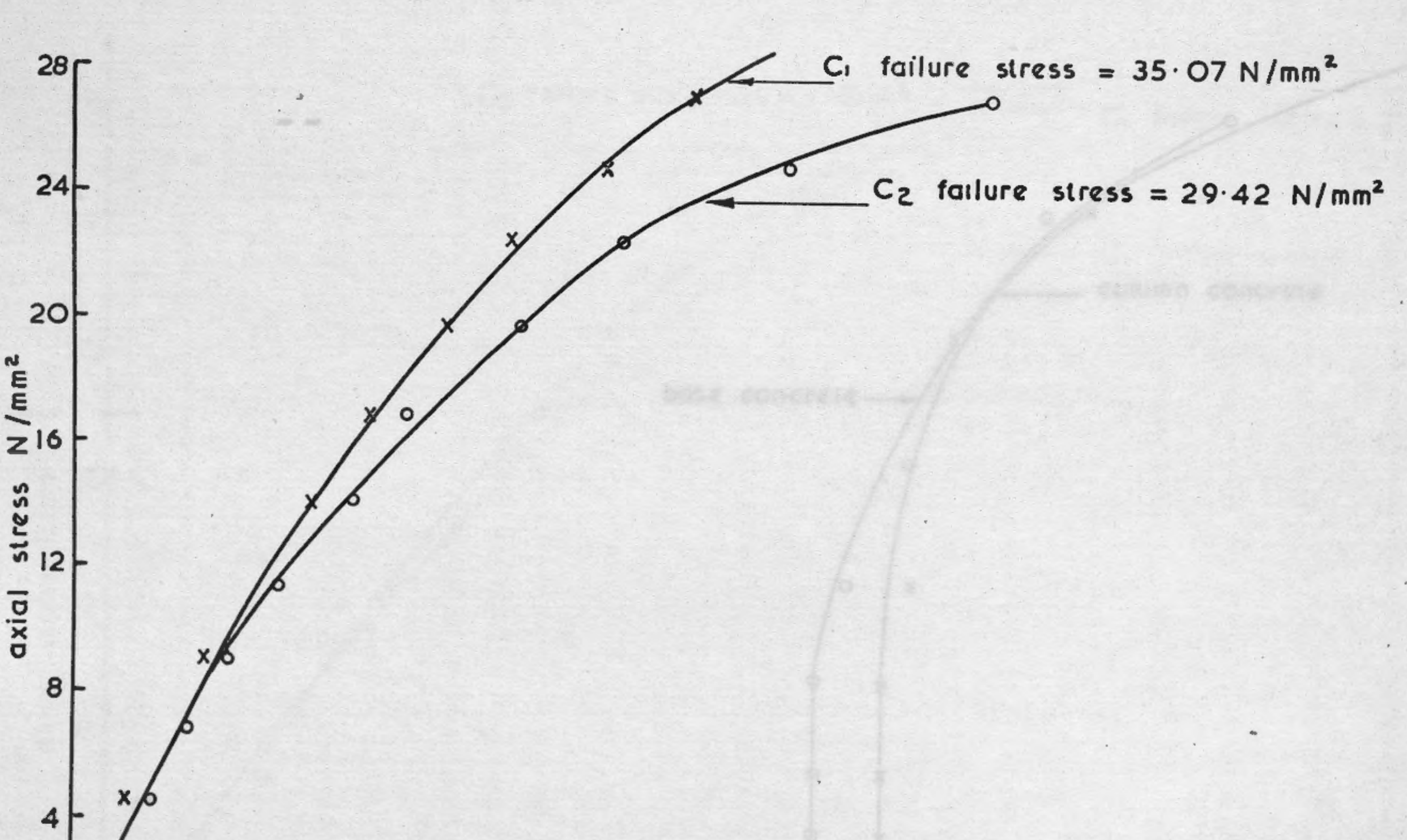

Fig. 3·2.1e. Axial stress v. lateral strain measured on cylinders for base concrete by electrical resistance strain gauges

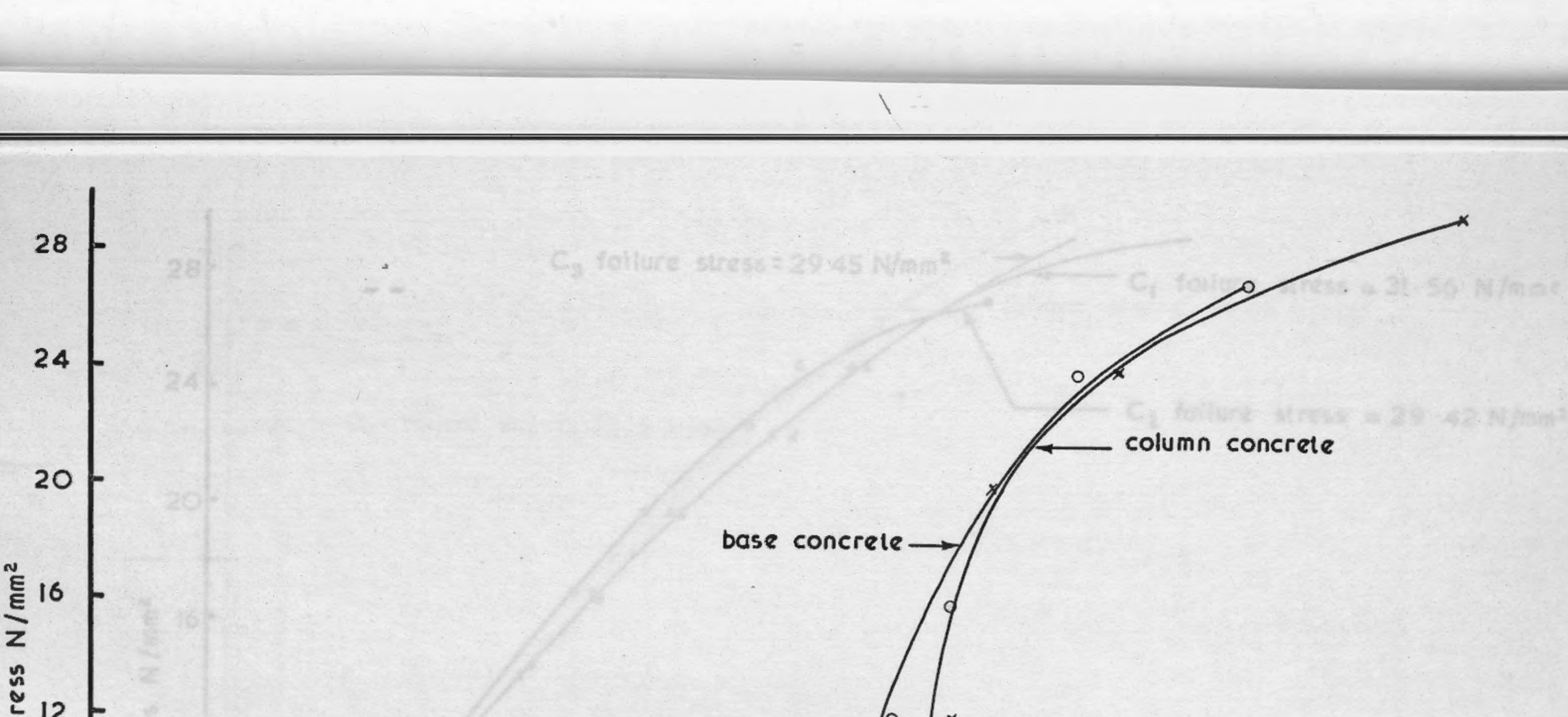

Fig. 3.2.1f. Axial stress v. Poission's ratio ν_c for column concrete and base concrete

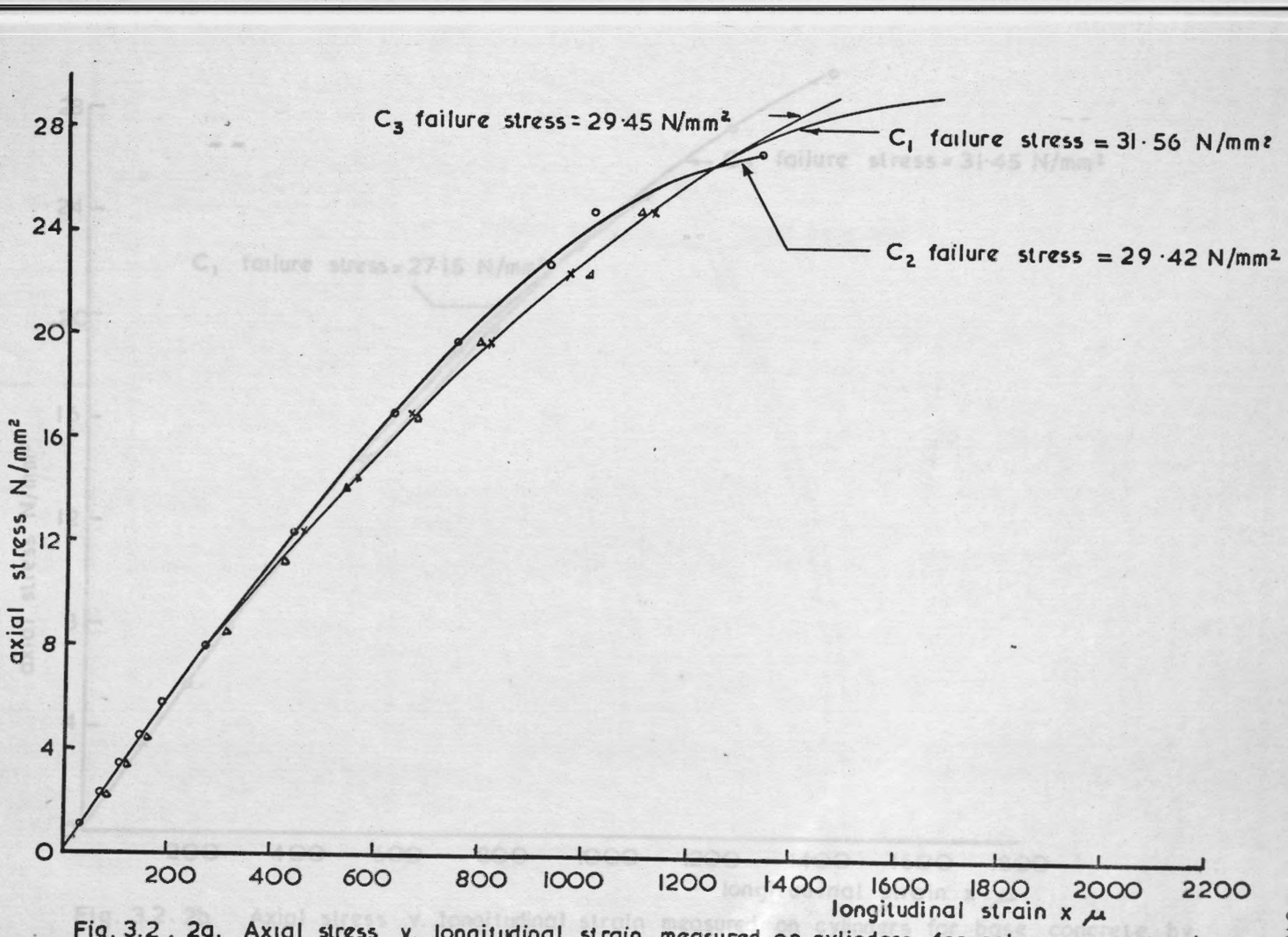

Fig. 3.2 . 2a. Axial stress v. longitudinal strain measured on cylinders for column concrete by electrical resistance strain gauges.

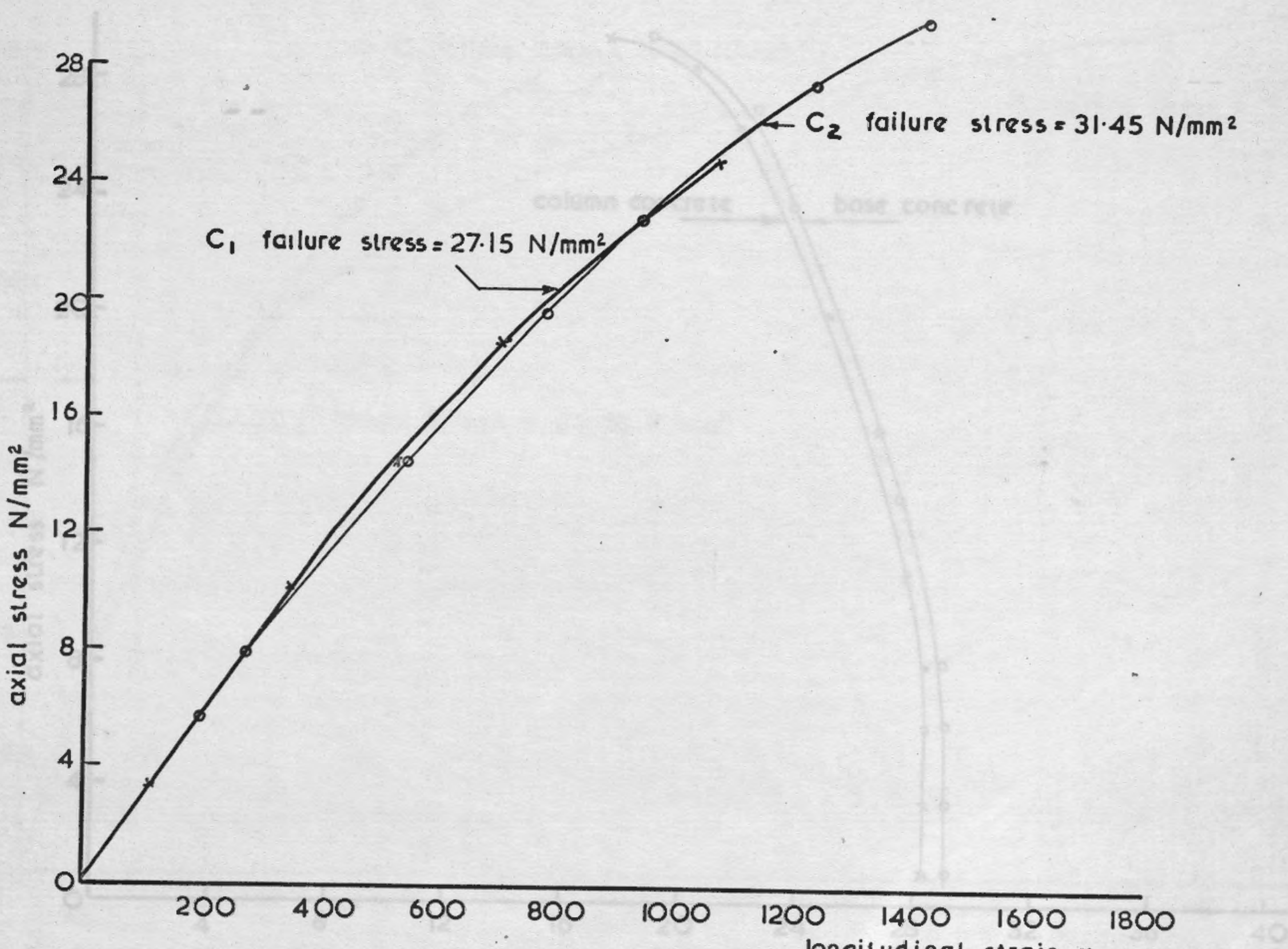

Fig. 3.2. 2b. Axial stress v. longitudinal strain measured on cylinders for base concrete by electrical resistance strain gauges.

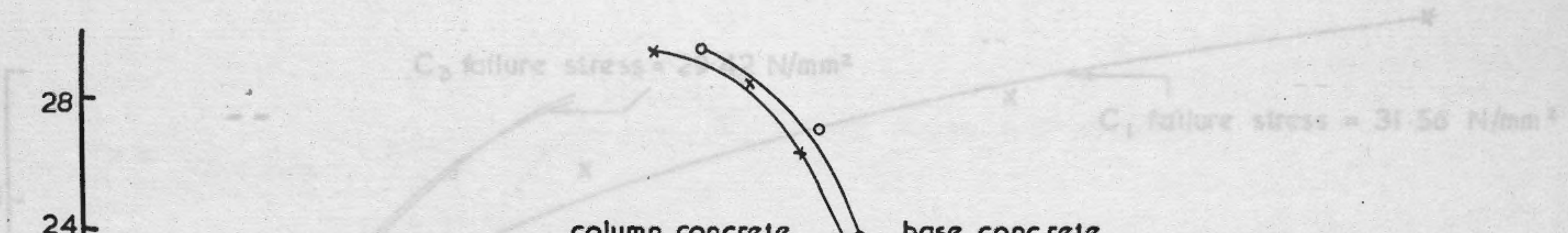

Fig.3.2.2c Axial stress v. modulus of elasticity for column concrete and for base concrete

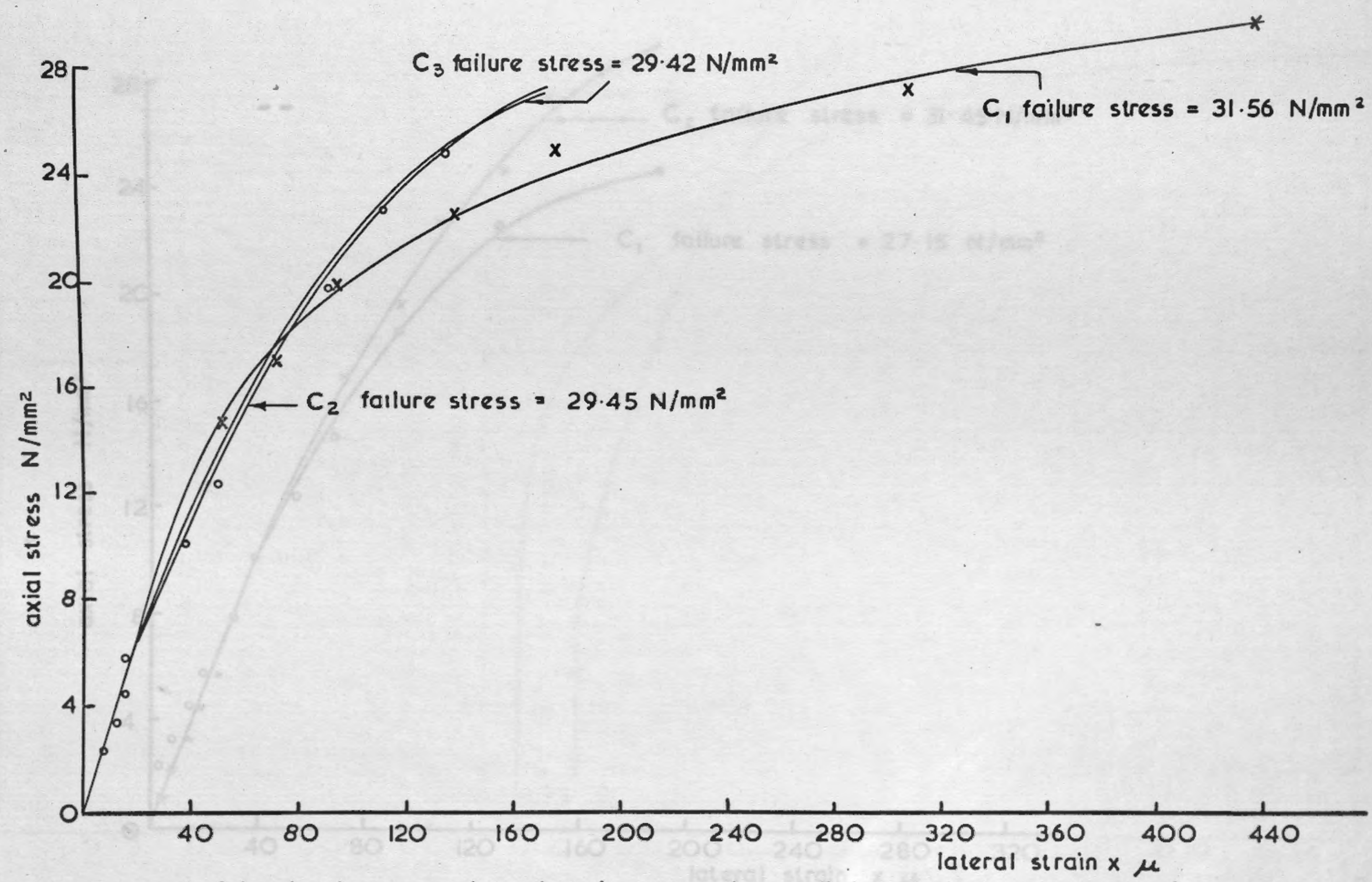

Fig. 3.2.2d. Axial stress v. lateral strain measured on cylinders for column concrete by electrical resistance strain gauges

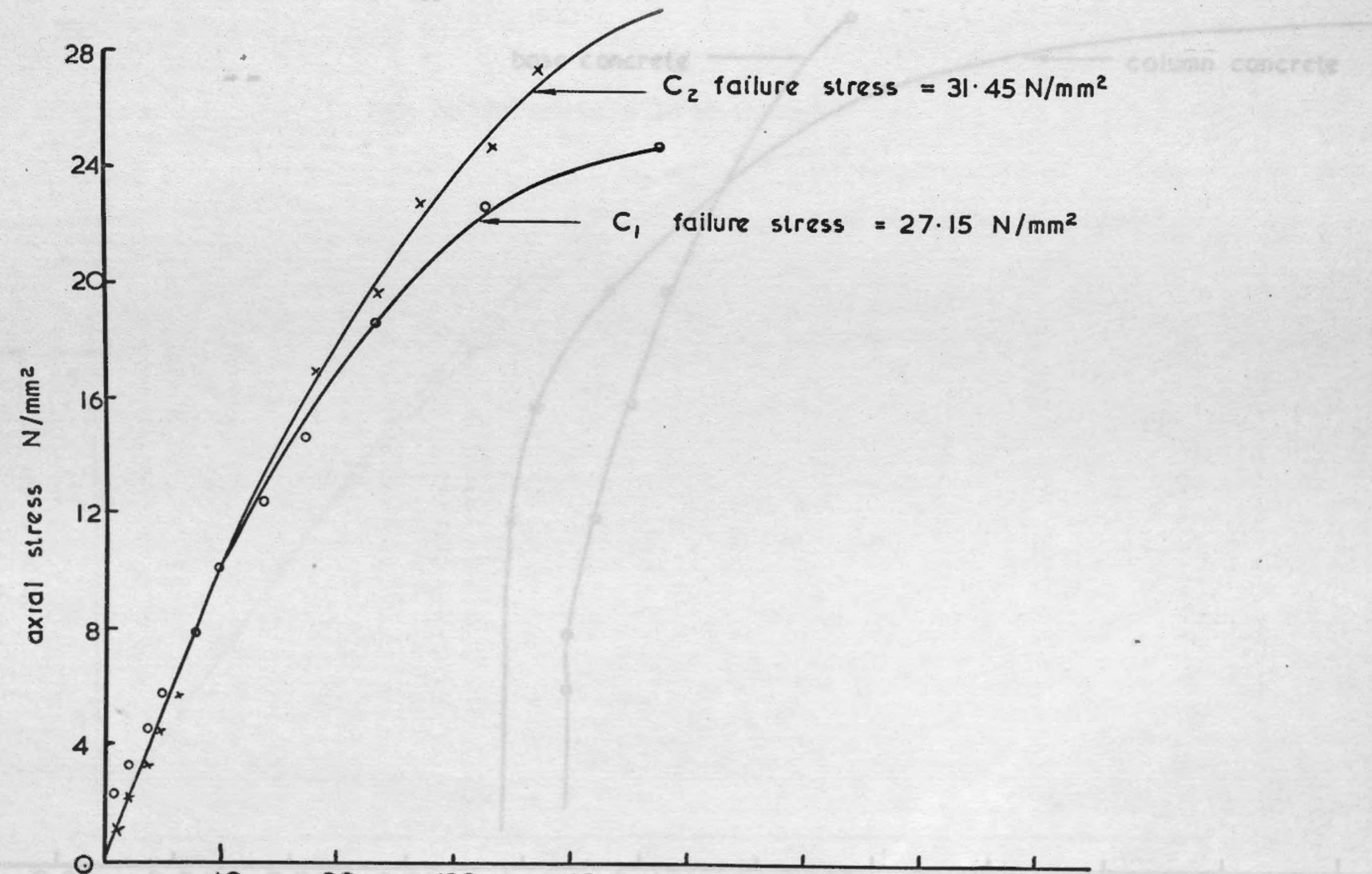

Fig. 3 . 2 . 2e. Axial stress v. lateral strain measured on cylinders for base concrete by electrical resistance strain gauges.

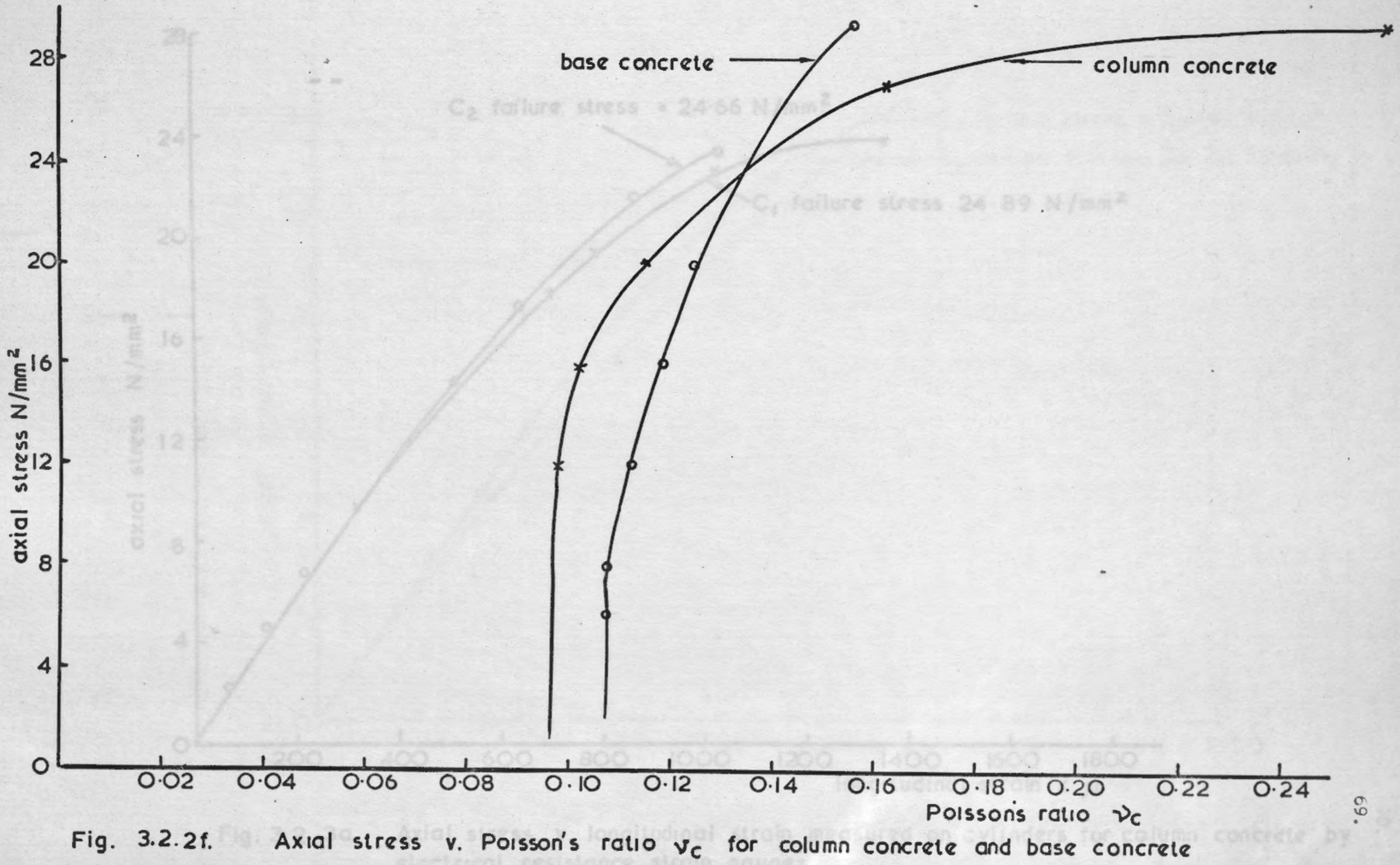

Fig. 3.2.2f. Axial stress v. Poisson's ratio ν_c for column concrete and base concrete

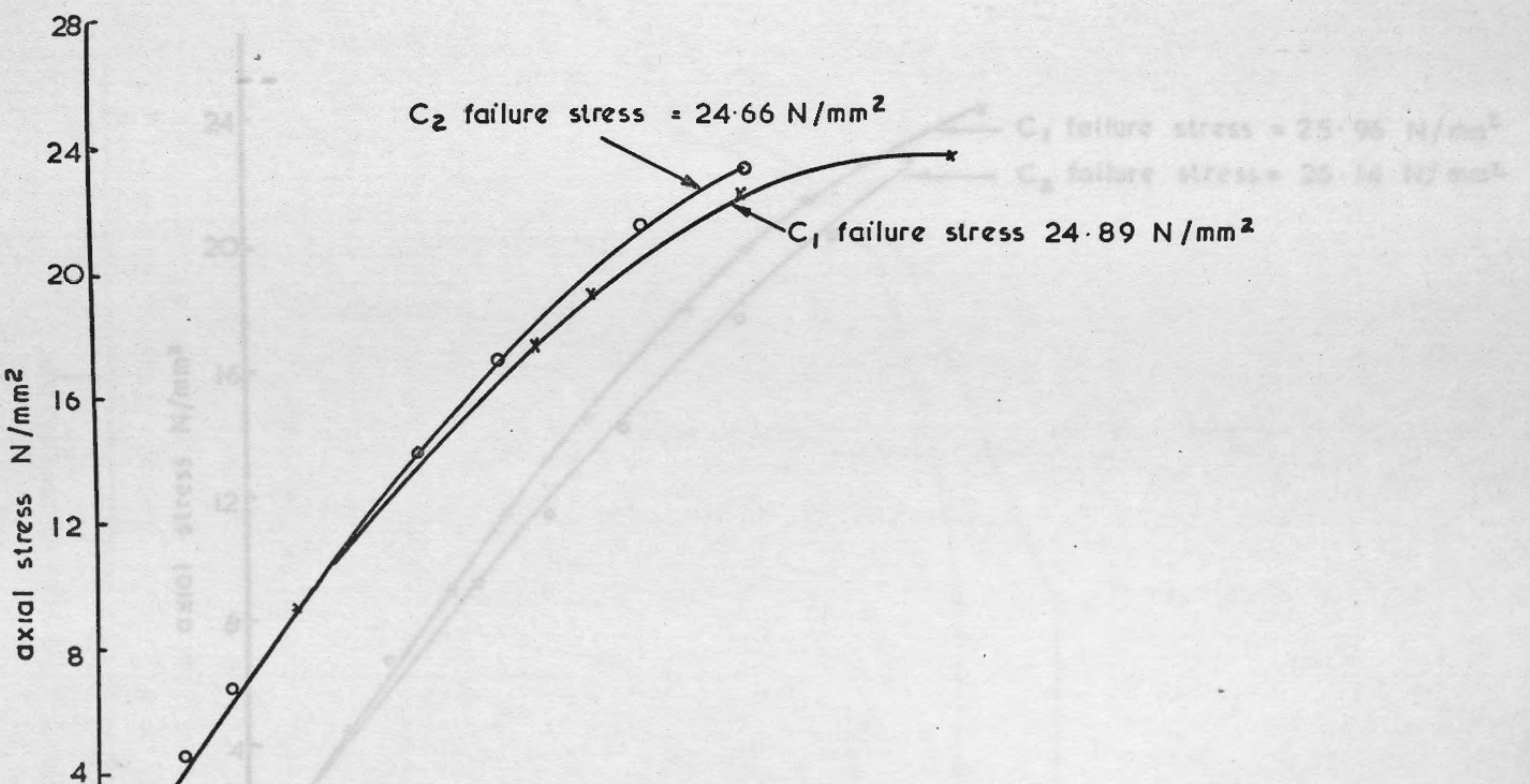

Fig. 3.2.3a Axial stress v. longitudinal strain measured on cylinders for column concrete by electrical resistance strain gauges.

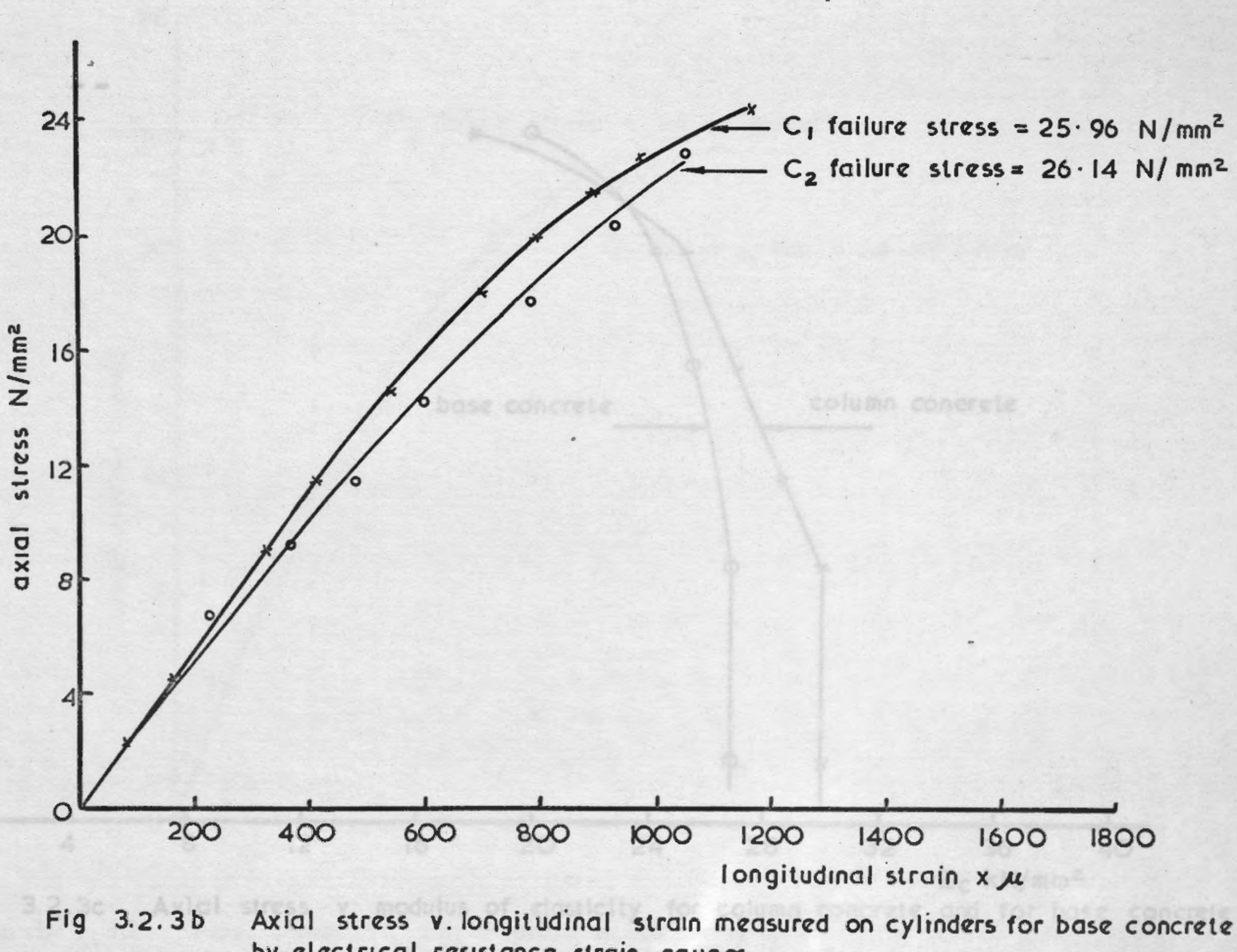

Fig 3.2.3b Axial stress v. longitudinal strain measured on cylinders for base concrete by electrical resistance strain gauges.

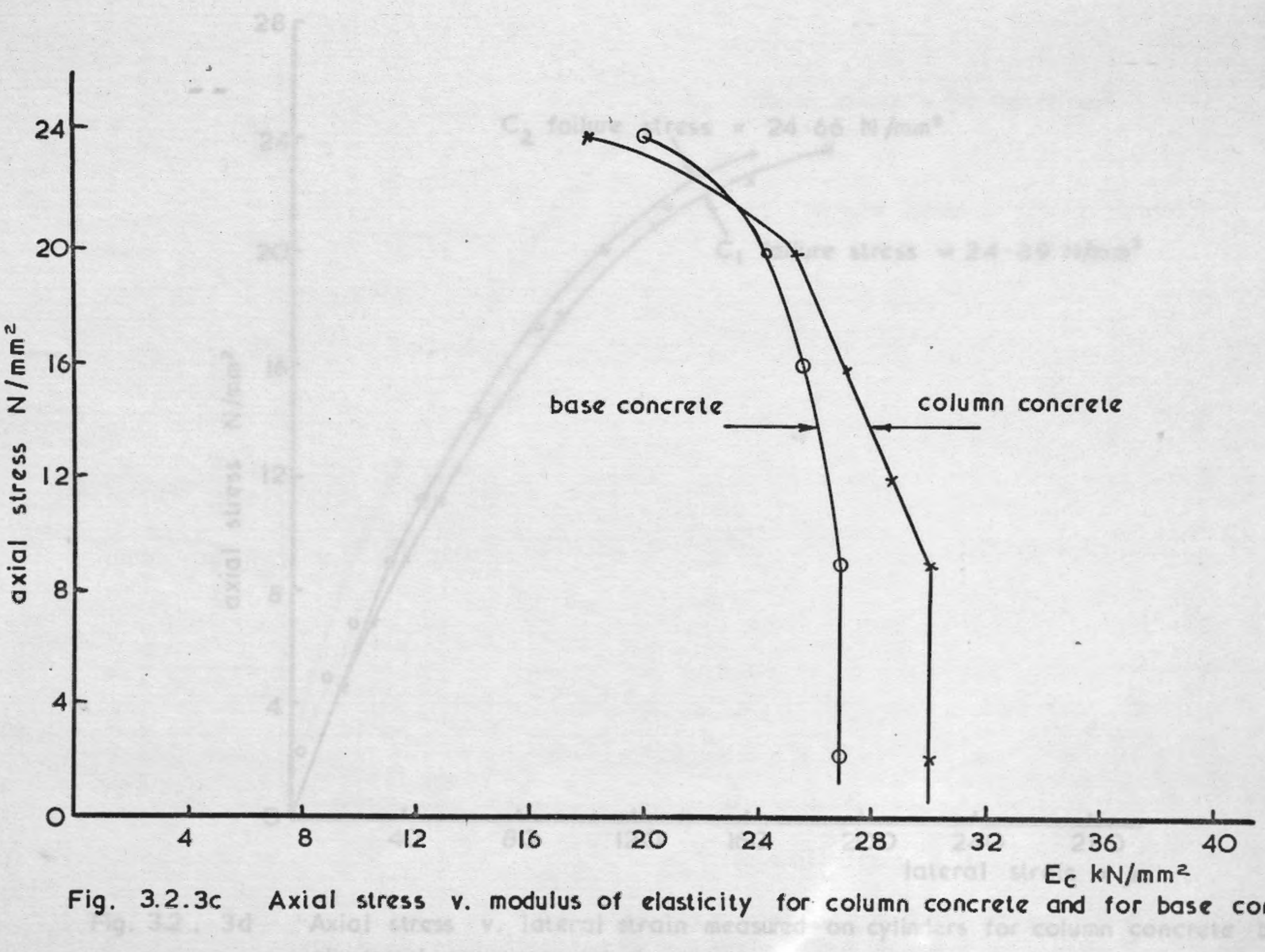

Fig. 3.2.3c Axial stress v. modulus of elasticity for column concrete and for base concrete

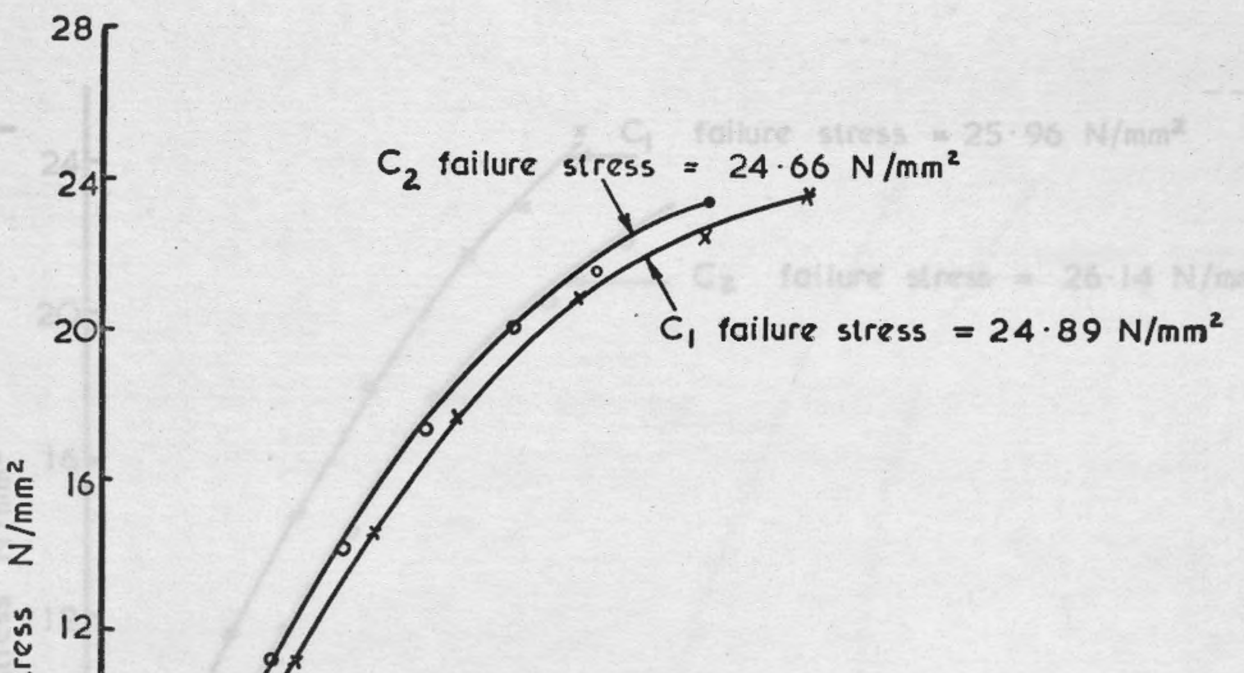

Fig. 3.2 . 3d Axial stress v. lateral strain measured on cylinders for column concrete by electrical resistance strain gauges.

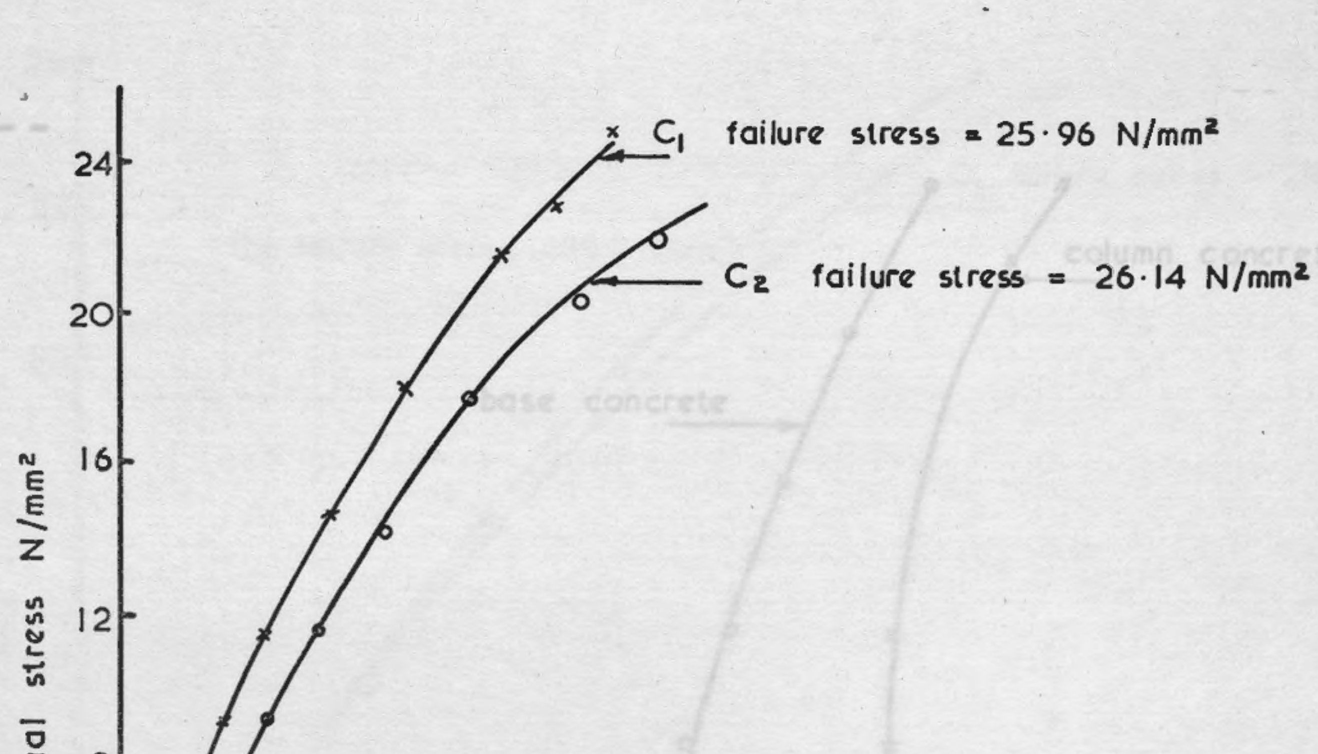

Fig. 3.2 . 3 e. Axial stress v. lateral strain measured on cylinders for base concrete by electrical resistance strain gauges.

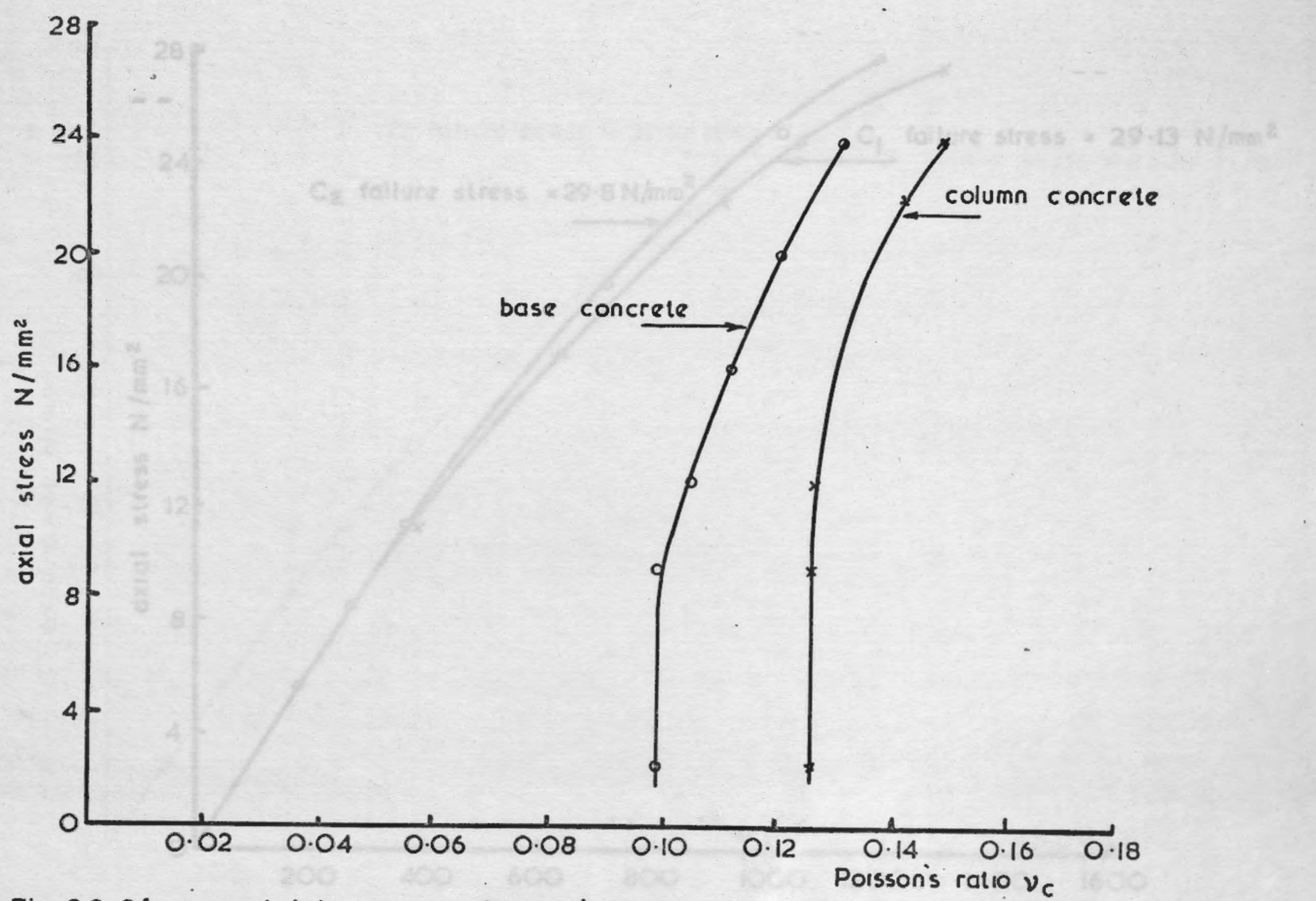

Fig. 3.2.3f Axial stress v. Poisson's ratio ν_c for column concrete and base concrete

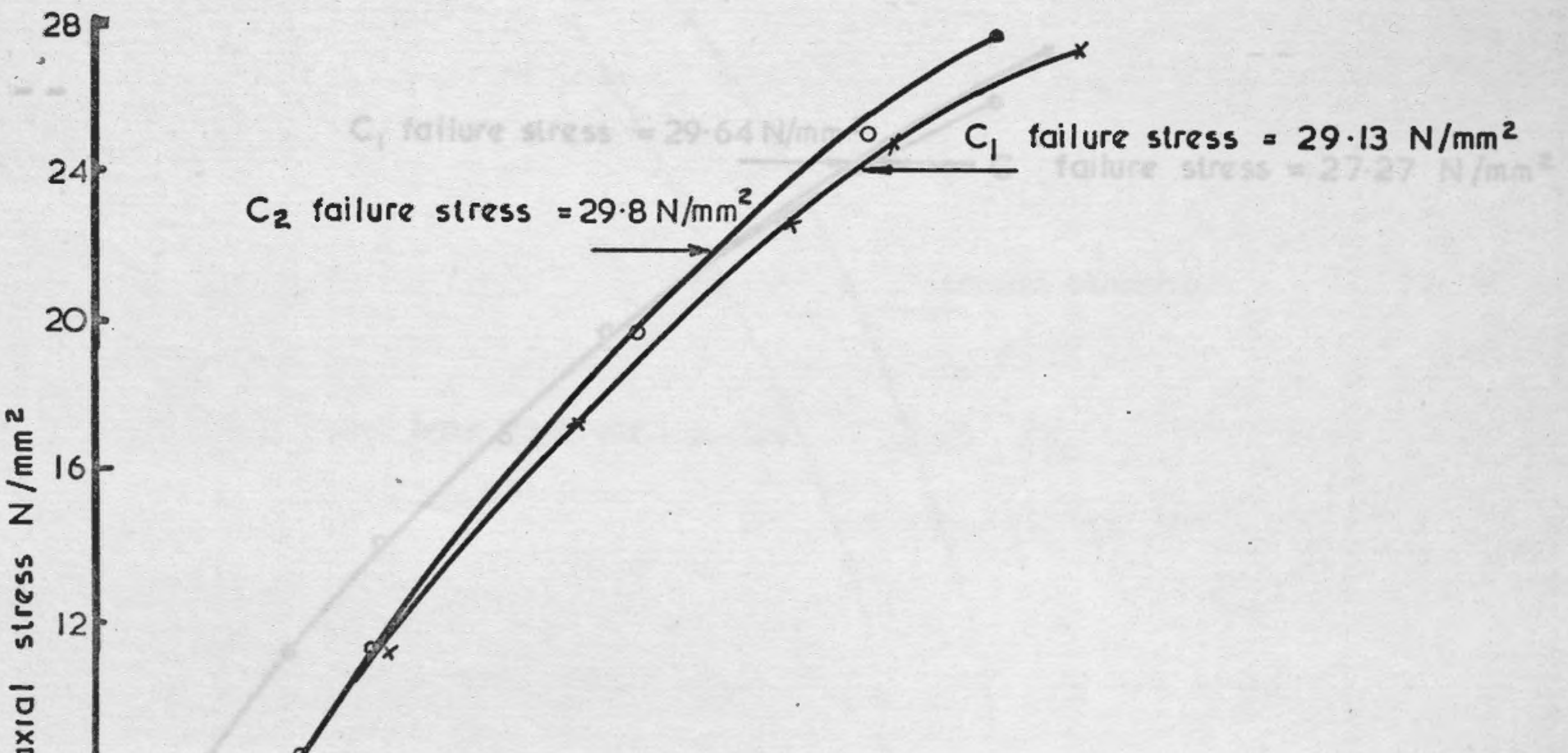

Fig. 3.2 . 4a. Axial stress v. longitudinal strain measured on cylinders for column concrete by electrical resistance strain gauges.

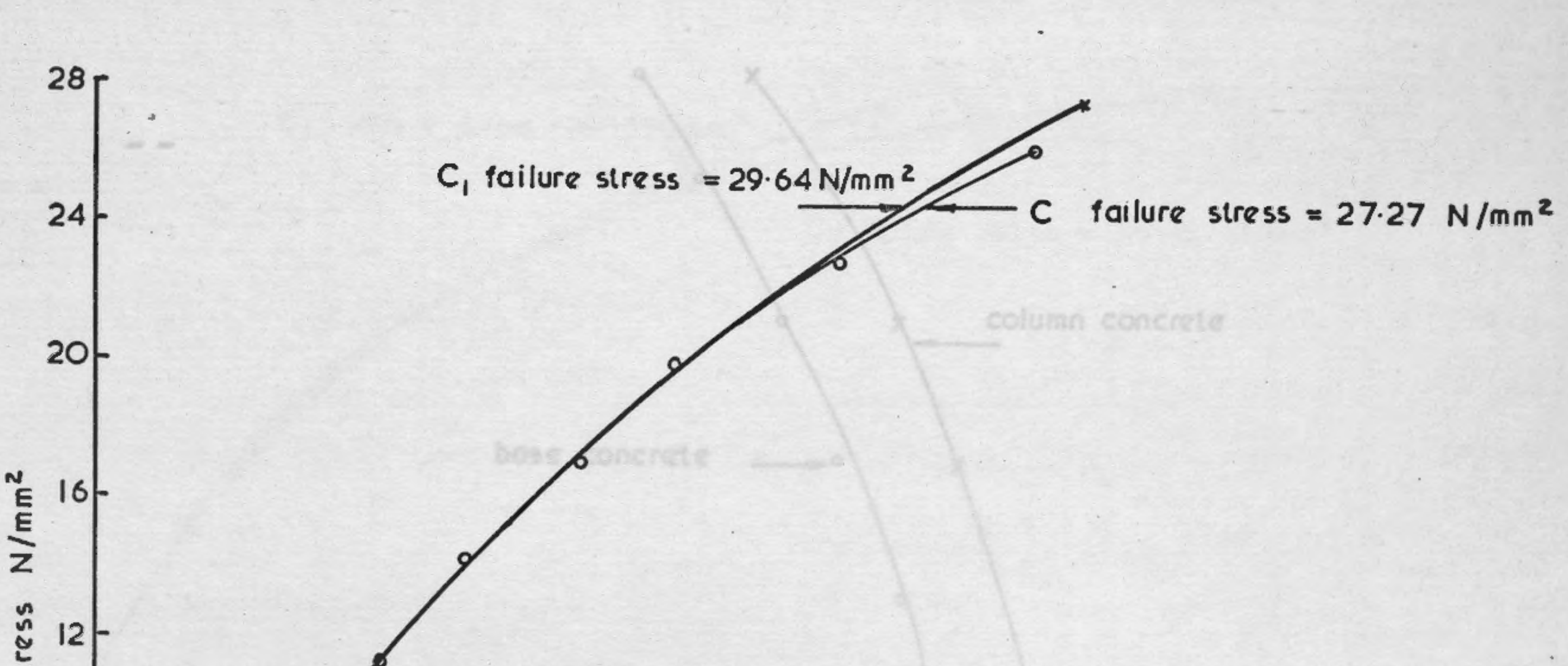

Fig 3.2.4b. Axial stress v. longitudinal strain measured on cylinders for base concrete by electrical resistance strain gauges.

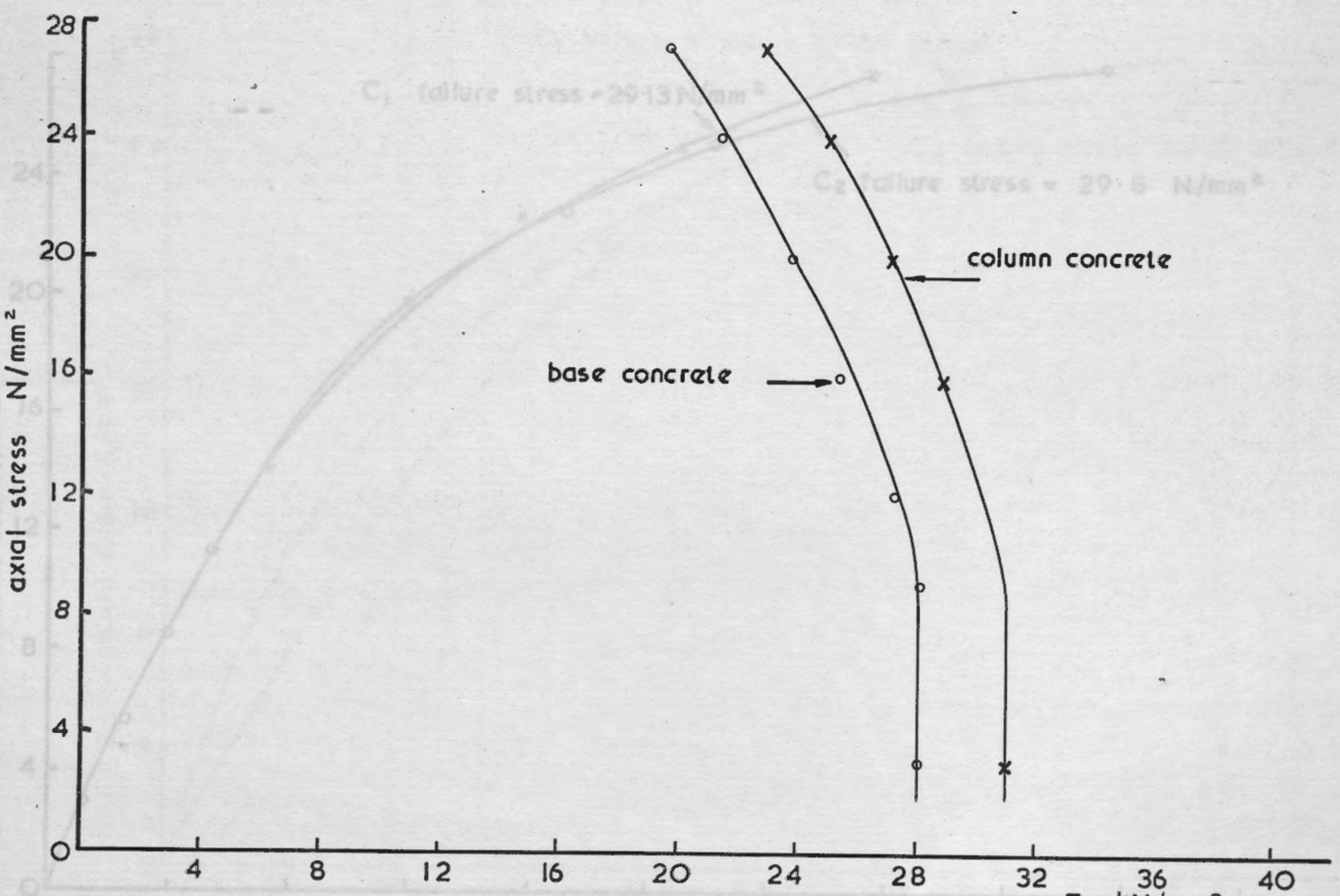

Fig. 3.2. 4c Axial stress v. modulus of elasticity for column concrete and for base concrete

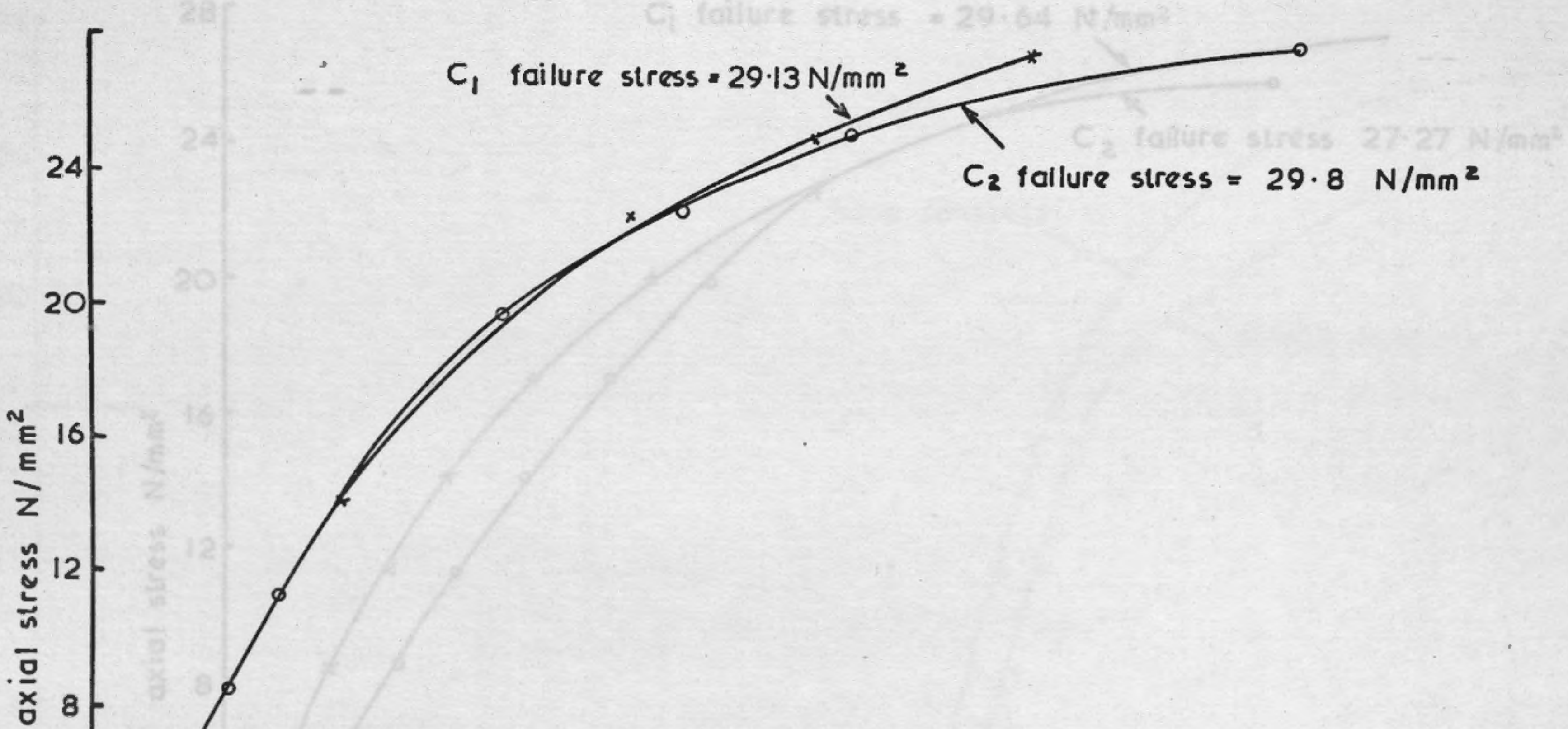

Fig. 3.2.4d Axial stress v. lateral strain measured on cylinders for column concrete by electrical resistance strain gauges.

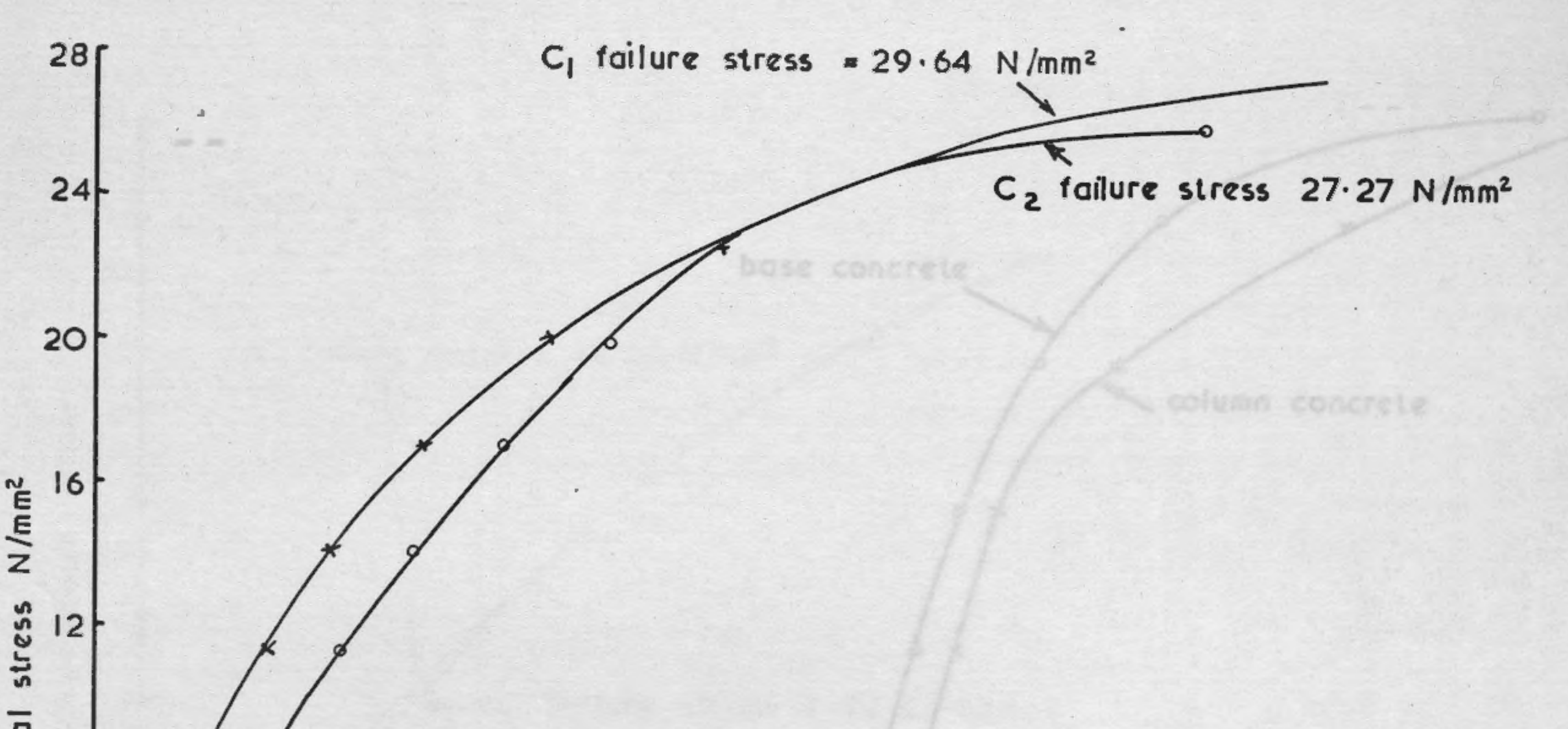

Fig. 3.2.4e. Axial stress v. lateral strain measured on cylinders for base concrete by electrical resistance strain gauges

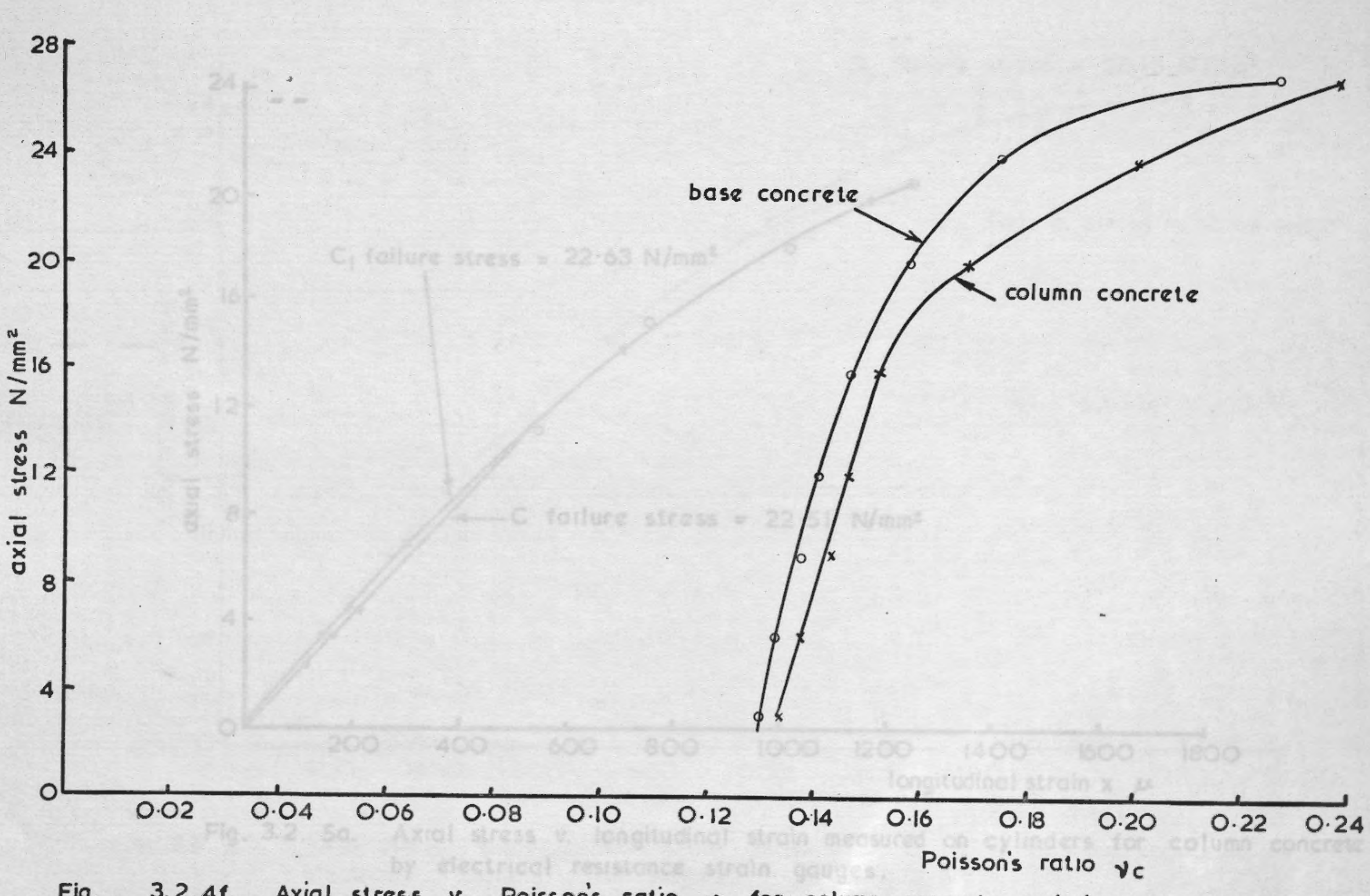

Fig. 3.2.4f. Axial stress v. Poisson's ratio ν_c for column concrete and base concrete

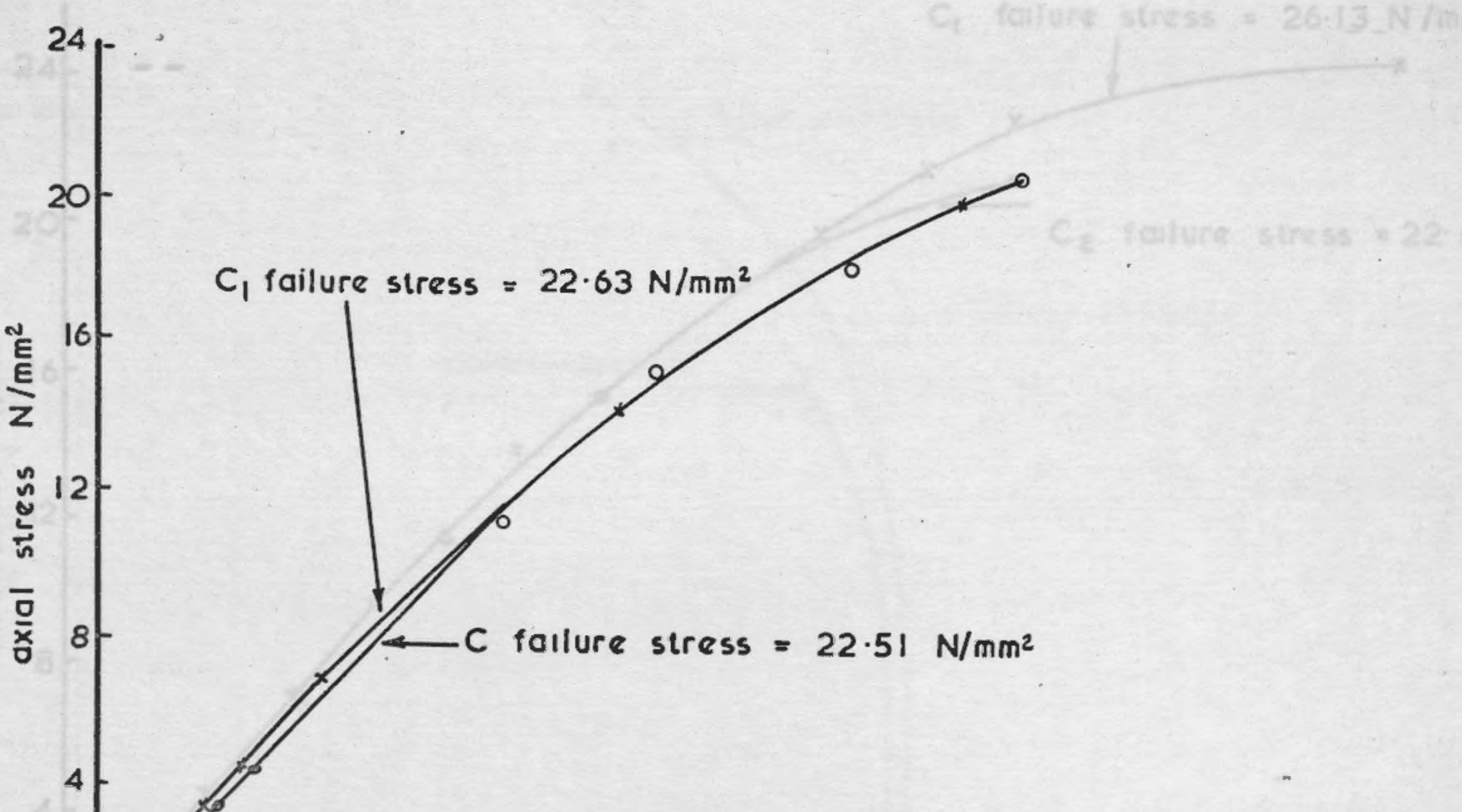

Fig. 3.2. 5a. Axial stress v. longitudinal strain measured on cylinders for column concrete by electrical resistance strain gauges.

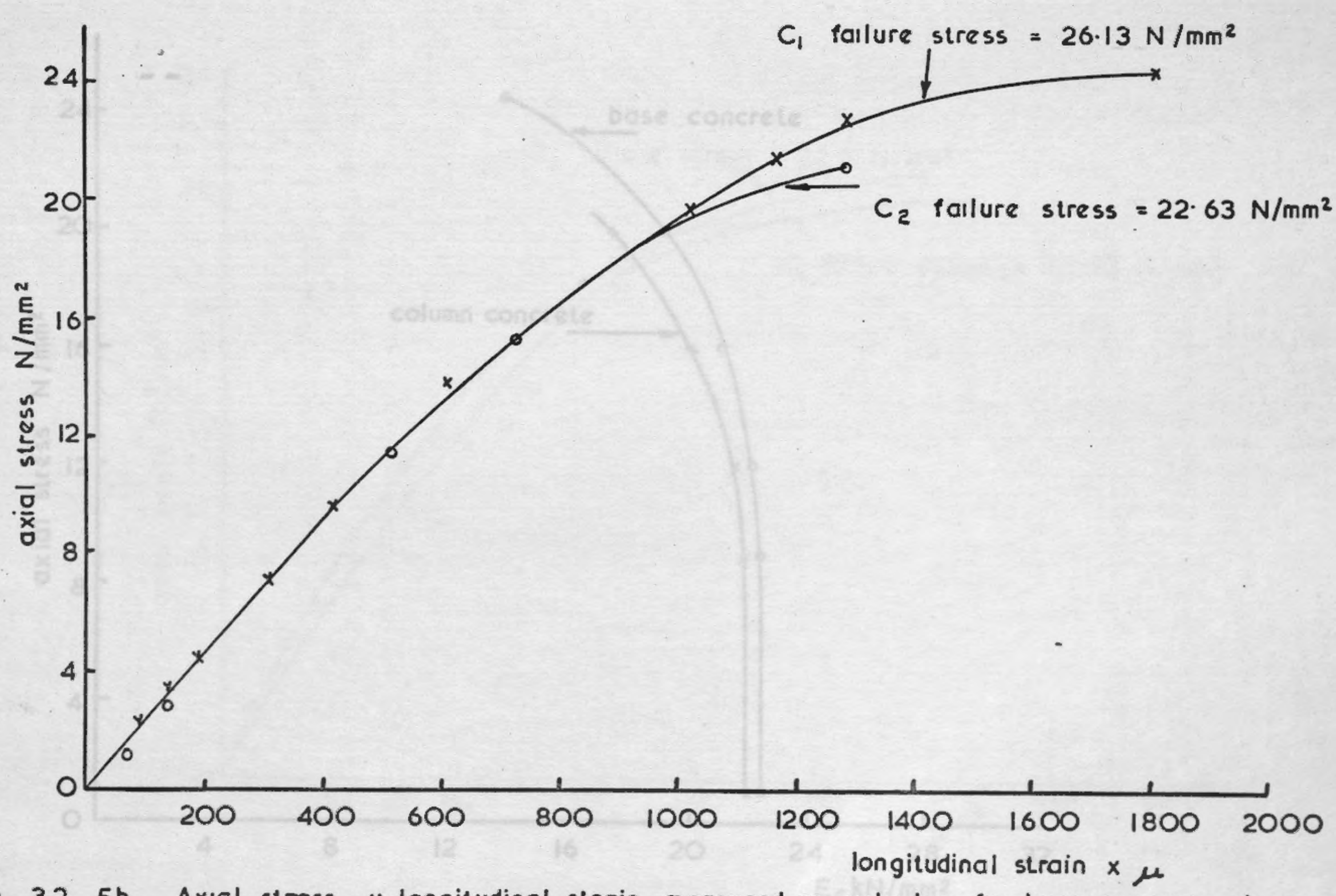

Fig. 3.2. 5b. Axial stress v. longitudinal strain measured on cylinders for base concrete by electrical resistance strain gauges.

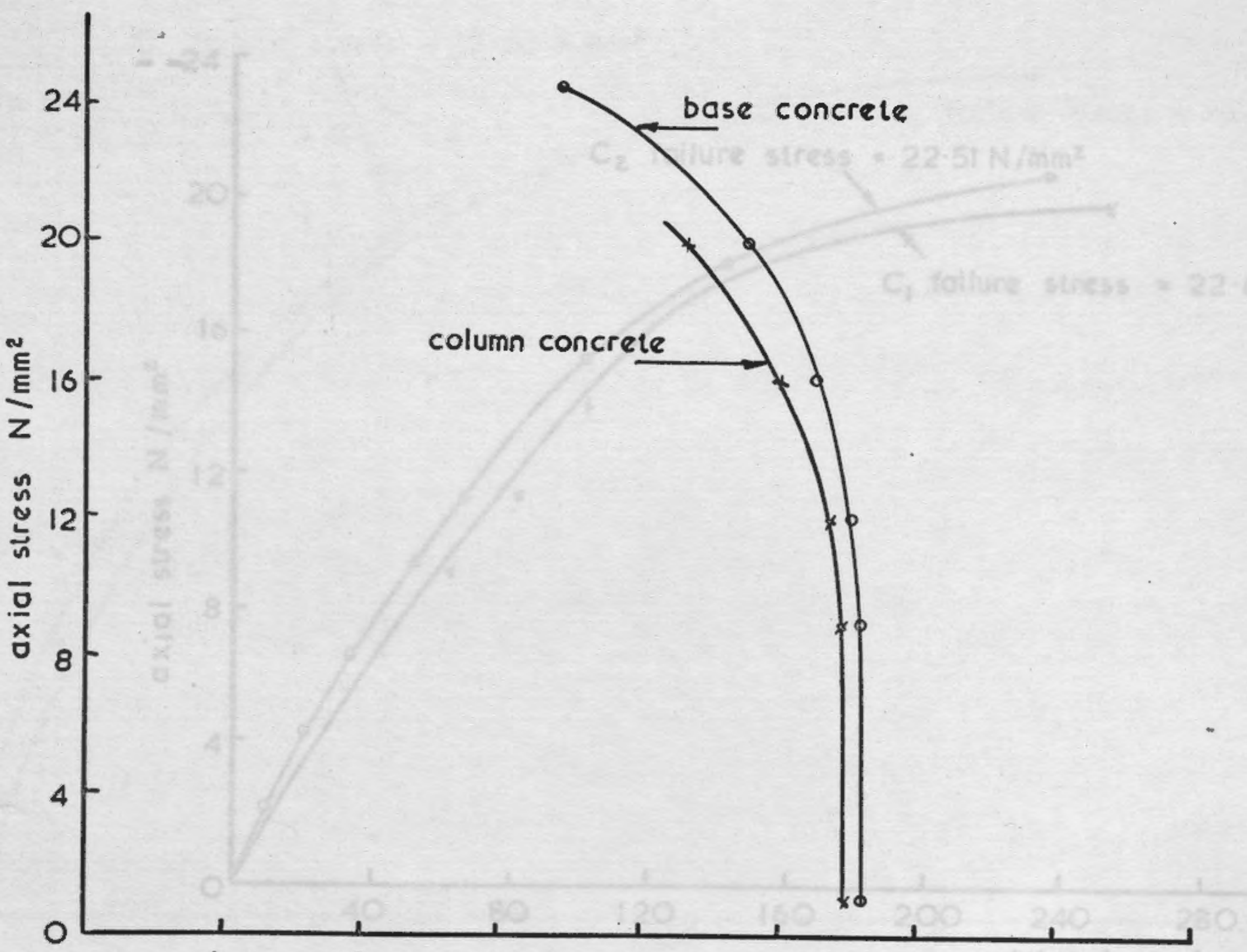

Fig.3.2 . 5c. Axial stress v. Modulus of elasticity for column concrete and for base concrete

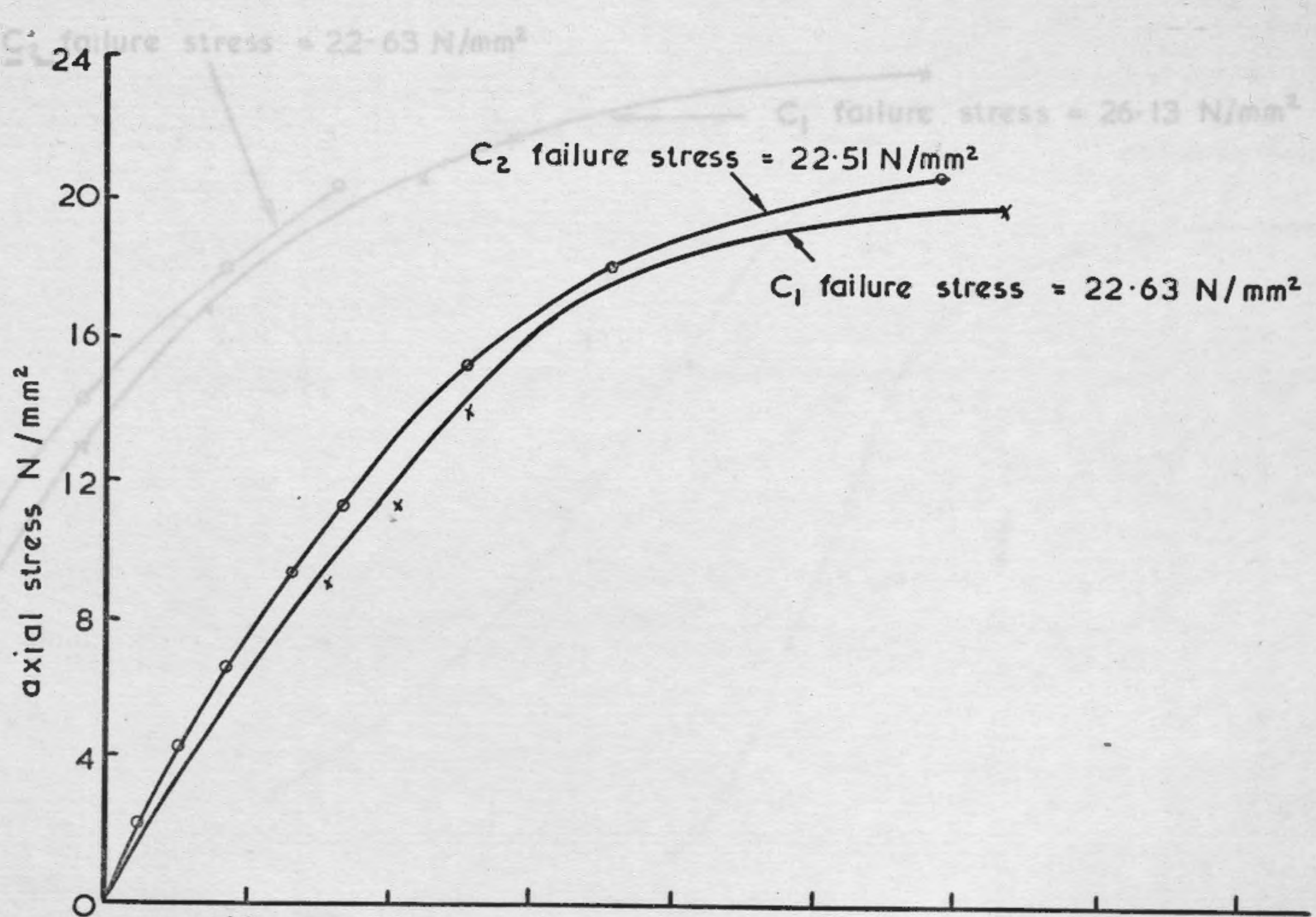

Fig. 3.2. 5d. Axial stress v. lateral strain measured on cylinders for column concrete by electrical resistance strain gauges.

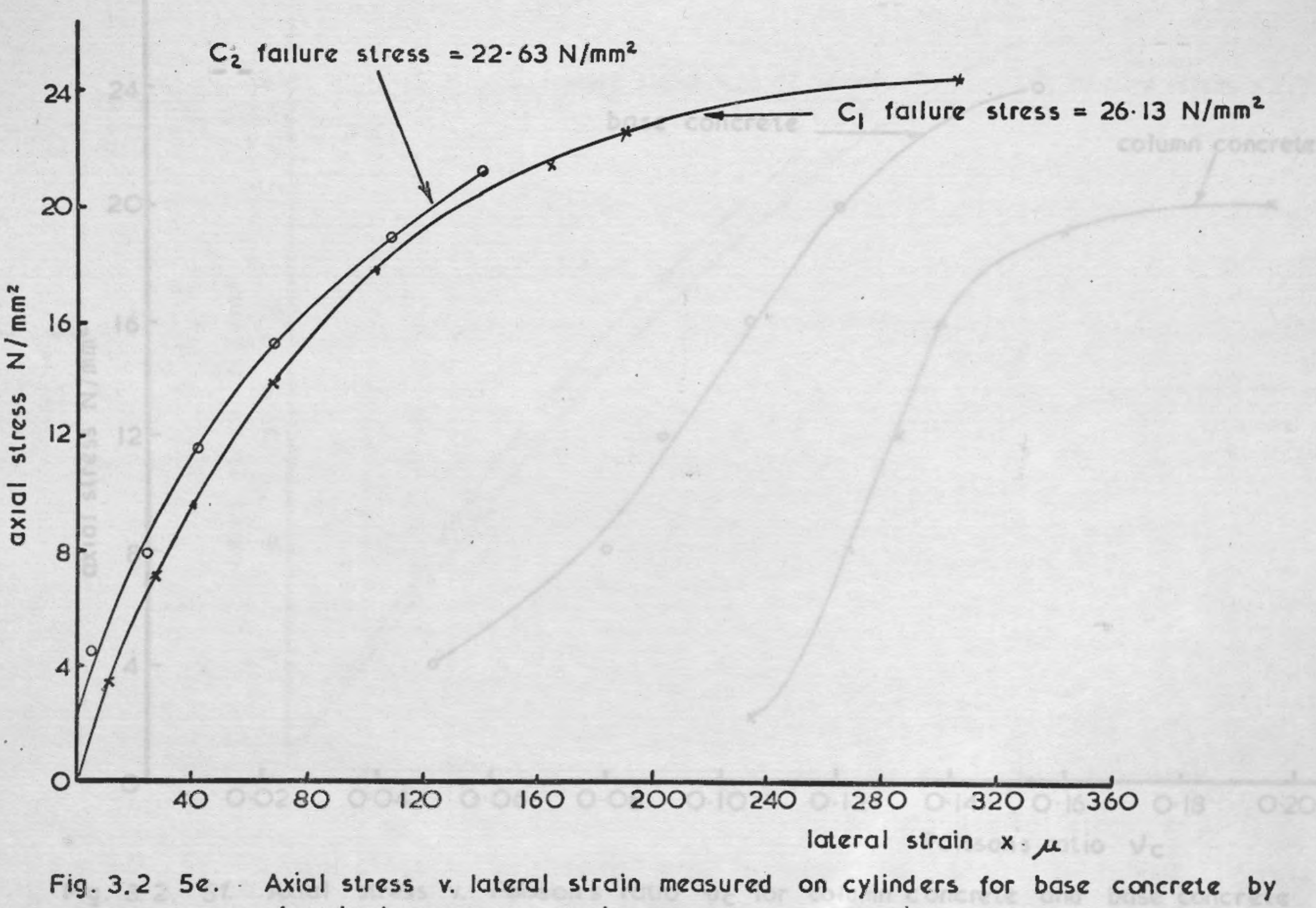

Fig. 3.2 5e. Axial stress v. lateral strain measured on cylinders for base concrete by electrical resistance strain gauges

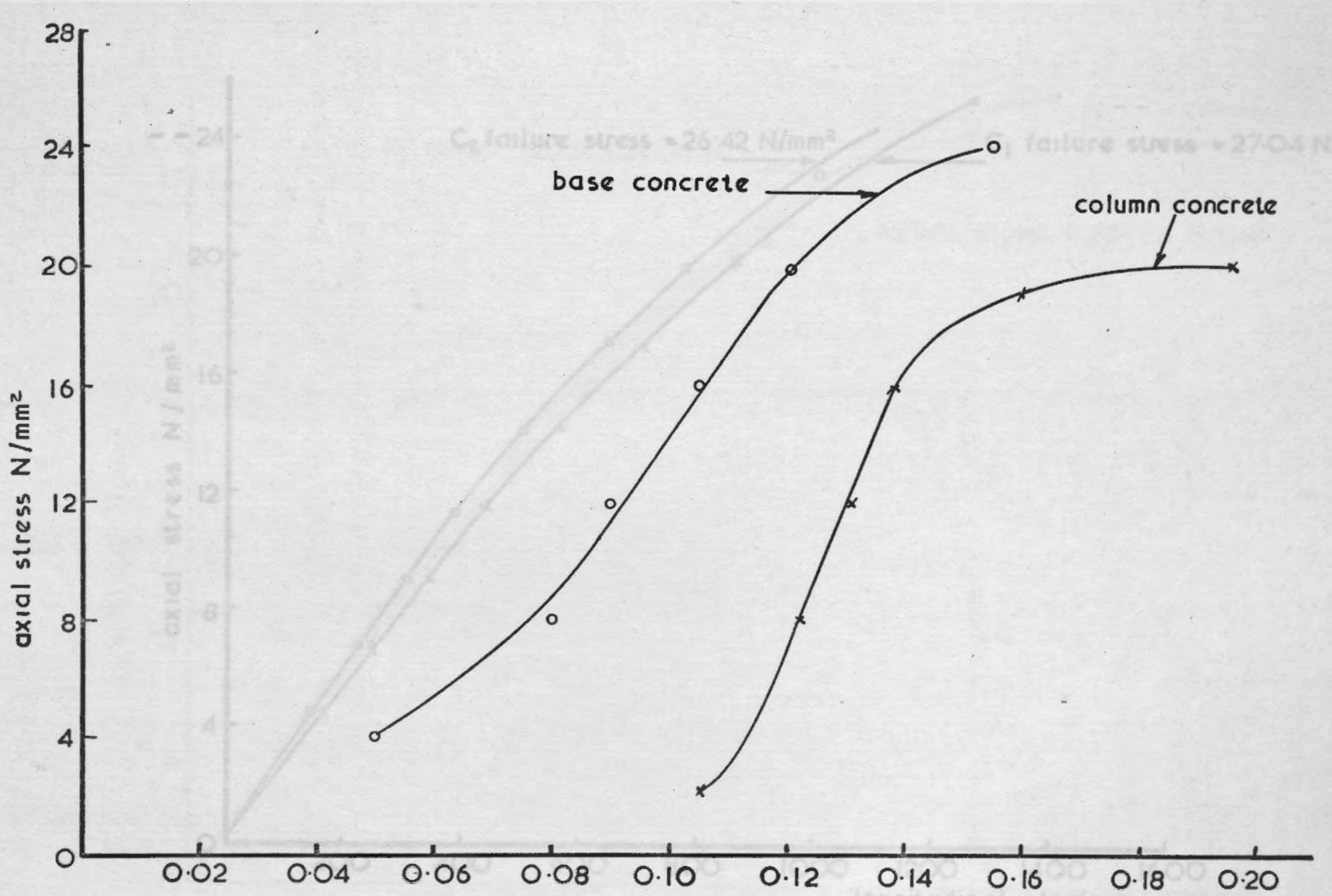

Fig. 3.2. 5f. Axial stress v. Poisson's ratio ν_c for column concrete and base concrete

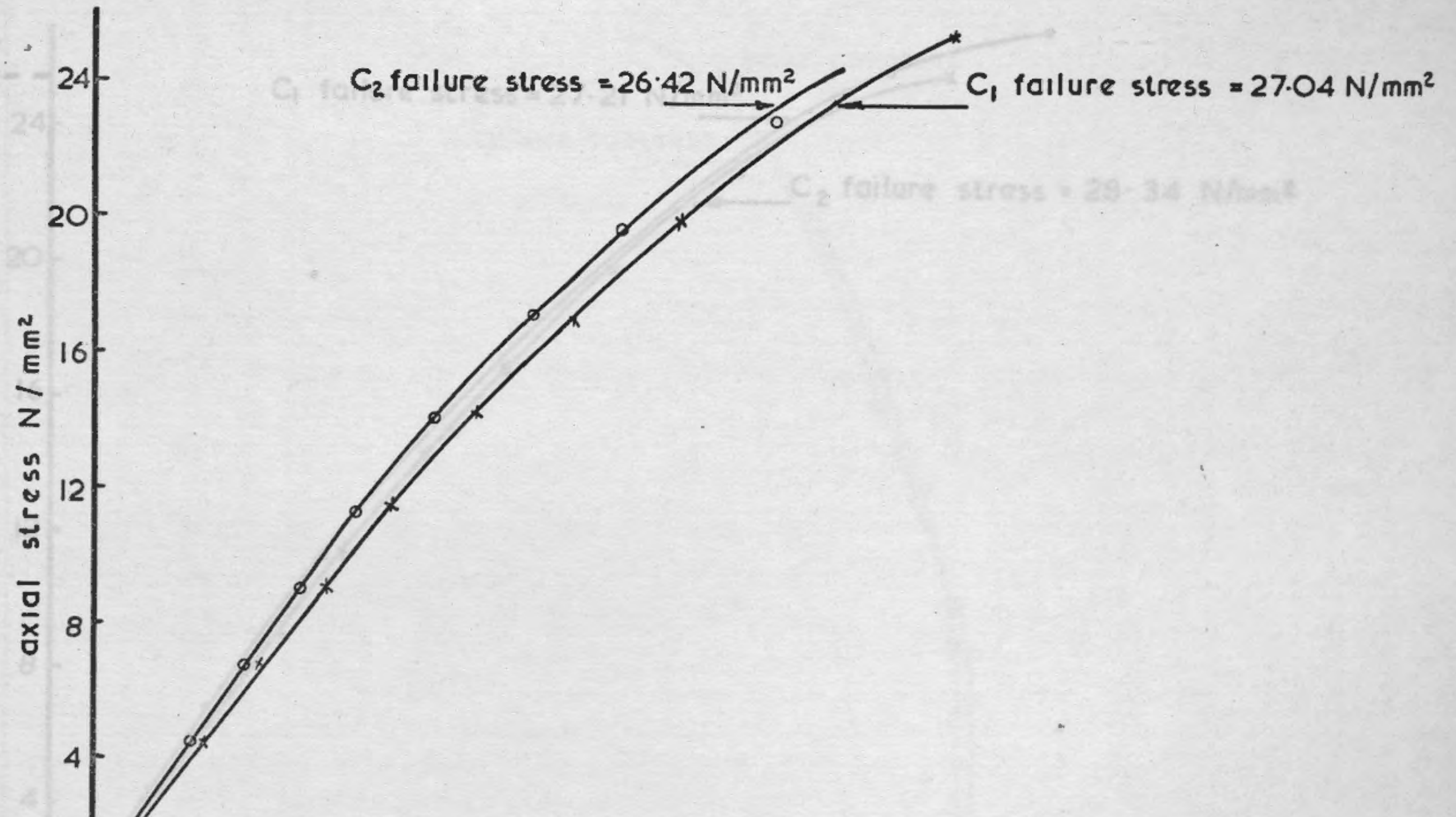

Fig 3.2 . 6a. Axial stress v. longitudinal strain measured on cylinders for column concrete by electrical resistance strain gauges.

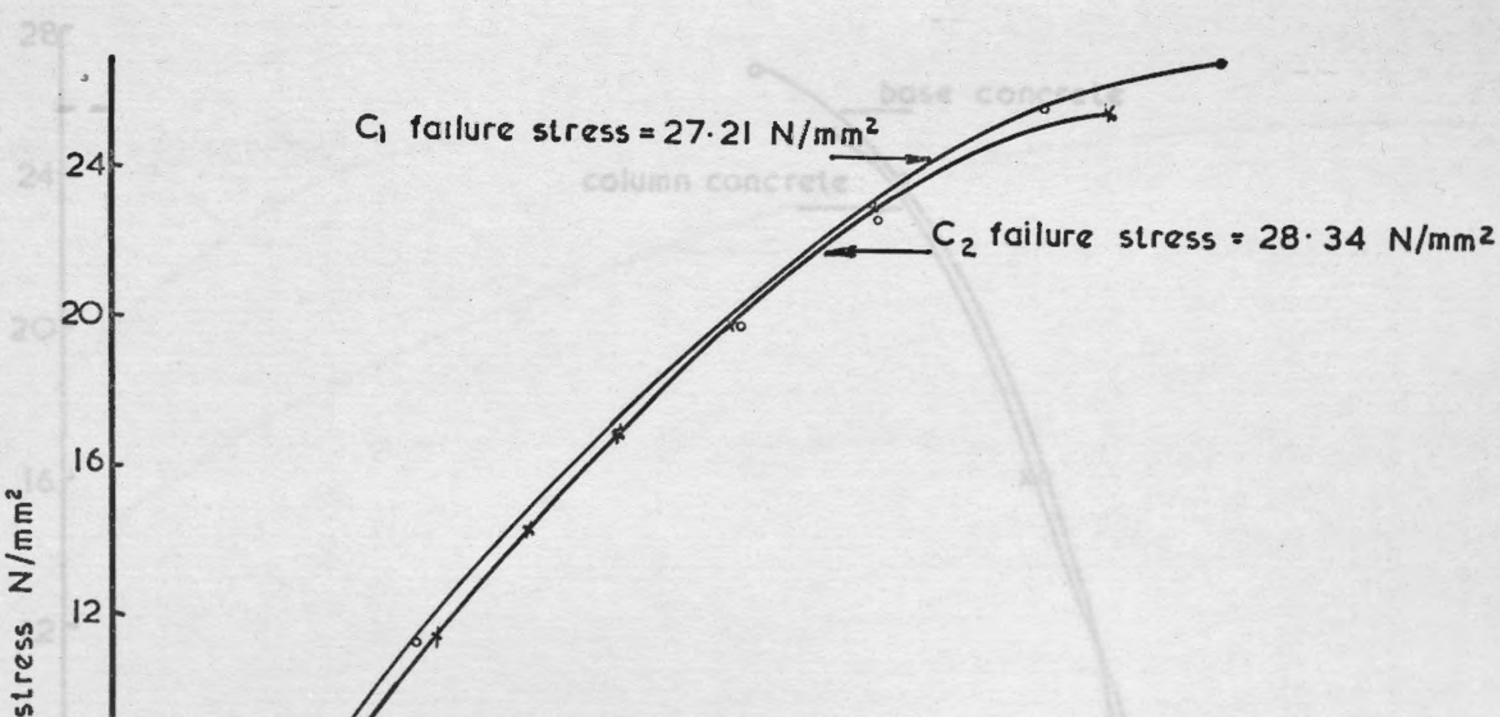

Fig. 3.2 . 6b. Axial stress v. longitudinal strain measured on cylinders for base concrete by electrical resistance strain gauges .

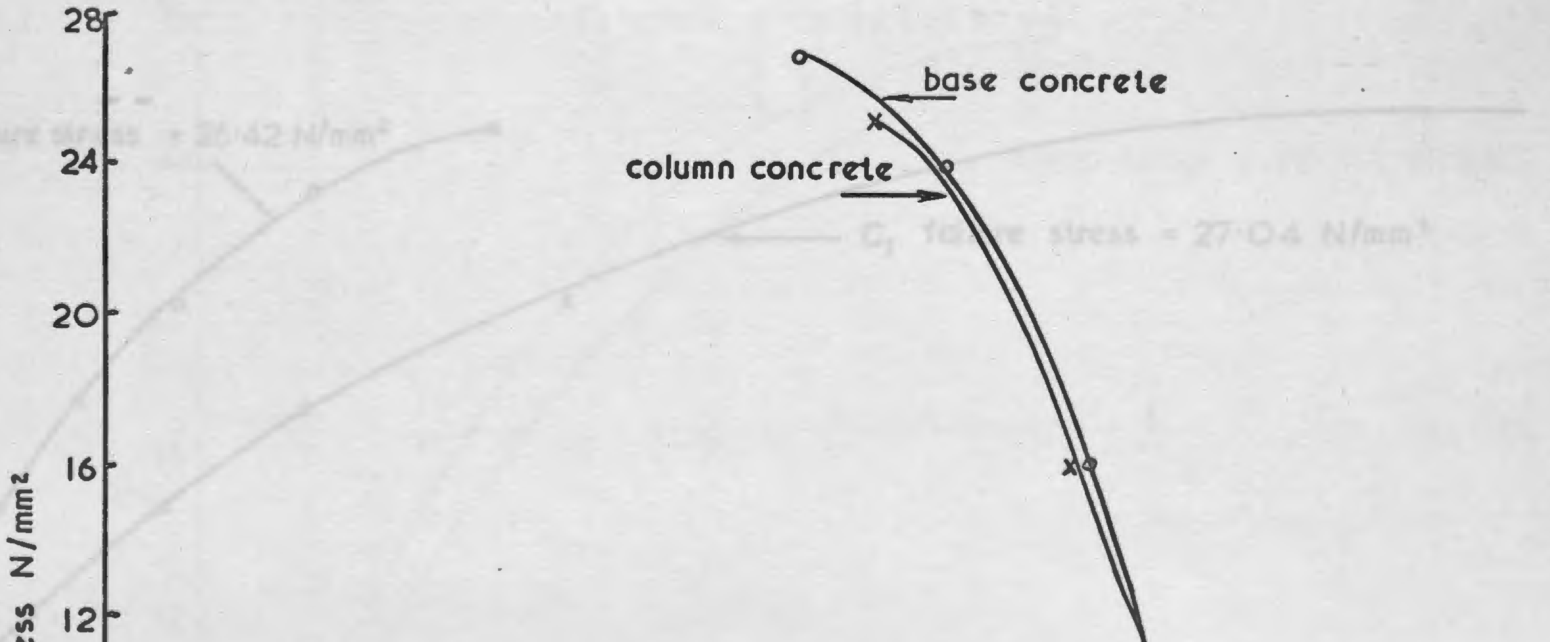

Fig. 3.2. 6c Axial stress v. Modulus of elasticity for column concrete and for base concrete

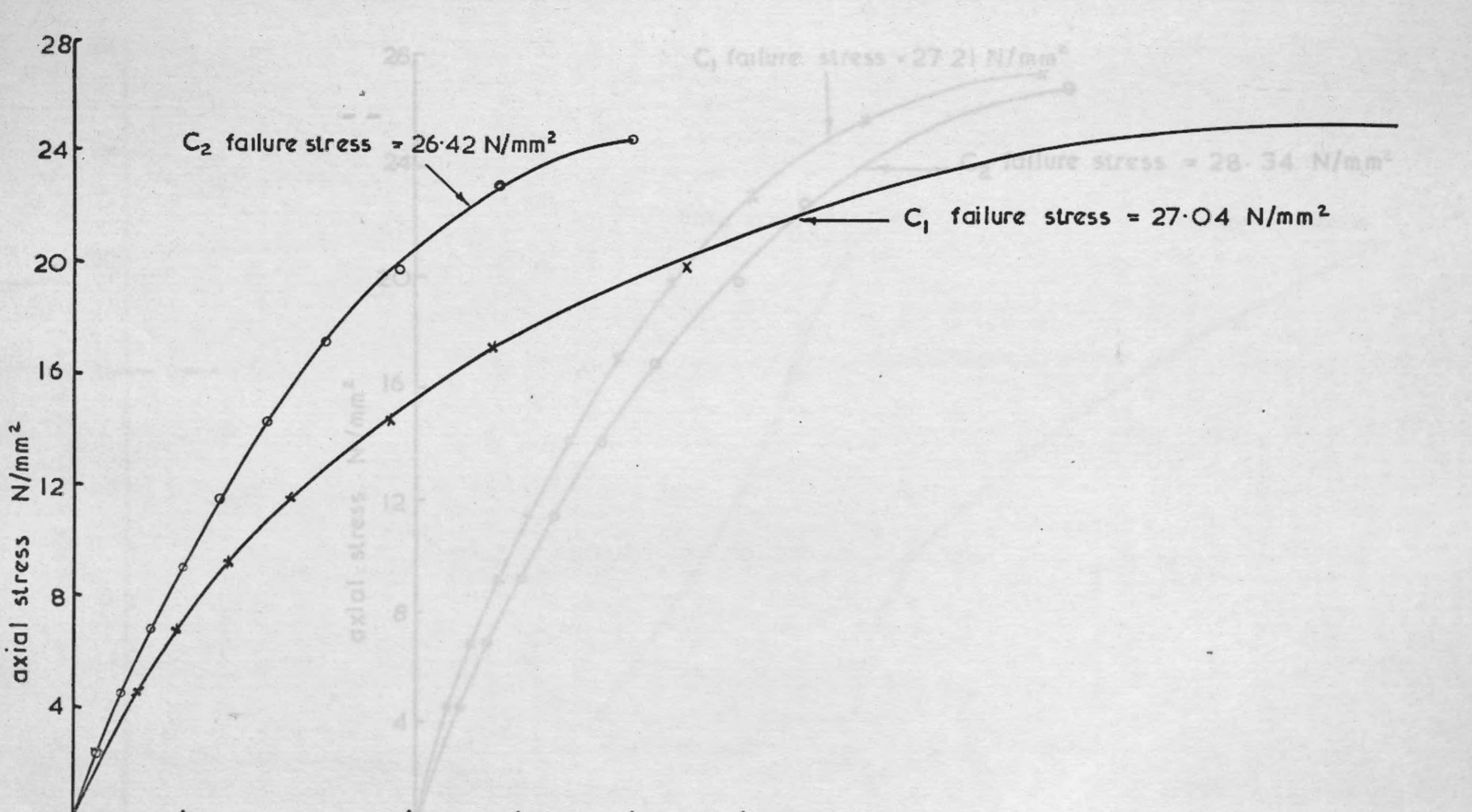

Fig. 3.2. 6d. Axial stress v. lateral strain measured on cylinders for column concrete by electrical resistance strain gauges

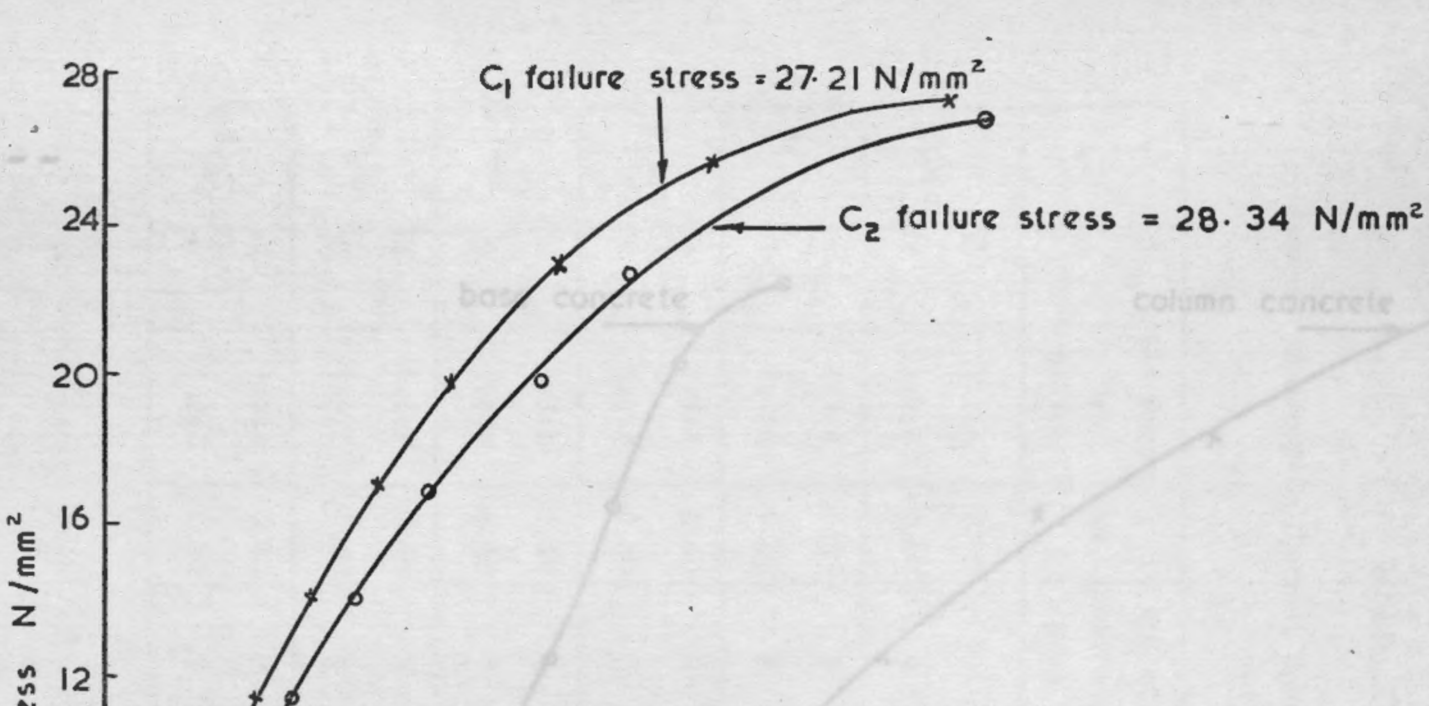

Fig.3.2. 6e Axial stress v. lateral strain measured on cylinders for base concrete by electrical resistance strain gauges.

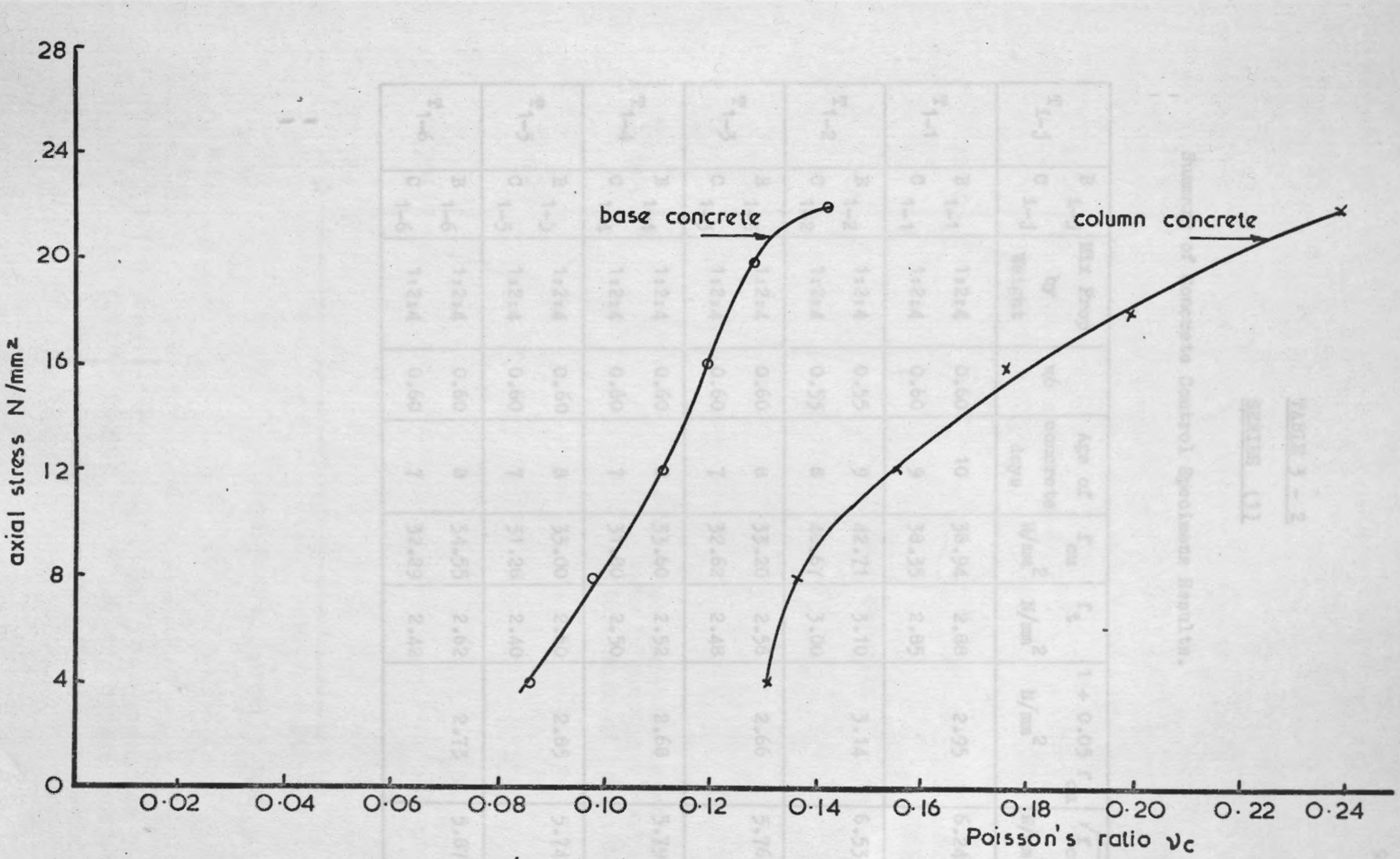

Fig. 3. 2. 6f   Axial stress v. Poisson's ratio ν_c for column concrete and base concrete

TABLE 3 - 2

SERIES (1)

Summary of Concrete Control Specimens Results.

T_{i-j}	B_{i-j} / C_{i-j}	Mix Prop. by Weight	w/c	Age of concrete days	f_{cu} N/mm^2	f_t N/mm^2	$1 + 0.05 f_{cu}$ N/mm^2	$\sqrt{f_{cu}}$ N/mm^2
T_{1-1}	B_{1-1}	1:2:4	0.60	10	38.94	2.88	2.95	6.240
	C_{1-1}	1:2:4	0.60	9	38.35	2.85		
T_{1-2}	B_{1-2}	1:2:4	0.55	9	42.71	3.10	3.14	6.535
	C_{1-2}	1:2:4	0.55	8	40.67	3.00		
T_{1-3}	B_{1-3}	1:2:4	0.60	8	33.20	2.56	2.66	5.762
	C_{1-3}	1:2:4	0.60	7	32.62	2.48		
T_{1-4}	B_{1-4}	1:2:4	0.60	8	33.60	2.52	2.68	5.797
	C_{1-4}	1:2:4	0.60	7	31.80	2.50		
T_{1-5}	B_{1-5}	1:2:4	0.60	8	33.00	2.60	2.85	5.745
	C_{1-5}	1:2:4	0.60	7	31.28	2.40		
T_{1-6}	B_{1-6}	1:2:4	0.60	8	34.55	2.62	2.73	5.878
	C_{1-6}	1:2:4	0.60	7	32.29	2.42		

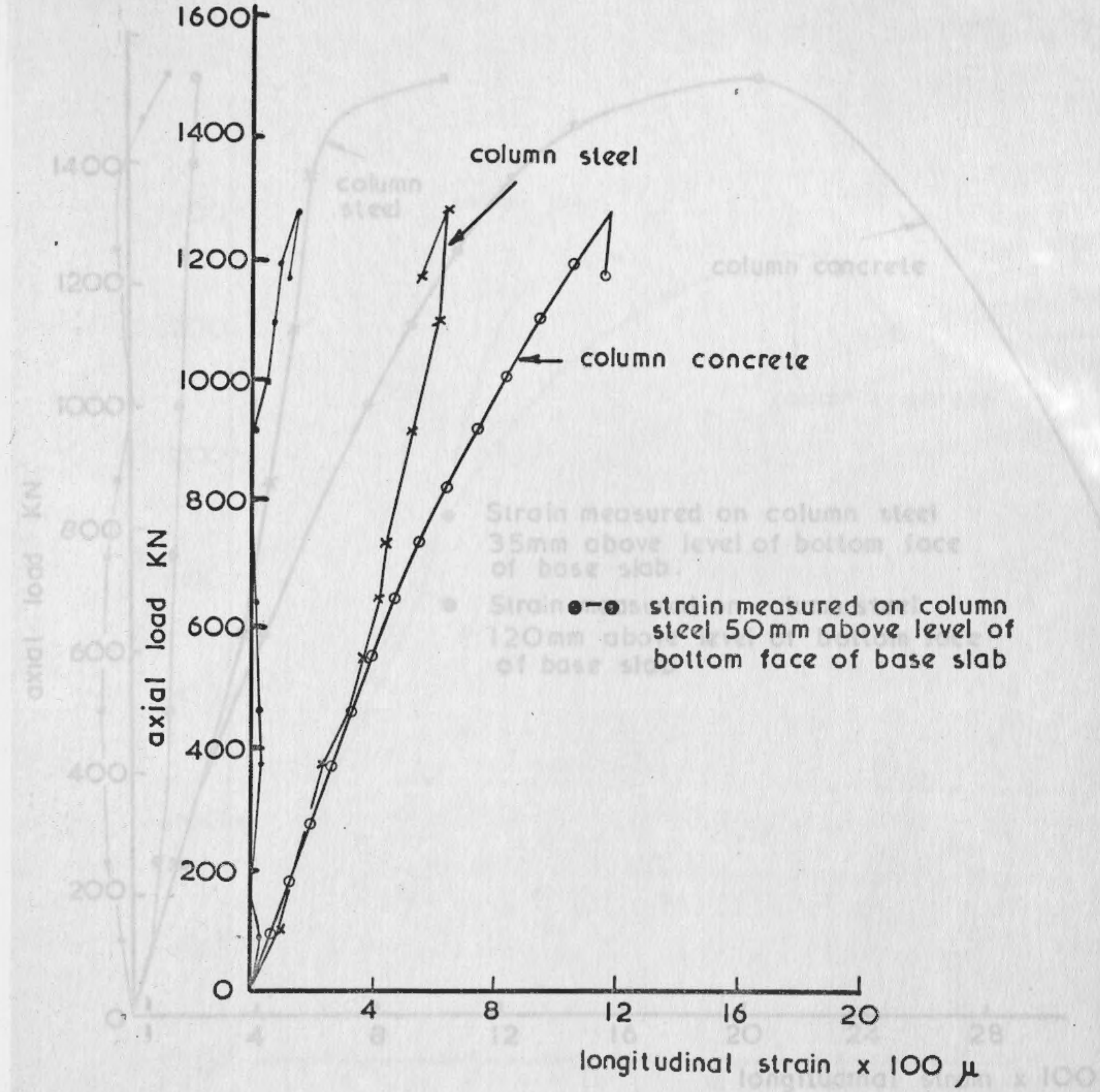

Fig. 3.3·1 Axial load v. longitudinal strain measured on column concrete by 8" demec gauges and on column steel by electrical resistance strain gauges (T_{1-1})

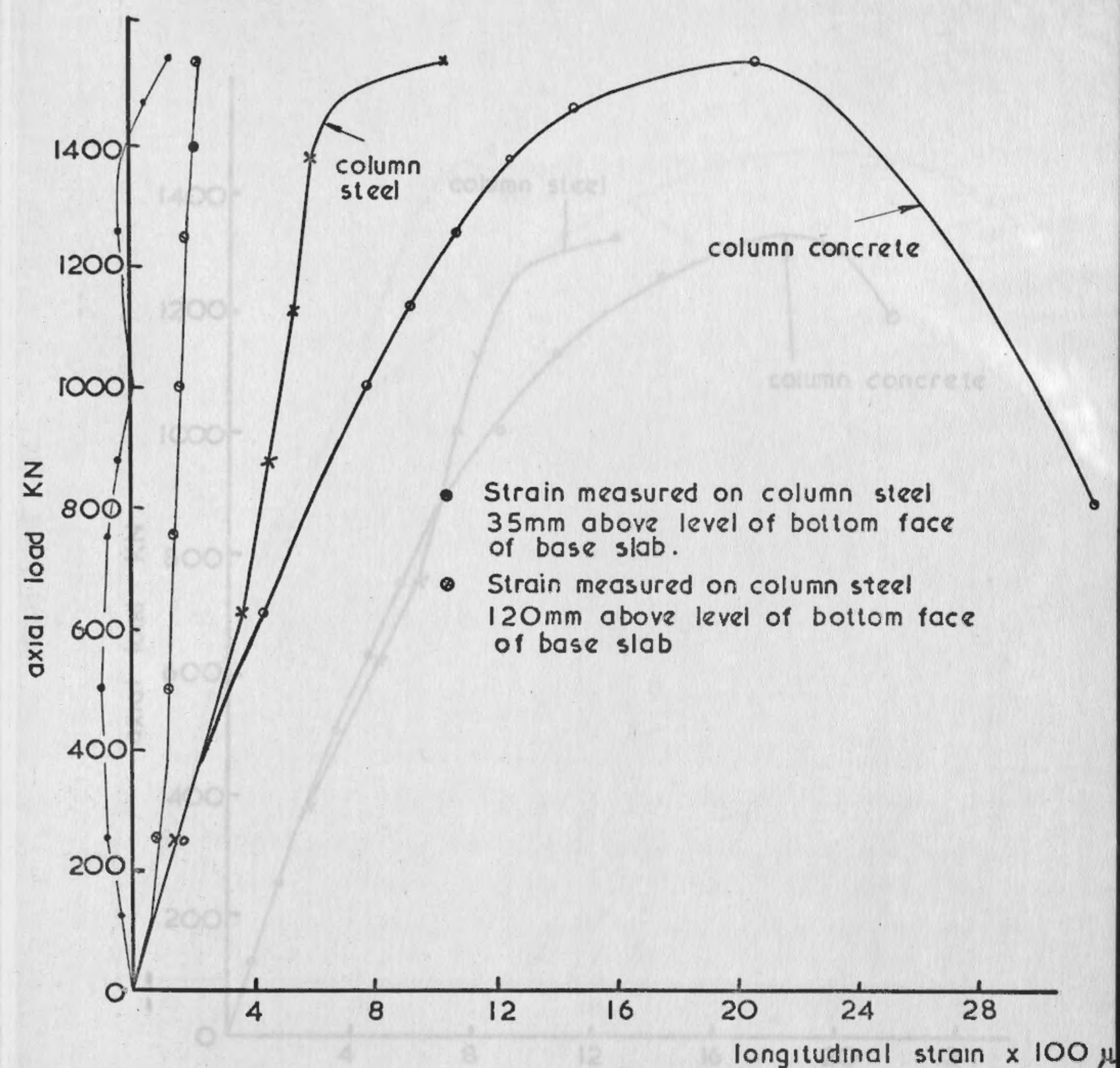

Fig. 3.3.2 Axial load v. longitudinal strain measured on column concrete by 8" demec gauges and on column steel by electrical resistance strain gauges (T_{1}-2)

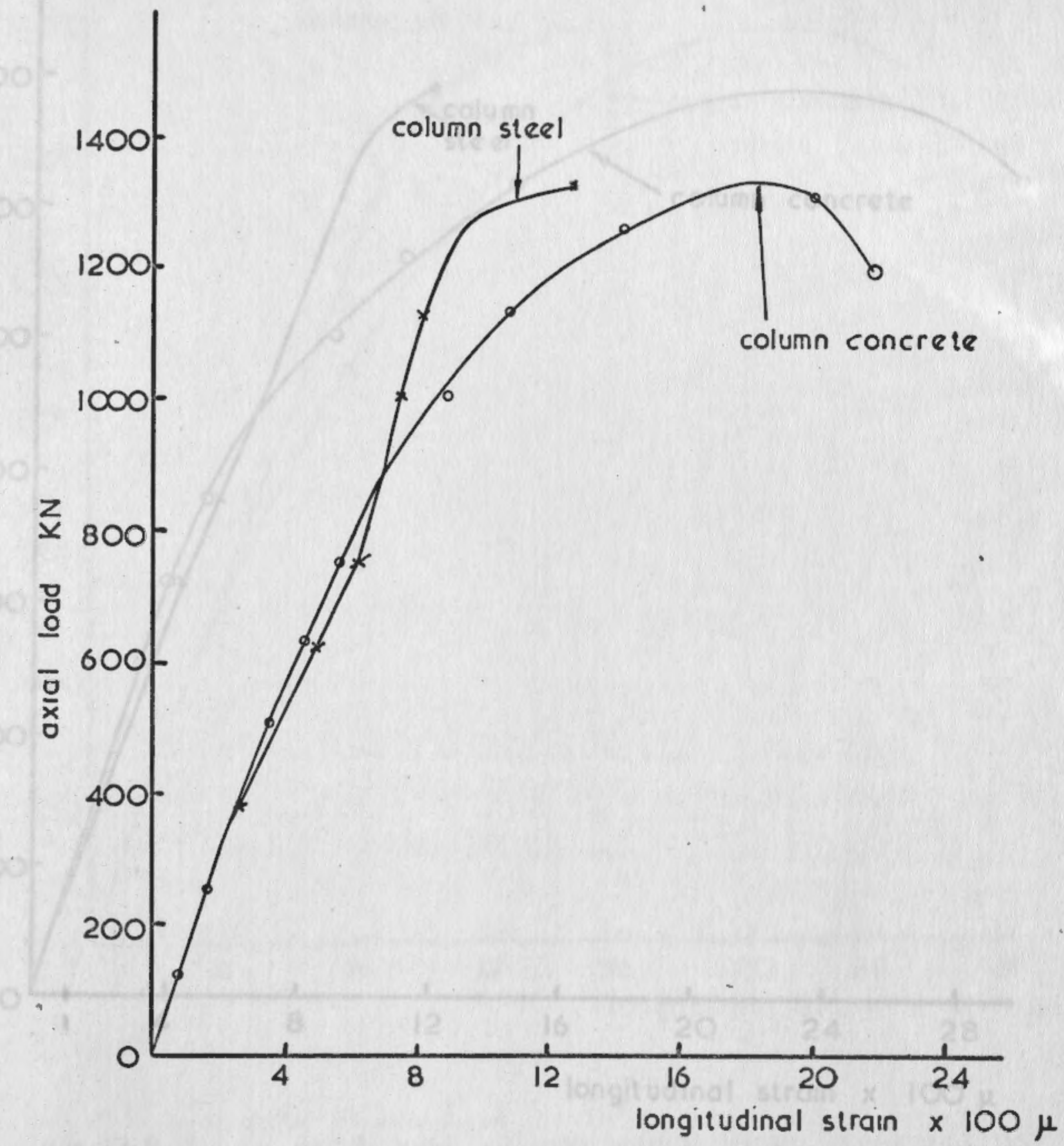

Fig. 3·3·3 Axial load v. longitudinal strain measured on column concrete by 8" demec gauges and on column steel by electrical resistance strain gauges (T_1 - 3)

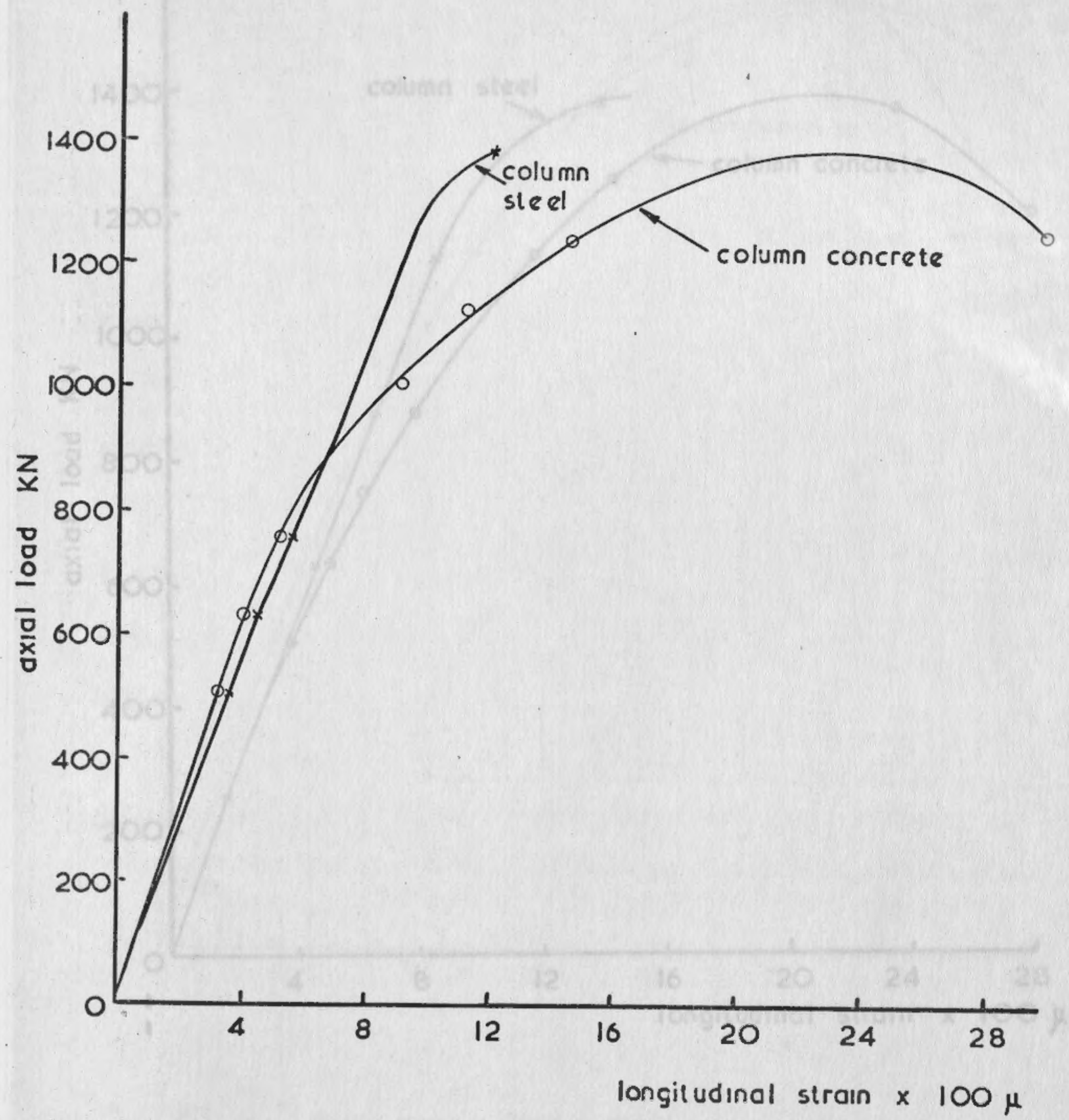

Fig. 3.3 . 4 Axial load v longitudinal strain measured on column concrete by 8 " demec gauges and on column steel by electrical resistance strain gauges (T_{1}-4)

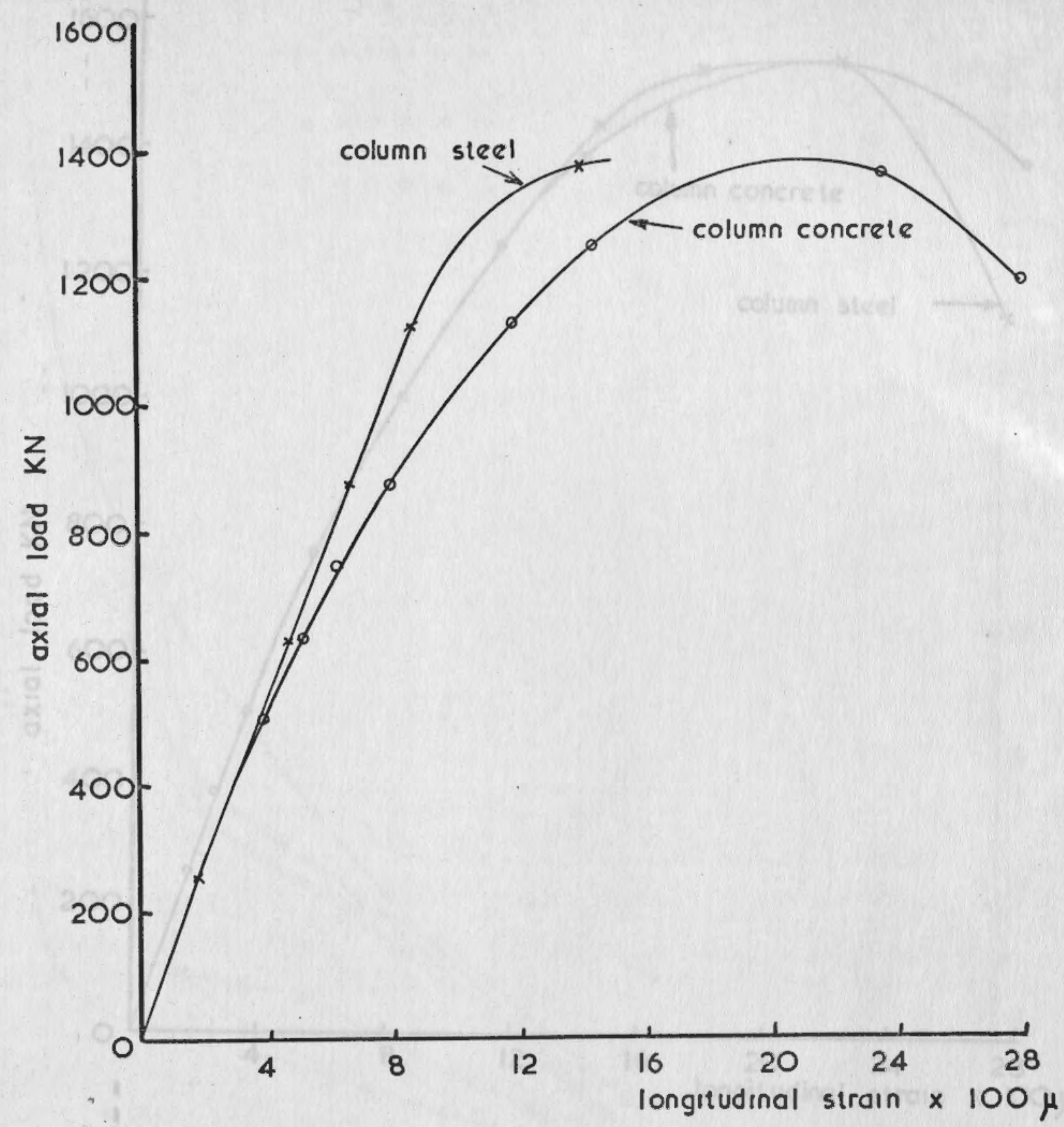

Fig. 3.3.5 Axail load v. longitudinal strain measured on column concrete by 8" demec gauges and on column steel by electrical resistance strain gauges (T1-5)

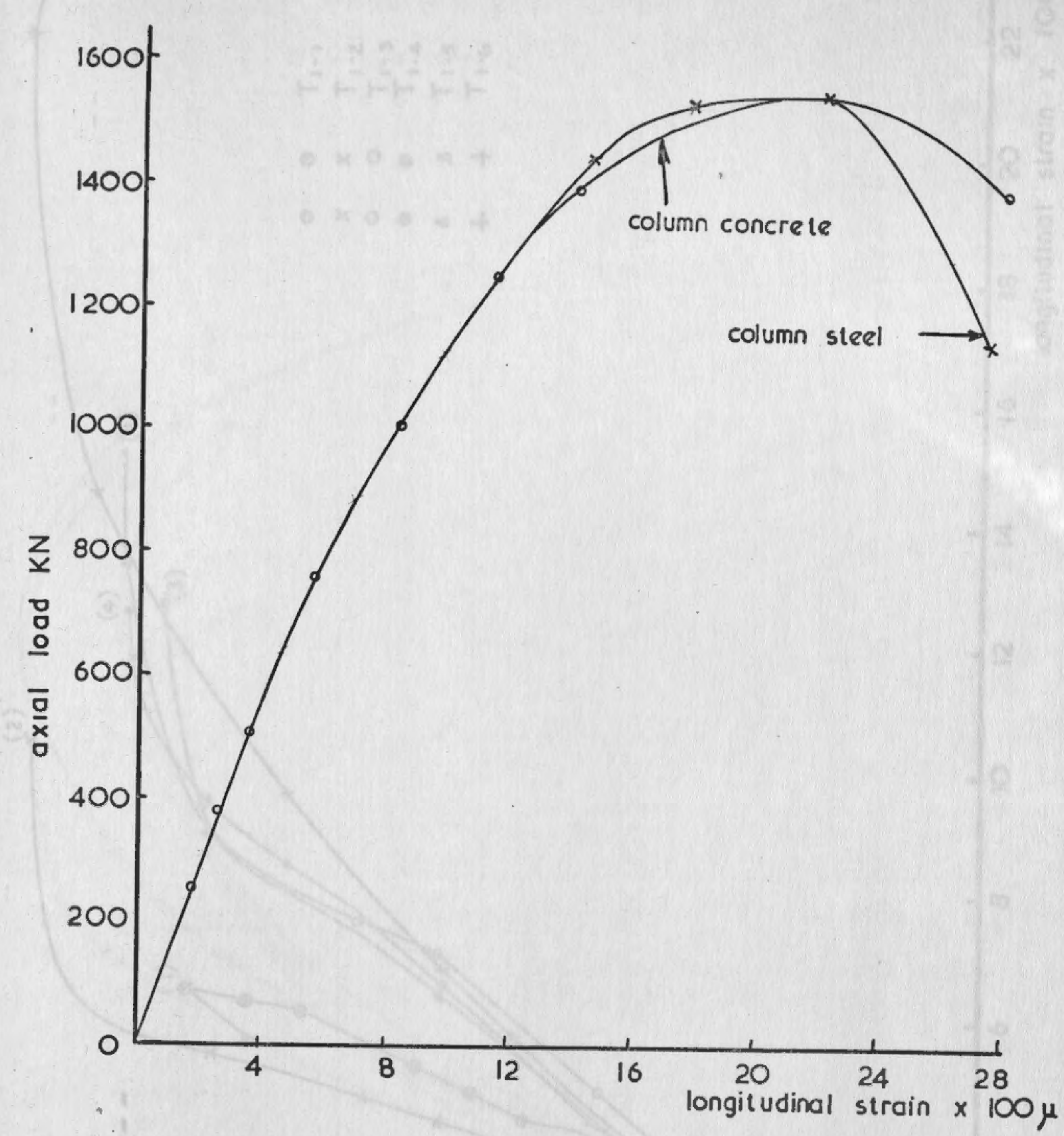

Fig. 3.3.6 Axial load v longitudinal strain measured on column concrete by 8" demec gauges and on column steel by electrical resistance strain gauges
(T1-6)

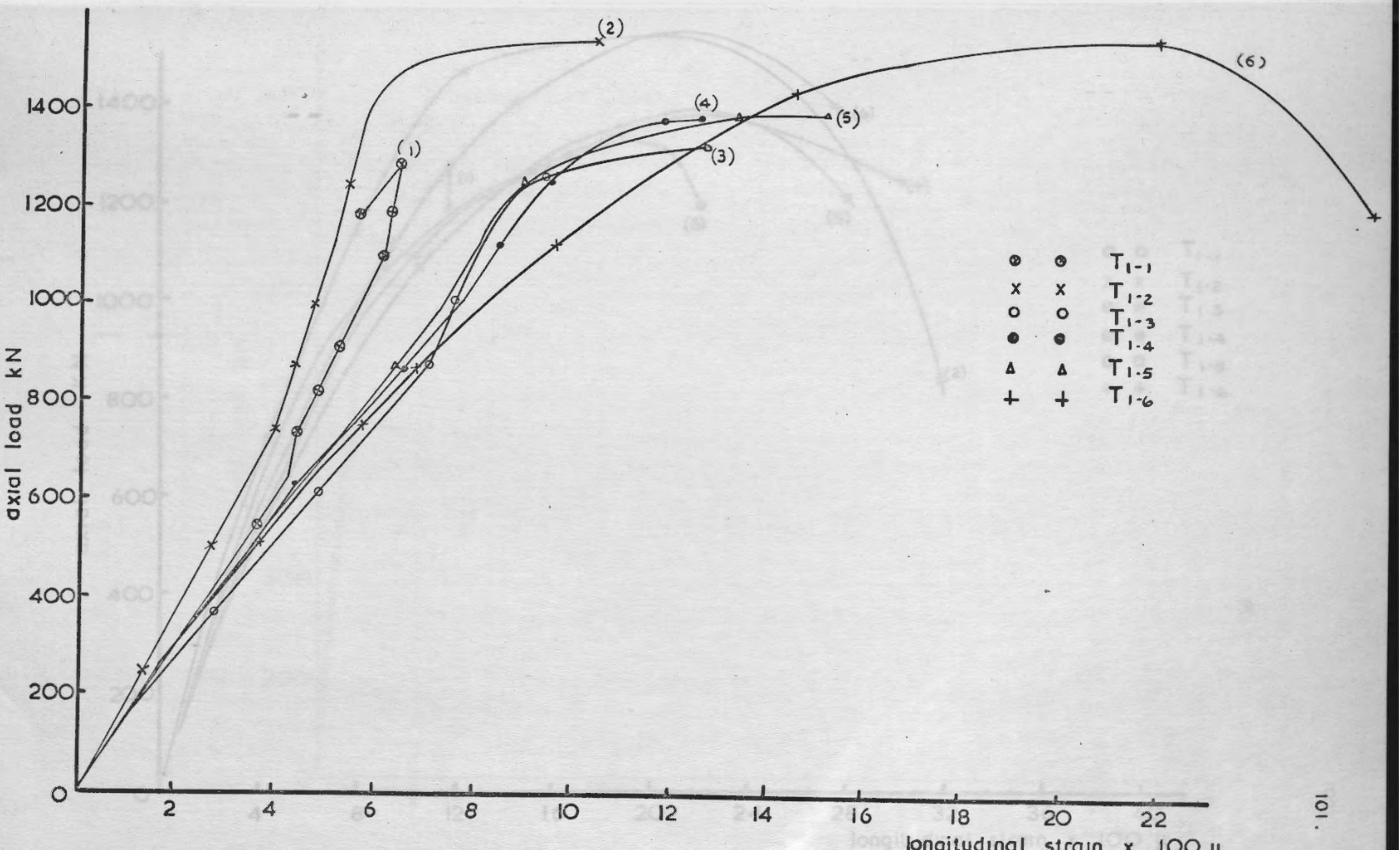

Fig 3. 3. a. Axial load v. longitudinal strain measured on column steel by electrical resistance strain gauges. for series (I.) specimens

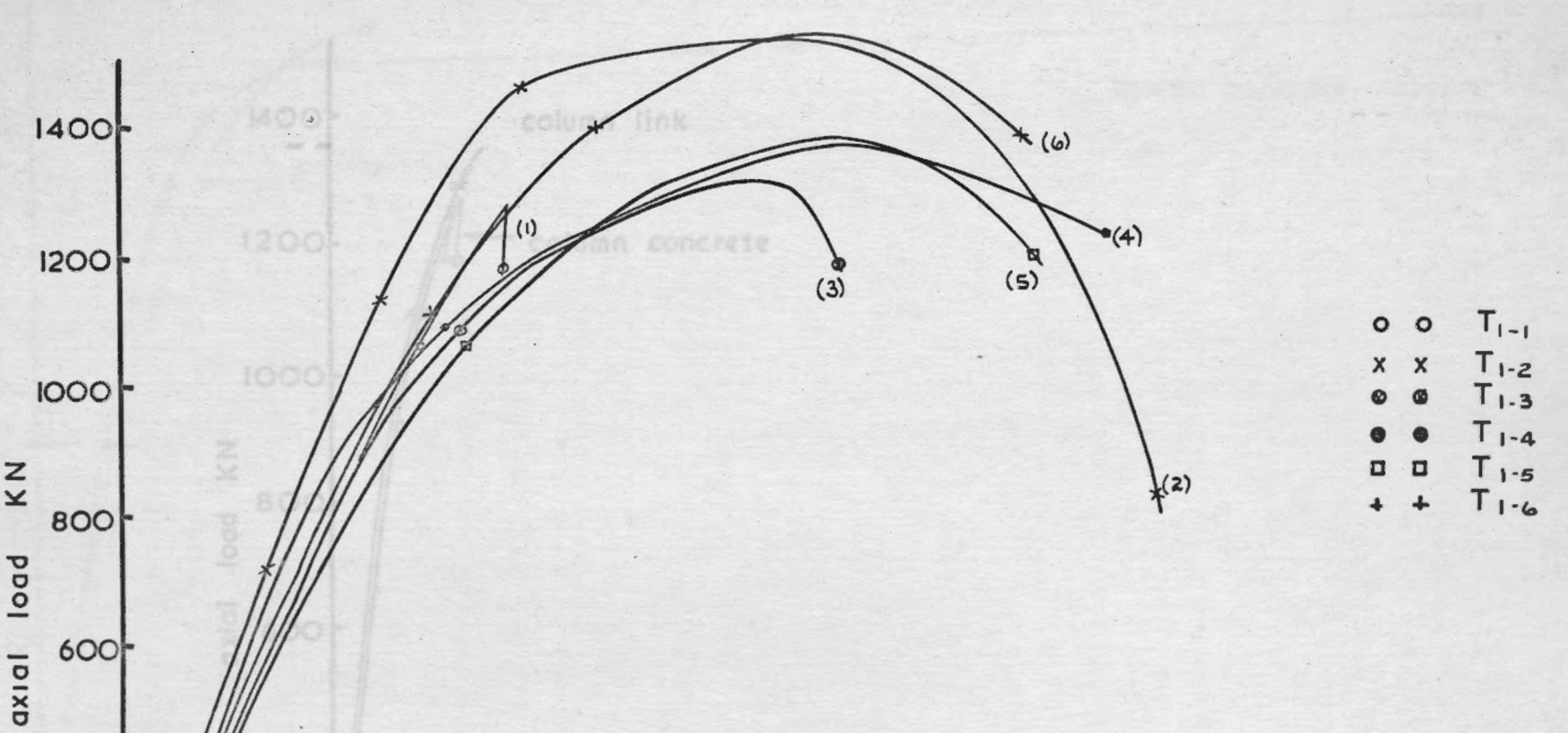

Fig 3.3. b Axial load v. longitudinal strain measured on column concrete by 8" demec gauges for series (1) specimens

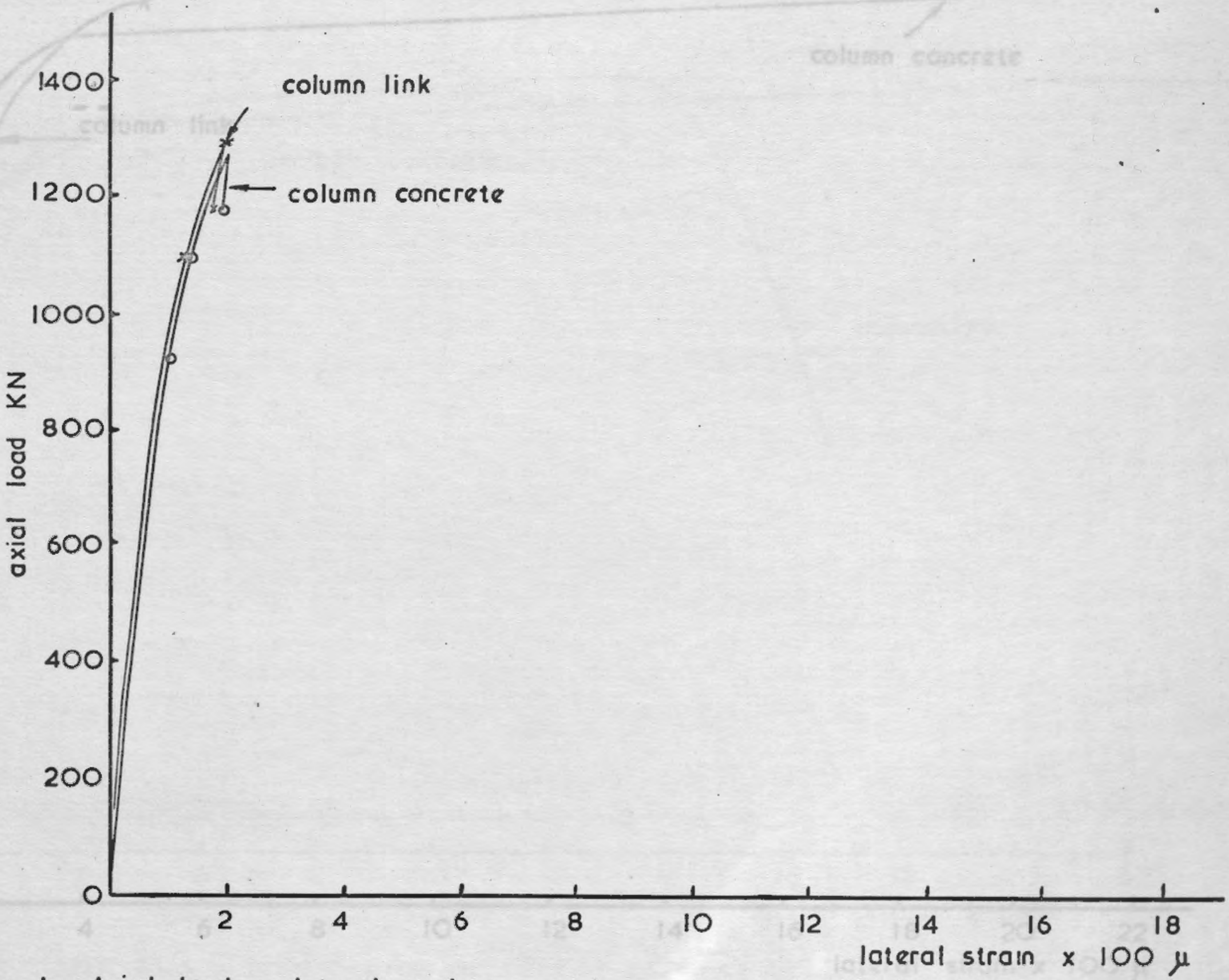

Fig. 3.4.1 Axial load v. lateral strain measured on column concrete by 6" demec gauges and on column links by electrical resistance strain gauges (T 1·1)

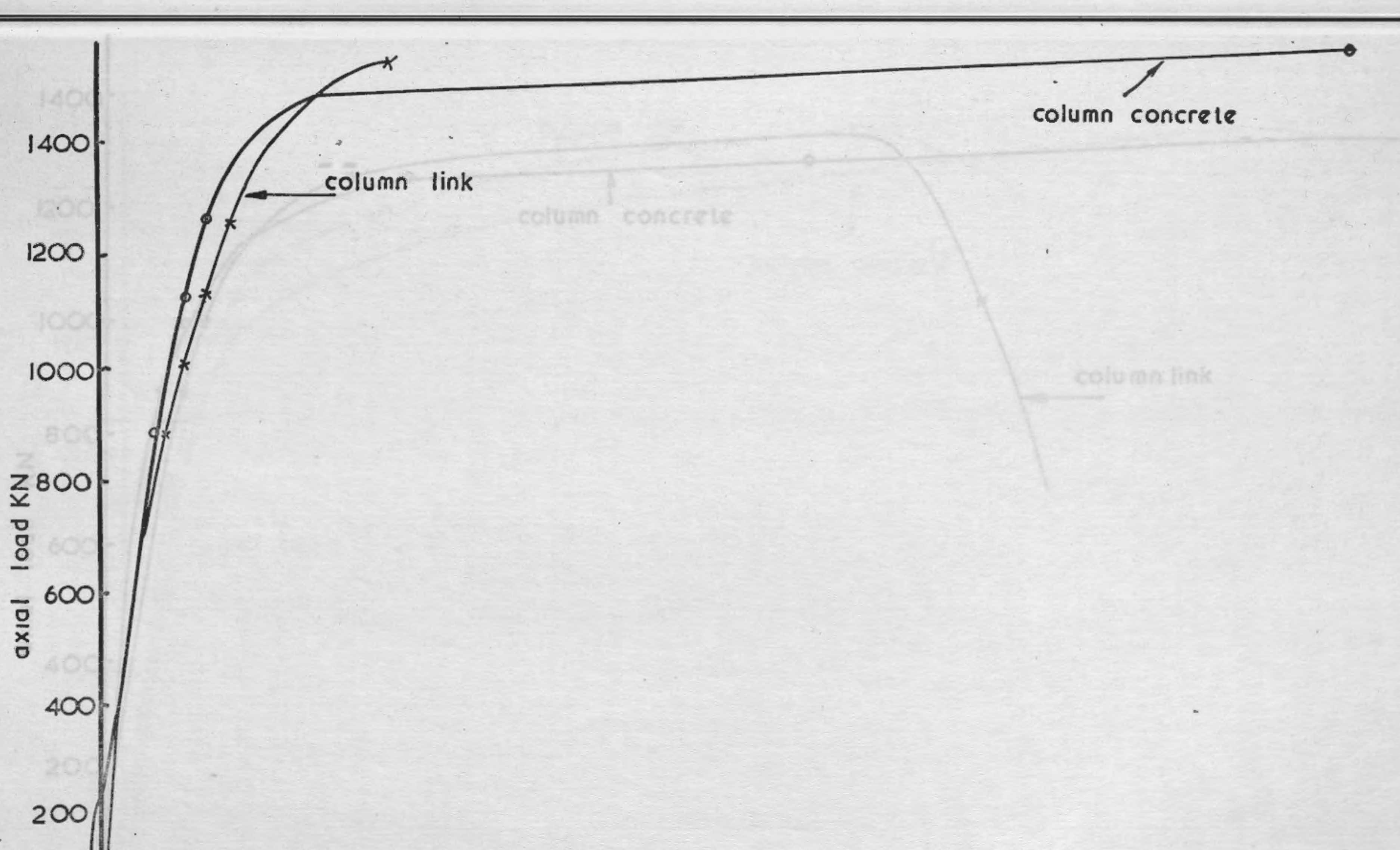

Fig. 3.4.2. Axial load v. lateral strain measured on column concrete by 6" demec gauges and on column links by electrical resistance strain gauges (T_{1-2})

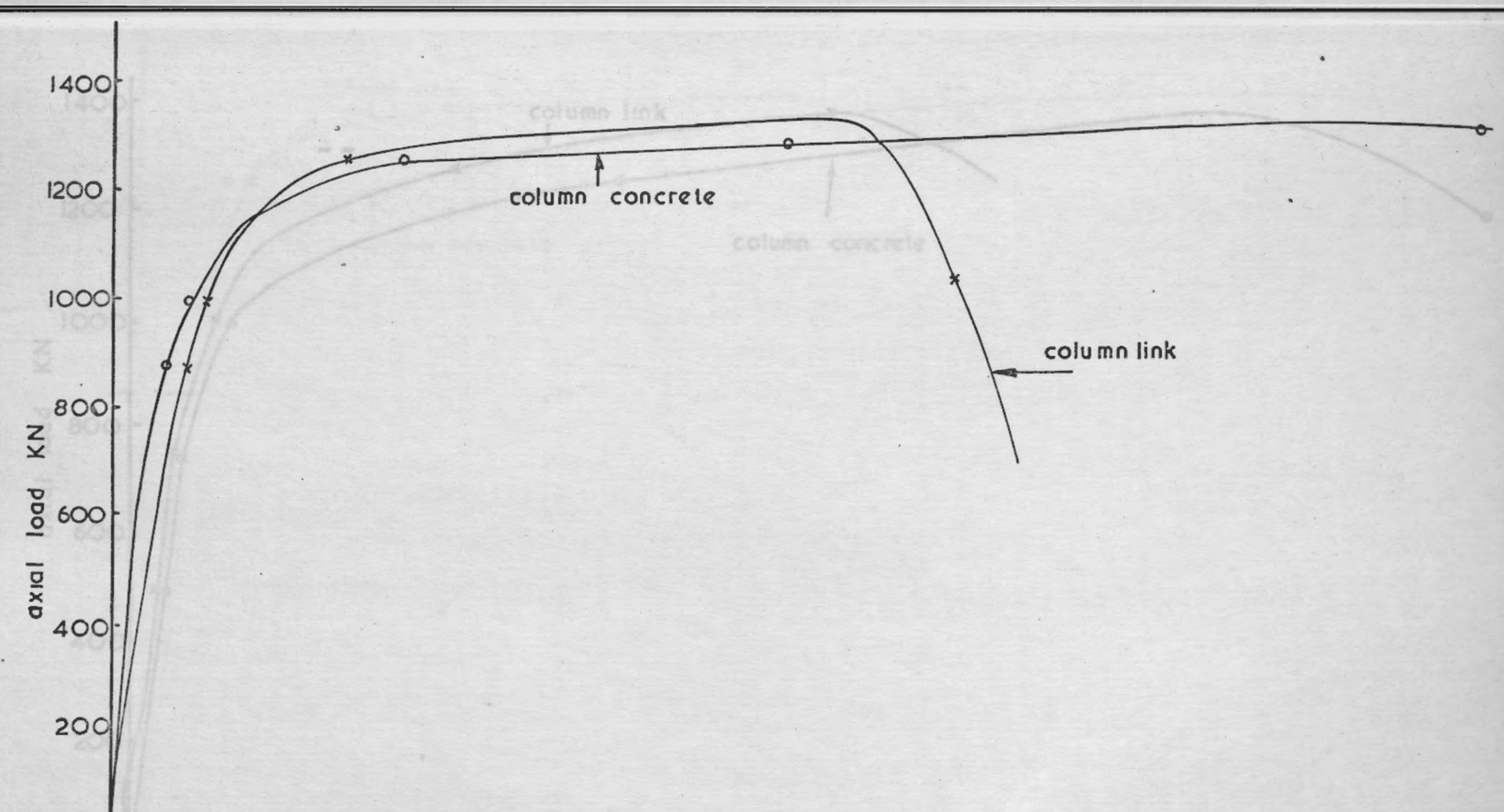

Fig. 3.4. 3 Axial load v. lateral strain measured on column concrete by 6" demec gauges and on column links by electrical resistance strain gauges (T_{1-3})

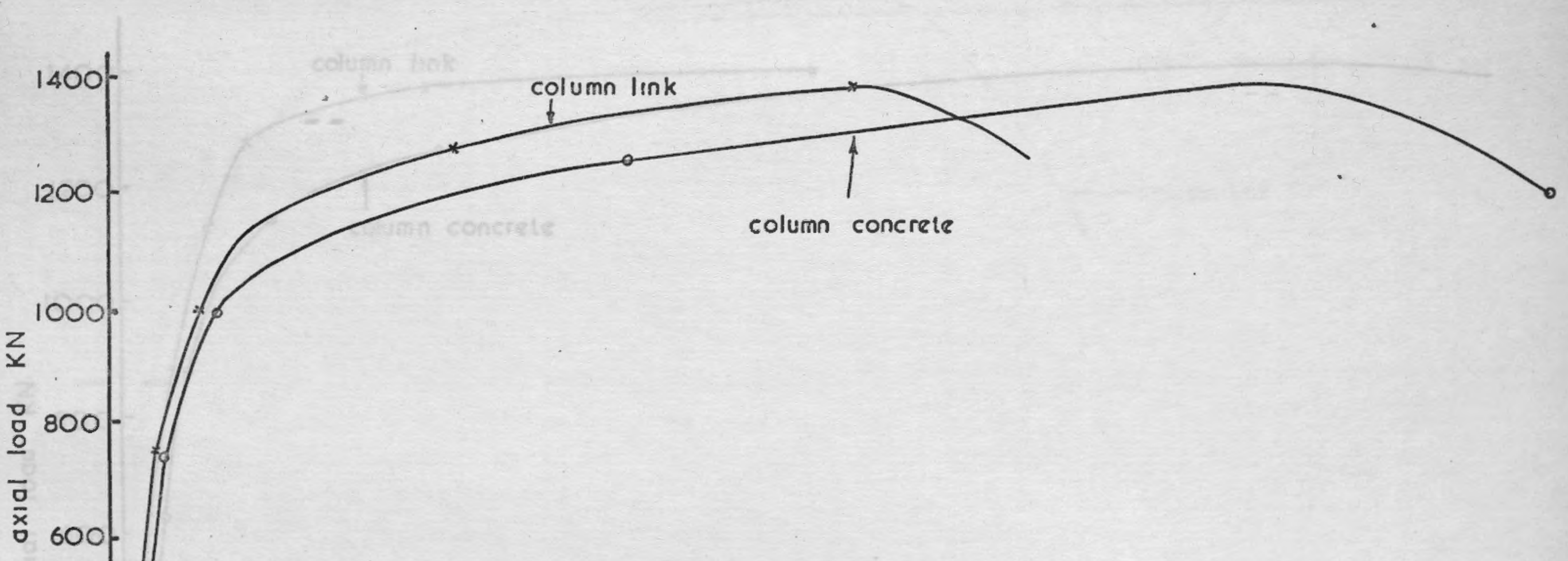

Fig. 3.4 · 4 Axial load v. lateral strain measured on column concrete by 6" demec gauges and on column links by electrical resistance strain gauges (T1-4)

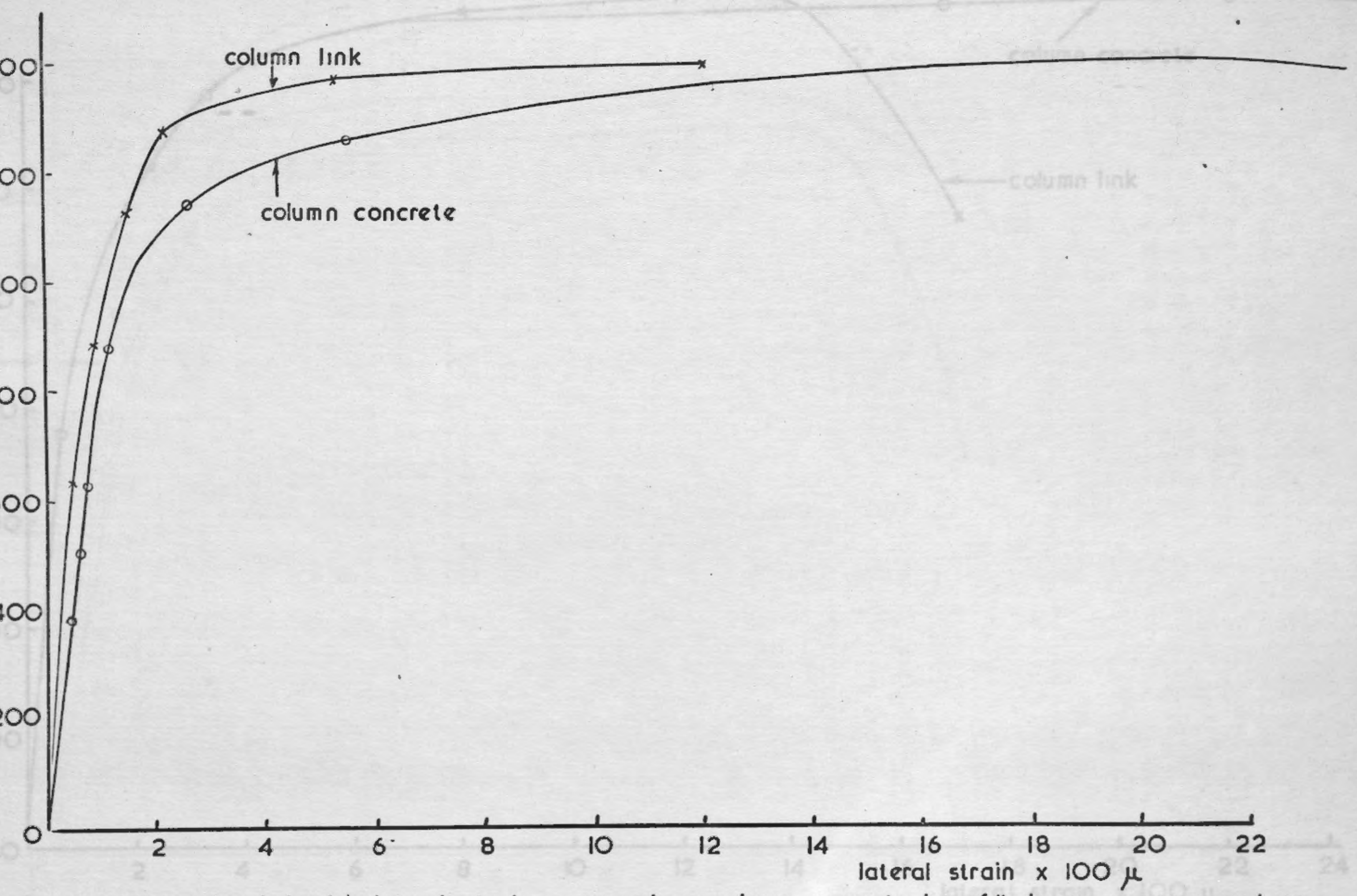

Fig. 3.4 · 5 Axial load v lateral strain measured on column concrete by 6" demec gauges and on column links by electrical resistance strain gauges ($T_{1,5}$)

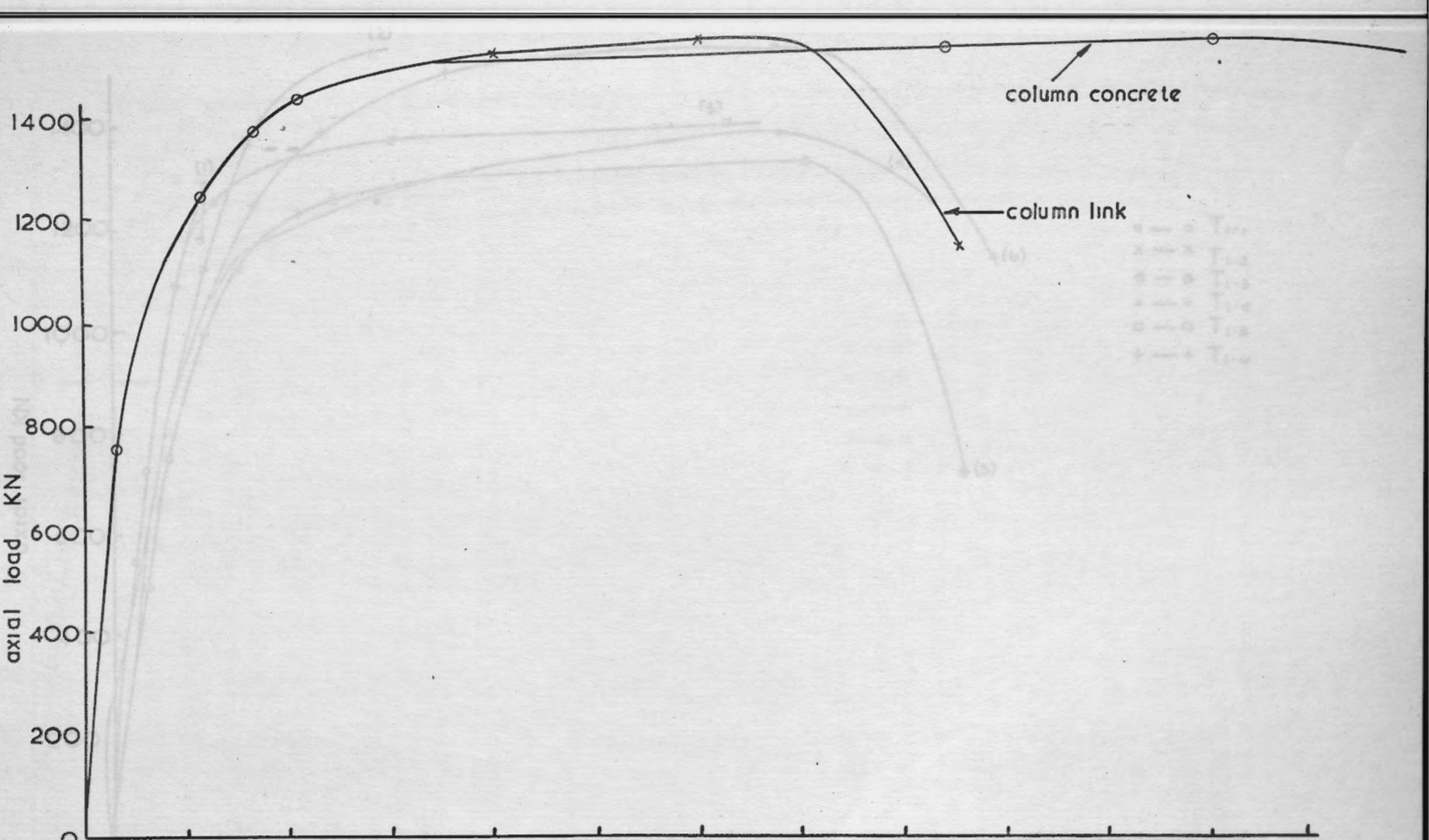

Fig. 3.4. 6 Axial load v lateral strain measured on column concrete by 6" demec gauges and on column links by electrical resistance strain gauges (T_{1-6})

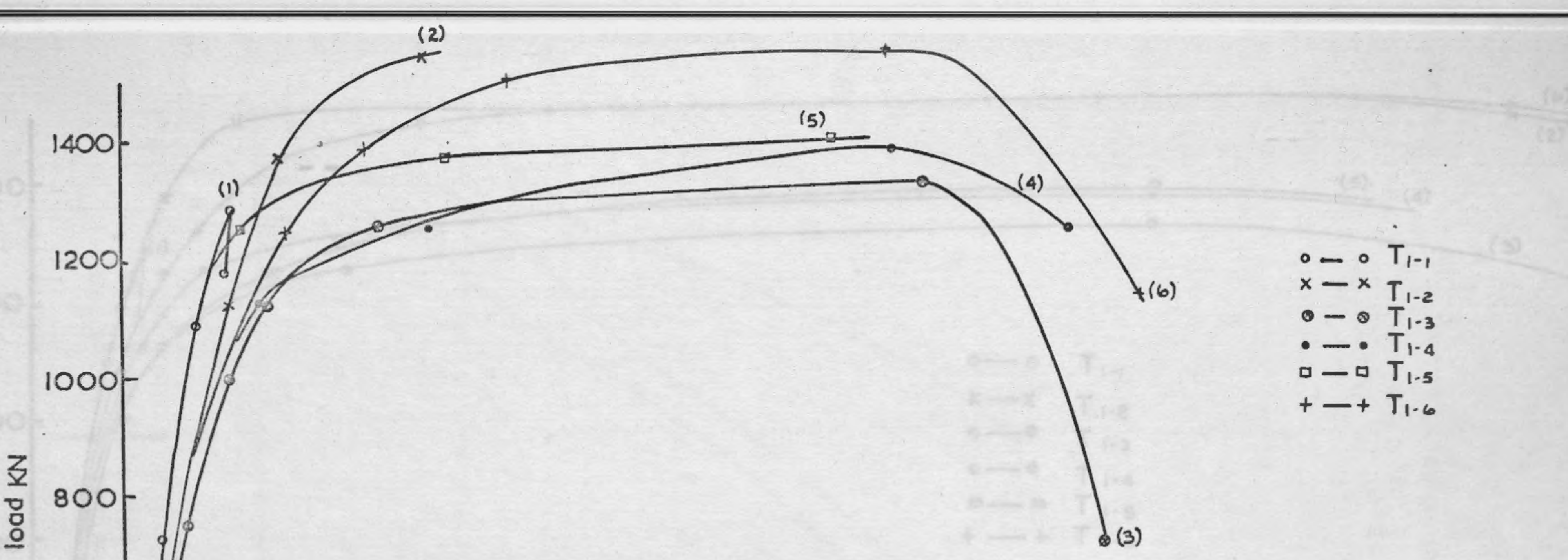

Fig 3.4 .a Axial load v lateral strain measured on column links by electrical resistance strain gauges for series (1) specimens

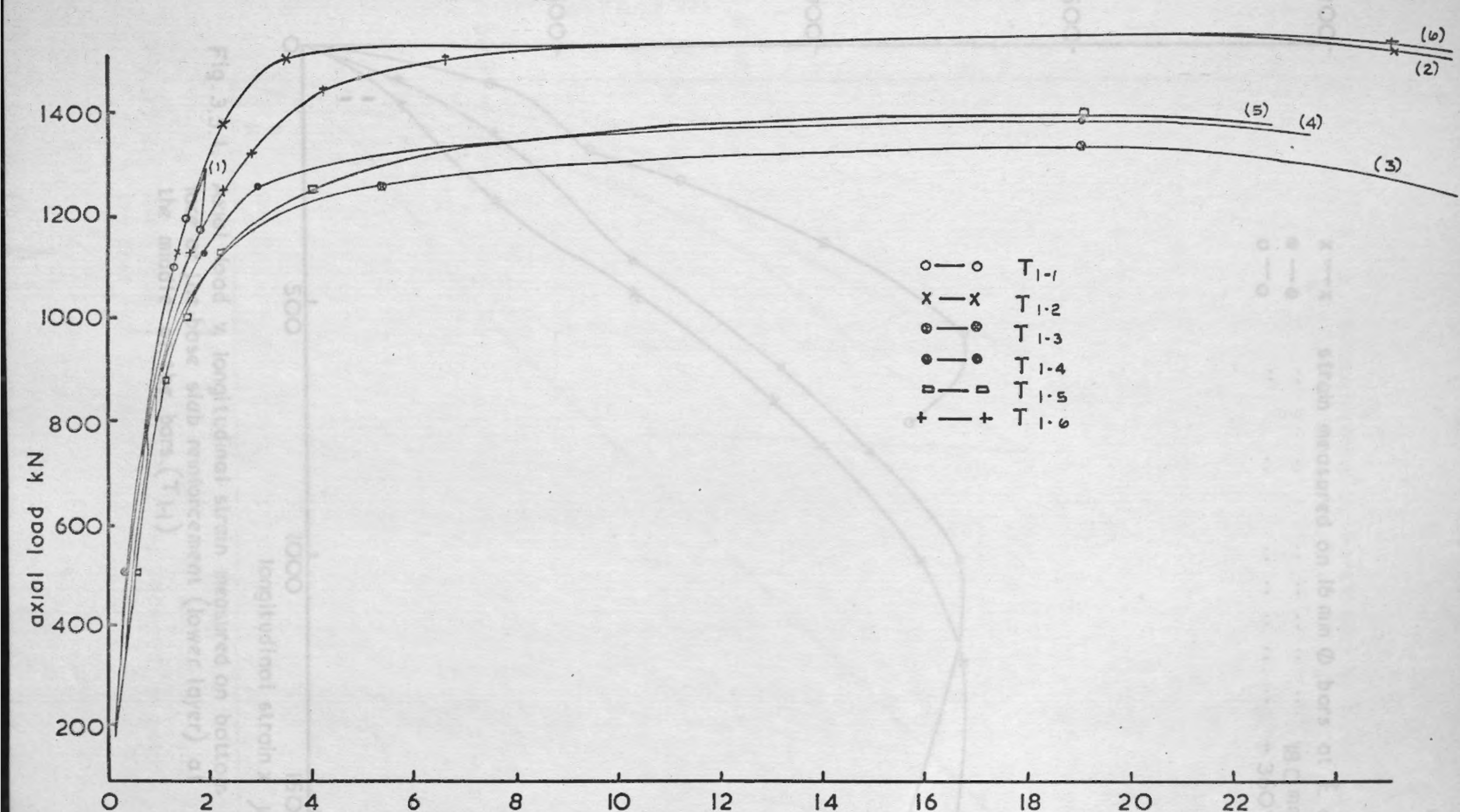

Fig. 3.4. b. Axial load v. lateral strain measured on column concrete by 6" demec gauges or series(1) specimens

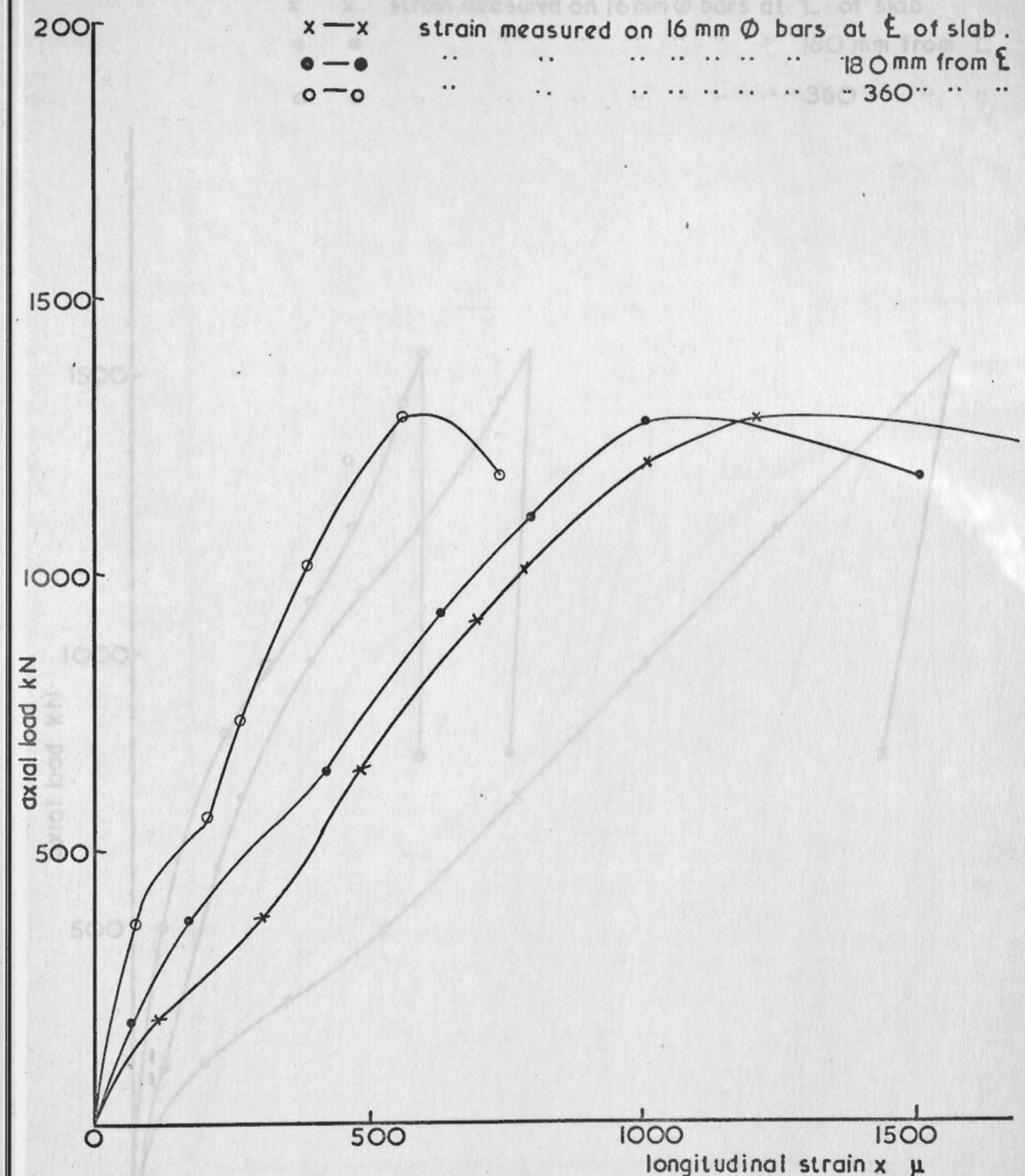

Fig. 3.5.1. Axial load v. longitudinal strain measured on bottom face of the base slab reinforcement (lower layer) at the middle of the bars. (T 1-1)

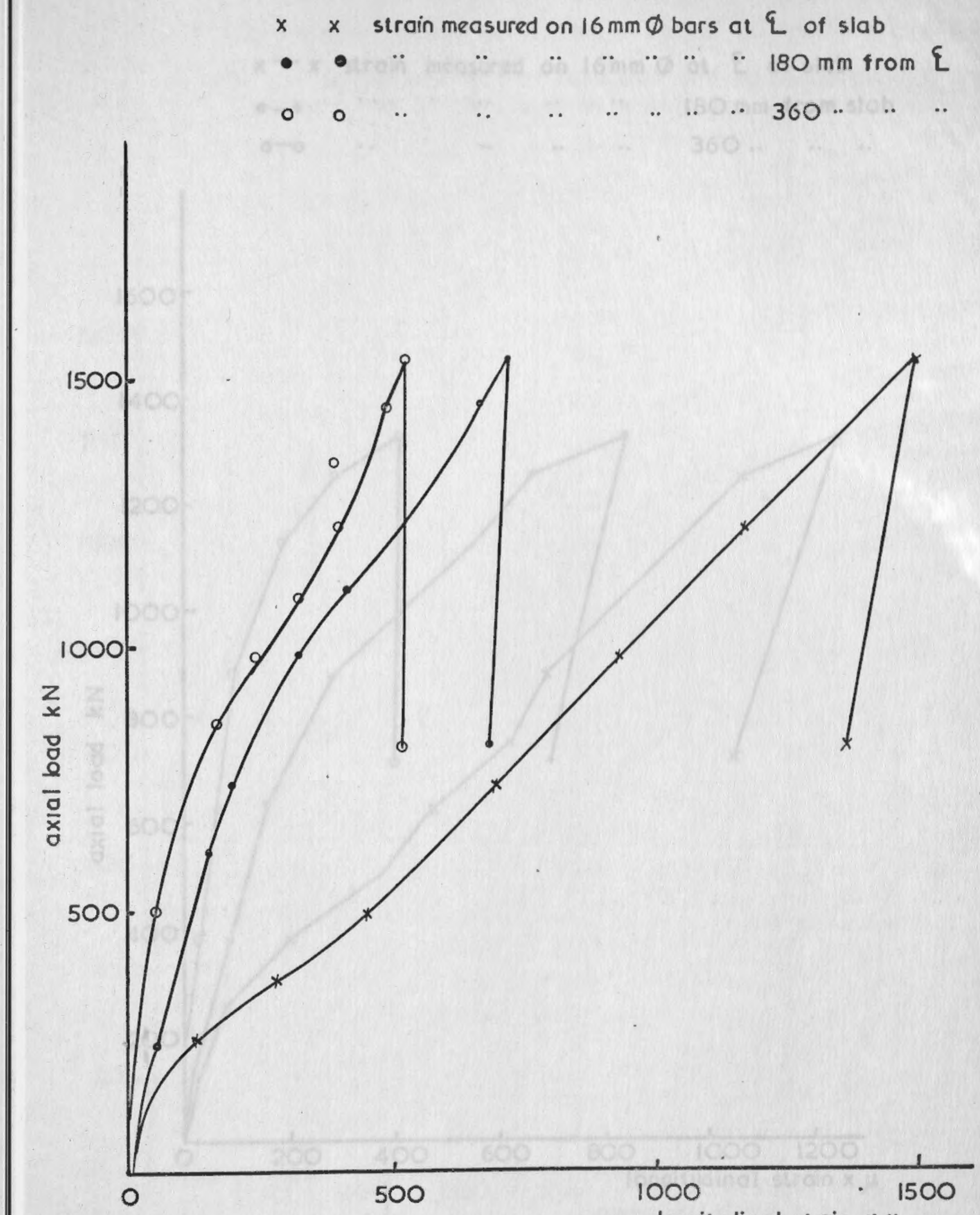

Fig. 3.5.2. Axial load v longitudinal strains measured on bottom face of the base slab reinforcement (lower layer) at the middle of bars. ($T_{1\cdot2}$)

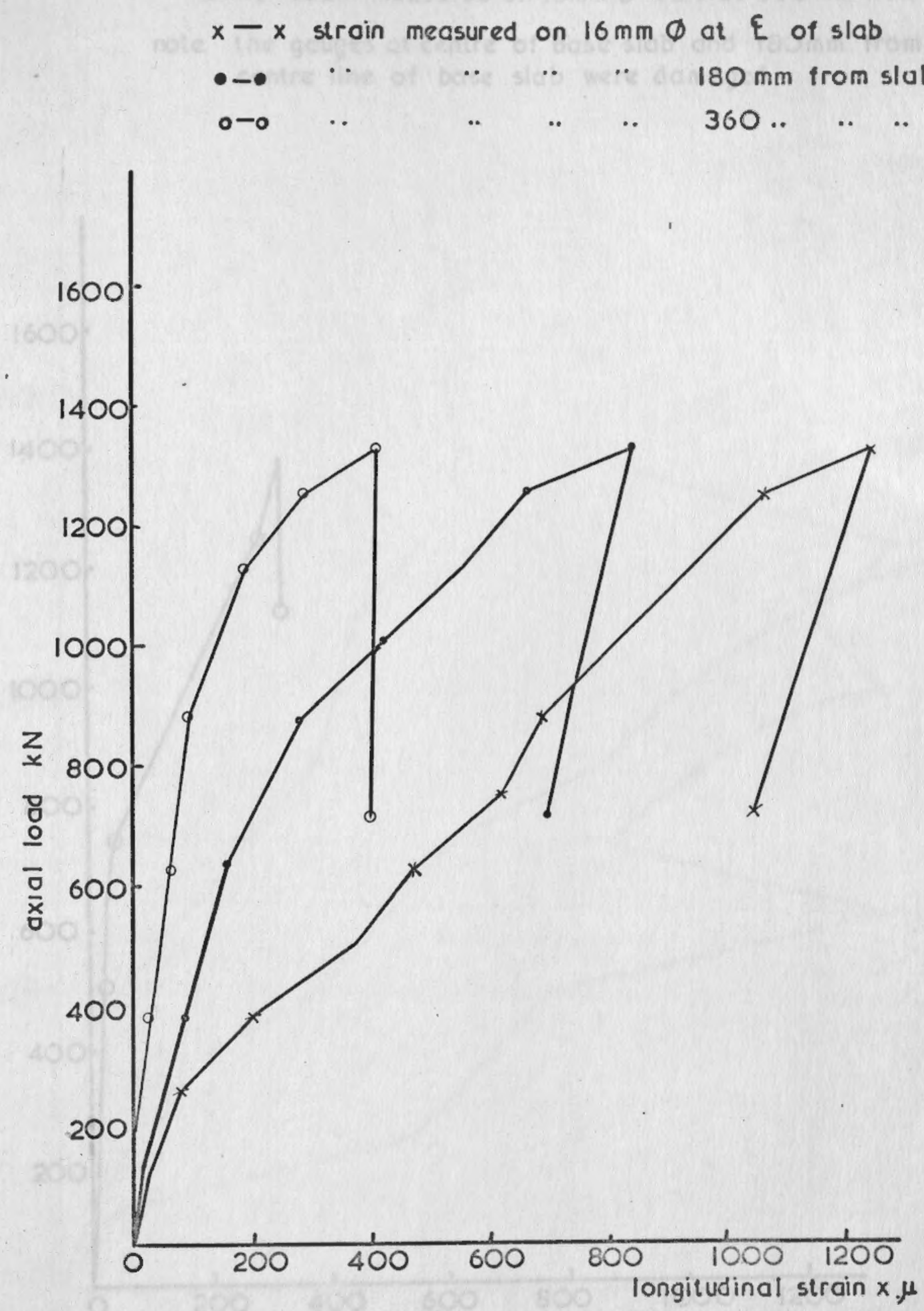

Fig. 3.5.3 Axial load v. longitudinal strains measured on bottom face of the base slab reinforcement (lower layer) at the middle of the bars. (T_1-3)

o—o strain measured on 16mm Ø bars at 360mm from ℄ of slab

note. the gauges at centre of base slab and 180mm from centre line of base slab were damaged

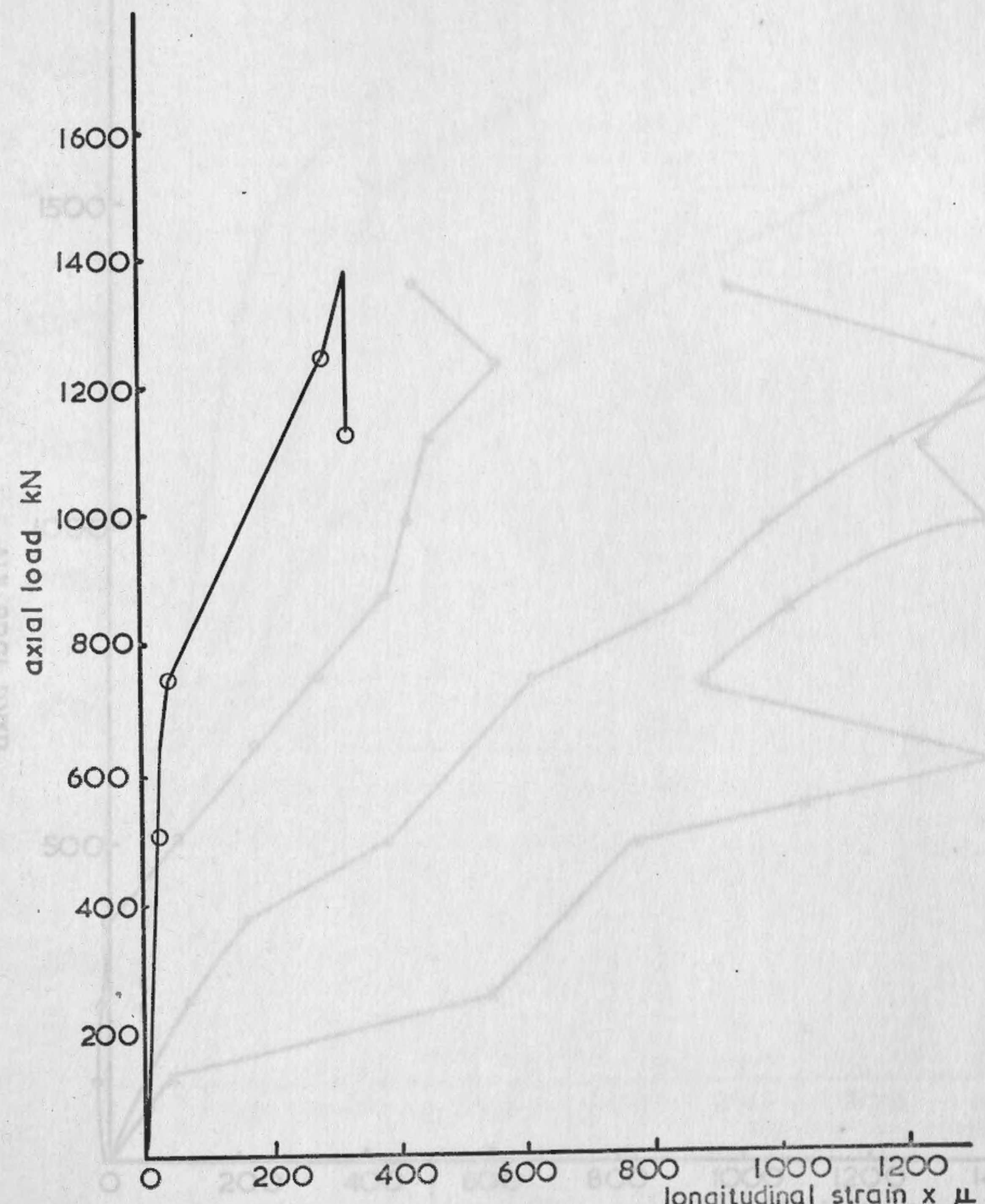

Fig. 3.5.4. Axial load v. longitudinal strains measured on bottom face of the base slab reinforcement (lower layer) at middle of bars (T_1-4)

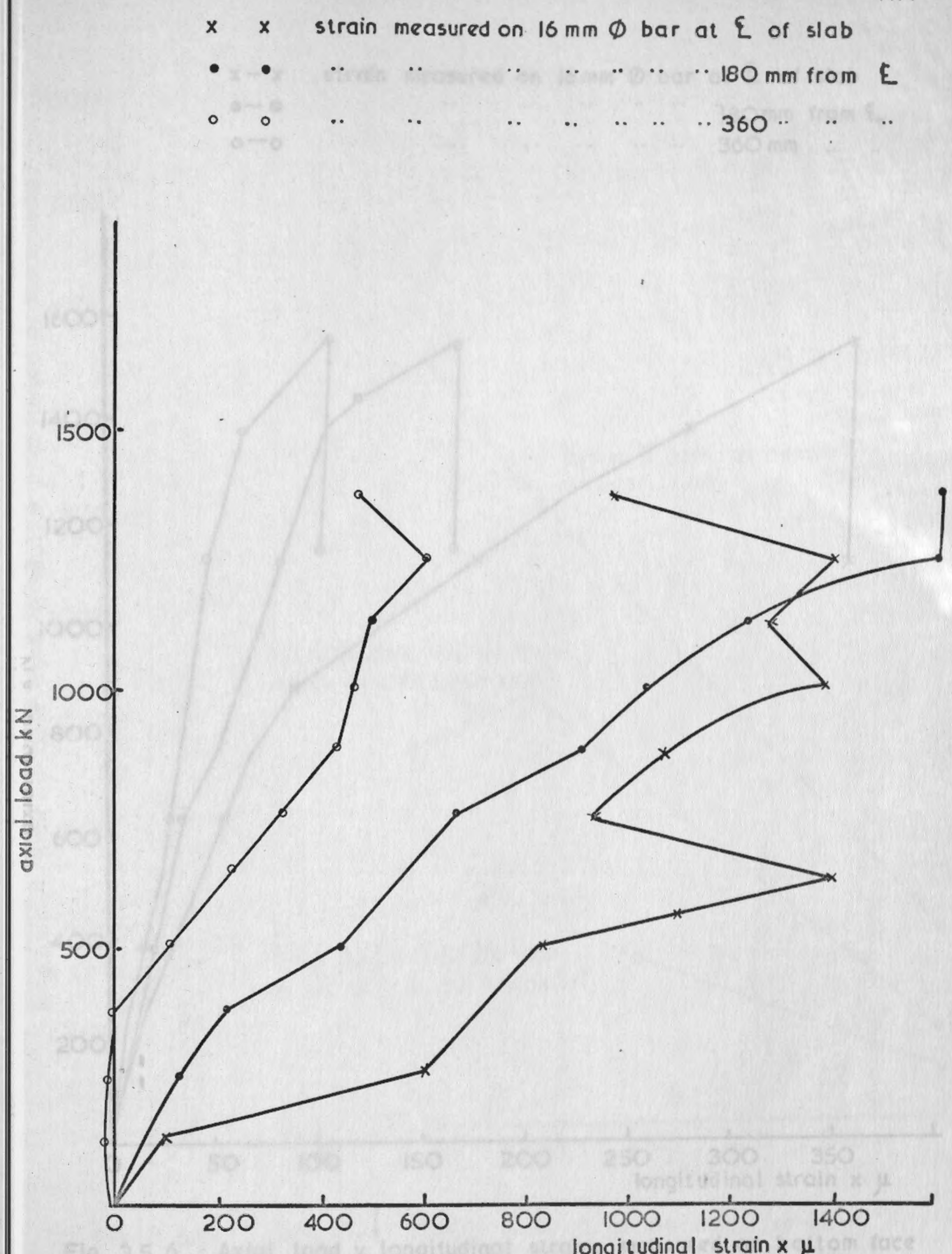

Fig. 3.5.5. Axial load v. longitudinal strains measured on bottom face of the base slab reinforcement (lower layer) at the middle of the bars. $(T_{1\text{-}5})$

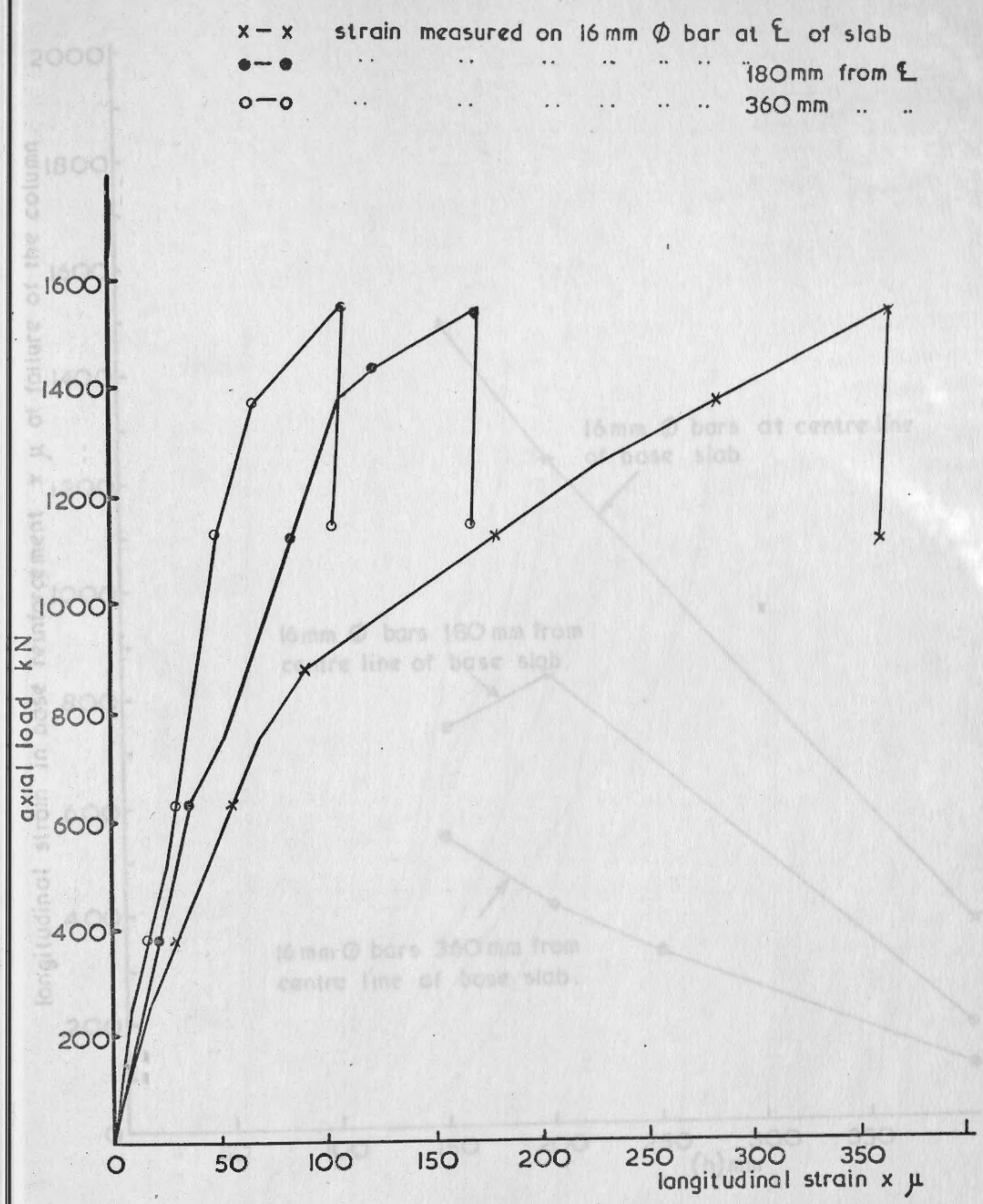

Fig. 3.5.6 Axial load v. longitudinal strains measured on bottom face of the base slab reinforcement (lower layer) at middle of bars (T1-6)

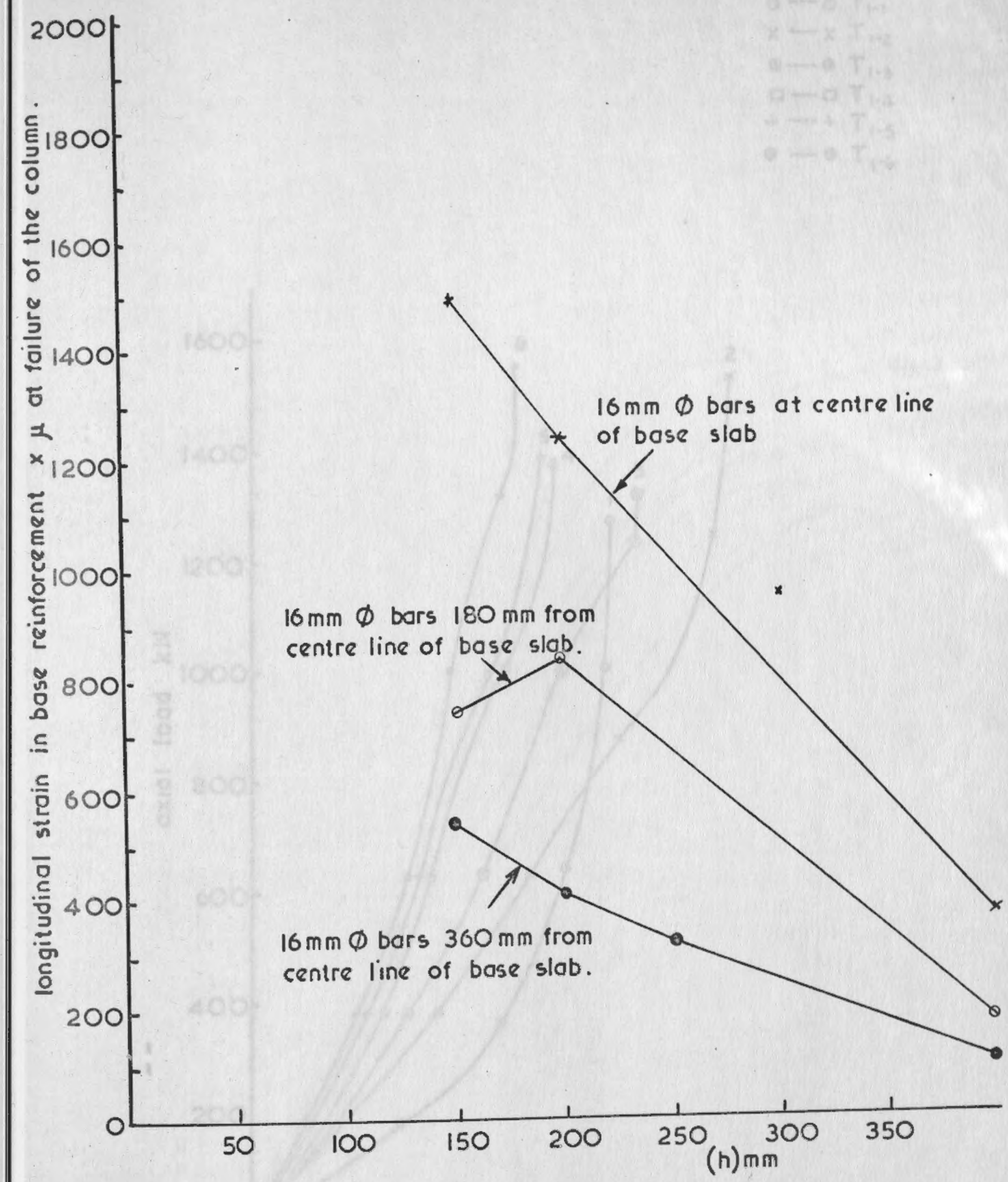

Fig. 3.5.a. Longitudinal strain measured at the middle of base slab reinforcement on the bottom face (lower layer) v overall depth of base slab (h) for series (1) specimens

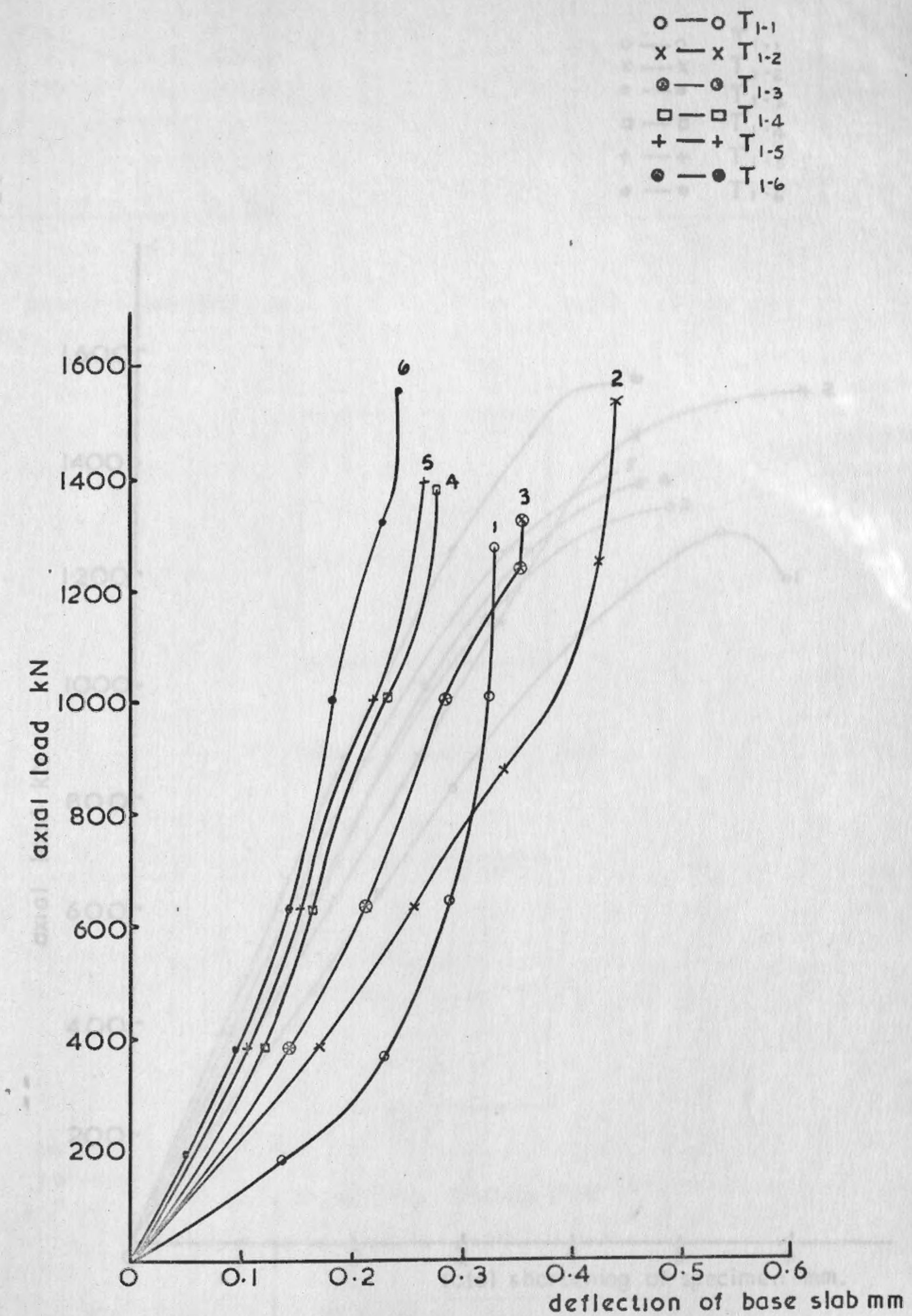

Fig. 3.6 Axial load v. average upward deflection of base slab at 105 mm from faces of column on the centre lines for series (1) specimens

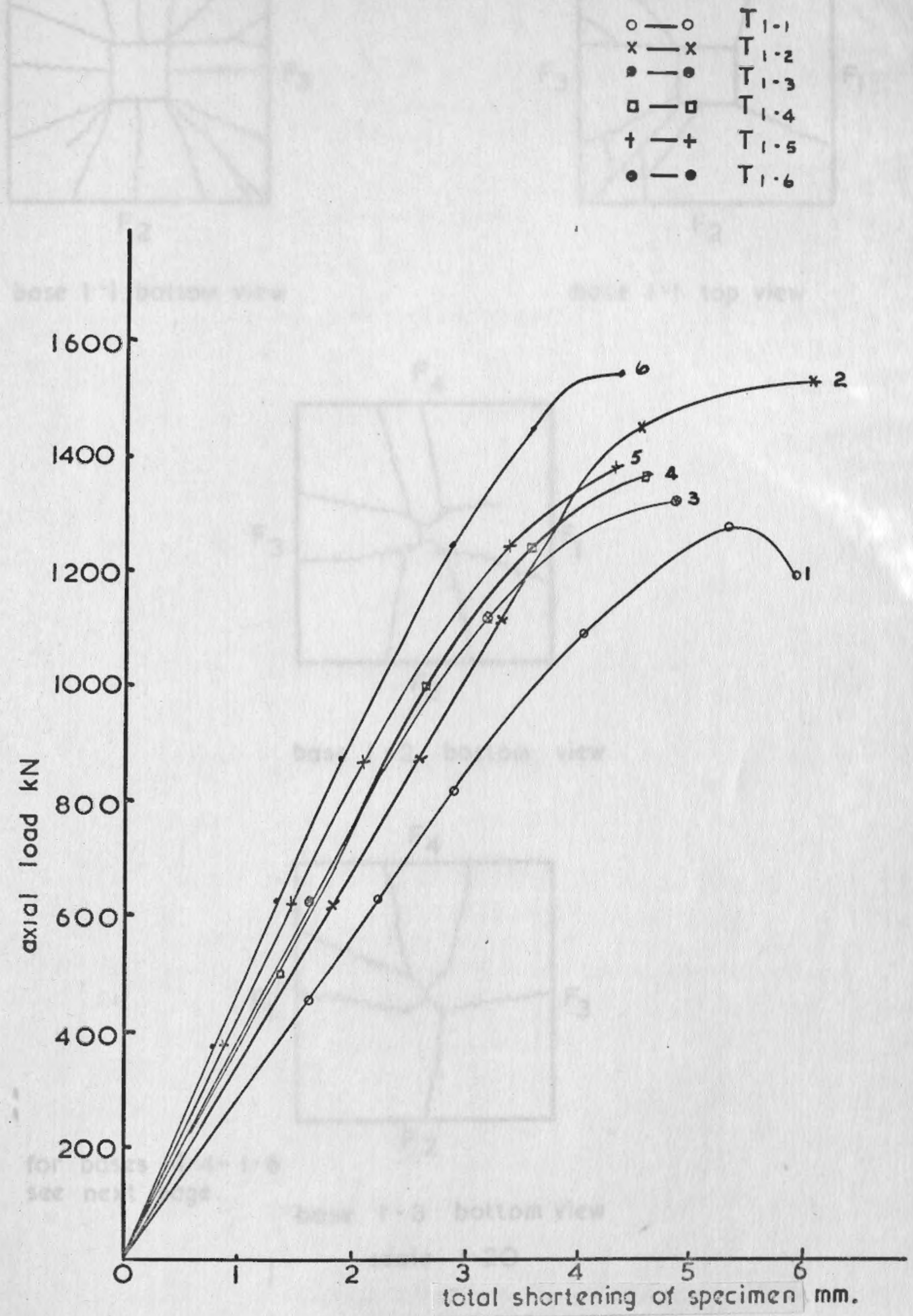

Fig. 3.7. Axial load v. total shortening of specimen for series (1) specimens

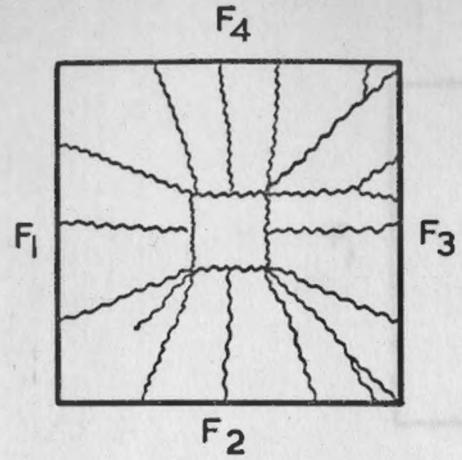

base 1-1 bottom view

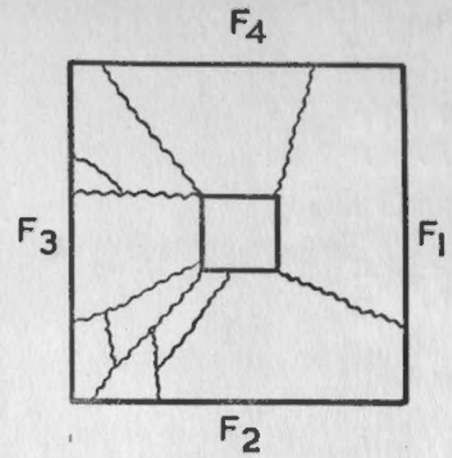

base 1-1 top view

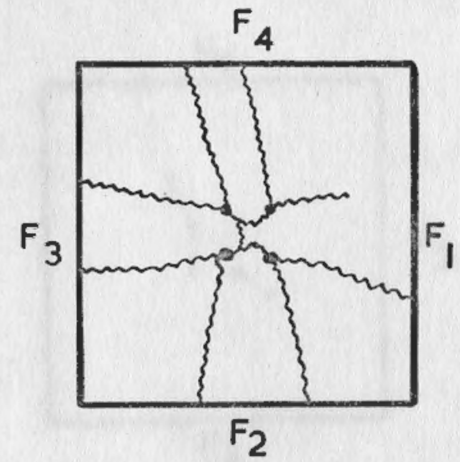

base 1-2 bottom view

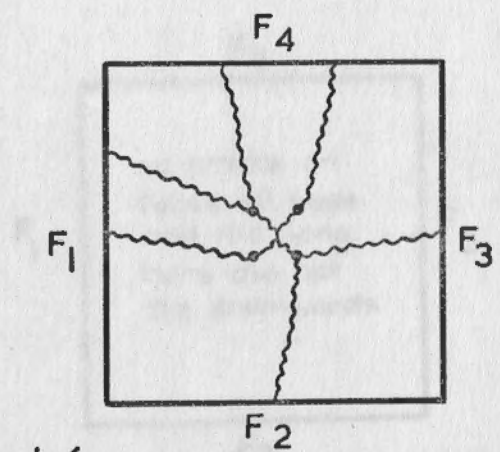

for bases 1·4–1·6
see next page.

base 1-3 bottom view

scale 1:20

Fig. 3.8. Views of base slabs after failure series (1) specimens

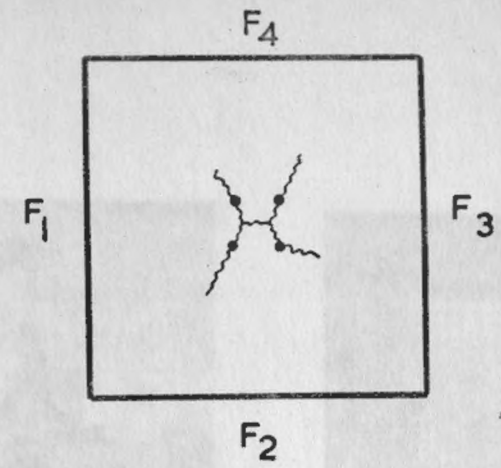

base 1 - 4 bottom view

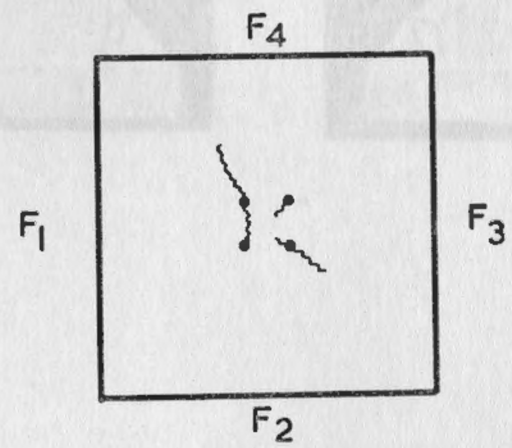

base 1 - 5 bottom view

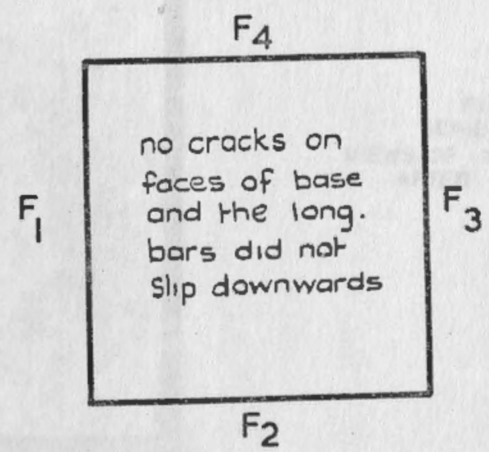

base 1-6 bottom view

scale 1:20

Fig. 3.8. Views of base slabs after failure series(I) specimens

FACE 2

FACE 3

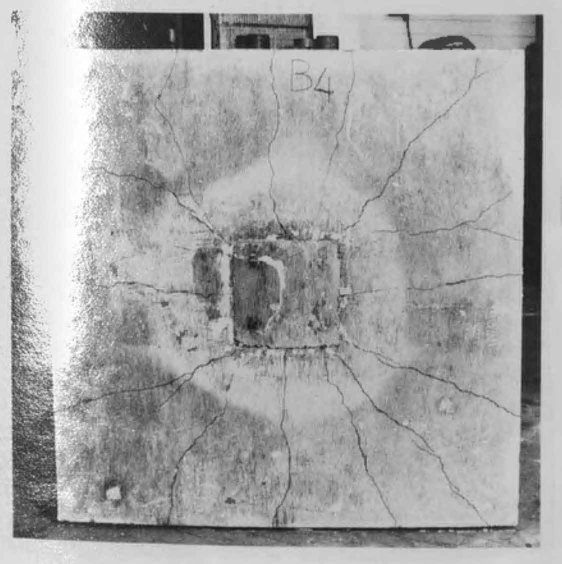

Bottom view of base

FIG. 39.1
SERIES (I)
VIEWS OF SPECIMEN T_{I-I}
AFTER FAILURE

FACE 1

FACE 2

FACE 3

FACE 4

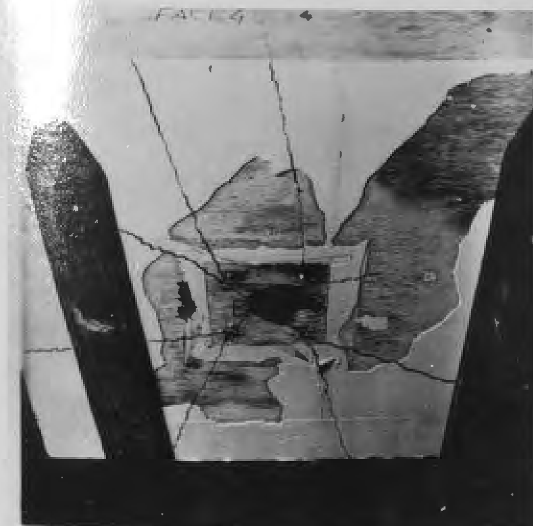

Bottom view of base

FIG. 3.92
SERIES (1)
VIEWS OF SPECIMEN $T_{1 \cdot 2}$
AFTER FAILURE

FACE 1

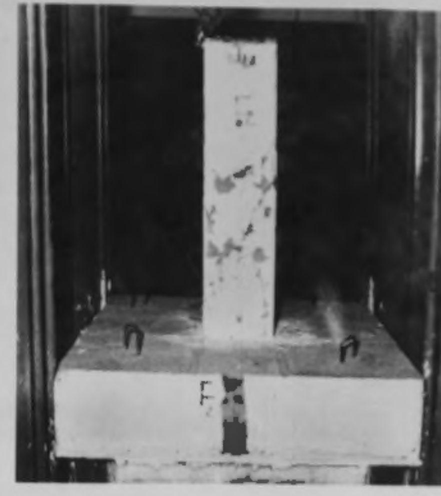

FACE 2

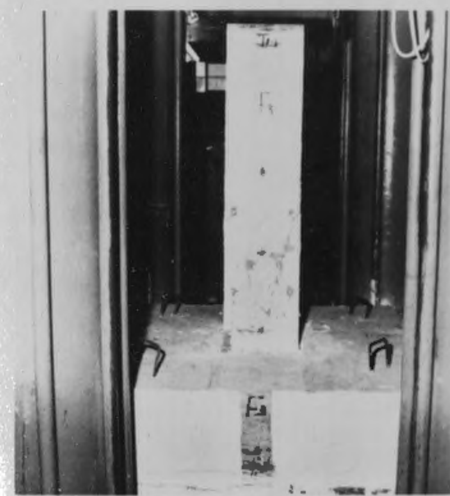

FACE 3

FACE 4

Bottom view of base

FIG. 3.9.3
SERIES (1)
VIEWS OF SPECIMEN $T_{1.3}$
AFTER FAILURE

FACE 1

FACE 2

FACE 3

FACE 4

Bottom view of base

FIG 3.9.4
SERIES (I)
VIEWS OF SPECIMEN T_1-4
AFTER FAILURE

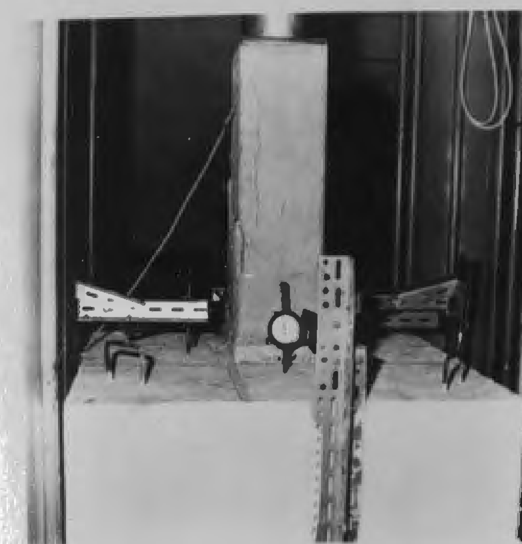

View of specimen after failure

View of specimen after breaking off the loose concrete

Bottom view of base

FIG. 3.9.5
SERIES (I)
VIEWS OF SPECIMEN $T_{1\cdot 5}$
AFTER FAILURE

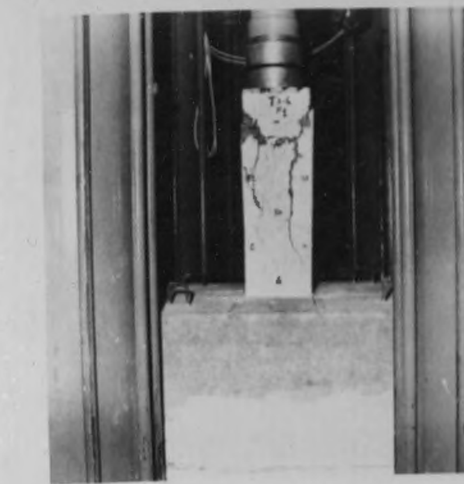

FACE 1

FACE 2

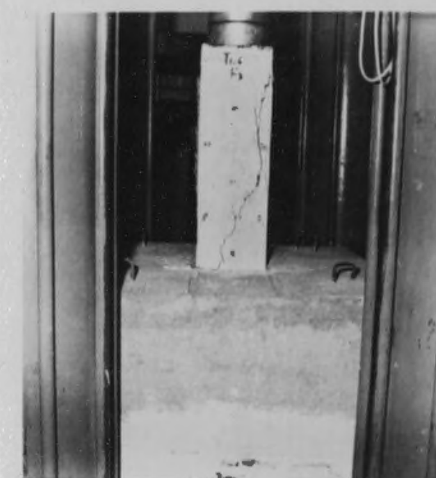

FACE 3

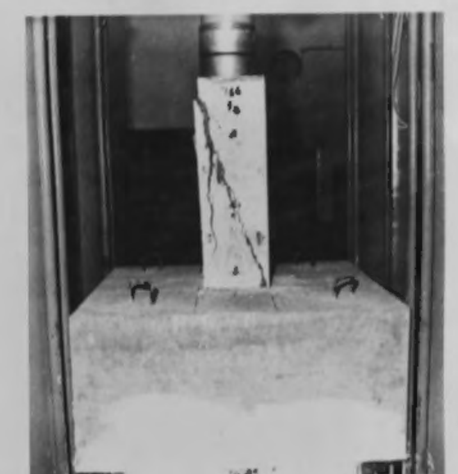

FACE 4

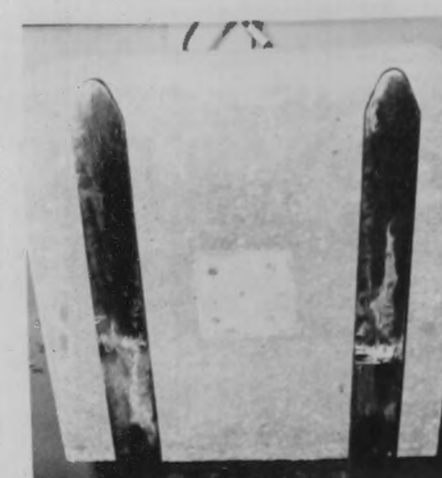

Bottom view of base

View of column after removing the loose concrete

FIG. 3.9·6 SERIES (1) VIEWS OF SPECIMEN T1·6 AFTER FAILURE

TABLE 3.3

SERIES (1)

Summary of specimens results and calculations

T_{i-j}	h mm.	d mm.	Pult. KN	Ptest KN	$\frac{Ptest}{Pult.}$	ε_s (av.) x μ	f_s (av.) N/mm^2	ε_s (max.) x μ	f_s (max.) N/mm^2
T_{1-1}	100	52	1718.2	1285	0.748	648	135.2	800	166.9
T_{1-2}	150	102	1790.1	1544	0.863	1050	219.0	1300	270.5
T_{1-3}	200	152	1511.8	1330	0.880	1270	259.0	1650	316.1
T_{1-4}	250	202	1529.7	1385	0.906	1264	298.0	1600	370.0
T_{1-5}	300	252	1499.1	1395	0.930	1520	313.8	1741	369.6
T_{1-6}	400	352	1552.1	1550	0.999	2206	414.0	3077	458.6

T_{i-j}	f_c N/mm^2	$\frac{f_c}{f_{cu}}$ for Column	$\frac{f_s(av.)}{f_y}$	$\frac{f_s(max.)}{f_y}$	f_{bs} (av.) N/mm^2	f_{bs} (max.) N/mm^2	f_{bs} (CP110) N/mm^2	f_{bs} (ACI) N/mm^2	$\frac{0.8f_{cu}A_c}{Pult.}$
T_{1-1}	28.78	0.75	0.289	0.357	7.22	8.91	3.15	5.84	0.692
T_{1-2}	32.75	0.805	0.468	0.578	7.98	9.85	3.20	6.12	0.704
T_{1-3}	25.93	0.795	0.585	0.714	6.48	7.90	2.86	5.40	0.669
T_{1-4}	26.09	0.820	0.620	0.769	5.96	7.40	2.88	5.43	0.644
T_{1-5}	25.83	0.826	0.671	0.790	5.23	6.16	2.85	5.38	0.647
T_{1-6}	26.58	0.823	0.850	0.941	5.18	5.73	2.93	5.51	0.645

Continued TABLE 3.3.

SERIES (1)

T_{i-j}	$\frac{f_{bs}\text{ (av.)}}{f_{cu}\text{ for base}}$	$\frac{f_{bs}\text{ (max.)}}{f_{cu}\text{ for base}}$	$\frac{f_{bs}\text{ (CP110)}}{f_{cu}\text{ for base}}$	$\frac{f_{bs}\text{ (ACI)}}{f_{cu}\text{ for base}}$	$\frac{f_{bs}\text{ (av.)}}{f_{bs}\text{(CP110)}}$	$\frac{f_{bs}\text{ (av.)}}{f_{bs}\text{ (ACI)}}$
T_{1-1}	0.185	0.229	0.081	0.150	2.29	1.24
T_{1-2}	0.187	0.231	0.075	0.143	2.49	1.30
T_{1-3}	0.195	0.238	0.086	0.163	2.27	1.20
T_{1-4}	0.177	0.220	0.086	0.162	2.07	1.10
T_{1-5}	0.159	0.187	0.086	0.163	1.84	0.97
T_{1-6}	0.150	0.166	0.085	0.160	1.77	0.94

Average value of f_c /(f_{cu} for column) for series (1) except T_{1-1} is 0.814.

Average value of 0.8 f_{cu} $A_c/P_{ult.}$ for series (1) except T_{1-1} is 0.662.

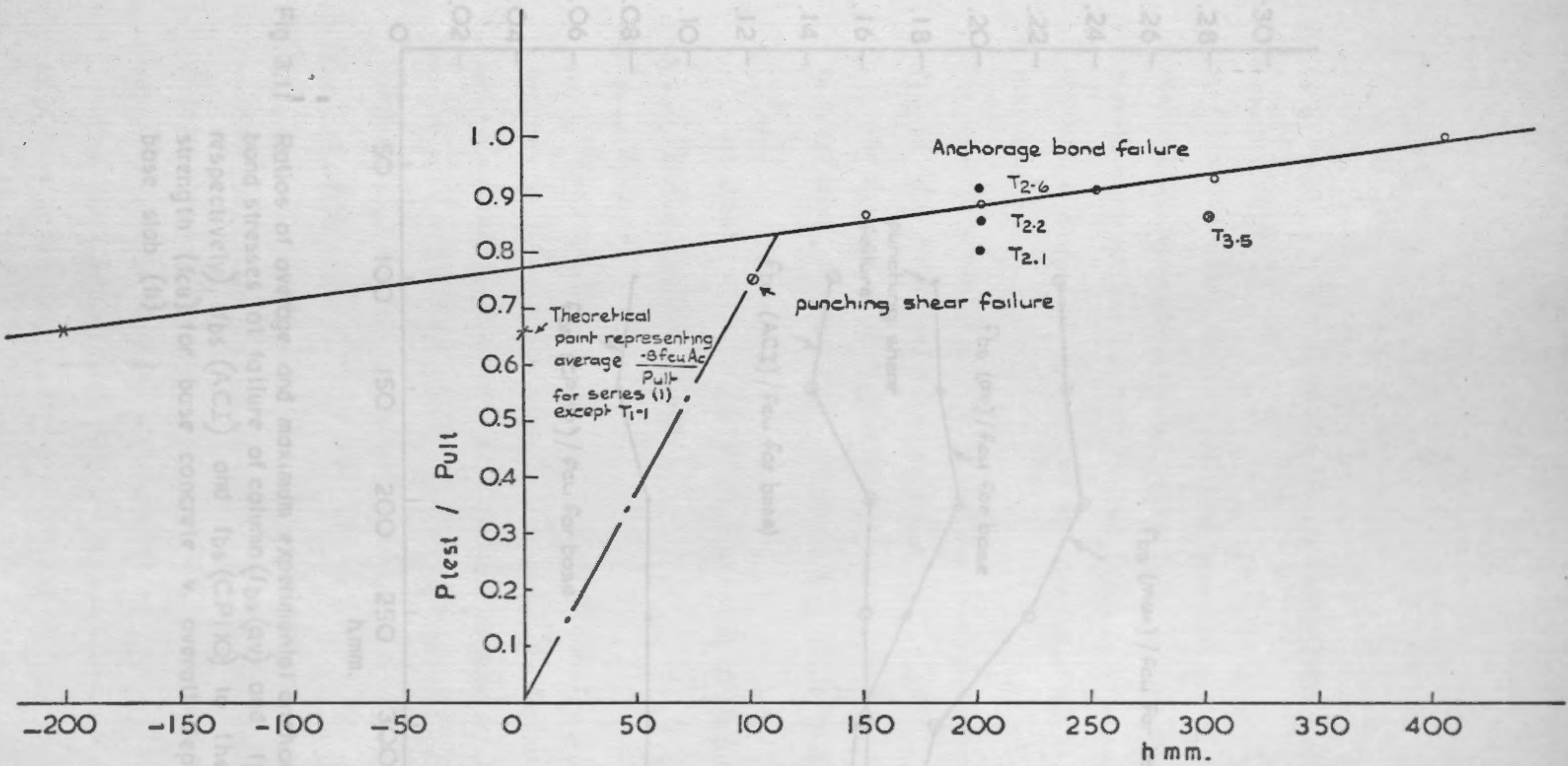

Fig. 3.10. Ratio of maximum experimental load on column (P test) to calculated ultimate axial load for column using eqn.(I)(Pult) v. overall depth of base slab (h)

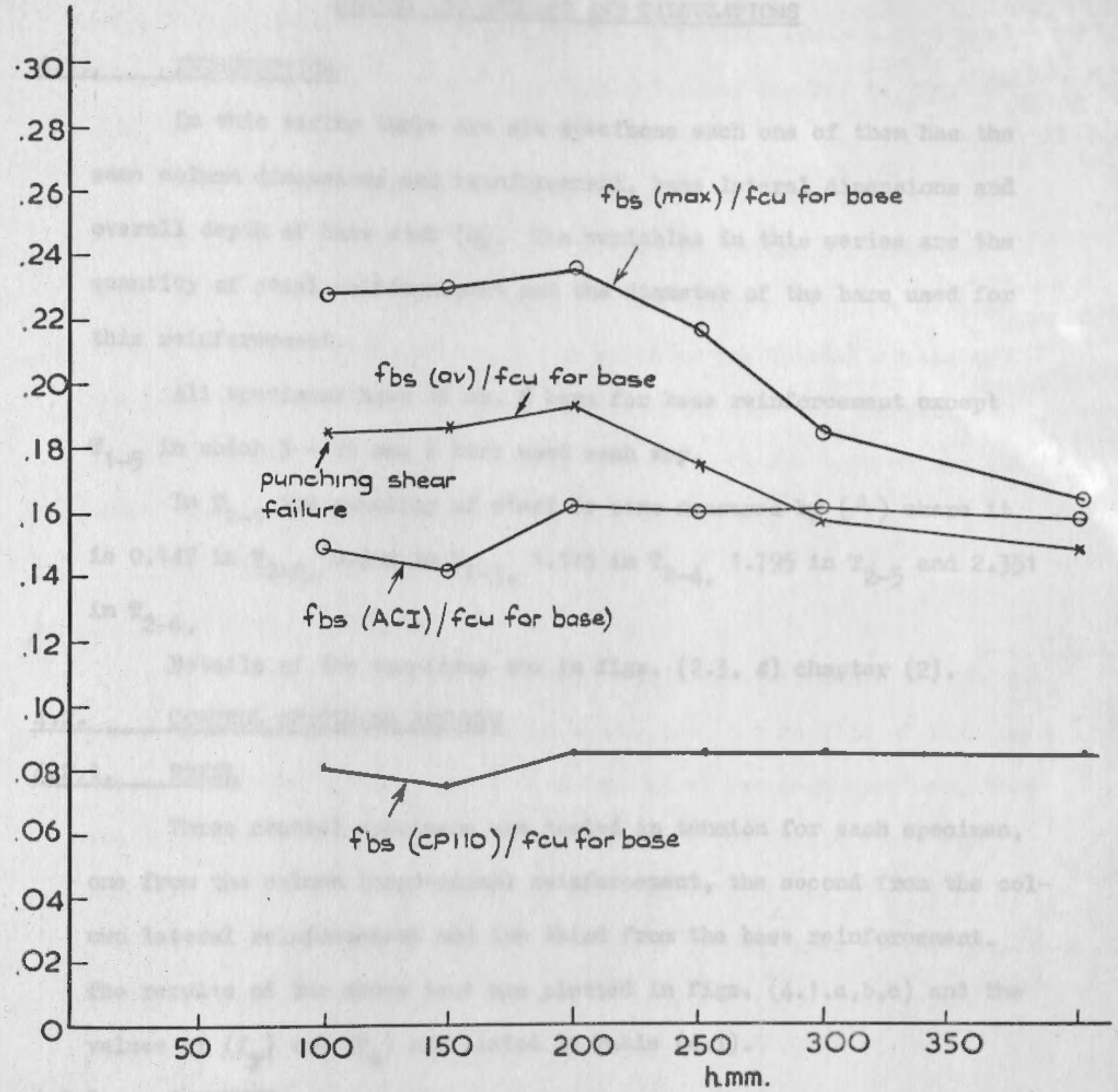

Fig. 3.11 Ratios of average and maximum experimental anchorage bond stresses at failure of column (f_{bs} (av) and f_{bs} (max) respectively), f_{bs} (ACI) and f_{bs} (CP110) to the cube strength (fcu) for base concrete v. overall depth of base slab (h).

CHAPTER 4.

SERIES (2) RESULTS AND CALCULATIONS

4.1. INTRODUCTION

In this series there are six specimens each one of them has the same column dimensions and reinforcement, base lateral dimensions and overall depth of base slab (h). The variables in this series are the quantity of steel reinforcement and the diameter of the bars used for this reinforcement.

All specimens have 16 mm. ∅ bars for base reinforcement except T_{1-5} in which 5 - 25 mm. ∅ bars used each way.

In T_{2-1} the quantity of steel is zero measured by (ρ) where it is 0.147 in T_{2-2}, 0.294 in T_{2-3}, 1.175 in T_{2-4}, 1.795 in T_{2-5} and 2.351 in T_{2-6}.

Details of the specimens are in figs. (2.3, 4) chapter (2).

4.2. CONTROL SPECIMENS RESULTS

4.2.1. STEEL

Three control specimens are tested in tension for each specimen, one from the column longitudinal reinforcement, the second from the column lateral reinforcement and the third from the base reinforcement. The results of the above test are plotted in figs. (4.1.a,b,c) and the values of (f_y) and (E_s) are listed in Table (4.1).

4.2.2. CONCRETE

The water cement ratio (w/c), mix proportion by weight, age of concrete, the compresive cube strength (f_{cu}) for base and column concrete and the tensile strength (f_t) for base and column concrete are tabulated in Table (4.2) for each specimen.

From the capped cylinder result of each specimen the axial stress is plotted against the longitudinal strain as in figs. (4.2.1a, 2a, 3a, 4a, 5a, 6a) for column concrete and figs. (4.2.1b, 2b, 3b, 4b, 5b, 6b) for base concrete. From these graphs the average secant modulus (E_c) is calculated then the axial stress is plotted against (E_c) for both column and base concrete, see figs. (4.2.1c, 2c, 3c, 4c, 5c, 6c).

Also the axial stress is plotted against the lateral strain as shown in figs. (4.2.1d, 2d, 3d, 4d, 5d, 6d) for column concrete and figs. (4.2.1e, 2e, 3e, 4e, 5e, 6e) for base concrete then the average Poisson's ratio (ν_c) is calculated by dividing the lateral strain on the longitudinal strain for each load increment and then the axial stress is plotted against the Poisson's ratio (ν_c) for both column and base concrete as shown in figs. (4.2.1f, 2f, 3f, 4f, 5f, 6f).

4.3. SPECIMENS RESULTS

4.3.1. LONGITUDINAL STRAIN

The average longitudinal strain is calculated from the results of the 8" Demec gauges on column concrete and from the results of the electrical resistance strain gauges on column steel for each specimen, then the experimental axial load is plotted against the longitudinal strain measured on both concrete and steel as shown in figs. (4.3.1, 2, 3, 4, 5 and 6) then the experimental axial load is plotted against the longitudinal strain for all the specimens as in fig. (4.3.a) for column steel, and fig. (4.3.b) for column concrete.

4.3.2. LATERAL STRAIN

The experimental axial load is plotted against the average lateral strain calculated from the results of the 6" Demec gauges on column concrete and from the electrical resistance strain gauges on column link for each specimen, see figs. (4.4.1, 2, 3, 4, 5, 6). Also the axial load is plotted against the lateral strain for all the specimens as shown in fig. (4.4.a) for column link and fig. (4.4.b) for column concrete.

4.3.3. STRAIN IN BASE SLAB REINFORCEMENT

The experimental axial load is plotted against the strain measured on the bottom face of the base lower layer reinforcement.

For T_{2-1} there is no reinforcement in the base slab. For T_{2-2} there is only 1-16 mm.∅ bar in the lower layer of base reinforcemen, on this bar the strain measured at the centre of the bar which is the centre of the base and 100 mm. on each side and their plot is shown in fig. (4.5.2).

In T_{2-3} there are two 16 mm.∅ bars in the lower layer of base reinforcement, on these bars the strain measured at the middle of each of them and the average of the two results is calculated since each bar is 225 mm. from the centre of the base slab. The plot of this strain is as in fig. (4.5.3.).

In T_{2-4} the strains are measured at the middle ofthe 16 mm. ∅ bars at 42 mm, 168.75 mm, 281.25 mm. and 393.75 mm. from the centre line of the base slab and they are plotted as in fig. (4.5.4).

T_{2-5} has the same spacing of bars as series (1) specimens, but the diameter of the bars is 25 mm. The strains are measured at the middle of the bars at the centre of the slab, 180 mm, and 360 mm. from the centre line of the base slab, and they are plotted as in fig. (4.5.5).

For T_{2-6} the strains are measured at the middle of the 16 mm. ∅ bars at 28.125 mm, 84.375 mm., 196.875 mm, 309.375 mm. and 412.5 mm. from the centre line of the base slab and they are plotted as in fig. (4.5.6). In fig. (4.5.a) the maximum longitudinal strain in the bar at the centre of the base as the nearest to it is plotted against (ρ), also the results of series (1) are plotted on the same graph.

4.3.4. DEFLECTION OF BASE SLAB AND TOTAL SHORTENING OF SPECIMEN

The experimental axial load is plotted against the average upward deflection of the base slab at 105 mm. from faces of column on the centre lines of the base slab as shown in fig. (4.6) and also plotted against the total shortening of the specimen as in fig. (4.7) for all the specimens.

4.4. MODE OF FAILURE

Specimens of this series all failed by anchorage bond failure between the column longitudinal reinforcement and base slab concrete.

In all tests the cracks first started on the bottom face of the base slab from the 20 mm. Ø bars and then propogated either to the inside or outside direction, those to the inside met each other while the others travelled until they reached the outsides of the base slab, then they extended upward until they reached near the top face of the slab, except T_{2-6} in which the bars slipped downwards without causing any cracks on the base slab, see figs. (4.8 and 4.9.6).

In the rest of the specimens the patterns of the cracks are similar to each other except for the number of cracks, in T_{2-1}, T_{2-2}, T_{2-3} and T_{2-4} the number of cracks increased as the quantity of steel in the base slab increased, see figs. (4.8, 4.9.1, 2, 3, 4) then in T_{2-5} which has different size reinforcement, but larger quantity of steel, the number of cracks was even smaller than T_{2-1} see figs. (4.8, 4.9.5).

For all the specimens as the cracks reached near the top of the base slab the amount of slip in the longitudinal column reinforcement became excessive and hence, the column concrete failed by compression.

4.5. CALCULATIONS

4.5.1. TABLE (4.3) AND GRAPHS

Using equation (1) the theoretical ultimate axial load (P_{ult}) is calculated and the maximum experimental axial load is recorded, hence, the ratio of (P_{test}/P_{ult}) is found for each specimen.

The average and maximum longitudinal strains for column reinforcement ε_s(av.) and ε_s(max.) are recorded, then the corresponding axial loads on the 20 mm. ϕ bars are calculated using the results of the steel control specimens and the above strains. The average axial load taken by the reinforcement is calculated and subtracted from P_{test} and the result is divided by the cross-sectional area of the column concrete (A_c). This gives the value (f_c) then the ratio of (f_c/f_{cu} for column) is calculated. (See example of calculations in 3.5.1).

The average and maximum stresses in the 20 mm. ϕ column reinforcement f_s(av.) and f_s (max.) respectively are calculated and their ratios to f_y are found. Then the average and maximum anchorage bond stresses f_{bs} (av.) and f_{bs} (max.) respectively are calculated using the average and maximum stresses in the 20 mm. ϕ bars.

From CP110: Part 1: 1972 Table (22) the allowable anchorage bond stress corresponding to f_{cu} for base f_{bs} (CP110) is read for all specimens.

Using equation (6.a) and assuming $f'_c = 0.8\ f_{cu}$ the allowable anchorage bond stress f_{bs} (ACI) for the American code is found to be equal to ($0.9366\ f_{cu}$). This value is calculated for all specimens.

The ratios of f_{bs} (av.), f_{bs} (max.), f_{bs} (CP110) and f_{bs} (ACI) to f_{cu} for base are calculated, also the ratios of f_{bs} (av.) to f_{bs} (CP110) and f_{bs} (ACI) are calculated.

All the above results and calculations are tabulated in table (4.3).

The ratio of ($P_{test}/P_{ult.}$) is plotted against the percentage of steel reinforcement in the base slab (ρ), also the results of series (1) and (3) are plotted as shown in fig. (4.10).

The ratios of f_{bs} (av.), f_{bs} (max.), f_{bs} (CP110) and f_{bs} (ACI) to f_{cu} for base are plotted against (ρ) and f_{bs} (av.) / f_{cu} for base of series (1) and (3) are also plotted on the same graph as shown in fig. (4.11).

4.5.2. PUNCHING SHEAR

The properties of T_{2-6} are used to determine the depth required to resist punching shear failure so that it can be compared with the depth required to resist anchorage bond failure.

The depth required to resist punching shear is calculated according to the following :-

1) CP110: Part 1: 1972

From tables (5) and (14) of the above code using T_{2-6} properties $v_c = 0.938$ N/mm^2.

Hence, using equation (3) the depth required = 360.4 mm.

2) ACI 318-1971

$f'_c = 0.8\ f_{cu} = 27.39$ N/mm^2.

Hence using equation (4) the depth required = 449.0 mm.

3) EQUATION (2)

Using equation (2) the depth required = 321.7 mm.

If punching shear failure was allowed all series (2) specimens would have failed by punching shear.

4.5.3. ANCHORAGE LENGTH FOR LONGITUDINAL COLUMN REINFORCEMENT

The anchorage length required to resist anchorage bond failure is calculated for T_{2-6} properties and the following :-

1) CP110: Part 1: 1972

From table (22) the allowable anchorage bond stress = 2.91 N/mm^2.

and the permissible stress in the column longitudinal reinforcement

$$= \frac{484.1 \times 2000}{2000 + 484.1}$$

$$= 389.76 \text{ N/mm}^2$$

Hence, using equation (5) gives

$$1 = 669.7 \text{ mm}.$$

2) ACI 318-1971

The yield stress corresponding to 0.35% strain for the 20 mm.

ϕ bars of T_{2-6} = 469.75 N/mm^2.

Hence equation (6.a) gives the maximum anchorage length.

That is $\quad l \; = \; 429.4$ mm.

4.6. DISCUSSION OF SPECIMENS RESULTS AND CALCULATIONS

4.6.1. COLUMN LONGITUDINAL STRAIN

The graphs for strains measured on steel and concrete at the beginning of each test are almost the same except for a small difference which may be due to the different methods of measurement used for steel and concrete. Then as the load increased the steel starts to lose some strain which is the beginning of small slipping after each slip the slope of the graph reduced due to the increase of strain difference compared with the previous reading. This is due to the gripping properties of the square twisted bars. As the bars continued to slip as the load increased the steel graph lags behind the concrete one until failure of the column concrete in compression. In all the tests the slope of the steel graph reduced sharply which means the strain increased sharply just before failure of the column concrete except T_{2-1} in which the failure of the base was severe since the cracks on the sides of the base slab reached the top of the base.

The shape of these graphs is the same for all specimens, see fig. (4.3.a) for column steel and fig. (4.3.b) for column concrete.

4.6.2. COLUMN LATERAL STRAIN

T_{2-4} graph for column link has compressive strain at the beginning of the test, see fig. (4.4.4) and in some of the tests the strain was zero at the beginning of the test, see fig. (4.4.1, 6).

As the load increased the strains increased and they become almost the same until the final stages of the test where the steel graph lags behind the concrete one and at failure, the strain measured on the concrete is more than double that measured on the column link.

In some of the specimens the two graphs at the beginning of the test are almost the same, see figs. (4.4.2, 3, 5). The difference between the graphs at the beginning of the tests is due to the different methods used to measure the strain on steel and concrete, also it is difficult to fix the strain gauges on the column link at the exact position, due to the geometric properties of the 6 mm. bar used.

Apart from the above differences, the steel graphs have the same shape, see fig. (4.4.a).

The concrete graphs have the same shape as shown in fig. (4.4.b).

4.6.3. STRAIN IN BASE SLAB REINFORCEMENT

From the strains measured on T_{2-2} reinforcement, it can be seen that the strain measured at the centre of the slab is greater than that measured at the face of the column which means that the bending moment at the centre is greater than that at the face of the column, and their ratio is = 1.456.

The rest of the graphs show that the strains measured on the bars near the centre of the base slab are greater than those measured on bars which are further away from the centre. This means that bending moment is not constant across the section at the centre line of the base slab, and confirms the finding in chapter (3). Fig. (4.5.6) shows that the strains measured on bars within the boundary of the column are almost the same. This applies for etrains measured on bars further than 309.375 mm. away from the centre of the base slab, this shows that bending moment is more uniform under the column then reduced as the distance increased further than its faces, then starts to level up as it reaches the outsides of the base on each side,

Fig. (4.5.5.) shows the strains measured for specimen T_{2-5}, which has the same spacing of bars as series (1) but the diameter of bars in 25 mm. ∅ instead of 16 mm. ∅, are less than those of T_{1-3} and the ratio of the one at the centre is more than four times than that at the edge compared with more than three times in series (1) fig. (3.5.3).

From fig. (4.5.a) it can be seen that as the value of (ρ) increases by increasing (A_s) the strain in the base steel reduces and from series (1) results the strain increases as (ρ) increases by reducing the overall depth of the base slab (h).

4.6.4. UPWARD DEFLECTION OF BASE SLAB AND TOTAL SHORTENING OF SPECIMEN

The graphs of the axial load against the average upward deflection of the base slab are not consistent with the value of (ρ) see fig. (4.6) in which the deflection of T_{2-6} and T_{2-1} are almost the same, and that of T_{2-4} is greater than that of T_{2-3}, but in general, if the results of T_{2-4} and T_{2-1} are neglected, then the deflection is reduced as the value of (ρ) increased for the same experimental axial load.

The shape of these graphs is the same as those of series (1), see fig. (3.6).

The graphs of the axial load against the total shortening of the specimen are also not consistent with (ρ) values, and it can be seen that the shortening of T_{2-1} and T_{2-6} are the same, also, the specimens have the same shortening at the early stages of the tests, see fig. (4.7).

4.6.5. TABLE (4.3) AND GRAPHS

The average value of the ratios of (f_c/f_{cu} for column) is 0.794 where the average for all the experimental program is 0.797 (except T_{1-1}).

Fig. (4.10) shows that by increasing the value of (ρ) from zero to 0.147 (ie. by increasing (A_s) from zero to 201 mm^2. where (d) is constant) the specimen strength increased by 5.5% compared with equation (1) and by increasing the value of (ρ) from 0.147 (A_s = 201 mm^2.) to 2.351 (A_s = 3217 mm^2) using bars of the same size, the column strength increased by only 5.7%. This shows that the strength increased sharply up till (ρ) = 0.147, then the slope of the graph flatten up until it reaches $\rho = 0.735$ then the graph flattens further.

If the size of the bars used in the base are increased for the same (ρ), which means the spacing of the bars (s_b) increased, the column strength reduced, see T_{2-5} on the same graph.

If T_{2-5} is compared with T_{1-3} since (s_b) is the same and equal to 180 mm. but A_s in T_{2-5} is 2.44 that of T_{1-3}, it is found that the column strength of T_{2-5} is slightly less than that of T_{1-3}. More tests are needed using different bar sizes in the base to confirm T_{2-5} results which means that for the same (A_s) using small size bars gives better results than using larger size bars.

By plotting the results of series (1) and (3) on fig. (4.10) it can be seen from series (1) results that by varying the effective depth of the base slab (d) and keeping (A_s) constant, the graph is a curve whose $P_{test}/P_{ult.} = 0.77$ at $\rho = \infty$ and at $\rho = 0.317$, $P_{test}/P_{ult.} = 1$. Hence a specimen having h = 150 mm. and $A_s = 1005$ mm^2. is the same as a specimen having h = 200 mm. and $A_s = 402$ mm^2. as far as the column strength is concerned, compared with equation (1). See T_{1-2} and T_{2-3} results.

Also series (3) results are all on the ($P_{test}/P_{ult.}$) axis since $A_s = 0$. Hence, a specimen with h = 300 mm. and $A_s = 0$ mm^2. is the same as a specimen with h = 200 mm. and $A_s = 402$ mm^2. as far as column strength is concerned, compared with equation (1).

Fig. (4.11) shows that the graphs of f_{bs} (av.) and f_{bs} (max.) ratios to (f_{cu} for base) have the same shape as that of fig. (4.10). The gap between these graphs reduces as the value of (ρ) increases, this means that the load is more uniform on the bars as the value of (ρ) increases.

The average ratios for series (2) are well above the values given by CP110: Part 1: 1972 and not that far from the values of the ACI 318 -

1971. The difference between the average ratios and the above codes increases as the value of (ρ) increases and at $\rho = 0$ the American results coincide with the test results.

The average ratios for series (1) and(3) are also plotted on the same graph and show that series (3) results are well below T_{2-1} results and those of series (1) are forming a straight line except that of T_{1-2} which means that the stresses increases as (d) decreases, then flatten as d reduced below 152 mm. The strains measured on the 20 mm. Ø Bars of T_{1-2} by one electrical resistance strain gauge on each bar whereon the other tests two gauges are used, placed opposite to each other. This could account for the low values of f_{bs} (av.) and f_{bs} (max.) in T_{1-2} test.

The value of f_c/f_{cu} for column is higher than the average value for T_{2-6}. This might be due to the increase in the base strength which then provides stronger holding for the column concrete above the base slab and then compression failure only occurs at higher f_c values, see also (3.6.5).

4.6.6. PUNCHING SHEAR

Using the properties of T_{2-6} the required depths to resist punching shear failure according to the British code, American code and equation (2) are listed in the following table.

(1)	(2)	(3)	(4)	(5)
Equation (2) mm.	Equation (3) (CP110) mm.	(2) / (1)	Equation (4) (ACI) mm.	(4/) / (1)
321.7	360.4	1.12	449.0	1.40

This table shows that for large values of (ρ) the British code gives thinner slabs than the American one for punching shear consideration.

4.6.7. ANCHORAGE LENGTH

For the properties of T_{2-6} the British code gives $l = 669.7$ mm. where the American code gives $l = 429.4$ mm. which shows that the American code gives shorter bond length than the British one, neither code makes any allowance for variation in slab steel when determining anchorage bond stress. The British code uses an allowable stress in the longitudinal steel of T_{2-6} column equal to $0.805\ f_y$ where the American code uses $0.970\ f_y$ which is higher than that obtained from T_{1-6} test and the pilot test of chapter (7).

4.6.8. PUNCHING SHEAR AND ANCHORAGE LENGTH

If punching shear failure can occur in series (2) tests, then all the specimens would have failed by punching shear according to equation (2).

4.7. CONCLUSIONS

From the results and calculations of series (2) specimens the following are concluded :-

1) Increasing (A_s) and hence (ρ) increases the bond strength and hence the column strength compared with equation (1) using the same bar size in the base.

2) For the same (A_s) using small diameter bars gives higher bond strength and hence higher column strength than using larger size bars.

3) Varying the value of (ρ) by varying (A_s) gives different results from that by varying (d).

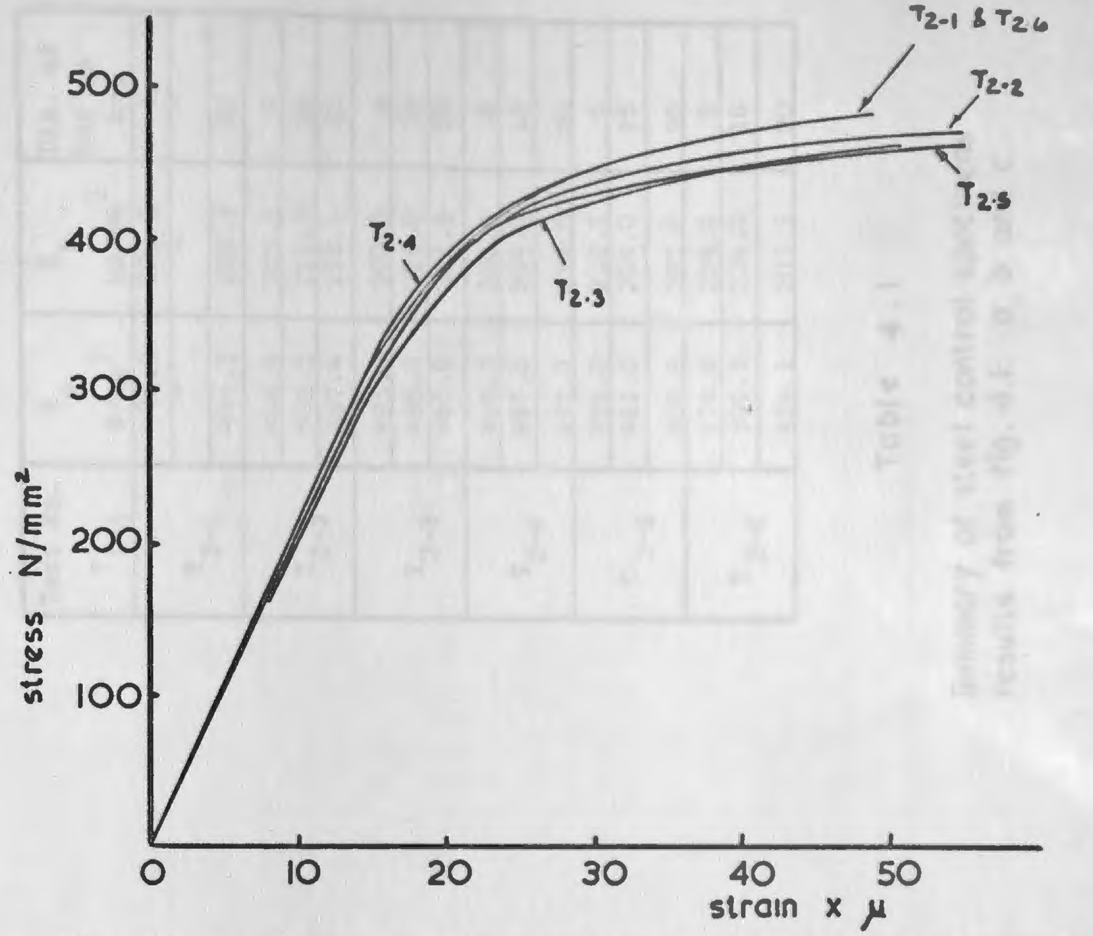

Fig 4.1. a. Stress v. strain for 20mm Ø HT square twisted steel bars

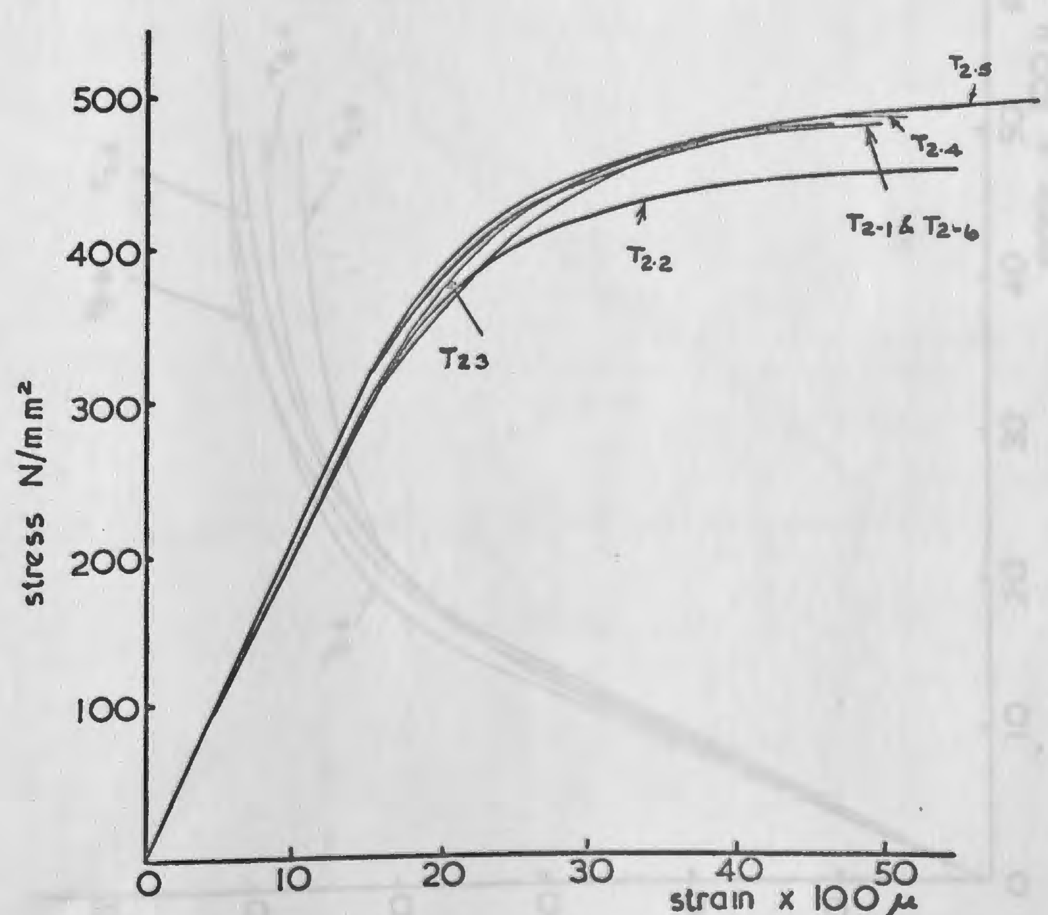

Fig. 4.1. b. Stress v. strain for 6mm Ø HT square twisted steel bars

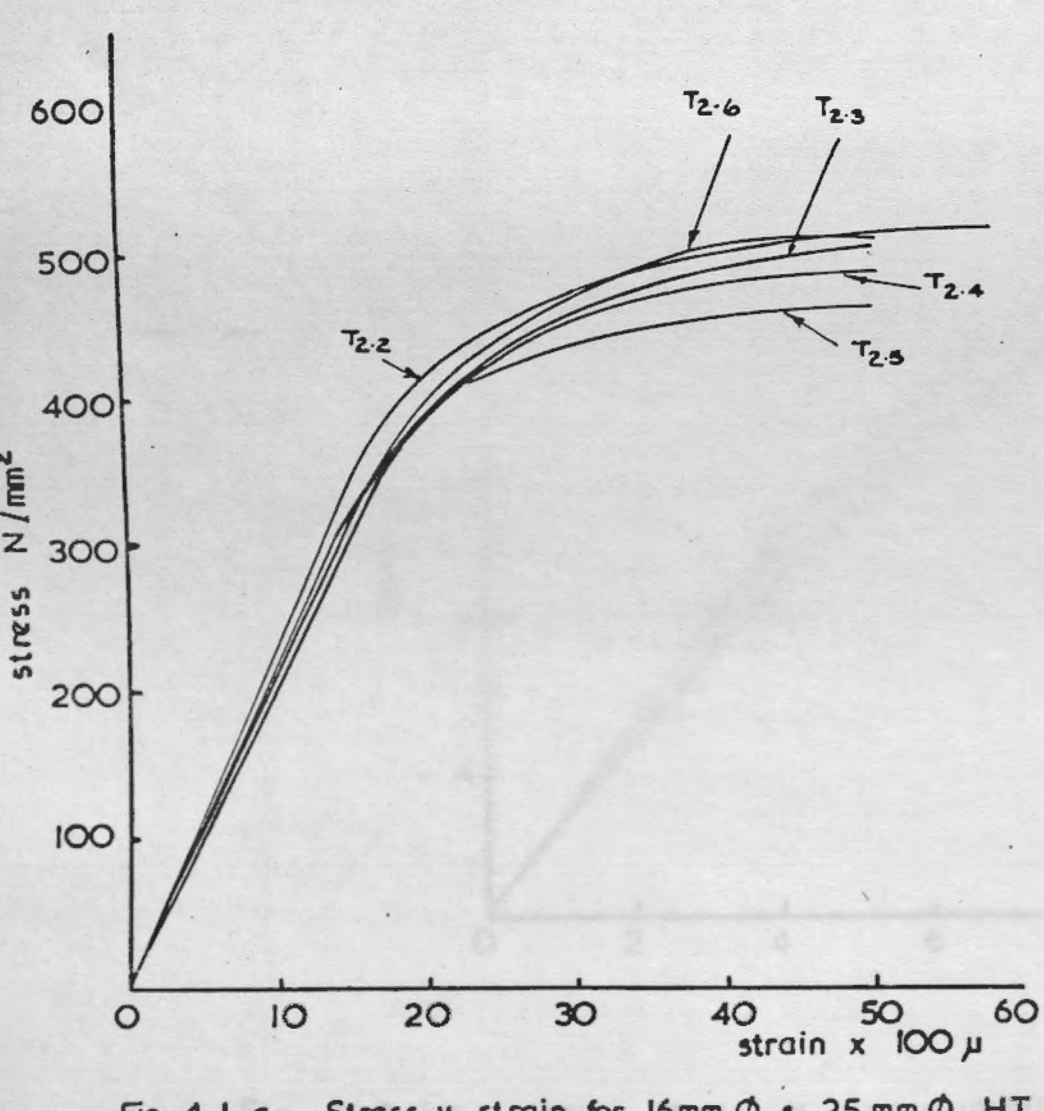

Fig 4.1.c. Stress v. strain for 16mm Ø & 25 mm Ø HT square twisted steel bars

Test No. T_{i-j}	f_y N/mm^2	E_s KN/mm^2	Dia. of bar in mm.
T_{2-1}	478.6	209.0	6
	-	-	-
	484.1	203.3	20
T_{2-2}	446.4	203.6	6
	502.5	228.9	16
	467.4	213.4	20
T_{2-3}	485.0	200.0	6
	495.0	225.0	16
	460.0	203.8	20
T_{2-4}	489.3	200.0	6
	487.6	204.0	16
	477.7	214.00	20
T_{2-5}	484.0	212.5	6
	461.0	209.0	25
	458.6	207.0	20
T_{2-6}	478.6	209.0	6
	502.5	214.0	16
	484.1	203.3	20

Table 4.1

Summary of steel control specimens results from fig. 4.1. a, b and c.

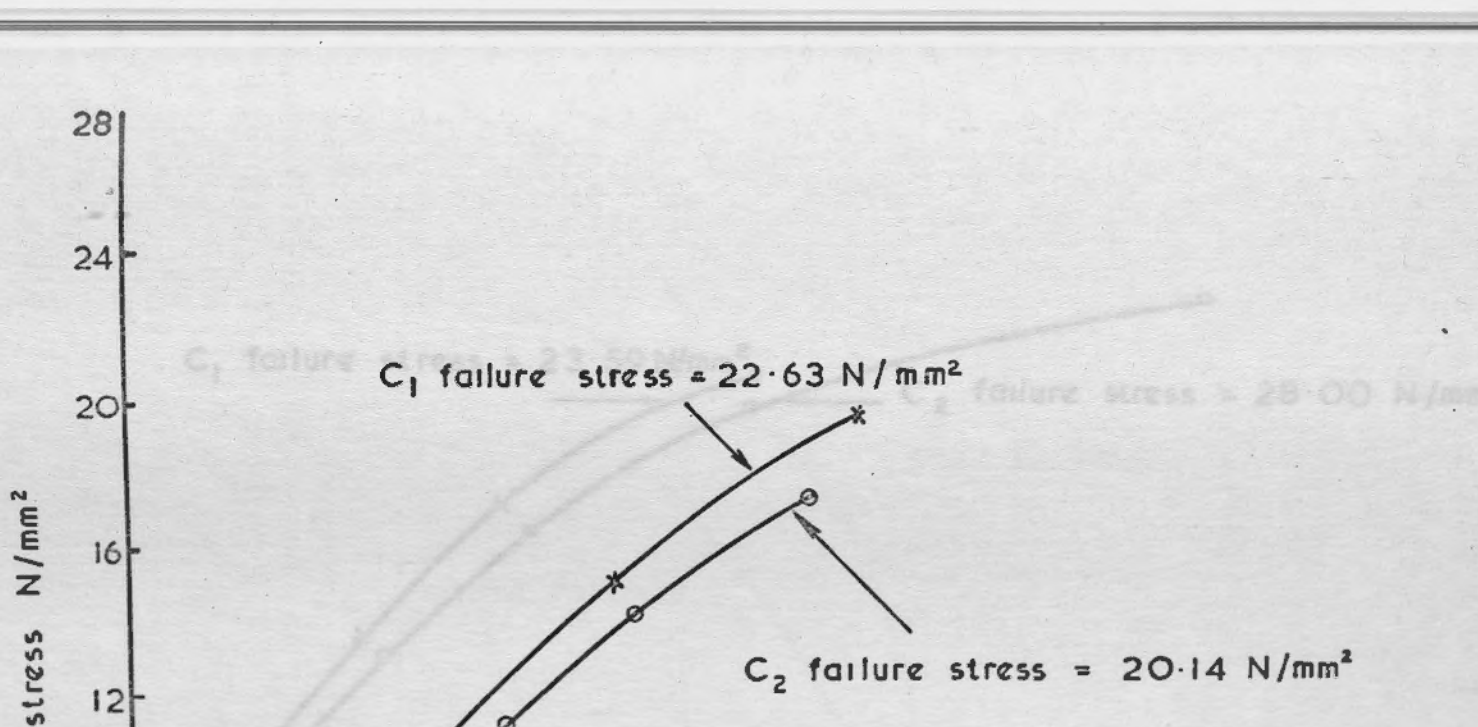

Fig. 4.2.1a. Axial stress v. longitudinal strain measured on cylinders for column concrete by electrical resistance strain gauges.

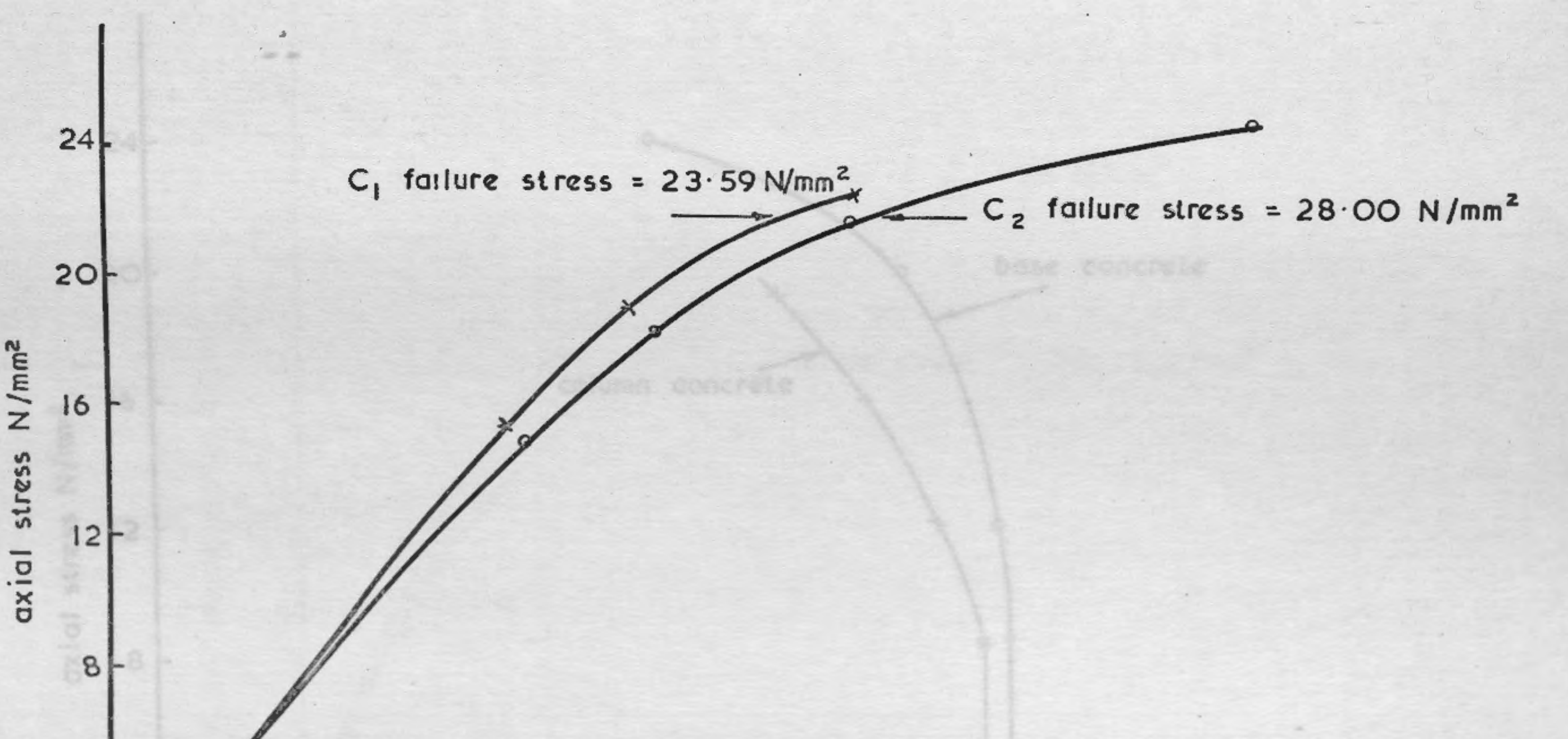

Fig. 4.2.1b. Axial stress v. longitudinal strain measured on cylinders for base concrete by electrical resistance strain gauges

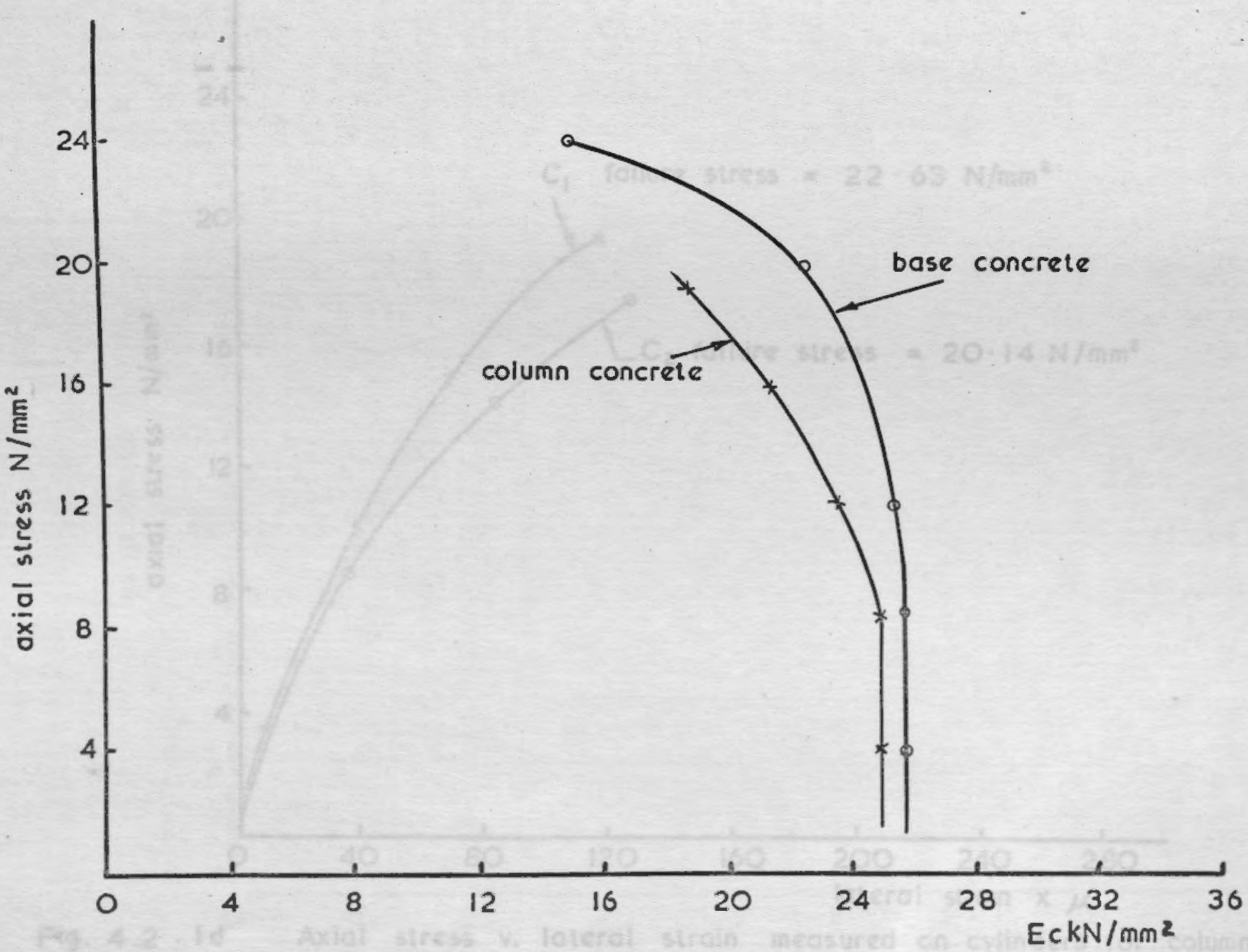

Fig. 4.2.1c Axial stress v. modulus of elasticity for column concrete and for base concrete

Fig. 4.2.1d Axial stress v. lateral strain measured on cylinders for column concrete by electrical resistance strain gauges.

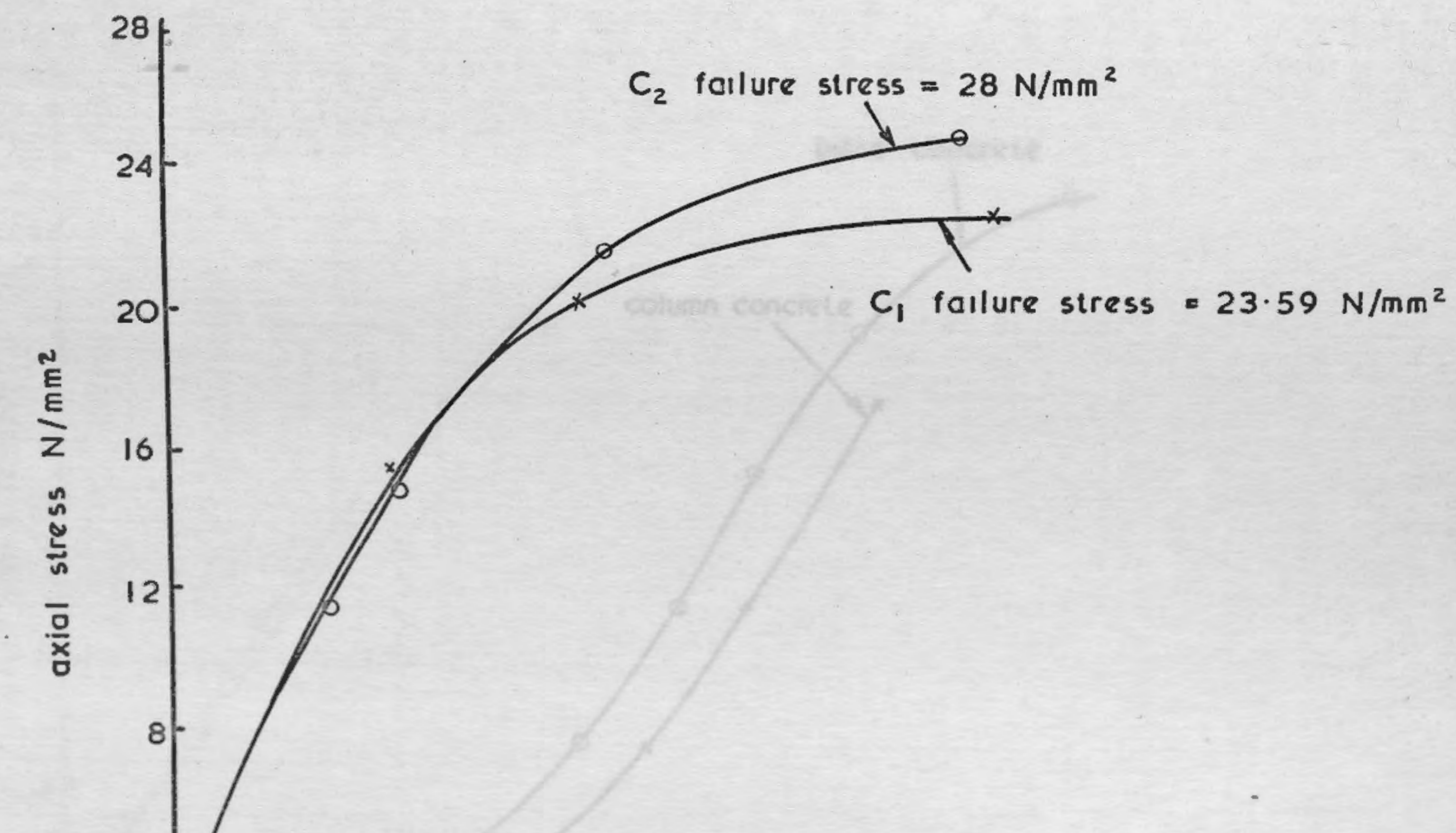

Fig. 4.2. 1e Axial stress v. lateral strain measured on cylinders for base concrete by electrical resistance strain gauges

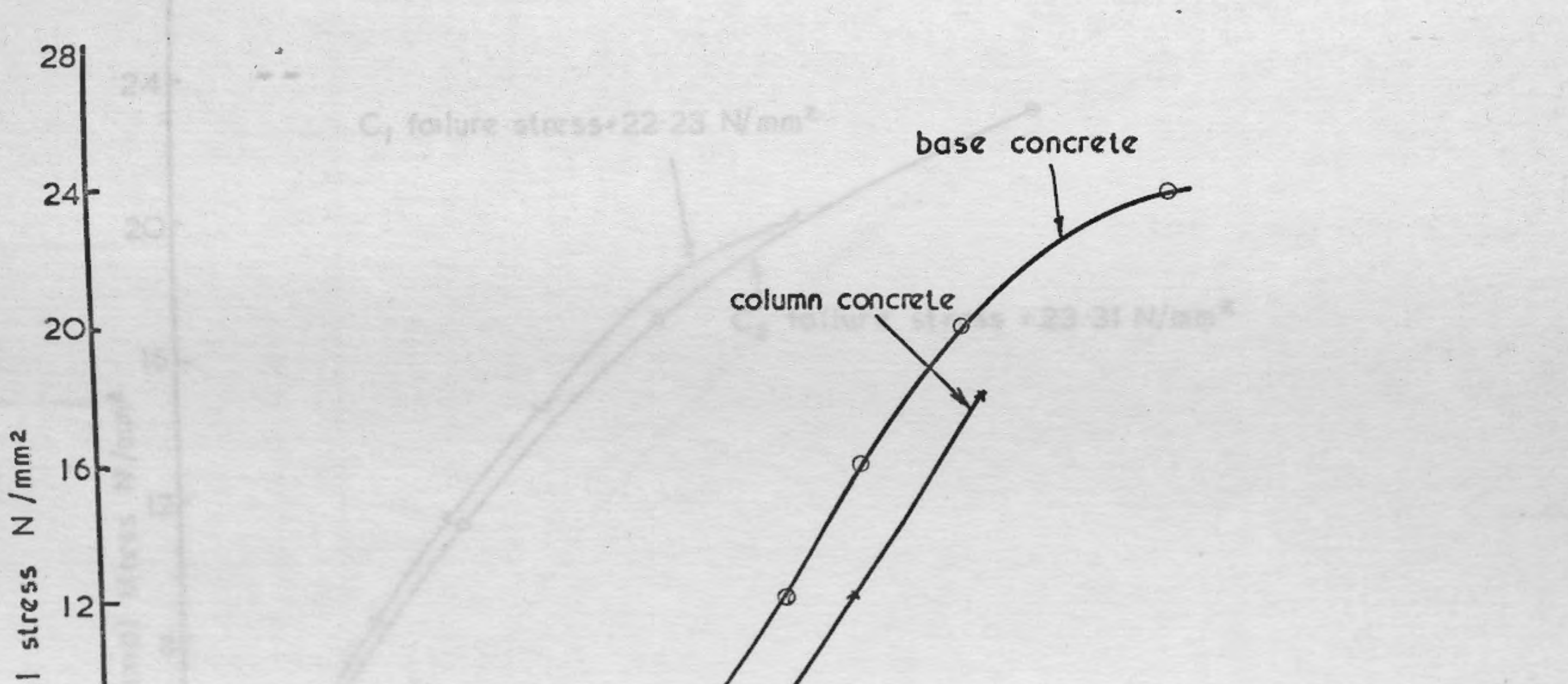

Fig. 4.2. 1f Axial stress v. Poissons ratio νc for column concrete and base concrete

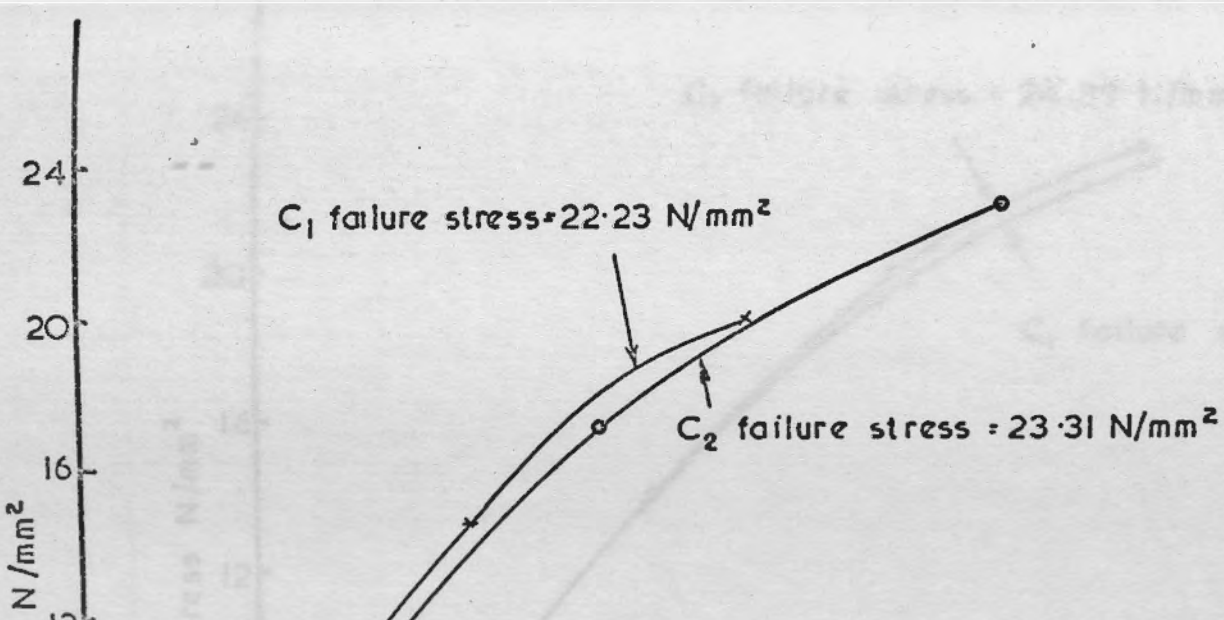

Fig. 4.2. 2a. Axial stress v longitudinal strain measured on cylinders for column concrete by electrical resistance strain gauges

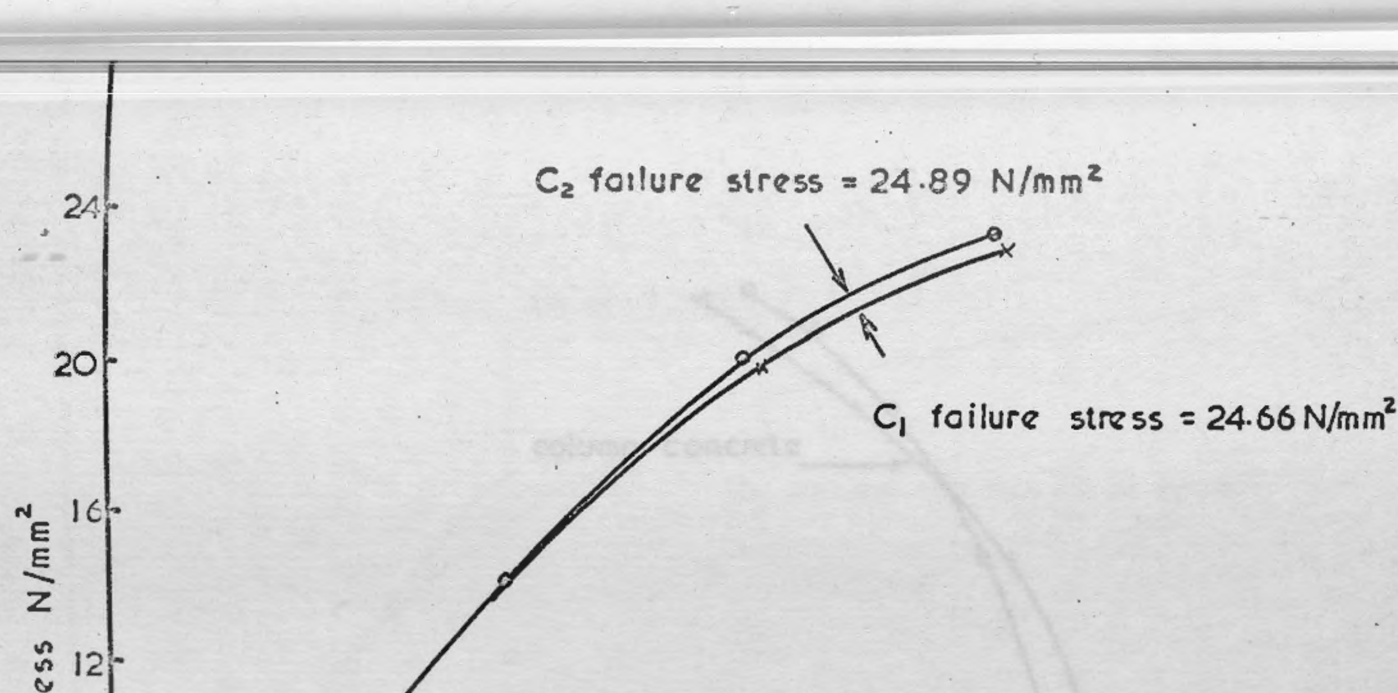

Fig. 4.2 .2b. Axial stress v. longitudinal strain measured on cylinders for base concrete by electrical resistance strain gauges.

Fig.4.2. 2c. Axial stress v. Modulus of elasticity for column concrete and for base concrete

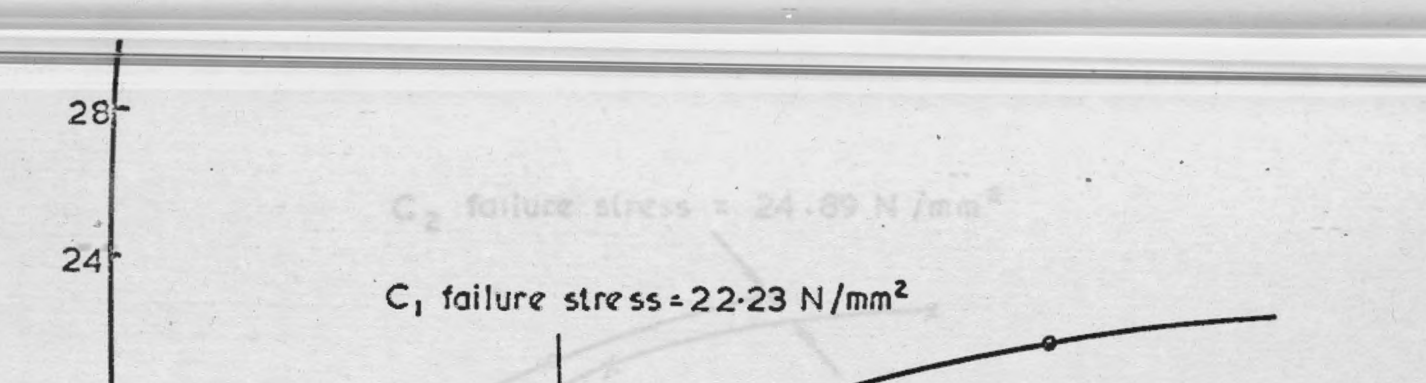

Fig. 4.2.2d. Axial stress v. lateral strain measured on cylinders for column concrete by electrical resistance strain gauges.

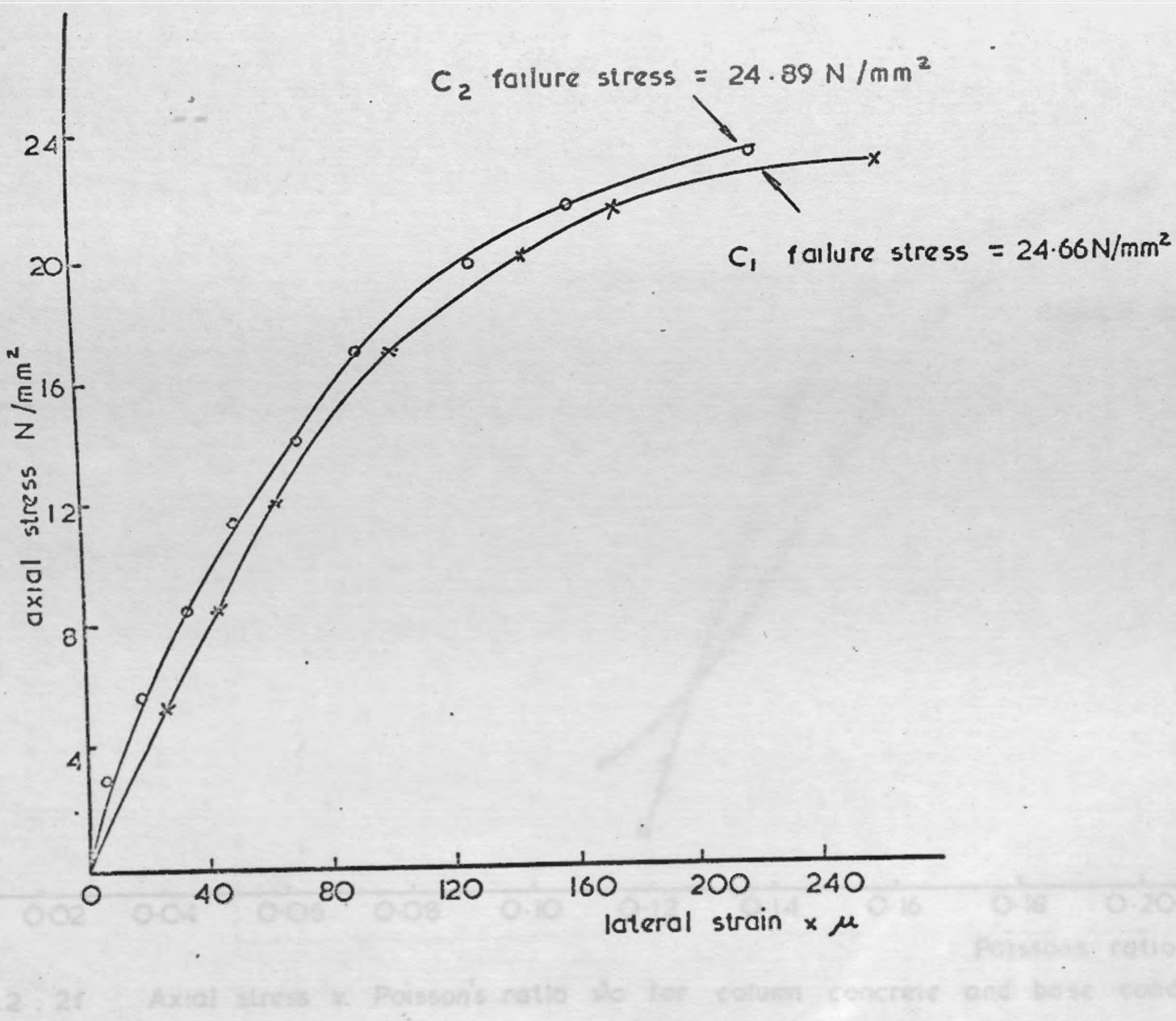

Fig. 4.2 .2e Axial stress v. lateral strain measured on cylinders for base concrete by electrical resistance strain gauges.

Fig. 4.2 . 2f Axial stress v. Poisson's ratio νc for column concrete and base concrete

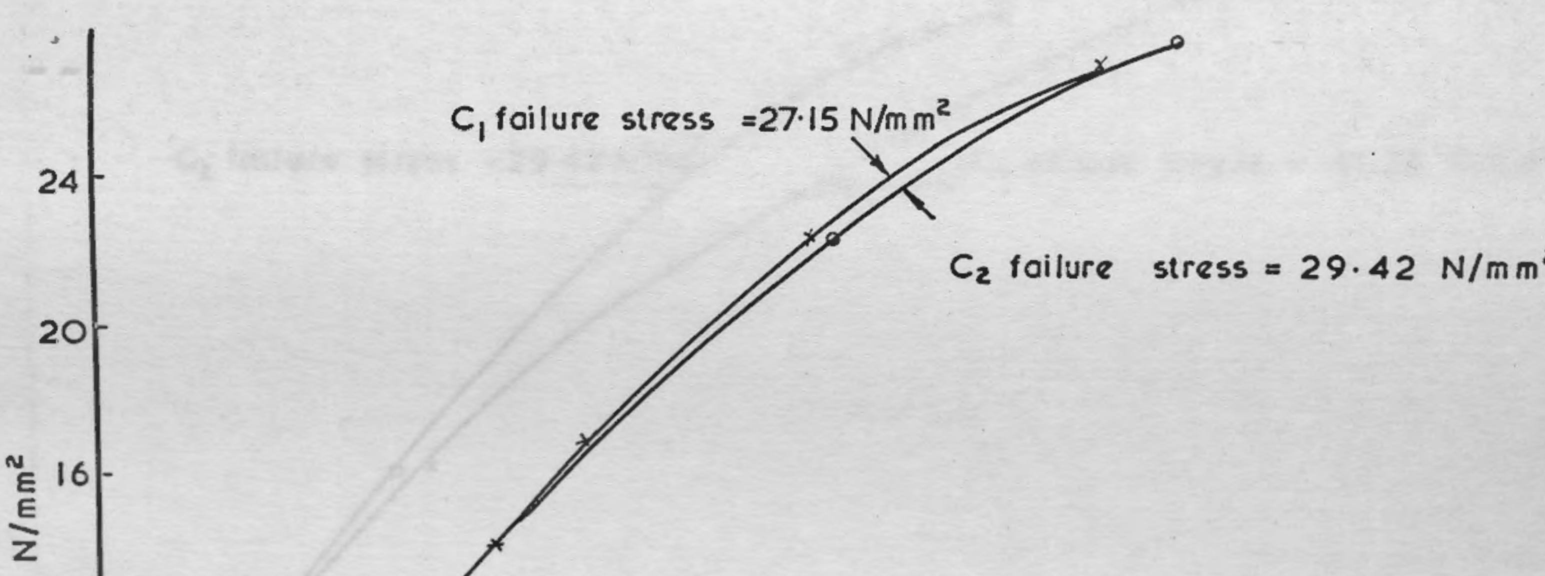

Fig. 4.2.3a. Axial stress v longitudinal strain measured on cylinders for column concrete by electrical resistance strain gauges.

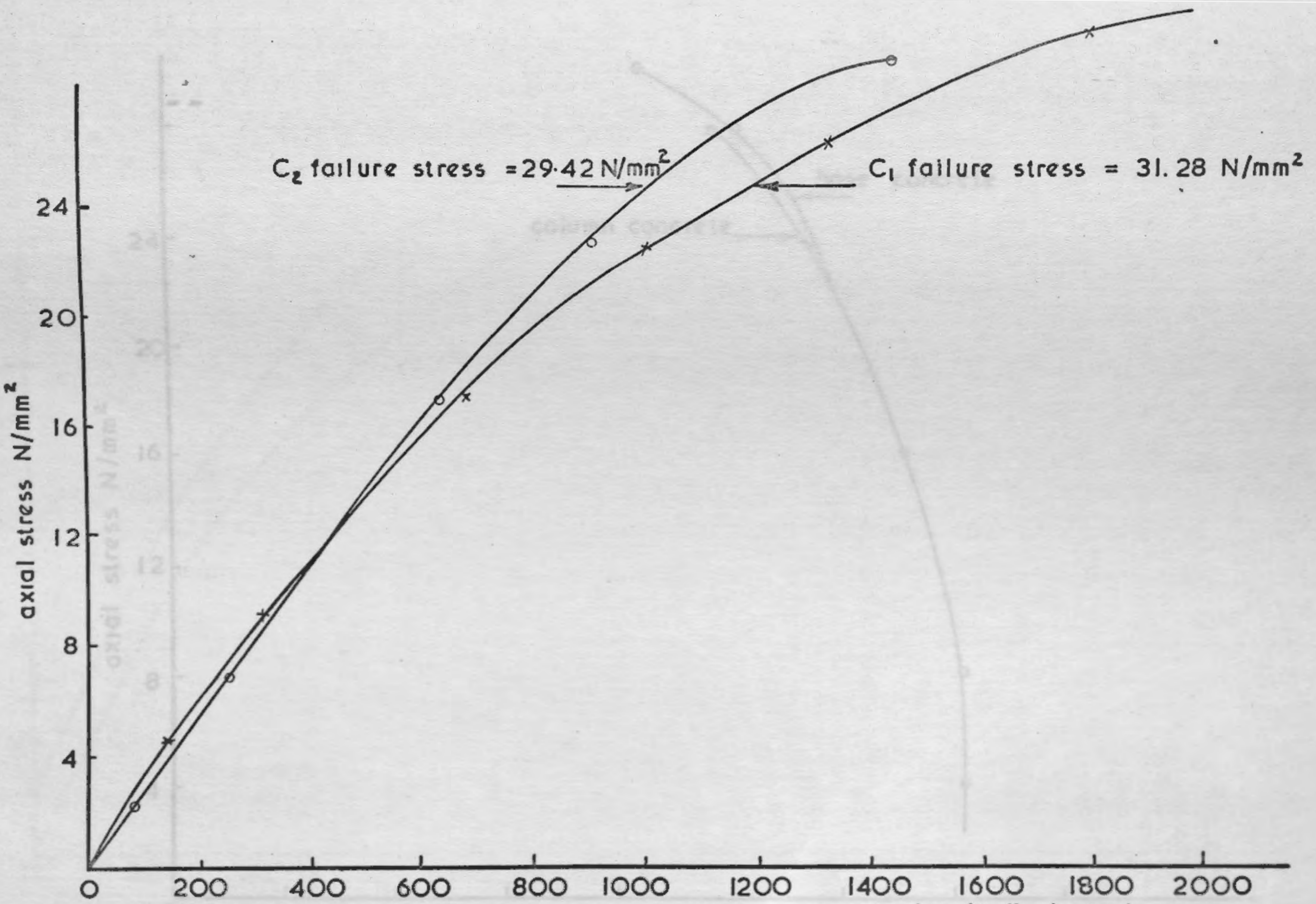

Fig. 4.2.3b. Axial stress v longitudinal strain measured on cylinders for base concrete by electrical resistance strain gauges.

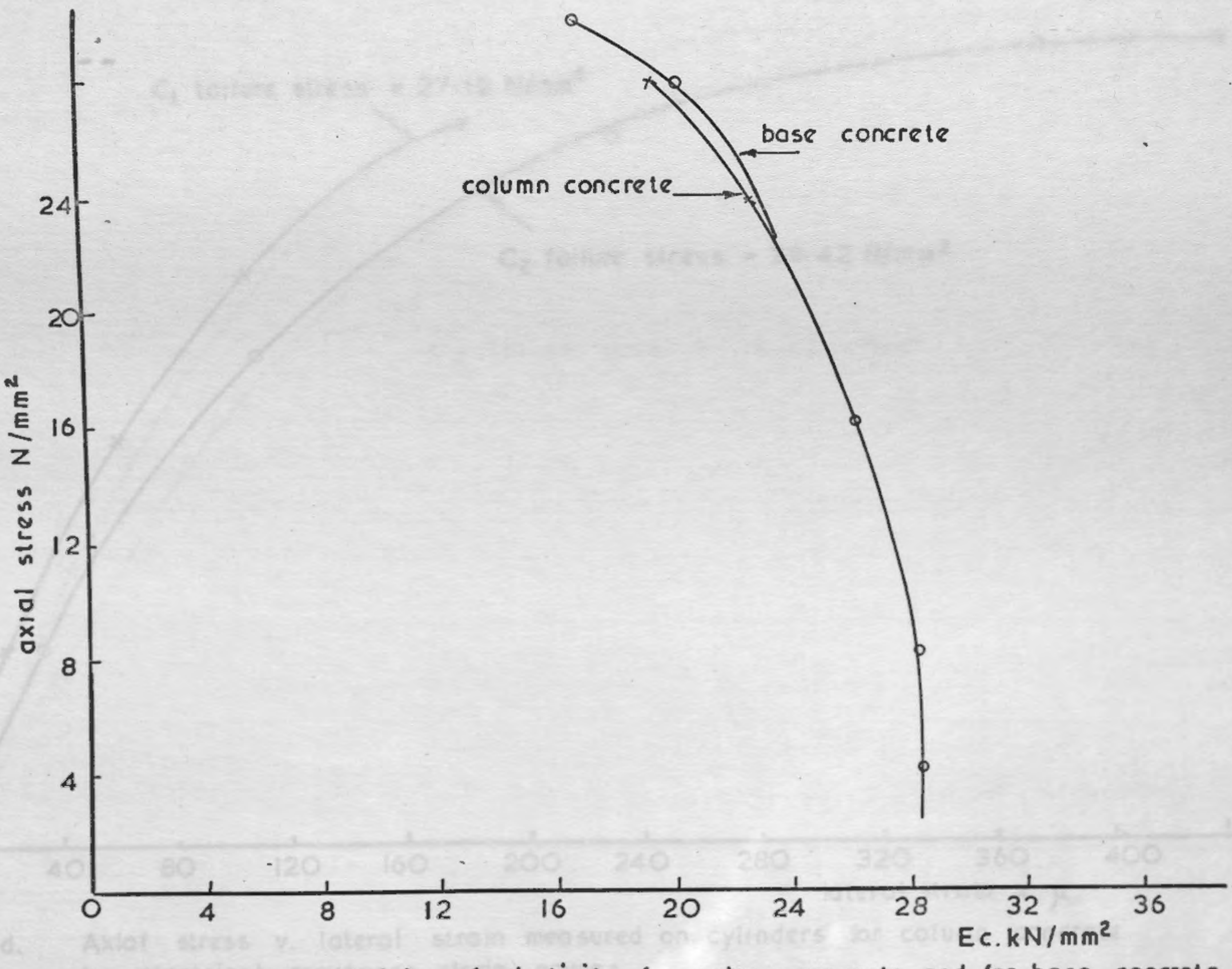

Fig. 4.2. 3c Axial stress v. Modulus of elasticity for column concrete and for base concrete

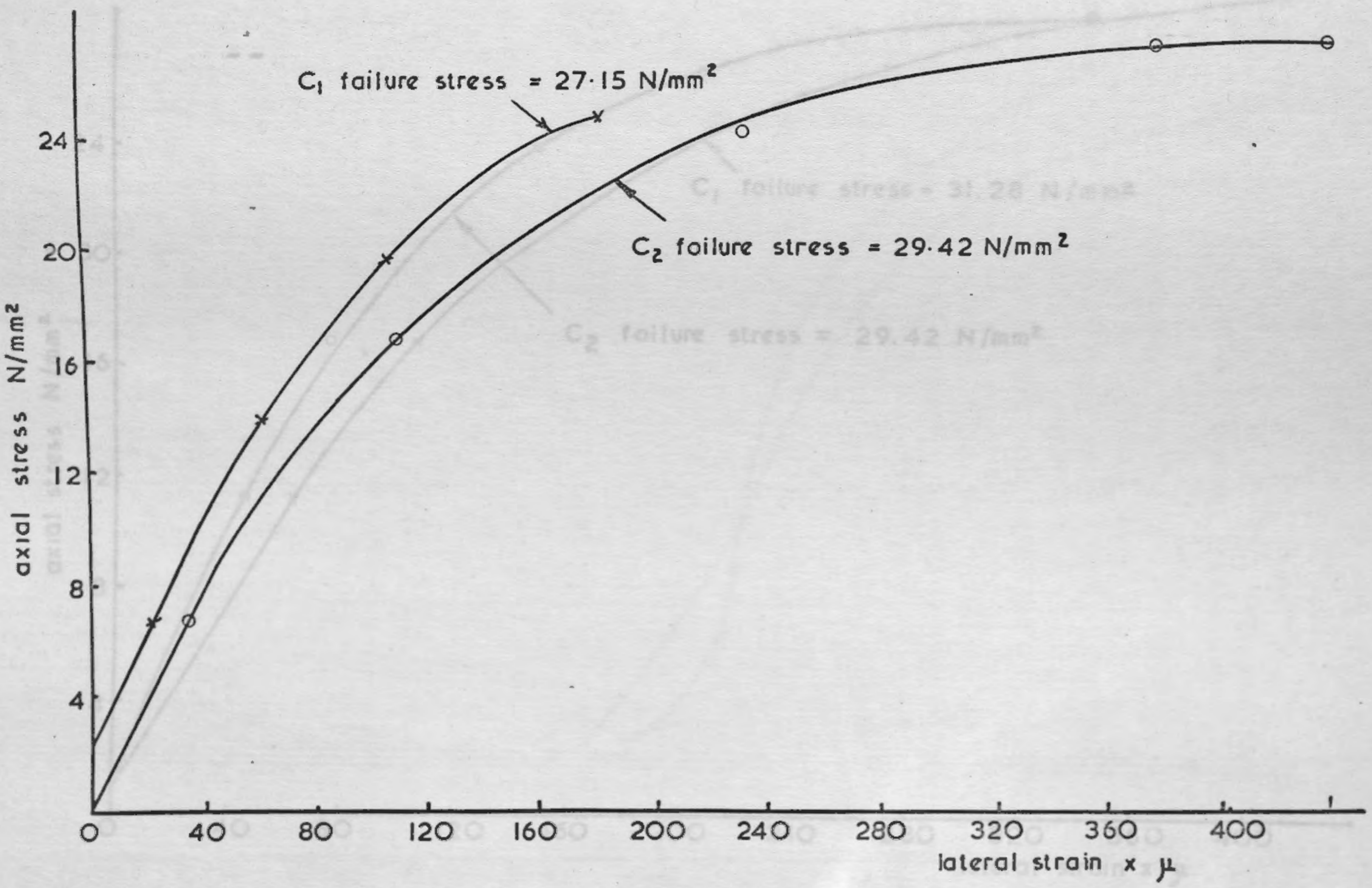

Fig. 4.2 . 3d. Axial stress v. lateral strain measured on cylinders for column concrete by electrical resistance strain gauges.

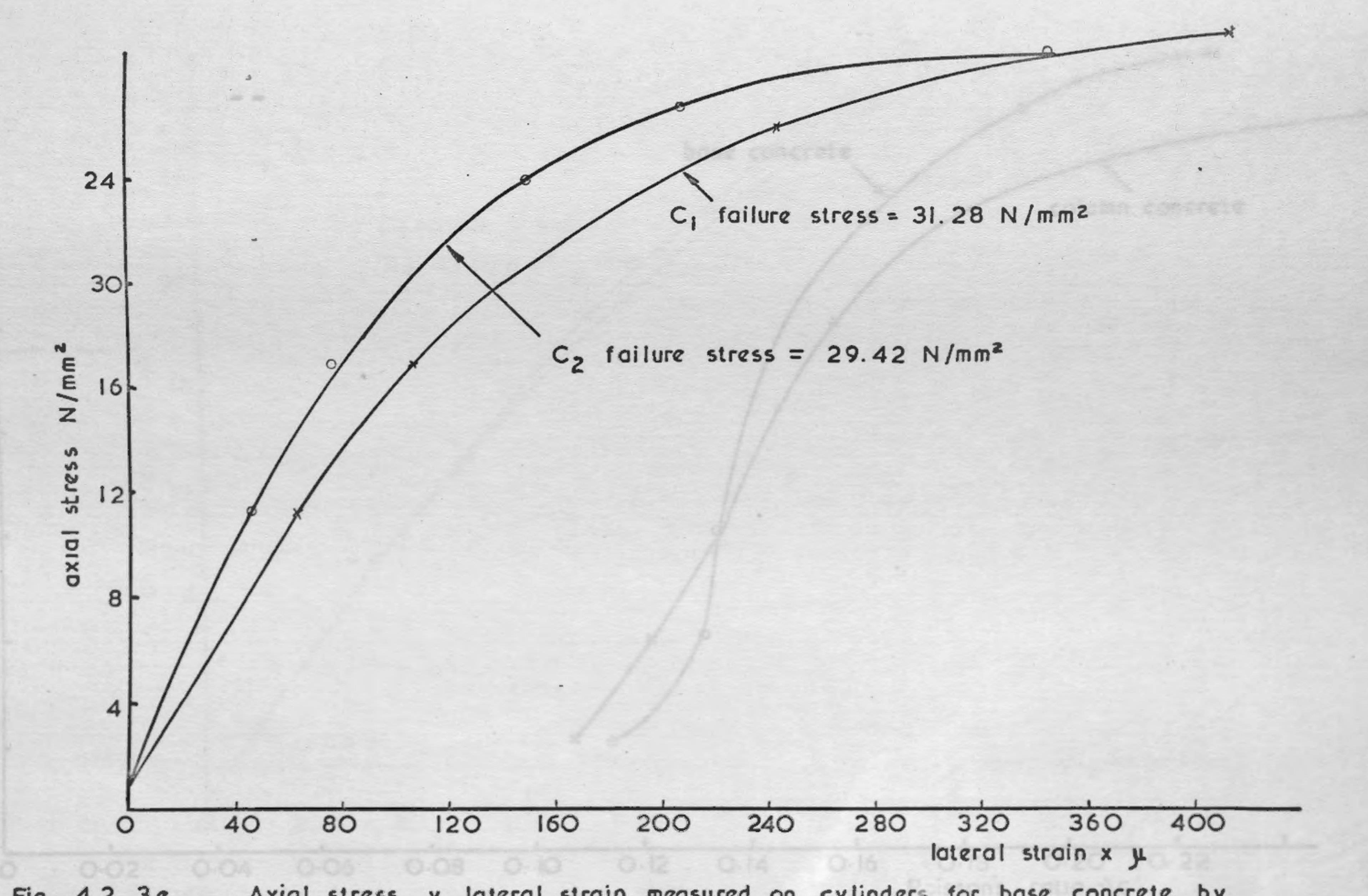

Fig. 4.2.3e. Axial stress v. lateral strain measured on cylinders for base concrete by electrical resistance strain gauges.

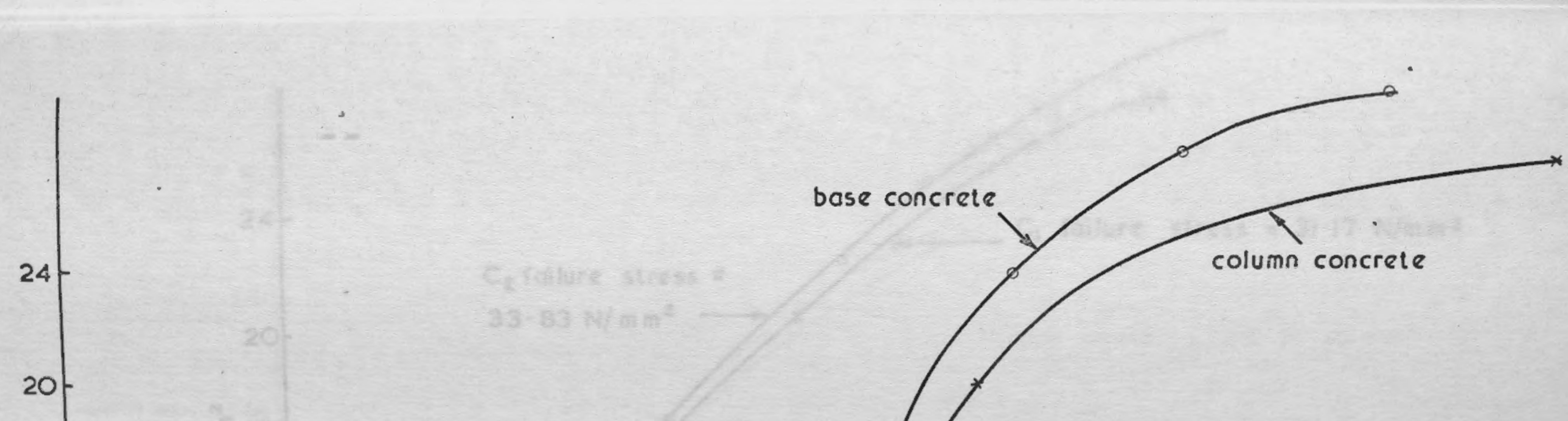

Fig. 4.2. 3f Axial stress v. Poisson's ratio νc for column concrete and base concrete.

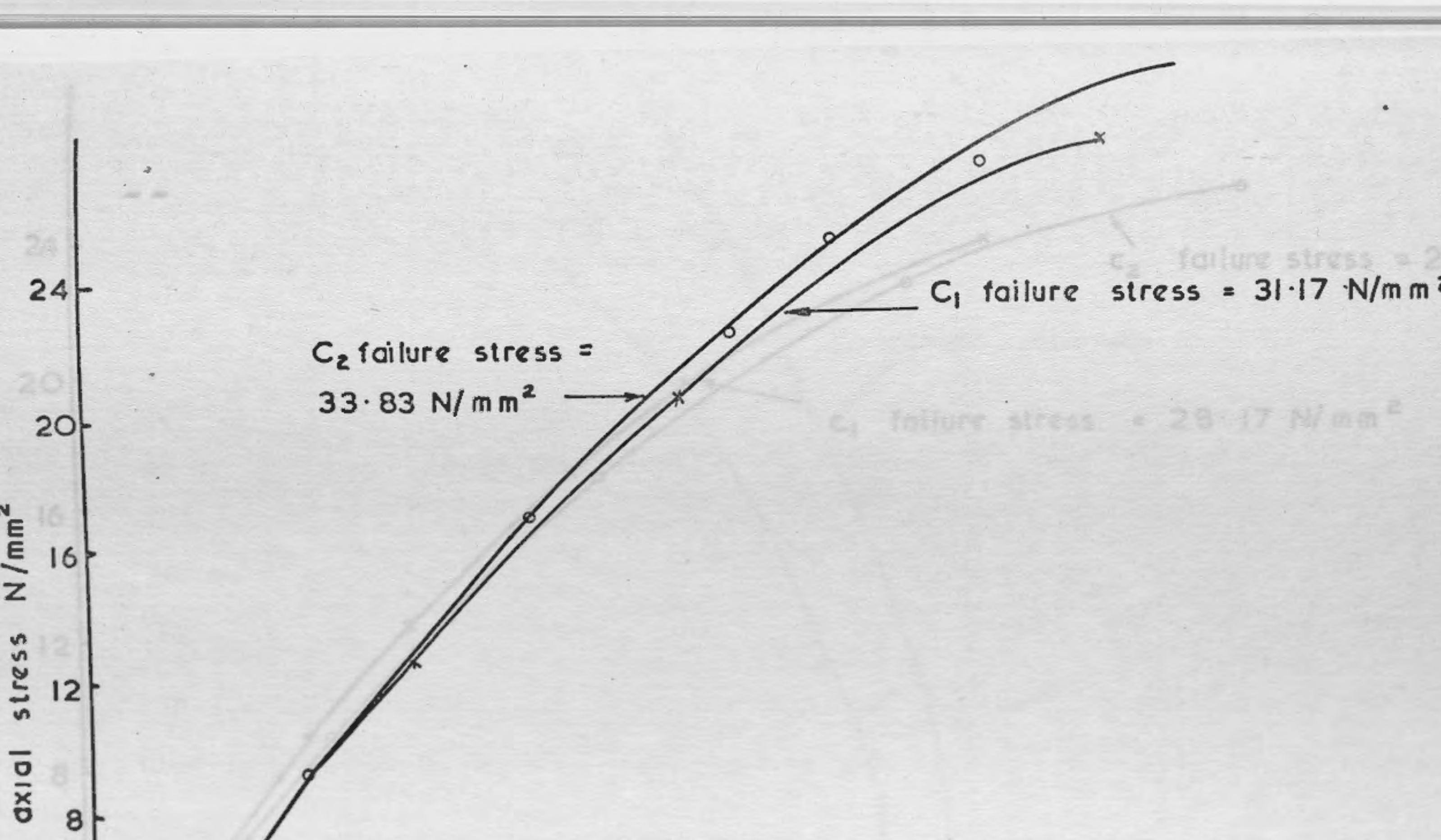

Fig. 4.2 . 4a. Axial stress v. longitudinal strain measured on cylinders for column concrete by electrical resistance strain gauges.

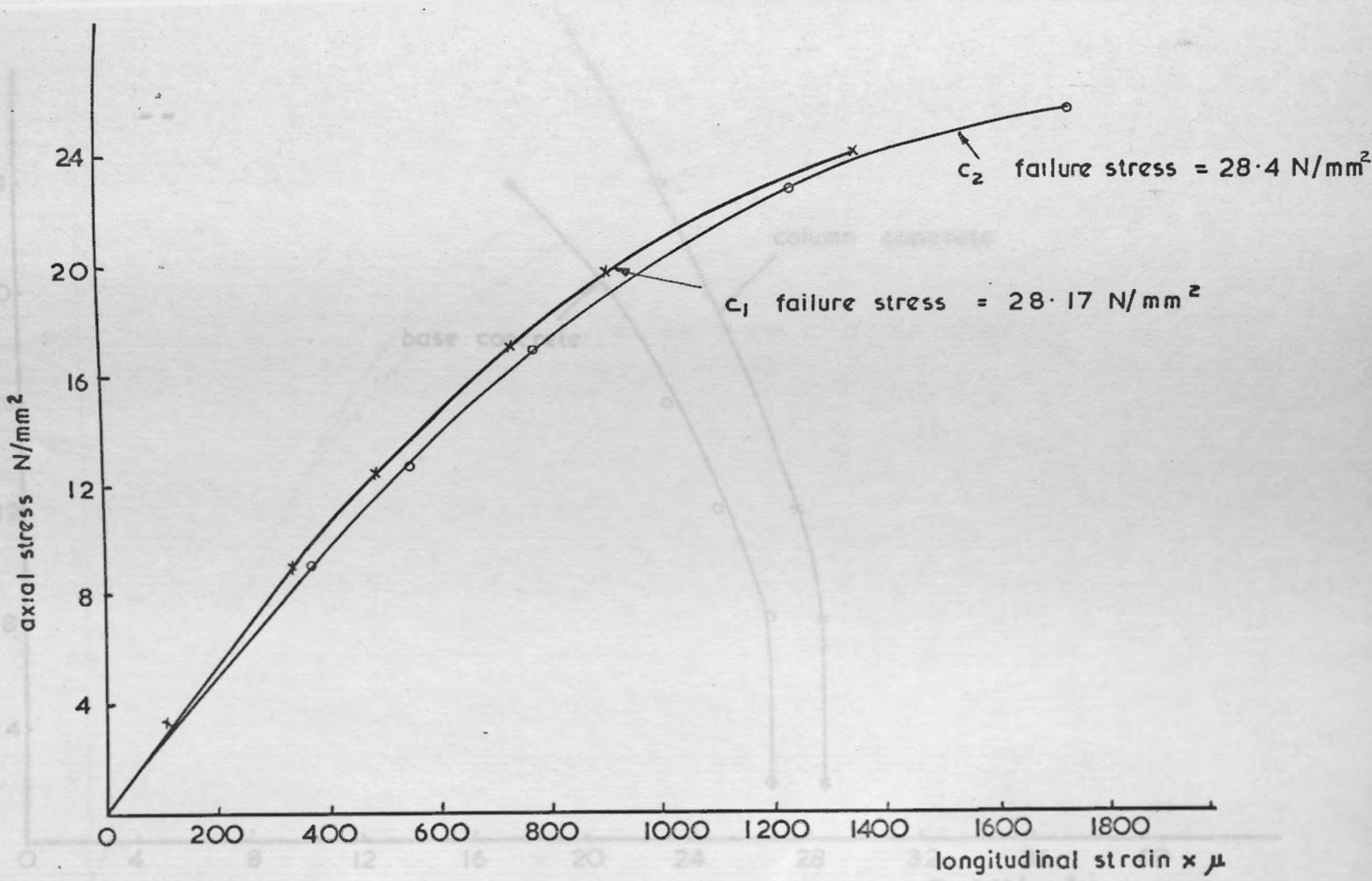

Fig. 4.2.4b. Axial stress v. longitudinal strain measured on cylinders for base concrete by electrical resistance strain gauges.

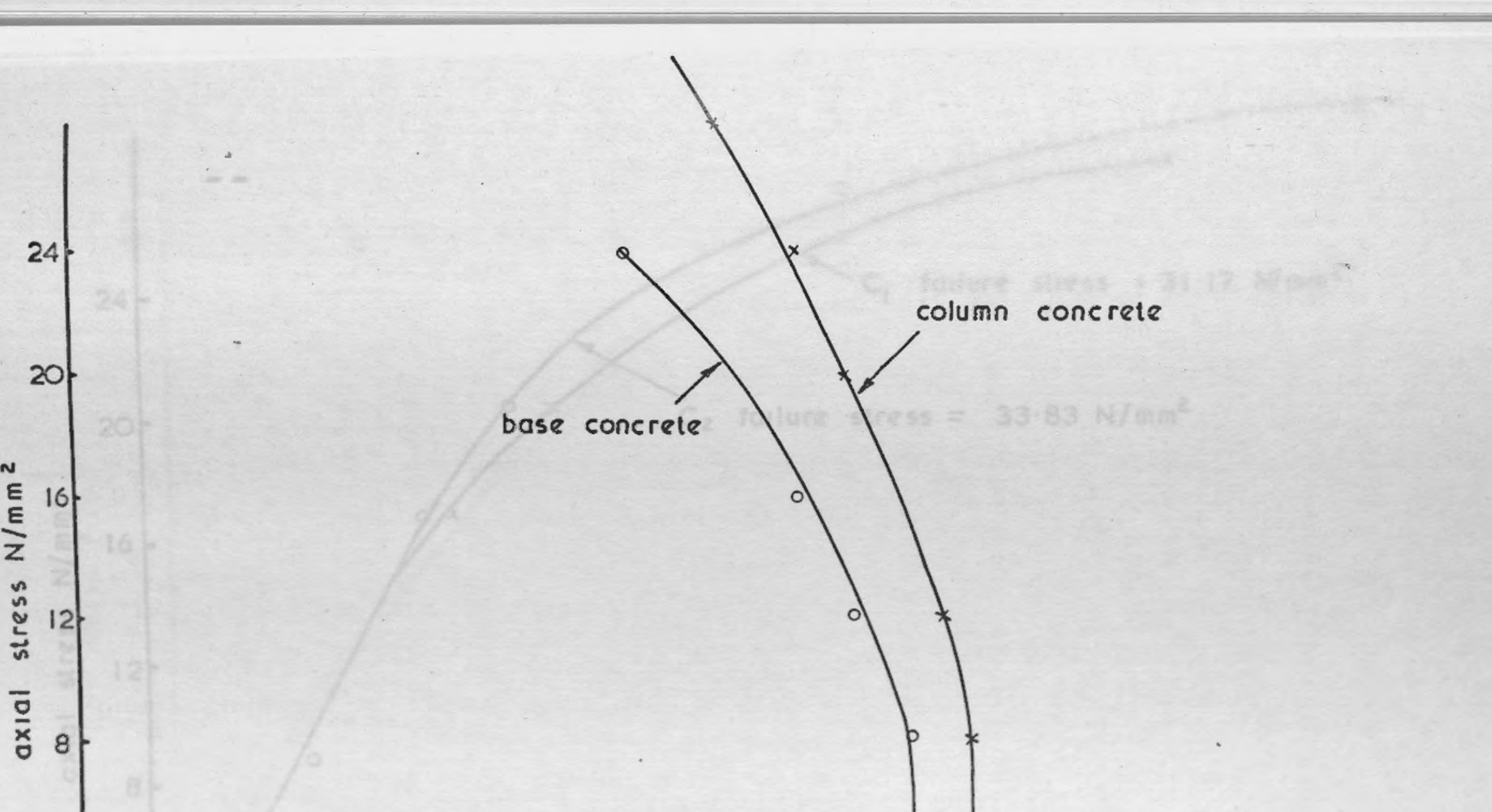

Fig. 4.2. 4c. Axial stress v. Modulus of elasticity for column concrete and for base concrete

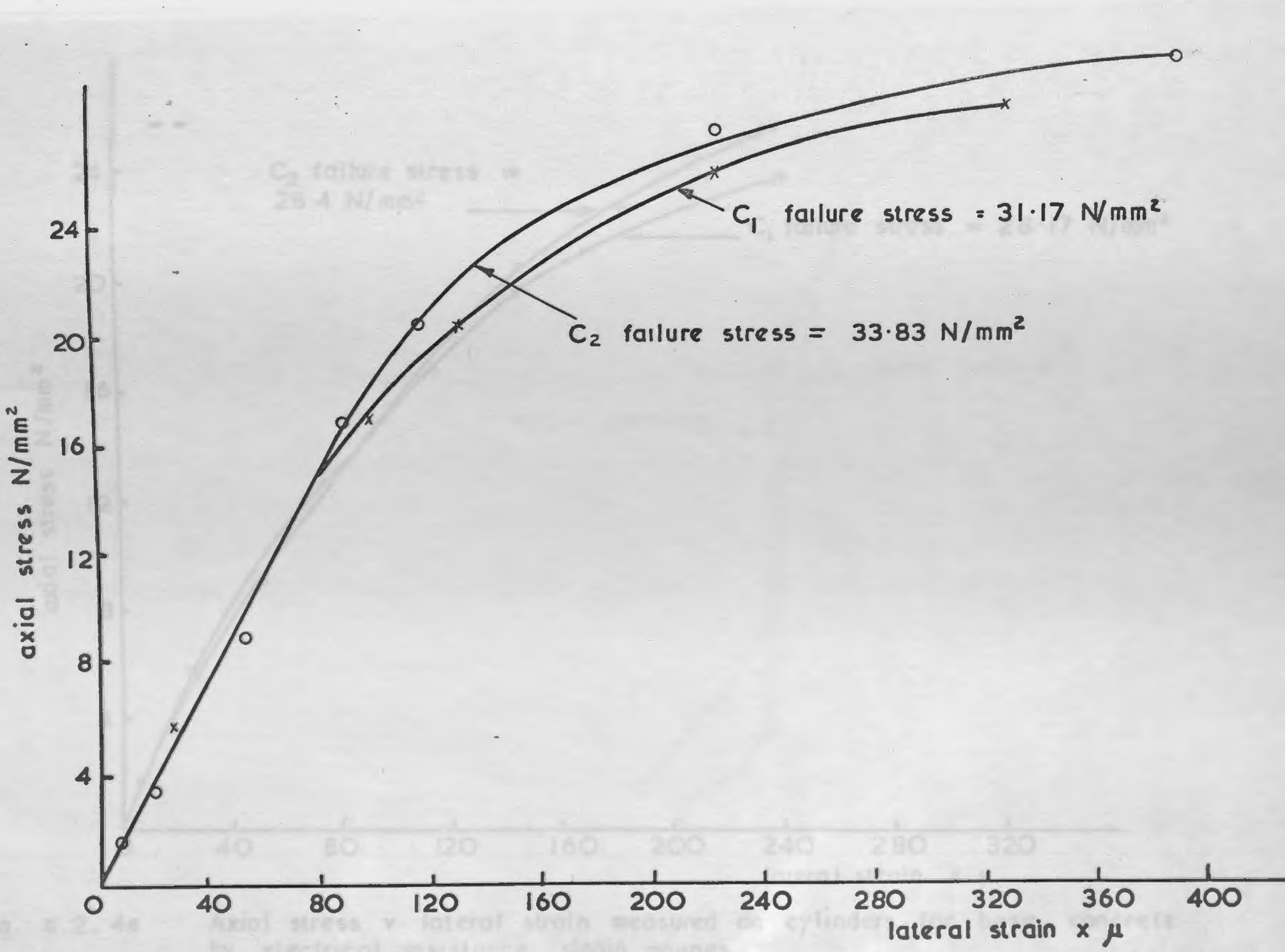

Fig. 4.2 . 4d. Axial stress v. lateral strain measured on cylinders for column concrete by electrical resistance strain gauges.

Fig. 4.2.4e Axial stress v lateral strain measured on cylinders for base concrete by electrical resistance strain gauges.

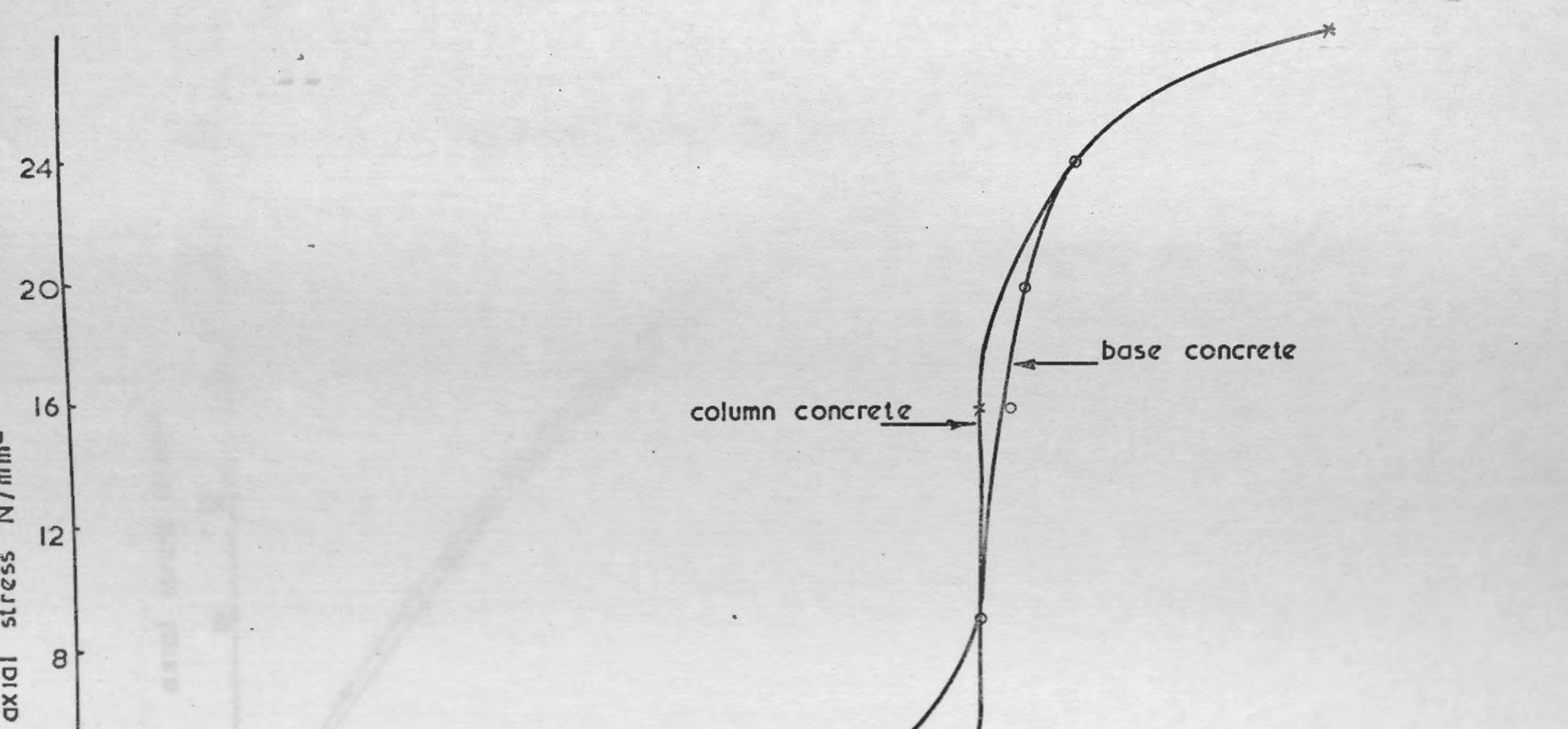

Fig. 4.2. 4f. Axial stress v. Poissons ratio νc for column concrete and base concrete

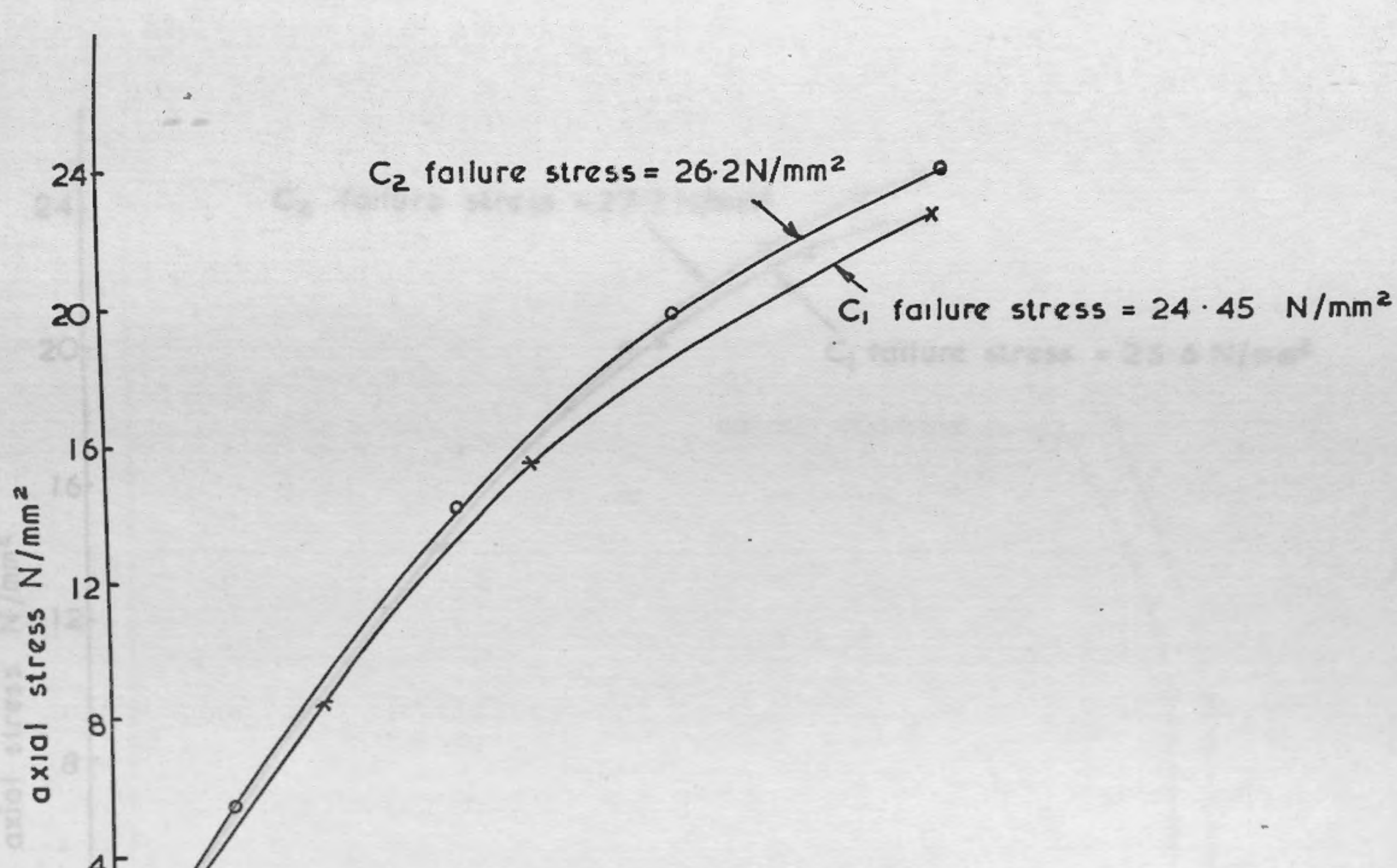

Fig. 4.2 . 5a. Axial stress v. longitudinal strain measured on cylinders for column concrete by electrical resistance strain gauges

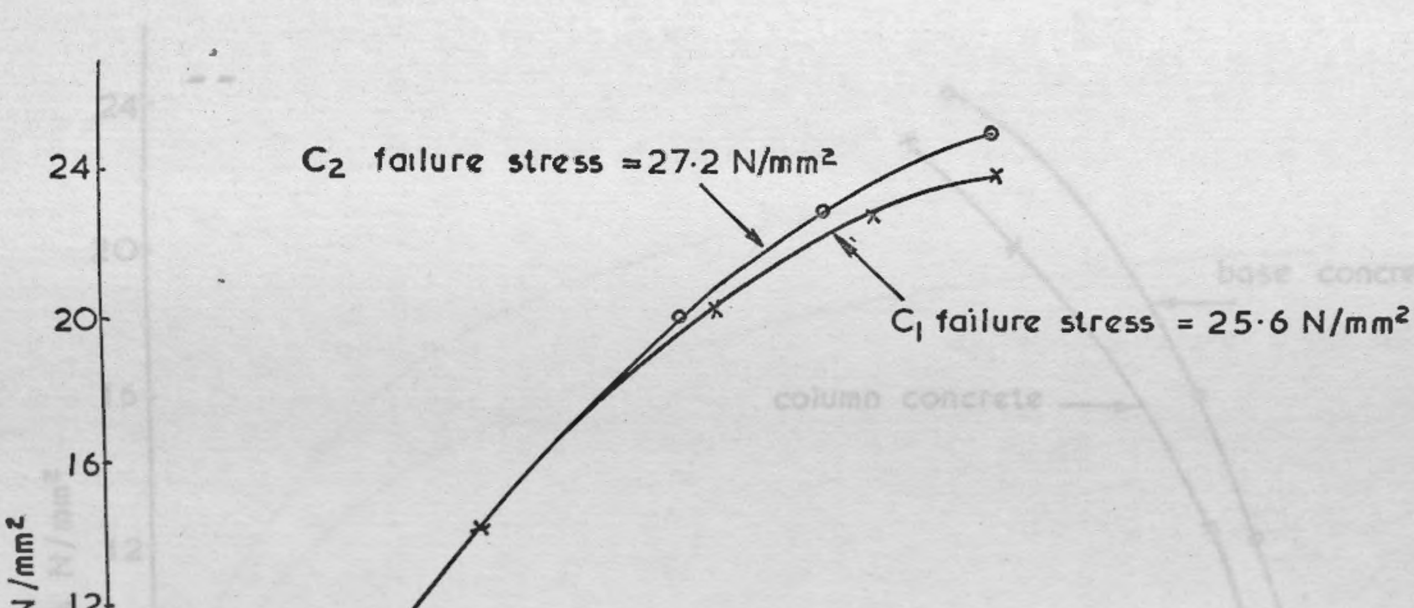

Fig.4.2.5b. Axial stress v. longitudinal strain measured on cylinders for base concrete by electrical resistance strain gauges.

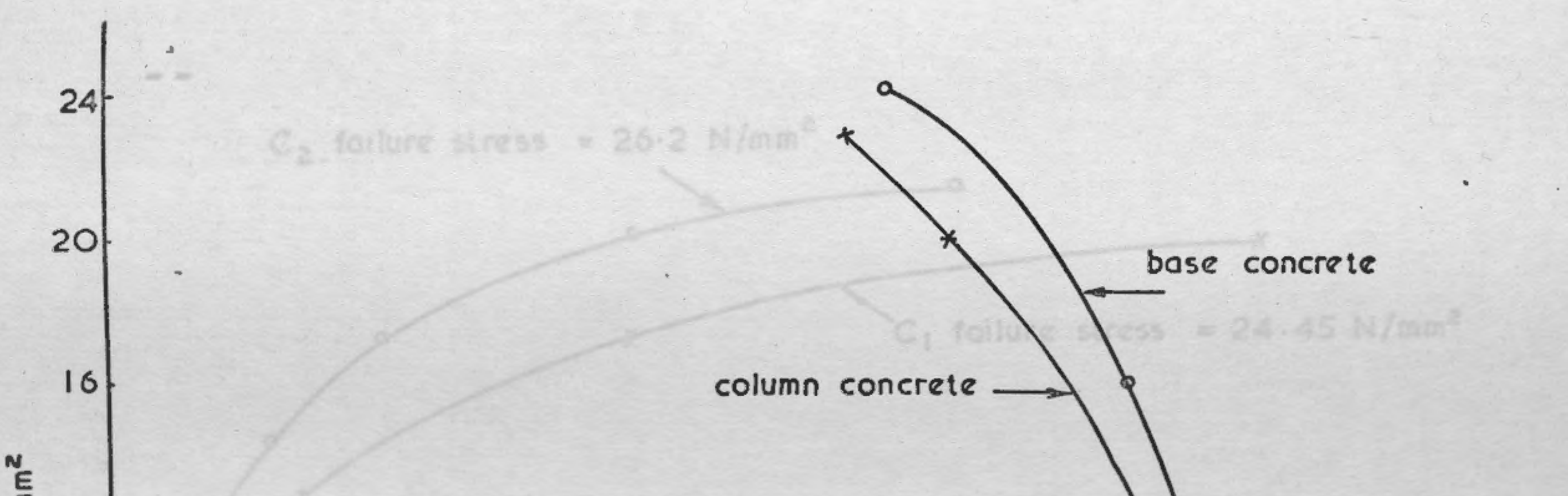

Fig. 4.2.5c Axial stress v. Modulus of elasticity for column concrete and for base concrete

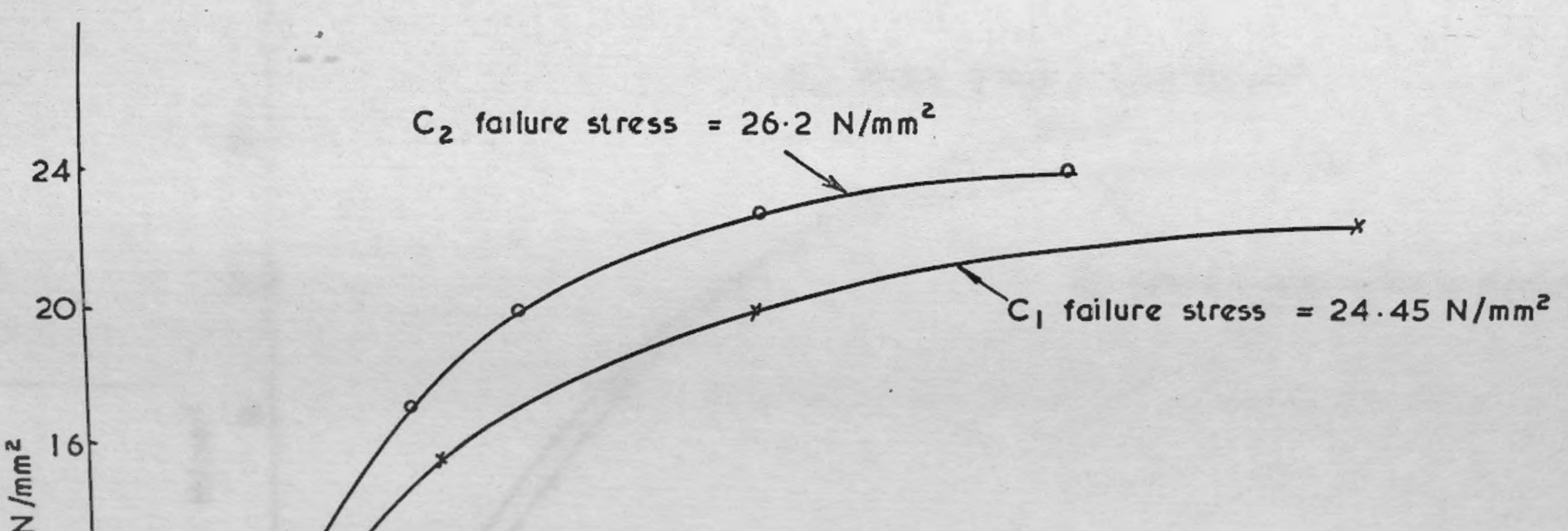

Fig. 4.2. 5d. Axial stress v. lateral strain measured on cylinders for column concrete by electrical resistance strain gauges.

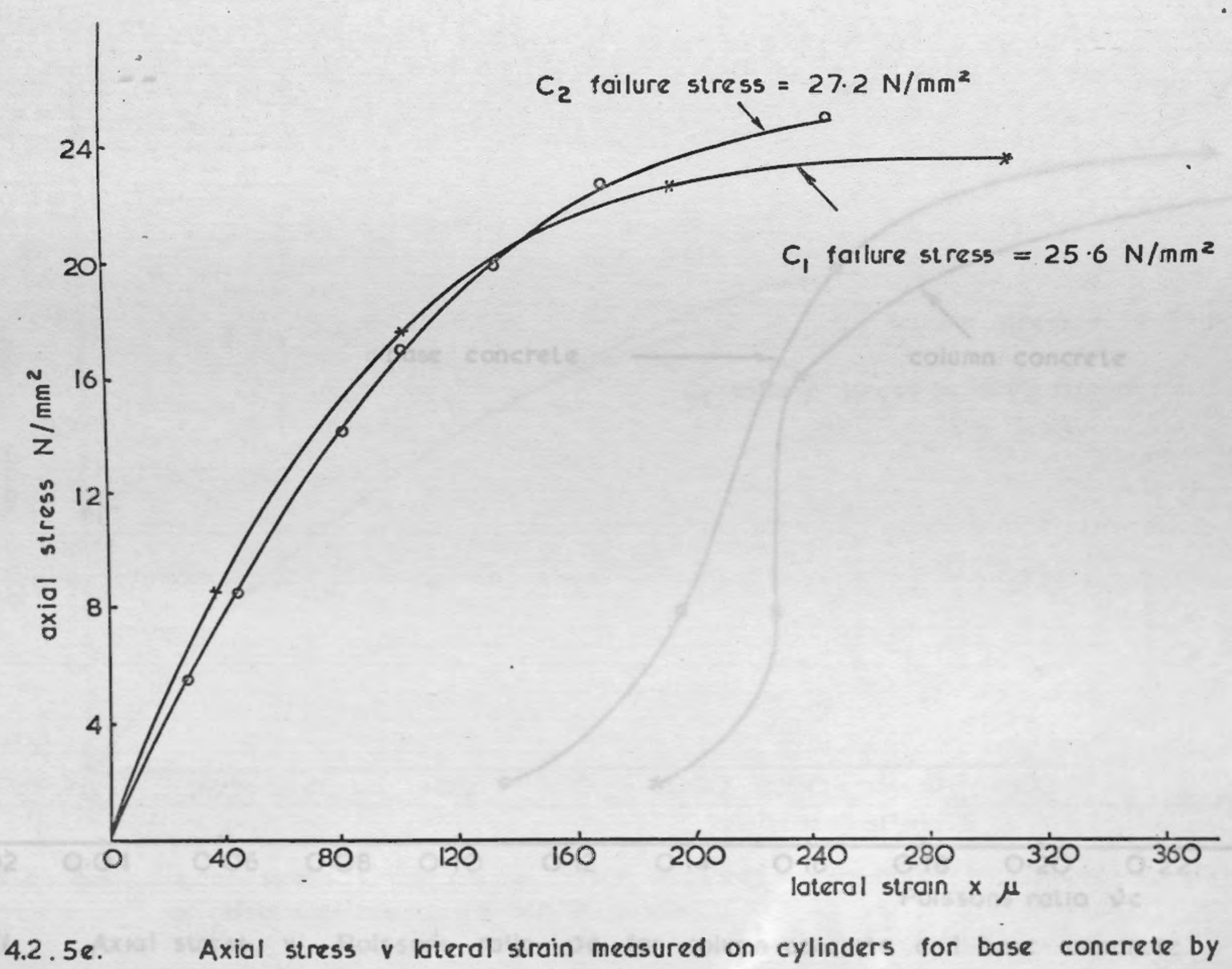

Fig. 4.2.5e. Axial stress v lateral strain measured on cylinders for base concrete by electrical resistance strain gauges

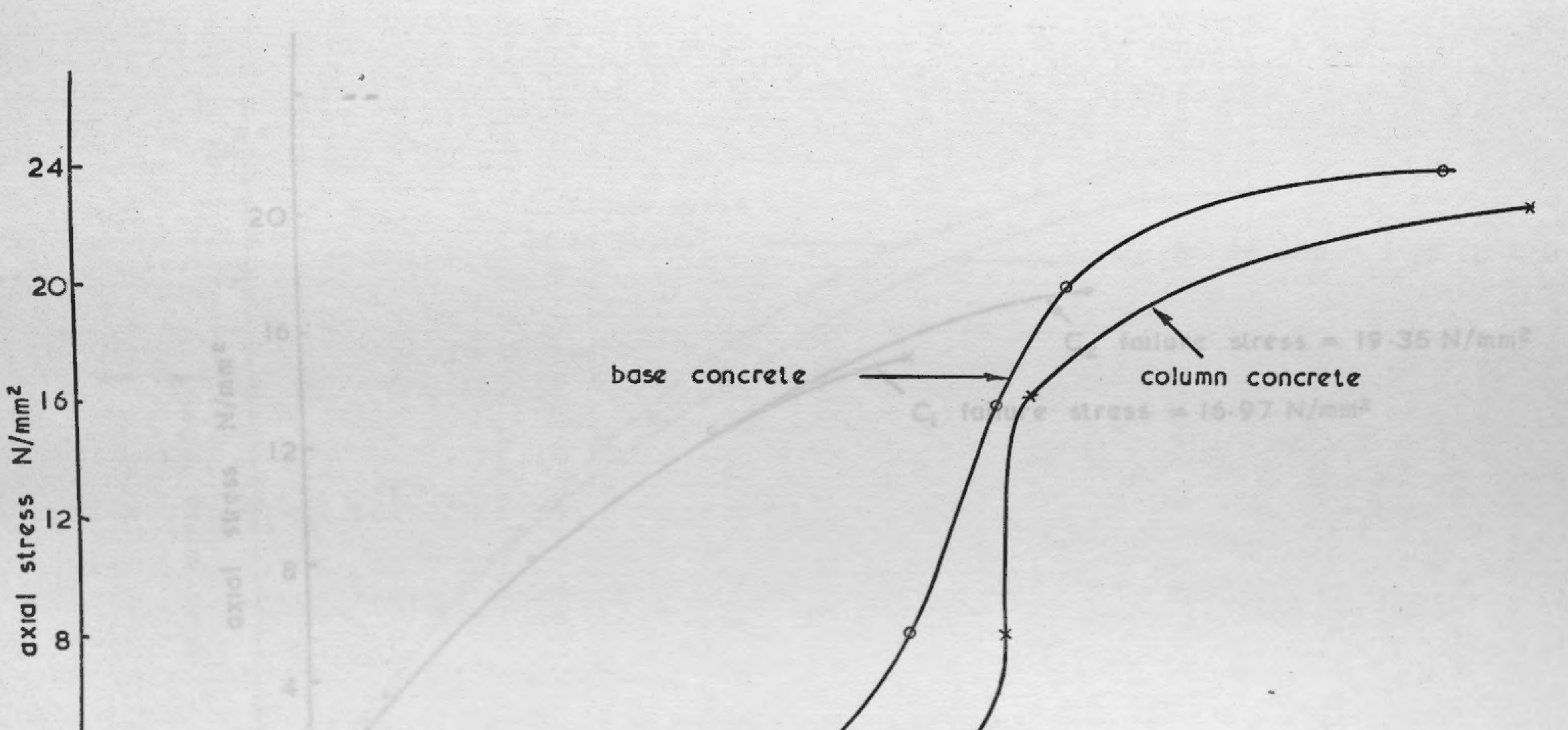

Fig. 4.2.5f. Axial stress v. Poisson's ratio νc for column concrete and base concrete

Fig. 4.2 . 6a. Axial stress v. longitudinal strain measured on cylinders for column concrete by electrical resistance strain gauges

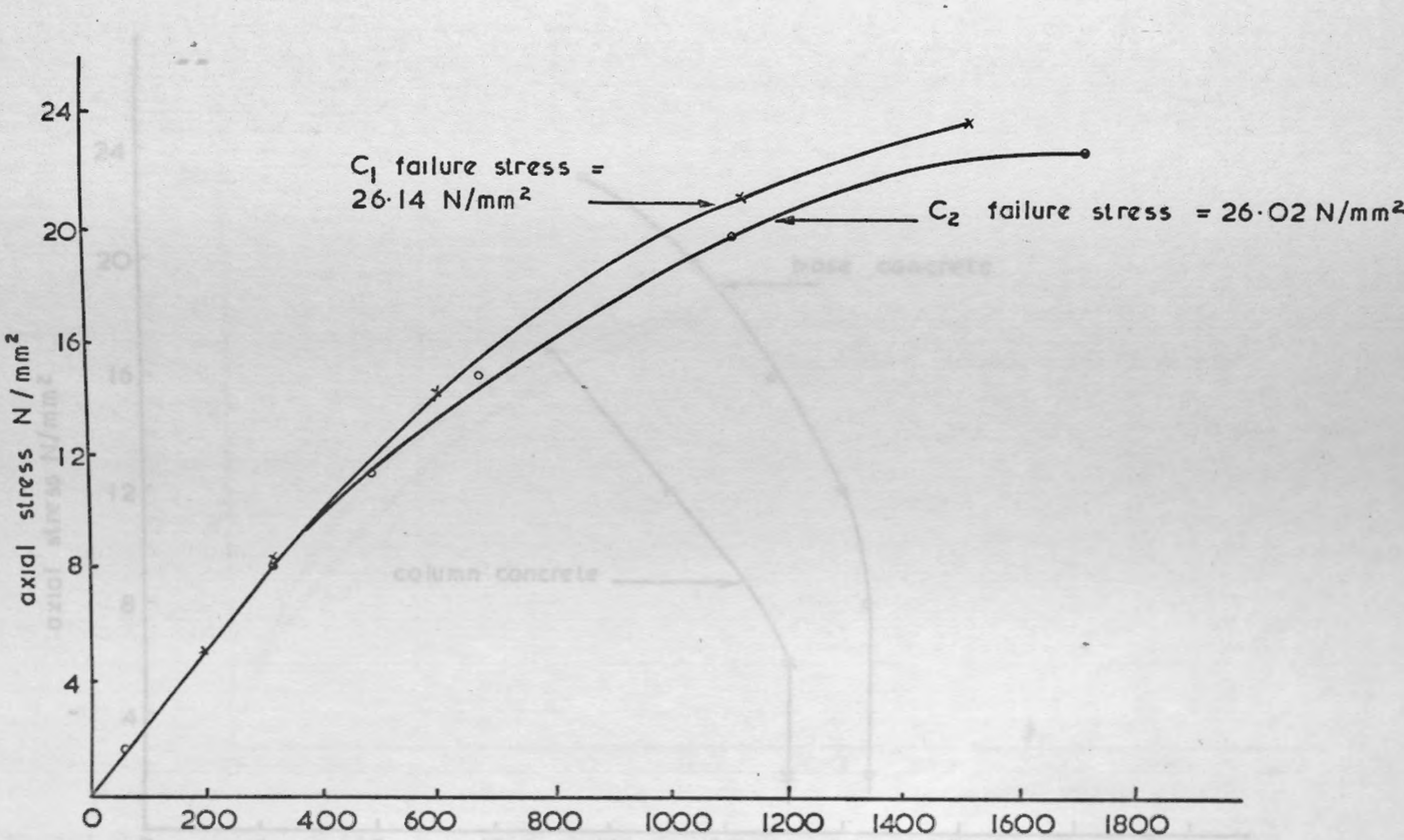

Fig. 4.2.6b. Axial stress v. longitudinal strain measured on cylinders for base concrete by electrical resistance strain gauges

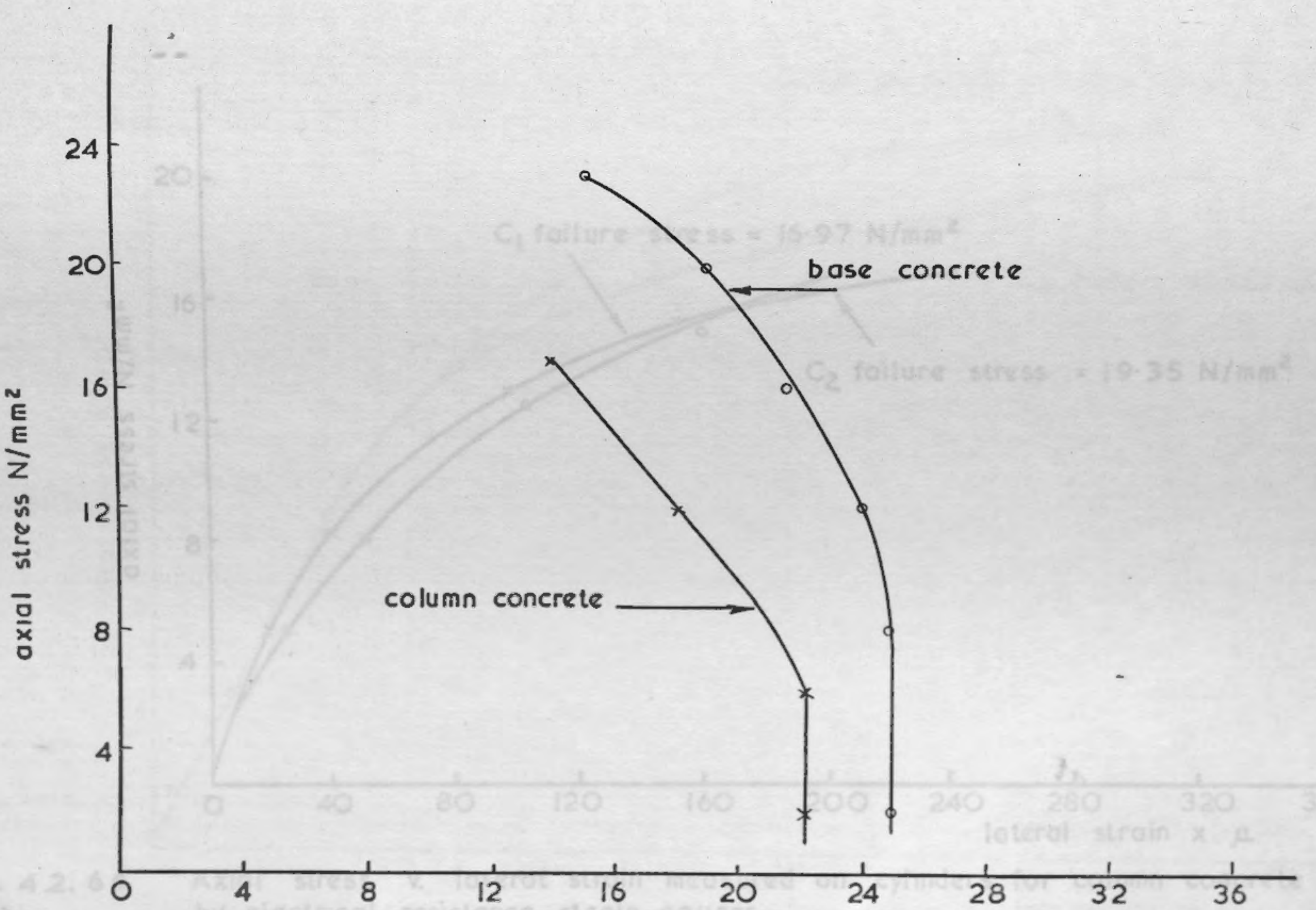

Fig. 4.2. 6c. Axial stress v. Modulus of elasticity for column concrete and for base concrete

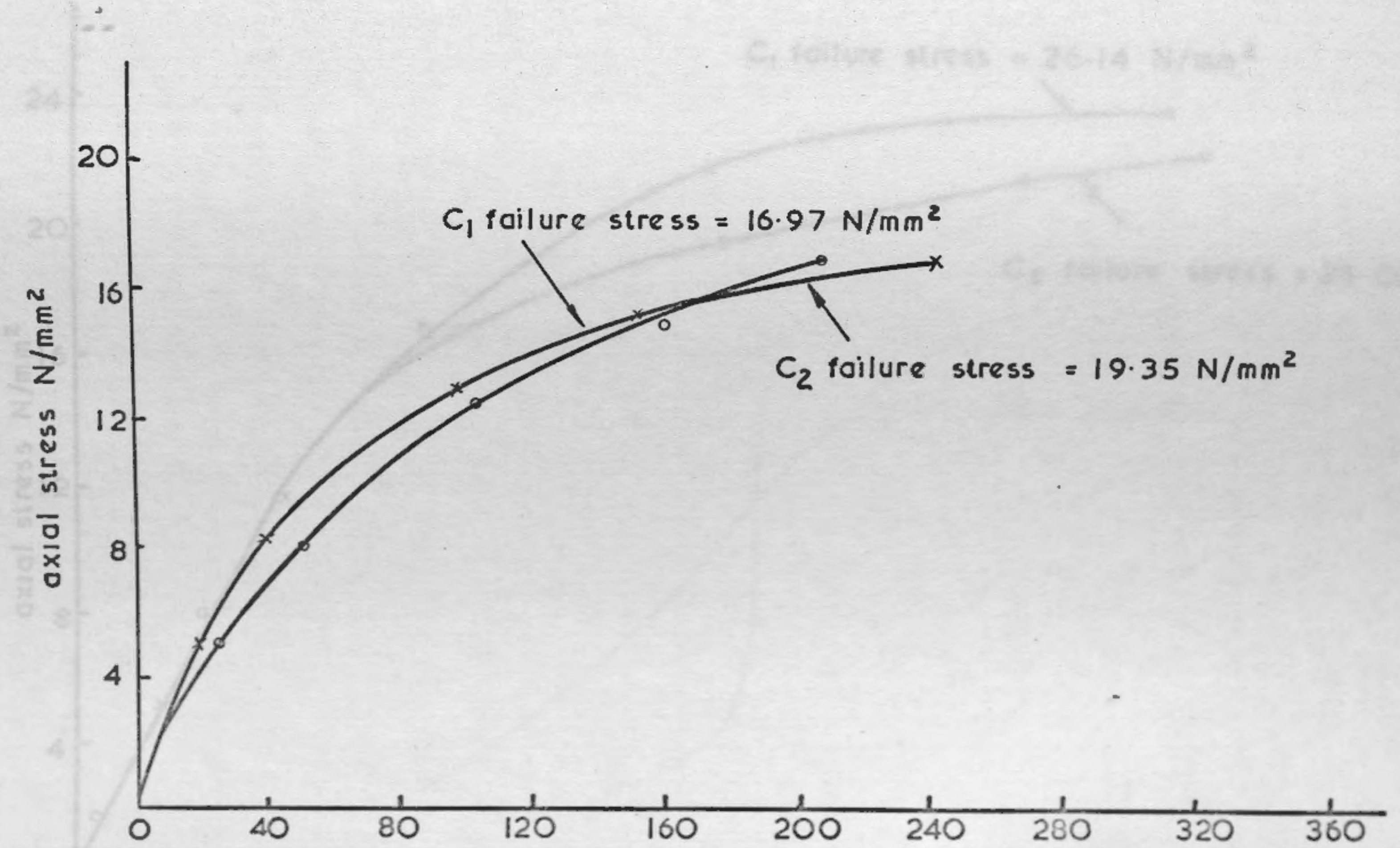

Fig. 4.2. 6d Axial stress v. lateral strain measured on cylinders for column concrete by electrical resistance strain gauges

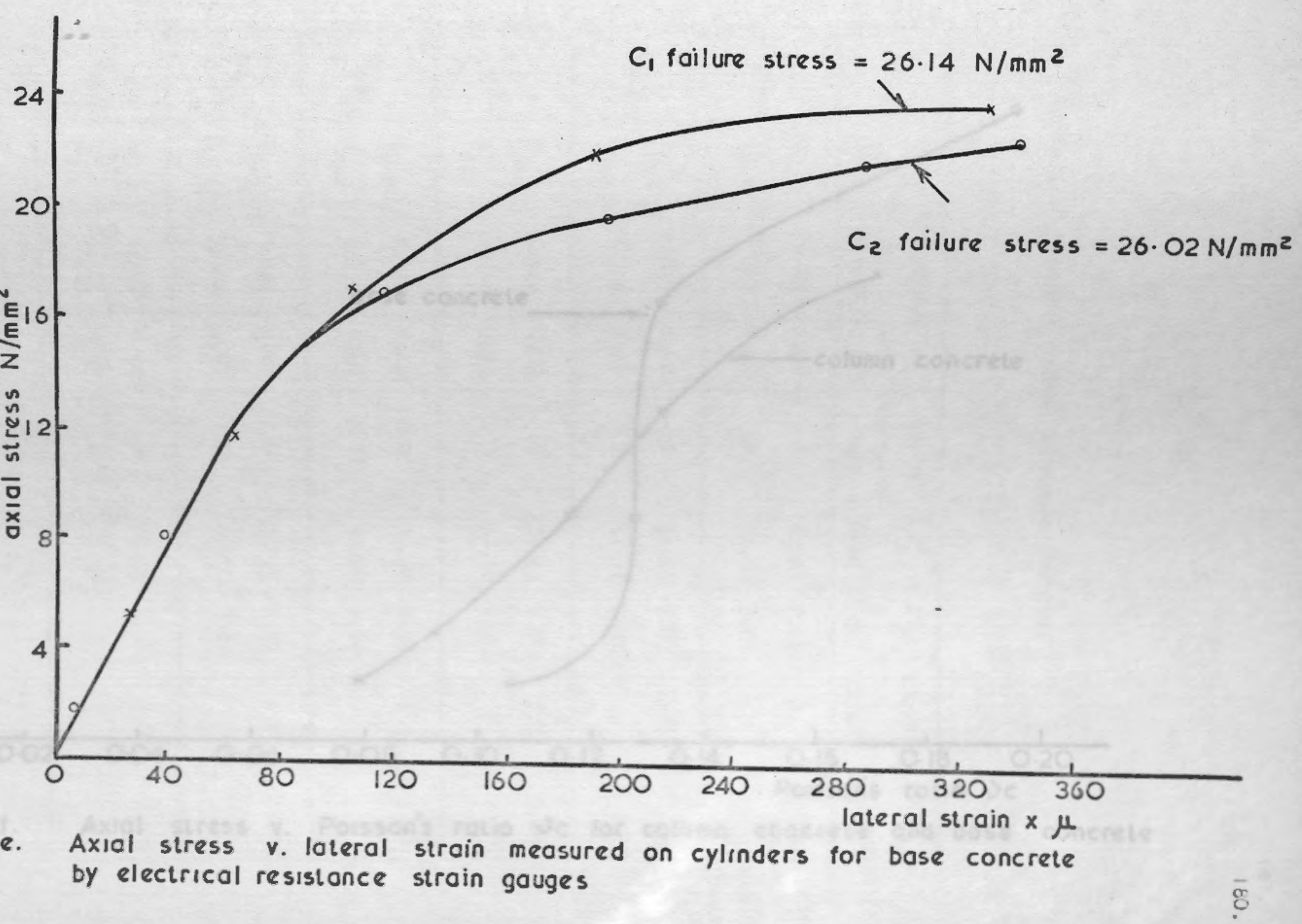

Fig. 4.2.6e. Axial stress v. lateral strain measured on cylinders for base concrete by electrical resistance strain gauges

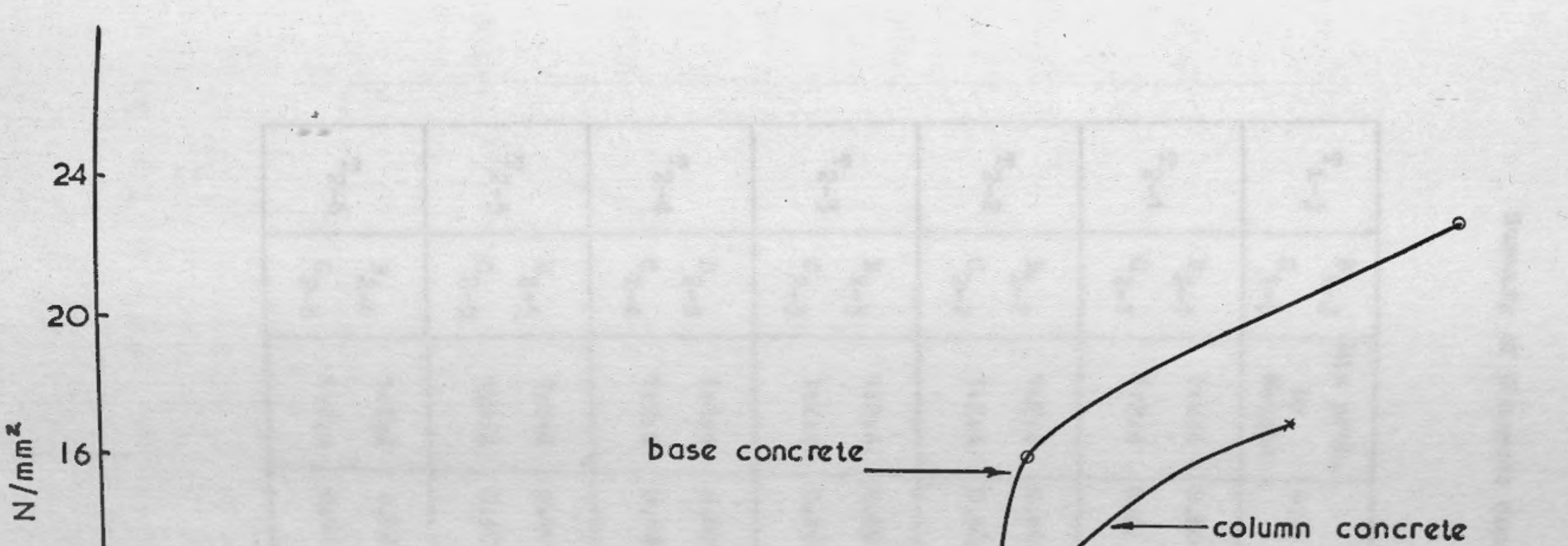

Fig. 4.2. 6f. Axial stress v. Poisson's ratio ν_c for column concrete and base concrete

TABLE 4-2

SERIES (2)

Summary of Concrete Control Specimens Results.

T_{i-j}	B_{i-j} C_{i-j}	Mix prop. by Weight	w/c	Age of Concrete days	f_{cu} N/mm^2	ft N/mm^2	$1+0.05 f_{cu}$ N/mm^2	$\sqrt{f_{cu}}$ N/mm^2
T_{2-1}	B_{2-1}	1:2:4	0.60	8	35.41	2.68	2.77	5.951
	C_{2-1}	1:2:4	0.60	7	32.30	2.49		
T_{2-2}	B_{2-2}	1:2:4	0.60	8	34.25	2.60	2.71	5.852
	C_{2-2}	1:2:4	0.60	7	32.60	2.52		
T_{2-3}	B_{2-3}	1:2:4	0.60	8	34.41	2.66	2.72	5.866
	C_{2-3}	1:2:4	0.60	7	34.12	2.58		
T_{2-4}	B_{2-4}	1:2:4	0.60	8	36.00	2.98	2.80	6.00
	C_{2-4}	1:2:4	0.60	7	40.00	3.04		
T_{2-5}	B_{2-5}	1:2:4	0.60	8	32.70	2.54	2.64	5.718
	C_{2-5}	1:2:4	0.60	7	30.50	2.40		
T_{2-6}	B_{2-6}	1:2:4	0.60	8	34.13	2.55	2.71	5.842
	C_{2-6}	1:2:4	0.60	7	25.87	2.21		

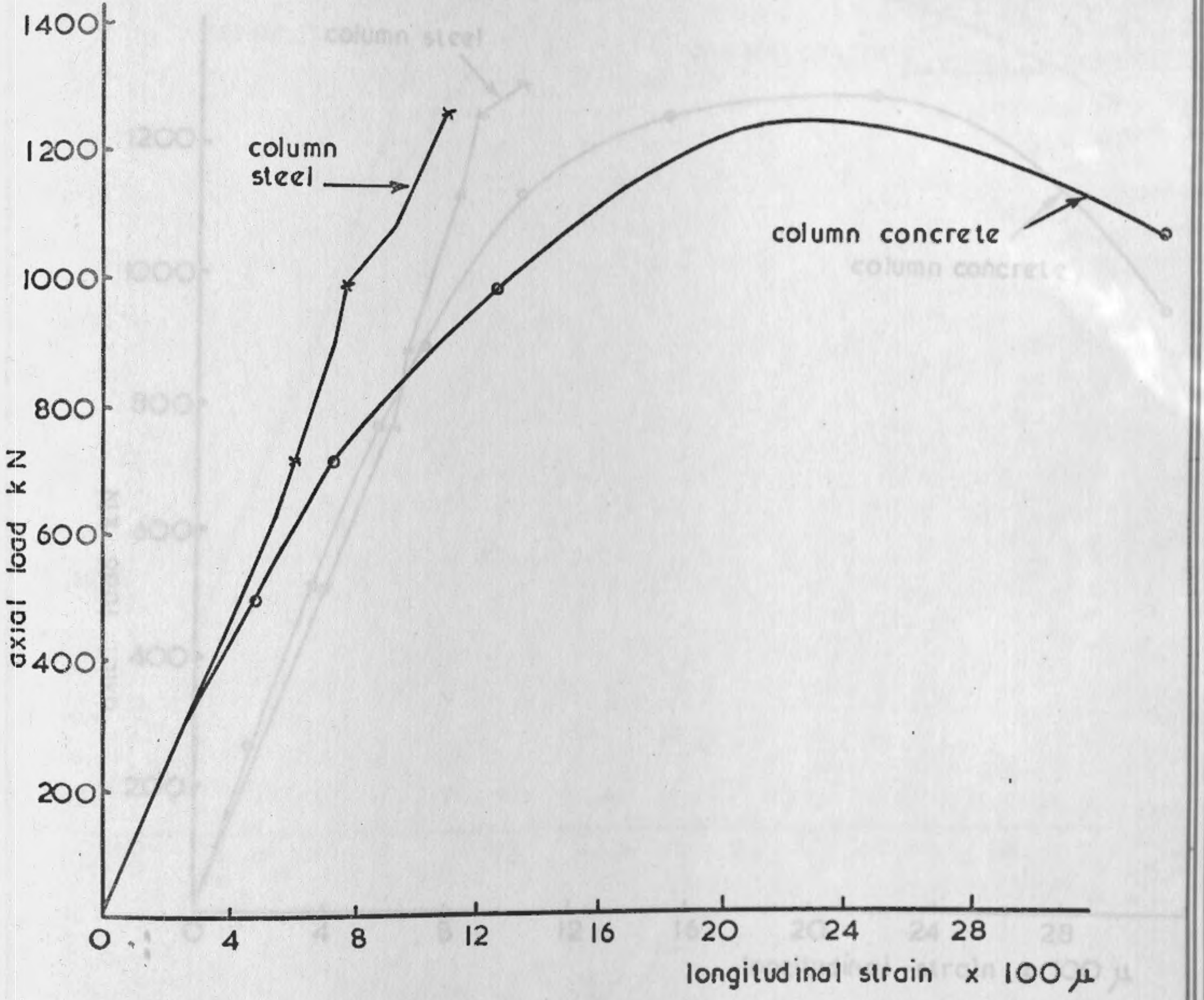

Fig. 4.3 .1. Axial load v. longitudinal strain measured on column concrete by 8" demec gauges and on column steel by electrical resistance strain gauges.(T_{2-1})

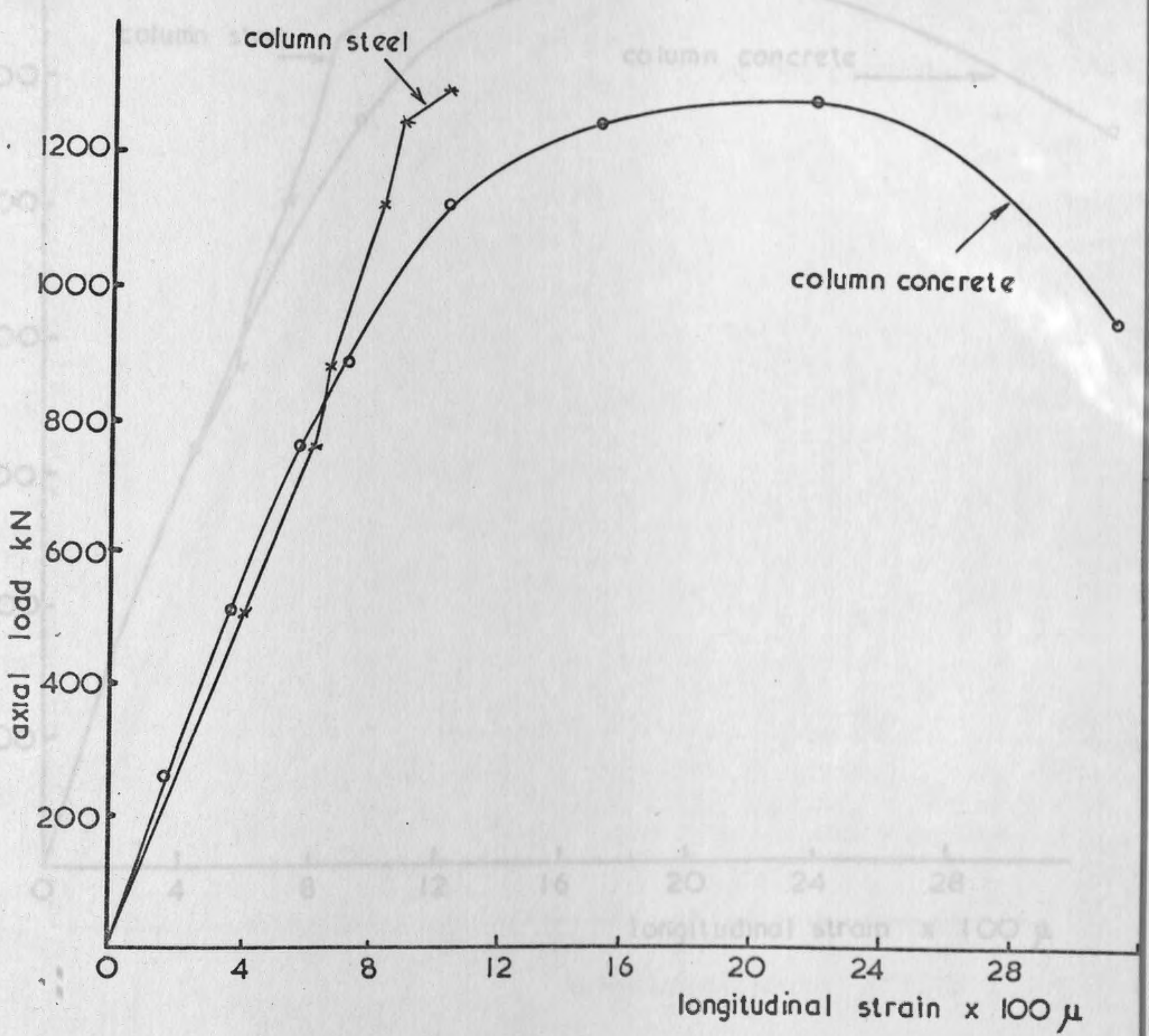

Fig. 4.3.2 Axial load v. longitudinal strain measured on column concrete by 8" demec gauges and on column steel by electrical resistance strain gauges (T_{2-2})

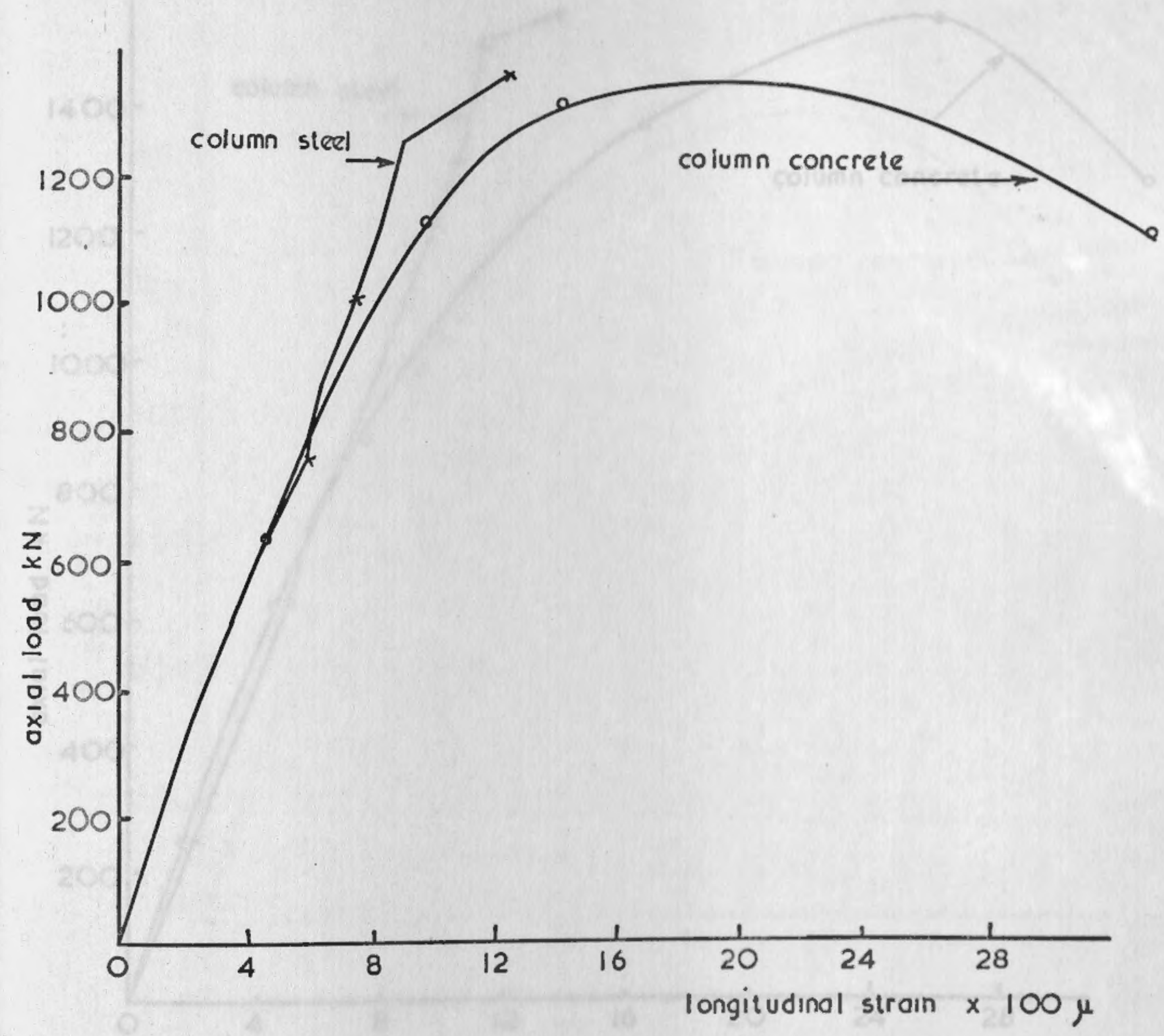

Fig. 4.3 . 3 Axial load v. longitudinal strain measured on column concrete by 8" demec gauges and on column steel by electrical resistance strain gauges. ($T_{2\cdot3}$)

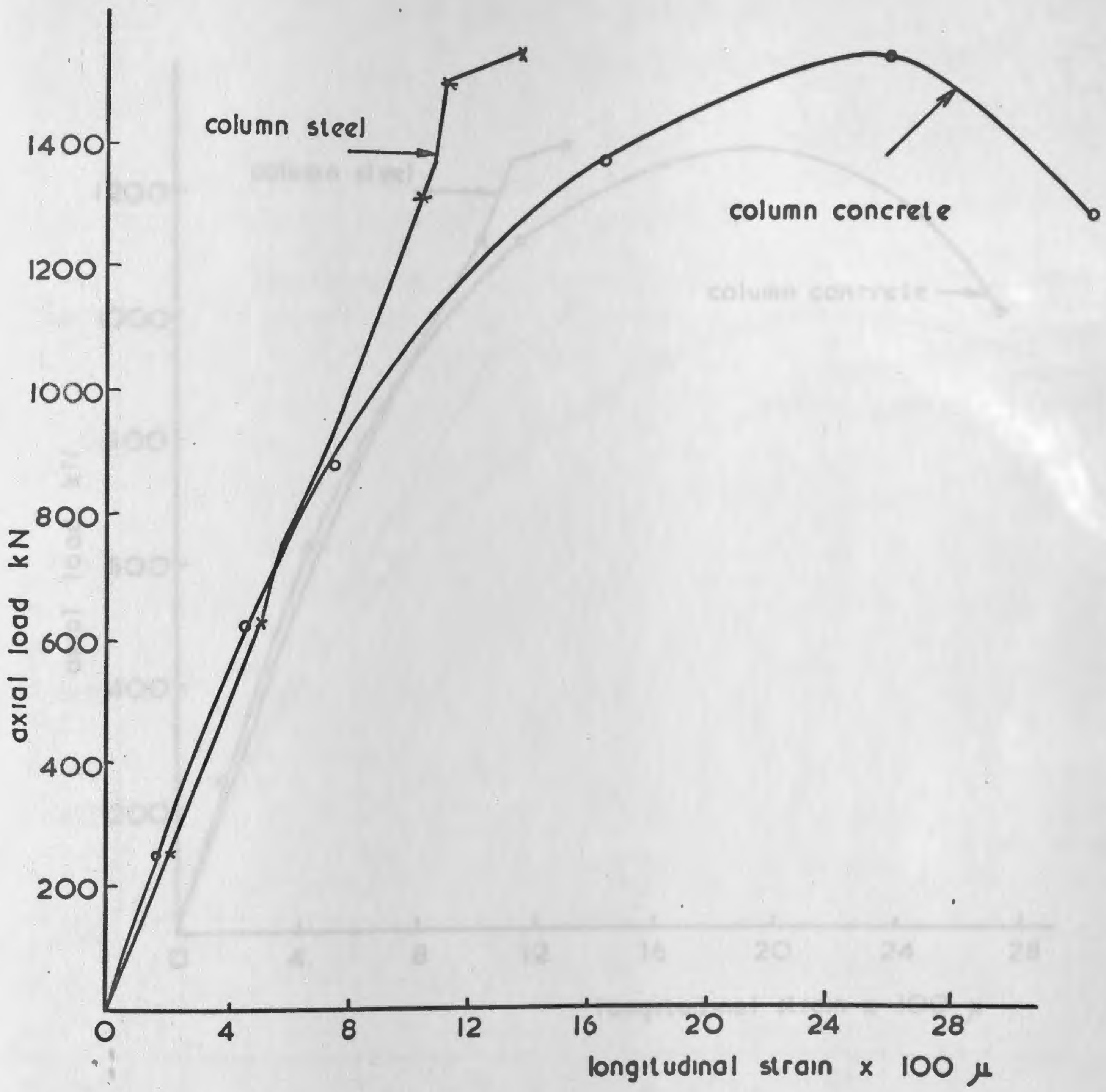

Fig. 4.3.4. Axial load v. longitudinal strain measured on column concrete by 8" demec gauges and on column steel by electrical resistance strain gauges (T_{2-4})

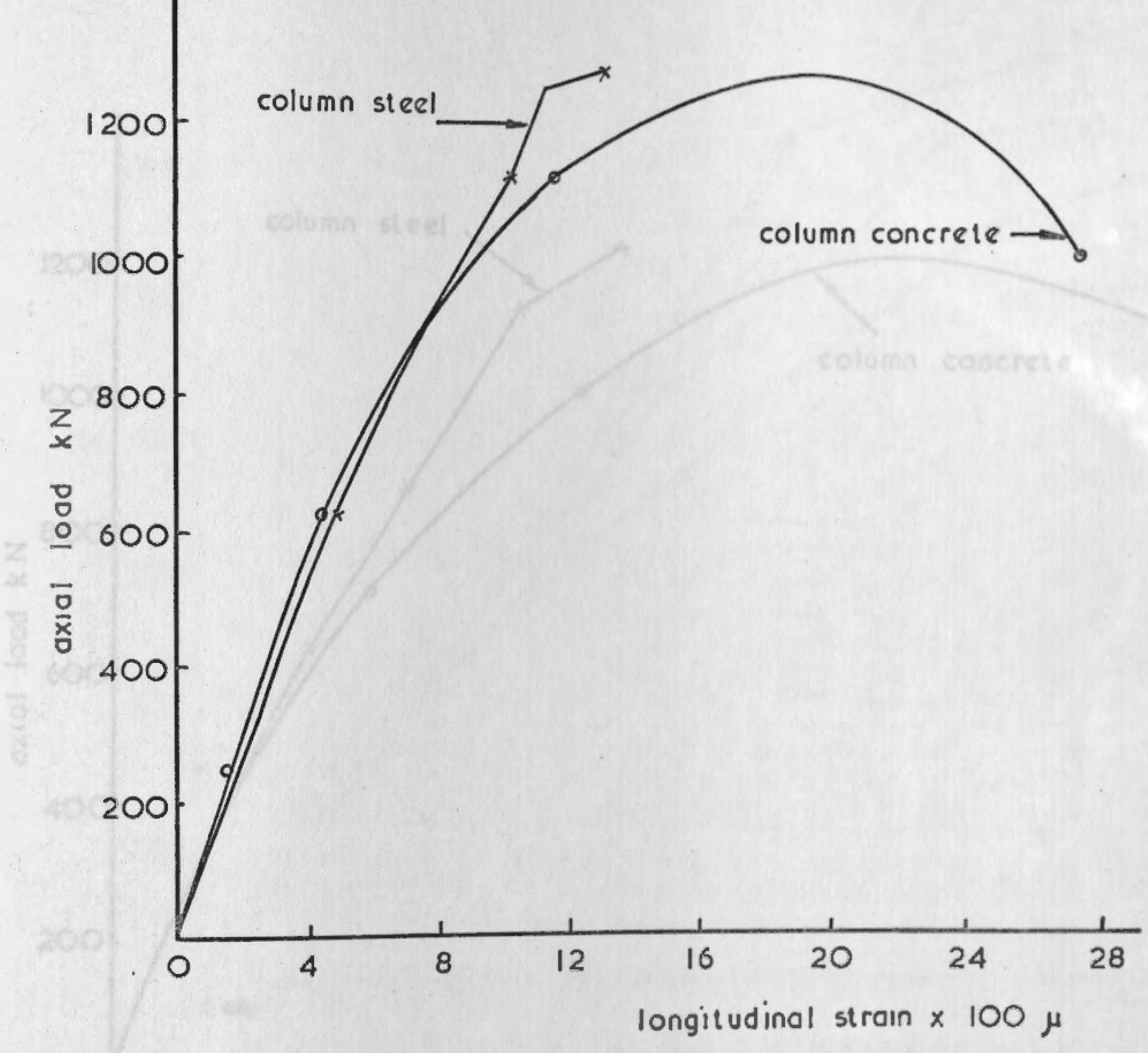

Fig.4.3.5 Axial load v longitudinal strain measured on column by 8" demec gauges and on column steel by electrical resistance strain gauges. (T_{2-5})

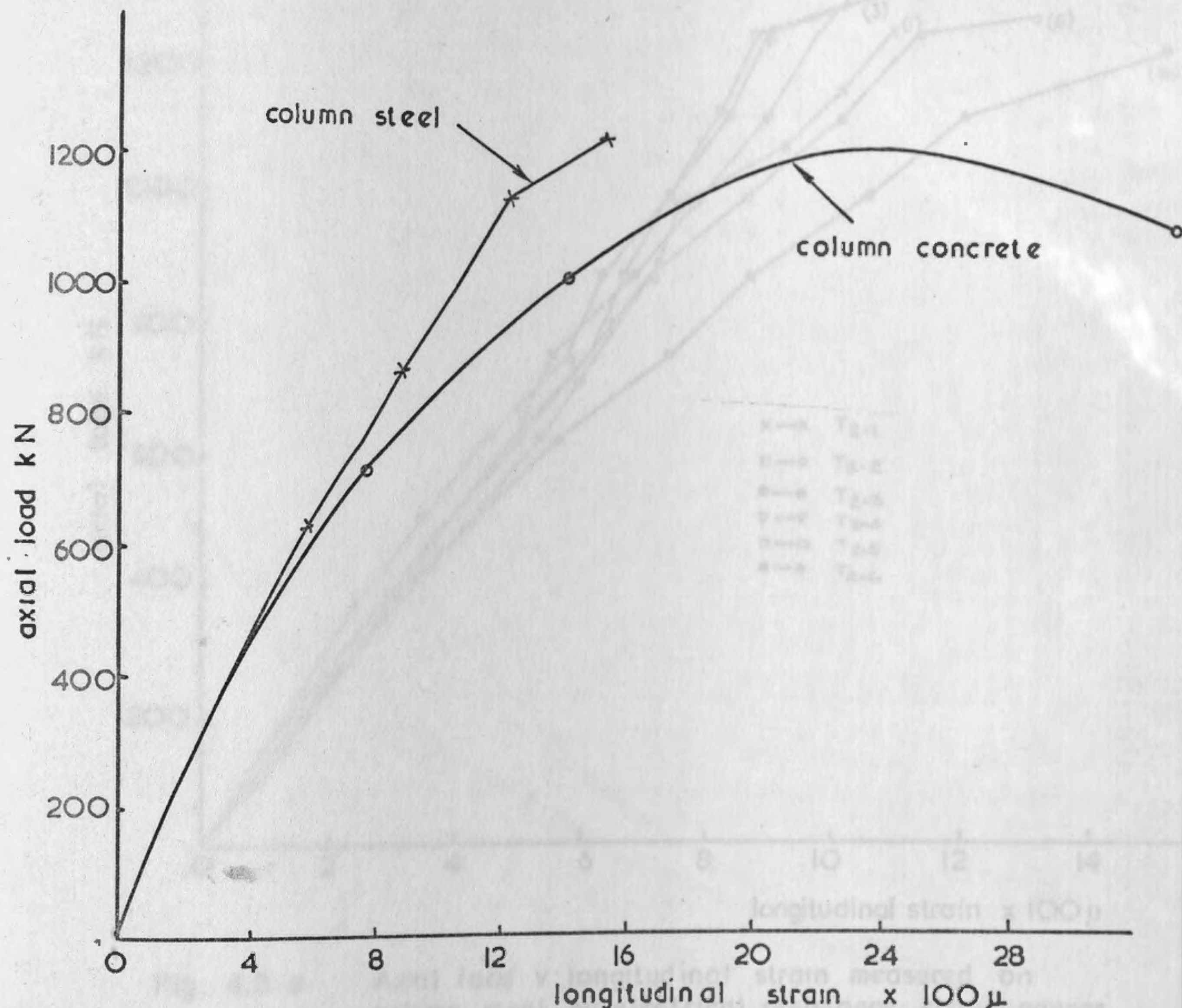

Fig. 4.3. 6. Axial load v. longitudinal strain measured on column concrete by 8" demec gauges and on column steel by electrical resistance strain gauges (T_{2-6})

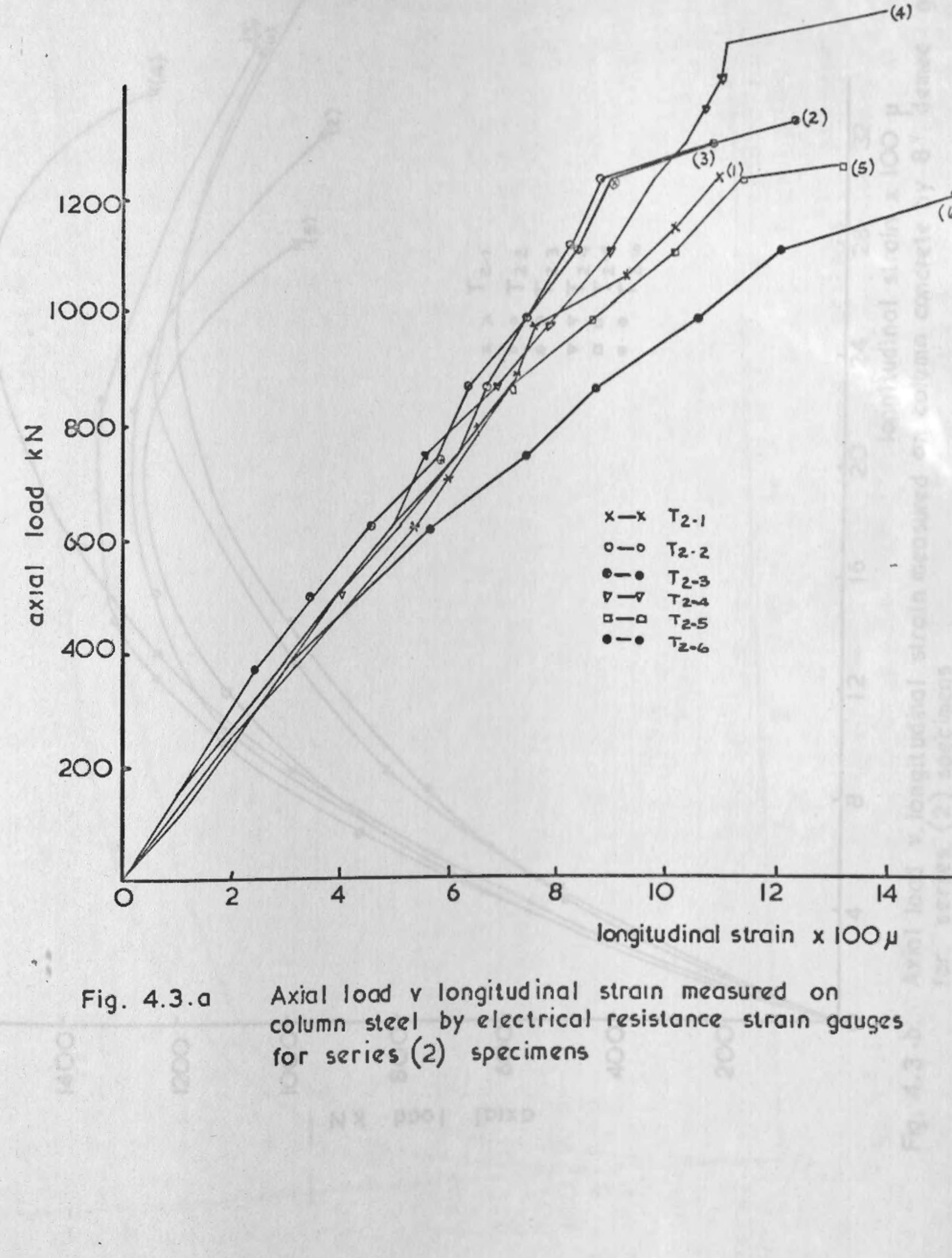

Fig. 4.3.a Axial load v longitudinal strain measured on column steel by electrical resistance strain gauges for series (2) specimens

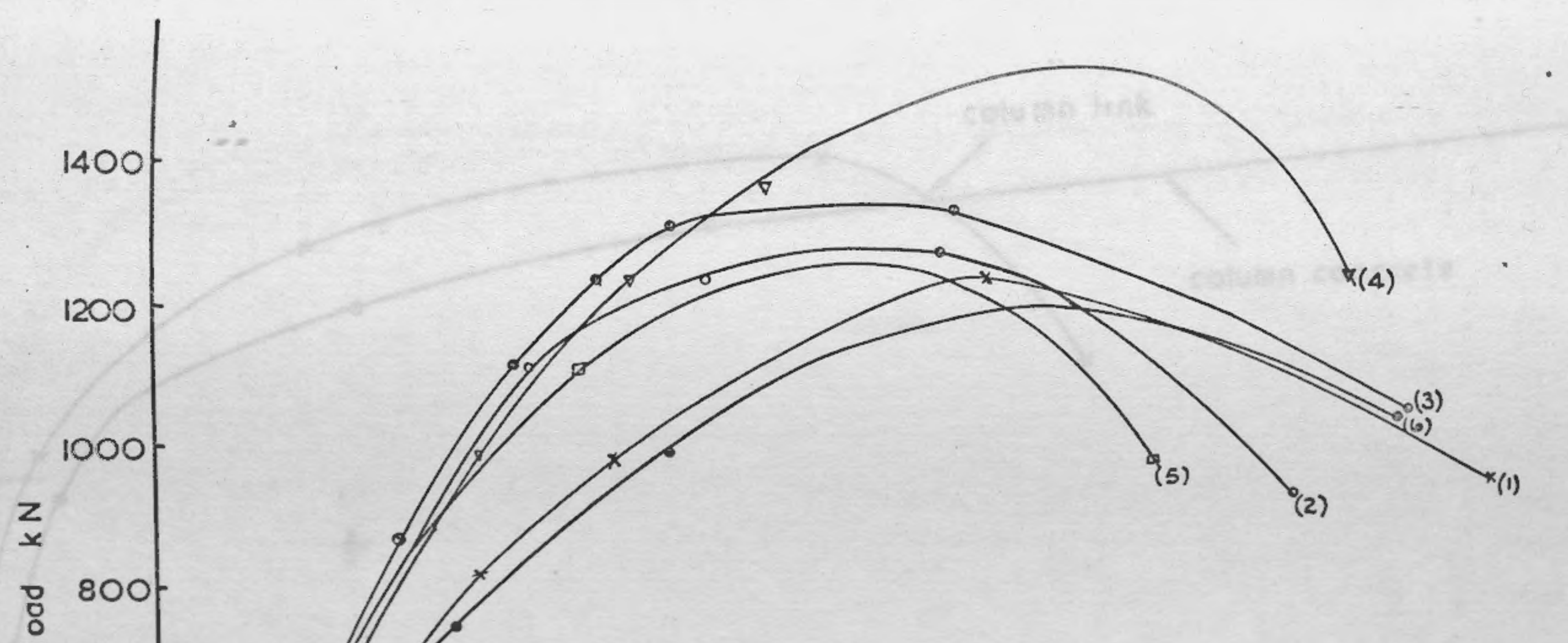

Fig. 4.3 -b. Axial load v. longitudinal strain measured on column concrete by 8" demec gauges for series (2) specimens

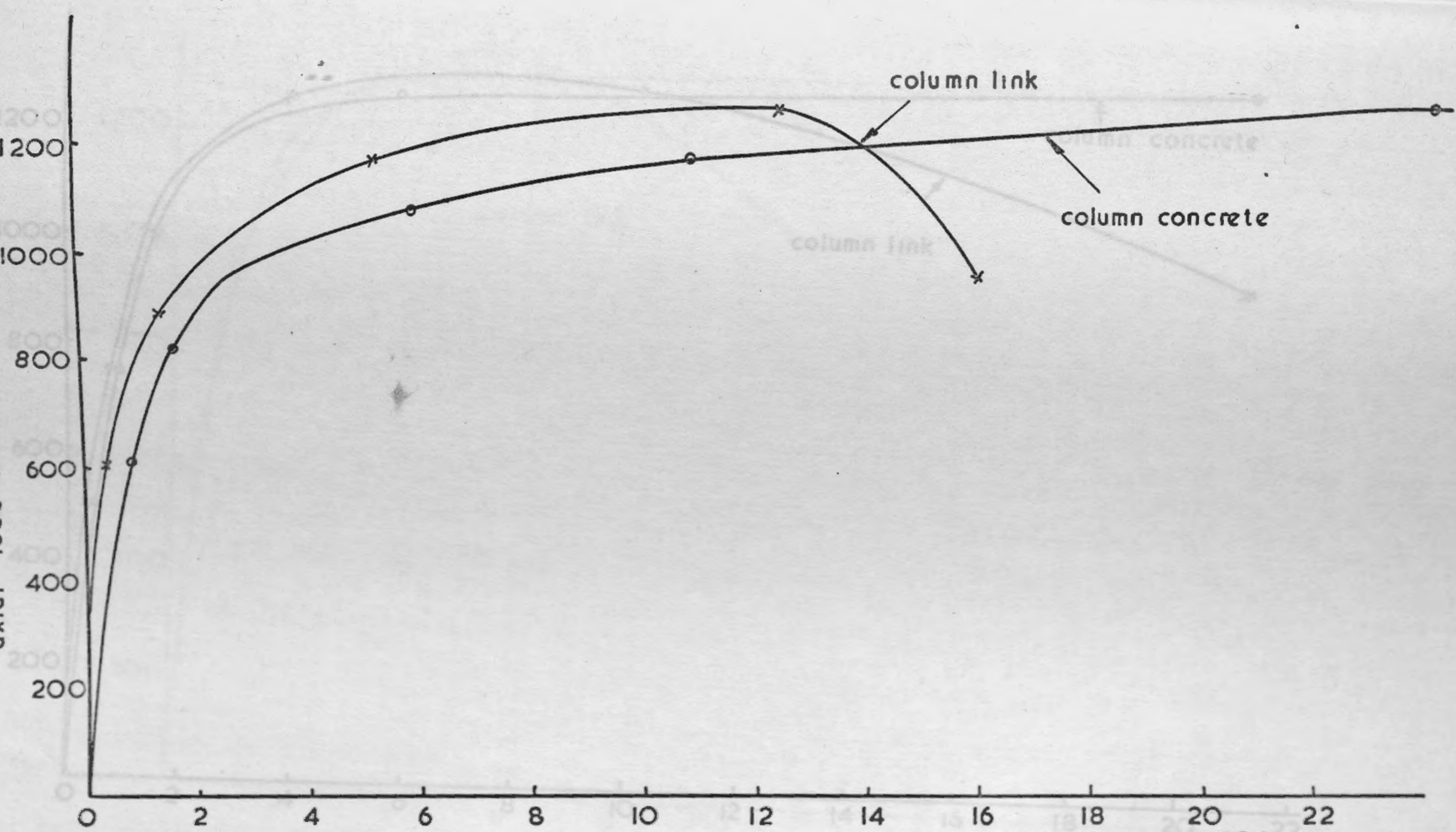

Fig. 4.4.1 Axial load v. lateral strain measured on column concrete by 6" demec gauges and on column links by electrical resistance strain gauges (T_{2-1})

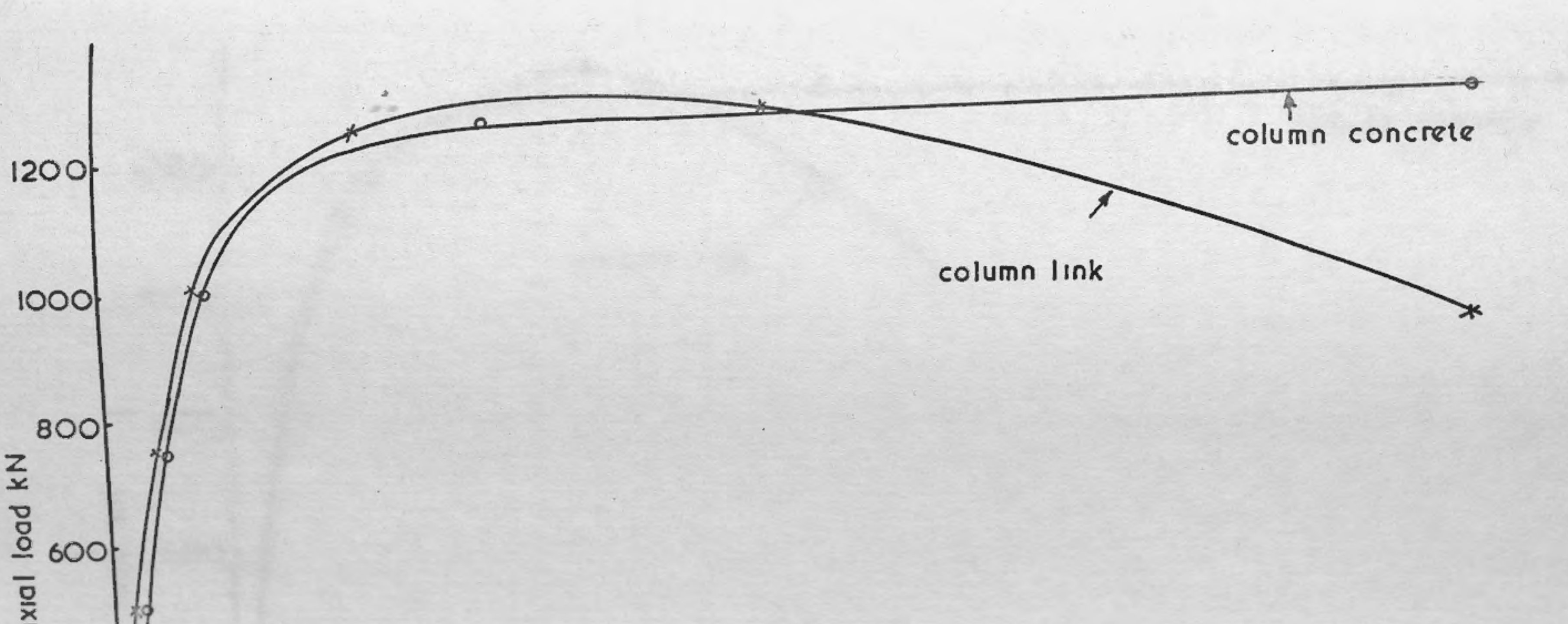

Fig. 4.4 .2. Axial load v. lateral strain measured on column concrete by 6" demec gauges and on column links by electrical resistance strain gauges. ($T_{2 \cdot 2}$)

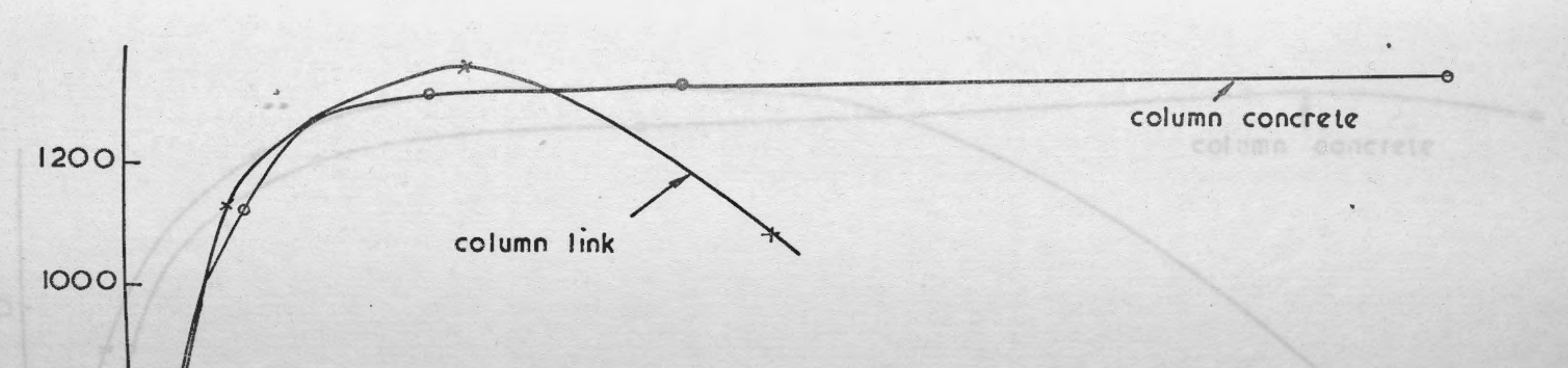

Fig. 4.4.3 Axial load v. lateral strain measured on column concrete by 6" demec gauges and on column links by electrical resistance strain gauges. ($T_{2\cdot3}$)

Fig. 4.4.4. Axial load v lateral strain measured on column concrete by 6" demec gauges and on column links by electrical resistance strain gauges ($T_{2.4}$)

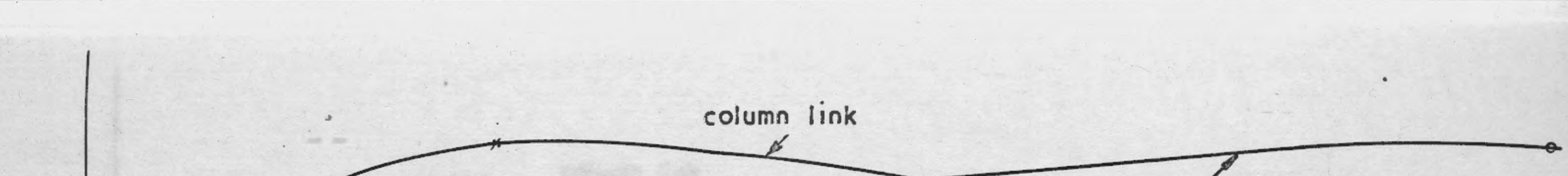

Fig. 4.4.5. Axial load. v lateral strain measured on column concrete by 6" demec gauges and on column links by electrical resistance strain gauges. ($T_{2\cdot5}$.)

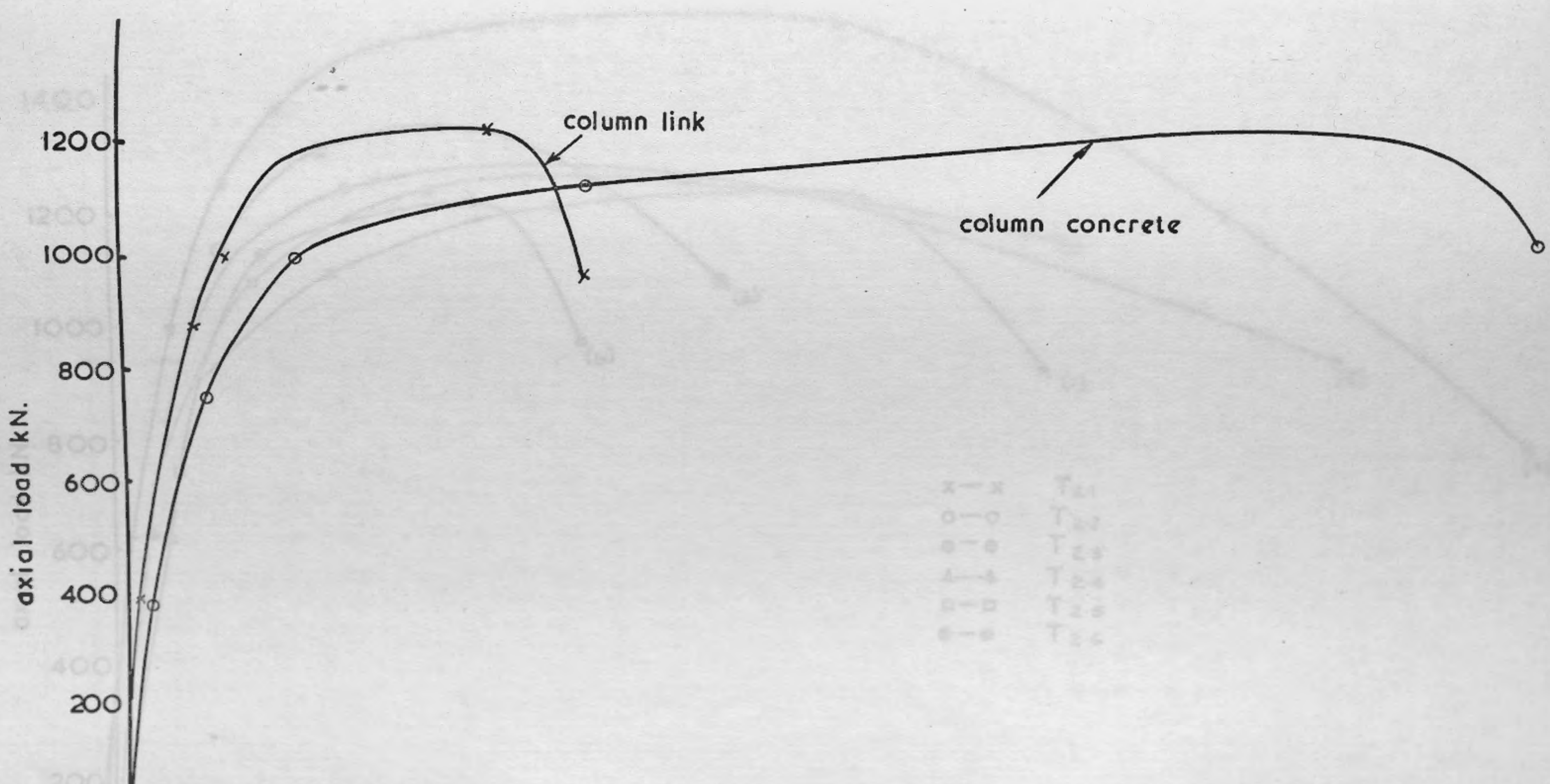

Fig. 4.4.6. Axial load v. lateral strain measured on column concrete by 6." demec gauges and on column links by electrical resistance strain gauges ($T_{2 \cdot 6}$)

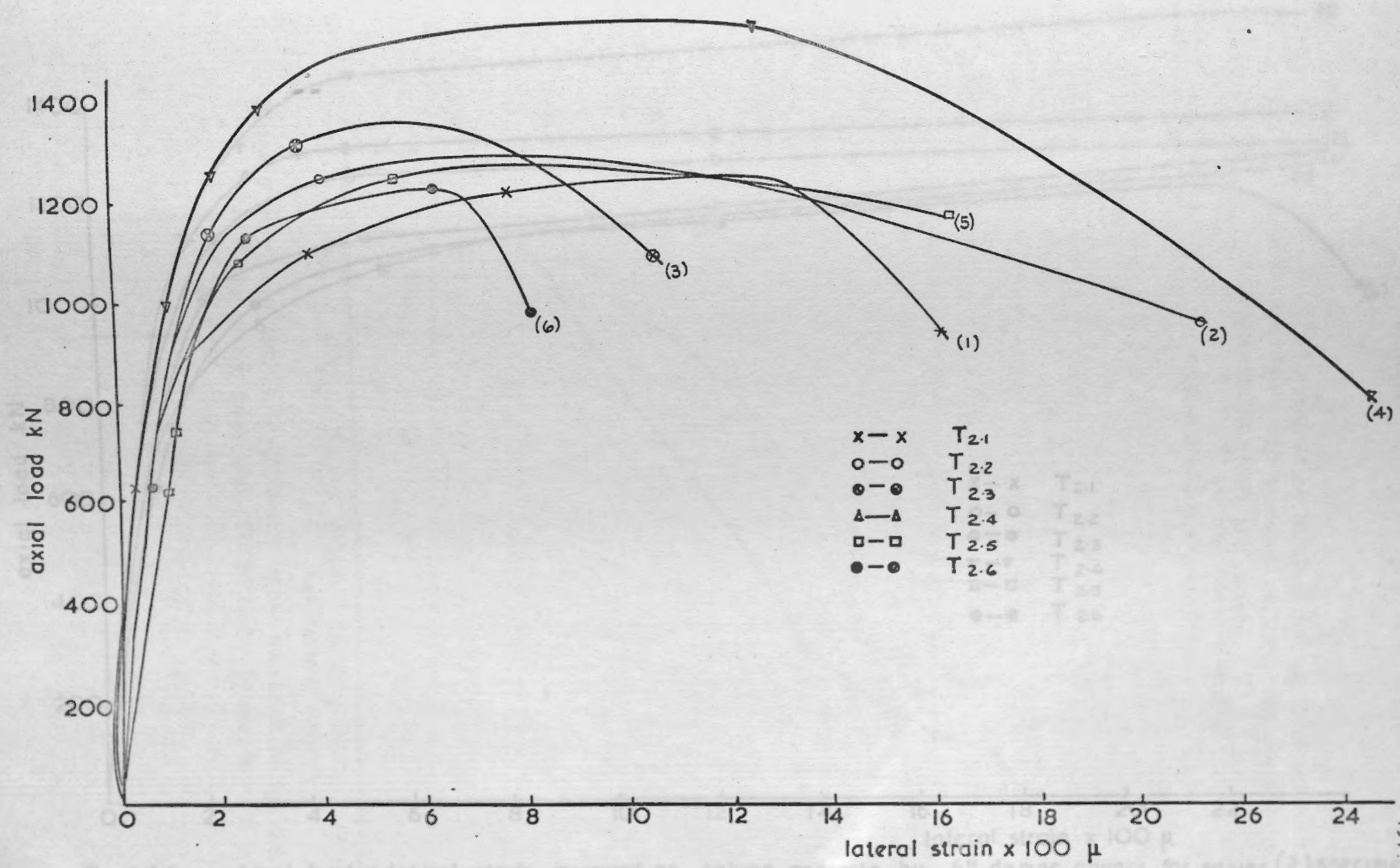

Fig. 4.4.a. Axial load v. lateral strain measured on column links by electrical resistance strain gauges. for series (2) specimens

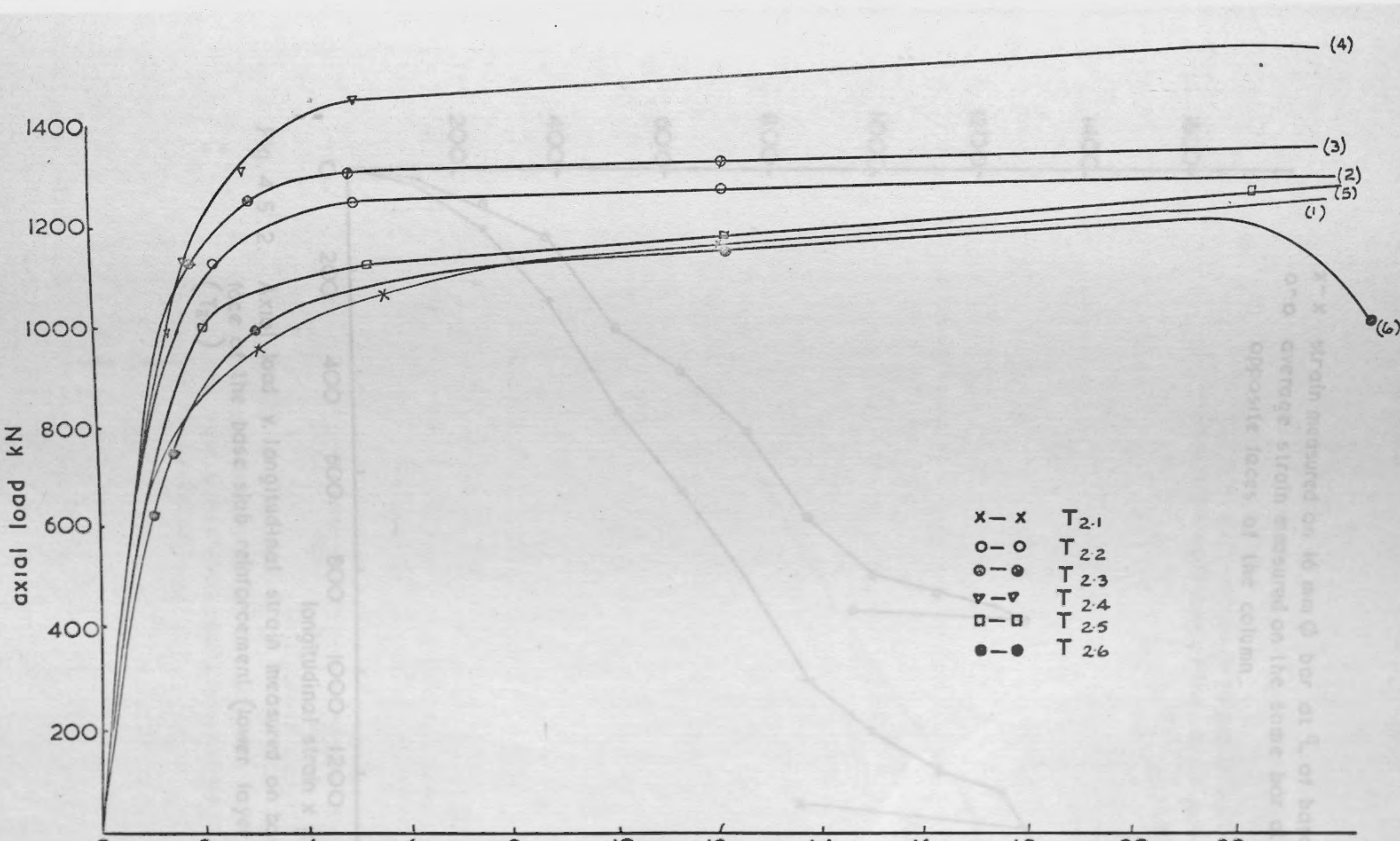

Fig 4.4.b. Axial load v. lateral strain measured on column concrete by 6" demec gauges. for series (2) specimens

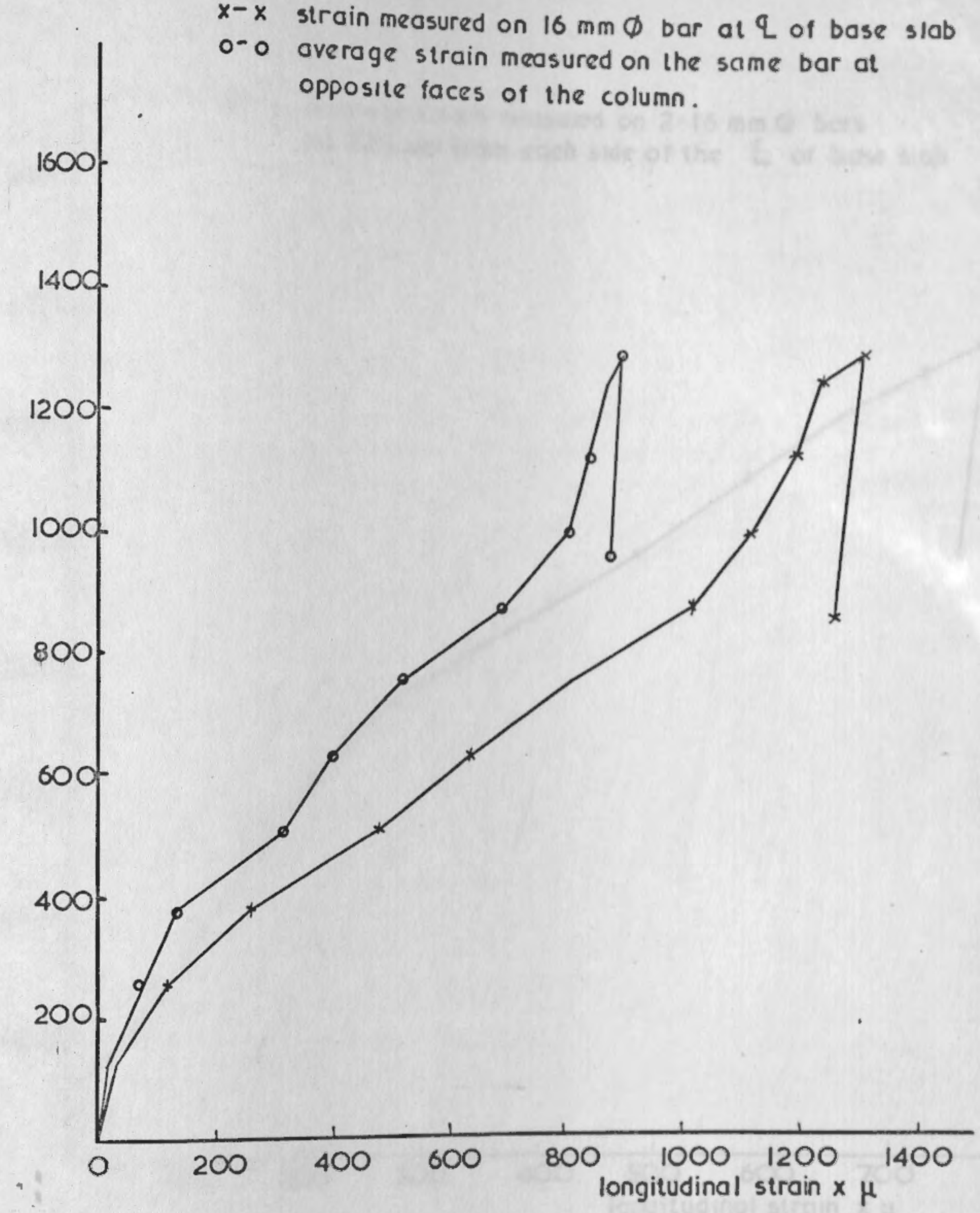

Fig. 4.5.2. Axial load v. longitudinal strain measured on bottom face of the base slab reinforcement (lower layer) ($T_{2\cdot2}$)

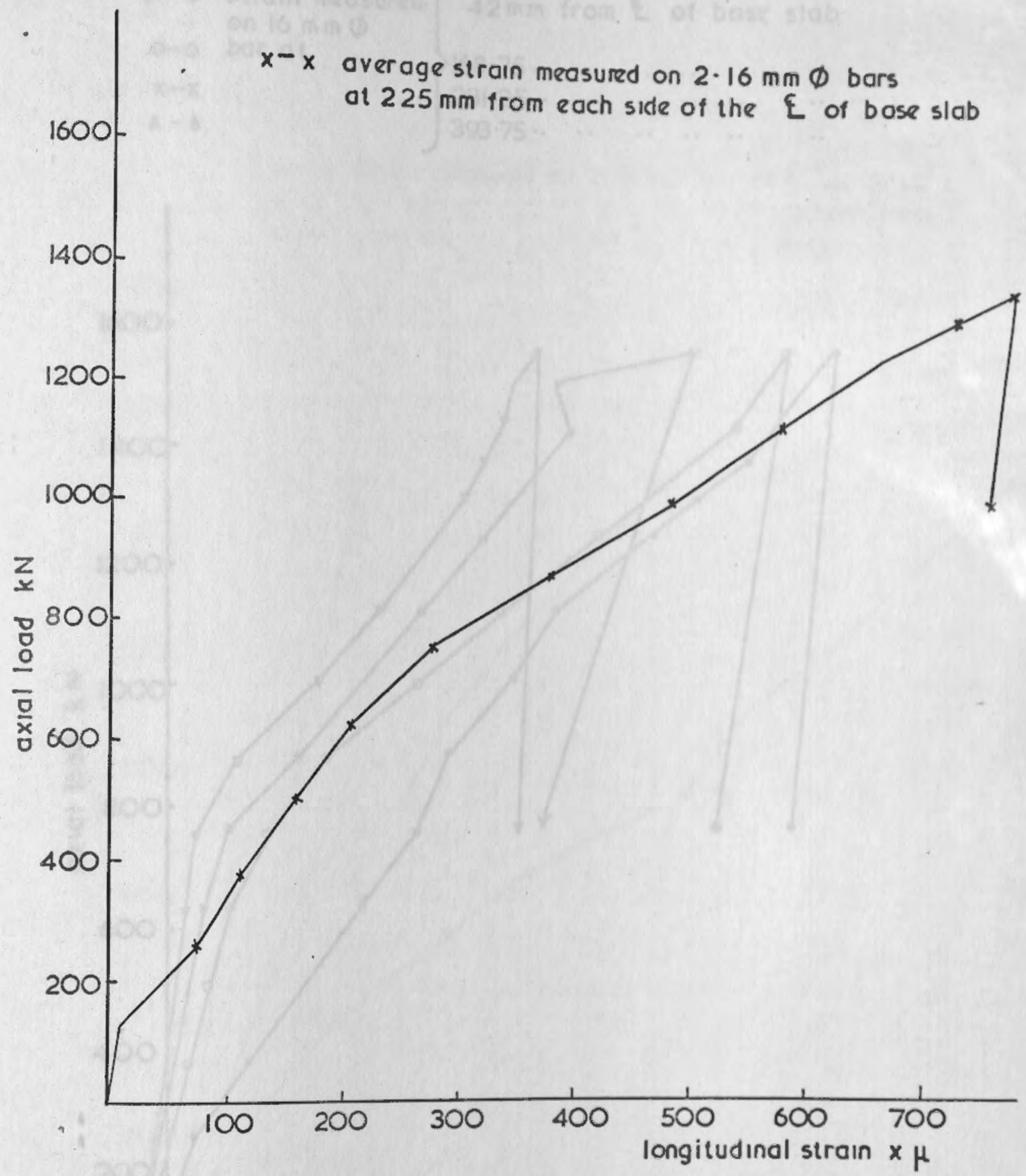

Fig. 4.5.3. Axial load v. longitudinal strain measured on the bottom face of the base slab reinforcement (lower layer) at the middle of the bars. ($T_{2\cdot3}$)

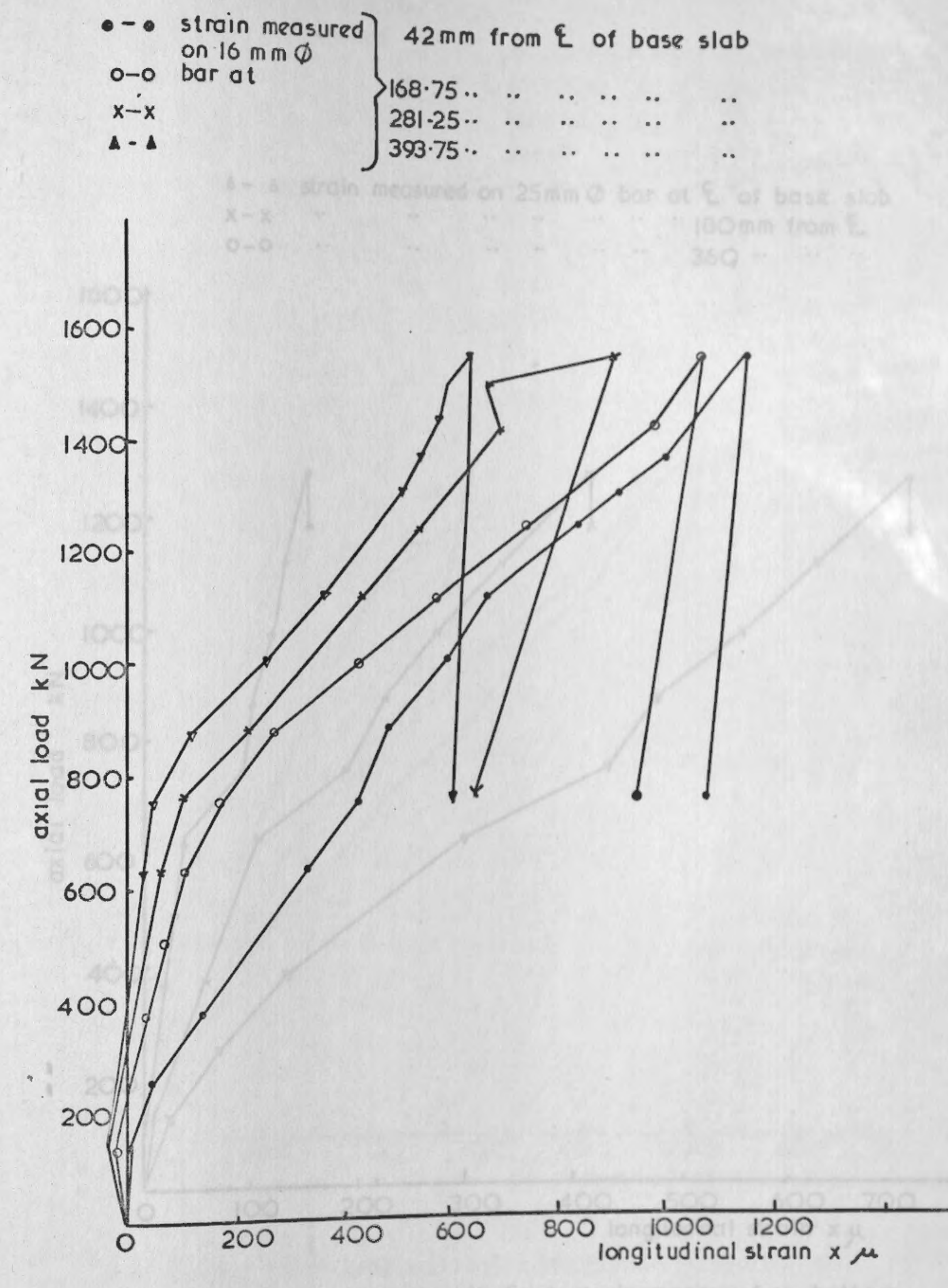

Fig. 4.5.4 Axial load v. longitudinal strains measured on bottom face of the base slab reinforcement (lower layer) at the middle of the bars ($T_{2.4}$)

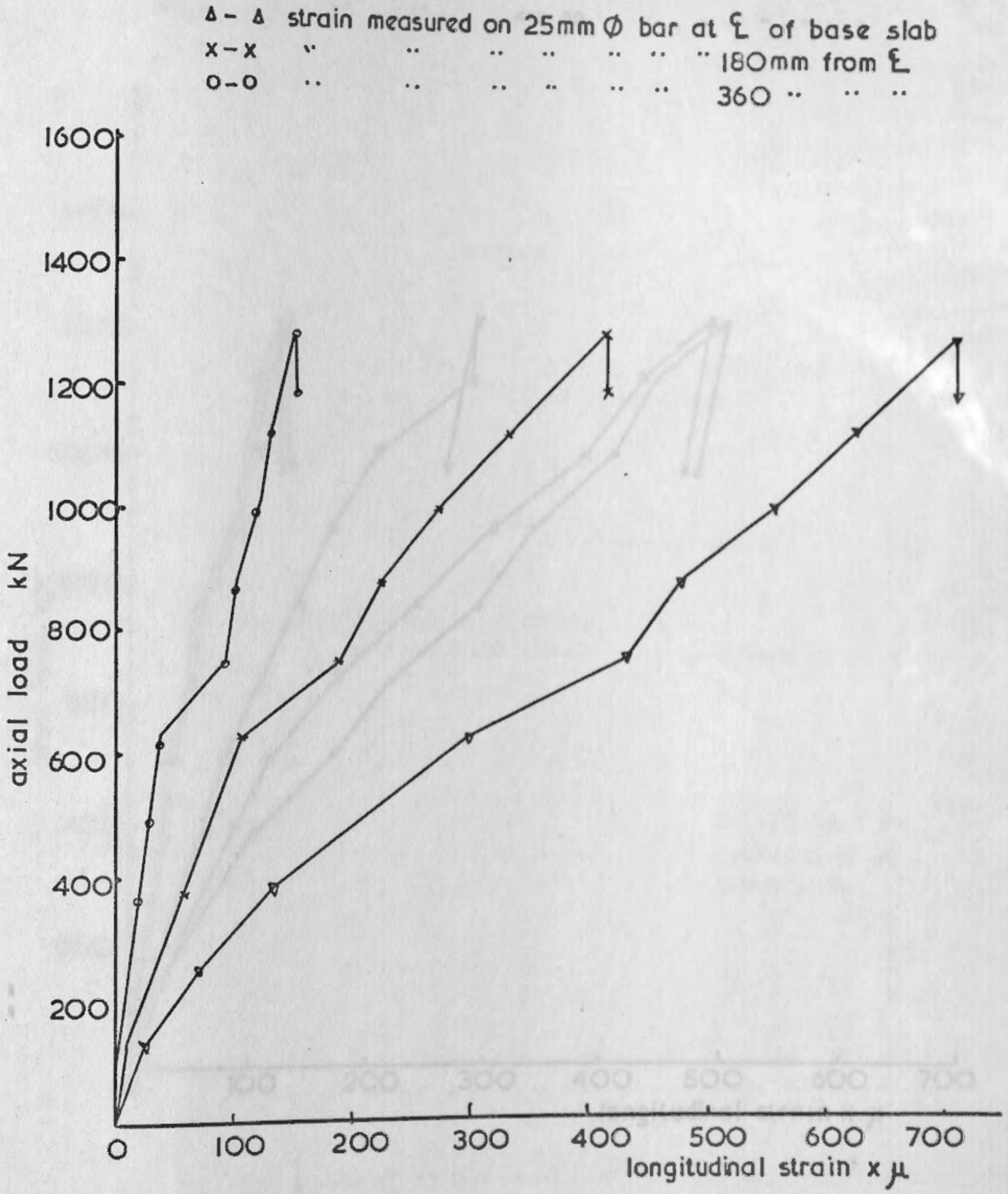

Fig. 4.5.5 Axial load v. longitudinal strain measured on bottom face of the base slab reinforcement (lower layer) at the middle of the bars. ($T_{2\cdot5}$)

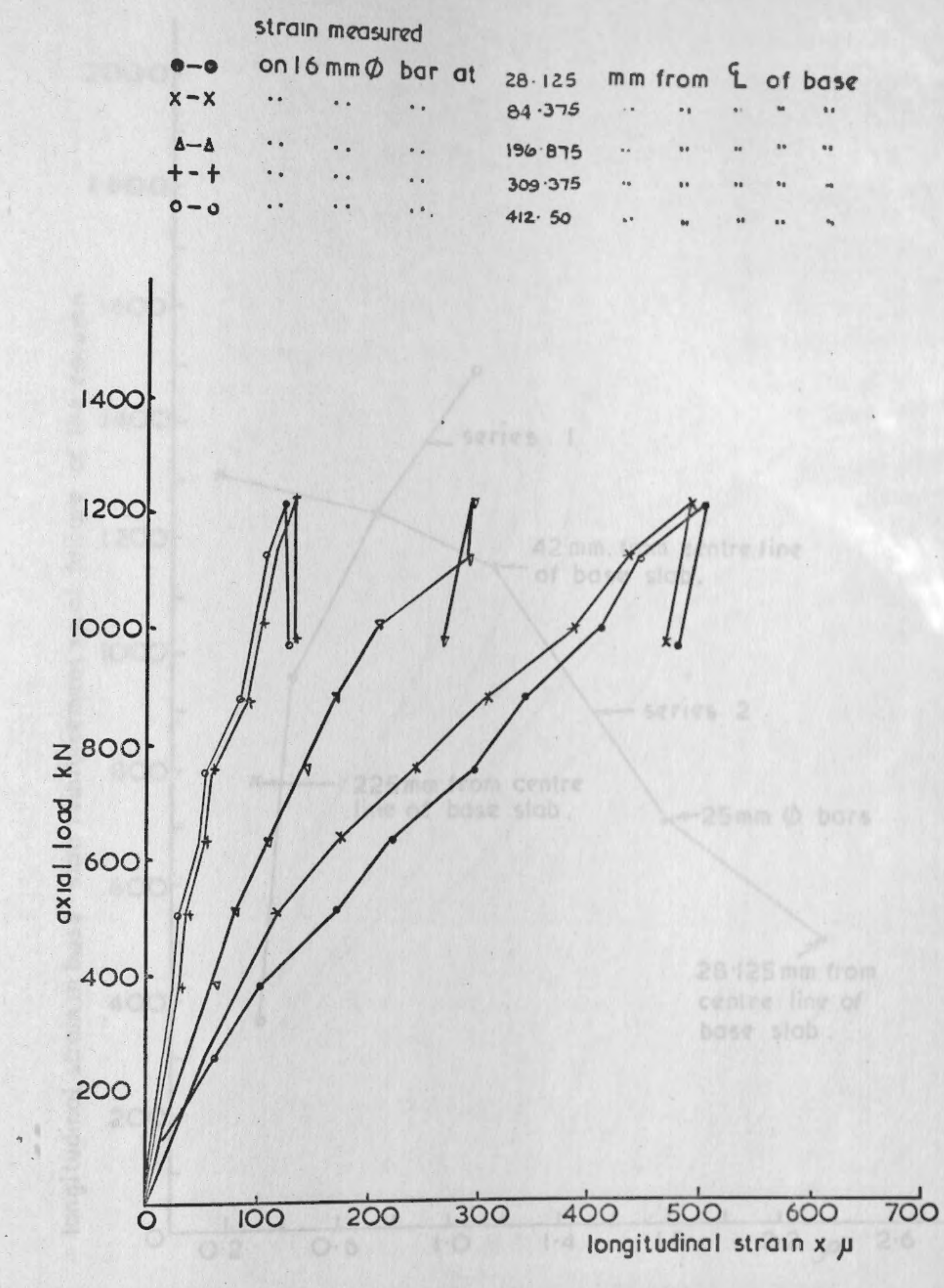

Fig. 4.5.6 Axial load v. longitudinal strain measured on bottom face of the base slab reinforcement (lower layer) at the middle of the bars. ($T_{2\cdot6}$)

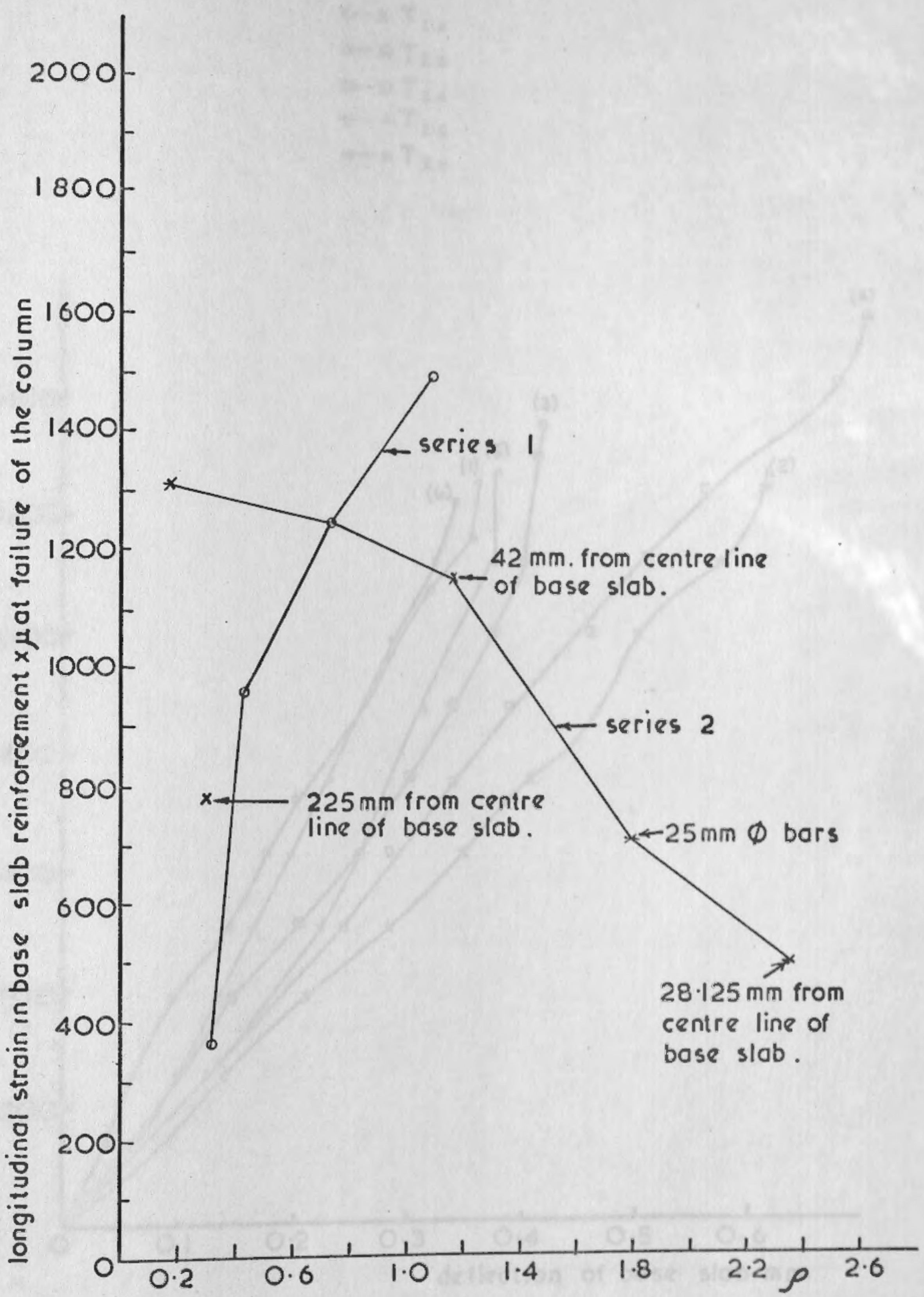

Fig. 4. 5a. Longitudinal strain measured at the middle of base slab reinforcement on the bottom face of bars at the ℄ or nearest to it (lower layer) v % of tensile reinforcement in base slab (ρ) for series (1) and (2) specimens

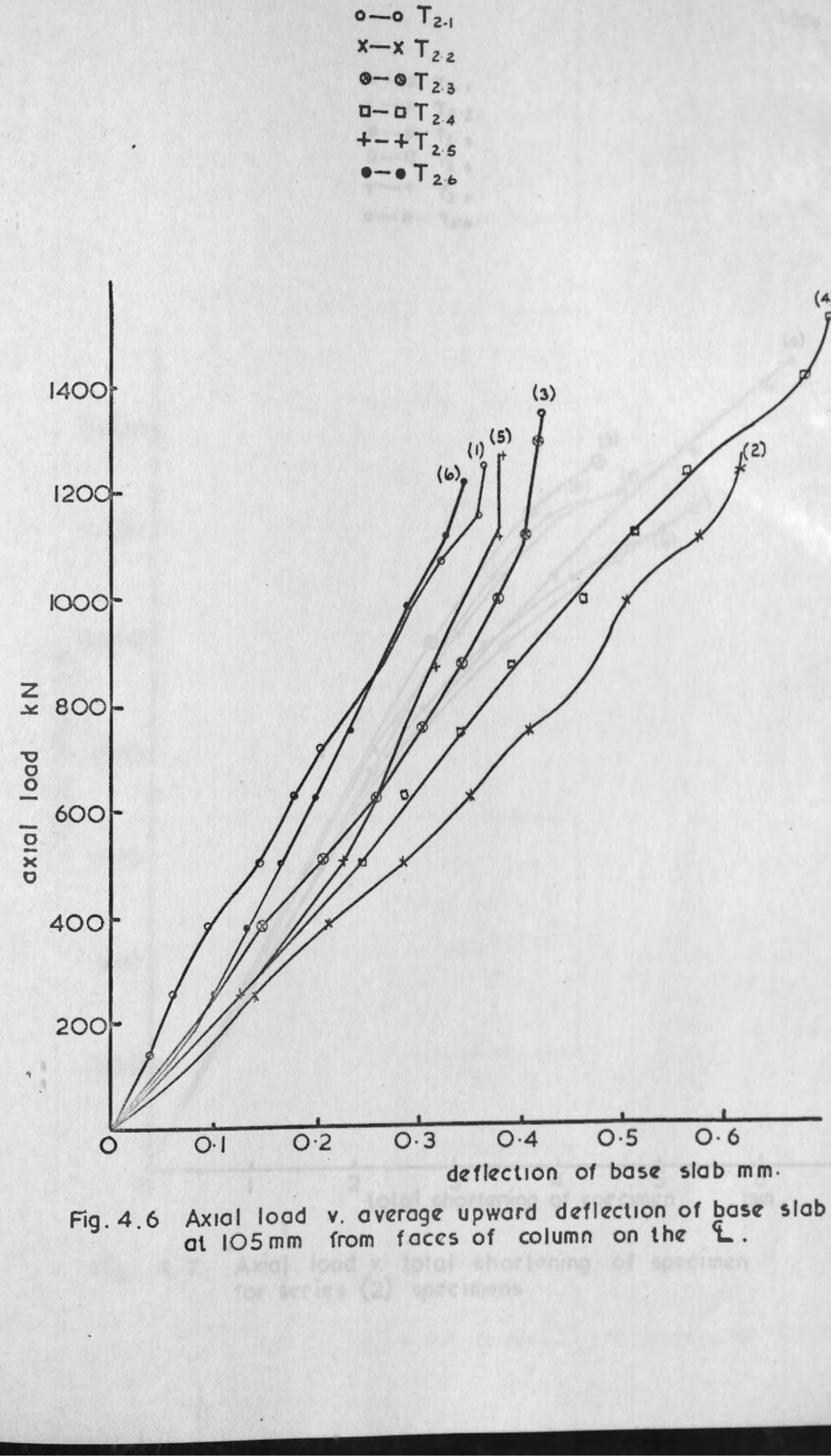

Fig. 4.6 Axial load v. average upward deflection of base slab at 105 mm from faces of column on the ℄.

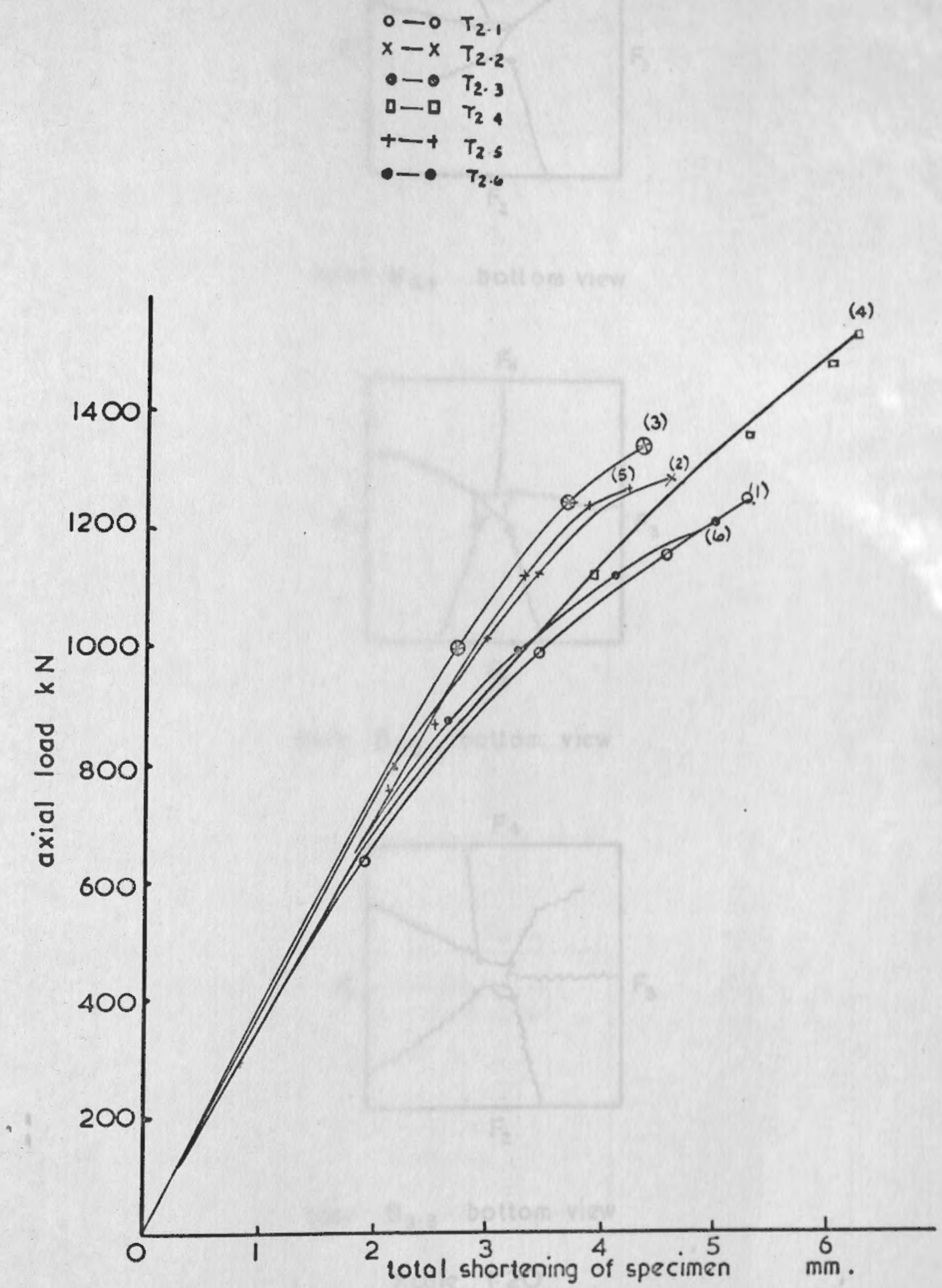

Fig. 4.7. Axial load v. total shortening of specimen for series (2) specimens

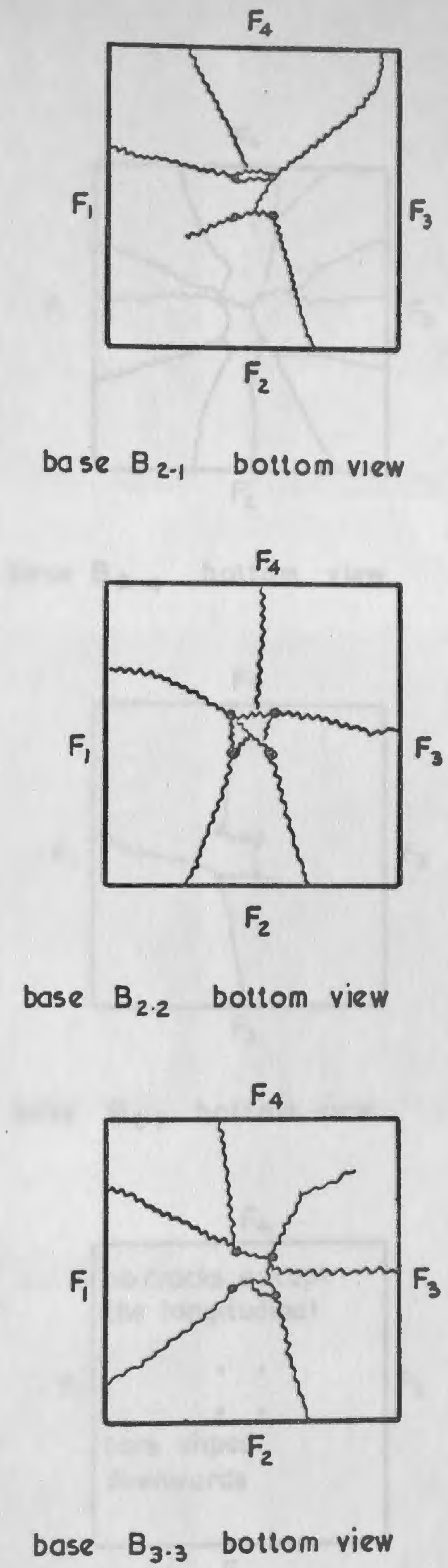

Scale 1:20

for bases $B_{2\cdot4}$ – $B_{2\cdot6}$ see next page

Fig. 4.8 Bottom views for series (2) specimens after failure

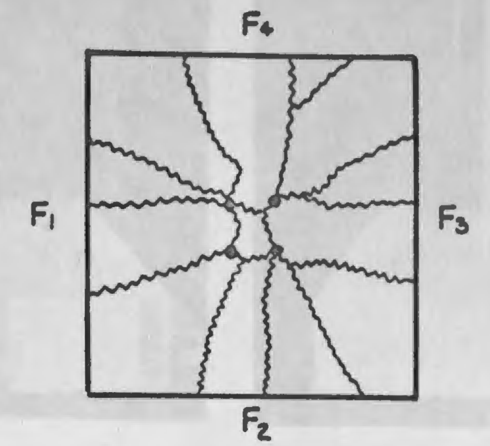

base $B_{2.4}$ bottom view

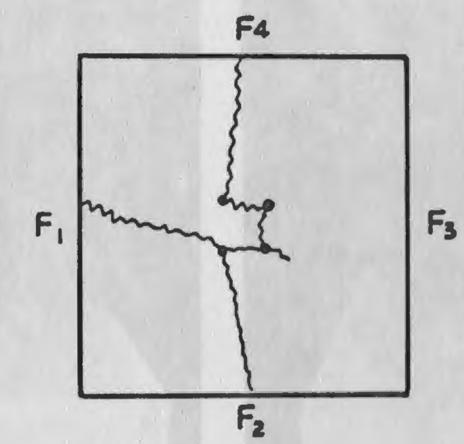

base $B_{2.5}$ bottom view

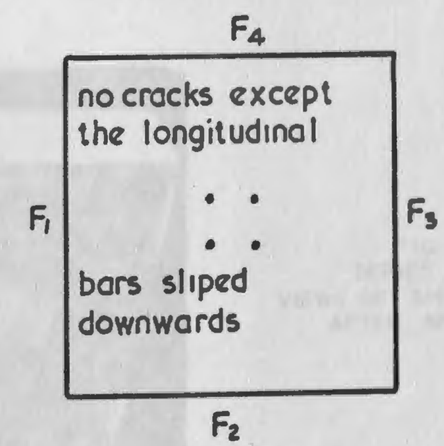

base $B_{2.6}$ bottom view

Scale 1:20

Fig. 4.8. Bottom views for series (2) specimens after failure

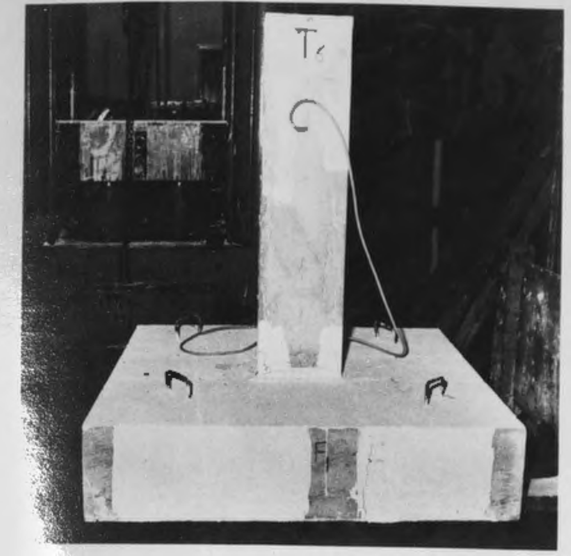

FACE 1

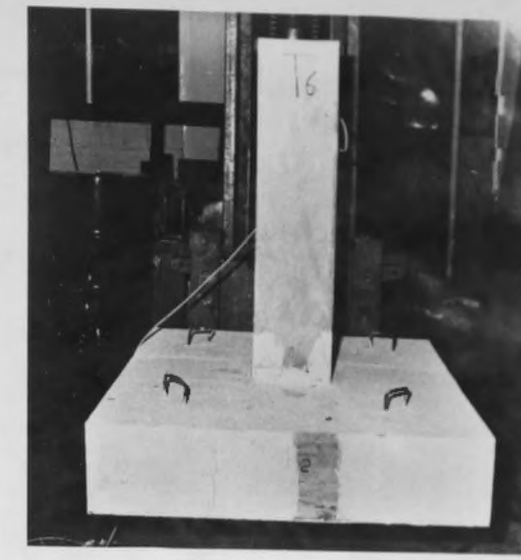

FACE 2

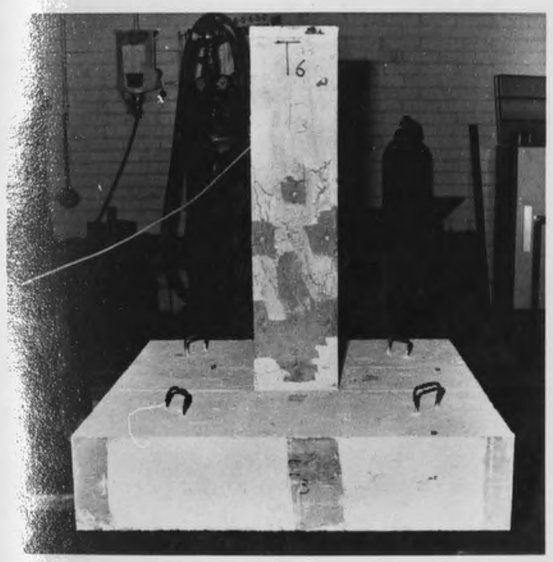

FACE 3

FACE 4

Bottom view of base

FIG. 4.9 ·1
SERIES (2)
VIEWS OF SPECIMEN $T_2 \cdot 1$
AFTER FAILURE

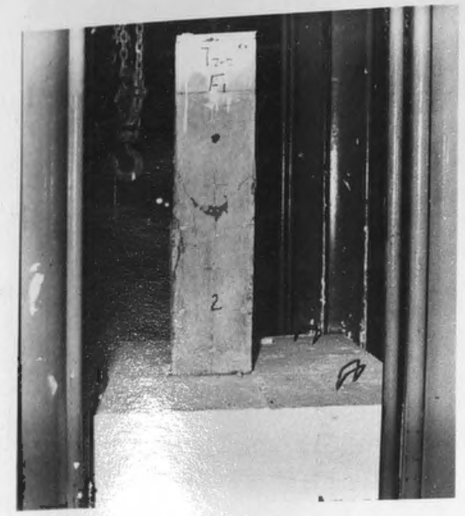

FACE 1

FACE 2

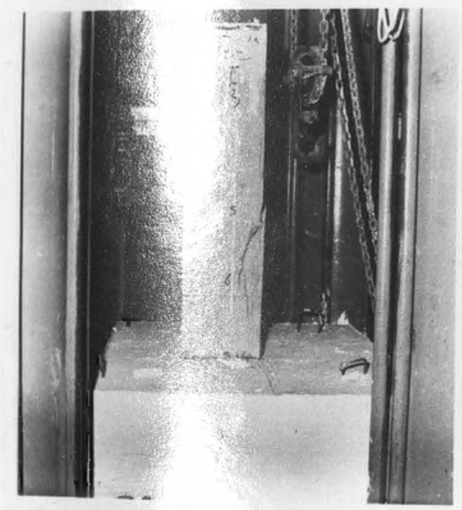

FACE 3

FACE 4

Bottom view of base

FIG. 4.9.2
SERIES (2)
VIEWS OF SPECIMEN $T_{2\cdot2}$
AFTER FAILURE

FACE 1

FACE 2

FACE 3

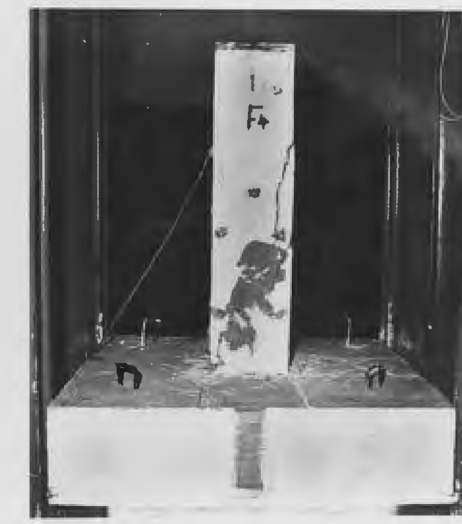

FACE 4

Bottom view of base

FIG. 4.9 ·3
SERIES (2)
VIEWS OF SPECIMEN $T_{2 \cdot 3}$
AFTER FAILURE

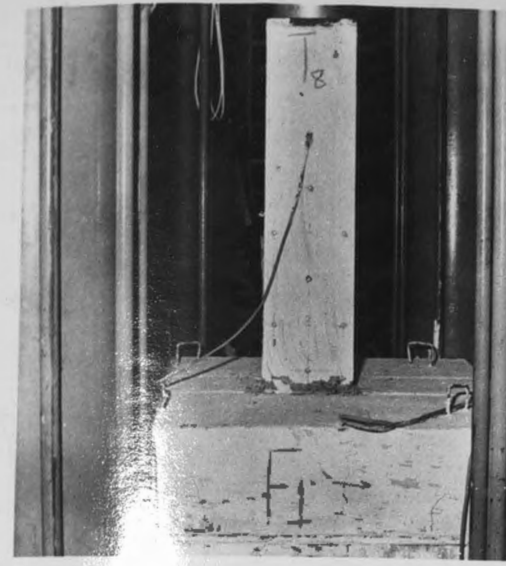

FACE .1

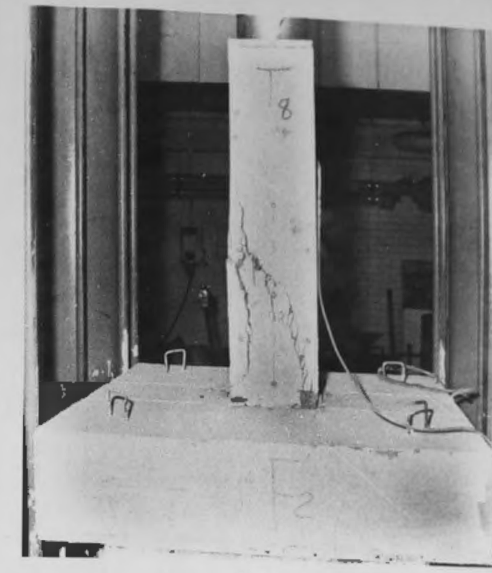

FACE 2

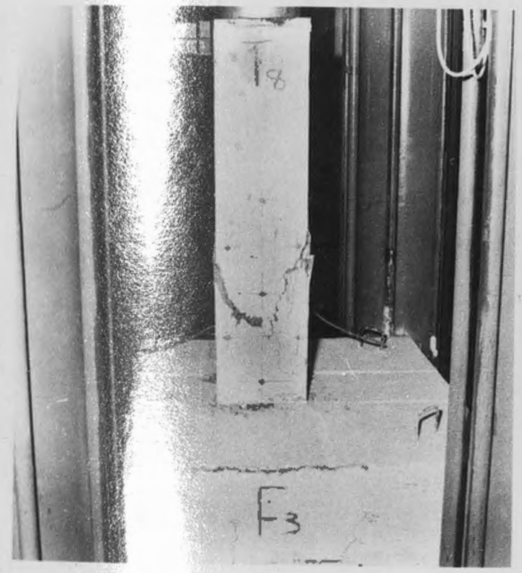

FACE 3

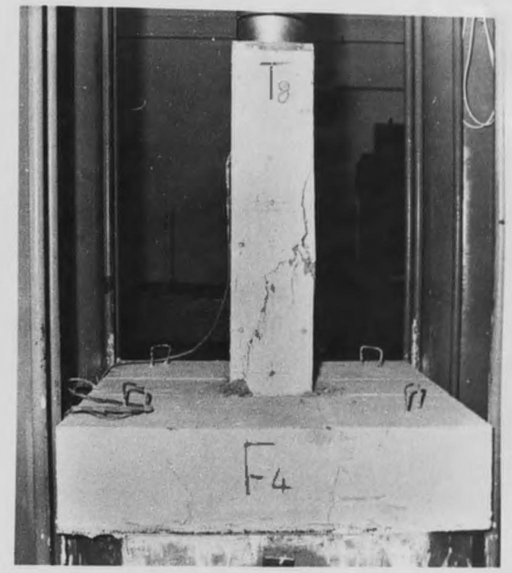

FACE 4

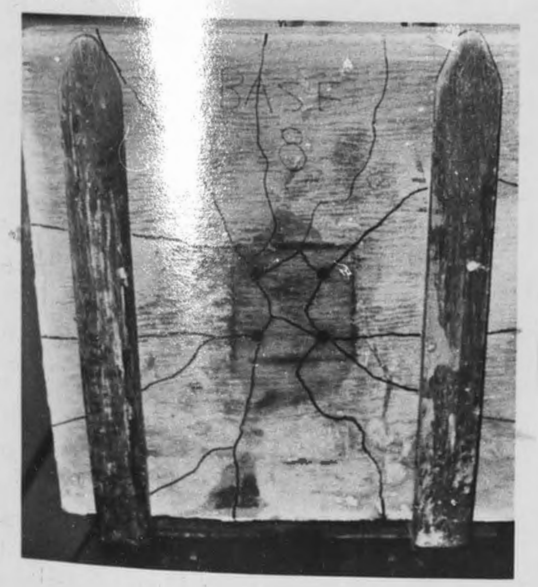

Bottom view of base

FIG 4.9 4
SERIES (2)
VIEWS OF SPECIMEN $T_{2\cdot 4}$
AFTER FAILURE

FACE I

FACE 2

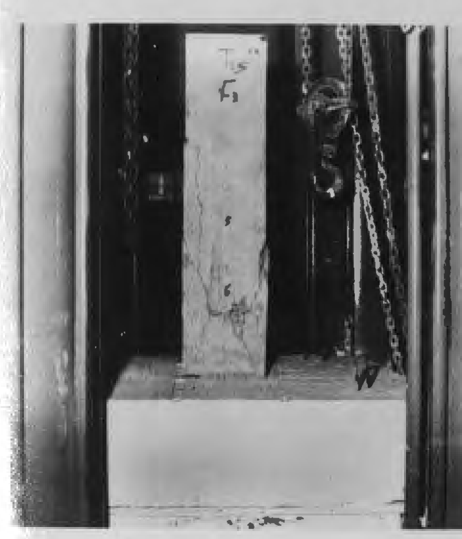

FACE 3

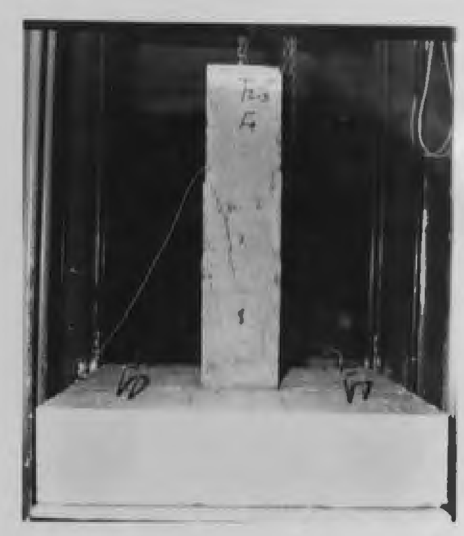

FACE 4

Bottom view of base

FIG. 4.9.5
SERIES (2)
VIEWS OF SPECIMEN $T_{2\cdot5}$
AFTER FAILURE

FACE 1

FACE 2

FACE 3

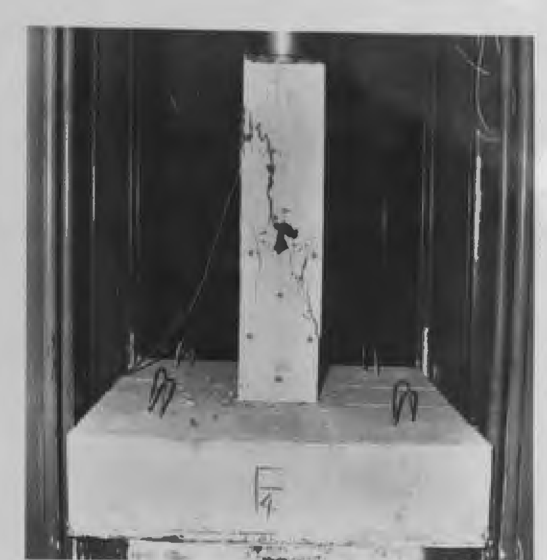

FACE 4

Bottom view of base

FIG 4.9.6
SERIES (2)
VIEWS OF SPECIMEN $T_{2\cdot6}$
AFTER FAILURE

TABLE 4-3

SERIES (2)

Summary of specimens results and calculations.

T_{i-j}	d mm.	ρ	$P_{ult.}$ KN	P_{test} KN	$\frac{P_{test}}{P_{ult.}}$	ε_s (av.) x μ	f_s (av.) N/mm^2	ε_s(max.) x μ	f_s(max.) N/mm^2
T_{2-1}	-	0	1548.8	1239.0	0.800	1100	223.4	1500	305.5
T_{2-2}	152	0.147	1535.2	1312.5	0.855	1123	239.6	1419	302.8
T_{2-3}	152	0.294	1578.0	1360.0	0.862	1235	251.5	1600	317.5
T_{1-3}	152	0.735	1511.8	1330.0	0.880	1270	259.0	1650	316.1
T_{2-4}	152	1.175	1780.0	1580.0	0.888	1355	290.0	1720	351.2
T_{2-5}	152	1.795	1463.9	1281.5	0.877	1305	269.0	1505	318.5
T_{2-6}	152	2.351	1349.5	1230.0	0.912	1580	321.2	1820	361.5

T_{i-j}	f_c N/mm^2	$\frac{f_c}{f_{cu}}$ for Column	$\frac{f_s(av)}{f_y}$	$\frac{f_s(max)}{f_y}$	f_{bs}(av) N/mm^2	f_{bs}(max) N/mm^2	f_{bs}(CP110) N/mm^2	f_{bs}(ACI) N/mm^2
T_{2-1}	24.71	0.765	0.465	0.630	5.59	7.62	2.97	5.57
T_{2-2}	26.10	0.801	0.513	0.648	5.99	7.57	2.91	5.48
T_{2-3}	26.94	0.790	0.547	0.690	6.29	7.94	2.92	5.50
T_{1-3}	25.93	0.795	0.585	0.714	6.48	7.90	2.86	5.40
T_{2-4}	31.38	0.785	0.607	0.735	7.25	8.78	3.00	5.62
T_{2-5}	23.95	0.799	0.587	0.695	6.74	7.96	2.84	5.36
T_{2-6}	21.33	0.824	0.664	0.747	8.03	9.03	2.91	5.47

T_{i-j}	f_{bs} (av.) / f_{cu} for base	f_{bs} (max.) / f_{cu} for base	f_{bs} (CP110) / f_{cu} for base	f_{bs} (ACI) / f_{cu} for base	f_{bs} (av.) / f_{bs} (CP110)	f_{bs} (av.) / f_{bs} (ACI)
T_{2-1}	0.158	0.215	0.084	0.157	1.682	1.004
T_{2-2}	0.175	0.221	0.085	0.160	2.058	1.093
T_{2-3}	0.183	0.231	0.085	0.160	2.154	1.144
T_{1-3}	0.195	0.238	0.086	0.163	2.27	1.200
T_{2-4}	0.201	0.244	0.083	0.156	2.380	1.290
T_{2-5}	0.206	0.243	0.087	0.164	2.373	1.257
T_{2-6}	0.235	0.265	0.085	0.160	2.759	1.468

Average value for f_c /(f_{cu} for column) for series (2) is 0.794.

All base slabs are 200 mm. thick.

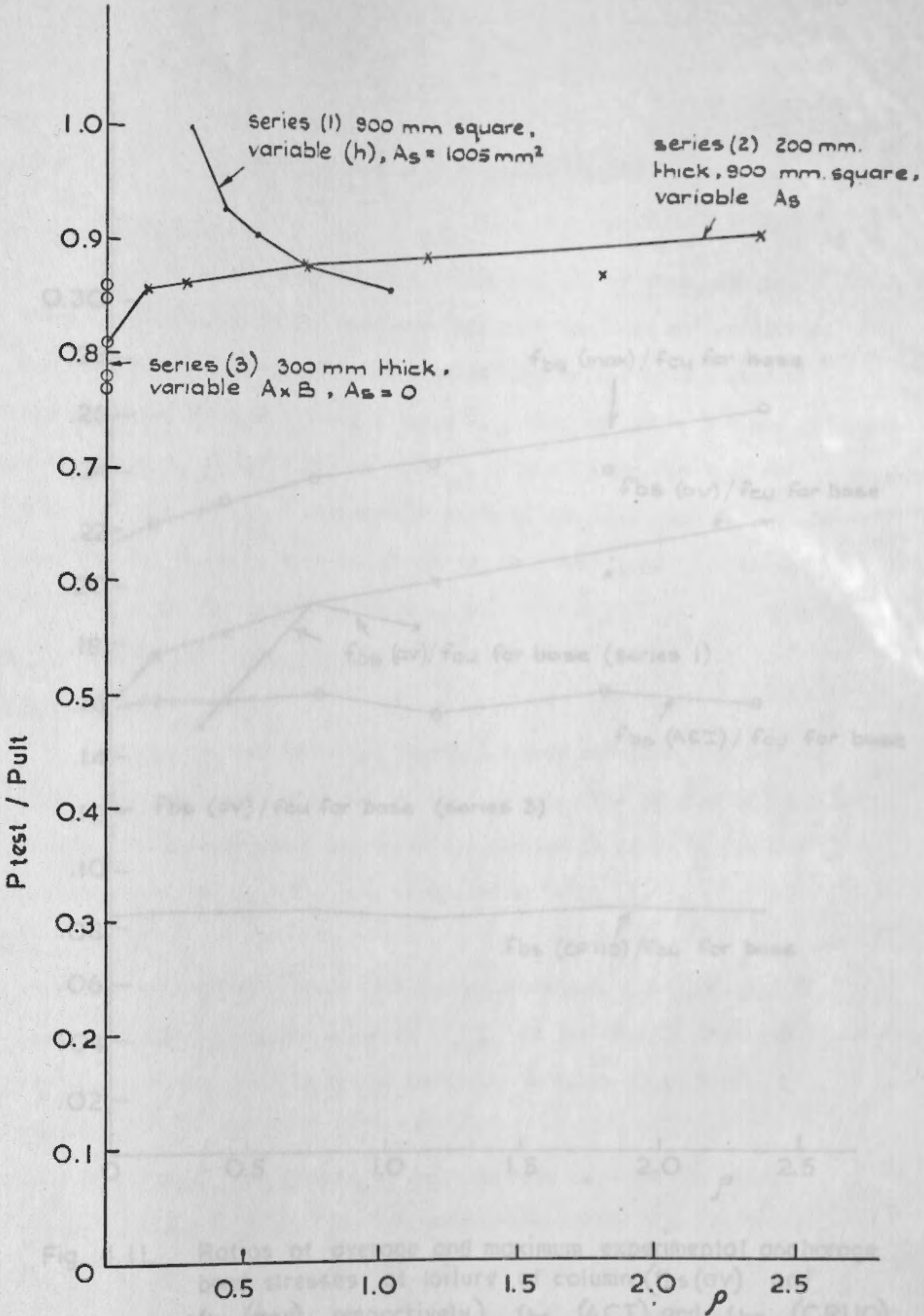

Fig. 4.10 Ratio of maximum experimental axial load on column (P_{test}) to calculated ultimate axial load for column using equ. (1) (P_{ult}) v % of tensile reinforcement in base slab (ρ).

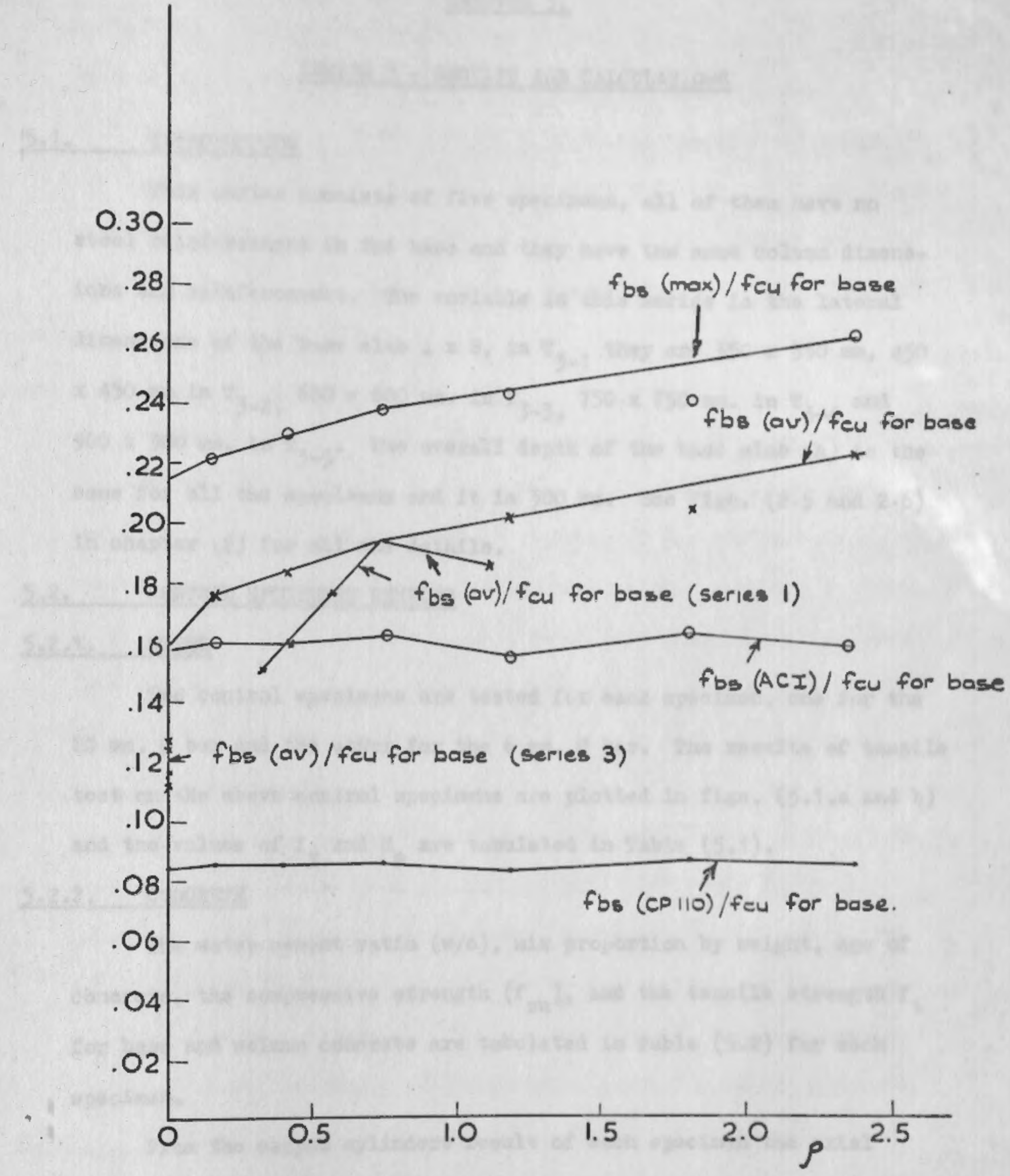

Fig. 4.11. Ratios of average and maximum experimental anchorage bond stresses at failure of column (f_{bs} (av) and f_{bs} (max) respectively), f_{bs} (ACI) and f_{bs} (CP110) to the cube strength (f_{cu}) for base concrete v % of tensile reinforcement in base slab (ρ).

CHAPTER 5.

SERIES 3 - RESULTS AND CALCULATIONS

5.1. INTRODUCTION

This series consists of five specimens, all of them have no steel reinforcement in the base and they have the same column dimensions and reinforcement. The variable in this series is the lateral dimensions of the base slab A x B, in T_{3-1} they are 350 x 350 mm, 450 x 450 mm. in T_{3-2}, 600 x 600 mm. in T_{3-3}, 750 x 750 mm. in T_{3-4} and 900 x 900 mm. in T_{3-5}. The overall depth of the base slab (h) is the same for all the specimens and it is 300 mm. See figs. (2·5 and 2·6) in chapter (2) for all the details.

5.2. CONTROL SPECIMENS RESULTS

5.2.1. STEEL

Two control specimens are tested for each specimen, one for the 20 mm. ∅ bar and the other for the 6 mm. ∅ bar. The results of tensile test on the above control specimens are plotted in figs. (5.1.a and b) and the values of f_y and E_s are tabulated in Table (5.1).

5.2.2. CONCRETE

The water cement ratio (w/c), mix proportion by weight, age of concrete, the compressive strength (f_{cu}), and the tensile strength f_t for base and column concrete are tabulated in Table (5.2) for each specimen.

From the capped cylinders result of each specimen the axial stress is plotted against the longitudinal strain in figs. (5.2·1a, 2a, 3a, 4a and 5a) for column concrete and figs. (5.2·1b, 2b, 3b, 4b and 5b) for base concrete. From these graphs the average secant modulus (E_c) is calculated, then the axial stress is plotted against (E_c) for both column and base concrete as in figs. (5.2·1c, 2c, 3c, 4c and 5c). Also the axial stress is plotted against the lateral strain as in figs. (5.2-1d, 2d, 3d, 4d, and 5d) for column concrete and figs. (5.2 1e, 2e, 3e, 4e, and 5e) for base concrete, then the average Poisson's ration (ν_c) is calculated by dividing the lateral strain on the longitudinal one for each load increment and then the axial stress is plotted against the Poisson's ratio (ν_c) for both column and base concrete in figs. (5.2 1f, 2f, 3f, 4f and 5f).

5.3. SPECIMENS RESULTS

5.3.1. LONGITUDINAL STRAIN

From the results of the 8" Demec gauges on column concrete and the results of the electrical resistance strain gauges on column steel, the average longitudinal strains are calculated for each specimen, then the experimental axial load is plotted against them as shown in figs. (5.3, 1, 2, 3, 4 and 5) then it is also plotted against the longitudinal strain for all the specimens as in fig. (5.3.a) for column steel and fig. (5.3.b) for column concrete.

5.3.2. LATERAL STRAIN

The experimental axial load is plotted against the average lateral strain calculated from the results of the 6" Demec gauges on column concrete and from the electrical resistance strain gauges on column link for each specimen as shown in figs. (5.4.1, 2, 3, 4 and 5) and also plotted against the lateral strain for all the specimens as in fig. (5.4.a) for column link and fig. (5.4.b) for column concrete.

5.3.3. DEFLECTION OF BASE SLAB AND TOTAL SHORTENING OF SPECIMEN

The experimental axial load is plotted against the average upward deflection of the base slab at 105 mm. from faces of the column and on the centre lines of the base slab for all the specimens except T_{3-1} whose base is not wide enough to fix the dial gauges on. See fig. (5.5). Then it is plotted against the total shortening of the specimen for all specimens as in fig. (5.6).

5.4. MODE OF FAILURE

All of the specimens of this series failed by anchorage bond failure between column longitudinal reinforcement and base concrete. In these specimens the cracks probably first started on the bottom face of the base slab from the column longitudinal 20 mm. ∅ bars, and then as the load increased they travelled inward until they met eachother within the 4-20 mm. ∅ bars and outward until they reached the sides of the base slab, after that they travelled upwards nearly to the top of the base slab, except T_{3-1} in which the cracks reached the top. Some of the cracks which reached the outsides of the base started from the point of intersection of two cracks started from two bars. The number of cracks differ from specimen to specimen but the mode of failure and the pattern of the cracks is similar, see figs. (5.7 and 5.8·1, 2, 3, 4, and 5).

In all the specimens as the 20 mm. ∅ bars slipped downward, the base slab cracked as above and then the column concrete failed by compression.

5.5. CALCULATIONS

5.5.1. TABLE (5.3) AND GRAPHS

Using equation (1) and the control specimens results, the theoretical ultimate axial load (P_{ult}) is calculated for each specimen, also the experimental axial load (P_{test}) is recorded, hence, the ratio of (P_{test}/P_{ult}) is found.

From the average and maximum longitudinal strains measured on column reinforcement (ε_s (av.))and (ε_s (max.)) respectively, the axial load on each of the 20 mm. ∅ bars is found for both ε_s (av.) and ε_s (max.), from that the average load taken by the longitudinal column reinforcement is found and subtracted from (P_{test}) and the result is divided by the cross-sectional area of the column concrete

(A_c) this gives the value of (f_c) then the ratio of (f_c/f_{cu} of column concrete) is found. See example of calculations in (3.5.1).

The average and maximum anchorage bond stresses f_{bs}(av.) and f_{bs} (max.) respectively are calculated from the average and maximum load on the 20 mm. Ø bars, then the ratios of (f_{bs} (av.) and f_{bs}(max.)) to f_{cu} of base concrete are calculated.

The average and maximum stresses in the 20 mm. Ø column reinforcement f_s(av.) and f_s (max.) respectively are calculated from ε_s (av.) and ε_s (max.) and the steel control specimens results then the ratios of these stresses to f_y are found.

From CP110:Part 1:1972 Table (22) the allowable anchorage bond stress corresponding to f_{cu} for base f_{bs} (CP110) is read for all specimens. Then the ratios of f_{bs} (CP110) / f_{cu} for base and f_{bs} (av.) / f_{bs} (CP110) are found.

Using equation (6.a) and assuming $f'_c = 0.8\ f_{cu}$ the allowable anchorage bond stress f_{bs} (ACI) for the American code is found to be equal to ($0.9366\ f_{cu}$). This value is calculated for all specimens, then the ratios of f_{bs} (ACI)/f_{cu} for base and f_{bs}(av.)/f_{bs}(ACI) are found.

For each specimen the ratio of ($0.8\ f_{cu}\ A_c/P_{ult}$) is calculated, then the average value of these ratios is found. This represents a theoretical point for the strength of the column when the longitudinal steel carries zero load and the base area equal to the area of the column, see also (3.5.1).

All the above results and calculations are tabulated in table (5.3).

The ratio of (P_{test}/P_{ult}) is plotted against the ratio of the loaded area of the base to the area of the column. On the same graph the results of T_{1-5} is plotted which has a (ρ) value = 0.443. The theoretical points for series (1) and this series are also plotted, see fig. (5.9). The ratios of f_{bs} (av.), f_{bs} (max.), f_{bs} (CP110) and f_{bs} (ACI) to f_{cu} for base are plotted against the ratio of the loaded area of the base to the area of the column. On the same graph f_{bs} (av.) / f_{cu} for base from T_{1-5} results is plotted, see fig. (5.10).

5.5.2. PUNCHING SHEAR

It is known from series (1) calculations that for such depths as those of series (3) the punching shear failure always occurs before anchorage bond failure. Hence, if punching shear failure is allowed all series (3) specimens would have failed by punching shear failure.

5.5.3. ANCHORAGE LENGTH FOR LONGITUDINAL COLUMN REINFORCEMENT

The required depth of base slab to resist anchorage bond failure using the properties of T_{3-5} and the following :-

1) CP110: Part 1: 1972

From Table (22) the allowable anchorage bond stress $= 2.94\ \text{N/mm}^2$.

The permissible stress in the column longitudinal

$$\text{reinforcement} = \frac{500 \times 2000}{2000 + 500}$$

$$= 400\ \text{N/mm}^2.$$

Hence using equation (5) gives

$$l = 680.3\ \text{mm}.$$

2) ACI 318 - 1971

$f'_c = 0.8\ f_{cu} = 27.8\ \text{N/mm}^2$.

and the yield stress corresponding to a strain of 0.35% for the 20mm. Ø bar of T_{3-5}.

$$= 490.5\ \text{N/mm}.$$

Hence equation (6.a) gives the maximum anchorage length,

that is, $l = 445.1$ mm.

5.6. DISCUSSION OF SPECIMENS RESULTS AND CALCULATIONS

5.6.1. COLUMN LONGITUDINAL STRAIN

At failure of all specimens of this series, the strain measured on the column longitudinal reinforcement is far less than that measured on the concrete where at the beginning of the tests they are almost the same apart from small difference due to the two different methods used to measure them, and as slipping started the steel graph lags behind until failure of the column concrete by compression. Just before failure all steel graphs except that of T_{3-5} have a very steep slope, see figs. (5.3.1, 2, 3, 4 and 5).

The shape of these graphs is the same for the strains measured on steel as in fig. (5.3.a) and on concrete as in fig.(5.3.b).

5.6.2. COLUMN LATERAL STRAIN

The tests of this series did not have compressive stress in the column link (i.e. contraction) apart from T_{3-2}, see fig. (5.4.2) but their strains both measured on column link and concrete have the same value at the beginning of the test apart from the difference due to the methods of measurement and the difficulty in fixing the gauges on the column link due to the gemometric properties of the 6 mm. ∅ bars, then as the load increased, the link strain starts to lag behind that measured on the concrete until failure of the column concrete in compression.

Apart from T_{3-2} at the beginning of the test otherwise all the specimens have the same shape of lateral strain graphs as in fig. (5.4.a) for column link and the graphs of lateral strains measured on the concrete have the same shape, see fig. (5.4.b).

5.6.3. UPWARD DEFLECTION OF BASE SLAB AND TOTAL SHORTENING OF SPECIMEN

The graphs of average deflection of the base slab at 105 mm. from the faces of the column on the centre lines of the base slab, increase sharply at the beginning of the tests, then as the load increased the graph starts to curve upward until failure of the specimen.

This series shows that as the lateral dimensions of the base slab increased, the deflection decreased for the same axial load, see fig. (5.5).

The axial load is proportional to the total shortening of the specimen at the beginning of the tests, then as the specimen starts to fail, this proportionality does not hold and the total shortening increases more rapidly, also this series shows that the total shortening is less for specimens with larger lateral dimensions at the same axial load. See fig. (5·6).

5.6.4. TABLE (5.3) AND GRAPHS

The average value of (f_c / f_{cu} for column) for all the specimens of this series is 0.783, where the average for all the experimental program except T_{1-1} is 0.797.

From fig. (5.9) the results can be represented by two straight lines, the first one is through T_{3-1}, T_{3-2}, T_{3-3} and T_{3-4} results. The equation of this line obtained by regression analysis is

$$\frac{P_{test}}{P_{ult}} = 7.15 \times 10^{-3} \left(\frac{AB - a_1 a_2}{a_1\ a_2} \right) + 0.753$$

The intercept of this line when $\frac{AB - a_1 a_2}{a_1\ a_2} = 0$ is 0.753.

The difference between the intercept and the theoretical point of series (1) results = 0.753 - 0.662 = 0.09 and this is less than 0.11 which corresponds to 200 mm. anchorage length, see fig. (3.10). The corresponding anchorage length to 0.09 is 163.6 mm.

The second line is through T_{3-4} and T_{3-5} results and it is flatter than the first one. This shows that by increasing the dimensions of the base slab from 350 x 350 mm^2. to 750 x 750 mm^2. the strength increased by 7.7% compared with equation (1) and by increasing the dimensions from 750 x 750 mm^2. to 900 x 900 mm^2. the strength increased only by 1.3%.

This shows that the effect of increasing the base lateral dimensions may be has no effect on the column strength after certain dimensions. If it is assumed that after $\frac{AB - a_1\ a_2}{a_1\ a_2}$ reaches (30) which is the same value suggested by Meyerhof (1953), Ersoy and Hawkins (1960) for the bearing capacity of concrete, then when the base dimensions are 108 x 108 mm^2. the bond strength and the column strength become constant. In increasing (A_s) from zero to 1005 mm^2. that is varying (ρ) from zero to 0.443 the column strength increased by 7%, see T_{3-5} and T_{1-5}.

From fig. (5.10) the graphs of f_{bs} (av.) / f_{cu} for base and f_{bs} (max.) / f_{cu} for base also consisting of two straight lines, the second line is flatter than the first one and having the same shape as that of fig. (4.9). These graphs indicate that the bond strength increases as the lateral dimensions of the base increases. This has not been provided for in the British or American code when determining the anchorage bond stresses.

The graph also shows that the American code gives anchorage bond stresses higher even than the maximum experimental anchorage bond stresses where the British code gives safe anchorage bond stresses well below the average experimental anchorage bond stresses.

T_{1-5} point shows that increasing (A_s) and hence (ρ) in the base slab increases the bond strength between the column longitudinal reinforcement and base concrete.

5.6.5. PUNCHING SHEAR AND ANCHORAGE LENGTH

From series (1) results and calculations, the specimens of series (3) would have failed by punching shear if it was allowed to take place.

The British code gives anchorage length larger than that given by the American code which uses higher allowable stress in the longitudinal column steel.

5.7. CONCLUSIONS

From the results and calculations of series (3) specimens the following are concluded :-

1) As the lateral dimensions of the base slab increased the average bond strength between the longitudinal column reinforcement and the base slab concrete increases.

2) After certain dimensions of the base slab the bond strength and hence the column strength graphs start to flatten which may indicate that reaching some dimensions after which bond strength and hence column strength becomes constant.

More tests after T_{3-5} are needed to verify this.

3) This series also indicates that part of the column length is acting as extra anchorage length apart from the base slab depth.

4) The use of stepped bases should be looked at very carefully since this reduces the confinement of the longitudinal column bars and hence reduces the bond and column strength if it is not wide enough.

For unreinforced bases with a column of 200 mm. square the width of the step should be not less than one meter.

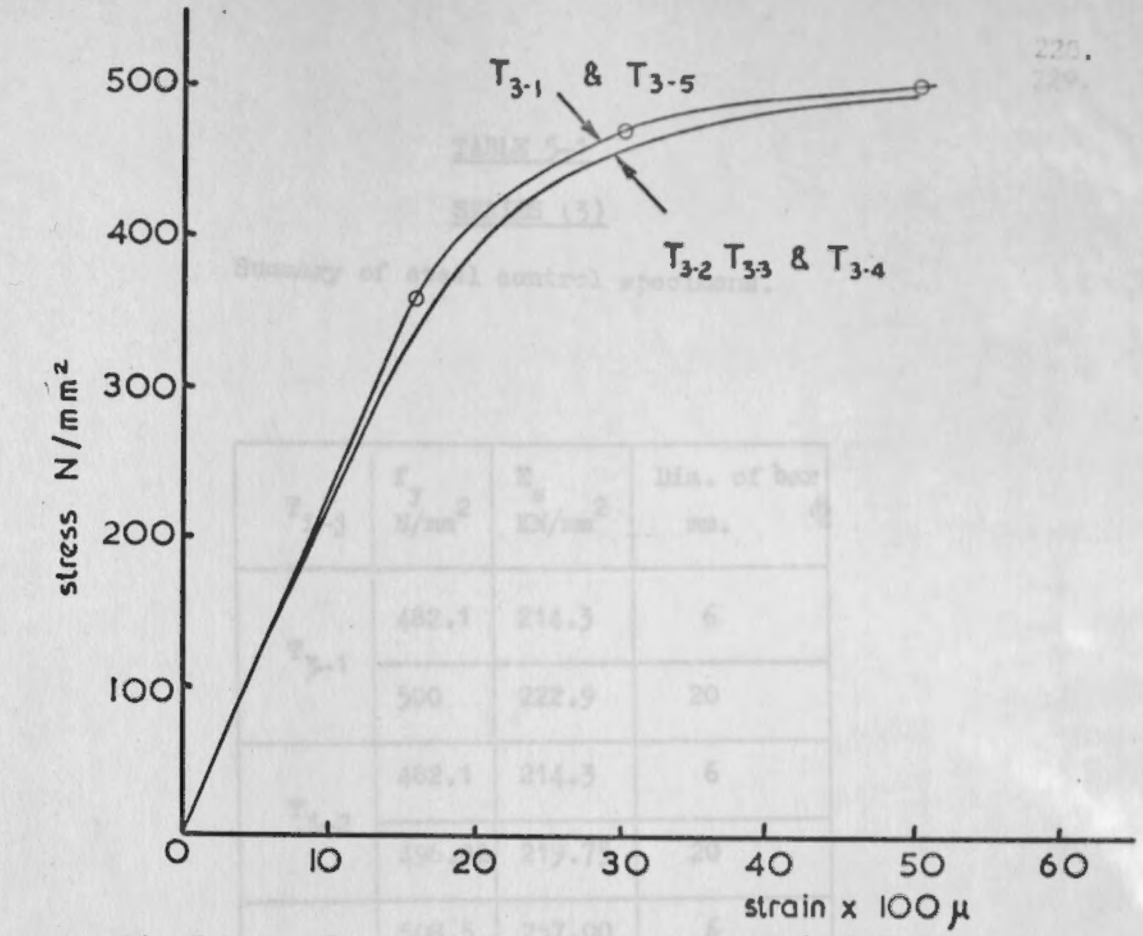

Fig. 5.1. a Stress v. strain for 20 mm Ø H-T square twisted steel bars

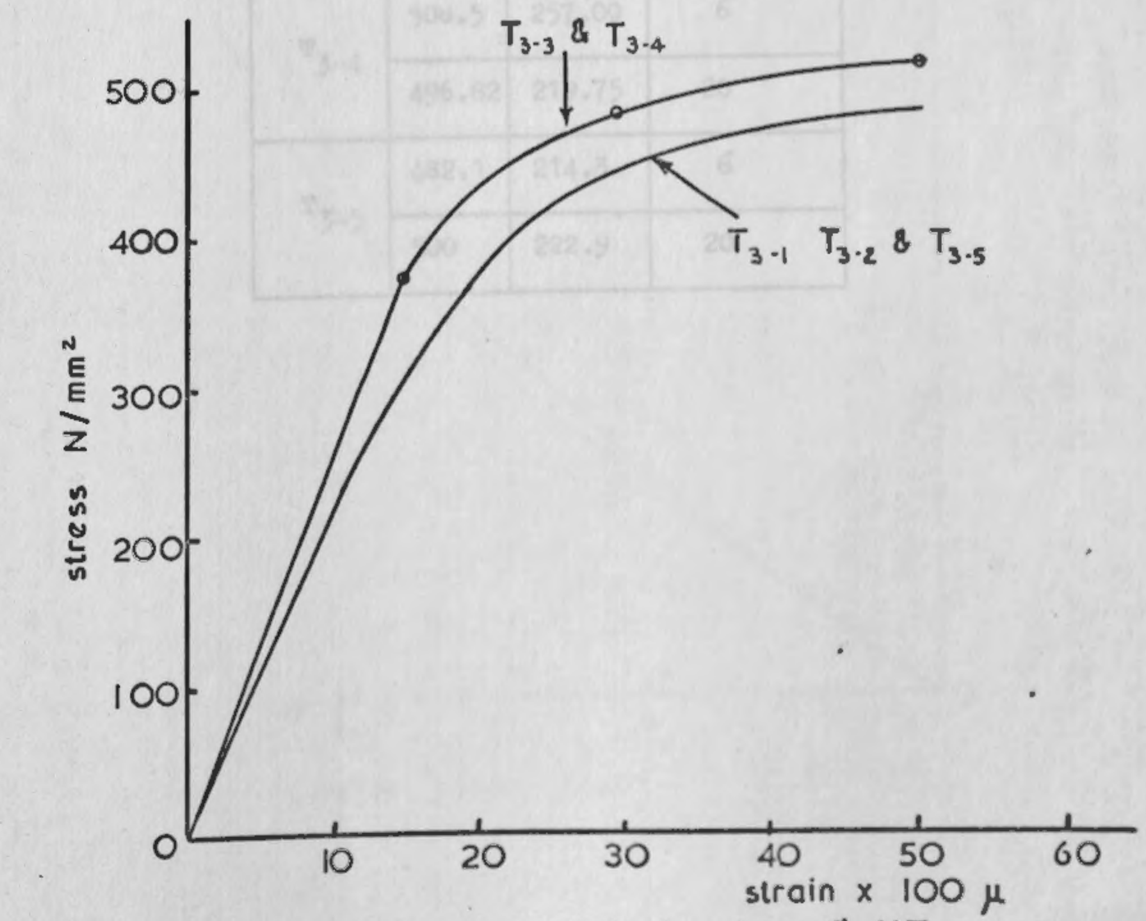

Fig. 5.1. b Stress v. strain for 6 mm Ø HT square twisted steel bars

TABLE 5-1

SERIES (3)

Summary of steel control specimens.

T_{i-j}	f_y N/mm^2	E_s KN/mm^2	Dia. of bar mm.
T_{3-1}	482.1	214.3	6
	500	222.9	20
T_{3-2}	482.1	214.3	6
	496.82	219.75	20
T_{3-3}	508.5	257.00	6
	496.82	219.75	20
T_{3-4}	508.5	257.00	6
	496.82	219.75	20
T_{3-5}	482.1	214.3	6
	500	222.9	20

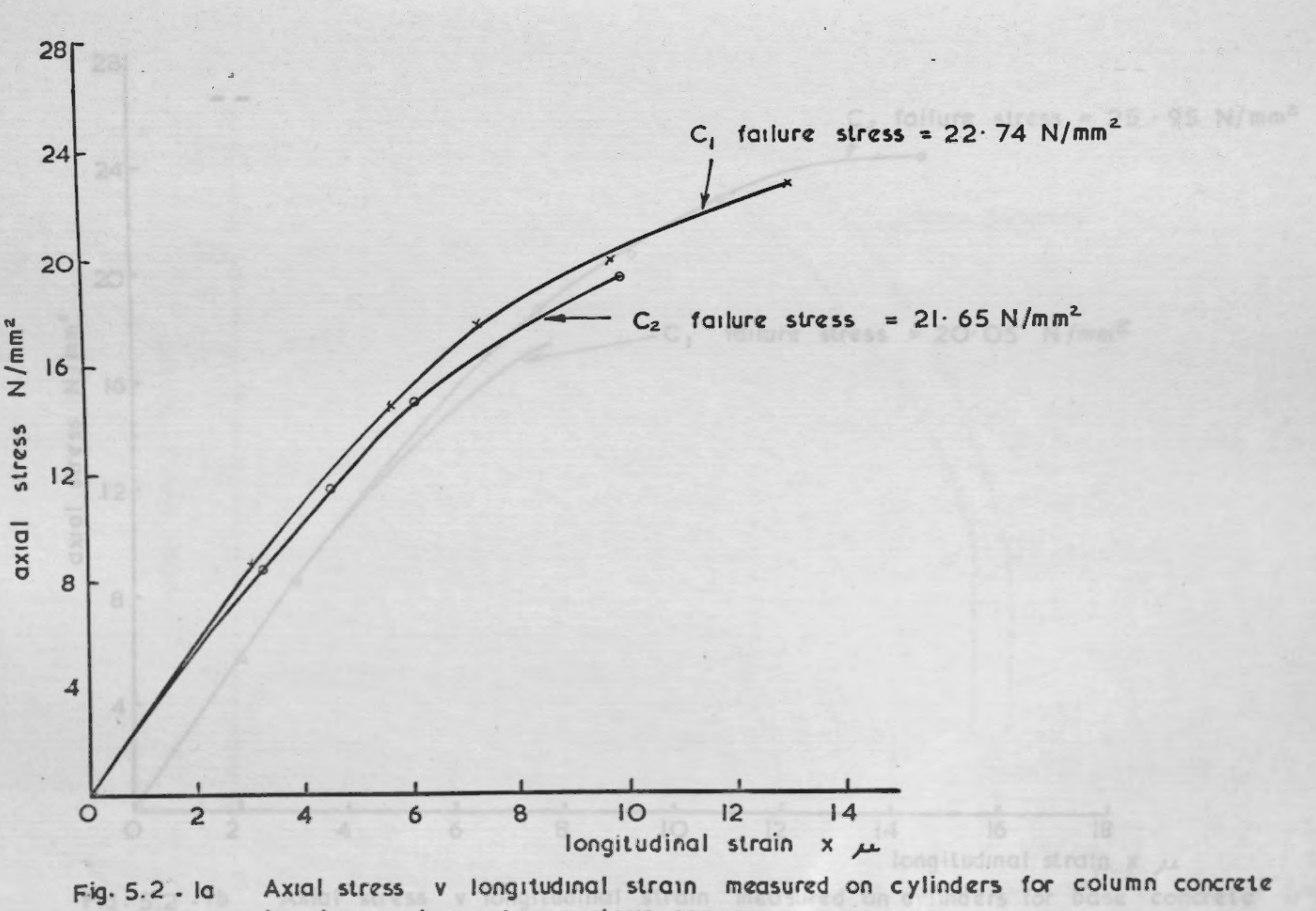

Fig. 5.2 · 1a Axial stress v longitudinal strain measured on cylinders for column concrete by electrical resistance strain gauges

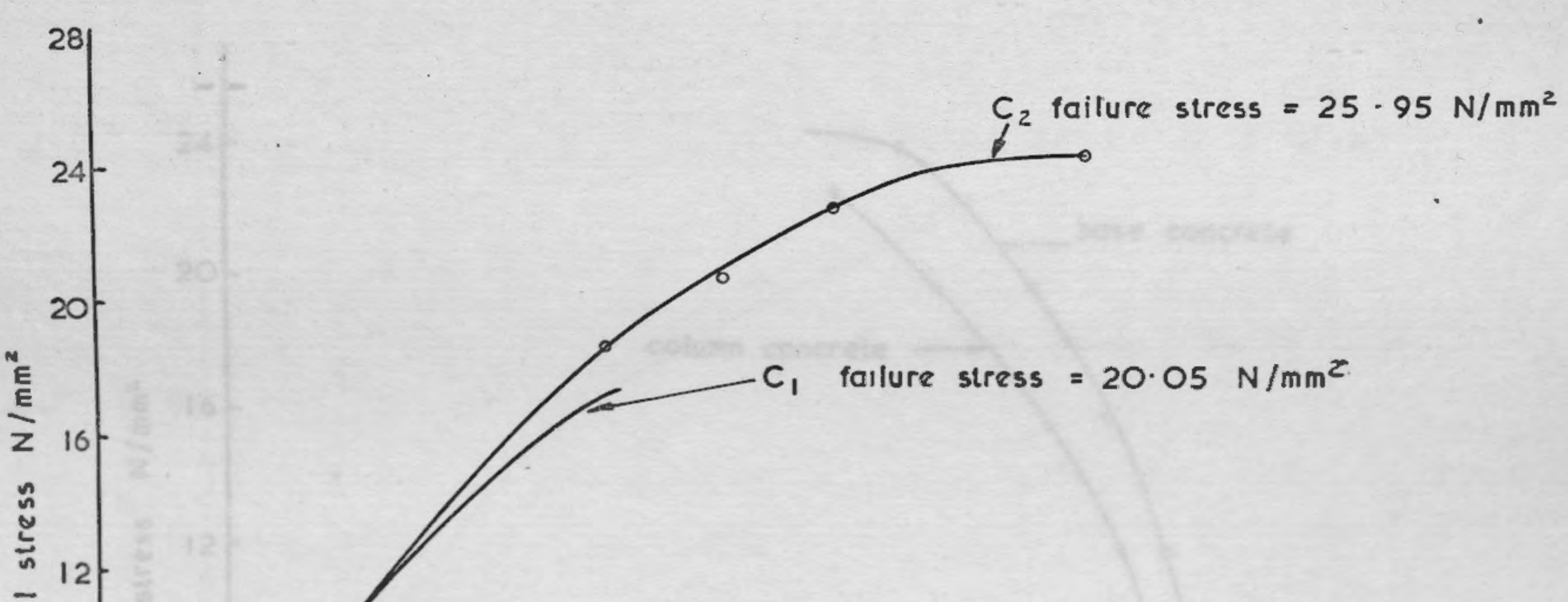

Fig. 5.2 · 1b Axial stress v longitudinal strain measured on cylinders for base concrete by electrical resistance strain gauges

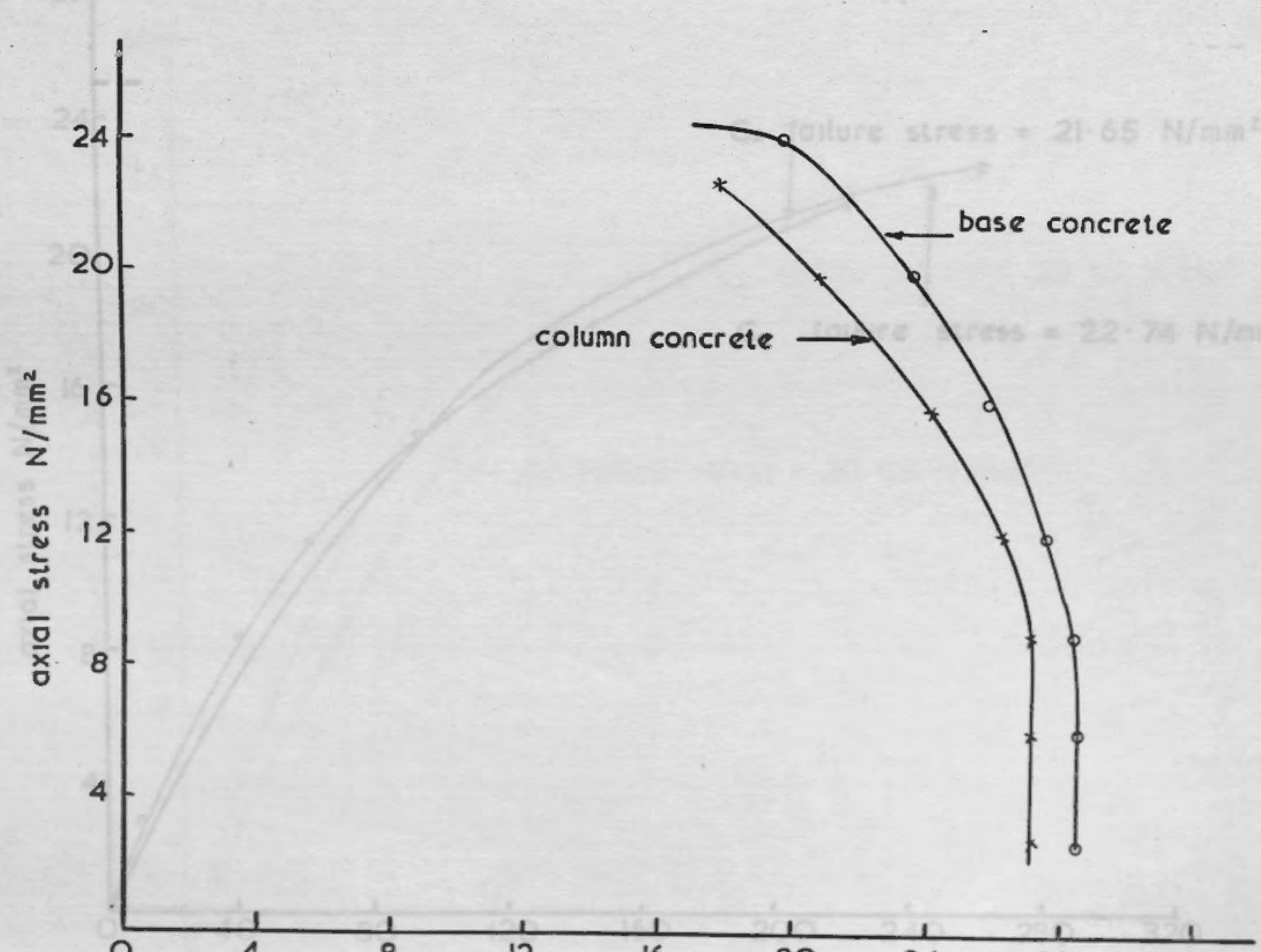

Fig. 5.2.1c Axial stress v modulus of elasticity for column concrete and for base concrete

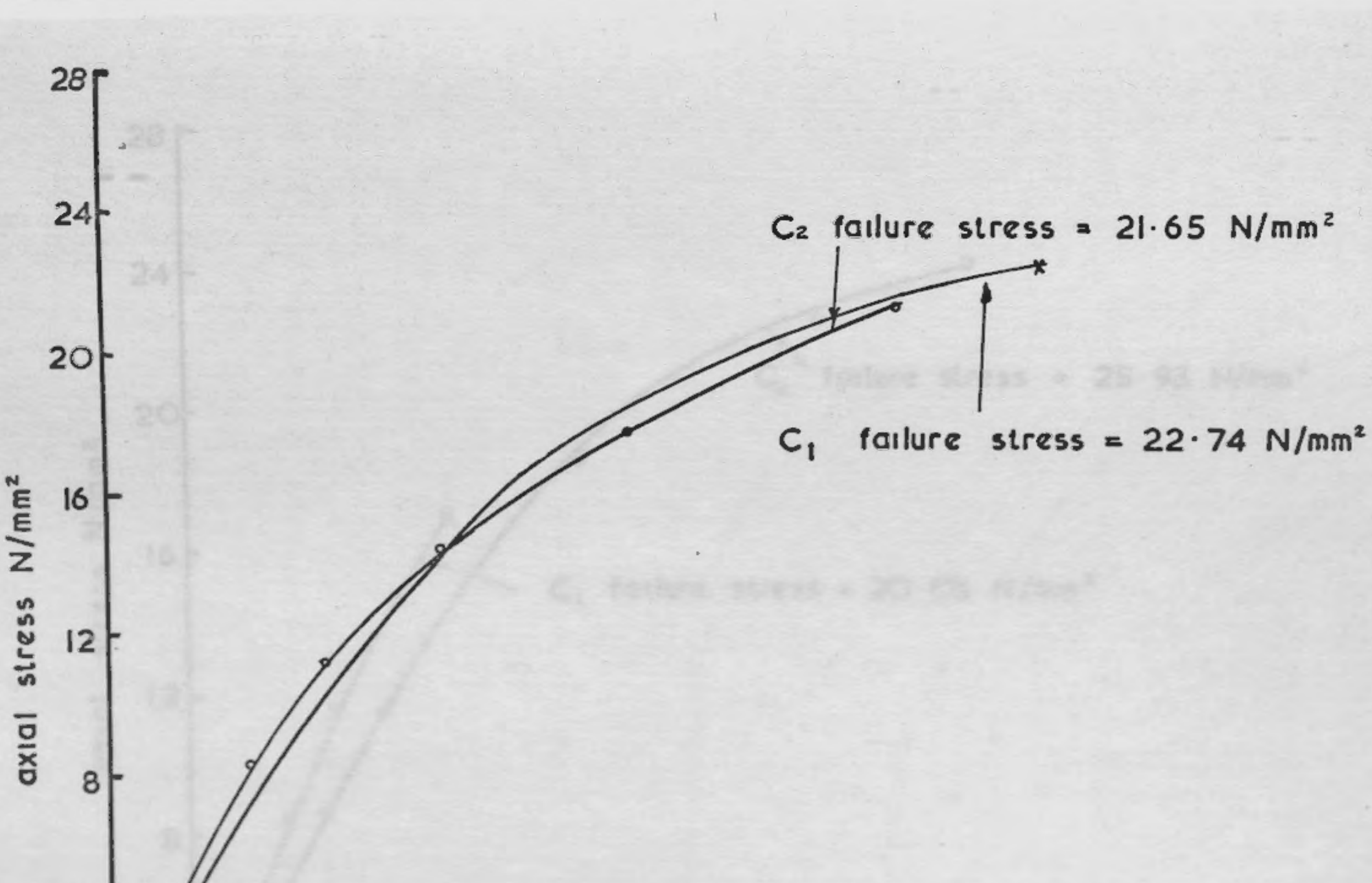

Fig. 5·2·1d. Axial stress v. lateral strain measured on cylinders for column concrete by electrical resistance strain gauges

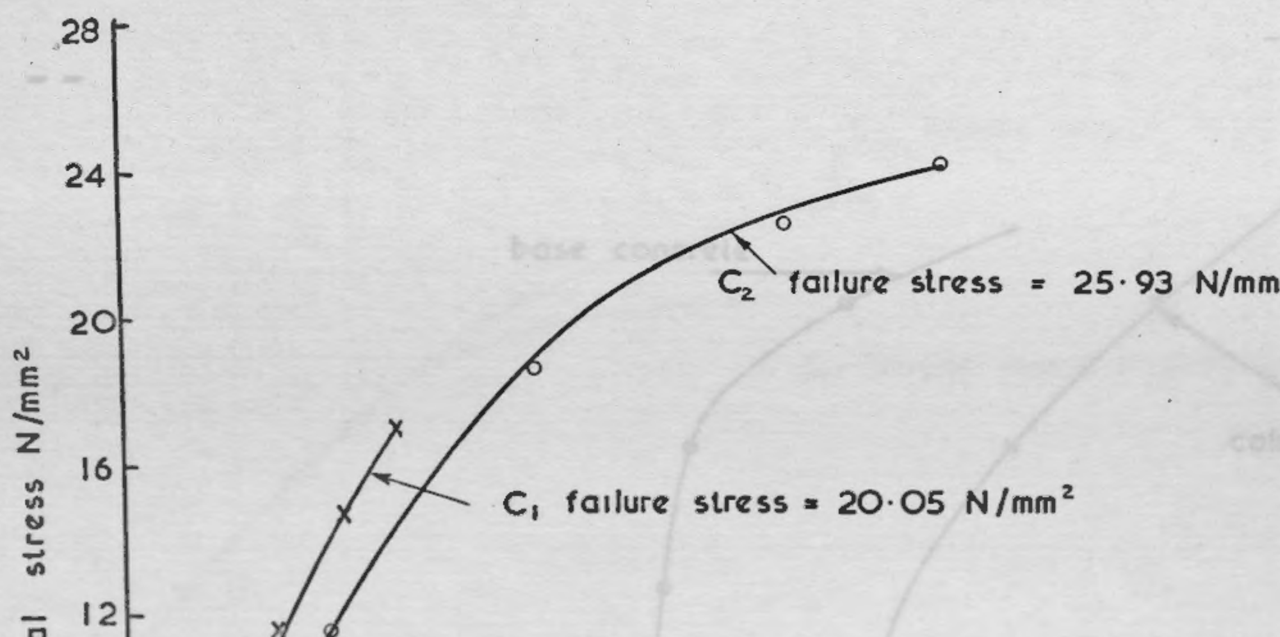

Fig. 5.2 · 1e. Axial stress v. lateral strain measured on cylinders for base concrete by electrical resistance strain gauges.

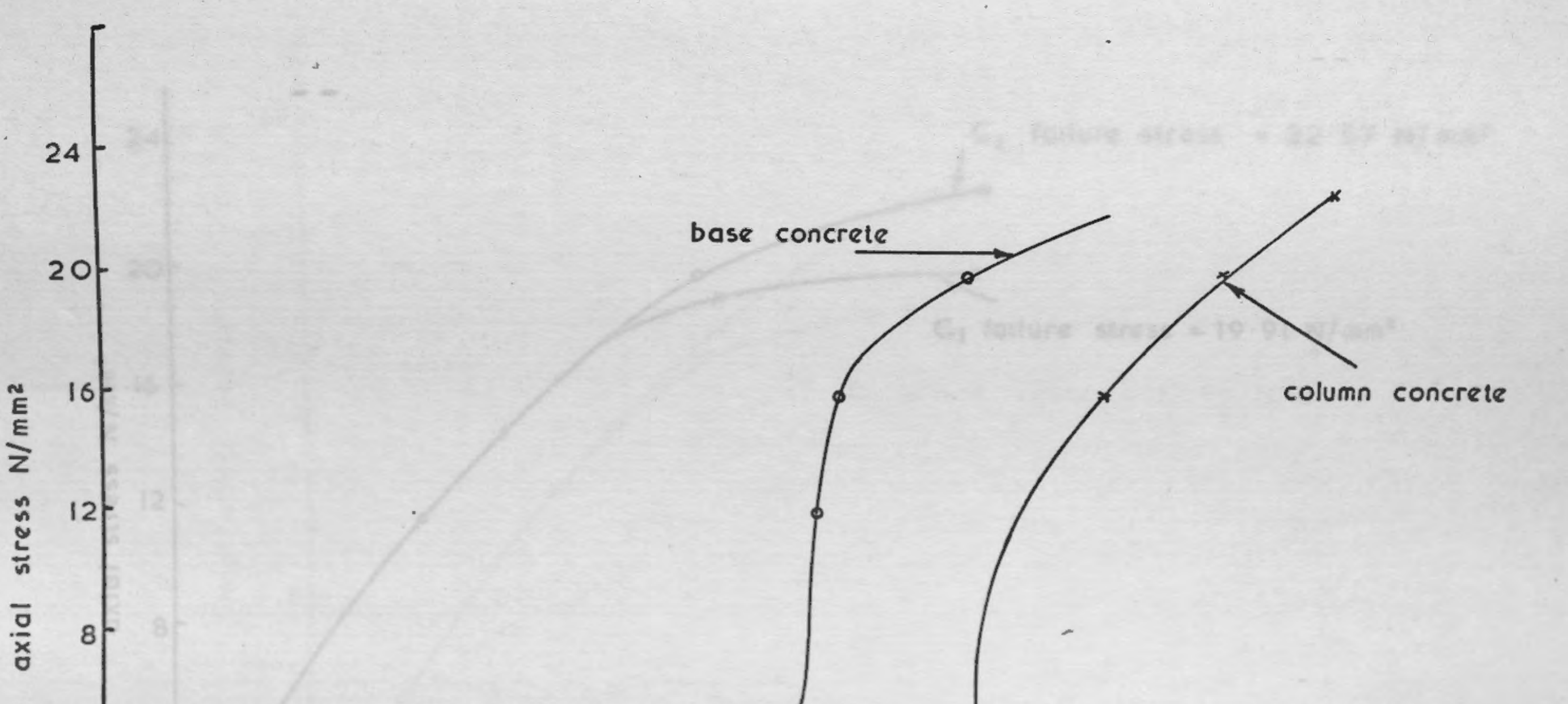

Fig. 5.2.1f. Axial stress v. Poisson's ratio νc for column concrete and base concrete.

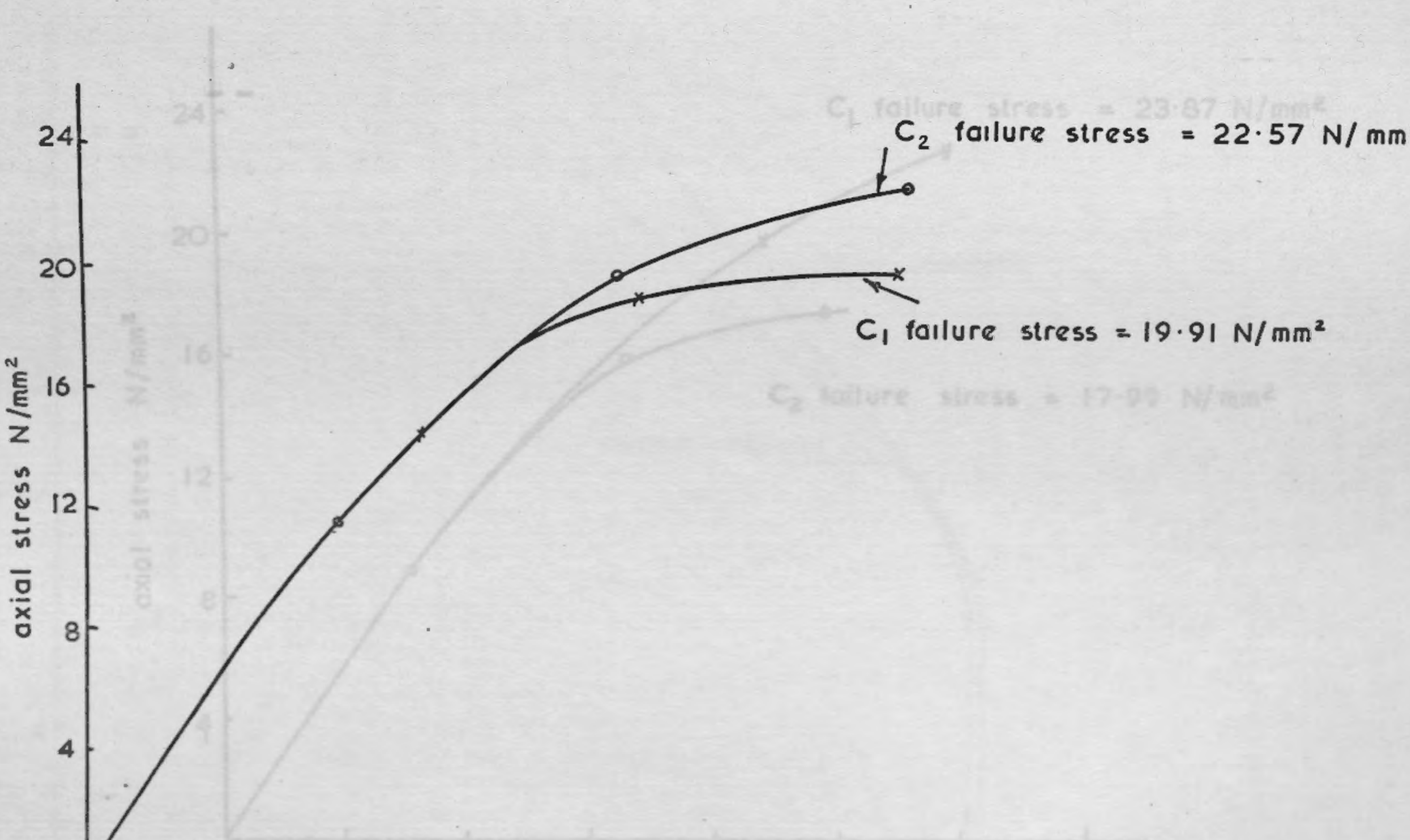

Fig. 5.2 2a. Axial stress v. longitudinal strain measured on cylinders for column concrete by electrical resistance strain gauges

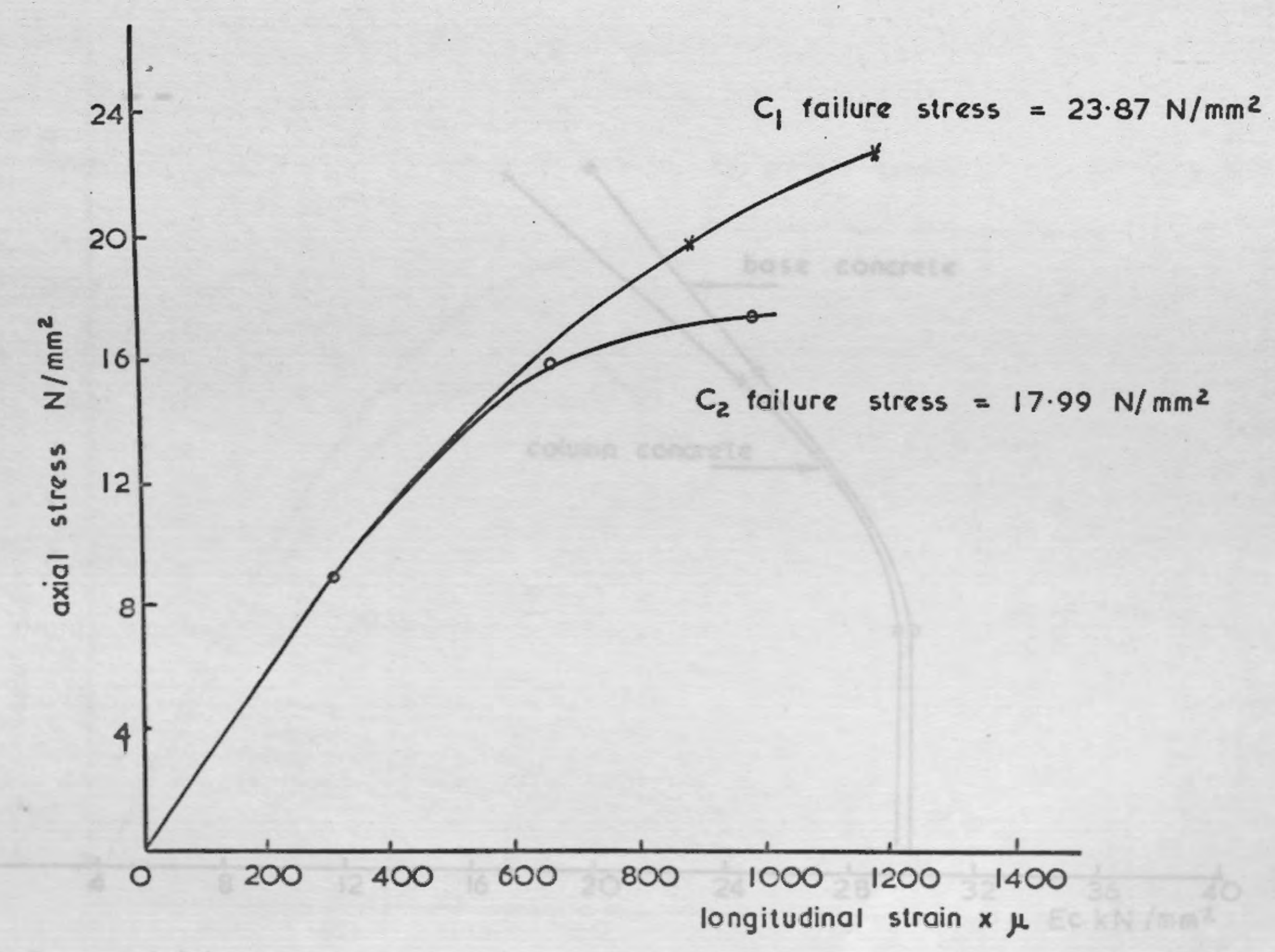

Fig. 5.2 2b. Axial stress v. longitudinal strain measured on cylinders for base concrete by electrical resistance strain gauges

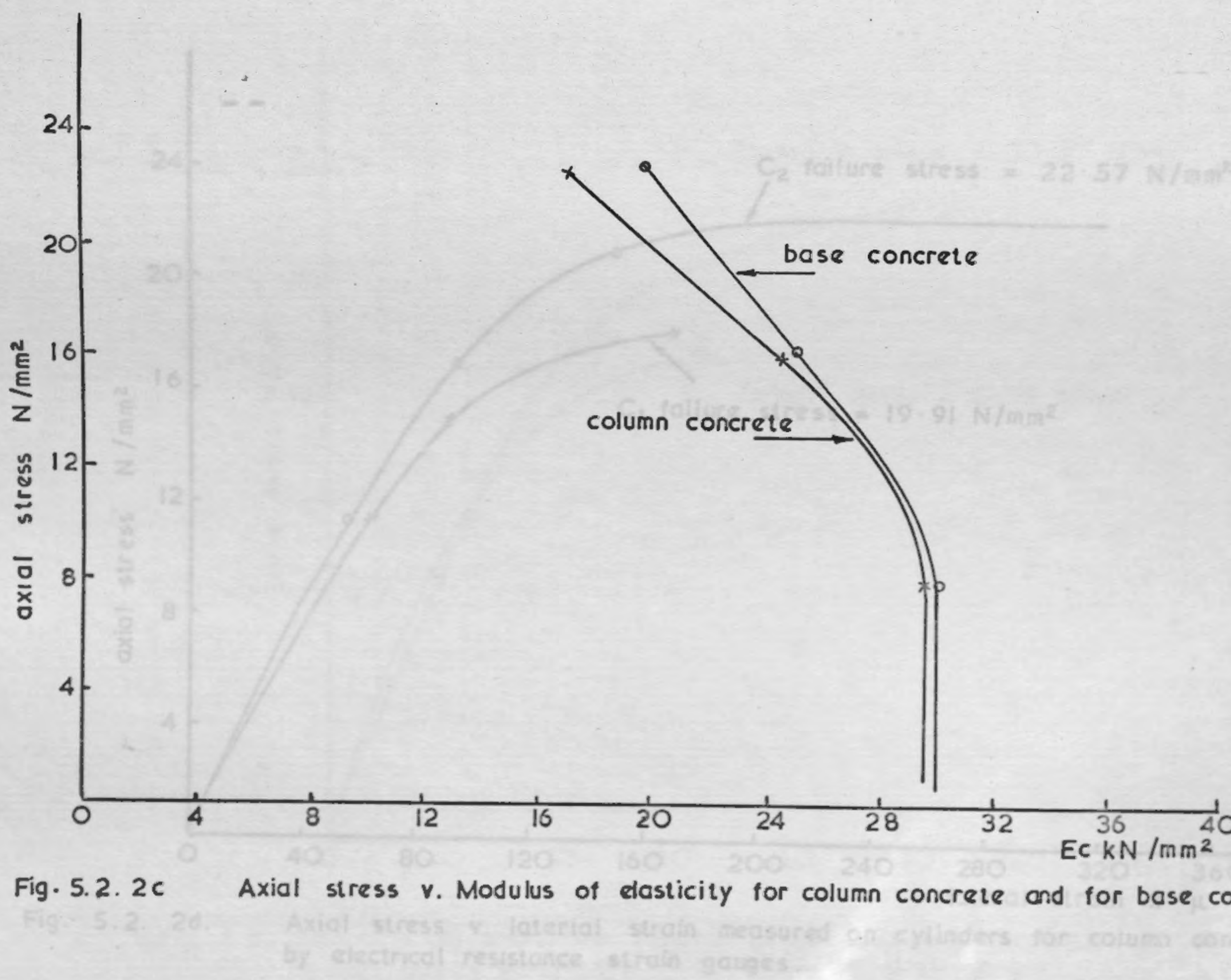

Fig. 5.2.2c Axial stress v. Modulus of elasticity for column concrete and for base concrete

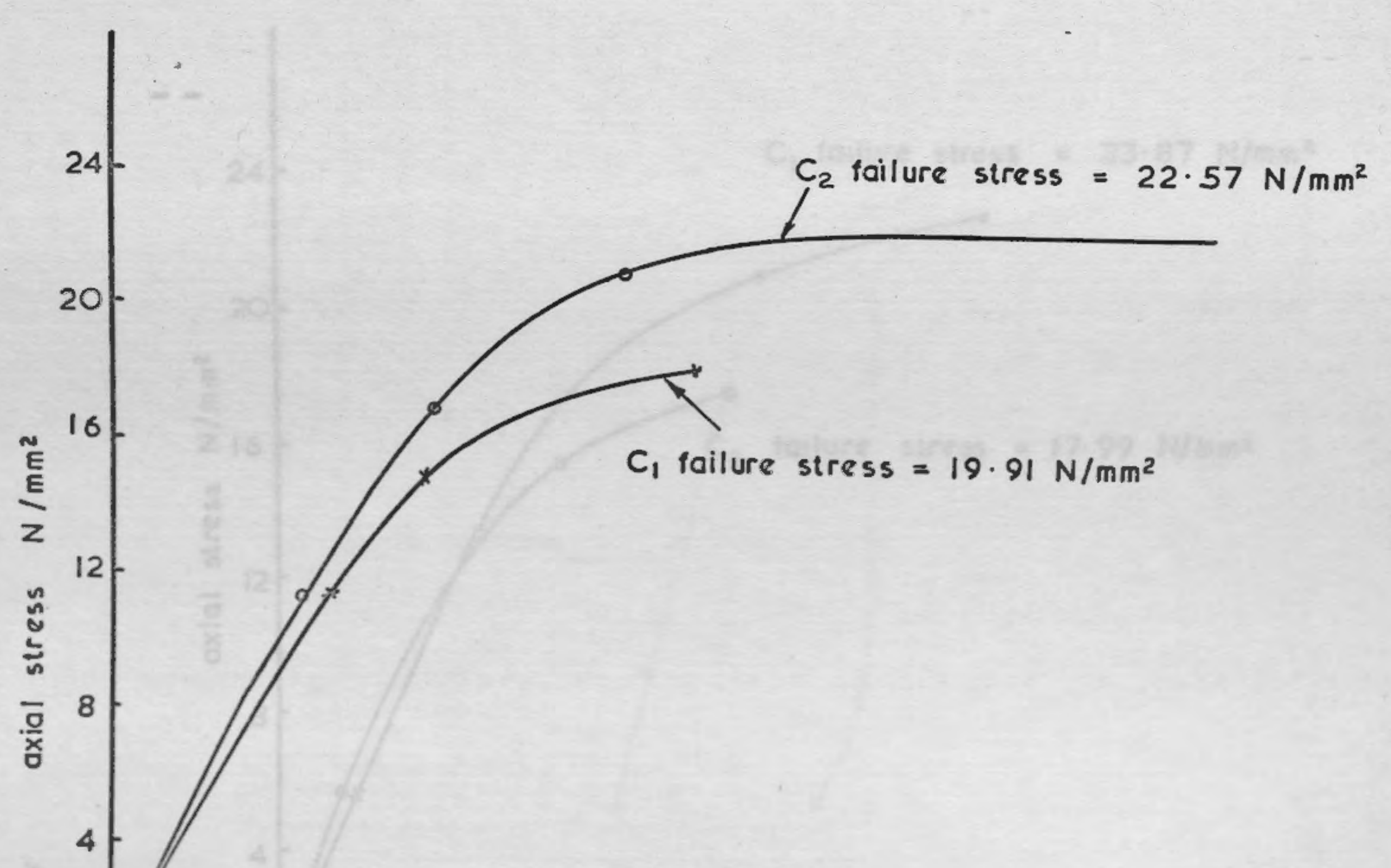

Fig. 5.2. 2d. Axial stress v. lateral strain measured on cylinders for column concrete by electrical resistance strain gauges.

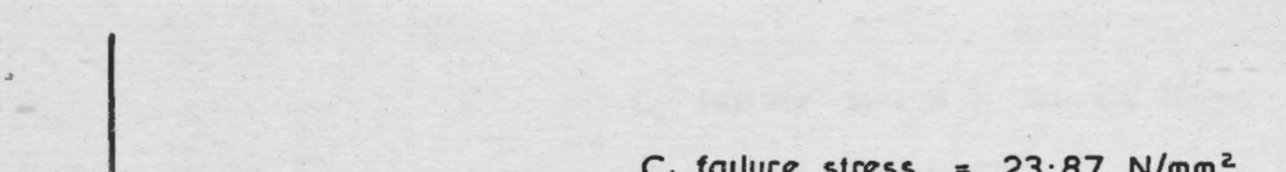

Fig. 5.2. 2e Axial stress v. lateral strain measured on cylinders for base concrete by electrical resistance strain gauges

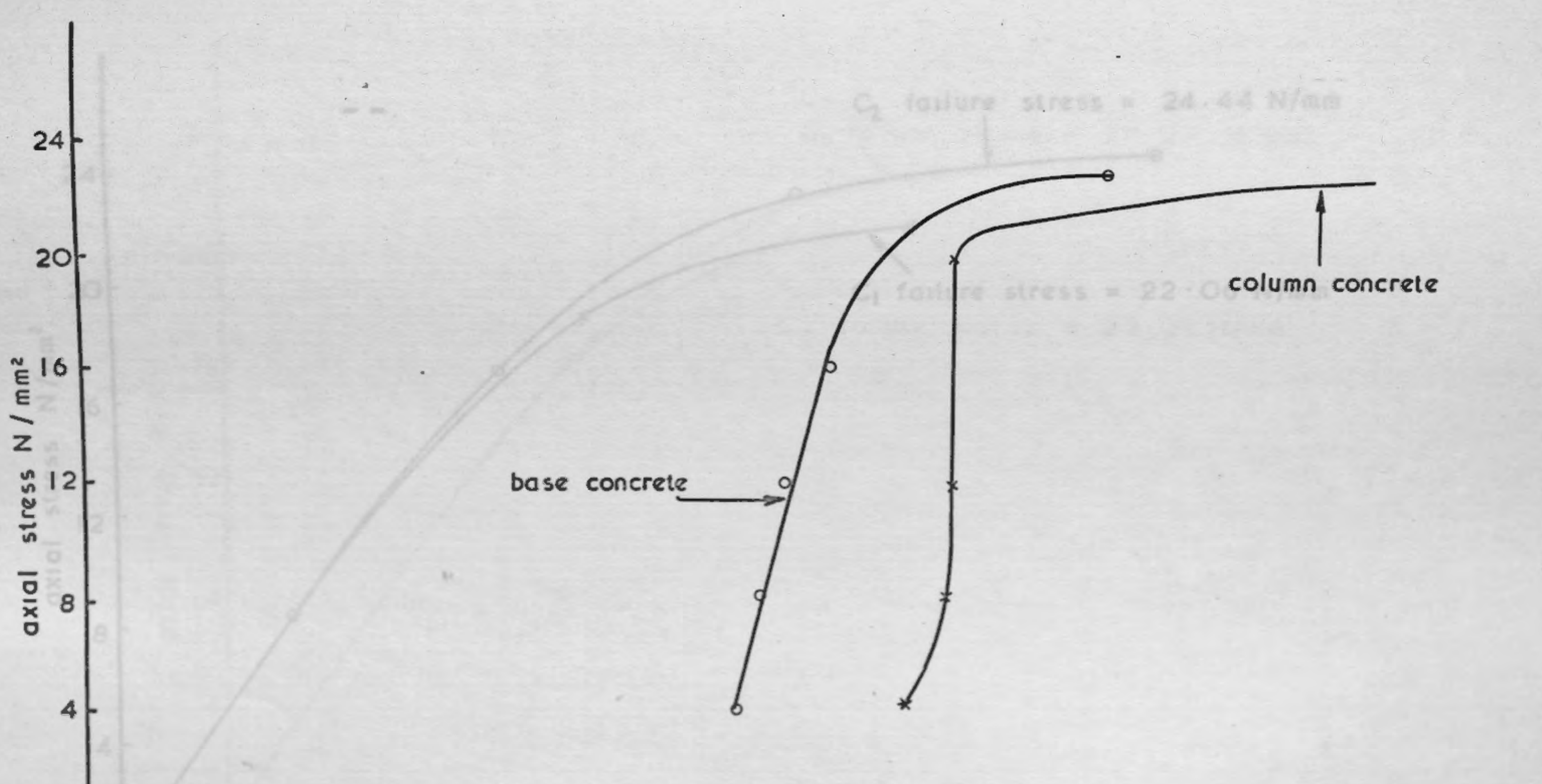

Fig. 5.2.2f Axial stress v. Poisson's ratio ϑc for column concrete and base concrete

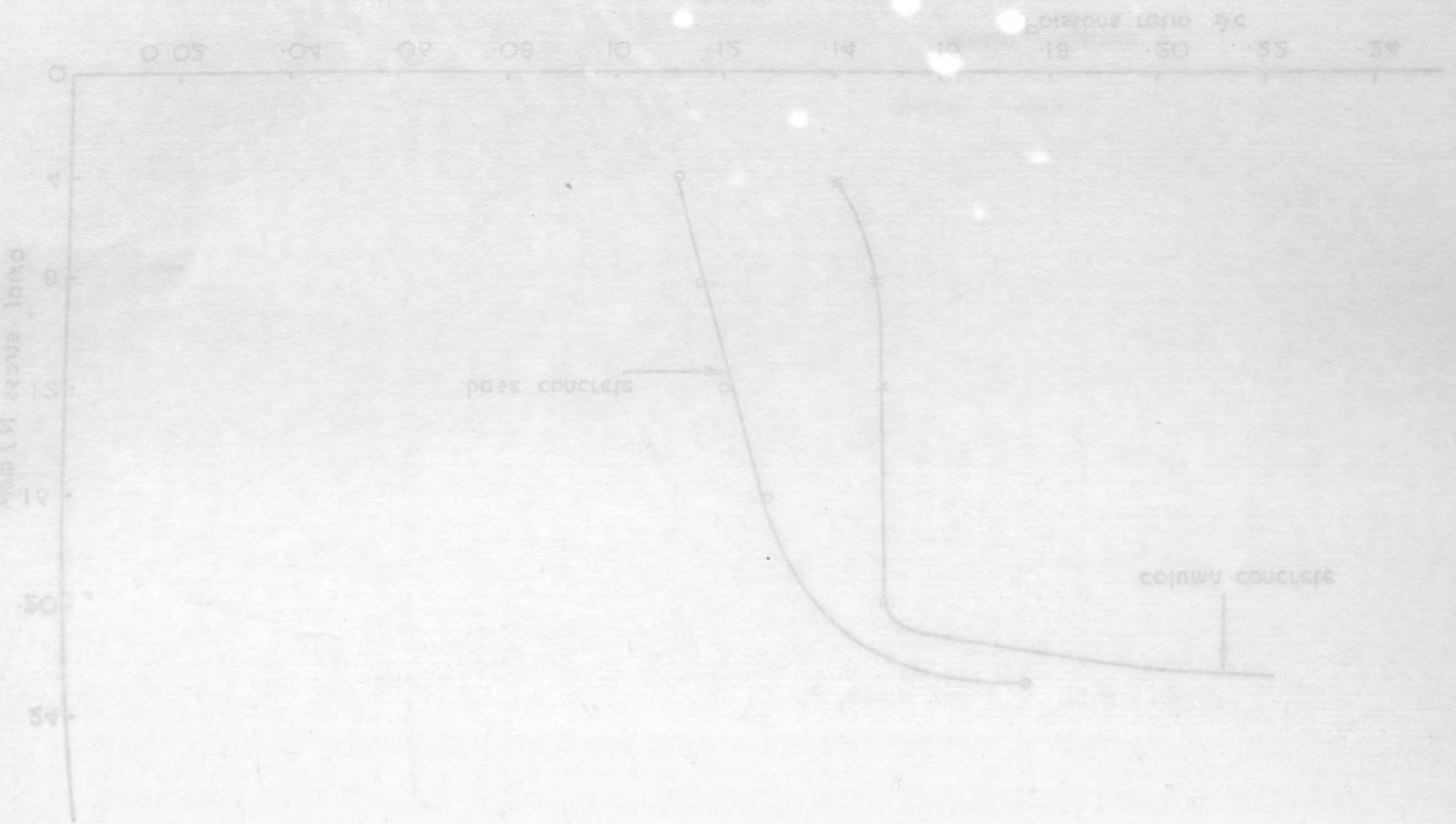

Fig 5.2.2d Axial stress v. Poissons ratio ʋc for column concrete and base concrete

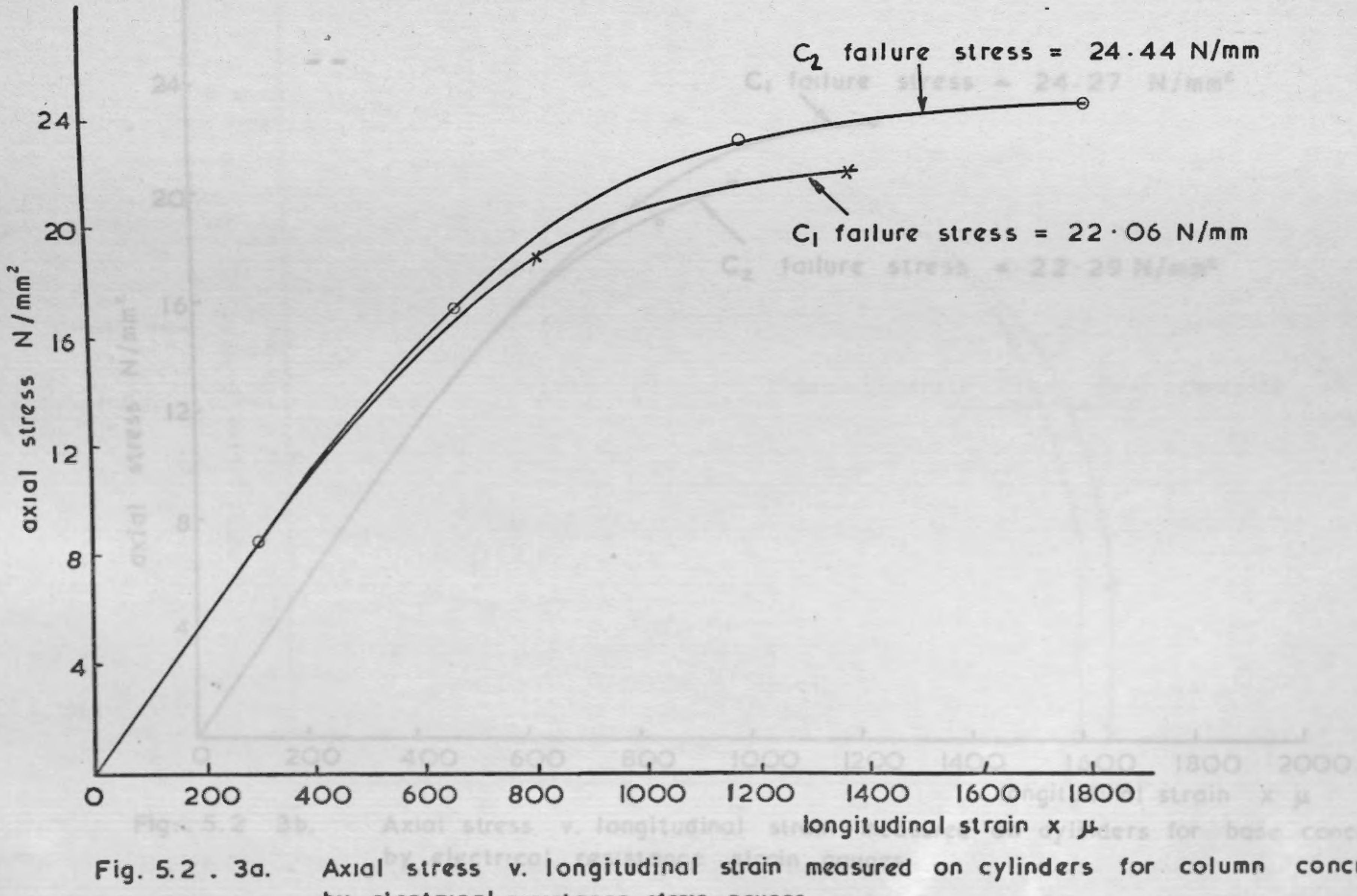

Fig. 5.2 . 3a. Axial stress v. longitudinal strain measured on cylinders for column concrete by electrical resistance strain gauges

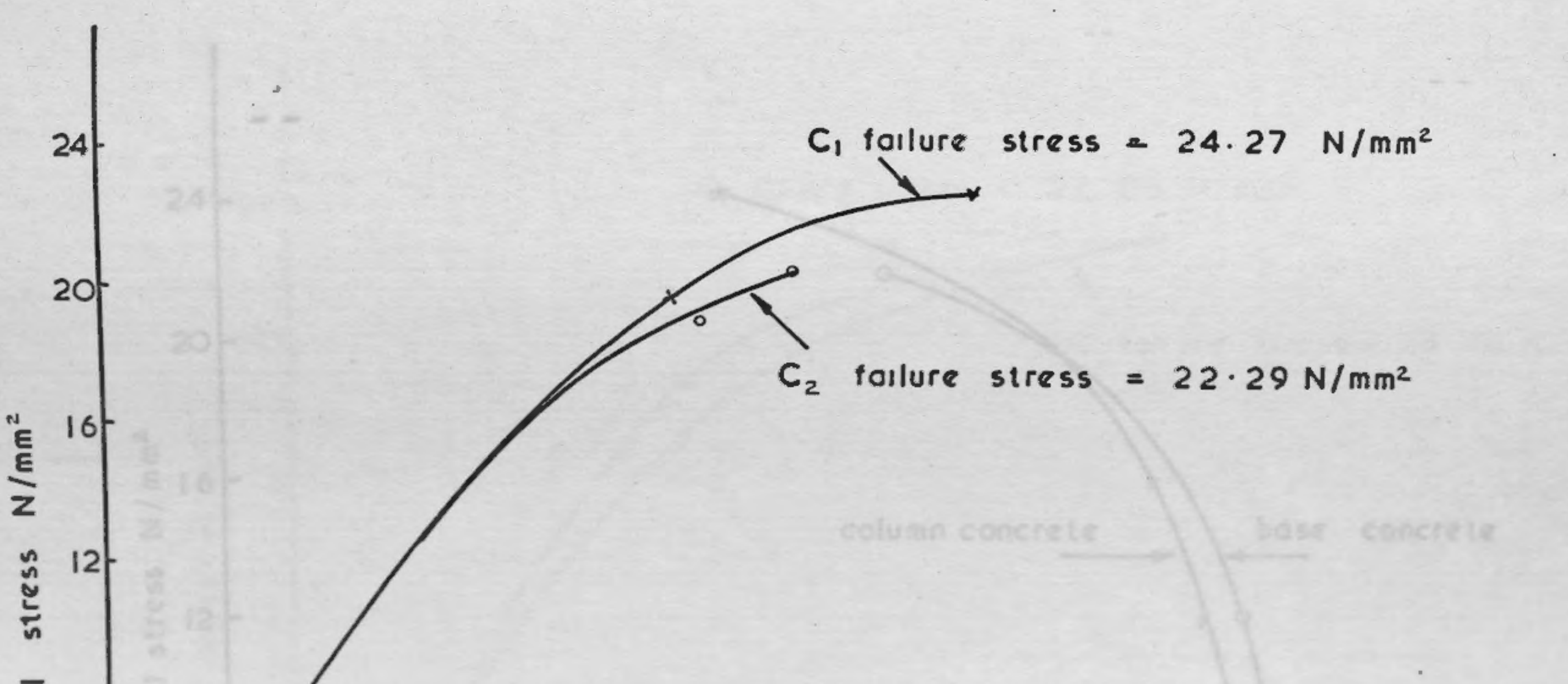

Fig. 5.2 3b. Axial stress v. longitudinal strain measured on cylinders for base concrete by electrical resistance strain gauges

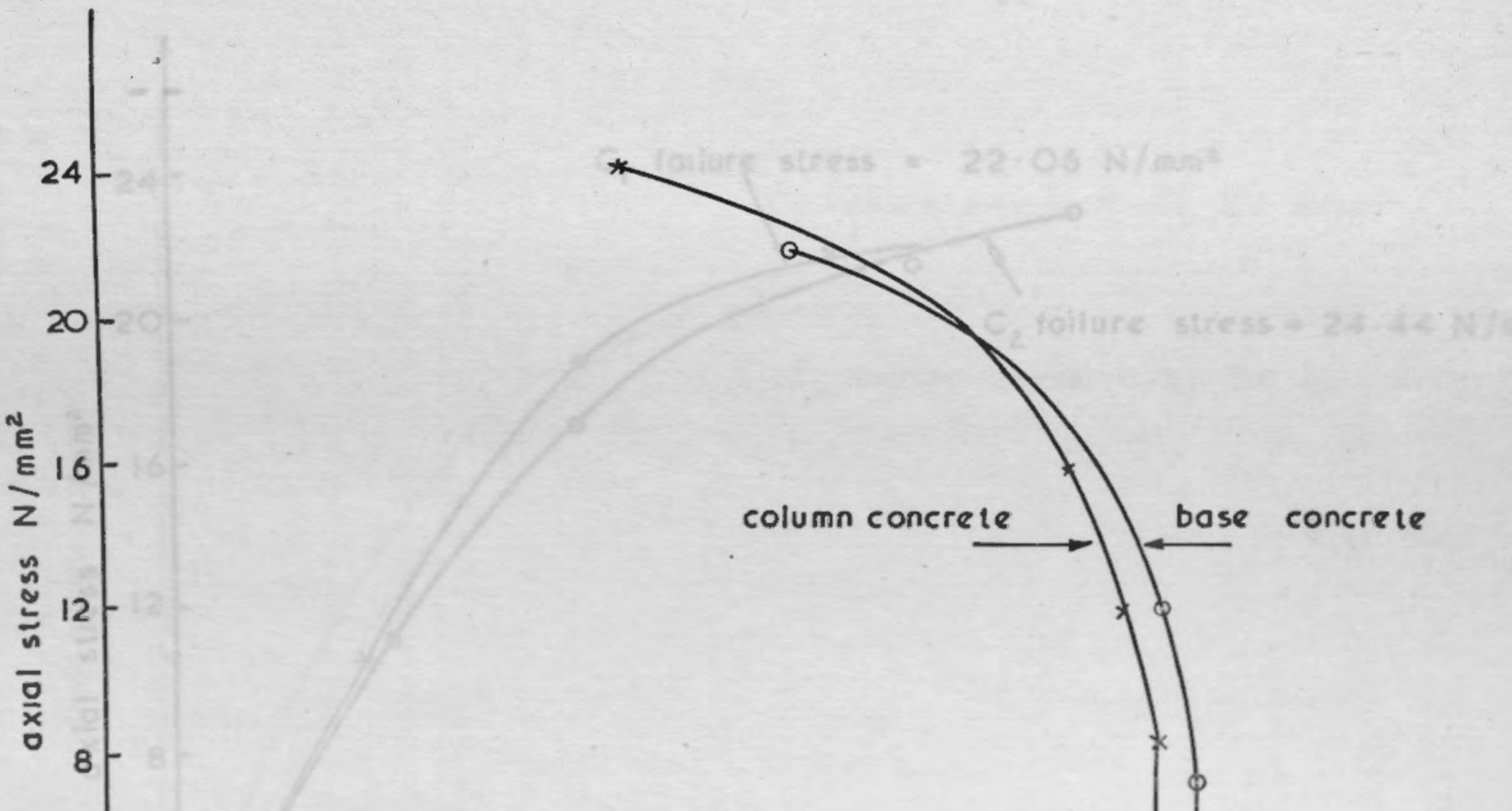

Fig. 5.2 . · 3c. Axial stress v. Modulus of elasticity for column concrete and for base concrete

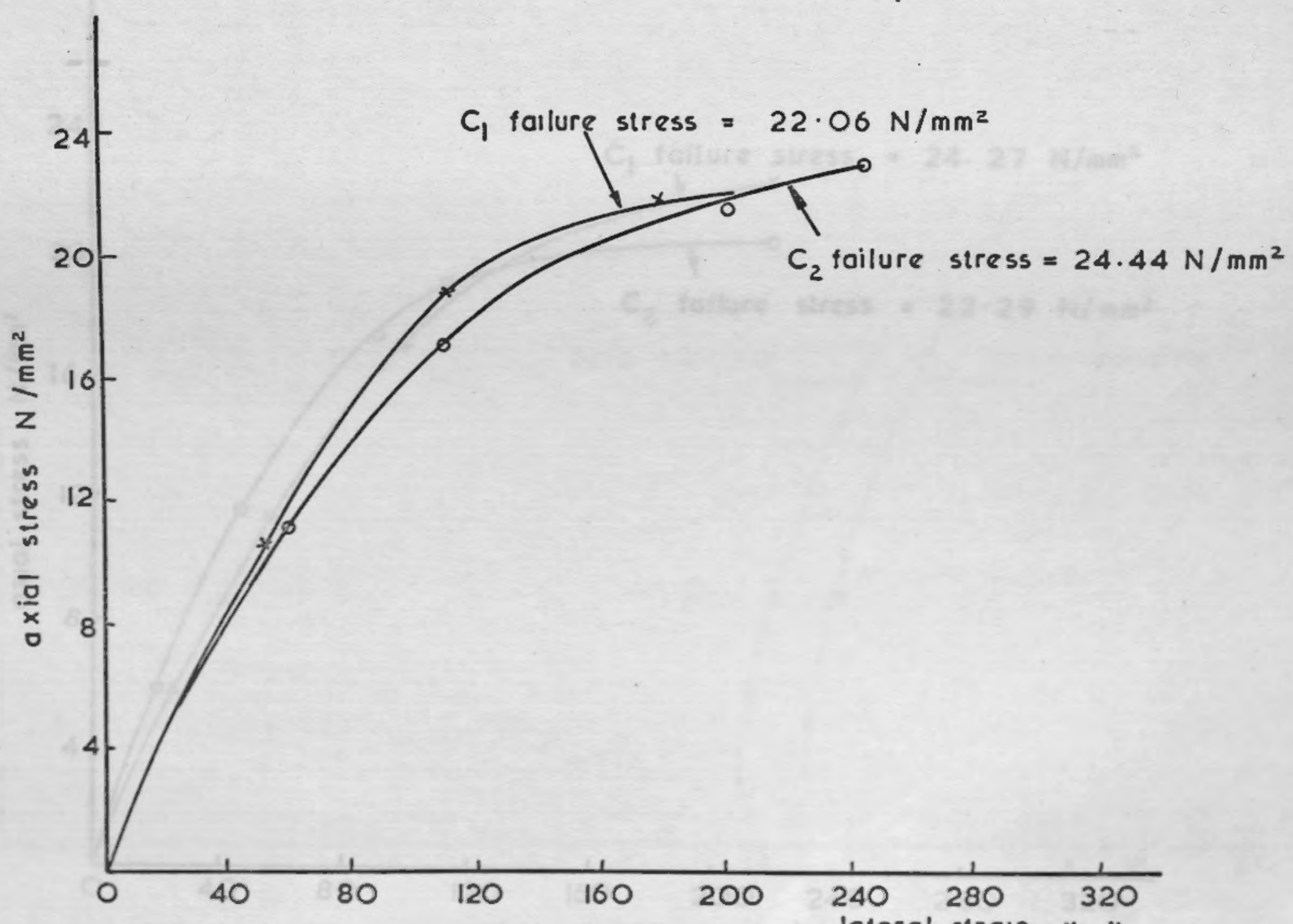

Fig. 5.2 - 3d. Axial stress v. lateral strain measured on cylinders for column concrete by electrical resistance strain gauges

Fig. 5.2 . 3e. Axial stress v. lateral strain measured on cylinders for base concrete by electrical resistance strain gauges.

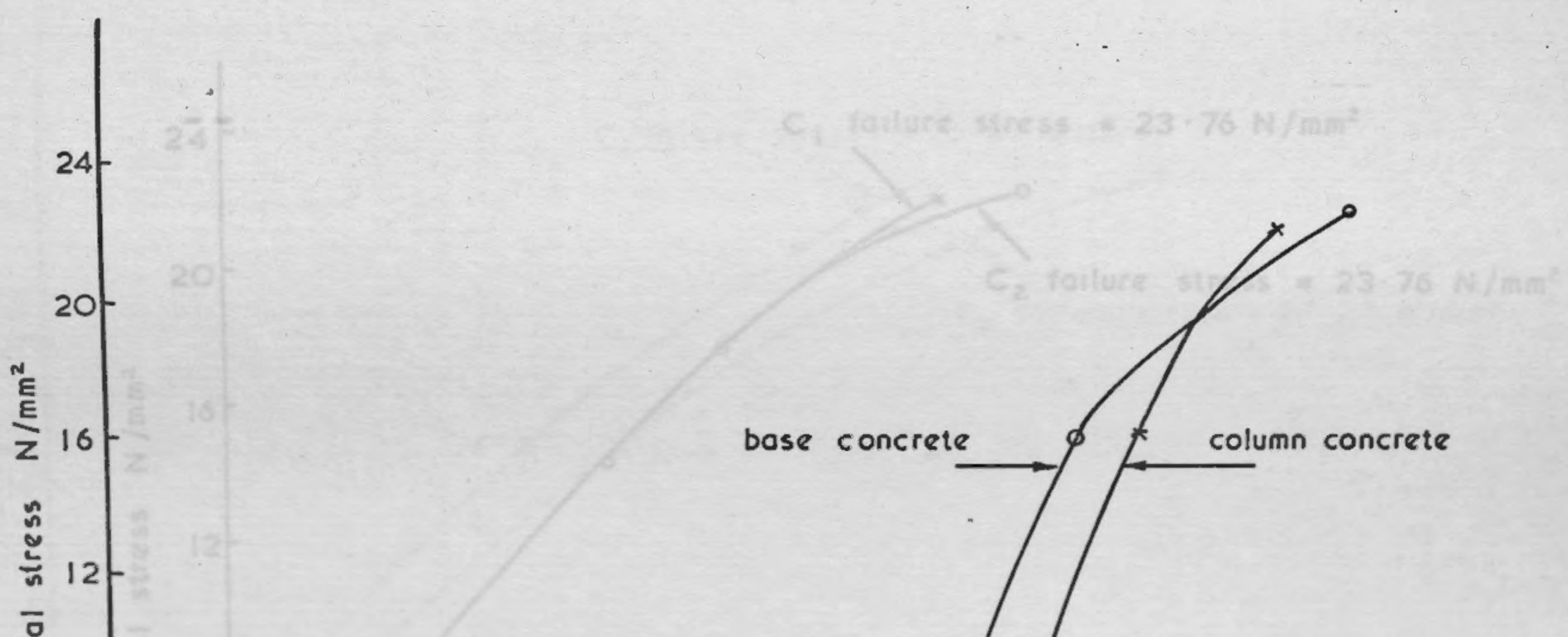

Fig. 5.2 3f Axial stress v Poisson's ratio νc for column concrete and base concrete

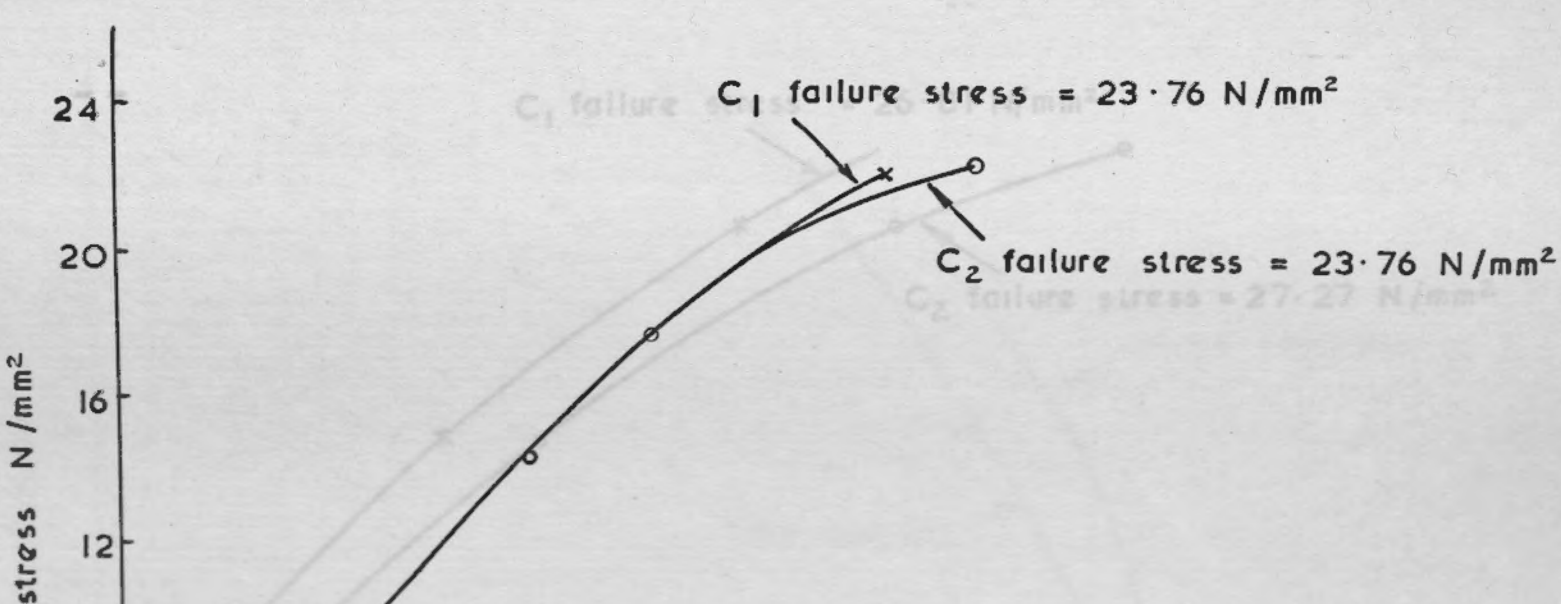

Fig. 5.2 .4a. Axial stress v. longitudinal strain measured on cylinders for column concrete by electrical resistance strain gauges

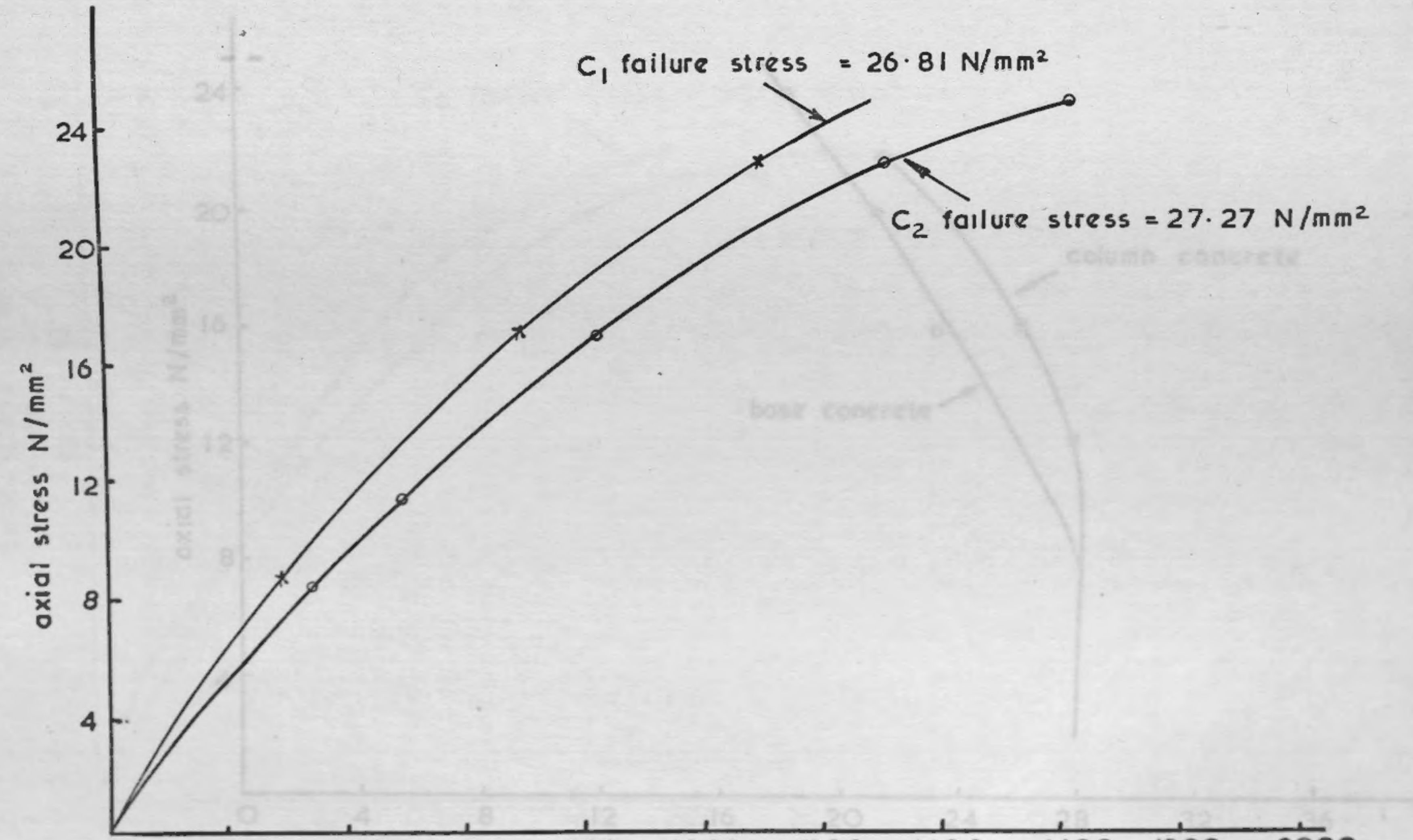

Fig. 5.2.4b. · Axial stress v. longitudinal strain measured on cylinders for base concrete by electrical resistance strain gauges

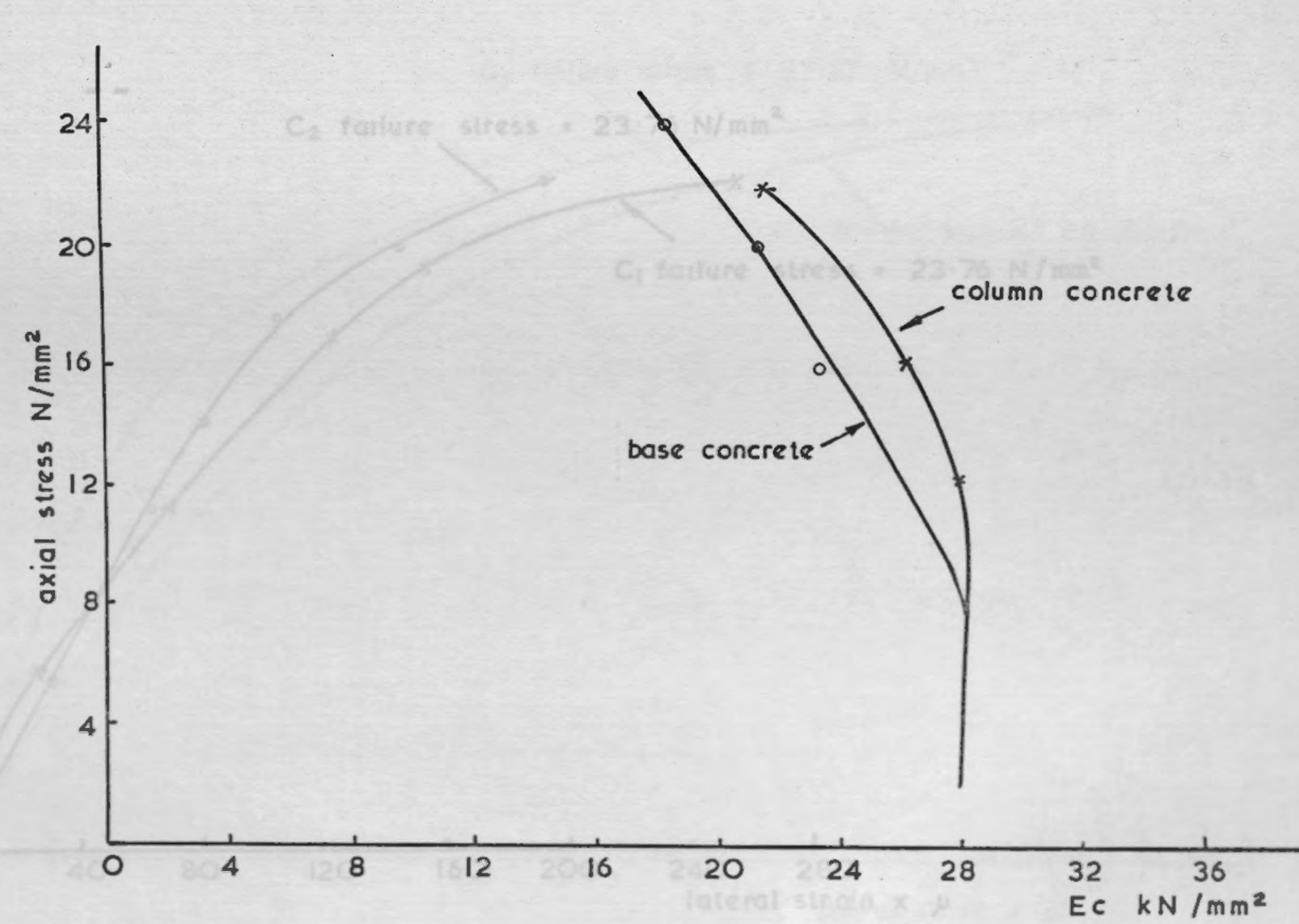

Fig. 5.2.4c. Axial stress v Modulus of elasticity for column concrete and for base concrete.

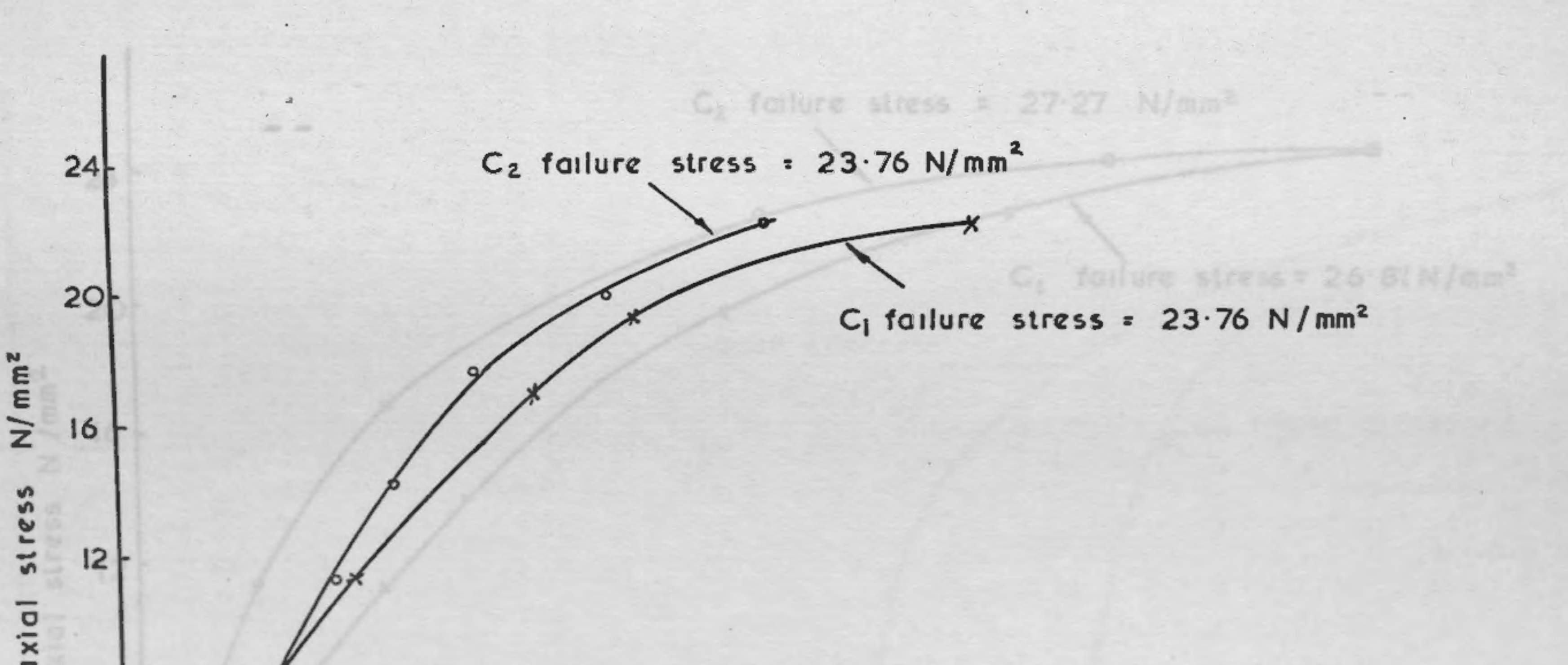

Fig. 5.2 . 4d. Axial stress v lateral strain measured on cylinders for column concrete by electrical resistance strain gauges

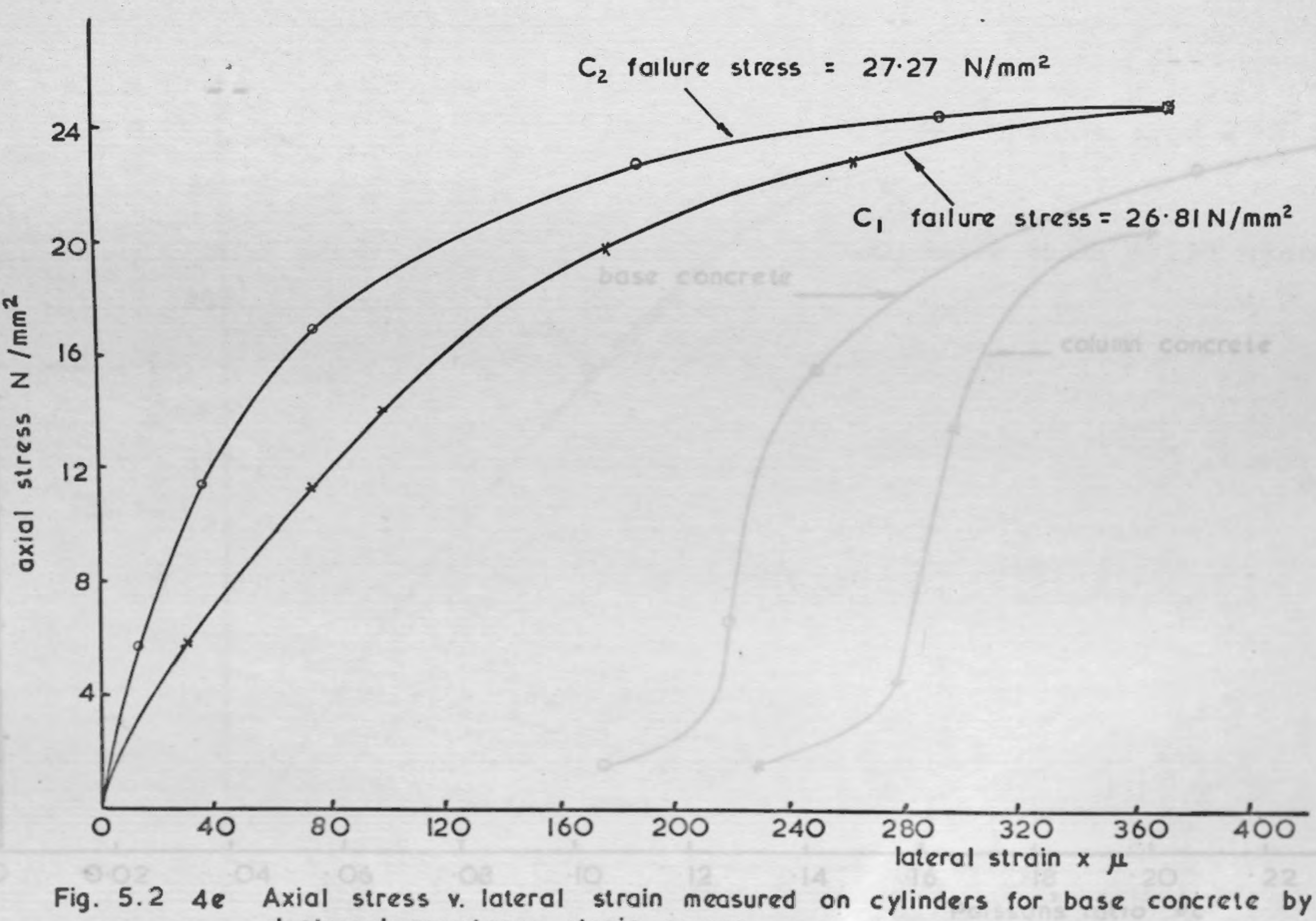

Fig. 5.2 4e Axial stress v. lateral strain measured on cylinders for base concrete by electrical resistance strain gauges.

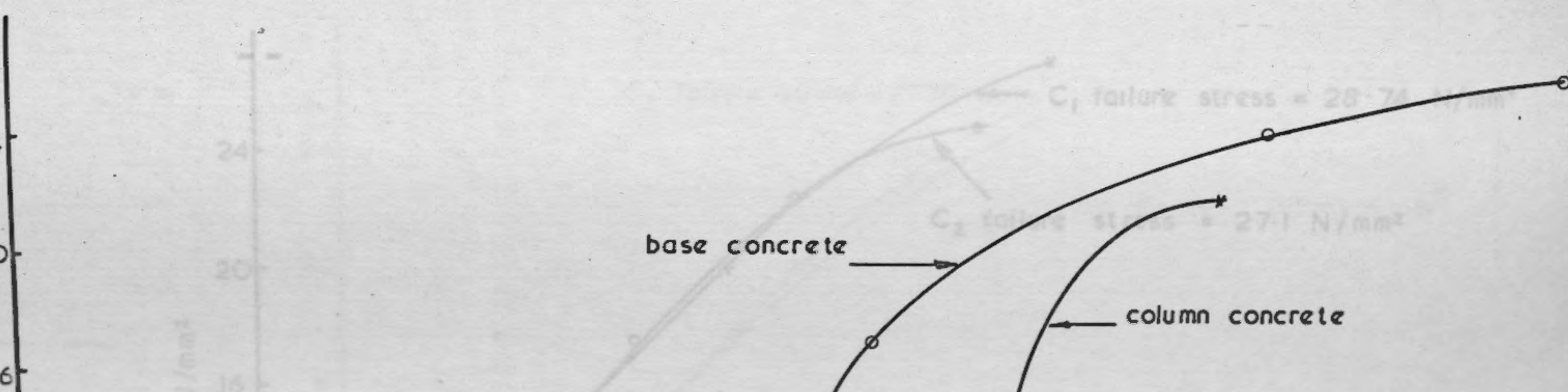

Fig. 5.2 4f Axial stress v. Poisson's ratio νc for column concrete and base concrete

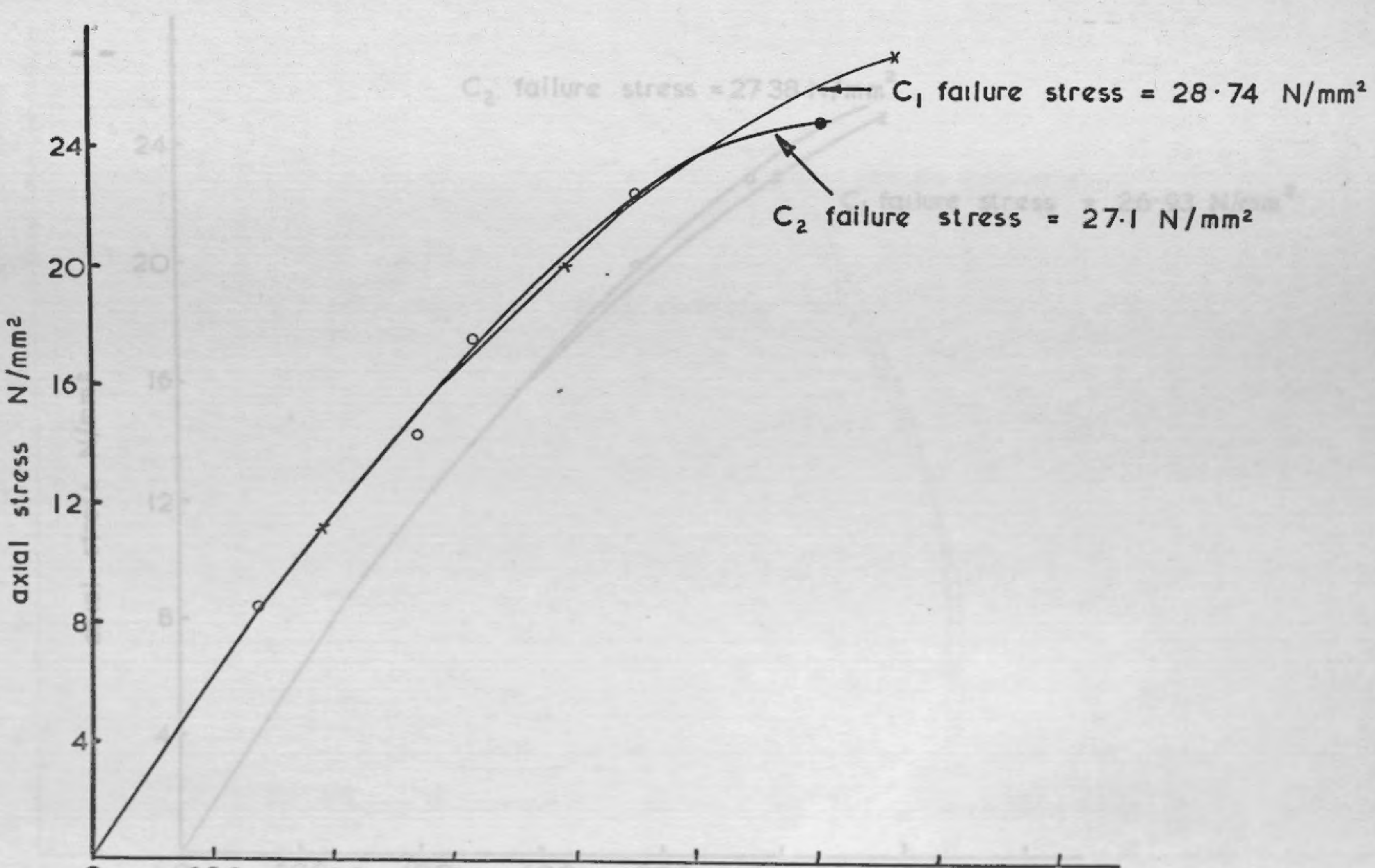

Fig. 5.2.5a. Axial stress v. longitudinal strain measured on cylinders for column concrete by electrical resistance strain gauges

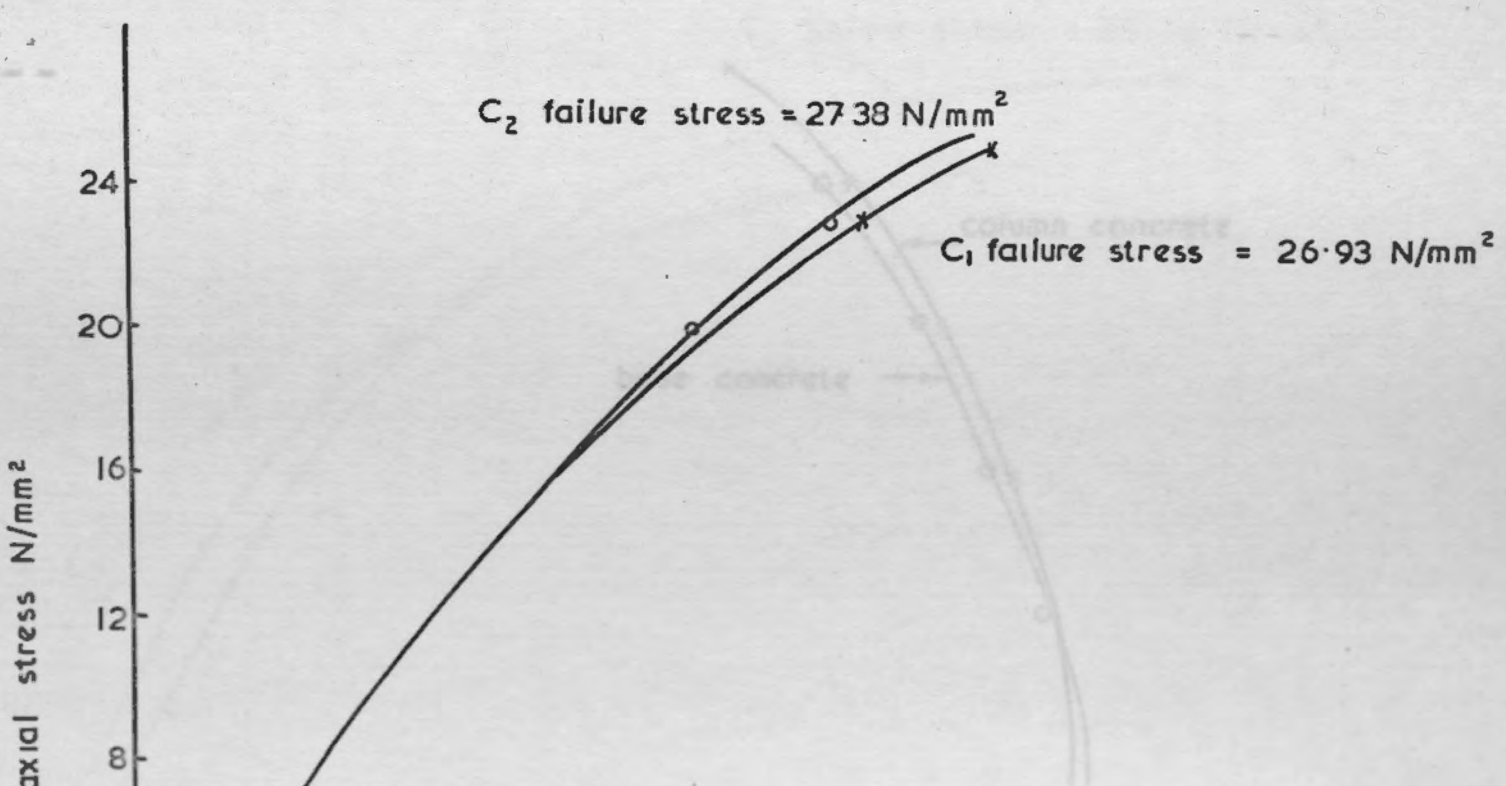

Fig. 5.2 . 5b. Axial stress v. longitudinal strain measured on cylinders for base concrete by electrical resistance strain gauges.

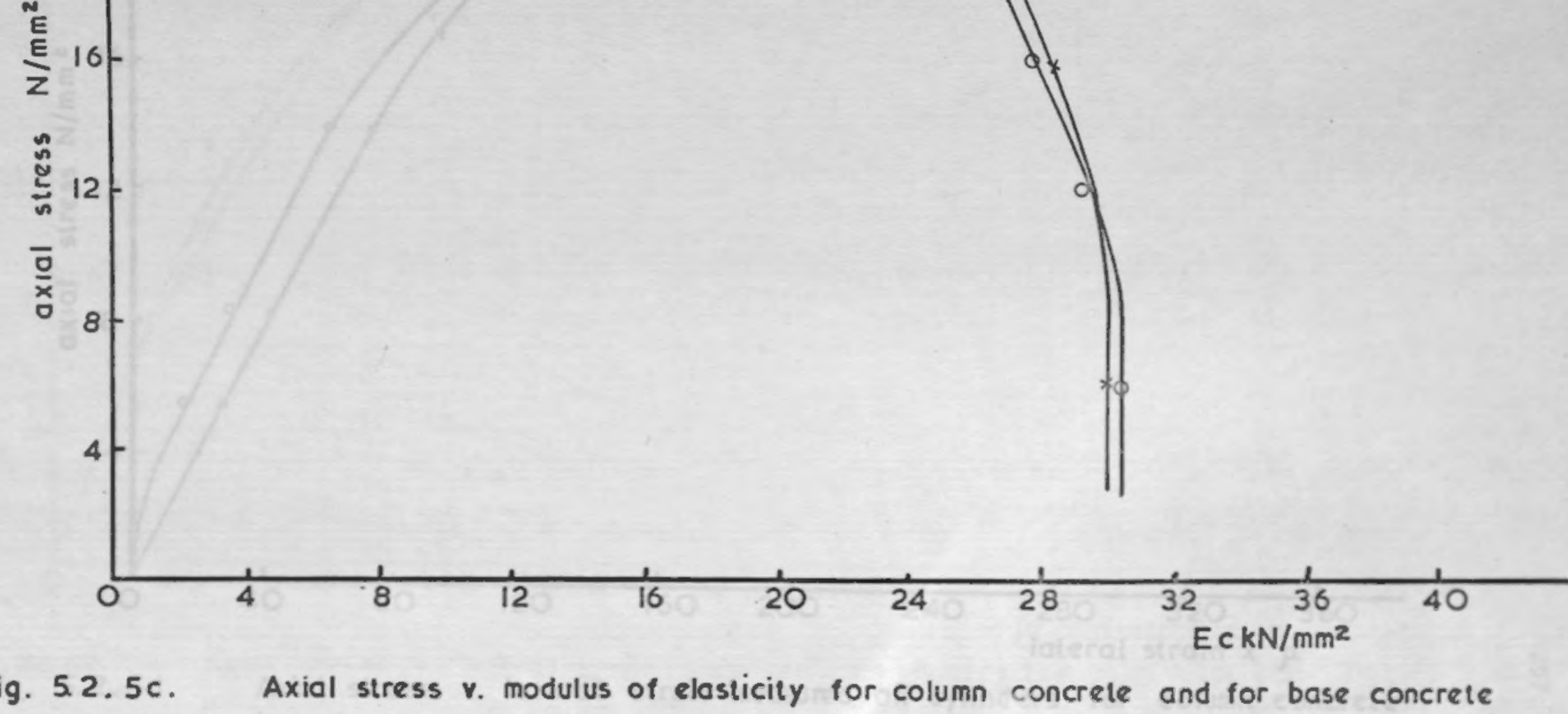

Fig. 5.2. 5c. Axial stress v. modulus of elasticity for column concrete and for base concrete

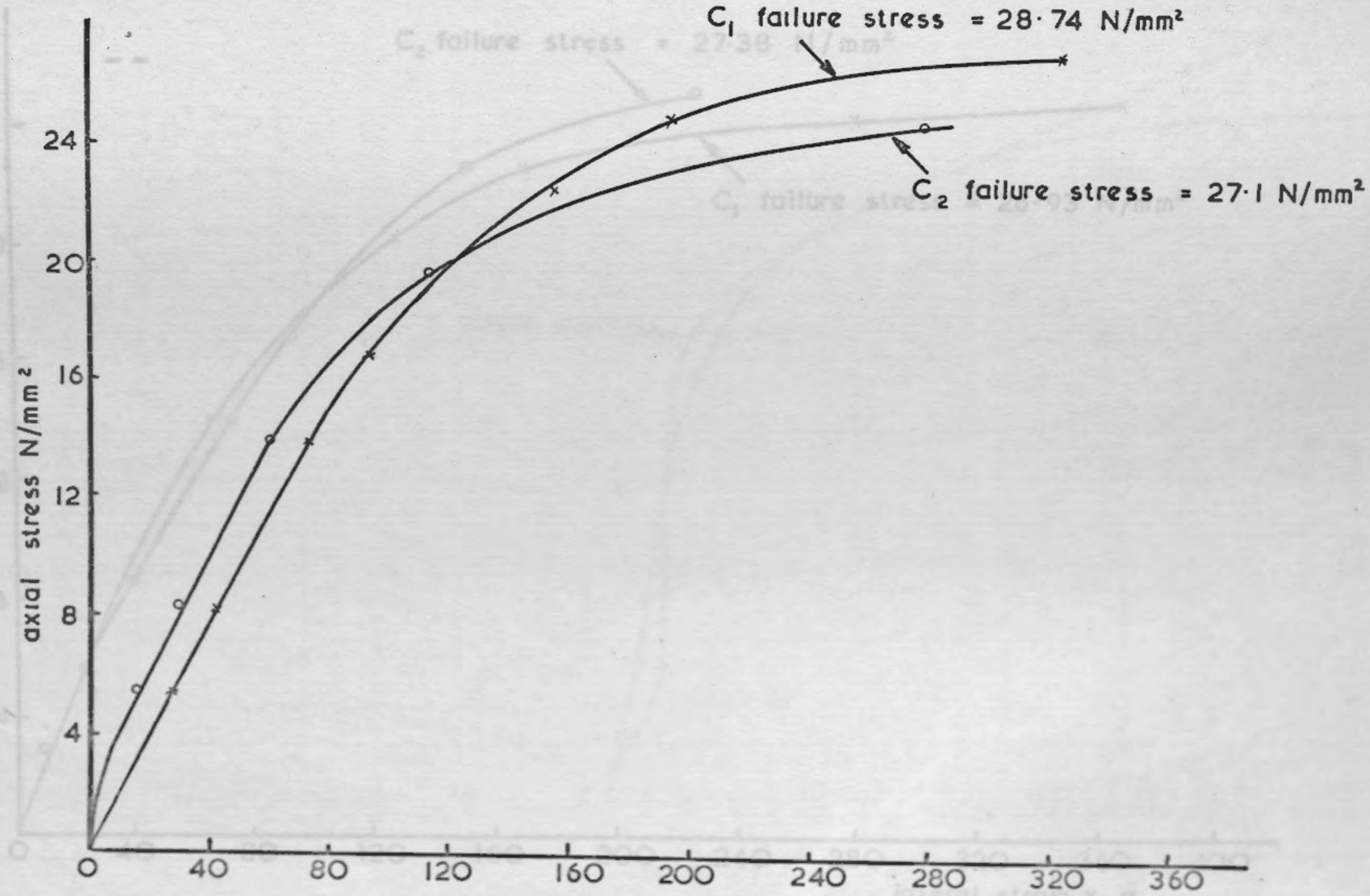

Fig. 5.2.5d. Axial stress v. lateral strain measured on cylinders for column concrete by electrical resistance strain gauges

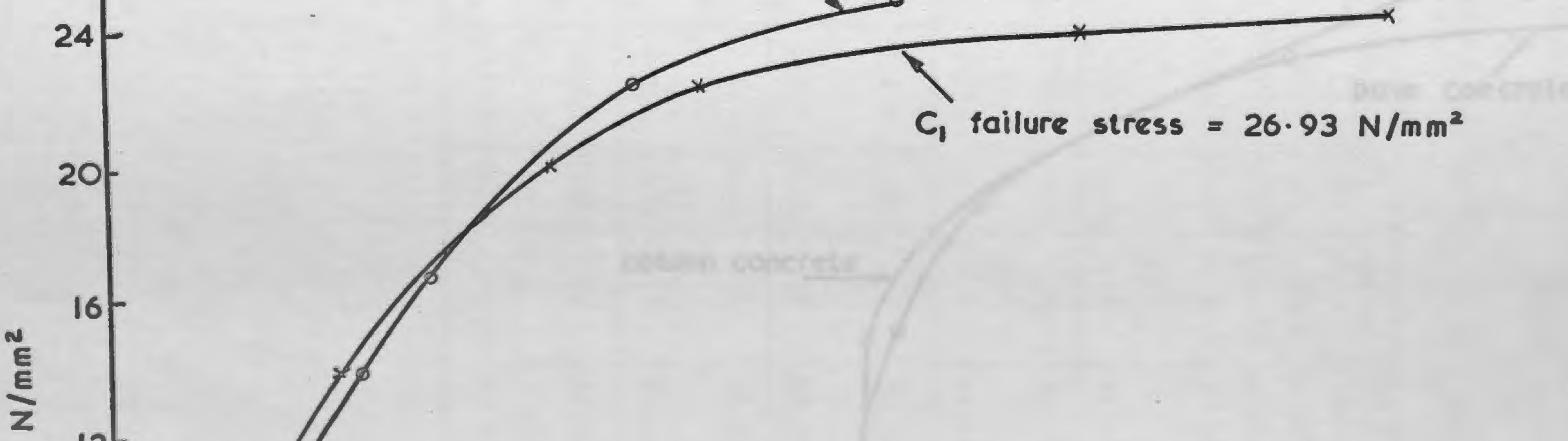

Fig. 5.2.5e. Axial stress v. lateral strain measured on cylinders for base concrete by electrical resistance strain gauges

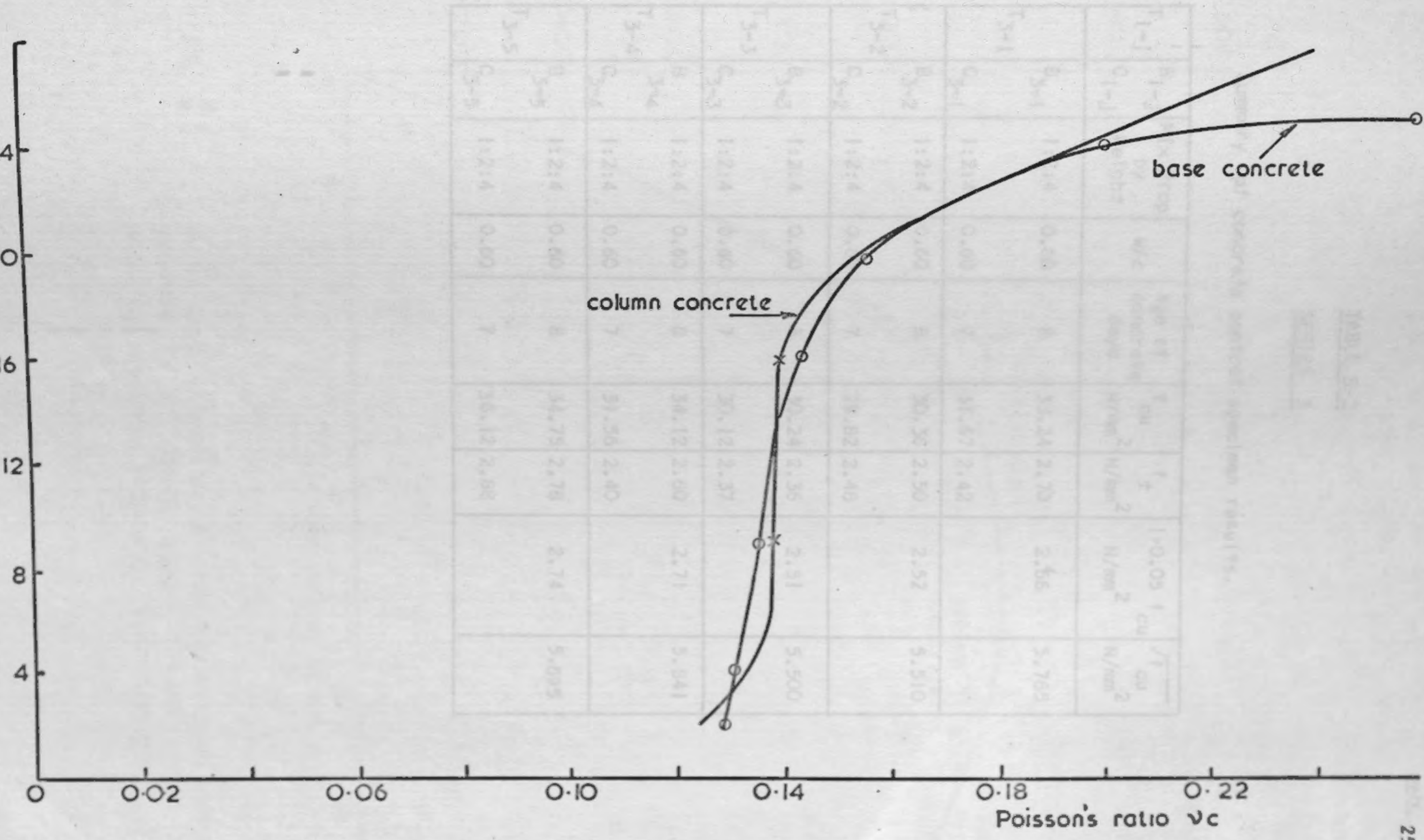

Fig. 5.2.5f. Axial stress v. Poissons ratio νc for column concrete and base concrete

TABLE 5-2

SERIES 3

Summary of concrete control specimen results.

T_{i-j}	B_{i-j} / C_{i-j}	Mix Prop by Weight	w/c	Age of concrete days	f_{cu} N/mm^2	f_t N/mm^2	$1+0.05 f_{cu}$ N/mm^2	$\sqrt{f_{cu}}$ N/mm^2
T_{3-1}	B_{3-1}	1:2:4	0.60	8	33.24	2.70	2.66	5.765
	C_{3-1}	1:2:4	0.60	7	31.67	2.42		
T_{3-2}	B_{3-2}	1:2:4	0.60	8	30.36	2.50	2.52	5.510
	C_{3-2}	1:2:4	0.60	7	29.82	2.48		
T_{3-3}	B_{3-3}	1:2:4	0.60	8	30.24	2.36	2.51	5.500
	C_{3-3}	1:2:4	0.60	7	30.12	2.37		
T_{3-4}	B_{3-4}	1:2:4	0.60	8	34.12	2.60	2.71	5.841
	C_{3-4}	1:2:4	0.60	7	31.56	2.40		
T_{3-5}	B_{3-5}	1:2:4	0.60	8	34.75	2.78	2.74	5.895
	C_{3-5}	1:2:4	0.60	7	36.12	2.88		

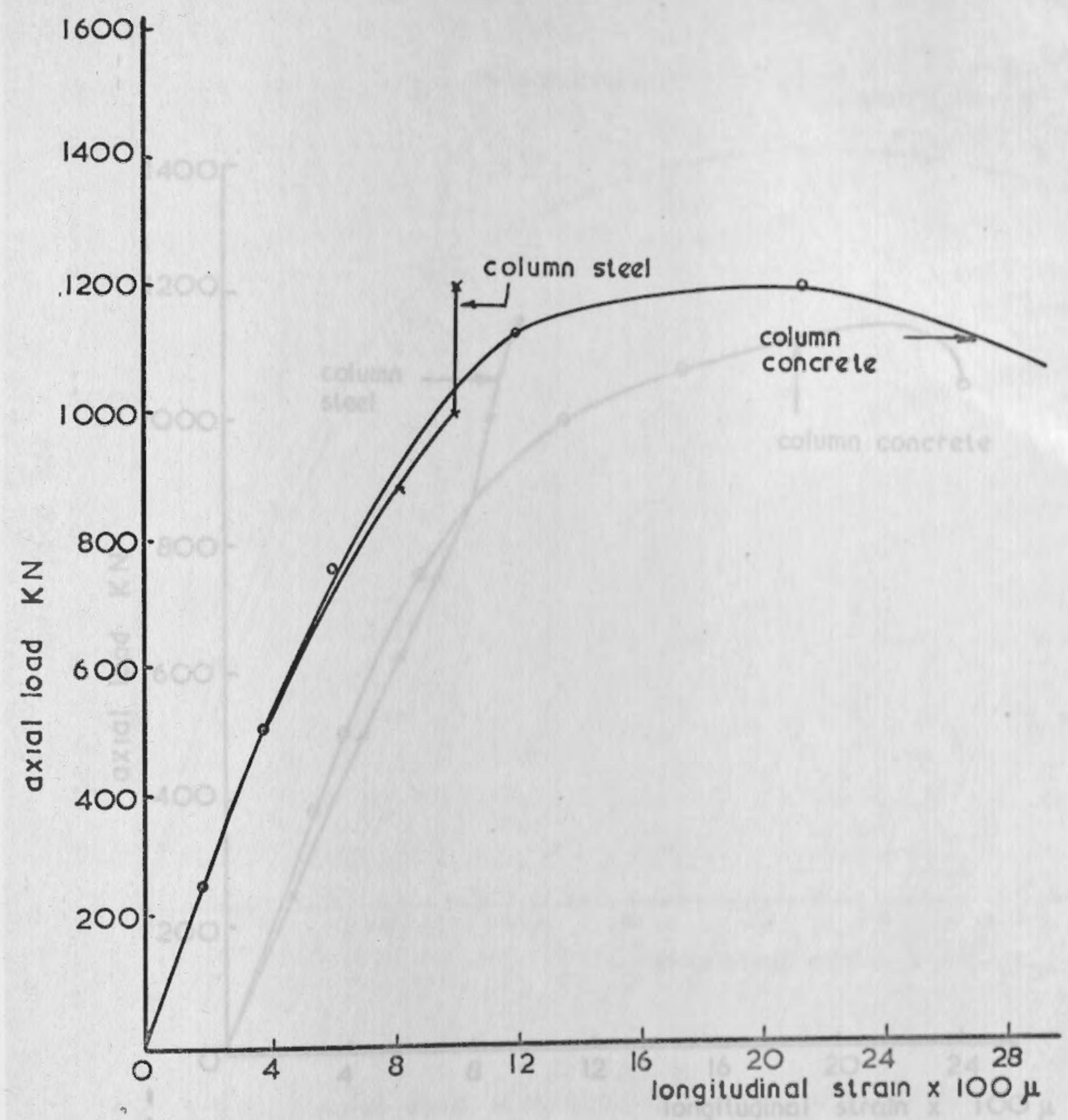

Fig 5.3.1 Axial load v longitudinal strain measured on column concrete by 8" demec gauges and on column steel by electrical resistance strain gauges (T_{3-1})

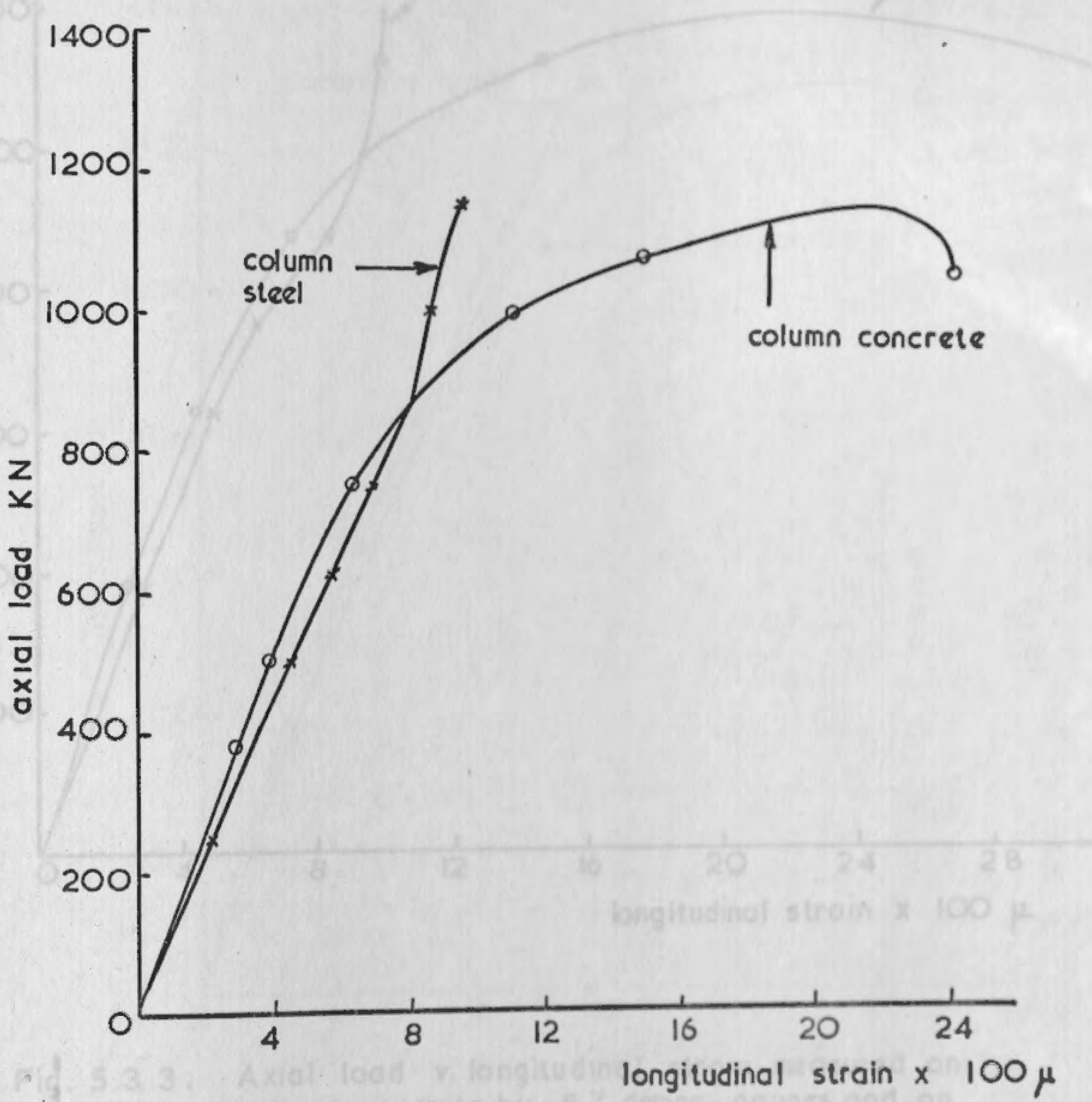

Fig 5.3.2 Axial load v longitudinal strain measured on column concrete by 8" demec gauges and on column steel by electrical resistance strain gauges ($T_{3\cdot2}$)

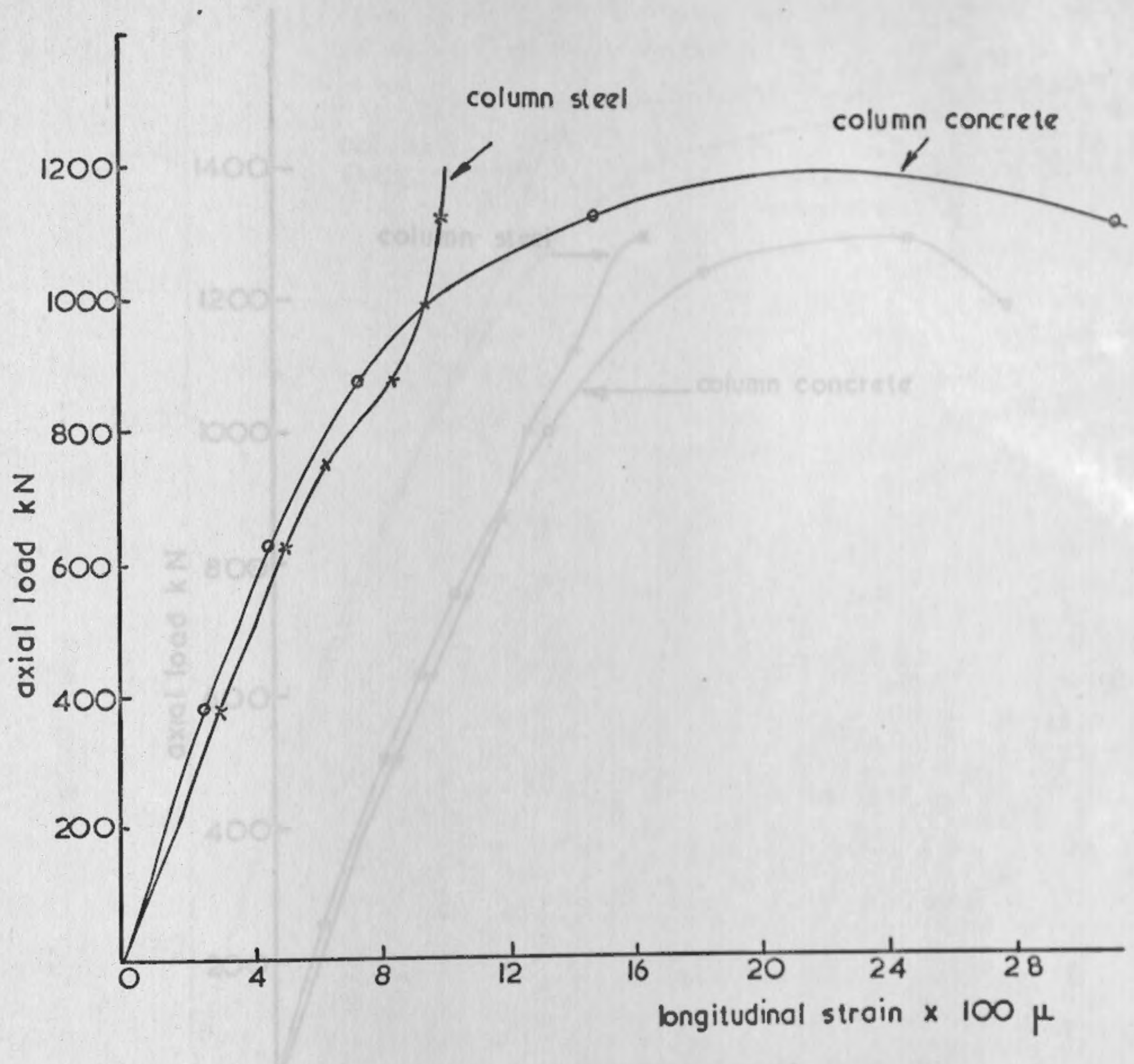

Fig. 5.3.3. Axial load v. longitudinal strain measured on column concrete by 8" demec gauges and on column steel by electrical resistance strain gauges. (T_{3-3})

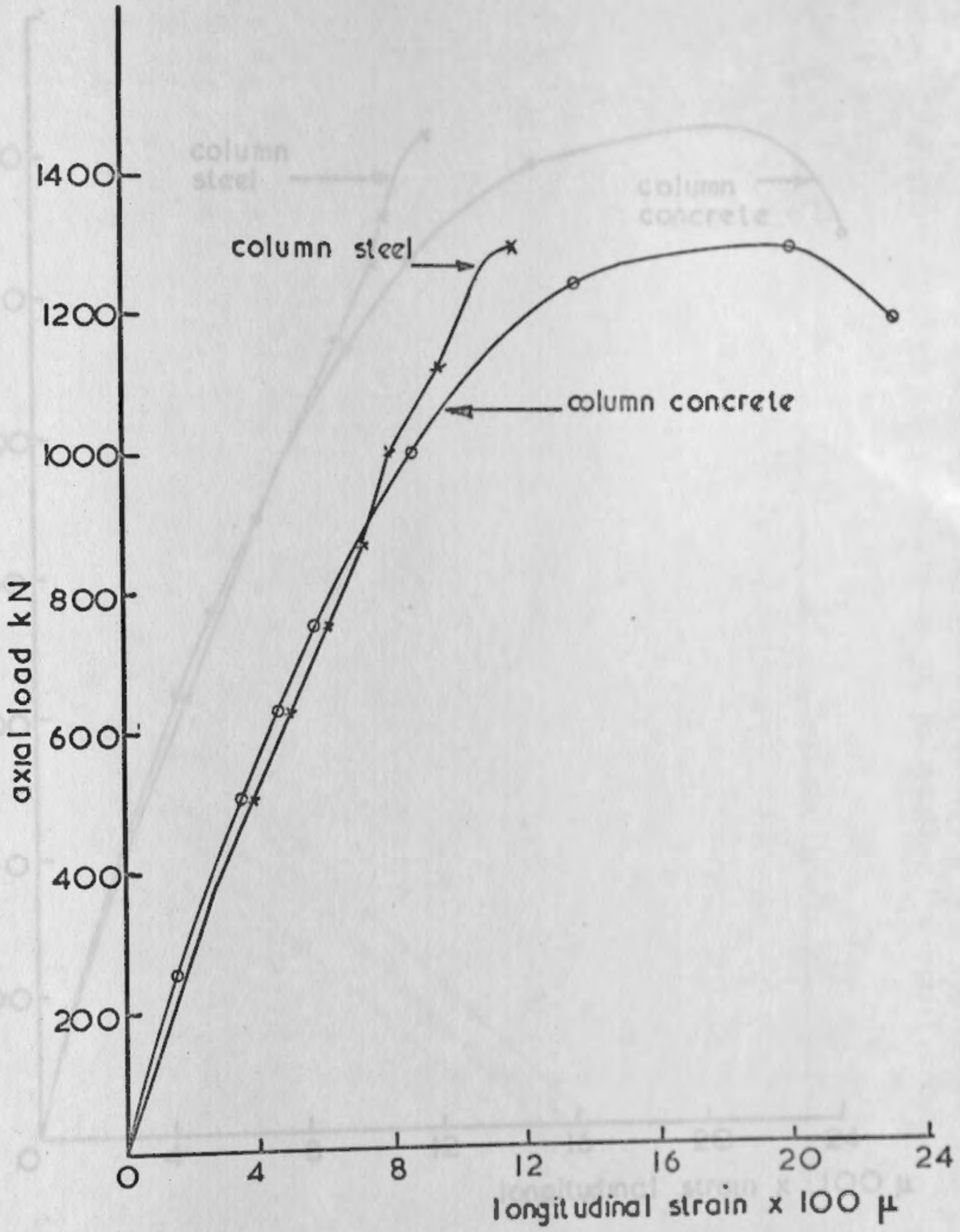

Fig. 5.3.4 Axial load v. longitudinal strain measured on column concrete by 8" demec gauges and on column steel by electrical resistance strain gauges ($T_{3.4}$)

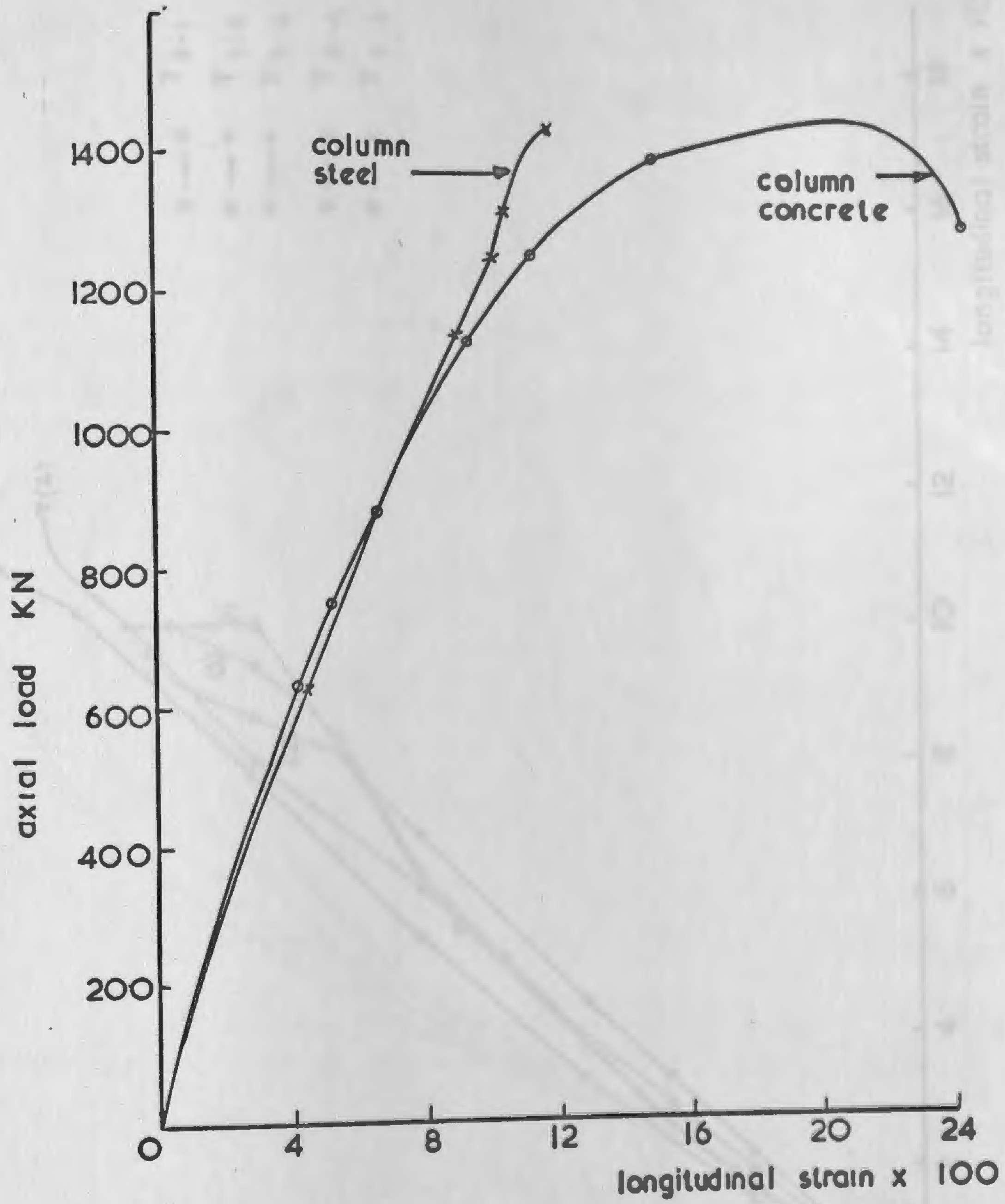

Fig 5.3.5 Axial load v longitudinal strain measured on column concrete by 8″ demec gauges and on column steel by electrical resistance strain gauges ($T_{3.5}$)

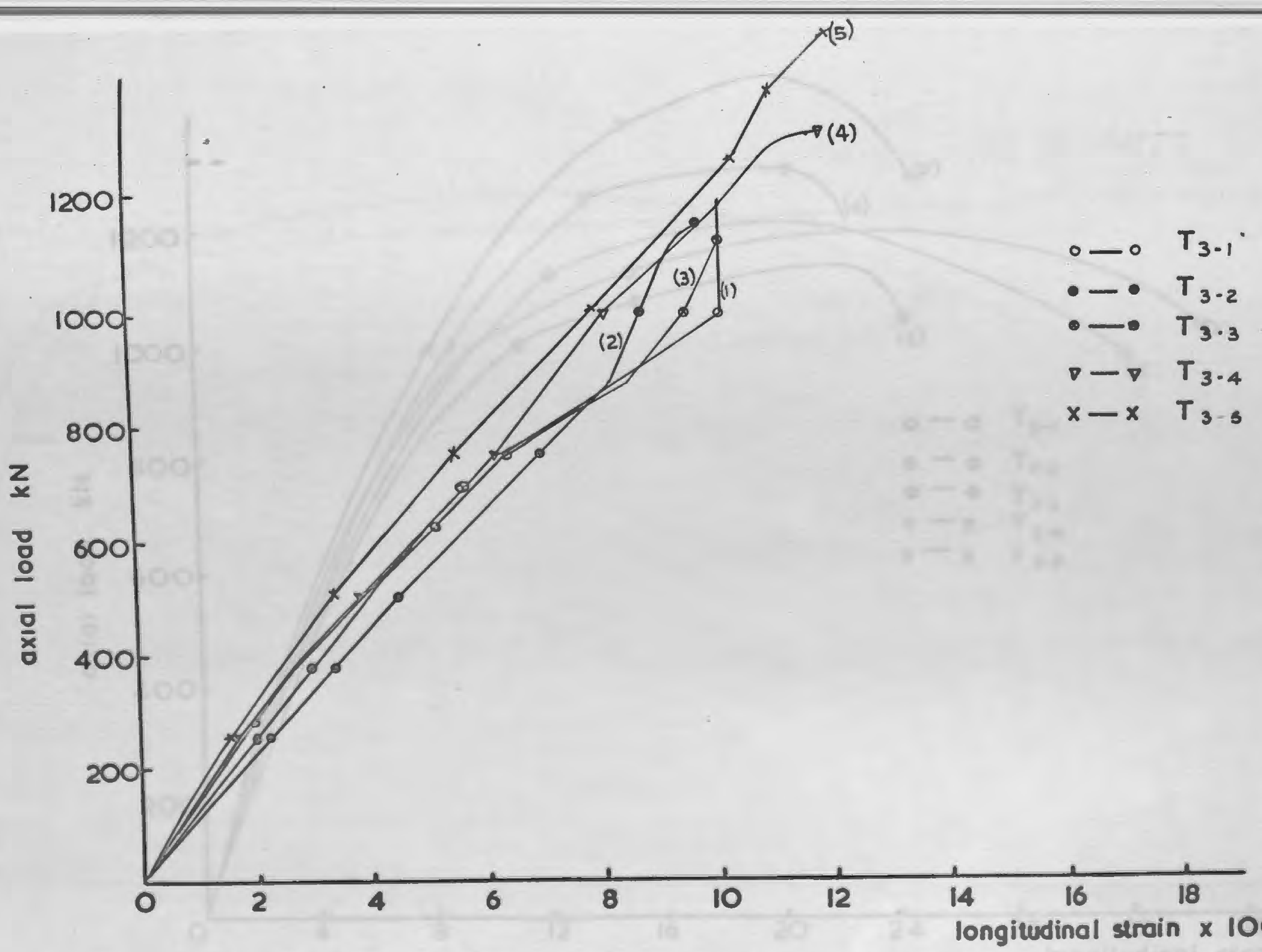

Fig. 5. 3. a Axial load v. longitudinal strain measured on column steel by electrical resistance strain gauges for series (3) specimens

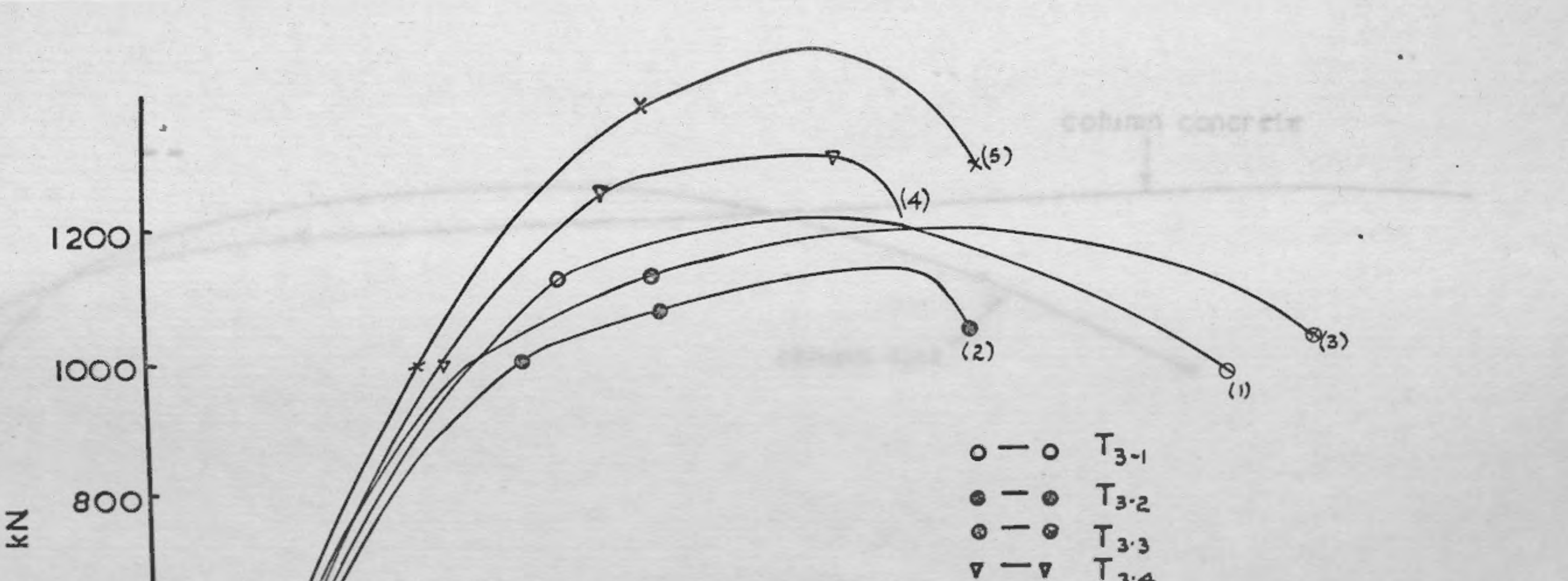

Fig. 5.3 . b. Axial load v. longitudinal strain measured on column concrete by 8" demec gauges for series (3) specimens

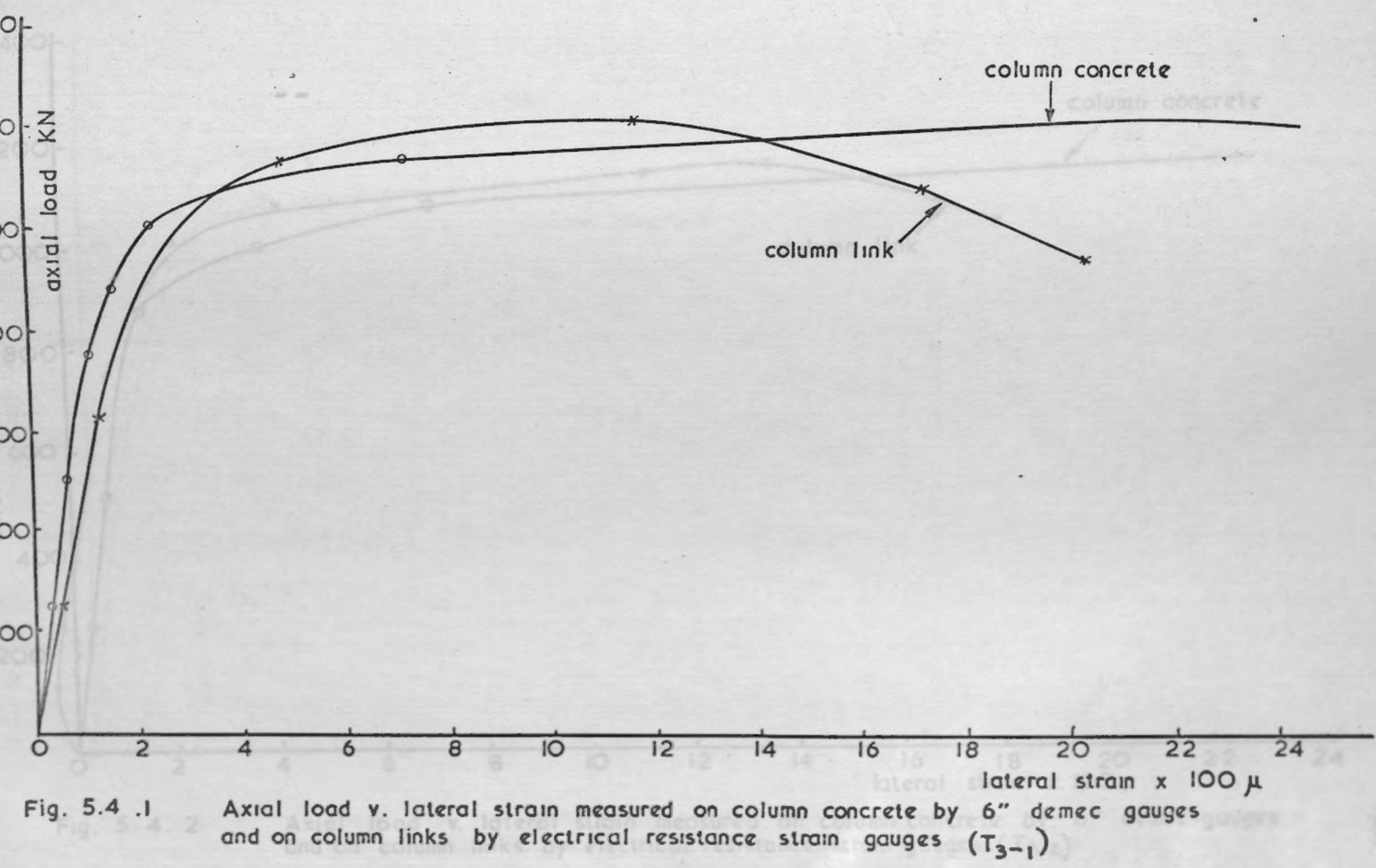

Fig. 5.4 .1 Axial load v. lateral strain measured on column concrete by 6" demec gauges and on column links by electrical resistance strain gauges (T_{3-1})

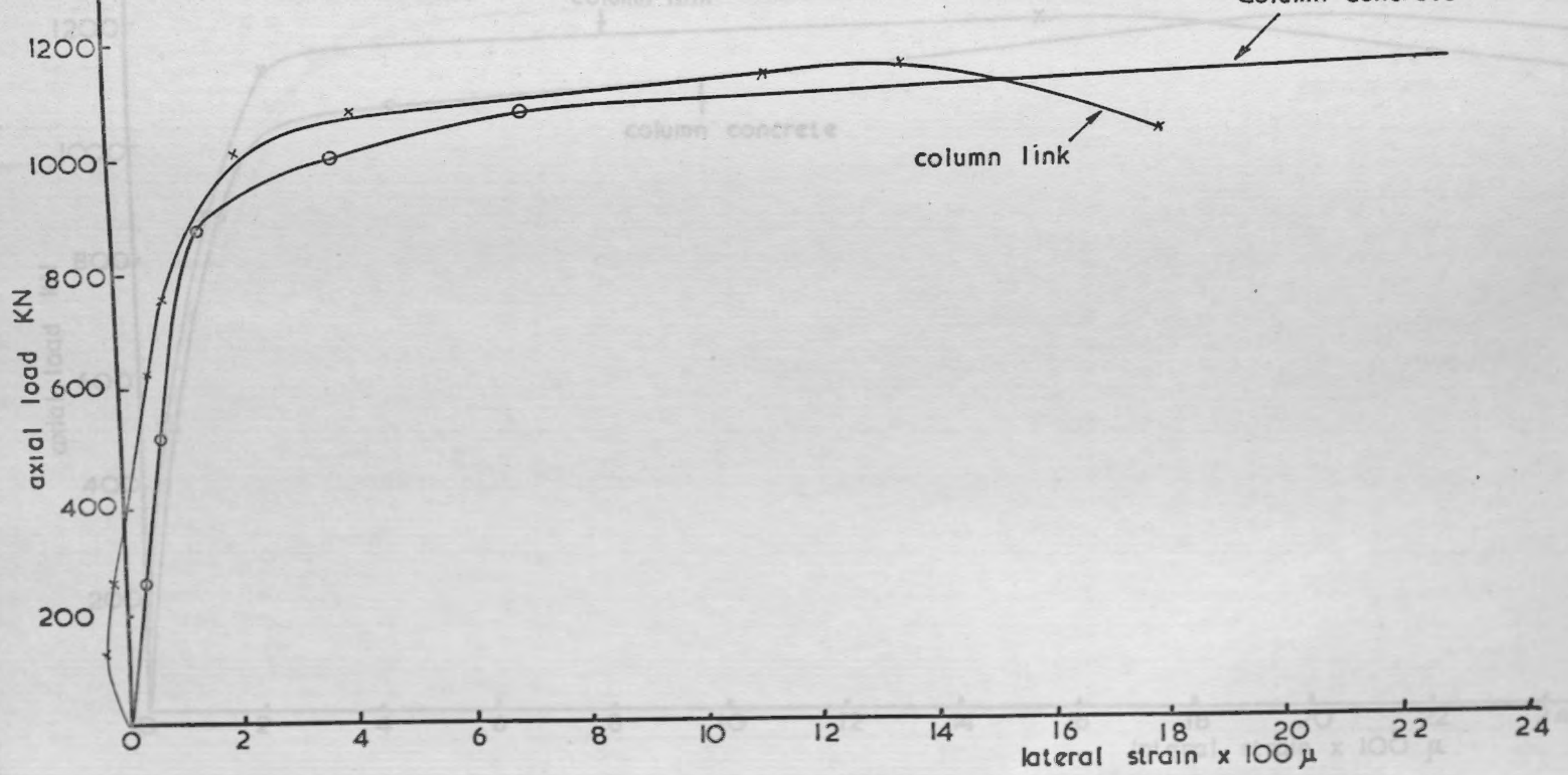

Fig. 5.4.2 Axial load v. lateral strain measured on column concrete by 6" demec gauges and on column links by electrical resistance strain gauges. (T_{3-2})

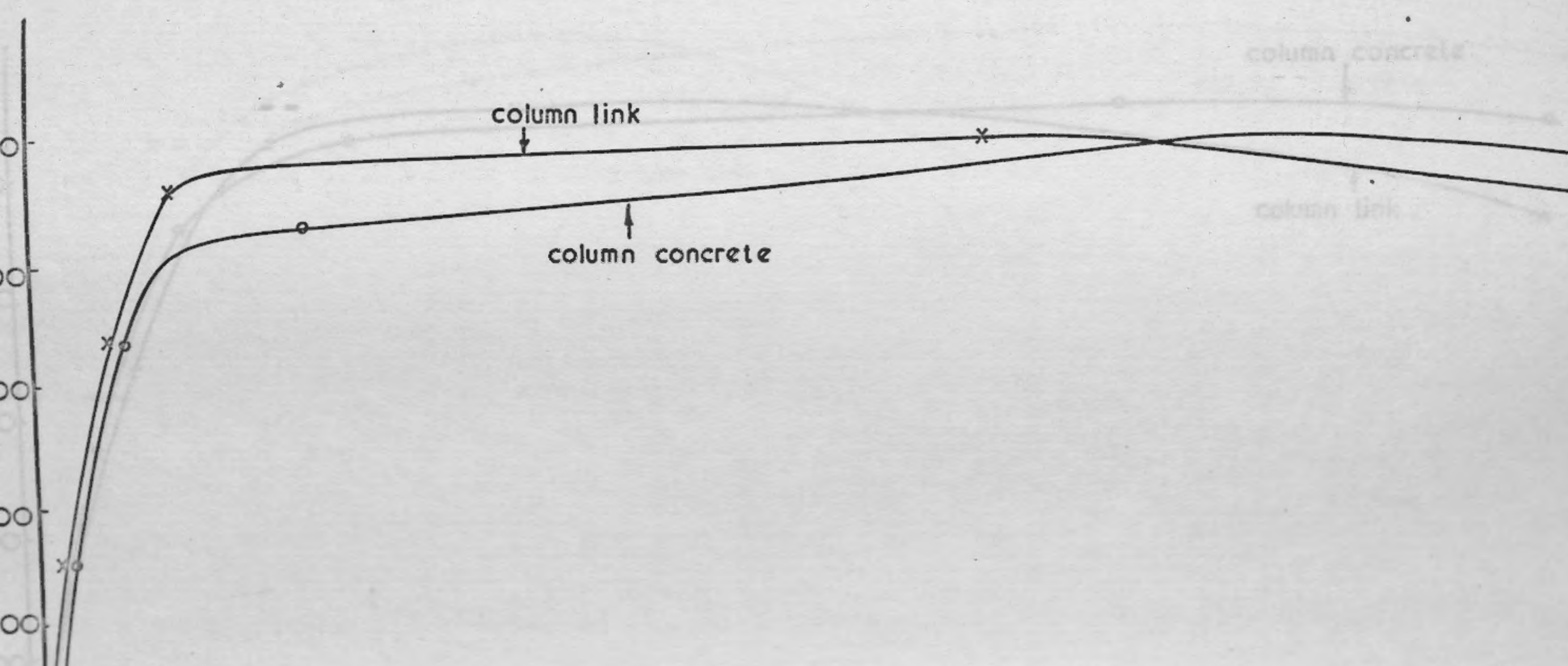

Fig. 5.4. 3 Axial load v lateral strain measured on colum concrete by 6" demec gauges and on column links by electrical resistance strain gauges. ($T_{3\text{-}3}$)

Fig. 5.4.4 Axial load v lateral strain measured on column concrete by 6″ demec gauges and on column links by electrical resistance strain gauges ($T_{3\text{-}4}$)

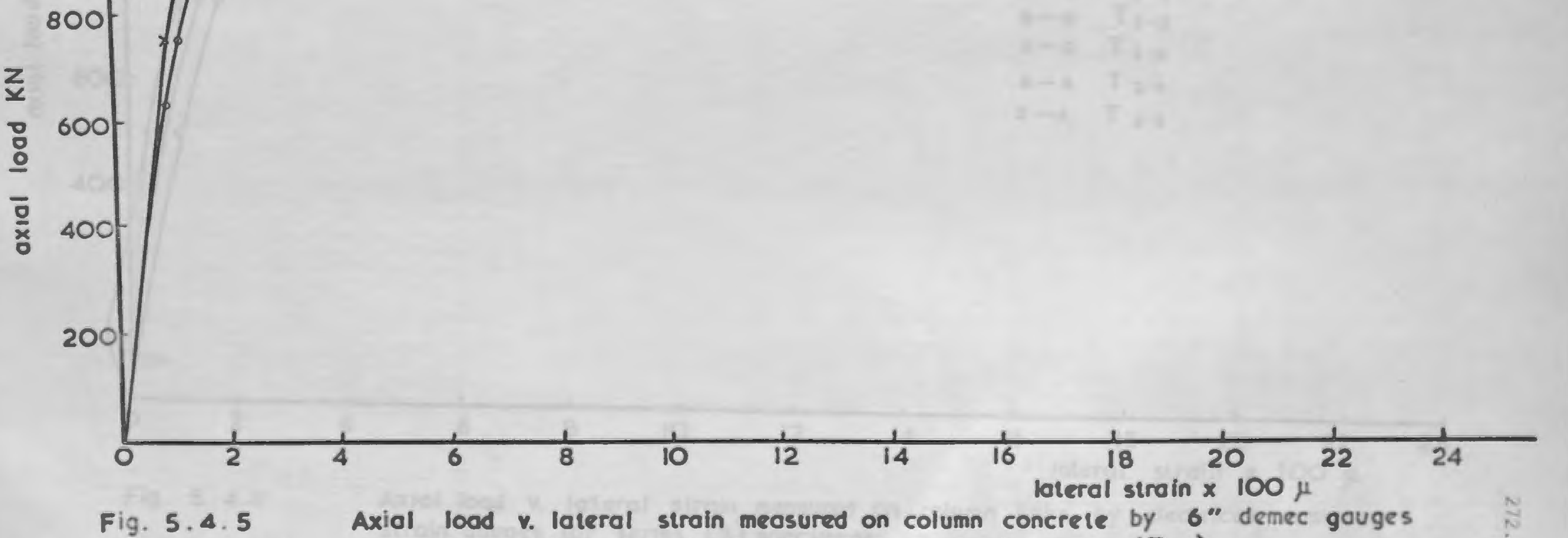

Fig. 5.4.5 Axial load v. lateral strain measured on column concrete by 6" demec gauges and on column links by electrical resistance strain gauges ($T_{3\cdot5}$)

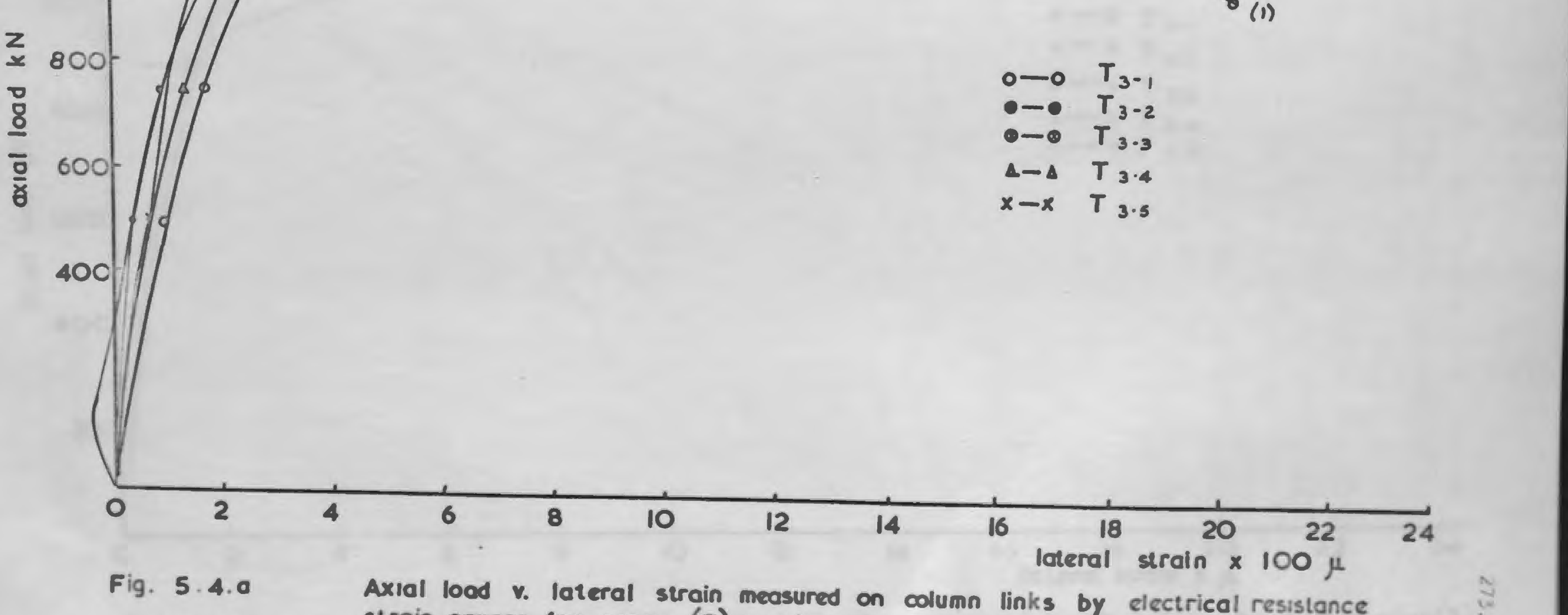

Fig. 5.4.a Axial load v. lateral strain measured on column links by electrical resistance strain gauges for series (3) specimens

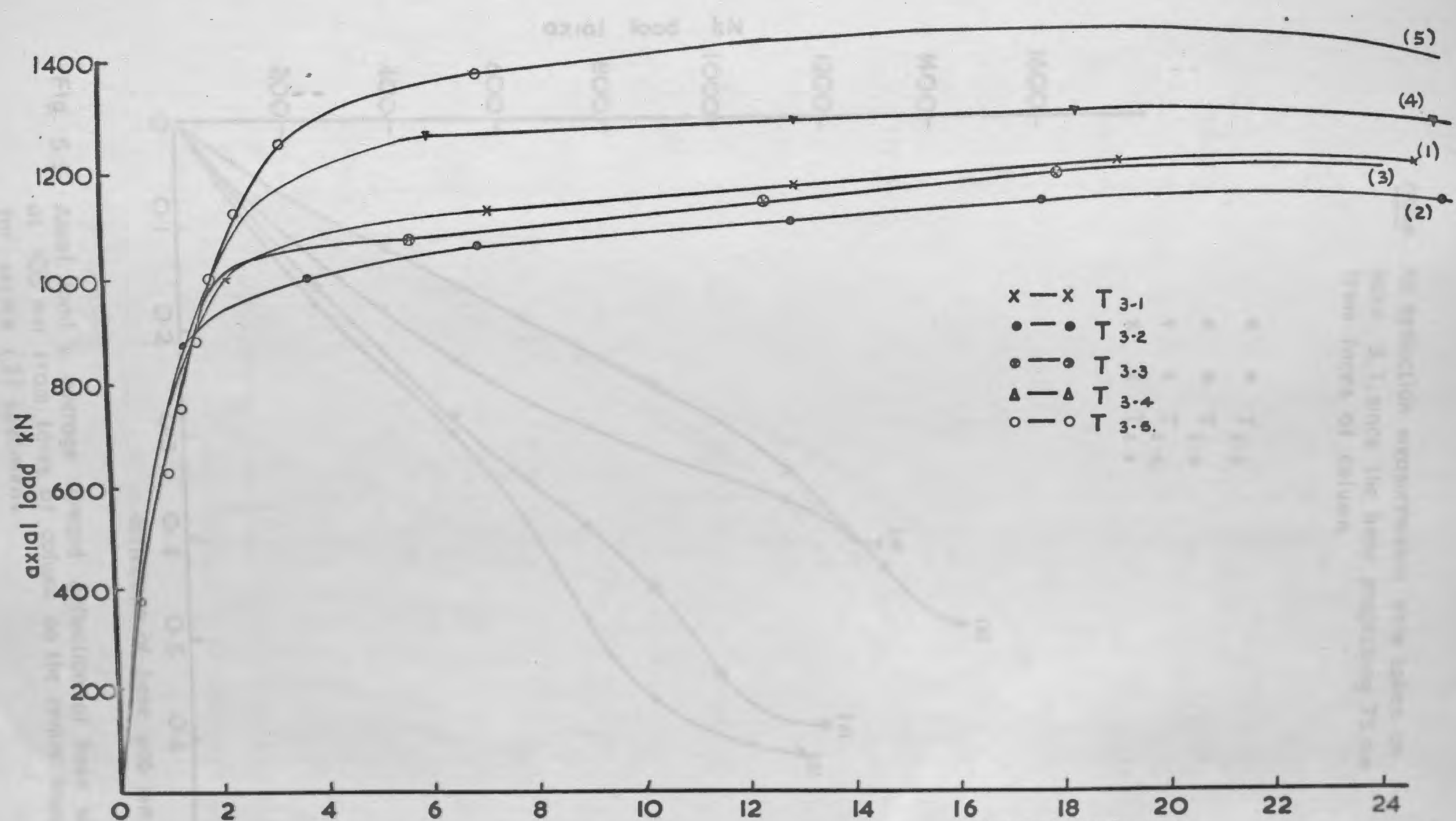

Fig. 5.4 . b. Axial load v. lateral strain measured on column concrete by 6" demec gauges for series (3) specimens

<u>note</u>. no deflection measurements were taken on base 3.1. since the base projecting 75 mm from faces of column

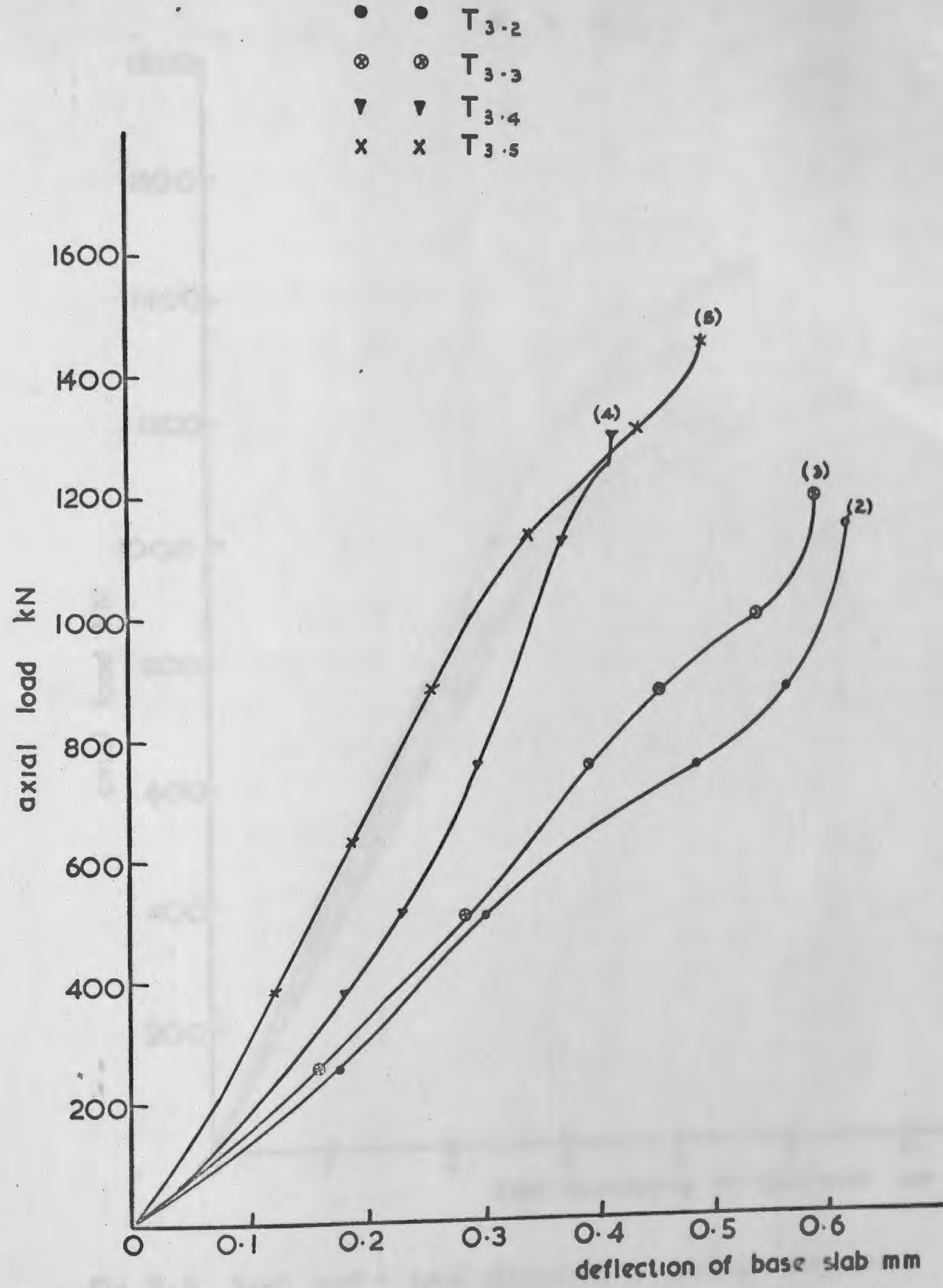

Fig. 5.5. Axial load v. average upward deflection of base slab at 105 mm from faces of column on the centre lines for series (3) specimens

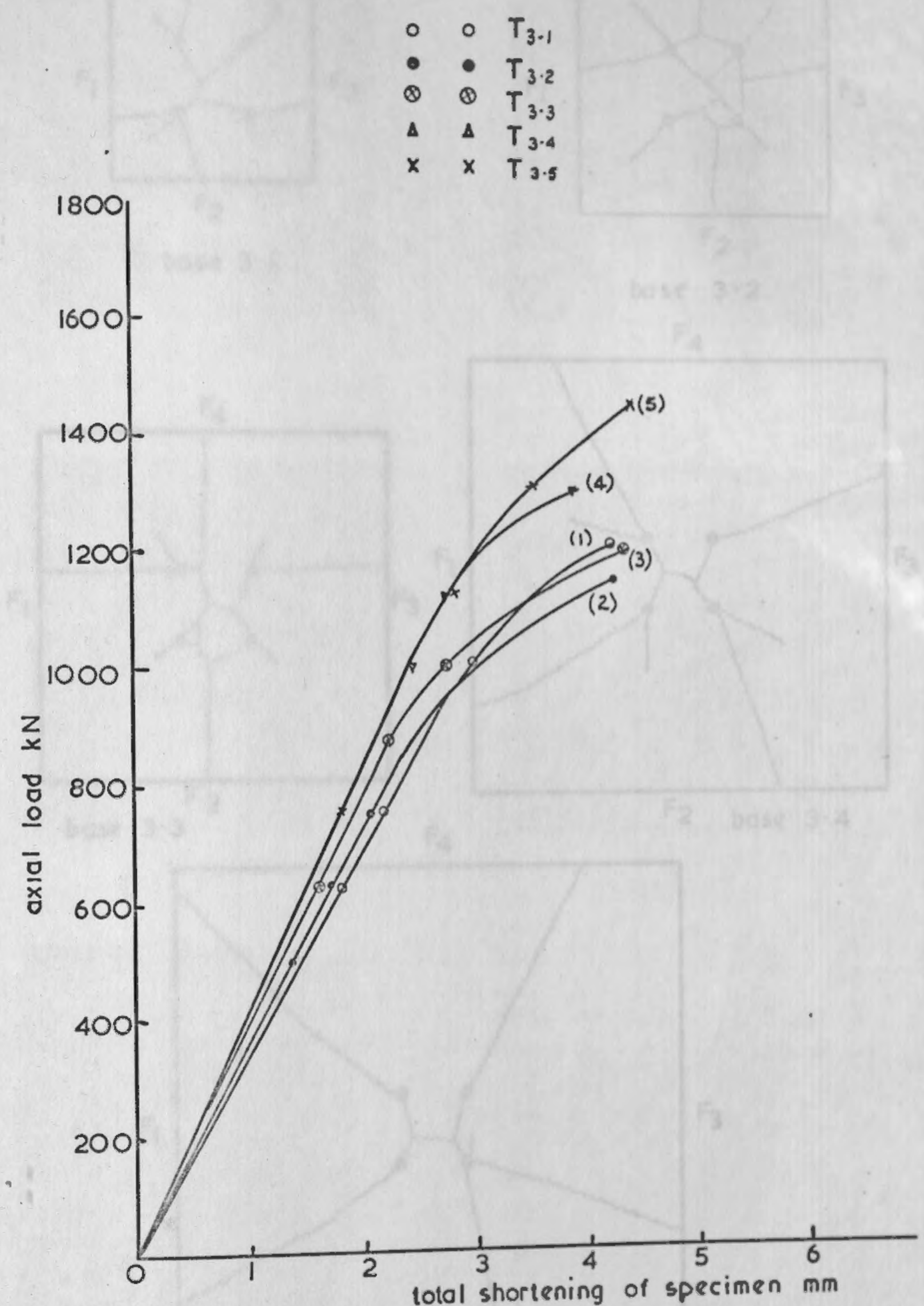

Fig. 5. 6. Axial load v. total shortening of specimen for series (3) specimens .

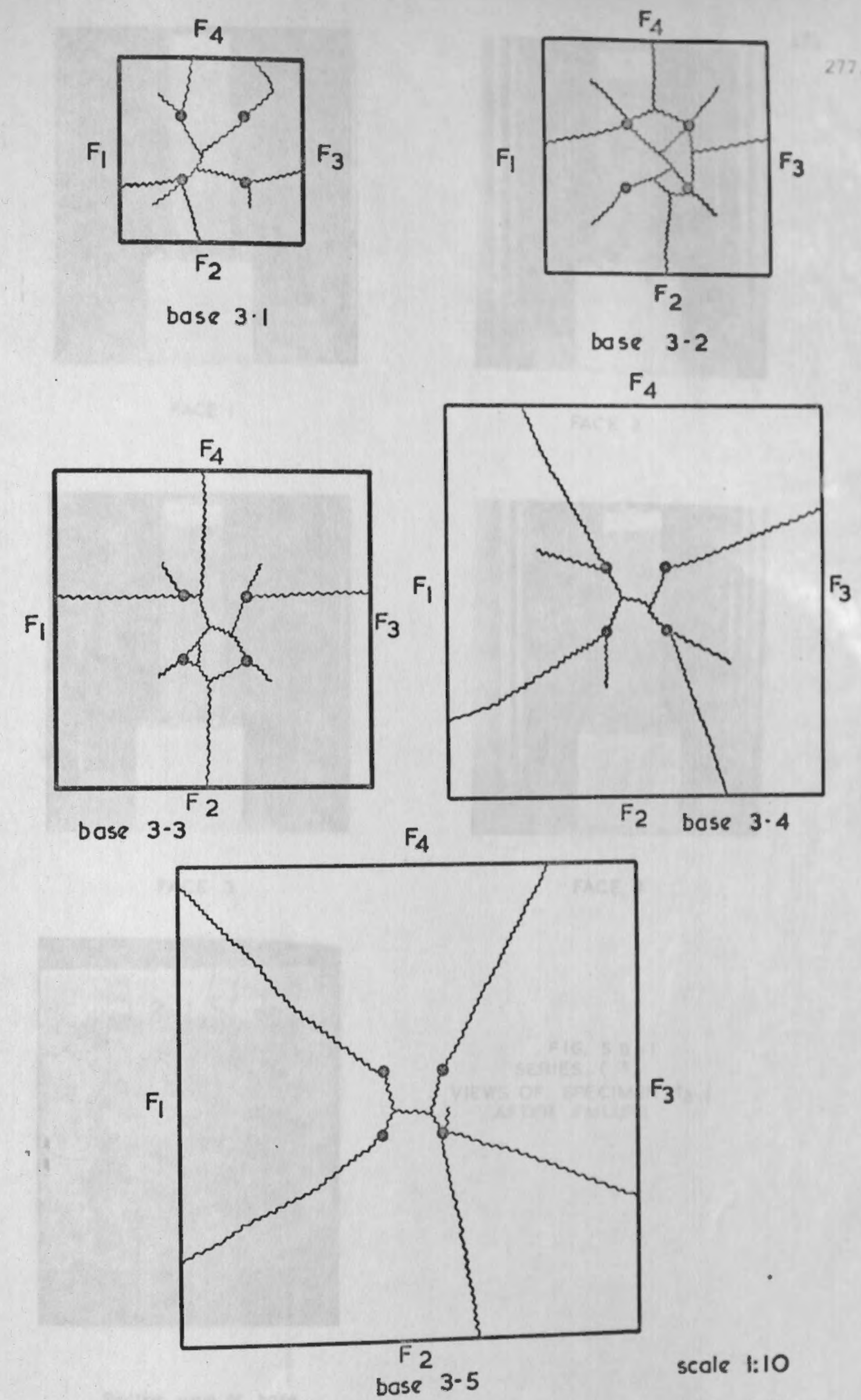

Fig. 5.7. Views of bottom faces of base slabs after failure for series (3) specimens

FACE 1

FACE 2

FACE 3

FACE 4

Bottom view of base

FIG. 5.8.1
SERIES (3)
VIEWS OF SPECIMEN T_{3-1}
AFTER FAILURE

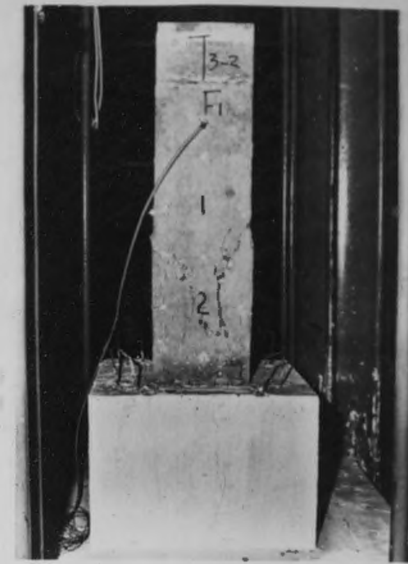

FACE 1

FACE 2

FACE 3

FACE 4

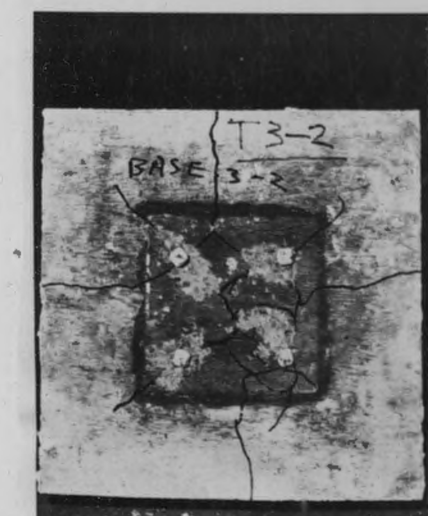

.Bottom view of base

FIG. 5.8.2
SERIES (3)
VIEWS OF SPECIMEN $T_{3\cdot2}$
AFTER FAILURE

FACE 1

FACE 2

FACE 3

FACE 4

Bottom view of base

FIG. 5.8.3
SERIES (3)
VIEWS OF SPECIMEN $T_{3 \cdot 3}$
AFTER FAILURE

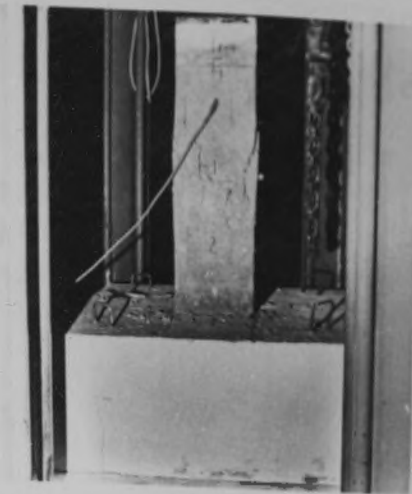

FACE 1

FACE 2

FACE 3

FACE 4

Bottom view of base

FIG. 5.8.4
SERIES (3)
VIEWS OF SPECIMEN $T_{3\cdot 4}$
AFTER FAILURE

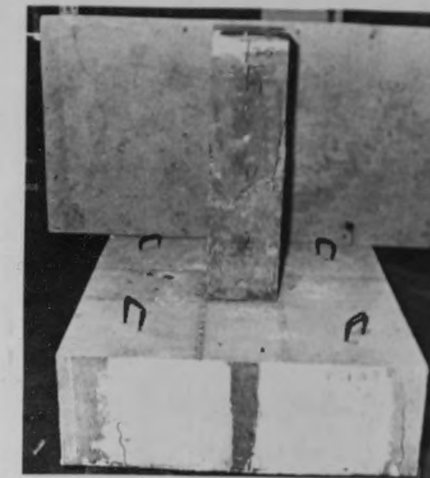

FACE 1

FACE 2

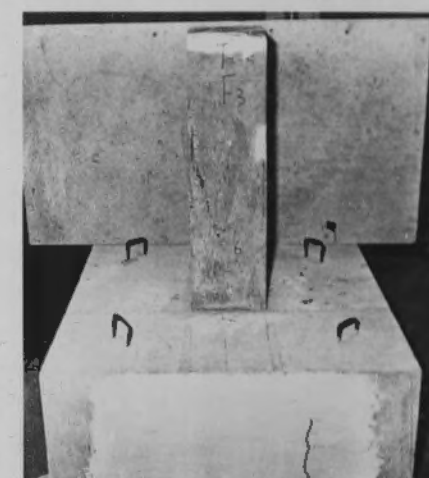

FACE 3

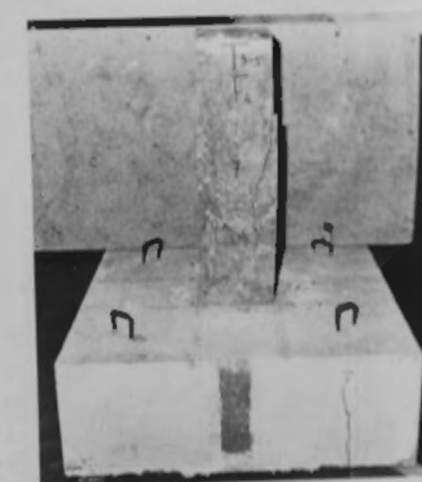

FACE 4

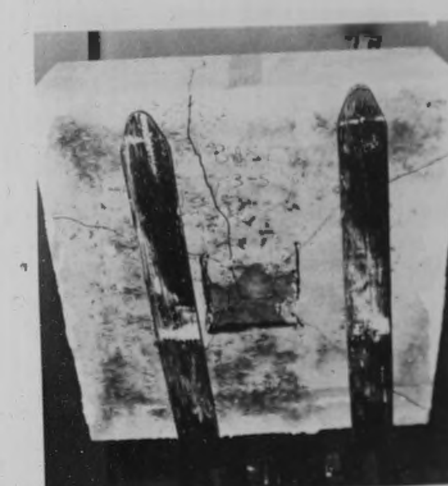

Bottom view of base

FIG. 5.8 - 5
SERIES (3)
VIEWS OF SPECIMEN T_{3-5}
AFTER FAILURE

TABLE 5.3

Summary of series (3) specimens results and calculations.

T_{i-j}	h mm.	$\frac{AB-a_1 a_2}{a_1 a_2}$	$P_{ult.}$	P_{test}	$\frac{P_{test}}{P_{ult.}}$	$\frac{0.8 f_{cu} A_c}{P_{ult.}}$	ε_s (av.) x μ	f_s (av.) N/ mm^2
T_{3-1}	300	2.063	1547.24	1192.5	0.770	0.635	1000	222.9
T_{3-2}	300	4.063	1486.37	1160.0	0.780	0.622	965	212.1
T_{3-3}	300	8.000	1495.6	1211.3	0.810	0.624	1030	226.3
T_{3-4}	300	13.063	1540.3	1305.0	0.847	0.635	1170	257.1
T_{3-5}	300	19.250	1685.2	1451.0	0.860	0.664	1180	263.0

T_{i-j}	ε_s(max) xμ	f_s(max) N/mm^2	f_c N/mm^2	$\frac{fc}{f_{cu}}$ for Column	$\frac{f_s(av)}{f_y}$	$\frac{f_s(max)}{f_y}$	f_{bs}(av) N/mm^2	f_{bs} (CP110) N/mm^2	f_{bs} (ACI) N/mm^2
T_{3-1}	1140	254.1	23.55	0.744	0.446	0.508	3.72	2.86	5.40
T_{3-2}	1100	241.7	23.06	0.773	0.427	0.487	3.53	2.72	5.16
T_{3-3}	1150	252.7	23.92	0.794	0.456	0.509	3.77	2.71	5.15
T_{3-4}	1450	312.1	25.34	0.803	0.518	0.628	4.29	2.91	5.47
T_{3-5}	1440	321.0	28.92	0.801	0.526	0.642	4.38	2.94	5.52

T_{i-j}	$f_{bs(max)}$ N/mm^2	$\frac{f_{bs(av)}}{f_{cu}}$ for base	$\frac{f_{bs(max)}}{f_{cu}}$ for base	$\frac{f_{bs(CP110)}}{f_{cu}}$ for base	$\frac{f_{bs(ACI)}}{f_{cu}}$ for base	$\frac{f_{bs(av)}}{f_{bs}(CP110)}$	$\frac{f_{bs(av)}}{f_{bs(ACI)}}$
T_{3-1}	4.24	0.112	0.128	0.0.86	0.162	1.300	0.689
T_{3-2}	4.03	0.116	0.133	0.090	0.170	1.298	0.684
T_{3-3}	4.21	0.129	0.139	0.090	0.170	1.391	0.732
T_{3-4}	5.20	0.126	0.153	0.085	0.160	1.474	0.784
T_{3-5}	5.35	0.126	0.154	0.085	0.159	1.490	0.794

Average value of f_c/f_{cu} for column = 0.783

Average value of 0.8 $f_{cu}A_c/P_{ult}$ except 3-5 = 0.630

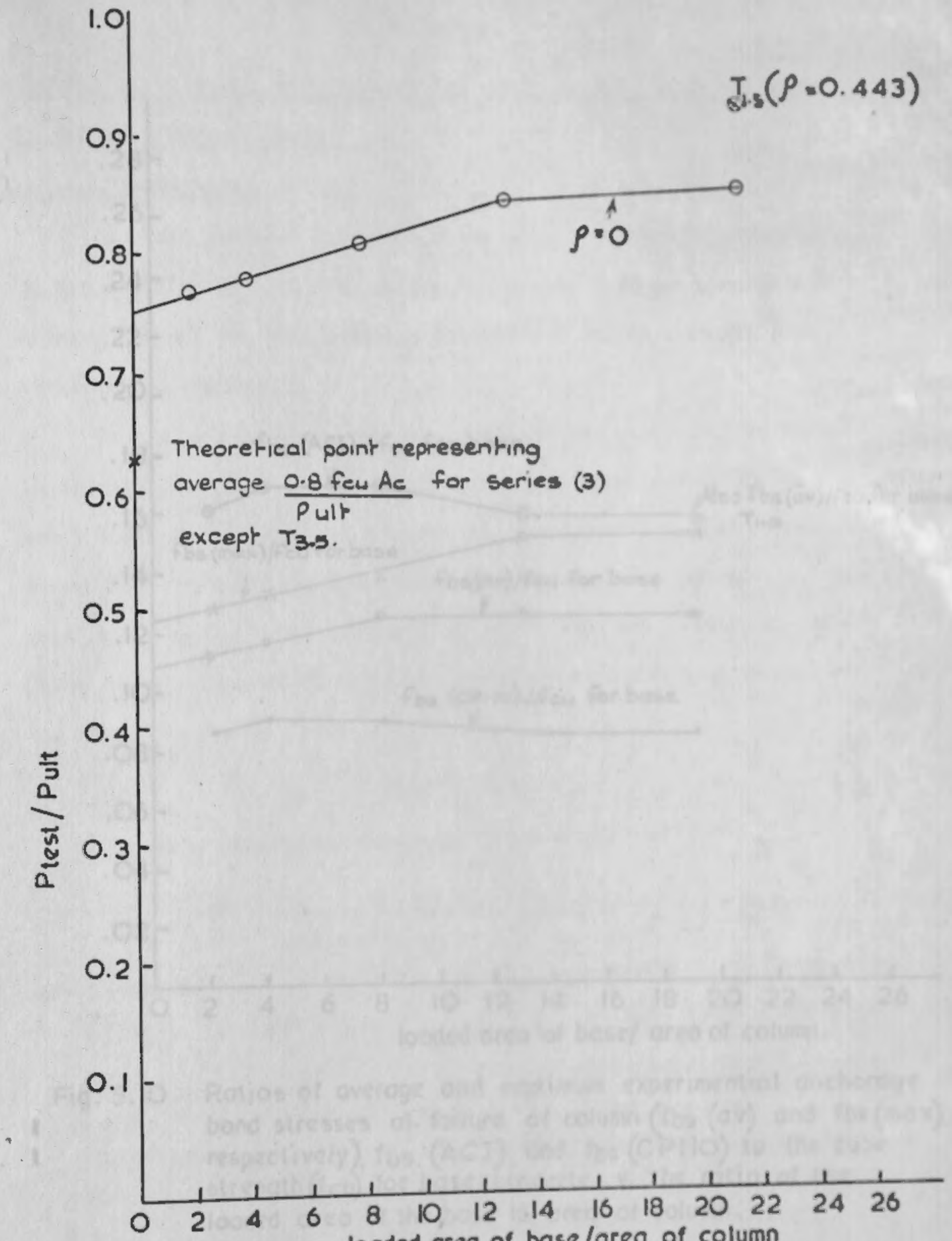

Fig. 5.9. Ratio of maximum experimental load on column (P test) to calculated ultimate axial load for column using eqn (1) (Pult) v. ratio of loaded area of base to area of column.

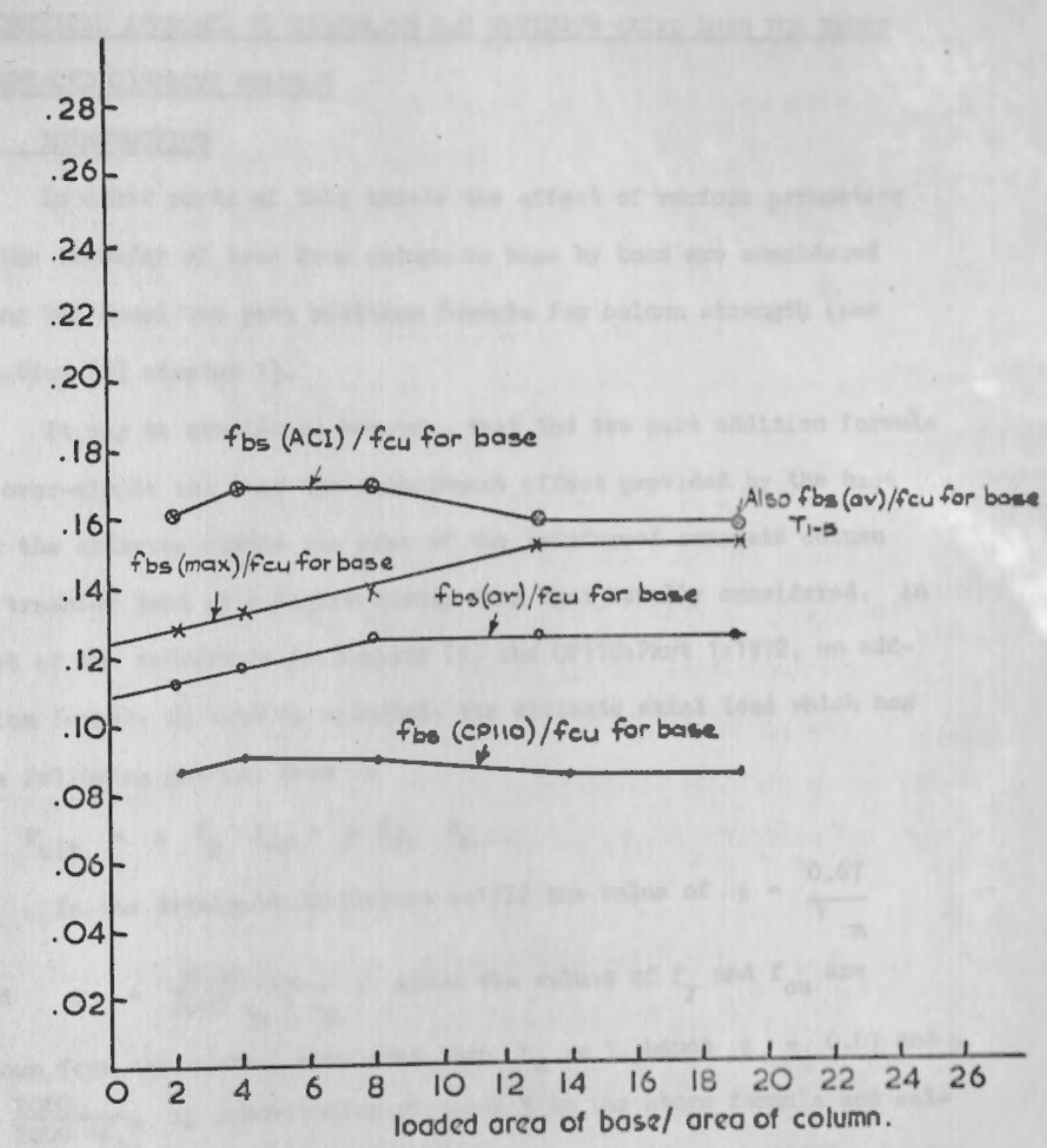

Fig. 5.10 Ratios of average and maximum experimential anchorage bond stresses at failure of column (fbs (av) and fbs (max) respectively), fbs (ACI) and fbs (CP110) to the cube strength (fcu) for base concrete v. the ratio of the loaded area of the base to area of column.

CHAPTER 6

THEORETICAL APPROACH TO CALCULATE THE ULTIMATE AXIAL LOAD FOR SHORT REINFORCED CONCRETE COLUMNS

6.1. INTRODUCTION

In other parts of this thesis the effect of various parameters on the transfer of load from column to base by bond are considered using the usual two part addition formula for column strength (see equation (1) chapter 1).

It may be considered however, that the two part addition formula is over-simple and that the containment effect provided by the base and the stirrups enable the core of the reinforced concrete column to transfer load at a higher stress than that usually considered. In most of the references in chapter (1) and CP110:Part 1:1972, an addition formula is used to calculate the ultimate axial load which has the following general form :-

$$P_{ult} = \alpha \; f_y \; A_{sc} + \beta \; f_{cu} \; A_c$$

In the developed CP110:Part 1:1972 the value of $\beta = \dfrac{0.67}{\gamma_m}$ and $\alpha = \dfrac{2000}{2000\;\gamma_m + f_y}$. Since the values of f_y and f_{cu} are known from the control specimens then $\gamma_m = 1$, hence $\beta = 0.67$ and $\alpha = \dfrac{2000}{2000 + f_y}$. By substituting for α and β in the above formula and calculating P_{ult} for specimen (1B) of Pfister and Mattock (1965), specimens (1), (3), (5) of Sommerville and Taylor (1972) and specimen T_{1-6} of this research programme, the ratio of $P_{test}/P_{ult.}$ is found as tabulated below.

	Test No	P_{test} KN	P_{ult} KN	P_{test}/P_{ult}
Pfister and Mattock (1963)	1B	3039.9	3031.0	1.003
Sommerville and Taylor (1972)	1	1700.0	1745.7	0.974
	3	2200.0	2202.8	0.999
	5	1960.0	1941.9	1.009
Research Program	T_{1-6}	1550.0	1330.7	1.165

The above table shows that the developed British code formula having $\gamma_m = 1$ gives low value of the ultimate axial strength of T_{1-6} but fits very well with others result. The T_{1-6} P_{test}/P_{ult} ratio is 16.5% higher than the others and that is why higher values of α and β are used in equation (1).

The increase in strength must be due to the base effect on the column strength.

Since the experimental program specimen gives higher strength than that calculated using the two parts addition formula used by many researchers and the code of practice in current use, therefore, the ultimate axial strength for short columns must be considered. All the above addition formulae treat the column concrete as one section, but in reality the concrete section consists of core concrete which is confined by the reinforcing cage and the cover concrete.

King (1949) showed on small scale tests that by increasing the core area using the same concrete and longitudinal reinforcement, the column strength increased which supports the idea of dividing the column section into the following :-

1 - Longitudinal steel whose cross-sectional area = A_{sc}

2 - Core concrete whose cross-sectional area = A_{core}

3 - Cover concrete whose cross-sectional area = $A_c - A_{core} = A_{cover}$.

6.2. ASSUMPTIONS AND FORMULAE

To calculate the ultimate axial load using the new approach of dividing the column section, the following assumptions are made :-

1) The longitudinal steel is unconfined and the stress in it is f_s(av.) from tests see Tables (3.3, 4.3 and 5.3) or for design use 0.9 f_y where full bond is attained.

2) The cover concrete is unconfined and its stress (f_2) at failure is the same as the average stress in the capped cylinders for the same longitudinal strain (ε_1).

3) The core concrete is partially confined by the cage of steel column reinforcement in the lateral direction. For the tests the longitudinal strain (ε_1) is the strain measured on the faces of the column by the 8" Demec gauges. The lateral strain (ε_s) is the strain measured on the column links by the electrical resistance strain gauges.

Therefore, using the assumption of (3) the stress in the core (f_1) can be found by solving the following equations

$$E_c \quad \varepsilon_1 = f_1 - 2\,\nu_c \quad f_3 \quad \text{and}$$

$$E_c \quad \varepsilon_3 = f_3 - \nu_c \quad (f_1 + f_3)$$

where f_3 is the lateral stress acting on the core concrete

ν_c is the poisson's ratio

E_c is the secant modulus of elasticity.

Hence

$$f_1 = \left[\varepsilon_1 (1 - \nu_c) + 2\,\nu_c \;\varepsilon_3\right] \frac{E_c}{(1-2\,\nu_c)\,(1+\nu_c)} \quad \ldots\ldots(7)$$

Where ε_3 has negative value when substituted in equation (7) since the core is expanding in the lateral direction.

Therefore, the ultimate axial load (P_1) can be calculated from

$$P_1 = f_1 \; A_{core} + f_2 \; A_{cover} + f_s \text{ (av.) } A_{sc} \quad \ldots\ldots\ldots\ldots\ldots(8)$$

The usual addition formula is also used in the following form for comparision with equation (8) results.

$$P_2 = f_s \text{ (av.) } \; A_{sc} + 0.8 \; f_{cu} \; A_c \ldots\ldots\ldots\ldots\ldots\ldots\ldots\ldots(9)$$

6.3. POISSON'S RATIO (ν_c) AND SECAND MODULUS OF ELASTICITY (E_c) FOR COLUMN CONCRETE

Plowman (1963) showed that the Poisson's ratio (ν_c) is independent of mix proportions, strength, age and humidity of curing and at the ultimate stress level there is a high rate of creep which makes the slope of the chord of the stress-strain curve at higher stresses a function of speed at which the test is conducted. He measured (ν_c) and (E_c) at stress level varying from zero to $f_{cu}/3$. Anson and Newman (1966) showed that the value of (ν_c) remains sensibly constant up to a stress of about 60% of the ultimate stress then increases significantly. This sharp increase in (ν_c) is due to the formation of large cracks or fissures which cause dilation of concrete.

Hence the value of the Poisson's ratio (ν_c) is read from figs. (3.2.1f, 2f, 3f, 4f, 5f, 6f, 4.2.1f, 2f, 3f, 4f, 5f, 6f, 5.2.1f, 2f, 3f, 4f and 5f) for series (1), (2) and (3) specimens respectively.

The above graphs showed that the value of the Poisson's ratio (ν_c) increases significantly after a stress of about 0.6 f_{cu}. The average value of (ν_c) at this level of stress for all the specimens is (0.161) where at 0.55 f_{cu} stress level it is (0.153) and (0.148) at 0.50 f_{cu} stress level. This shows that the value of (ν_c) does not vary significantly below 0.6 f_{cu} stress level. Since the value of (ν_c) is independent of strength and age therefore, the average value at 0.6 f_{cu} stress level for all the experimental program is used in equation (7) calculations. At the same stress level of 0.6 f_{cu} the value of (E_c) is read from figs. (3.2.1c, 2c, 3c, 4c, 5c, 6c, 4.2.1c, 2c, 3c, 4c, 5c, 6c, 5.2.1c, 2c, 3c, 4c and 5c), for series (1), (2) and (3) specimens respectively.

The value of (E_c) for each specimen is used in equation (7) calculations. See Table (6.1) for these values.

6.4. ε_1, ε_s(av.) AND ε_3 VALUES FROM TESTS

From figs. (3.4.1, 2, 3, 4, 5, 6, 4.4.1, 2, 3, 4, 5, 6, 5.4.1, 2, 3, 4 and 5) of series (1), (2) and (3) respectively, it can be seen that after an axial load of about 0.9 P_{test} the lateral strain measured on the faces of the column by the 6" Demec gauges increases rapidly indicating the formation of cracks and then failure will follow shortly. Hence to avoid the excessive cracking the above strains are read at 0.9 P_{test} axial load from the above figures for (ε_3) and from figs. (3.3.1, 2, 3, 4, 5, 6, 4.3.1, 2, 3, 4, 5, 6, 5.3.1, 2, 3, 4, and 5) for (ε_1) and ε_s(av.).

The strains (ε_1) and (ε_3) are used in equation (7) calculations where (ε_s(av)) is used to calculate (f_s(av.)) then substituted in equation (8). There is no relation between (ε_3) and (ε_1) or ε_s(av.) see Table (6.2).

6.5. CALCULATIONS

Substituting the average value of (ν_c) = 0.161, the corresponding (E_c) value, (ε_1) and (ε_3) in equation (7) gives the value of the stress in the core (f_1) for each specimen.

The stress in the cover (f_2) is calculated from the compatibility conditions using (ε_1) values and figs. (3.2.1a, 2a, 3a, 4a, 5a, 6a, 4.2.1a, 2a, 3a, 4a, 5a, 6a, 5.2.1a, 2a, 3a, 4a and 5a).

For all columns the values of A_{sc} = 1257 mm^2, A_{core} = 18343 mm^2 and A_{cover} = 20400 mm^2.

Hence substituting in equation (8) for f_1, f_2, f_s(av.), A_{sc}, A_{core} and A_{cover} gives P_1 values and then P_1 / P_{test} is calculated for each specimen.

The ratios of f_1, and f_2 to f_{cu} for column are calculated all the above results are tabulated in Table (6.2). The value of P_2 and then P_2/P_{test} are calculated and tabulated in table (6.3). In P_2 calculations the stress f_s(av.) is taken at failure of the column.

6.6. DISCUSSION

From table (6.2) the average value of $\frac{P_1}{P_{test}}$ is 0.971 and the coefficient of variation is = 9% compared with the average value of 1.004 and the coefficient of variation is 2.1% for P_2/P_{test} from table (6.3).

This shows that the addition formula (9) gives more accurate estimate for the ultimate axial load than equation (8). To estimate the ultimate axial load using equation (8), the values of ν_c, ε_1, ε_3 and ε_s(av.) or f_y are needed to be known. This means that any error in these values leads to an error in the ultimate axial load.

Using the addition formula (9) to estimate the axial load only f_{cu} and ε_s(av.) or f_y values are needed, hence less variables and less error in estimating the axial load than that of equation (8). Equation (8) can be written in the following form in terms of f_{cu} and f_s(av.) or f_y :-

$$P_3 = (\beta_1 A_{core} + \beta_2 A_{cover})\, f_{cu} + f_s(av.)\, A_{sc}$$

From table (6.2) the values of β_1 and β_2 are taken as the average values of f_1 / f_{cu} and f_2 / f_{cu} respectively, hence rewriting the above equation gives

$$P_3 = (0.91\, A_{core} + 0.75\, A_{cover})\, f_{cu} + f_s(av.)\, A_{sc} \quad \ldots\ldots\ldots\ldots (10)$$

where f_s(av.) is the stress in the steel at failure of the column. Equation (10) treats the column concrete section as in equation (8) but it is in the same form of equation (9) and having the same number of variables. It gives accurate estimat value of the ultimate axial load and the average value of P_3 / P_{test} is 1.029 and the coefficient of variation is 2%.

Equation (10) fits very well with the test results of this experimental program but to use it in design more tests are needed in which the column section is varied keeping the cover and spacing of links within the nominal requirements of the British Code hence the ratio of the core area to cover area varies.

6.7. CONCLUSIONS

From Tables (6.1), (6.2) and (6.3) the following are concluded :

1) Equations(8) and (10) agree very well with the test results. This shows that the core concrete carries more load than the

cover concrete for the same cross-sectional area and hence the load from the column core concrete is transferred to the base slab at a higher stress than that from the column cover concrete.

2) Equation (10) can be used to estimate the ultimate axial load of short columns provided that they have the same section as those in this experimental program, but for different column sections the addition formula in the form of equation (1) should be used where full bond strength is attained.

In both equations $f_s(av.) = 0.9\ f_y$.

3) The average Poisson's ratio of the concrete used in this experimental program is found to be 0.161 and the coefficient of variation is 11% at a stress level of 0.6 f_{cu}.

TABLE (6.1)

Summary of (E_c) and (ν_c) values at 0.6 f_{cu} stress level for all specimens.

T_{i-j}	fcu for column N/mm^2	$0.6f_{cu}$ N/mm^2	E_c KN/mm^2	ν_c
T_{1-1}	38.35	23.01	22.70	0.167
T_{1-2}	40.67	24.40	23.09	0.138
T_{1-3}	32.62	19.57	25.42	0.136
T_{1-4}	31.80	19.08	27.65	0.163
T_{1-5}	31.28	18.77	18.05	0.156
T_{1-6}	32.29	19.37	24.52	0.210
T_{2-1}	32.30	19.38	18.70	0.132
T_{2-2}	32.60	19.56	23.56	0.171
T_{2-3}	34.12	20.47	24.51	0.159
T_{2-4}	40.00	24.00	22.75	0.160
T_{2-5}	30.50	18.30	24.40	0.170
T_{2-6}	25.87	15.52	15.37	0.154
T_{3-1}	31.67	19.00	21.50	0.178
T_{3-2}	29.82	17.89	24.01	0.149
T_{3-3}	30.12	18.07	24.82	0.153
T_{3-4}	31.56	18.94	24.28	0.174
T_{3-5}	36.12	21.67	25.50	0.168

The average calue of ν_c for all the specimens = 0.161

Coefficient of variation is 11%

TABLE (6.2)

Summary of equation (7) calculations for all specimens.

T_{i-j}	P_{test} KN	$0.9\ P_{test}$ KN	ε_s (av.) xμ	ε_1 xμ	$-\varepsilon_3$ xμ	f_1 N/mm^2	f_2 N/mm^2
T_{1-1}	1285.0	1157.0	620	1010	140	23.13	23.00
T_{1-2}	1544.0	1390.0	580	1280	290	28.76	27.10
T_{1-3}	1330.0	1197.0	880	1240	320	30.26	23.8
T_{1-4}	1385.0	1247.0	940	1500	520	38.32	29.46
T_{1-5}	1395.0	1256.0	1010	1440	200	26.23	22.57
T_{1-6}	1550.0	1395.0	1390	1430	360	33.74	26.73
T_{2-1}	1239.0	1115.0	960	1580	390	28.51	21.39
T_{2-2}	1312.5	1181.0	860	1170	270	26.77	22.52
T_{2-3}	1360.0	1224.0	890	1150	240	27.64	25.30
T_{2-4}	1580.0	1422.0	1090	1760	350	39.41	32.50
T_{2-5}	1281.5	1153.0	1040	1240	320	29.05	25.33
T_{2-6}	1230.0	1107.0	1190	1650	230	25.59	18.16
T_{3-1}	1192.5	1073.0	1000	1060	360	21.13	21.00
T_{3-2}	1160.0	1044.0	880	1300	340	29.92	21.20
T_{3-3}	1211.3	1090.0	980	1320	220	32.66	22.90
T_{3-4}	1305.0	1175.0	1000	1140	340	26.12	23.50
T_{3-5}	1451.0	1306.0	1040	1250	320	30.64	27.92

continued....

TABLE (6.2)

Summary of equation (7) calculations for all specimens.

T_{i-j}	f_1A_{core} KN	f_2A_{cover} KN	$fs(av)A_{sc}$ KN	P_1 KN	$\frac{P_1}{P_{test}}$	$\frac{f_1}{f_{cu}}$	$\frac{f_2}{f_{cu}}$
T_{1-1}	424.3	469.2	162.6	1056.1	0.822	0.603	0.600
T_{1-2}	527.5	552.8	152.1	1232.4	0.798	0.707	0.666
T_{1-3}	555.1	485.5	225.5	1265.7	0.952	0.928	0.730
T_{1-4}	702.9	601.0	278.5	1582.8	1.143	1.205	0.926
T_{1-5}	481.2	460.4	264.8	1206.4	0.865	0.839	0.722
T_{1-6}	618.9	545.3	356.1	1520.3	0.981	1.045	0.828
T_{2-1}	523.0	436.4	204.5	1163.8	0.939	0.883	0.662
T_{2-2}	491.1	459.4	230.7	1181.2	0.900	0.821	0.691
T_{2-3}	507.1	516.1	228.0	1251.2	0.920	0.810	0.742
T_{2-4}	722.9	663.0	293.2	1679.1	1.063	0.985	0.813
T_{2-5}	532.9	516.7	270.6	1320.2	1.030	0.953	0.830
T_{2-6}	469.3	370.5	304.1	1143.9	0.930	0.989	0.702
T_{3-1}	387.6	428.4	280.2	1096.2	0.919	0.667	0.663
T_{3-2}	548.9	432.5	243.1	1224.5	1.056	1.003	0.711
T_{3-3}	599.1	467.2	270.7	1336.9	1.104	1.084	0.760
T_{3-4}	479.1	479.4	276.2	1234.7	0.946	0.828	0.745
T_{3-5}	562.0	569.6	291.4	1423.0	0.981	0.842	0.773

Average value of P_1/P_{test} = 0.97, Coefficient of variation 9%

Average value of f_1/f_{cu} = 0.91, Coefficient of variation 14.8%

Average value of f_2/f_{cu} = 0.75, Coefficient of variation 9.2%

T_{1-1} results are not included in calculating the above averages since the column did not fail.

TABLE (6.3)

Summary of equations (9) and (10) calculations for all specimens.

T_{i-j}	$f_s(av)A_{sc}$ KN	$0.8f_{cu}A_c$ KN	P_2 KN	$\frac{P_2}{P_{test}}$	$0.91f_{cu}$	$0.75f_{cu}$ cover KN	P_3 KN.	$\frac{P_3}{P_{test}}$
T_{1-1}	169.9	1188.6	1358.5	1.057	640.1	586.8	1396.8	1.087
T_{1-2}	275.3	1260.5	1535.8	0.995	678.9	622.3	1576.5	1.021
T_{1-3}	325.6	1011.0	1336.6	1.005	544.5	499.1	1369.2	1.029
T_{1-4}	374.6	985.6	1360.2	0.982	530.8	486.5	1391.9	1.005
T_{1-5}	394.5	969.5	1364.0	0.978	522.1	478.6	1395.2	1.000
T_{1-6}	520.4	1000.8	1521.2	0.982	539.0	494.0	1553.4	1.002
T_{2-1}	280.8	1001.1	1281.9	1.035	539.2	494.2	1314.2	1.061
T_{2-2}	301.2	1010.4	1311.6	0.999	544.2	498.8	1344.2	1.024
T_{2-3}	316.1	1057.5	1373.6	1.010	569.5	522.0	1407.6	1.035
T_{2-4}	364.5	1239.8	1604.3	1.015	667.7	612.0	1644.2	1.041
T_{2-5}	338.1	945.3	1283.4	1.002	509.1	466.7	1314.9	1.026
T_{2-6}	403.7	801.8	1205.5	0.980	431.8	395.8	1231.3	1.001
T_{3-1}	280.2	981.6	1261.8	1.058	528.6	484.6	1293.4	1.085
T_{3-2}	266.6	924.3	1190.9	1.027	497.8	456.2	1220.6	1.052
T_{3-3}	284.5	933.6	1218.1	1.006	502.8	460.8	1248.1	1.030
T_{3-4}	323.2	978.2	1301.3	0.997	526.8	482.9	1332.9	1.021
T_{3-5}	330.6	1119.5	1450.1	0.999	602.9	552.6	1486.1	1.024

The average value of P_2/P_{test} = 1.004 Coefficient of variation 2.1%

The average value of P_3/P_{test} = 1.029 Coefficient of variation 2%

T_{1-1} result was not included in averaging the above ratios since the column did not fail.

CHAPTER 7

AXIAL LOAD TREANSFERENCE BETWEEN COMPRESSION STEEL REINFORCEMENT AND CONCRETE

7.1. INTRODUCTION

In all current codes of practice and the calculations which have been done to calculate the anchorage bond stresses for specimens of series (1), (2) and (3), the first assumption is that the anchorage bond stress is constant along the anchorage length (1).

From the literature review on the work which is relative to this topic, it can be suggested that the above assumption is not the case, and hence, an experimental program is needed to verify that the axial load distribution along the anchorage length is not linear.

Due to the limit of time only one pilot test is carried out using the same type of rinforcement, concrete mix and concrete materials as those used in the previous specimens of series (1), (2) and (3).

7.2. LITERATURE REVIEW

There is a lot of work done on pull out test to find the average anchorage bond stress between concrete and tensile steel reinforcement using different types of reinforcement and concrete and many other factors but Wilkins (1951) reported his work on the load distribution in bond tests. He also carried a pull out test using a bright drawn steel tube reinforcement of 1"external diameter and having smooth, fine knurl, and heavy knurl external surface and embedment length in a 6" diameter concrete cylinder of 16", 12" and 8", also have a very uniform dimensions along their length.

The 16" length is done for the smooth surface only where an extra test is done for the 8" length on G."Hi-Bond" pattern.

Electrical resistance strain gauges are fixed on the inside surface of the steel tube and their readings are recorded at each load increment until anchorage bond failure between the tube and the concrete.

He indicated that bond may be caused by adhesion, friction and mechanical wedging.

There is a definite length of bar which develops resistance to withdrawal from the concrete, and added length of embedment provides little extra resistance. The average bond stress is dependent on the length of embedment. Bond resistance is first developed at the loaded end, and part of the tube may be free from load in the early stages of the test. The maximum bond stress moves towards the free end as load increases and first slip at the free end is observed when the bond stress at that end reaches its limiting value. For a smooth surface at failure, the part of the tube near the pull-out end has zero anchorage bond stress and at the free end the stress is a maximum where as for a heavy knurl surface high bond stresses are also developed at the pull out end by mechanical wedging and these may cause fracture of the concrete cylinder.

Wilkins also did some preliminary tests with black tubing, which had the type of surface corresponding to normal reinforcement steel, and they gave very erratic results and that was due to the variable dimensions of the tube itself.

Using a tube does not have the same relative deformation characteristics as a solid bar and it is very difficult to fix the gauges on the inside surface specially for small diameter bars in which drilling a hole becomes even more difficult, but in this method, the outside surface is kept free from any water proofing material which could affect the surface properties of the reinforcement.

The author could not find any work done on load transference between concrete and a reinforcing steel bar in compression apart from the theoretical work done by Mattes and Poulos (1968) on the analysis of settlement of single compressible pile - In their analysis they use linear elastic theory to analyse the behaviour of a compressible floating pile of circular cross-section in an ideal elastic soil mass.

This work has some relation to the above topic since the pile in soil is similar to a reinforcing bar in compression in concrete but since their analysis is only for circular or cylinderical pile, this can only apply to plain bars.

In their work the compatibility condition must be satisfied for the pile and the soil that is, if at top parts of the pile shear stresses reach their top value, this analysis can only hold for the rest of the pile and only vertical displacement was considered.

The vertical displacement of the soil due to the shear stress along the pile (same as anchorage bond stress between reinforcing steel bar and concrete) may be obtained by double integration of the Mindlin equation for vertical displacement and the pile was divided into ten equal elements.

The influence of the compressibility of the pile on load transfer along it is examined. The compressibility of the pile K is

$$\frac{\text{E for pile}}{\text{E for soil}} \times \frac{\text{4 Area of pile}}{\pi\,(\text{external diameter of pile})^2}$$

which is for a reinforcing bar in concrete $\frac{E_s}{E_{ce}}$. They found that for small values of K that is, $K \leq 50$ and $\frac{l}{\phi} = 25$ for soils Poisson's ratio of 0-0·5 the shear stress distribution is high at the top of the pile and low at the bottom end where is for $K = 5000$ the shear stress is almost uniform with high concentration near the bottom end which is the same finding by Paulos and Davis (1968) for incompressible pile for $\frac{l}{\phi} > 20$ and soils Poisson's ratio of 0.5 but for $\frac{l}{\phi} < 20$ the shear stresses are high at both ends and low at the middle parts of the pile.

So the calculations for compressible and incompressible piles does not agree with the pull out tests by Wilkins (1951) for smooth surface circular tubes but for a heavy knurl circular tube there is a stress concentration at the pull out end as well due to mechanical wedging action which is not included in the above theoretical analysis. Since the values for K using series (1), (2) and (3) specimens results are < 10 and $\frac{l}{\phi} \leq 20$ therefore an experimental program is needed to see how the anchorage bond stresses between the steel bar incompression and concrete are distributed along the anchorage length and whether they follow the pile analysis or not or are they like the pull out tests.

7.3. PILOT SPECIMEN DESIGN AND PREPARATION

Since there could be many factors affecting the anchorage bond stresses along the anchorage length such as the K value, $\frac{l}{\phi}$, spacing of the bars and whether these stresses reached their ultimate value at any part of the anchorage length or not etc. and since only one pilot test is going to be performed, the specimen is chosen so that it has four reinforcing 20 mm. ϕ square twisted H.T. steel bars which have the same spacing as those used as longitudinal column reinforcement for series (1), (2) and (3) specimens. The anchorage length l = 300 mm. so that $\frac{l}{\phi} = 15$ and both situations when the anchorage bond stresses reached its ultimate value or not can be observed since it is known from T_{1-5} and series (3) specimens that anchorage bond failure governs for this anchorage length. Also it is known that the maximum axial load which is taken by the column steel of T_{3-3} which has the same base dimensions as this pilot specimen is 284.5 KN. The tops of the four bars are welded to a 200 x 200 mm. square by 20 mm. thick steel plate as in series (1), (2) and (3) specimens, but in this time the bars are also welded with the bottom of the plate all around.

At the bottom of the bars a 22 mm. square by 20 mm. high holes are left under them by inserting wooden blocks of the same dimensions before casting. These wooden blocks are removed with the wooden mould so that slipping of the bars can take place without any end bearing. From the original 20 mm. Ø square twisted H.T steel bar a steel control specimen of 450 mm. long is prepared.

Electrical resistance strain gauges of 5 mm. length, 2.04 gauge factor and 120 Ohm gauge resistance are fixed on the bars in the way stated in chapter (2).

The water proof material used to protect the gauges in the specimen is M. coat G which is 100% solids polysulfide/epoxy compound. The positions of the gauges are as in fig. (7.1) and they are in pairs at each position placed one opposite to the other.

Two of these gauges are fixed above the concrete level to measure the axial load on each bar.

The concrete mix is 1:2:4 by weight and w/c = 0.6 and two batches are enough for the specimen, five 150 mm. cubes and four 150 x 300 mm. cylinders. The specimen and concrete control specimens casted and cured in the same way as those of series (1), (2) and (3).

The steel and concrete control specimens are tested in the same way stated in chapter (2).

The test of specimen and its concrete control specimens are tested after eight days of casting.

The total settlement of the bottom face of the steel plate is measured by a dial gauge reading to the nearest 0.01 mm. This dial gauge is fixed to the top beam of the testing rig and hence it also includes in its readings the deflection of the testing rig due to the load applied. The measurement of the settlement can be also used to know when the bars will slip, through the concrete. For position of the dial gauge see fig. (7.1).

7.4. CONTROL SPECIMENS RESULTS AND CALCULATIONS

From the steel control specimen results a graph of axial stress V. longitudinal strain is plotted from which E_s is found to be 207 KN/mm^2. and f_y = 461.8 N/mm^2 see fig. 7.2.

From the concrete control specimen results the average value of f_{cu} is calculated to be equal to 31.05 N/mm^2. from the cubes results, f_t is calculated from the uncapped cylinders results and it is equal to 2.50 N/mm^2., and from the capped cylinders results axial stress is plotted against the longitudinal and lateral strains see figs. (7.3.a,b) respectively, from these two graphs another two are plotted which are axial stress V. E_c and ν_c see figs. (7.3.c and d) respectively. E_{ce} is calculated from the initial tangent of fig. (7.3.a) and it is equal to 24.20 KN/mm^2.

7.5. TESTING, MODE OF FAILURE, RESULTS, AND CALCULATIONS FOR THE PILOT SPECIMEN

The specimen is set in the testing rig as shown in fig. (7.4.a).

The compulog data logger is programmed to print the strains in the steel bars automatically from the electrical resistance strain gauges at each load increment. The load increased in 10KN. increments until failure. The reading of the dial gauges is recorded at each load increment.

The mode of failure of the specimen is as shown in fig. (7.4.b) which shows the four 20 mm. ∅ bars slipped through the concrete and some cracks started from the bars to the outside face of the concrete block. The total axial load on the 4-20 mm. ∅ bars is plotted against the dial gauge reading as shown in fig. (7.5). From zero load to 30 KN. the graph is a straight line, then after that the bars started to slip. Since most of the previous specimens the average slip of the bars was about 3mm. after failure of the columns, then by drawing a line parallel to the first straight part of the graph at 3 mm. on the dial gauge axis it cuts the graph at a total axial load of about 195 KN. After a load of 240 KN the bars slipped suddenly about 4 mm, then they grip again and the graph becomes a straight line again until a load of 400 KN. then it starts to curve as the bars begin to yield, and then they yielded at a load of 525 KN. At a load of 195 KN. which corresponds to 3mm. slip f_{bs} (av.) = 2.59 N/mm^2, f_{bs}(av.) / f_{cu} = 0.083 and at a load of 240 KN which corresponds to a slip greater than 3 mm. f_{bs} (av.) = 3.19 N/mm^2, f_{bs} (av.) /f_{cu} = 0.103.

Also at yielding failure of the pilot specimen the average stress in the 20 mm. ∅ bars = 417.7 N/mm^2 which is 0.905 f_y.

The dial gauge readings include the deflection of the testing rig.

7.6. DISCUSSION OF THE PILOT SPECIMEN RESULTS

At an average total slip of about 3.00 mm. for T_{3-3} column longitudinal reinforcement , the total load carried by the column steel = 284.5 KN. where for the same amount of slip the load carried by the pilot specimen bars is 195 KN. The difference between the two loads = 89.5 KN. which is equivalent to an anchorage length = 138 mm. This confirms that parts of the column length is acting as an extra anchorage length. Where if the failure load is taken to be 240 KN. then the difference is 44.5 KN which is equivalent to 57 mm. extra anchorage length. From the yielding failure of the bars it can be seen that the maximum stress in these bars is 0.905 f_y which again justify the use of 0.9 as a factor for f_y in equation (1).

The bars after slipping took more than double the slipping failure load and this was due to the geometric properties of the square twisted steel bars which when slip might cause some interlocking of the aggregate and hence prevent the bars from slipping any further.

7.7. THEORETICAL PREDICTIONS OF THE VARIATION OF ANCHORAGE BOND STRESS (OR AXIAL LOAD) ALONG THE ANCHORAGE LENGTH USING SERIES (1) RESULTS

7.7.1. INTRODUCTION

Inspection of Mattes and Paulos (1968) fig. (2) and Paulos and Davis (1968), fig. (5) shows two sorts of curve.

1) For an elastic pile having $l/\phi = 25$ and $K < 50$, maximum shear stress (anchorage bond stress) occurs at the top of the pile and minimum shear stress at the bottom.

2) For a rigid pile having small l/ϕ value, maximum shear stress occurs at top and bottom with a minimum in the middle.

Both curves are complex and cannot be formulated in a simple way for design use. However, if it could be shown that a parabola or a cubic curve plus a constant would be sufficiently accurate, this could be more easily handled.

Further inspection of the test results and T_{1-6} results were used to calculate the basic values required for each of the above simple curves. Then using the upper part of the curves for shallower bases, it was possible to show that the parabola gave reasonable values.

7.7.2. ASSUMPTIONS AND FORMULAE

Assume that the anchorage bond stress has either of the following two distributions along the anchorage length, but in both cases the anchorage bond stress attained a maximum value f (max.) and does not exceed it for specimens failed by anchorage bond failure and having the same base slab properties, apart from the depth variation. Since T_{1-6} just failed by yielding of the column longitudinal bars, its results are used to calculate the unknowns required to solve the assumed curves and then used as reference for the rest of series (1) specimens.

1) DISTRIBUTION ONE

The anchorage bond stress has a maximum value f (max.) at the top of the anchorage length (l_{1-6}) and at the bottom end its value is (K_{1-6}) see fig. (7.6).

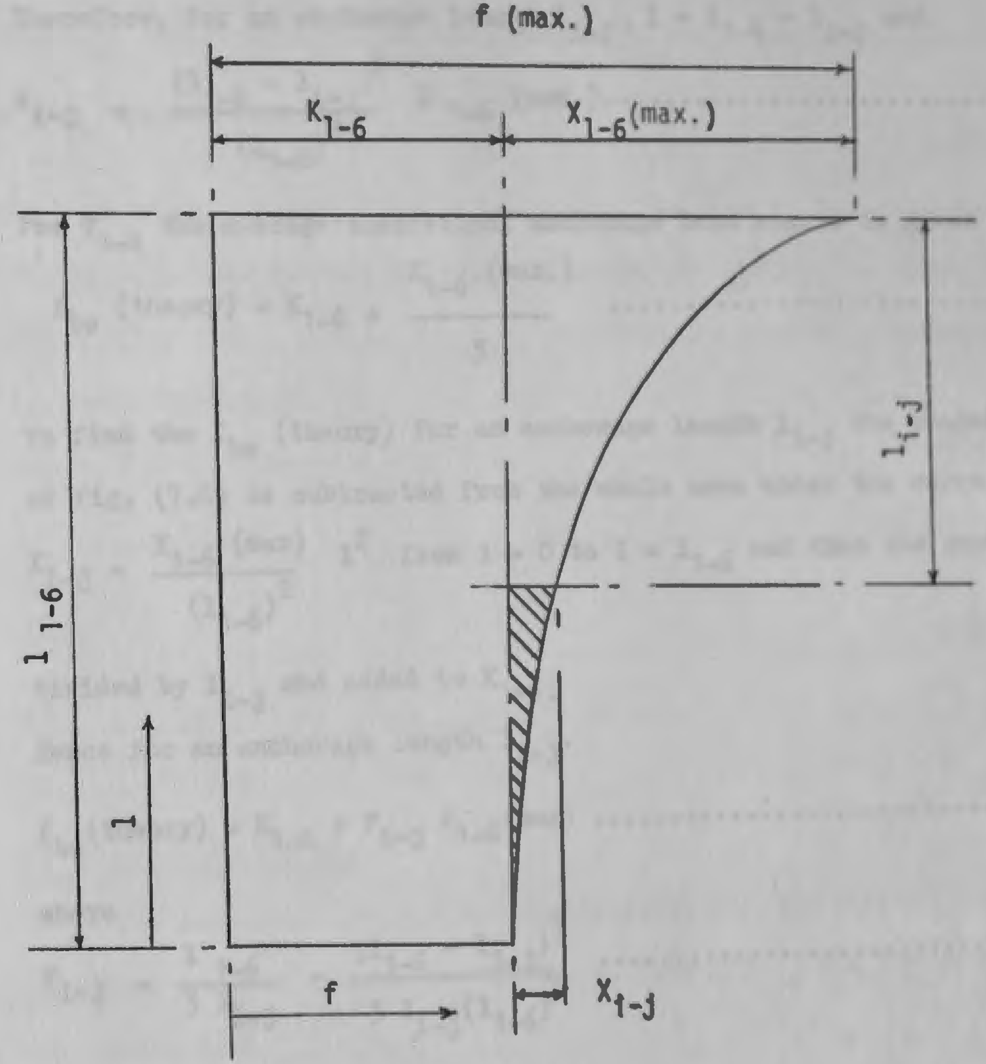

Fig. 7.6.

The anchorage bond stress (f) is given by

$$f = K_{1-6} + X_{i-j}$$

where X_{i-j} is either

i)

$$X_{i-j} = al^2$$

at $l = l_{1-6}$, $X_{i-j} = X_{1-6}$ (max.)

$$\therefore \; X_{i-j} = \frac{X_{1-6}\text{ (max.)}}{(l_{1-6})^2} \; l^2 \quad \text{..............................(11)}$$

The origin from which (l) is measured is taken as the bottom of the anchorage length (l_{1-6}).

Therefore, for an anchorage length l_{i-j}, $l = l_{1-6} - l_{i-j}$ and

$$X_{i-j} = \frac{(l_{1-6} - l_{i-j})^2}{(l_{1-6})^2} \; X_{1-6}\,(\text{max.}) \quad \ldots\ldots (11a)$$

For T_{1-6} the average theoretical anchorage bond stress is given by

$$f_{bs}\;(\text{theory}) = K_{1-6} + \frac{X_{1-6}\,(\text{max.})}{3} \quad \ldots\ldots (11b)$$

To find the f_{bs} (theory) for an anchorage length l_{i-j} the shaded area of fig. (7.6) is subtracted from the whole area under the curve

$X_{i-j} = \frac{X_{1-6}\,(\text{max})}{(l_{1-6})^2}\, l^2$ from $l = 0$ to $l = l_{1-6}$ and then the result is divided by l_{i-j} and added to K_{1-6}.

Hence for an anchorage length l_{i-j}.

$$f_{bs}(\text{theory}) = K_{1-6} + F_{i-j}\, X_{1-6}(\text{max}) \quad \ldots\ldots (11c)$$

where

$$F_{i-j} = \frac{l_{1-6}}{3\, l_{i-j}} - \frac{(l_{1-6} - l_{i-j})^3}{3\, l_{i-j}(l_{1-6})^2} \quad \ldots\ldots (11d)$$

ii)

$$X_{i-j} = a\, l^3$$

at $l = l_{1-6}$ $X_{i-j} = X_{1-6}(\text{max})$

$$\therefore X_{i-j} = \frac{X_{1-6}(\text{max.})}{(l_{1-6})^3}\; l^3 \quad \ldots\ldots (12)$$

The origin from which (l) is measured is taken as the bottom of the anchorage length l_{1-6}.

Therefore, for an anchorage length l_{i-j}, $l = l_{1-6} - l_{i-j}$ and

$$X_{i-j} = \frac{(l_{1-6} - l_{i-j})^3}{(l_{1-6})^3}\; X_{1-6}\,(\text{max.}) \quad \ldots\ldots (12a)$$

For T_{1-6} the average theoretical anchorage bond stress is given by

$$f_{bs}(\text{theory}) = K_{1-6} + \frac{X_{1-6}\,(\text{max})}{4} \quad \text{.........................(12b)}$$

To find the f_{bs}(theory) for an anchorage length l_{i-j} the shaded area of fig. (7.6) is subtracted from the whole area under the curve of equation (12) from $l = 0$ to $l = l_{1-6}$ and then the result is divided by l_{i-j} and added to K_{1-6}.

Hence, for an anchorage length l_{i-j}

$$f_{bs}\,(\text{theory}) = K_{1-6} + F_{i-j}\;X_{1-6}\,(\text{max}) \quad \text{.........................(12c)}$$

where

$$F_{i-j} = \frac{l_{1-6}}{4\,l_{i-j}} - \frac{(l_{1-6} - l_{i-j})^4}{4\,l_{i-j}\,(l_{1-6})^3} \quad \text{.............................(12d)}$$

2) DISTRIBUTION TWO

The anchorage bond stress distribution has the maximum value f (max.) at the two ends of the anchorage length l_{1-6} and its value at the middle of l_{1-6} is K_{1-6}.

This leads to the same formulae of (1) but $l_{i-j} = l_{i-j}/2$ and the origin from which l is measured is taken to be at $l_{1-6}/2$.

7.7.3 ANCHORAGE LENGTH (l_{i-j})

From series (1) results and the pilot test it is concluded that part of the column is acting as an extra anchorage length.

Hence for 7.7.1 (1) and (2) the anchorage length is

(1) l_{i-j} = Overall depth of the base slab (h_{i-j})

or

(2) $l_{i-j} = h_{i-j} + 90$ mm.

Since series (1) results give (200 mm.) extra anchorage length and pilot specimen gives (138 mm.) extra anchorage length, but the stress measured at (90 mm.) above the top surface of the base, so this must be used as an extra anchorage length for these calculations, and it is assumed to be the same as increasing the depth of the base slab by (90 mm.).

7.7.4. CALCULATIONS

To calculate the average anchorage bond stress from the above formulae, the value of K_{1-6} and X_{1-6} (max.) are needed to be known, and to find them the average experimental anchorage bond stress of T_{1-6} is used to find X_{1-6} (max.) in terms of K_{1-6}, then assuming a value of K_{1-6} to calculate X_{1-6}(max.) from equations (11a) and (12a) so that it gives the best fit with the other experimental results using equations (11c, 11d, 12c, and 12d) and the f_{cu} values of the base concrete and this is obtained by trial and error, see example below.

For 7.7.2(2) using $\frac{l_{i-j}}{2}$ and $\frac{l_{1-6}}{2}$ instead of l_{i-j} and l_{1-6} respectively in 7.7.2.(1) formulae, it gives exactly the same results of 7.7.2.(1).

After calculating the average theoretical anchorage bond stress f_{bs} (theory), the ratio (R) of the experimental results f_{bs}(av.) to f_{bs} (theory) is calculated then divided by f_{cu} and $\sqrt{f_{cu}}$ to see how the results are vary best with f_{cu} or $\sqrt{f_{cu}}$ by comparing the coefficients of variation which are the smallest values given by the assumed values of K_{1-6}.

The best results of the above calculations are tabulated as follows:-

For 7.7.2.(1-i, 1-ii) and $l_{i-j} = h_{i-j}$ in table 7.1.

For 7.7.2.(1-i, 1-ii) and $l_{i-j} = h_{i-j}$ + 90 mm. in table 7.2.

Example of calculations :-

Table 7.1. (1) :-

From T_{1-6} results, equation (11) gives

$$5.18 = K_{1-6} + \frac{X_{1-6}\,(max)}{3}$$

Assume $K_{1-6} = 3.5$ N/mm^2

Then $X_{1-6}(max.) = 5.04$ N/mm^2 and

$f(max.) = 8.54$ N/mm^2.

Then from equation (11d) the values of F_{i-j} is calculated for all the specimens, then this is used to find $F_{i-j}\ X_{1-6}(max)$ and then from equation (11c) the value f_{bs}(theory) is obtained and then the value of R is calculated where $R = f_{bs}(av.)/f_{bs}(theory)$. Then R/f_{cu} and $R/\sqrt{f_{cu}}$ are calculated. The average value of R/f_{cu}, $R/\sqrt{f_{cu}}$ and the coefficients of variation are calculated. Then the value of K_{1-6} is reduced or increased until the smallest value of the coefficient of variation is obtained.

Table 7.1 (2) :-

From T_{1-6} results, equation (12) gives

$$5.18 = K_{1-6} + \frac{X_{1-6}\,(max)}{4}$$

Assume $K_{1-6} = 3.75$ N/mm^2 then

$X_{1-6}(max) = 5.72$ N/mm^2 and

$f(max) = 9.47$ N/mm^2.

Then the calculations continued as for Table 7.1 (1), but using equations(12c and 12d).

Table 7.2 (1) and (2) :-

The calculations of this table are the same as in Table 7.1 (1) and (2) except for $l_{i-j} = h_{i-j} + 90$ mm.

7.7.5. DISCUSSION

Summary of the Tables.

TABLE	7.1 (1)	7.1 (2)	7.2 (1)	7.2 (2)
Average R/f_{cu}	0.029	0.029	0.029	0.028
Coefficient of variation	3.6%	4.1%	5.3%	6.7%
Average $R/\sqrt{f_{cu}}$	0.170	0.170	0.170	0.169
Coefficient of variation	3.5%	3.1%	1.8%	1.8%

All the tables give an average value of $R/f_{cu} = 0.029$ and $R/\sqrt{f_{cu}} = 0.170$ except table 7.2 (2).

From the coefficient of variation it can be seen that the results are best related to $\sqrt{f_{cu}}$ and using $l_{i-j} = h_{i-j} + 90$ mm. gives better results than using $l_{i-j} = h_{i-j}$ and finally using parabolic distribution of 7.7.2(1-i) is better than using a cubic one

Hence,

$R = 0.17\sqrt{f_{cu}}$ and the results of T_{1-6} for $l_{1-6} = 490$ mm. can be used to determine the average anchorage bond stress, but since there is not enough information on the extra anchorage length from the column length a part of series (1) and the pilot tests therefore, more tests are needed before it can be used in design calculations, but the above results can be used to calculate the anchorage length and then using it as the depth of the base slab, for the same type of column reinforcement, amount of A_s and base lateral dimensions.

7.8 CONCLUSIONS

1) From the pilot tests and T_{3-3} it is also concluded that part of the column length is acting as an extra anchorage length and it is $= 138$ mm.

2) From the theoretical distribution of the anchorage bond stress it is concluded that it is better to relate the average anchorage

bond stress to $\sqrt{f_{cu}}$ rather than f_{cu} and the best curve is a parabolic one of the form given by (11c and 11d) for $l_{i-j} = h_{i-j} + 90$ mm. and showed that the average anchorage bond stress is dependent on the anchorage length confirming Wilkins (1951) conclusion for pull out tests.

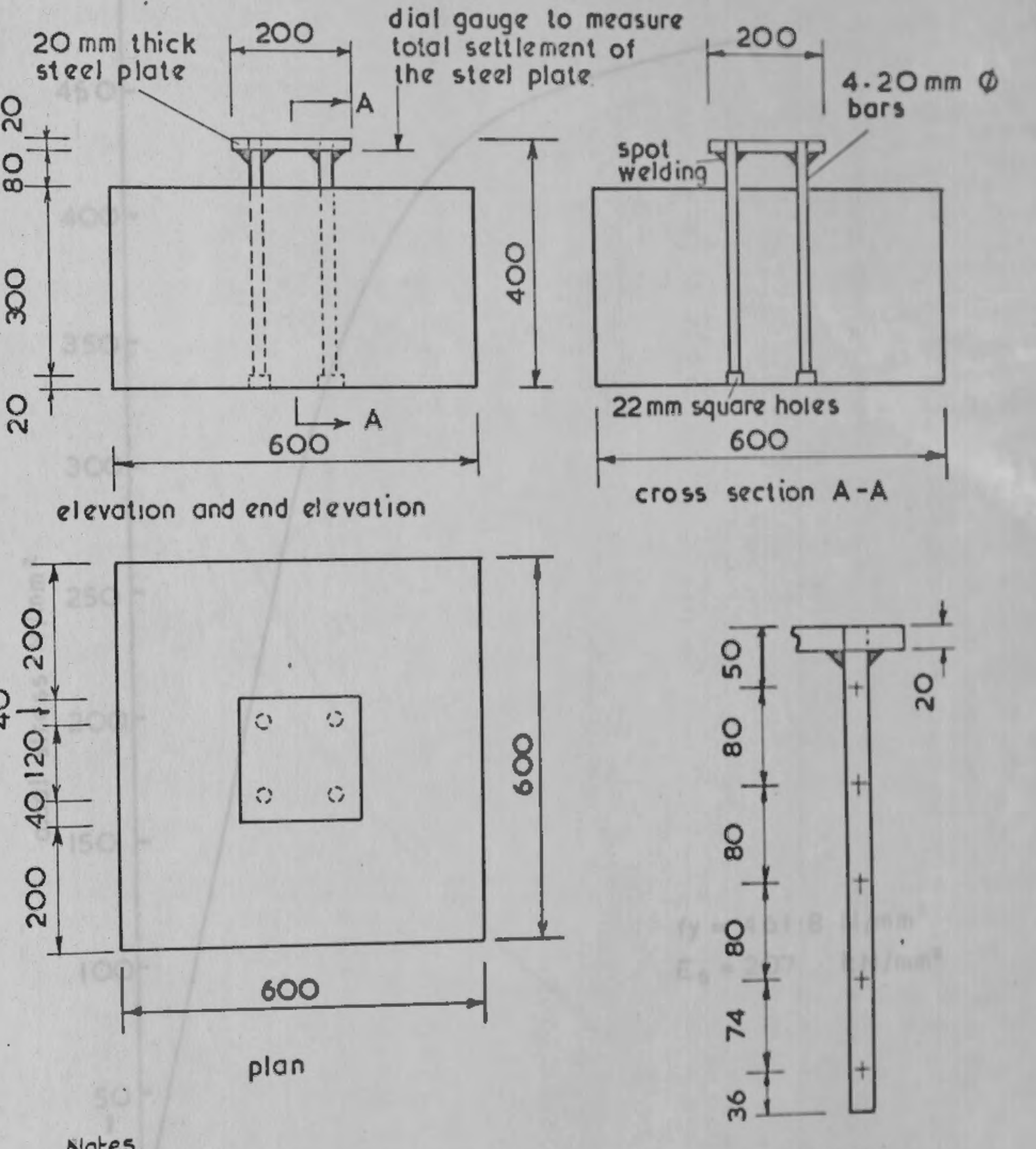

Notes.

1. All dimensions are in mm.
2. Scale 1:10 or as shown.
3. Two electrical resistance strain gauges are fixed at each position one opposite to the other

scale 1:5

Position of 5 mm electrical resistance strain gauges on each of the 20 mm Ø bars.

Fig. 7.1. Details of pilot specimen

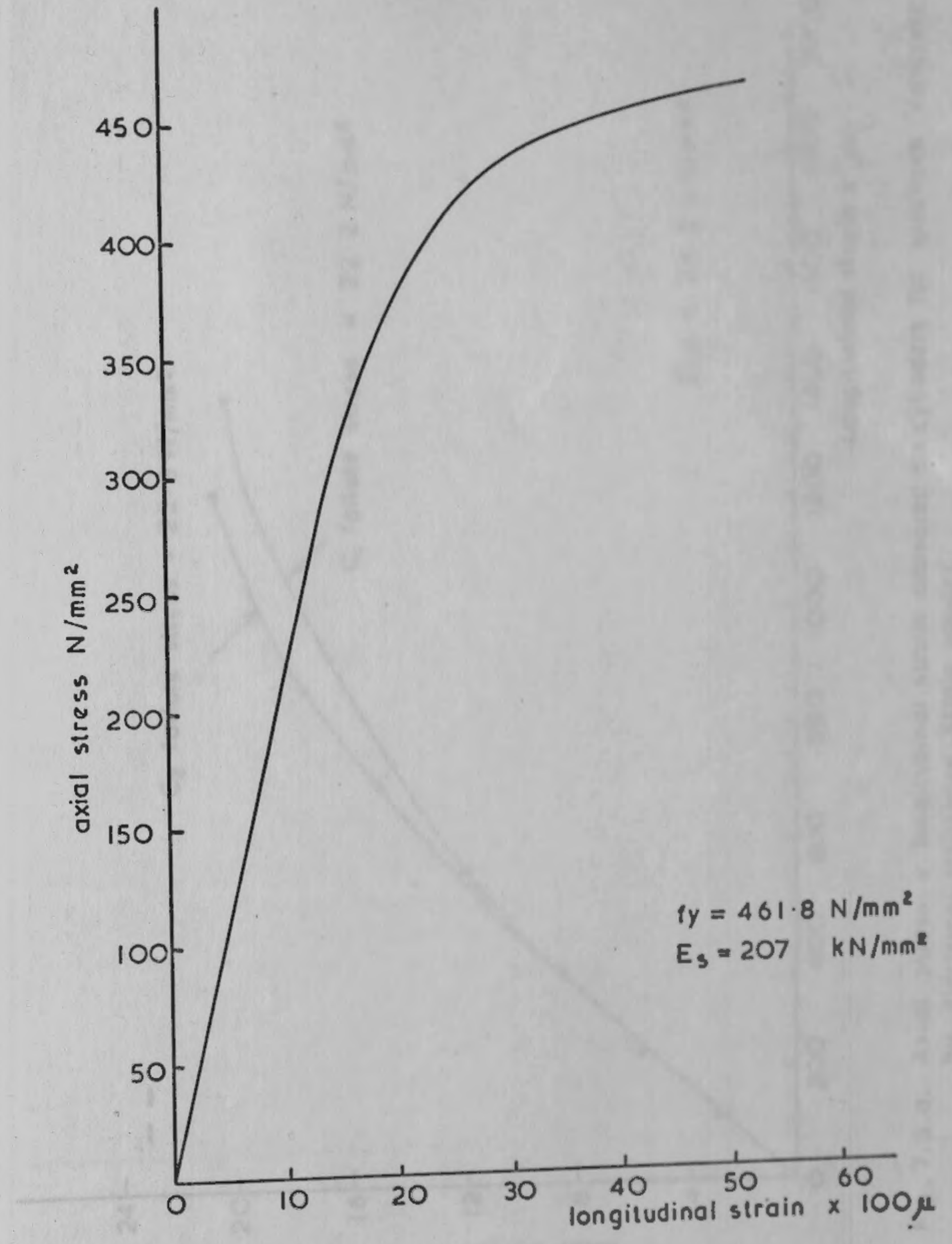

Fig. 7.2. Stress v. strain for 20mm Ø H.T. square twisted steel bar.

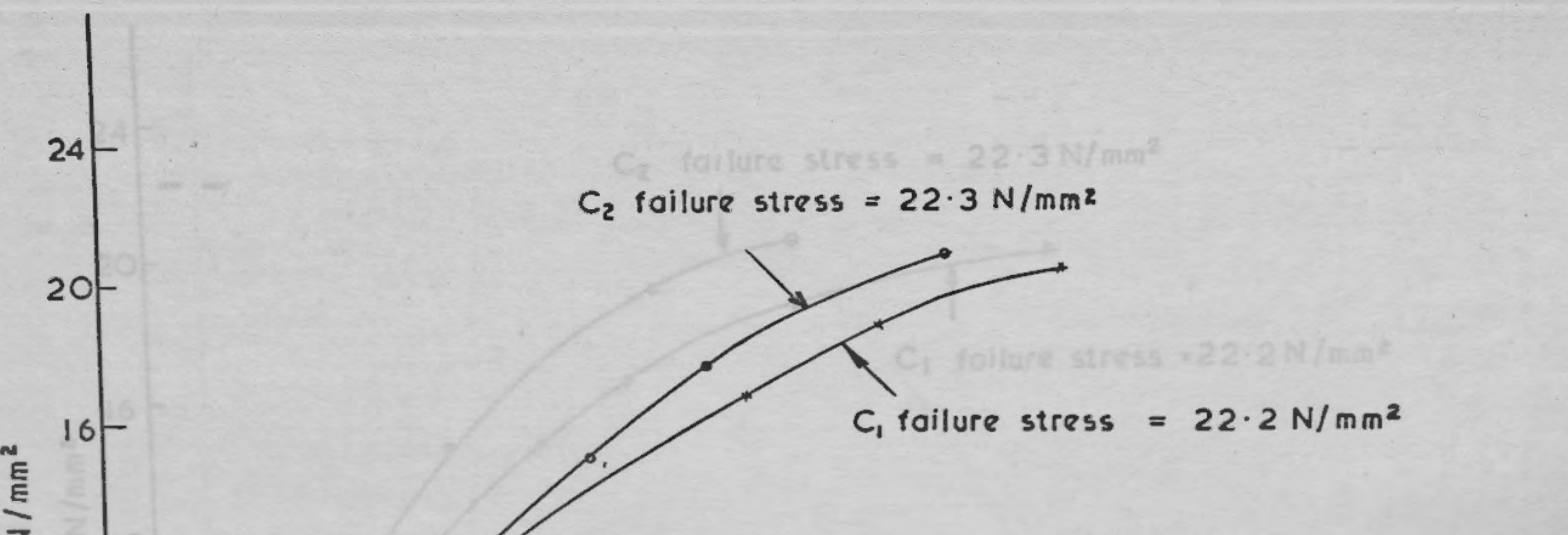

Fig. 7.3.a Axial stress v longitudinal strain measured on cylinders for specimen concrete by electrical resistance strain gauges

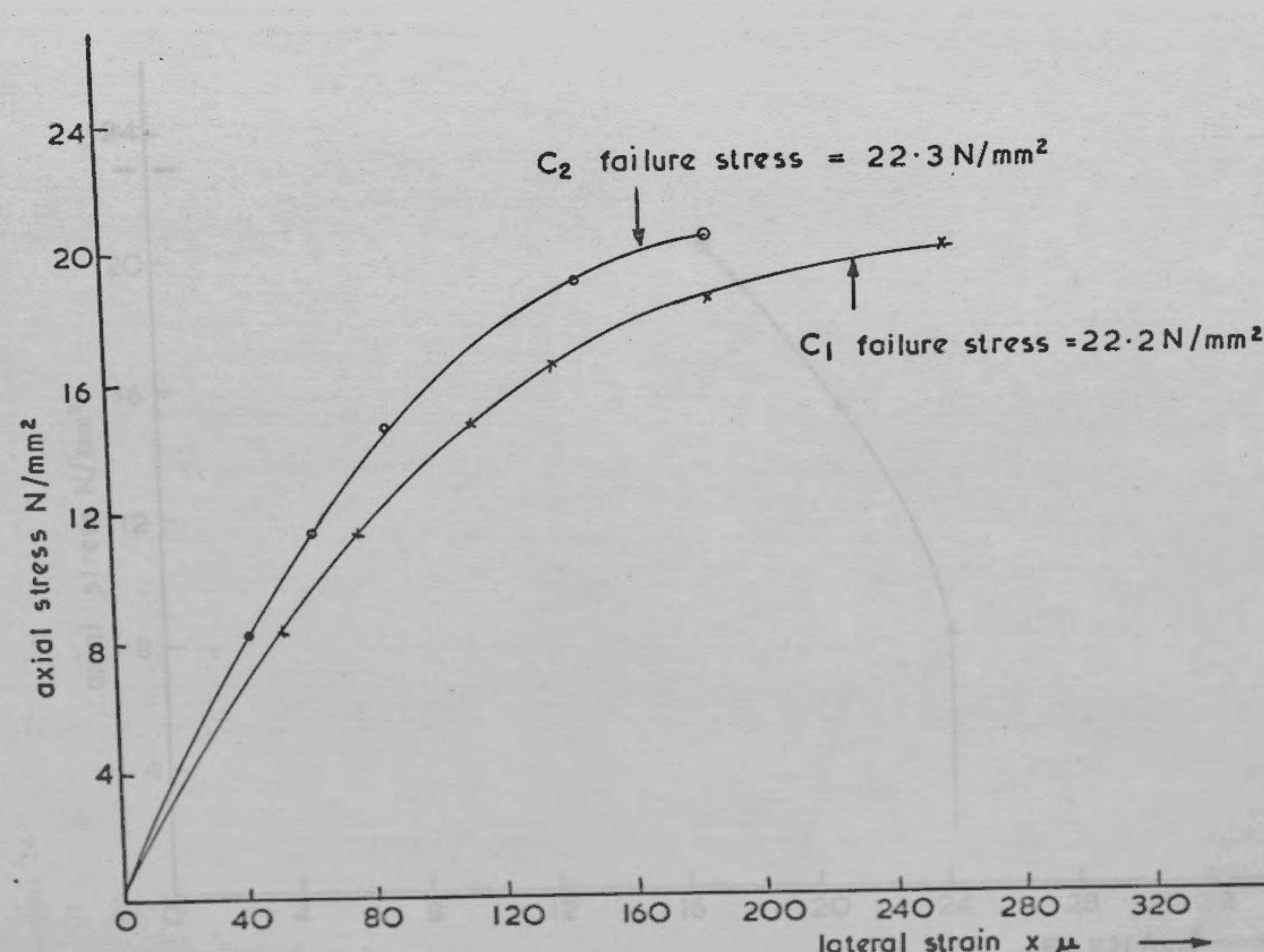

Fig. 7.3.b. Axial stress v. lateral strain measured on cylinders for specimen concrete by electrical resistance strain gauges

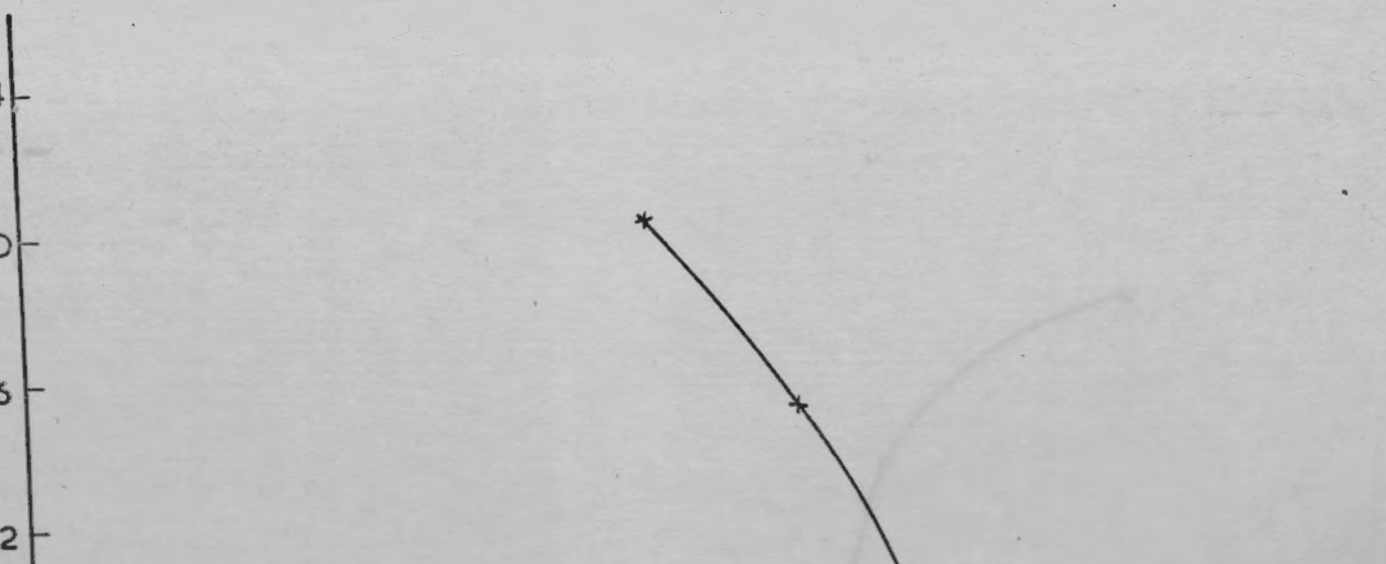

Fig. 7 .3.c Axial stress v. Modulus of elasticity for specimen concrete Ec

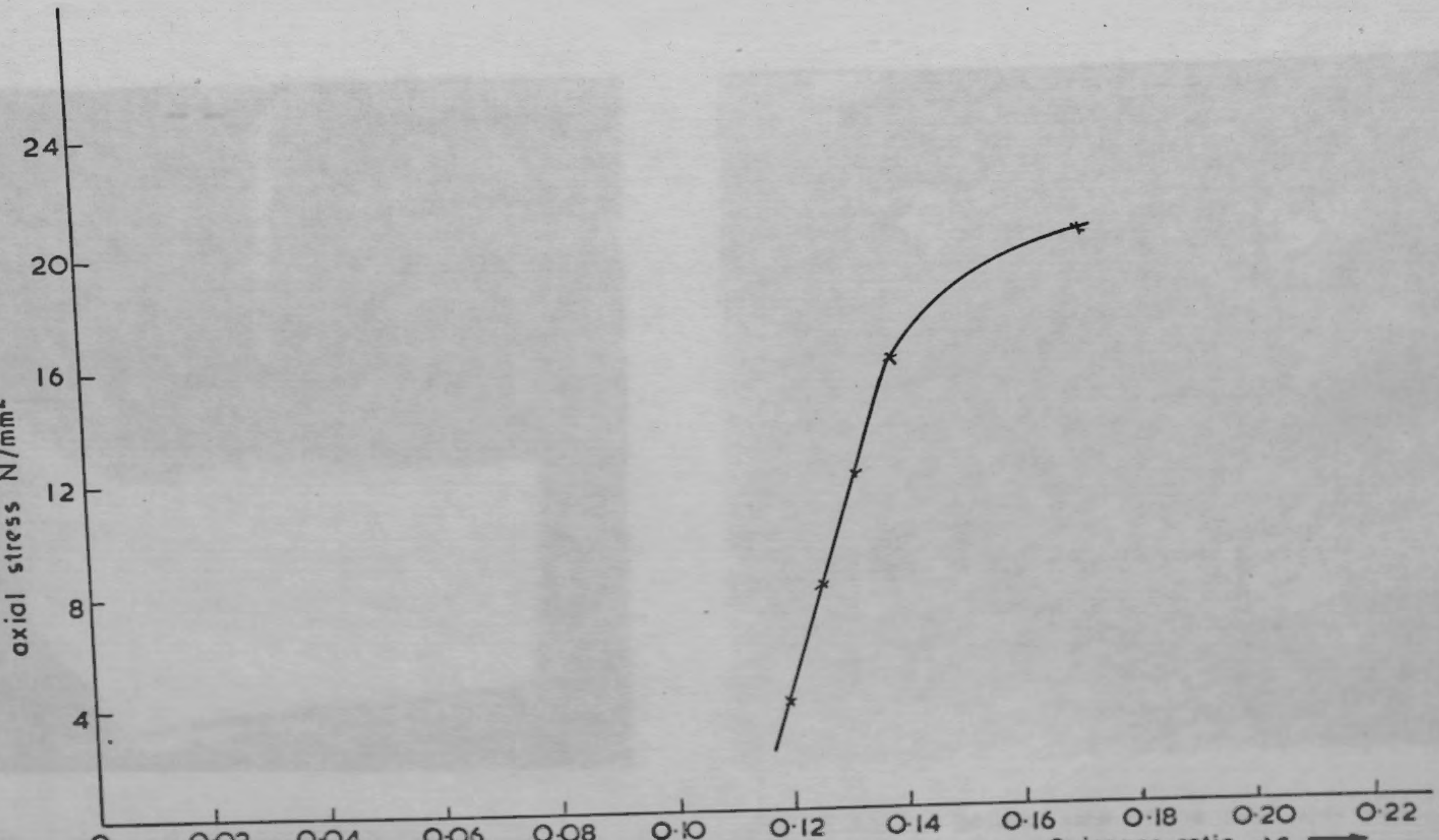

Fig. 7.3.d. Axial stress v Poisson's ratio νc for specimen concrete

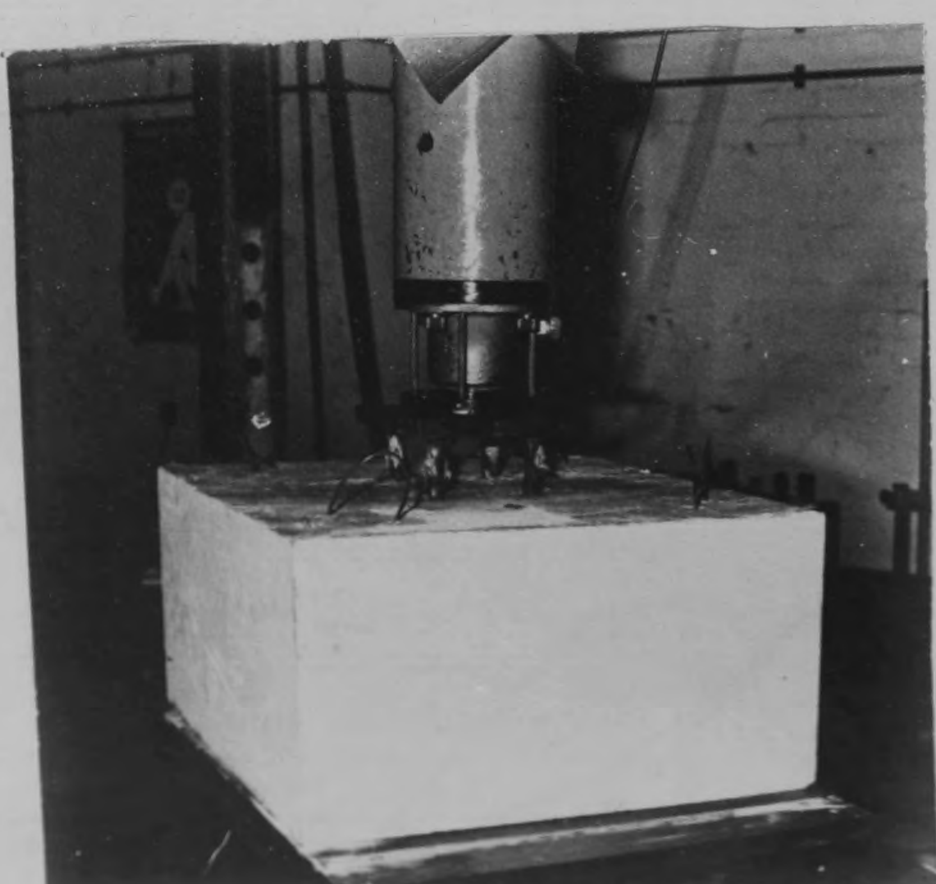

Fig 7.4.a Pilot specimen in the testing rig

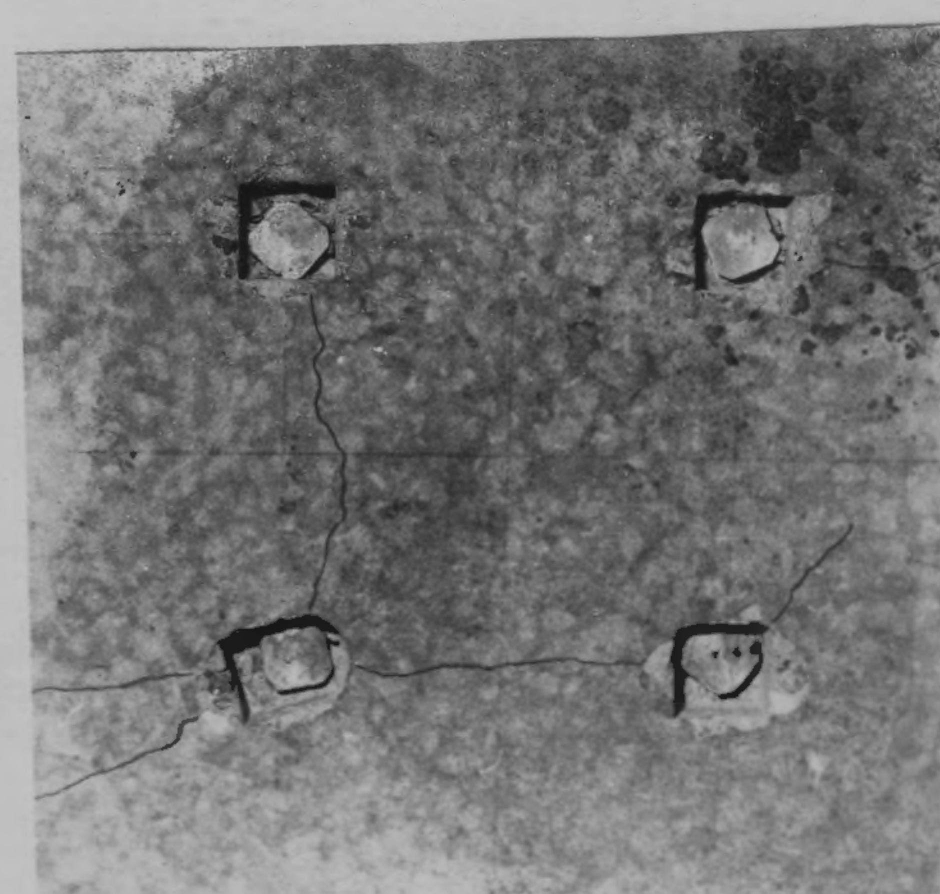

Fig 7.4.b Bottom view of the pilot specimen after failure.

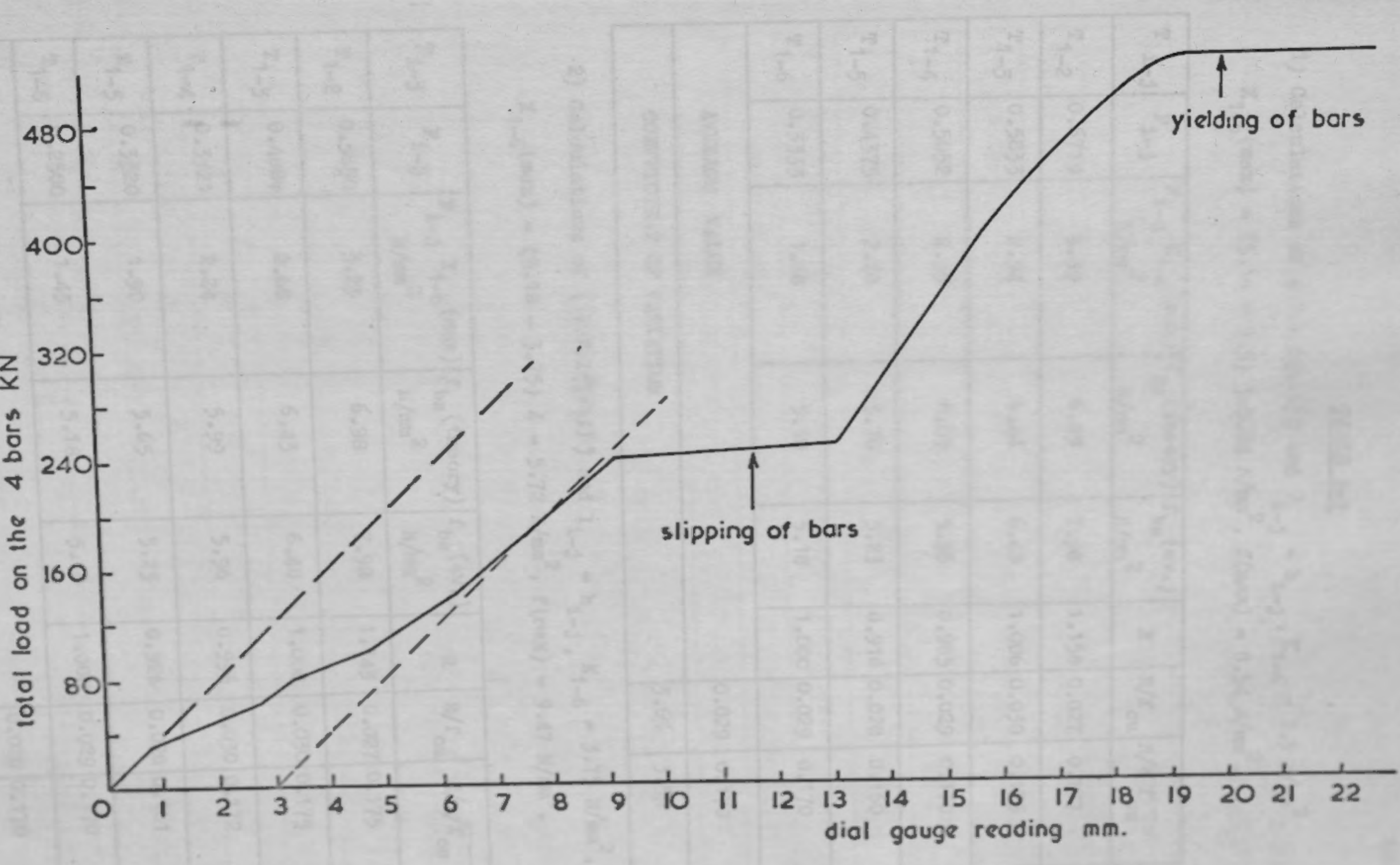

Fig. 7.5. Total load on the 4-20 mm Ø bars v. dial gauge reading at the bottom of the steel plate

TABLE 7-1

1) Calculations of (7.7.2(1-i)) and $l_{i-j} = h_{i-j}$, $K_{1-6} = 3.5$ N/mm^2,
$X_{1-6}(\max) = (5.18 - 3.5)\ 3 = 5.04$ N/mm^2, $f(\max) = 8.54$ N/mm^2.

T_{i-j}	F_{i-j}	$F_{i-j}\ X_{1-6}(\max)$ N/mm^2	f_{bs}(theory) N/mm^2	f_{bs}(av.) N/mm^2	R	R/f_{cu}	$R/\sqrt{f_{cu}}$
T_{1-2}	0.6719	3.39	6.89	7.98	1.158	0.027	0.177
T_{1-3}	0.5833	2.94	6.44	6.48	1.006	0.030	0.175
T_{1-4}	0.5052	2.55	6.05	5.96	0.985	0.029	0.170
T_{1-5}	0.4375	2.20	5.70	5.23	0.918	0.028	0.160
T_{1-6}	0.3333	1.68	5.18	5.18	1.000	0.029	0.170
AVERAGE VALUE						0.029	0.170
COEFFICIENT OF VARIATION						3.6%	3.5%

2) Calculations of (7.7.2(1-ii)) and $l_{i-j} = h_{i-j}$, $K_{1-6} = 3.75$ N/mm^2,
$X_{1-6}(\max) = (5.18 - 3.75)\ 4 = 5.72$ N/mm^2, $f(\max) = 9.47$ N/mm^2.

T_{i-j}	F_{i-j}	$F_{i-j}\ X_{1-6}(\max)$ N/mm^2	f_{bs}(theory) N/mm^2	f_{bs}(av.) N/mm^2	R	R/f_{cu}	$R/\sqrt{f_{cu}}$
T_{1-2}	0.5650	3.23	6.98	7.98	1.143	0.027	0.175
T_{1-3}	0.4688	2.68	6.43	6.48	1.008	0.030	0.175
T_{1-4}	0.3921	2.24	5.99	5.96	0.995	0.030	0.172
T_{1-5}	0.3320	1.90	5.65	5.23	0.926	0.028	0.161
T_{1-6}	0.2500	1.43	5.18	5.18	1.000	0.029	0.170
AVERAGE VALUE						0.029	0.170
COEFFICIENT OF VARIATION						4.1%	3.1%

TABLE 7-2

1) Calculations of (7.7.2(1-i)) and $l_{i-j} = h_{i-j} + 90$ mm. $K_{1-6} = 3.8$ N/mm^2, $X_{1-6} = (4.23 - 3.8)\ 3 = 1.29\ N/mm^2$, $f(max) = 5.09\ N/mm^2$.

T_{i-j}	F_{i-j}	$F_{i-j}\ X_{1-6}(max)$ N/mm^2	f_{bs}(theory) N/mm^2	f_{bs}(av.) N/mm^2	R	$R/\ f_{cu}$	$R/\sqrt{f_{cu}}$
T_{1-2}	0.5902	0.76	4.56	4.99	1.094	0.026	0.167
T_{1-3}	0.5250	0.68	4.48	4.47	0.998	0.030	0.173
T_{1-4}	0.4666	0.60	4.40	4.38	0.996	0.030	0.172
T_{1-5}	0.4152	0.54	4.34	4.02	0.926	0.028	0.165
T_{1-6}	0.3333	0.43	4.23	4.23	1.000	0.029	0.170
AVERAGE VALUE						0.029	0.170
COEFFICIENT OF VARIATION						5.3%	1.8%

2) Calculations of (7.7.2.(1-ii)) and $l_{i-j} = h_{i-j} + 90$ mm. $K_{1-6} = 3.8$ N/mm^2, $X_{1-6} = (4.23 - 3.8)\ 4 = 1.72\ N/mm^2$, $f(max) = 5.52\ N/mm^2$.

T_{i-j}	F_{i-j}	$F_{i-j}\ X_{1-6}(max)$ N/mm^2	f_{bs}(theory) N/mm^2	f_{bs}(av.) N/mm^2	R	$R/\ f_{cu}$	$R/\sqrt{f_{cu}}$
T_{1-2}	0.4758	0.82	4.62	4.99	1.080	0.025	0.165
T_{1-3}	0.4107	0.71	4.51	4.47	0.991	0.030	0.172
T_{1-4}	0.3571	0.61	4.41	4.38	0.993	0.030	0.171
T_{1-5}	0.3136	0.54	4.34	4.02	0.926	0.028	0.165
T_{1-6}	0.2500	0.43	4.23	4.23	1.000	0.029	0.170
AVERAGE VALUE						0.028	0.169
COEFFICIENT OF VARIATION						6.7%	1.8%

CHAPTER 8.

CONCLUSIONS AND SUGGESTIONS FOR DESIGN AND FURTHER RESEARCH

8.1. CONCLUSIONS

Although each of the previous chapters contains its own conclusions, this section will show the general conclusions of this research project and they are as follows :-

1) The column base joint strength compared with equation (1) varies linearly with the anchorage length which is the overall depth of the base slab (h) plus part of the column length acting as an extra anchorage length. This extra anchorage length is (200 mm.) for specimens of series (1), (163.6 mm.) from series (3) specimens and (138 mm.) from the pilot specimen and T_{3-3} results. This shows that the extra anchorage length is not constant for the same column.

2) The anchorage bond stress is dependent on the anchorage length. For specimen just failed by yielding of the longitudinal column reinforcement, the anchorage bond stress has a parabolic distribution plus a constant value along the anchorage length. For shallower bases, the upper part of the distribution may be used to calculate the average theoretical anchorage bond stress.

3) The anchorage bond strength for the column bars increases as the value of (ρ) increases by increasing the cross-sectional area of the tensile base slab reinforcement (A_s). For the same value of (A_s) it is better to use small diameter bars closely spaced than large bars widely spaced. The strength of the column base joint increases as the value of (ρ) increases by increasing (A_s) and keeping the effective depth (d) constant where it reduces as the value of (ρ) increases by reducing (d) and keep

ing (A_s) constant..

4) The anchorage bond strength for the column bars increases as the lateral dimensions of the base slab increase and tends to reach a limiting value as the dimensions increase beyond 900 x 900 mm. square corresponding to $\frac{AB - a_1 a_2}{a_1 a_2} = 19.25$.

5) The ultimate axial load transferred from the short column to the base can be calculated from the following equation for columns having the same properties as those used in this experimental program :-

$$P_3 = (0.91 A_{core} + 0.75 A_{cover}) f_{cu} + 0.9 f_y A_{sc}.$$

This means that the axial load transferred to the base from the core concrete at a higher stress than that from the cover concrete. The constants 0.91 and 0.75 cannot be related to any of the variables in the tests.

6) For specimen just failed by yielding of the column 20 mm. Ø square twisted H.T steel longitudinal reinforcement. The maximum average stress in the bars is 0.85 f_y and the maximum stress in any bar is 0.941 f_y whereas the maximum average stress is 0.905 f_y when the column contained no concrete.

8.2. SUGGESTIONS FOR DESIGN

Since this research program did not cover all the variables, it is difficult at this stage to draft any general conclusions for design, but for columns and bases having the same properties as those used in this project it is possible to suggest the following :-

1) Use three part addition formula to calculate the ultimate axial load transferrable from short columns to bases as in equation (10) and using the values of γ_m recommended by CP110:Part 1: 1972.

2) Assuming that the column does not provide any extra anchorage length for square twisted H.T. steel bars, an anchorage bond stress of 5.18 N/mm^2 can be used to calculate the anchorage length. Alternatively an anchorage bond stress of 4.23 N/mm^2 can be used to calculate the anchorage length where the column provides an extra anchorage length equal to the core size.

Also for other columns and bases the following are suggested :-

1) Use two part addition formula to calculate the ultimate axial load transferrable from short columns to bases as in equation (1) and γ_m values are given by CP110:Part 1: 1972.

2) Use CP110: Part 1: 1972 - table (22) for the ultimate anchorage bond stresses to calculate the anchorage lengths since it is on the safe-side until the suggestions for further research are completed.

8.3. SUGGESTIONS FOR FURTHER RESEARCH.

To complete this research program the following are suggested to be done :-

1) For square twisted H.T. steel bars reinforcement, the following should be done :-

i) Obtain a family of curves for different values of tensile base slab reinforcement (A_s) by varying (h) as in fig. (3.10) and hence to calculate the anchorage length required to resist anchorage bond failure for each value of (A_s).

ii) To investigate the effects of varying the geometrical properties of column concrete section and the bar size of the column reinforcement.

iii) To find experimentally the distribution of the anchorage bond stress along the anchorage length.

iv) To find the value of the column length which is acting as an extra anchorage length to be used in design by carrying out some tests with columns contained no concrete.

v) To find the effect of varying f_{cu} from (20 - 40) N/mm^2.

2) To repeat the research above using ribbed bars reinforcement.

3) To repeat the research above using plain bars reinforcement.

4) To draft a complete recommendation for design purposes.

REFERENCES

ABRAMS, D.A. (1913), "Test of bond between concrete and steel". University of Illinois, Engineering Experimental Station, Bulletin No. 71, December, 1913.

A.C.I. Standards (1974), Building code requirements for reinforced concrete. (ACI 318-71) October, 1974.

ALLEN, A. H. (1972), "Concrete design to CP110- Simply explained". P.20, Cement and Concrete Association, 1972.

ANIS, N. N. (1970) "Shear strength of reinforced concrete slabs without shear reinforcement". Ph.D Thesis, London University, 1970.

ANSON, M., and NEWMAN, K. (1966), "The effect of mix proportions and method of testing on Poisson's ratio for mortars and concrete" Magazine of Concrete Research: vol. 18, No. 56: Sept. 1966. pp. 115 - 130.

AU, T., and BAIRD, D.L. (1960), "Bearing capacity of concrete blocks". J. Am. Concr. Inst., Vol. 31, March, 1960. pp. 869 - 879.

BACH, C., and GRAF, O. (1915), "Tests of square and rectangular reinforced concrete slabs supported on all sides. "(Versuche mit allseitig aufliegenden, quandratischen and recteckigen eis en etoplatten. (In German), Deutchen Ausschus fur Eisen beton. Vol. 30, Berlin, 1915. pp. 1 - 309.

BASE, G.D. (1959), "Some tests on punching shear strength of reinforced concrete slabs". Cement and Concrete Association, Technical report TRA/321, July, 1959.

BRITISH STANDARDS INSTITUTION, (1972), "The structural use of Conrete". British Standard Code of practice. CP110:Part 1: 1972. (Design materials and workmanship). London.

ERSOY, U., and HAWKINS, M.M. (1960), "Bearing Capacity of Concrete blocks". J.Am.Concr.Inst., Vol. 31, September, 1960, pp. 1467-1479.

FERGUSON, Phil. M. (1966),"Bond stress the state of the art". J.Am. Concr. Inst., Vol. 63, No. 11, November, 1966, pp. 1161-1189.

FERGUSON, Phil M., and THOMPSON, J. Neils. (1962)."Development length of high strength reinforcing bars in bond". J.Am.Concr.Inst., Vol. 59, No. 7, July, 1962, pp. 887-922.

FORSELL, C. and HOLMBERG, A. (1946),"Concentrated load on concrete slabs." (Stampellast pa plattor av betong.) Betong, Stockholm, Vol. 31, (2), 1946, pp. 95 - 123.

GHOSH, S.K. SARGIN, M., and HANDA, V.K.(1971),"The effectiveness of cover in reinforced concrete compression members". Proceedings of the Institution of Civil Engineers, Vol. 50, November, 1971, P. 353, (Synopsis).

GRAF,O,(1938) (2). "Tests of reinforced concrete slabs under concentrated load applied near one support". (Versuche uber die wiederstands - fahigkeit von eisenbeton platten unter konzentrierter last nahe einem auflagen). (In German) Deutscher Ausschuss fur Eisenbeton (Be lin), Heft 73, 1933.

GRAF,O.(1938) (2)."Strength tests of thick reinforced concrete slabs supported on all sides under concentrated loads." (Versuche uber die wiederstands fahigkeit von allseitigen aufliegenden dicken eisenbeton platten unter einzellasten). (In German), Deutcher Ausschuss fur Eisenbeton (Berlin,) Heft 88, 1938, pp. 1 - 26.

HALSTEAD, P.E. (1969)."The Significance of Concrete cube tests". Magazine of Concrete Research: Vol. 21, No. 69, December, 1969, pp. 187 - 194.

"Discussion of the above paper"
Magazine of Concrete Research: Vol. 22, No.73, December, 1970, pp. 239 - 242.

HAWKINS, N.M. (1968) (1). "The bearing strength of concrete loaded through rigid plates". Magazine of Concrete Research: Vol,20, No. 62: March, 1968, pp. 31 - 40.

HAWKINS, N.M. (1968)(2). "The bearing strength of concrete loaded through flexible plates." Magazine of Concrete Research: Vol. 20, No. 63, June, 1968, pp. 95 - 102.

HIGGINS, J.B. and HOLLINGTON, M.R. (1973), "Design and detailed (CP110: 1972) p. 22. Cement and Concrete Association, 1973.

HOGNESTAD, E. (1953),"Shearing strength of reinforced concrete column footings". J.Am.Concr.Inst., November, 1953, Proceedings, 50, pp. 189 - 208.

HOGNESTAD, E., ELSTNER, R.C.(1956),"Shearing strength of reinforced concrete slabs". J.Am.Concr.Inst., July, 1956, Proceedings, 53, pp. 29 - 58.

HOGNESTAD, E., ELSTNER, R.C. and HANSON, J. (1964),"Shear strength of reinforced structural lightweight concrete slabs". J.Am.Concr. Inst., June, 1964, Proceedings, 61, pp. 643 - 656.

IR.M.DRAGOSAVIC and IR. A.VAN DENBEUKEL(1974),(IBBC-TNO) "Punching Shear" HERON, Vol. 20, No.2, 1974, Delft, The Netherlands.

IVY, C.B. (1966),"The diagonal tension resistance of structural lightweight concrete slabs". Ph.D. Dissertion, Graduate College of The Texas A and M University, January, 1966.

KING, J.W.H. (1949),"Some investigations of the effect of core size and steel and concrete quality in short reinforced concrete columns". Magazine of Concrete Research; June, 1949, pp. 47 - 56.

KINNUNEN, S. (1963),"Punching of concrete slabs with two-way reinforcement". Paper No. 198, Transactions of the Royal Institute of Technology, Stockholm, 1963.

LONG, A.E. (1967) (1), "Punching failure of reinforced concrete slabs under combined loading conditions". The Institution of Civil Engineers, Northern Ireland Association, February, 1967.

LONG, A.E.(1967) (2), "Punching failure of reinforced concrete slabs". Ph.D. Thesis, The Queen's University of Belfast, May, 1967.

LONG, A.E. and BOND, D. (1967), "Punching failure of reinforced concrete slabs". Paper No. 7002, Proceedings, The Institution of Civil Engineers, Vol. 37, May, 1967.

MARSHALL, W.T. (1944), "Experiments on reinforced concrete column bases". Paper No. 5383, Proceedings, The Institution of Civil Engineers, Vol. 22, 1944, pp. 49 - 52.

MATTES, N.S., and POULOS, H.G. (1968), "The settlement of a single compressible pile". Civil Engineering. Res.Rep. No. R94, University of Sydney 1968.

MEDINA, O. Jr.(1961), "Strength of non-monolithic connections between a flat plate slab and concrete column". M.Sc. Thesis, Graduate School of the University of Texas, June, 1961.

MEYERHOF, G.F.(1953) ,"The bearing capacity of concrete and rock". Magazine of Concrete Research, April, 1953, Vol. 4, pp. 107 - 116.

MOE, J. (1961),"Shearing strength of reinforced concrete slabs and footings under concentrated loads". Bulletin D.49, Development Department, Portland Cement Association, Illinois, April, 1961.

NYLANDER, H., and KINNUNEN, S. (1960),"Punching of concrete slabs without shear reinforcement." Paper No. 158, Transactions of the Royal Institute of Technology, Stockholm, 1960.

PFISTER, J.F, and MATTOCK, A.H. (1963) ,"High Strength bars as concrete reinforcement; Part 5, lapped bars in concentrically loaded column". Journal of the Portland Cement Association, Vol. 5, No. 2, May, 1963, pp. 27 - 40.

PLOWMAN, J.M. (1963),"Youngs modulus and Poisson's ratio of concrete at various humidities". Magazine of Concrete Research, vol. 15, No. 44, July, 1963, pp. 77 - 82.

POULOS, H.G. and DAVIS, E.H. (1968), "The settlement behaviour of single axially loaded incompressible piles and piers". Geotechnique, 18, pp. 351-371, 1968.

REGAN, P.E. (1974),"Design for punching shear". The Structural Engineer, June, 1974, No.6, Vol. 52, pp. 197 - 207.

REMEDIOS, N.C. and WOOD, W.G. (1969), "Stress diffusion from an end loaded reinforcing bar to plane matrix". Proceedings of the Institution of Civil Engineers, Vol. 42, March, 1969, pp. 397 - 411.

RICHART, F.E. (1948), "Reinforced concrete wall and column footings". J.Am.Concr.Inst., October - November, 1948, Proceedings, 45, pp. 97 - 127, 237 - 260.

ROBERTS, N.P. (1973),"Behaviour and design of tensile lapped joints in reinforced concrete beams". Civil Engineering and Public Works Review, January, 1973, pp. 33 - 45.

SARGIN, M., GHOSH, S.K., and HANDA, V.K. (1971) ,"Effect of lateral reinforcement upon the strength and deformation properties of concrete". Magazine of Concrete Research, Vol. 23, No. 75 - 76, June - September, 1971. pp. 99 - 110.

SHELSON, W. (1957),"Bearing capacity of concrete". J.Am.Concr.Inst., Vol. 29, November, 1957, pp. 405 - 414.

SOMERVILLE, G. (1971),"Structural joints in precast concrete and the compression bond problem". Ph.D.Thesis City University, 1971.

SOMERVILLE, G. AND TAYLOR, H.P.J.,(1972), "The influence of reinforcement detailing on the strength of concrete structures. "(Joggled splices in columns). The Structural Engineer, January, 1972. No.1. Vol. 50, pp. 10 - 12.

STAMEN KOVIC. A.(1969),"Local strength of flat slabs at column leads". Ph.D Thesis, University of London, September, 1969.

STAMENKOVIC, A., and CHAPMAN, J.C.(1972),"Local strength at column leads in flat slabs subjected to a combined vertical and horizontal loading". Paper No. 7633, Proceedings, Part 2, The Institution of Civil Engineers, 1972, pp. 205 - 232.

TALBOT, A.N.(1913),"Reinforced concrete wall footings and column footings". University of Illinois Engineering Experiment Station, Bulletin No. 67, March, 1913, pp. 1 - 114.

TANKUT, T. (1969),"Behaviour of flat plate structures subjected to various combinations of vertical and horizontal loads". Ph.D Thesis. University of London, 1969.

WESTLEY, J.W. (1966),"Some experiments on concrete cubes with non-plane surfaces".
Magazine of Concrete Research, Vol. 18, No. 54, March, 1966, pp. 35 - 37.

WHITNEY,C.S. (1957),"Ultimate shear strength of reinforced concrete flat slabs, footings, beams, and frame members without shear reinforcement". J.Am.Concr.Inst.Vol. 54, No.4. October, 1957. pp. 265 - 298.